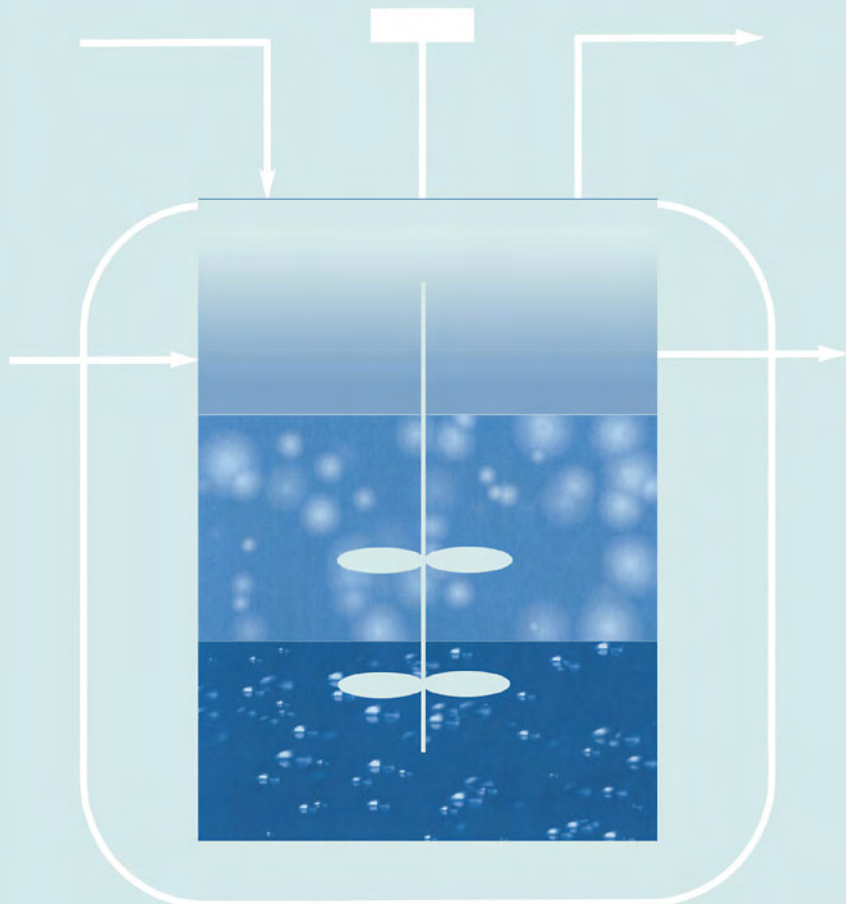


# Multiphase Bioreactor Design



Edited by  
Joaquim M.S. Cabral, Manuel Mota and Johannes Tramper

**Also available as a printed book**  
see title verso for ISBN details

# Multiphase Bioreactor Design



# Multiphase Bioreactor Design

Edited by

**Joaquim M.S.Cabral**

*Centre for Biological and Chemical Engineering  
Instituto Superior Técnico, Lisbon  
Portugal*

**Manuel Mota**

*Department of Biological Engineering  
University of Minho  
Portugal*

and

**Johannes Tramper**

*Wageningen Agricultural University  
Food and Bioprocess Engineering Group  
The Netherlands*



London and New York

First published 2001 by Taylor & Francis 11 New Fetter Lane, London EC4P 4EE  
Simultaneously published in the USA and Canada by Taylor & Francis Inc, 29 West 35th Street,  
New York, NY 10001

*Taylor & Francis is an imprint of the Taylor & Francis Group*

This edition published in the Taylor & Francis e-Library, 2005.

"To purchase your own copy of this or any of Taylor & Francis or Routledge's collection of thousands of eBooks please go to [www.eBookstore.tandf.co.uk](http://www.eBookstore.tandf.co.uk)."

© 2001 Taylor & Francis

All rights reserved. No part of this book may be reprinted or reproduced or utilised in any form or by any electronic, mechanical, or other means, now known or hereafter invented, including photocopying and recording, or in any information storage or retrieval system, without permission in writing from the publishers.

Every effort has been made to ensure that the advice and information in this book is true and accurate at the time of going to press. However, neither the publisher nor the authors can accept any legal responsibility or liability for any errors or omissions that may be made. In the case of drug administration, any medical procedure or the use of technical equipment mentioned within this book, you are strongly advised to consult the manufacturer's guidelines.

*British Library Cataloguing in Publication Data* A catalogue record for this book is available from the British Library

*Library of Congress Cataloging in Publication Data* A catalogue record has been requested

ISBN 0-203-30304-0 Master e-book ISBN

ISBN 0-203-34644-0 (Adobe eReader Format)

ISBN 0-415-27209-2 (Print Edition)

# CONTENTS

Preface	vii
Contributors	ix
1 New Methodologies for Multiphase Bioreactors 1:Hydrodynamic and Mass Transfer Characteristics of Multistage Slurry Reactors <i>Jindřich Zahradník</i>	1
2 New Methodologies for Multiphase Bioreactors 2: Image Analysis and Multiphase Bioreactors <i>Eugénio C.Ferreira, Manuel Mota and Marie-Noëlle Pons</i>	27
3 New Methodologies For Multiphase Bioreactors 3: Data Acquisition, Modelling and Control <i>Sebastião Feye de Azevedo, Rui Oliviera and Bernhard Sonnleitner</i>	57
4 Design and Modelling of Immobilised Biocatalytic Reactors <i>Bruno S.Ferreira, Pedro Fernandes and Joaquim M.S.Cabral</i>	90
5 Advances in the Selection and Design of Two-Liquid Phase Biocatalytic Reactors <i>Gary J.Lye and John M.Woodley</i>	122
6 Enzymatic Membrane Reactors <i>Duarte Miguel F.Prazeres and Joaquim M.S.Cabral</i>	145
7 Reversed Micellar Bioreaction Systems: Principles and Operation <i>Cristina M.L.Carvalho and Joaquim M.S.Cabral</i>	191
8 Solid-to-Solid Bioconversions: Batch or Continuous? <i>M.J.F.Michielsen, Rene H.Wijffels, Johannes Tramper and H.H.Beeltink</i>	238
9 Solid/Gas Systems, Theory and Applications <i>Sylvain Lamare, T.Maugard and Marie D.Legoy</i>	261
10 Biofilm Reactors <i>Luis F.Melo and Rosário Oliveira</i>	288
11 Pulsing Bioreactors <i>Juan M.Lema, Enrique Roca, Angeles Sanromán, M. José Núñez, M.Teresa Moreira and Gumerindo Feijoo</i>	328
12 Design of Liquid-Liquid-Solid Fluidised-Bed Bioreactors <i>Erik van Zessen, Arjen Rinzema and Johannes Tromper</i>	353
13 Flocculation Bioreactors <i>António A.Vicente, Manuel Mota and José A.Teixeira</i>	387
14 Bioreactor Design For Plant Cell Suspension Cultures <i>Patricia M.Kieran</i>	417

15	Lethal Effects of Bubbles in Animal-Cell Culture <i>Dirk E.Martens, Michel F.Muller, Cornelis D.de Gooijer and Johannes Tromper</i>	453
16	A Low-Cost Technology for Entomopathogenic Nematode Large-Scale Production <i>José Neves, Nelson Simões and Manuel Mota</i>	491
17	Marine Sponges as Biocatalysts <i>René H.Wijffels, Ronald Osinga, Shirley Pomponi and Johannes Tromper</i>	506
	Index	526

## PREFACE

The term bioreactor was not widely accepted for many years and initially, the term fermentor was preferred. The science-based approach to studying fermentors, using all the available knowledge from Chemical Engineering Science on the one hand, and the widespread use of reactors to perform enzyme-catalysed reactions on the other, gradually made the term bioreactor the most appropriate term to encompass every container where a controlled biological reaction may take place.

A bioreactor is defined as “A vessel in which a biological reaction or change takes place, usually a fermentation or a biotransformation, including tank bioreactors, immobilised cell bioreactors, hollow fibre and membrane bioreactors and digestors” (*“Biotechnology—from A to Z”, William Bains, Oxford Univ. Press, 2000*).

For a long time, bioreactors were able to accomplish a single biotransformation, and to contain a single species of an organism. Even when a mixed microbial population was present, the predominance of a certain species allowed for a model simplification, where only the dominant species was taken into account.

An attempt to classify bioreactors in two main groups according to the source of power and the degree of homogeneity was made by the Working Party of Bioreactor Performance of the European Federation of Biotechnology (*“Physical Aspects of Bioreactor Performance”, Dechema, W.Crueger (Ed.), 1987*). Even so, the authors noted that “...Many designs of bioreactor attempt to keep the whole of their volume homogeneous. Most stirred volumes are in this category although, as the scale increases, total homogeneity becomes progressively more difficult. There is no such thing as a true plug-flow bioreactor (except for immobilised bioconversions), since the characteristic fermentation time is of a magnitude greater than the outflow rate. Nevertheless, some bioreactors do aim to cycle the conditions; the deep shaft effluent treatment reactor is a good example. Oxygen is absorbed at the high pressures in the bottom, while carbon dioxide is desorbed best near the surface. In other configurations the designer may consciously decide to let the conditions vary within acceptable limits (e.g. the temperature in a reactor with an external cooling loop). These designs represent an intermediate case.”

The omnipresence of mixed populations in natural systems has always been the rule rather than the exception. Every bioprocess engineer working with single species cultures is deeply conscious of how relentless his strife against external contamination has to be.

Today, there is a generalised recognition of wastewater treatment systems as mixed population bioreactors, where a cohort of protozoa and many bacterial species cohabit and co-operate to remove contaminants from water. Furthermore, with the enormous liquid volumes dealt with by these systems—many billions of gallons of wastewater are processed each day around the world—there is no more excuse for excluding mixed species bioreactors as an important field of research.

Even when a single species is present, there is often the need for considering different developmental stages or physiological states, of which only one is responsible for the

production of the active substance that is sought after. On the other hand, more and more complex biotransformations are taking place within bioreactors. Some of them involve different phases, namely in biocatalysis in organic media, and the interplaying reactions are sometimes difficult to explain with the conventional models.

The same applies to gas-solid, liquid-solid or solid-solid transformations where in several instances it will be the structure of one of the phases, or its distribution inside the bioreactor that is going to control the final product yield.

Recently bioreactors were proposed for large-scale production of complex metazoan organisms. New problems arose, especially in those cases where sexual reproduction is compulsory. The problems will be still more complex whenever sexes exhibit different morphologies or physical properties. Another level of complexity will then be brought about, because the consideration of extra solid phases will be unavoidable.

All the aforementioned cases deal with multiphase bioreactors. In most of them, the quest for homogeneity is no longer a matter of concern. On the contrary, the absence of homogeneity is the rule. The number of liquid or solid phases may be greater than one, and, in several cases—membrane bioreactors, high-density cell cultures, fixed-film bioreactors, among others—phase segregation is a must, in order to optimise products recovery. We are thus obliged to consider the appropriate design of a multiphase bioreactor, each of which may be a special case with totally new questions to solve.

Research on this field will need new methodologies, able to deal with the different phases interplaying within the same time window. Eventually, new mathematical tools will be necessary, as well as new experimental methodologies.

That is why the present work was divided into three different parts. Part I presents new methodologies that are being successfully applied to the study of multiphase bioreactors. Part II is devoted to the presentation of bioreactors that, by their very own design, are specially fitted to deal with multiphase bioprocesses, and which may, in some instances, be the first solution for a multiphase reaction. Part III is devoted to the presentation of several case studies, where different approaches were used to solve real multiphase reaction problems.

We are convinced that, in the forthcoming years, a very active and flourishing area will emerge, dealing with these special kinds of bioreactors. We expect that this work will be helpful to all those who are at present struggling to increase the productivity of a bioprocess where multiple phases are playing a central role.

Joaquim Cabral  
Manuel Mota  
Johannes Tramper

# **CONTRIBUTORS**

## **H.H.Beefink**

Food and Bioprocess Engineering Group  
Wageningen University  
P.O. Box 8129  
6700 EV Wageningen  
The Netherlands

## **Joaquim M.S.Cabral**

Centre for Biological and Chemical Engineering  
Instituto Superior Técnico  
Av. Rovisco Pais  
1049–001 Lisboa  
Portugal

## **Cristina M.L.Carvalho**

Faculdade de Farmácia de Lisboa  
Universidade de Lisboa  
Av. Prof. Gama Pinto  
1649–003 Lisboa  
Portugal

## **Cornelis D. de Gooijer**

Food and Bioprocess Engineering Group  
Wageningen University  
P.O. Box 8129  
6700 EV Wageningen  
The Netherlands

## **Gumersindo Feijoo**

Department of Chemical Engineering  
Institute of Technology  
University of Santiago de Compostela  
Av. das Ciencias s/n  
E-15706 Santiago de Compostela  
Spain

## **Pedro Fernandes**

Universidade Lusófona de Humanidades e Tecnologies  
Av. do Campo Grande, 376  
1749–024 Lisboa

Portugal

**Eugénio C.Ferreira**

Department of Biological Engineering  
Universidade do Minho  
4710–057 Braga  
Portugal

**Bruno S.Ferreira**

Centre for Biological and Chemical Engineering  
Instituto Superior Técnico  
Av. Rovisco Pais  
1049–001 Lisboa  
Portugal

**Sebastião Fayo de Azevedo**

Department of Chemical Engineering  
Faculty of Engineering  
Universidade do Porto  
Rua Dr. Roberto Frias  
4200–465 Porto  
Portugal

**Patricia M.Kieran**

Department of Chemical Engineering  
University College Dublin  
Belfield, Dublin 4  
Ireland

**Sylvain Lamare**

Laboratoire du Génie Protéique et Cellulaire  
Université de La Rochelle  
Avenue Marillac  
17042 La Rochelle, Cedex 1  
France

**Marie D.Legoy**

Laboratoire du Génie Protéique et Cellulaire  
Université de La Rochelle  
Avenue Marillac  
17042 La Rochelle, Cedex 1  
France

**Juan M.Lema**

Department of Chemical Engineering  
Institute of Technology

University of Santiago de Compostela  
Av. das Ciencias s/n  
E-15706 Santiago de Compostela  
Spain

**Gary J.Lye**  
The Advanced Centre for Biochemical Engineering  
University College London  
Torrington Place  
London WC1E 7JE  
UK

**Dirk E.Martens**  
Food and Bioprocess Engineering Group  
Wageningen University  
P.O. Box 8129  
6700 EV Wageningen  
The Netherlands

**T.Maugard**  
Laboratoire du Génie Protéique et Cellulaire  
Université de La Rochelle  
Avenue Marillac  
17042 La Rochelle, Cedex 1  
France

**Luis F.Melo**  
Department of Chemical Engineering  
University of Porto  
Rua Dr. Roberto Frias  
4200-465 Porto  
Portugal

**M.J.F.Michielsen**  
Food and Bioprocess Engineering Group  
Wageningen University  
P.O. Box 8129  
6700 EV Wageningen  
The Netherlands

**M.Teresa Moreira**

Department of Chemical Engineering  
Institute of Technology  
University of Santiago de Compostela  
Av. das Ciencias s/n  
E-15706 Santiago de Compostela  
Spain

**Manuel Mota**

Department of Biological Engineering  
Universidade do Minho  
4710-057 Braga  
Portugal

**Michel F.Muller**

Food and Bioprocess Engineering Group  
Wageningen University  
P.O. Box 8129  
6700 EV Wageningen  
The Netherlands

**José Neves**

Departamento de Biologia e Centro de Investigação em Recursos Naturais  
Universidade dos Açores  
9501-801 Ponta Delgada  
Portugal

**M.José Núñez**

Department of Chemical Engineering  
Institute of Technology  
University of Santiago de Compostela  
Av. das Ciencias s/n  
E-15706 Santiago de Compostela  
Spain

**Rosário Oliveira**

Department of Biological Engineering  
Universidade do Minho  
4710-057 Braga  
Portugal

**Rui Oliveira**

Department of Chemical Engineering  
Faculty of Engineering  
Universidade do Porto

Rua Dr. Roberto Frias  
4200–465 Braga  
Portugal

**Ronald Osinga**  
Food and Bioprocess Engineering Group  
Wageningen University  
P.O. Box 8129  
6700 EV Wageningen  
The Netherlands

**Shirley Pomponi**  
Division of Biomédical Marine Research  
Harbor Branch Oceanographie Institution  
5600 US1 North  
Fort Pierce FL 34946  
USA

**Marie-Noëlle Pons**  
Laboratoire des Sciences du Génie Chimique  
CNRS-ENSIC-INPL  
1 Rue Grandville BP 451  
F-54001 Nancy Cedex  
France

**Duarte Miguel F.Prazeres**  
Centre for Biological and Chemical Engineering  
Instituto Superior Técnico  
Av. Rovisco Pais  
1049–001 Lisboa  
Portugal

**Arjen Rinzema**  
Food and Bioprocess Engineering Group  
Wageningen University  
P.O. Box 8129  
6700 EV Wageningen  
The Netherlands

**Enrique Roca**  
Department of Chemical Engineering  
Institute of Technology  
University of Santiago de Compostela  
Av. das Ciencias s/n  
E-15706 Santiago de Compostela  
Spain

**Angeles Sanromán**

Department of Chemical Engineering  
Institute of Technology  
University of Santiago de Compostela  
Av. das Ciencias s/n  
E-15706 Santiago de Compostela  
Spain

**Nelson Simões**

Departamento de Biologia e Centro de Investigação em Recursos Naturais  
Universidade dos Açores  
9501-801 Ponta Delgada  
Portugal

**Bernhard Sonnleitner**

Department of Chemistry  
Zurich University of Applied Sciences  
P.O. Box 805  
CH-8401 Winterthur  
Switzerland

**José A. Teixeira**

Department of Biological Engineering  
Universidade do Minho  
4710-057 Braga  
Portugal

**Johannes Tramper**

Food and Bioprocess Engineering Group  
Wageningen University  
P.O. Box 8129  
6700 EV Wageningen  
The Netherlands

**Erik van Zessen**

Food and Bioprocess Engineering Group  
Wageningen University  
P.O. Box 8129  
6700 EV Wageningen  
The Netherlands

**António A. Vincente**

Department of Biological Engineering  
Universidade do Minho  
4710-057 Braga  
Portugal

**Rene H.Wijffels**

Food and Bioprocess Engineering Group  
Wageningen University  
P.O. Box 8129  
6700 EV Wageningen  
The Netherlands

**John M.Woodley**

The Advanced Centre for Biochemical Engineering  
University College London  
Torrington Place  
London WC1E 7JE  
UK

<sup>†</sup>**Jindřich Zahradník**

Institute of Chemical Process Fundamentals  
Academy of Sciences of the Czech Republic  
Rozvojová 135  
165–02 Prague, 6-Suchdol  
Czech Republic

# **CHAPTER ONE**

## **NEW METHODOLOGIES FOR MULTIPHASE BIOREACTORS 1: HYDRODYNAMIC AND MASS TRANSFER CHARACTERISTICS OF MULTISTAGE SLURRY REACTORS**

JINDŘICH ZAHRADNÍK<sup>†</sup>

*Institute of Chemical Process Fundamentals, Academy of Sciences of the  
Czech Republic, Rozvojová 135, 165 02 Prague 6-Suchdol, Czech  
Republic*

### **ABSTRACT**

The advantageous features of multistage bubble column reactors for aerated slurry systems have been illustrated by the results of an extensive experimental study aimed at examining the effect of selected construction and operating variables (number of reactor stages, distributing plate geometry, gas and liquid flow rates, solid phase concentration) on hydrodynamic and mass transfer characteristics of multistage aerated slurry reactors. Experimental results proved the favourable effect of column sectionalisation on gas holdup and  $k_{LaL}$  values, and on the energy effectiveness of gas-liquid contacting. The effect of increasing solid concentration on these system characteristics was negative within the whole region of experimental conditions. The relationship between  $k_{LaL}$  and gas holdup was independent of the solid phase concentration and gas flow rate. However, the value of  $k_{LaL}$  corresponding to the given gas holdup ratio increased substantially with the increasing number of column stages. Axial mixing of the liquid (slurry) phase was well described by the model of perfectly mixed tanks in series with backflow, for the number of series terms equal to the number of column stages. Evaluation of the backflow coefficient stressed the importance of plate design optimisation for particular flow conditions. Implications of the experimental findings for the performance and applicability of multistage slurry reactors has been discussed thoroughly. Recommendations for future research have been given, aimed at clarifying particular aspects of multistage reactors performance with slurry systems and ultimately at providing reliable basis for the design and scale-up of such reactors.

<sup>†</sup> deceased

## INTRODUCTION

According to their operation mode, the multistage bubble column reactors sectionalised by internal plates represent a class of reactors with dispersed gas phase, distinguished by the energy input with gas compression and by spatially distributed energy dissipation in the reactor (Schügerl, 1983). Although it has been commonly acknowledged that sectionalisation of bubble column reactors can significantly improve their mass transfer characteristics and, at the same time, substantially reduce the degree of backmixing in contacted phases (Schügerl *et al.*, 1977; Shah *et al.*, 1978; Shah *et al.*, 1982; Deckwer, 1985), the multistage bubble column reactors have been only scarcely applied to chemical or biotechnological processes in aerated slurry systems. This type of slurry reactor has been received little coverage even in scientific literature. Accordingly, the multistage bubble column reactors were not even mentioned in the comprehensive treatment of reactors for gas-liquid-solid systems published by Shah (1979), and they were touched only marginally in the respective part of the more recent book on heterogeneous reactions authored by Doraiswamy and Sharma (1984). The Solvay towers, used in soda production (Shah *et al.*, 1978), thus still represent the proverbial exception proving the rule, regarding the industrial application of sectionalized bubble columns for g-l-s systems. In the bioreactors area, performance of a laboratory-scale multistage tower fermentor was studied by Prokop and co-workers (1969) and the application prospects of staged bubble column fermentors were subsequently discussed e.g. by Sittig and Heine (1977) and by Schügerl (1980, 1983). On the industrial scale, various modifications of internal-loop airlift reactors with dual-flow plates in the riser have been reportedly used for SCP production by the Japanese companies Kanefuchi and Mitsubishi Co. (Schügerl, 1983) and, most notably, a similar construction principle has been employed in the 1500 m<sup>3</sup> pressure cycle fermenter designed for the ICI PRUTEEN plant (Westlake, 1986). These applications have not, however, found many followers and the multistage tower fermenters were not even listed in the review paper of Mersmann and co-workers (1990), devoted to the selection and design of aerobic bioreactors. Apparently, it is the fear of plate holes choking and/or solid phase sedimenting on internal plates which has been primarily responsible for the reluctant approach to the application of staged bubble columns for systems with a suspended solid phase. While these phenomena may, indeed, represent a definite threat, namely in rapidly sedimenting systems, sectionalized bubble columns can be, according to our opinion, advantageously employed for pseudohomogeneous (non-sedimenting) suspensions of fine particles and/or in cases of small density differences between the solid and the liquid phases. Obviously, this latter condition is generally fulfilled in biological systems. Furthermore, the danger of plates choking can be to a large degree circumvented by the use of plates with downcomers, i.e. with the separate passage of gas and slurry phases.

Our previous study (Vlaev and Zahradník, 1987) demonstrated superior energy effectiveness of sectionalised bubble columns in comparison with other types of tower reactors for aerated slurry systems, including single-stage bubble column, tower reactor with an ejector distributor, and multistage rotating-discs reactor. In the following, the advantageous features of multistage bubble column reactors for aerated slurry systems will be illustrated with the results of the experimental study (Zahradník *et al.*, 1992) aimed at examining the effect of selected construction and operating variables (number of

column stages, distributing plate geometry, gas and liquid flow rates, solid phase concentration) on hydrodynamic and mass transfer characteristics of multistage aerated slurry reactors. The particular objectives of the reported work included:

- Evaluating the effect of column sectionalisation on liquid or suspension phase backmixing in the reactor and on the values of gas holdup and volumetric coefficient of mass transfer between the gas and liquid phases ( $k_{LaL}$ );
- Derivating and experimentally verifying physically realistic model of liquid phase (suspension) residence time distribution in a multistage bubble column sectionalised by perforated plates with downcomer tubes without overflow weirs and investigating the effect of operating regime on the extent of liquid backflow between the adjacent column stages;
- Experimentally determining the effect of solid phase concentration on gas holdup values and on the rate of gas-liquid mass transfer, i.e. on the values of  $k_{LaL}$ ; Evaluating the effect of column sectionalisation and solid phase concentration on the energy effectiveness of bubble bed formation and of gas-liquid interfacial mass transfer.

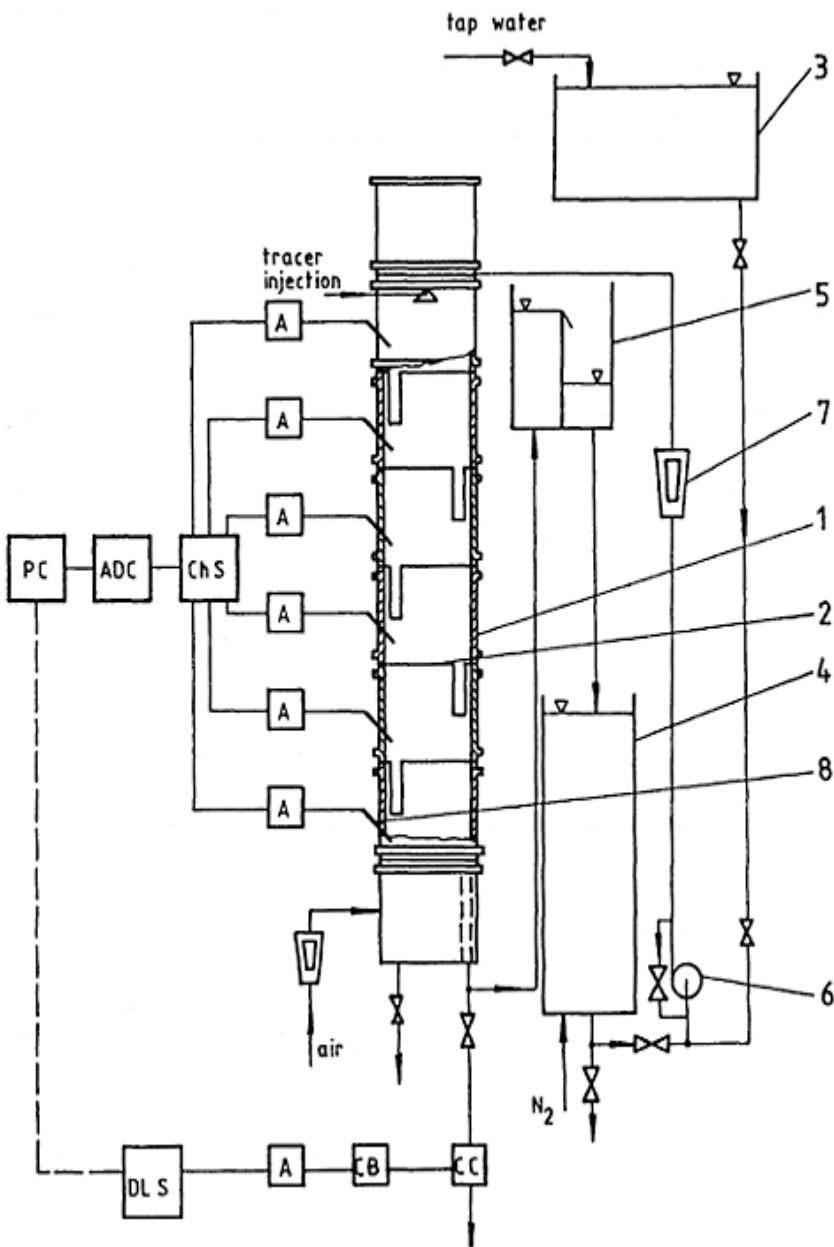
## EXPERIMENTAL

The experiments were carried out in a bubble column reactor 0.29 m in diameter and 2 m in height. The column was built of glass cylinders mounted between metal flanges and could be alternatively divided into three or six stages (stage height 0.6 m or 0.3 m respectively) by internal perforated plates with downcomer tubes without overflows. The plates were made of brass sheets 2 mm thick, free plate area ratio was 0.25%, holes diameter 1.8 mm. The downcomer tubes were 0.1 m long and 0.04 m in diameter; some preliminary experiments in the three-stage column were performed also with the tube length 0.42 m. The scheme of the experimental set-up is given in Figure 1.1; constructing details of distributing plates (position of downcomer tubes and placing of orifices) can be found elsewhere (Zahradník *et al.*, 1992). Experiments were carried out in a *countercurrent flow arrangement* with systems air-water and air-aqueous suspension of ZnO respectively. The characteristic particle dimension was 2.3  $\mu\text{m}$ , 90% of the particles were smaller than 3  $\mu\text{m}$  (see Kratochvíl *et al.*, 1985). Experiments were performed within the range of solid phase concentrations  $c_s=1\text{--}5$  wt.%. Experimental regions of gas and liquid (slurry) flow rates,

$$Q_G = 1.67\text{--}4.44 \times 10^{-3} \text{ m}^3\text{s}^{-1},$$

$Q_L$  (or  $Q_{SL}$ ) =  $0\text{--}2.11 \times 10^{-3} \text{ m}^{-3}\text{s}^{-1}$  corresponded to the superficial velocities  $u_{oG}=0.025\text{--}0.067 \text{ m s}^{-1}$  and  $u_{oL}$  (or  $u_{osl}$ ) =  $0\text{--}0.029 \text{ m s}^{-1}$ . Supposedly, such phase velocities covered the common operating regions of single-stage bubble column reactors while the plate geometry guaranteed uniform gas distribution within the whole experimental range of  $u_{oG}$  values (Zahradník *et al.*, 1982b).

Residence time distribution of the liquid or slurry phase was determined by the pulse response technique using aqueous solution of KCl as a tracer and the electrical conductivity detection method. A tracer pulse was injected into the feed stream in the upper column stage, the injection time fulfilled in the whole experimental region of liquid (slurry) flow rates condition for the satisfactory simulation of the pulse input signal,  $\Delta t_i/t_{av}$

**Figure 1.1** Experimental set-up

1—bubble column, 2—perforated plates, 3—storage tank, 4—auxiliary tank for circulation flow regime, 5—

overflow vessel, 6—pump, 7—rotameters, 8—oxygen electrodes; A—amplifier, ChS—channel selector, CC—conductivity cell, ADC—analog-digital converter, PC—personal computer, DLS—data logging system, CB—compensating bridge.

<0.05 (Kaštánek *et al.*, 1993). The tracer concentration in the exit stream was measured continuously by means of a conductivity cell installed at the column outlet (see Figure 1.1). The amplified electrode signal was sampled and stored in a PC and the experimental response curves were subsequently transformed to a dimensionless form, corresponding to the system response to a unit pulse signal (Dirac function). On the basis of previous analysis (Kaštánek and Zahradník, 1973), values of the abscissa of curve maximum ( $\theta_{Y_{\max}}$ ) and ordinate at  $\theta=1$  ( $Y_{\theta=1}$ ) were selected as suitable criteria for a simple comparison of experimental RTD curves with those calculated from respective mixing models. Values of the liquid backflow coefficient,  $E_{i+1,i}$ , defined as the ratio of the liquid backflow between the adjacent column stages to the net liquid throughput,  $Q_L$ , were measured by the stationary colorimetric method. Solution of methylene blue dye was continuously dosed to the lower column stage and its concentration in samples taken from individual column stages under steady state conditions was determined by the photometer Spekol-2 (Carl Zeiss Jena). Values of the backflow coefficient were then calculated from the relation

$$E_{i+1,i} = 1 / [(c_{i+1}/c_i) - 1] \quad (1)$$

derived from the steady state tracer balance (column stages are numbered from the top). Comparison of experimental RTD curves proved, in agreement with the literature (Kato and co-workers, 1972; Vlaev and Zahradník, 1987), that the presence of the solid phase had negligible effect on the liquid phase residence time distribution within the whole range of experimental conditions. Values of the backflow coefficient were therefore measured only in the air-water system.

The stationary method was employed for determining values of the volumetric gas-liquid mass transfer coefficient,  $k_{L}a_L$ . Deoxygenised liquid or slurry phase was continuously fed to the upper column stage and steady state concentration of dissolved oxygen in individual column stages was measured by polarographic electrodes of the Clark type. Respective  $k_{L}a_L$  values were then calculated from the oxygen balance equations assuming plug flow of the gas phase. Liquid (slurry) mixing in the column was described, on the basis of our RTD measurements, by the model of perfectly mixed tanks in series with backflow, for values of the backflow coefficients determined at respective flow conditions.

The average values of gas holdup ratio (bubble bed voidage) in individual column stages were determined by the method of pressure differences modified for the application in slurry systems. Values of wetted plate pressure drop were calculated from readings of pressure taps situated below and above the respective distributing plates.

## RESULTS AND DISCUSSION

### Preliminary Tests

The solid phase distribution in the reactor volume was virtually uniform within the whole range of experimental conditions. The suspension of ZnO particles was therefore further treated as a pseudohomogeneous continuum, characterized for each particular solid concentration by appropriate values of slurry density and viscosity, evaluated from relations proposed by Brinkman (1952) and Roscoe (1952):

$$\rho_{sl} = \varepsilon_s \rho_s + (1 - \varepsilon_s) \rho_L \quad (2)$$

$$\mu_{sl} = \mu_L (1 - \varepsilon_s)^{-2.5} \quad (3)$$

Results of pressure loss measurements in the sectionalised column ( $N=3$  and  $6$ ) showed its "autoregulation" behaviour. The total pressure drop of the column, defined as the sum of wetted plates pressure drop and of the hydrostatic pressure of the liquid phase (slurry) in the column, was constant for given values of liquid flow rate and solid phase concentration within the whole region of gas flow rates. Obviously, this implies that the increase of plates pressure drop with increasing gas flow rate was appropriately compensated by the simultaneous decrease of overall liquid (slurry) holdup in the column (see Table 1.1).

### Longitudinal Liquid Phase (Slurry) Mixing

Evaluation of RTD characteristics proved that the axial mixing of the liquid phase or suspension in the sectionalised reactor was appropriately described by the two-parameter model of perfectly mixed tanks in series with backflow between the adjacent tanks, for the number of series terms equal to the real number of column stages. Values of the second parameter,  $E_{i+1,i}$ , obtained from independent measurements proved further that the extent of liquid backflow was appreciably suppressed by the proper design of internal plates e.g. in comparison with the data obtained in our previous study (Kaštánek *et al.*, 1974) in a three-stage column of identical diameter for free plate area ratios  $\varphi=4$  and 8% respectively (Table 1.2). Formation of gas cushions below the internal sectionalising plates was observed within the regions of gas and liquid superficial velocities,  $U_{oG}=0.025\text{--}0.050 \text{ m s}^{-1}$ ,  $u_{oL}=0.013\text{--}0.029 \text{ m s}^{-1}$ , and consequently, liquid or suspension backflow was virtually negligible at such flow conditions ( $E_{av}\leq 0.1$ ). In this operation region, liquid mixing was satisfactorily described by the simple tanks-in-series model. Incidentally, the same result was reported by Poncin *et al.* (1990) from experiments in a six-stage countercurrent-flow bubble column sectionalised by dual-flow plates. An increase of backflow coefficients observed at  $u_{oG}>0.050 \text{ m s}^{-1}$  can be ascribed to the partial conversion of the plates working regime at such conditions. Due to the sharp increase of plates pressure drop at these  $u_{oG}$  values, a certain portion of gas passed upwards through the downcomer tubes causing excessive liquid entrainment. Based upon such results, the optimum operating region of internal plates can be defined by the gas velocity range  $u_{oG}=1\text{--}2 \text{ (}u_{oG}\text{)}_{crit}$ , where  $(u_{oG})_{crit}$  is the critical value of superficial gas

velocity corresponding for particular plate geometry to the onset of its stable and uniform distributing performance, characterised by the critical value of Weber number,  $(We_n)_{crit} = [(u_{oG})_{crit}^2 \rho_G d_n / \varphi^2 \sigma] = 3$ , determined experimentally in our former study (Zahradník *et al.*, 1982b). For the plates used in the present study ( $\varphi=0.0025$ ,  $d_n=0.0018$  m) and air-water system,  $(u_{oG})_{crit}$  equals to  $0.025$  m s<sup>-1</sup>.

**Table 1.1** Liquid holdup in the staged bubble column ( $c_s=0$ )

$u_{oG}$ m/s	$V_L$ m <sup>3</sup>											
	N= 3 m/s						N= 6 m/s					
	$u_{oL}$ ,						$u_{oL}$ ,					
0	0.004	0.008	0.012	0.017	0.029	0	0.004	0.008	0.012	0.017	0.029	
0.025	0.099	0.100	0.101	0.101	0.102	0.106	0.096	0.095	0.095	0.096	0.097	0.101
0.033	0.098	0.099	0.099	0.100	0.101	0.105	0.091	0.092	0.092	0.093	0.094	0.097
0.042	0.096	0.097	0.098	0.098	0.099	0.103	0.087	0.088	0.088	0.089	0.090	0.094
0.050	0.094	0.094	0.095	0.096	0.097	0.100	0.081	0.082	0.082	0.083	0.084	0.088
0.058	0.091	0.091	0.092	0.093	–	–	0.074	0.075	0.075	0.076	–	–

**Table 1.2** Average value of liquid backflow coefficient in multistage bubble columns

a) This work:  $D_t=0.292$  m,  $\eta=0.25\%$ ,  $d_n=1.8$  mm

$u_{oL}$ m/s	$u_{oG}$ m/s	E N=3	v N=6
0.004	0.025	0.34	0.28
	0.033	0.52	0.49
	0.042	0.75	0.61
	0.050	1.09	1.14
	0.058	1.92	1.89
0.010	0.025	0.04	0.04
	0.033	0.13	0.06
	0.042	0.17	0.11
	0.050	0.22	0.30
	0.058	0.32	0.55
0.013	0.025	0.03	0.02
	0.033	0.05	0.04

	0.042	0.07	0.06
	0.050	0.09	0.12
	0.058	0.20	0.24
0.017	0.025	0.02	0.01
	0.033	0.02	0.02
	0.042	0.02	0.02
	0.050	0.03	0.04
0.029	0.025	0	0
	0.033	0	0
	0.042	0	0
	0.050	0	0

b) Kaštánek, Zahradník, Rylek (1974):  $D_t=0.292$  m,  $N=3$ ,  $d_h=1.6$  mm

$u_{oL}$ m/s	$10^3$	$u_{oG}$ m/s	E $\varphi=4\%$	v $\varphi=8\%$
2.5		0.008	1.35	1.79
		0.025	2.05	2.40
		0.042	3.04	2.93
7.5		0.008	0.12	0.29
		0.025	0.27	0.45
		0.042	0.53	0.76

**Table 1.3** Comparison of characteristic coordinates of experimental and calculated RTD curves

$u_{oL}$ m/s	$u_{oG}$ m/s	Number of stages column							
		N=3				N=6			
		$\theta$ exp	$Y_{max}$ calc	$Y$ exp	$\theta=1$ calc	$E_{av}$	$\theta$ exp	$Y_{max}$ calc	$Y$ exp
0.004	0.025	0.60	0.57	0.62	0.60	0.34	0.73	0.70	0.80
	0.033	0.54	0.52	0.55	0.54	0.52	0.69	0.65	0.77
	0.042	0.48	0.47	0.53	0.52	0.75	0.67	0.63	0.72
	0.050	0.46	0.44	0.51	0.49	1.09	0.63	0.62	0.65
	0.058	0.38	0.36	0.48	0.48	1.93	0.53	0.51	0.57
0.017	0.025	0.69	0.68	0.71	0.70	0.02	0.84	0.84	0.99
	0.033	0.68	0.68	0.70	0.70	0.02	0.84	0.83	1.01

	0.042	0.67	0.68	0.70	0.70	0.02	0.83	0.83	0.99	0.98	0.02
	0.050	0.67	0.67	0.70	0.69	0.03	0.82	0.82	0.96	0.97	0.04
0.029	0.025	0.69	0.70	0.72	0.72	0	0.84	0.85	1.02	1.00	0
	0.033	0.69	0.70	0.71	0.72	0	0.83	0.85	0.99	1.00	0
	0.042	0.70	0.70	0.72	0.72	0	0.84	0.85	1.02	1.00	0
	0.050	0.70	0.70	0.73	0.72	0	0.83	0.85	1.00	1.00	0

Experimental RTD curves agreed well with those calculated from the model equations for respective values of the backflow coefficient obtained from independent measurements. The comparison of characteristic coordinates of experimental and calculated curves ( $\theta_{Y_{\max}}$  and  $Y_{\theta=1}$ ) presented in Table 1.3, demonstrates a good fit of experimental RTD data with appropriate mixing models (tanks-in-series with backflow and tanks-in-series, respectively) within the whole region of recommended working conditions.

### Gas Holdup

Experimental results proved the favourable effect of gas redispersion by internal plates on values of gas holdup ratio (Figure 1.2). The effect of solid phase content was negative within the whole experimental region of its concentration. The increase of effective slurry viscosity (see Eq.(3)) with increasing solid phase concentration was too small ( $\mu_{sl}=1.006-1.026$  mPa s for  $c_s=1-5$  wt.%) to justify the analogy with the coalescence enhancement in viscous media, proposed in the literature as a possible explanation of the

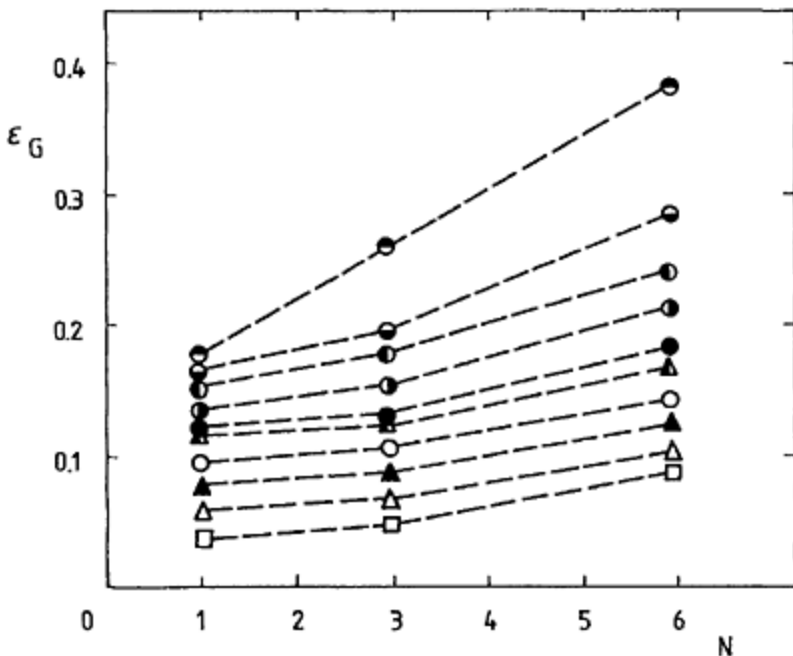


**Figure 1.2** Dependence of gas holdup on the number of column stages  $c_s=0$ :

$u_{oG}=0.025 \text{ m s}^{-1}$ ,  $\bullet u_{oG}=0.033 \text{ m s}^{-1}$ ,  
 $\bullet u_{oG}=0.042 \text{ m s}^{-1}$ ,  $\bullet u_{oG}=0.050 \text{ m s}^{-1}$ ,  
 $\bullet u_{oG}=0.058 \text{ m s}^{-1}$ ,  $\bullet u_{oG}=0.066 \text{ m s}^{-1}$ ;  
 $c_s=2.5 \text{ wt.\%}$ :  $\Delta u_{oG}=0.025 \text{ m s}^{-1}$ ,  $\blacktriangle u_{oG}=0.033 \text{ m s}^{-1}$ ,  $\blacktriangle u_{oG}=0.050 \text{ m s}^{-1}$ ;  
 $c_s=5 \text{ wt.\%}$ :  $\square u_{oG}=0.025 \text{ m s}^{-1}$ .

gas holdup decrease in pseudohomogeneous slurries (see e.g. Epstein, 1983). Accordingly, the negative effect of the solids content on gas holdup has to be ascribed in our case solely to the coalescence enhancement due to the presence of solid particles at gas interface. This observation has been in full agreement with our former data from a single-stage bubble column (Kratochvíl *et al.*, 1985); however, it contradicts the increase of gas holdup and specific interfacial area with the addition of solids, reported for pseudohomogeneous suspensions of fine inert particles in the literature (Sada *et al.*, 1986; Pandit and Joshi, 1986; Khare and Joshi, 1990). The ostensibly controversial information on the effect of inert microparticles can be possibly related to opposite effect of the particles presence at the interface on bubble coalescence in different bubbling regimes, i.e. at different levels of micro-scale turbulence at the gas-liquid interface. While the increase of gas holdup in the presence of fine inert particles has been commonly ascribed to the hindered bubble coalescence due to the accumulation of particles at the gas-liquid interface (Pandit and Joshi, 1986; Wilkinson *et al.*, 1992), it can be envisioned that, at a

higher level of micro-scale turbulence, the microparticles penetrate the intervening film between colliding bubbles and thus increase the rate of film drainage and ultimately enhance bubble coalescence. While this hypothesis has to be indeed further examined, it seems to be supported by the fact that significant increase of gas holdup due to the addition of fine inert particles has been observed under experimental conditions (small superficial gas velocity, low aspect ratio, porous sparger) favourising the existence of the homogeneous bubbling regime, typically exhibiting low levels of micro-scale turbulence (Sada *et al.*, 1986; Khare and Joshi, 1990). As can be seen from Table 1.4, the relative decrease of gas holdup in the slurry system, as compared with the standard two-phase air-water system,  $\Delta\epsilon_G = [((\epsilon_G)_{2F} - (\epsilon_G)_{3F})/(\epsilon_G)_{3F}] \times 100$ , was, to a certain extent, suppressed by the column sectionalisation. Obviously, this observation further confirmed the favourable effect of gas redispersion in multi-stage sieve-tray columns.

The effect of liquid flow rate on gas holdup was negligible within the whole region of working conditions. The dependence of gas holdup on the superficial gas velocity was formally described by the well known Reith-Mashelkar equation (Reith and Beek, 1971; Mashelkar, 1970) commonly used for gas-liquid systems,

$$\epsilon_G = u_{oG}/(2u_{oG} + U_{bs}) \quad (4)$$

where, however, bubble swarm velocity,  $U_{bs}$ , was in our case assumed to be a function of solid phase concentration and of the number of column stages (the latter parameter

**Table 1.4** Relative decrease of gas holdup with the solid phase concentration

$C_s$ , % wt.	$\Delta\epsilon$ , %		
	N= 1	N=3	N=6
1	20	20	18
2	29	28	26
3	37	36	34
4	46	48	38
5	55	50	42

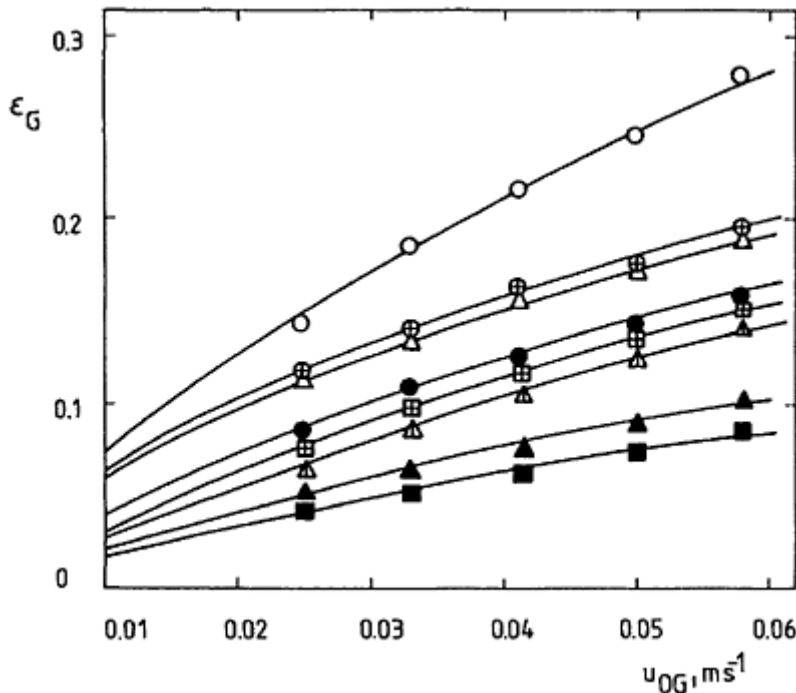


**Figure 1.3**  $k_{LAL}$  as a function of superficial gas velocity

$N = 6$ : ○  $c_s = 0$ , ●  $c_s = 1$  wt.%, ⊕  $c_s = 2.5$  wt.%, ⊖  $c_s = 5$  wt.%

$N = 3$ : ⊖  $c_s = 0$ , ⊕  $c_s = 1$  wt.%, ⊖  $c_s = 2.5$  wt.%, ⊖  $c_s = 5$  wt.%

$N = 1$ : ⊖  $c_s = 0$ , ⊖  $c_s = 1$  wt.%, ⊖  $c_s = 2.5$  wt.%, ⊖  $c_s = 5$  wt.%

full line: data from an ejector distributor reactor (Zahradník *et al.*, 1982a);  $D_r = 0.29$  m,  $H = 2$  m,  $c_s = 0$

**Table 1.5** Values of empirical coefficients in Eq. (5)

N	1	3	6
K <sub>1</sub>	0.050	0.058	0.068
K <sub>2</sub>	1.014	0.912	0.372
K <sub>3</sub>	0.221	0.177	0.107

representing the effect of gas redisposition by internal plates). According to Reith's derivation (Reith and Beek, 1971), coefficient 2 in the denominator of Eq.(4) corresponds to a single-loop circulation observed visually in individual column stages. Obviously,

such a clearly defined flow pattern was, in this case, induced by the liquid cross-flow due to downcomers position. Figure 1.3 shows good agreement of experimental data with gas holdup values calculated from Eq.(4) for

$$u_{hs} = K_1 c_s^k + K_3 \quad (5)$$

**Table 1.6** Comparison of gas holdup data for different plate designs (system air-water)

$u_{oG}$ , m/s	G			
	N=3		N=6	
	This work	Perforated plates ( $\varphi=0.04; 0.08$ )	This work	Dual-flow plates
0.01	0.049	0.026	0.072	0.030
0.02	0.087	0.052	0.123	0.059
0.03	0.122	0.076	0.170	0.085
0.04	0.154	0.097	0.211	0.110
0.05	0.180	–	0.249	0.132
0.06	0.207	–	0.280	0.152

where values of empirical coefficients  $K_1$ ,  $K_2$  and  $K_3$ , obtained for respective numbers of column stages from experimental data, are summarised in Table 1.5.

In Table 1.6, our experimental results are compared with analogical data obtained by Poncin *et al.* (1990) in a six stage column sectionalised by dual-flow plates ( $\varphi=0.25$ ,  $d_n = 15$  mm). Also compared are the data from the three-stage column obtained at otherwise identical conditions in the present study and in our former work (Zahradník and Kaštánek, 1974) at different values of free plate area  $\varphi=0.0025$  and  $\varphi=0.04$  or 0.08 respectively. Data given in the table clearly show the superiority of the plate design employed in this work. Moreover, the values of the plate pressure drop measured at working conditions in our present study were by 20–50% lower than the data reported at identical gas and liquid flow rates for dual-flow plates (Poncin *et al.*, 1990).

### Volumetric Gas-Liquid Mass Transfer Coefficient

The effect of individual independent variables,  $u_{oG}$ ,  $c_s$ , and N on  $k_{LaL}$  values is apparent from the data plotted in Figure 1.4. Within the whole range of experimental conditions,  $k_{LaL}$  increased with increasing number of column stages and decreased with increasing solids content (again in agreement with the analogous data of Kratochvíl *et al.* (1985) from a single-stage bubble column). Unlike gas holdup values,  $k_{LaL}$  decreased slightly with increasing liquid or slurry flow rate. As can be seen from Figure 1.5 a-c, the relationship between  $k_{LaL}$  and gas holdup was, however, independent of the solid phase concentration. Obviously, this observation implies that, within the whole region of experimental conditions, the solids content did not influence the mechanism of gas-liquid mass transfer (and thus even  $k_L$  values) and the decrease of  $k_{LaL}$  with increasing  $c_s$  could

be ascribed, similarly to the two-phase systems, solely to the decrease of the interfacial area caused by the enhanced bubble coalescence in the system. In general  $k_L$  may, however, vary with the level of micro-scale turbulence (i.e. with the bubbling mode) and with the particle size, wettability,

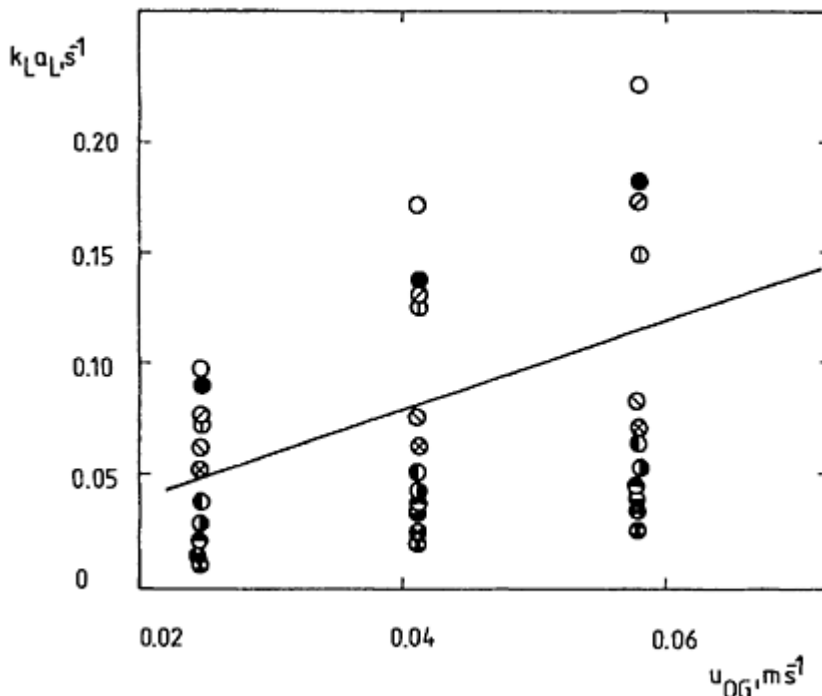


**Figure 1.4**  $k_{LaL}$  as a function of superficial gas velocity

$N = 3$ :  $\bigcirc$   $c_s = 0$ ,  $\otimes$   $c_s = 1$  wt.%,  $\bullet$   $c_s = 2.5$  wt.%,  $\blacksquare$   $c_s = 5$  wt.%

$N = 1$ :  $\bullet$   $c_s = 0$ ,  $\blacksquare$   $c_s = 1$  wt.%,  $\otimes$   $c_s = 2.5$  wt.%,  $\bigcirc$   $c_s = 5$  wt.%

$N = 6$ :  $\bigcirc$   $c_s = 0$ ,  $\bullet$   $c_s = 1$  wt.%,  $\otimes$   $c_s = 2.5$  wt.%,  $\blacksquare$   $c_s = 5$  wt.%

full line: data from an ejector distributor reactor (Zahradník *et al.*, 1982a);  $D_r=0.29$  m,  $H=2$  m,  $c_s=0$

sphericity and adsorbing capacity for the gas component (Alper *et al.*, 1980; Miyachi *et al.*, 1981; Brück and Hammer, 1986; Pandit and Joshi, 1986). Values  $k_{LaL}$  corresponding to given gas holdup increased substantially with the increasing number of column stages, i.e. with the number of internal plates. Obviously, such a variation of the functional dependence  $k_{LaL}=f(G)$  can be explained by the relatively weak dependence of bubble rise

velocity on bubble diameter, reported for the range of bubble sizes encountered in our work (Valentin, 1967). The increase of gas holdup due to longer residence time of smaller bubbles in the bed was thus less pronounced than the increase of interfacial area corresponding to the smaller size of bubbles. The secondary gas dispersion in sectionised bubble columns thus has obviously even more positive effect on the extent of interfacial area and thus consequently on  $k_{LaL}$  values than on gas holdup (bubble bed voidage).

### **Energy Effectiveness of Gas-Liquid Contacting**

It has been proved for gas-liquid reactors that for each particular mode of phases contacting and corresponding reactor type, there is an unambiguous relation between the

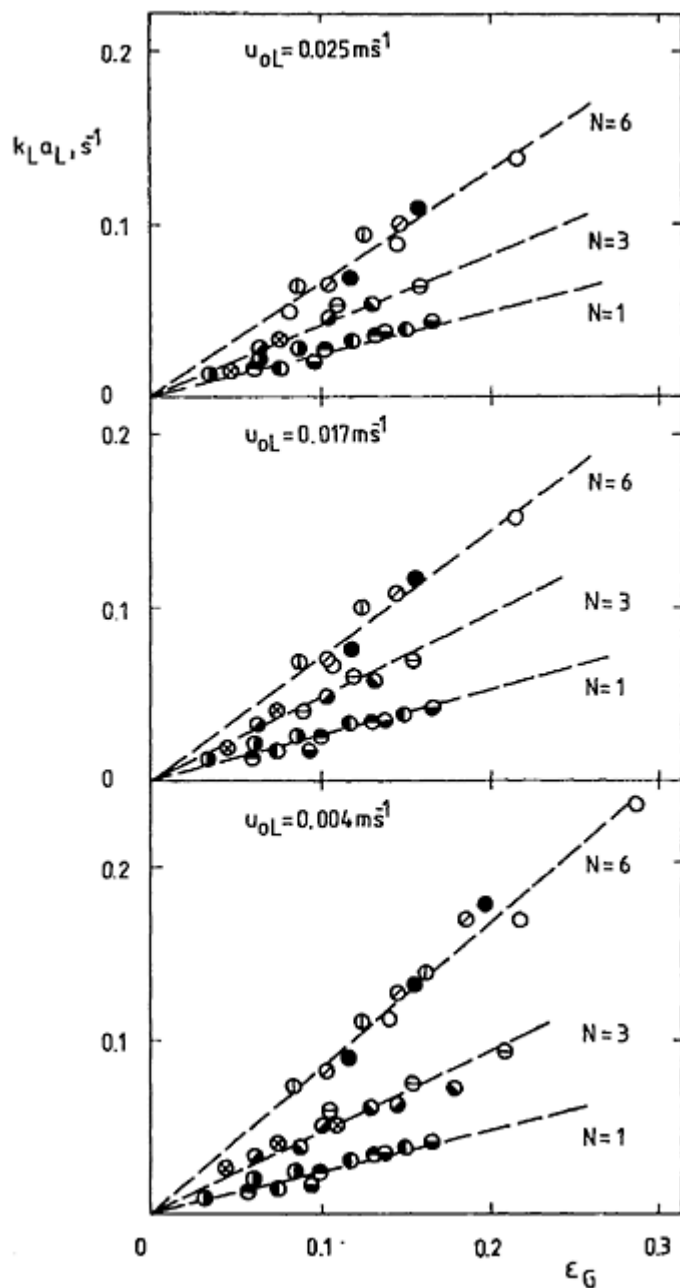


**Figure 1.5** Dependence of  $k_L a_L$  on gas holdup ratio

$$\begin{aligned}
 N = 6: & \bigcirc c_s = 0, \bullet c_s = 1 \text{ wt.\%}, \ominus c_s = 2.5 \text{ wt.\%}, \textcircled{1} c_s = 5 \text{ wt.\%} \\
 N = 3: & \bigcirc c_s = 0, \bullet c_s = 1 \text{ wt.\%}, \bullet c_s = 2.5 \text{ wt.\%}, \textcircled{2} c_s = 5 \text{ wt.\%} \\
 N = 1: & \textcircled{2} c_s = 0, \textcircled{1} c_s = 1 \text{ wt.\%}, \bullet c_s = 2.5 \text{ wt.\%}, \textcircled{1} c_s = 5 \text{ wt.\%}
 \end{aligned}$$

rate of energy dissipation in the place of dispersion formation and the rate of interfacial mass transfer represented by  $k_L a_L$  values (see e.g. Kaštánek *et al.*, 1993). Large rate of energy dissipation is therefore generally required to ensure large intensity of phases contacting in a reactor. At the same time, however, minimisation of the overall energy input (energy costs) has lately become one of the decisive factors to be considered in the process of reactor selection for specific processes in gas-liquid or gas-liquid-solid (slurry) systems (Kaštánek *et al.*, 1993). To solve optimally these two mutually contradicting tasks, it is therefore necessary to chose a reactor type with the most favourable relation between the energy dissipation rate and the intensity of gas-liquid contacting and subsequently to minimise, by an appropriate reactor design, the fraction of total power input which is not directly utilised for gas dispersion.

In principle, the overall rate of energy dissipation in a multistage bubble column sectionalised by perforated plates consists of the two basic contributions,

$$E_d = (\Delta P_b + \Delta P_w) Q_G \quad (6)$$

While the first term, representing the energy dissipation in bubble beds in individual stages,

$$\Delta P_b Q_G = \left( \sum_{i=1}^N H_{oi} \rho_{si} g \right) Q_G \quad (7)$$

directly determines the intensity of gas-liquid interfacial contact in the reactor (Kaštánek, 1977), the second term,  $\Delta P_w Q_G$ , represents the fraction of energy inefficiently dissipated due to the distributing plates pressure drop (Zahradník *et al.*, 1982a). The specific rate of energy dissipation related to a mass unit of a respective slurry system in the reactor,  $e_d$ , can be then defined by the relation

$$e_d = u_{oG} g + (\Delta P_w / \rho_{si}) \sum_{i=1}^N H_{oi} \rho_{si} g Q_G \quad (8)$$

where  $\Delta P_w$  is the total pressure drop of wetted plates in the column. Eq.(8) clearly indicates the importance of the optimum plates design aimed at minimising their pressure drop at given phases flow rates while ensuring their stable, uniform distributing performance.

Graph  $k_L a_L$  vs  $e_d$  plotted in Figure 1.6 clearly proves that the efficiency of utilisation of the dissipated energy for gas-liquid contacting increased with the increasing number of reactor stages while the effect of solid phase concentration was negative. To compare the energy effectiveness of gas-liquid contacting in different reactor types, the energy effectiveness criterion  $\Phi = k_L a_L / e_d$  was introduced in our former work (Zahradník *et al.*, 1982a). Multiplied by the respective concentration difference, representing mass transfer driving force, coefficient  $\Phi$  subsequently yields the amount of gas transferred across the gas-liquid interface per unit of dissipated energy. Graph  $\Phi$  vs  $k_L a_L$ , shown in Figure 1.7,

demonstrates superior energy effectiveness of sectionalised bubble columns in comparison with single-stage units and with the ejector-loop reactors (Zahradník *et al.*, 1982a).

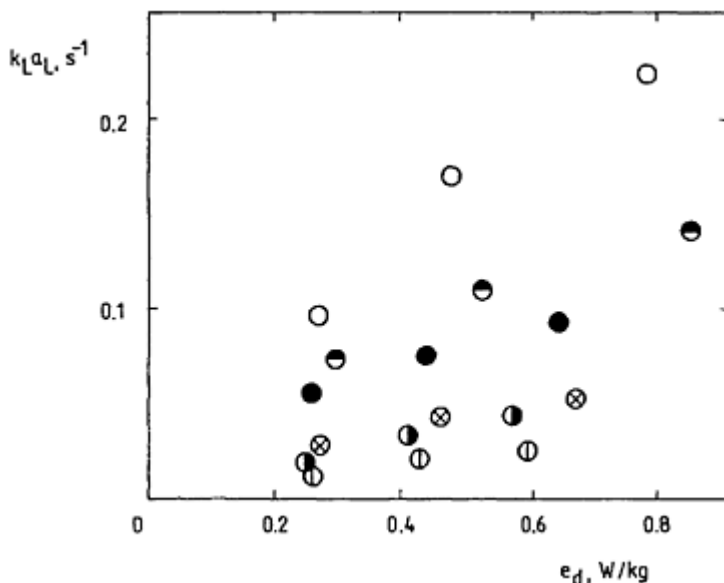


**Figure 1.6** Dependence of  $k_L a_L$  on the rate of energy dissipation;

$u_{oG} = 0.025\text{--}0.058 \text{ m s}^{-1}$ ,  $u_{oL} = 0.004$   
 $c_s = 0$ :  $\bullet$   $N = 1$ ,  $\bullet$   $N = 3$ ,  $\circ$   $N = 6$   
 $c_s = 5 \text{ wt.\%}$ :  $\oplus$   $N = 1$ ,  $\otimes$   $N = 3$ ,  $\bullet$   $N = 6$

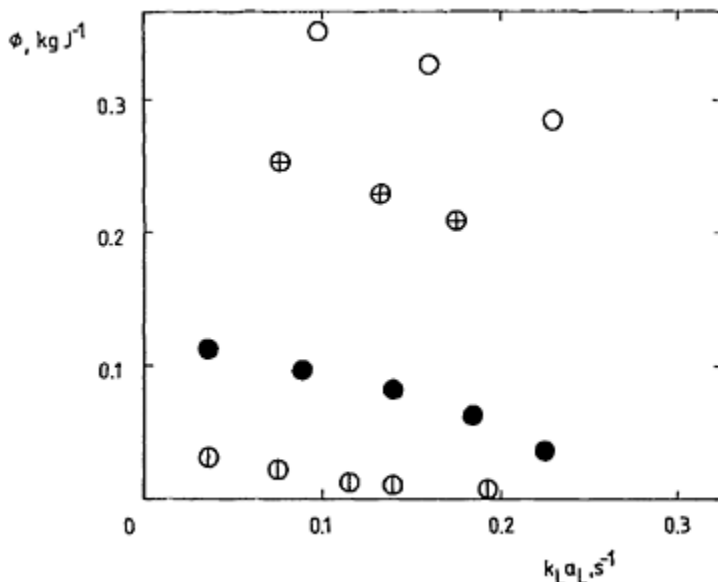


**Figure 1.7** Relation between the energy effectiveness criterion ( $\Phi$ ) and  $k_L a_L$  six stage column:  
 ○  $u_{ol} = 0.004 \text{ m s}^{-1}$ , ⊕  $u_{ol} = 0.025 \text{ m s}^{-1}$ ; ● single stage column (Zahradník *et al.*, 1982a); ⊖ ejector distributor reactor (Zahradník *et al.*, 1982a).

## CONCLUSIONS

Hydrodynamic and mass transfer characteristics of multi-stage three-phase slurry reactors were studied experimentally as functions of selected construction and operating parameters including number of column stages, distributing plate geometry, gas and liquid flow rates and solid phase concentration. Experimental results confirmed favourable effect of bubble column sectionalisation on the rate of mass transfer between the gas and the liquid phases and on the energy effectiveness of their contacting. It has been proved that the liquid phase (slurry) backflow between the adjacent column stages can be significantly suppressed or even eliminated by the proper design of sectionalising plates. Axial mixing of the liquid or slurry phase can be then appropriately described by the model of perfectly mixed tanks in series for the number of series terms equal to the real number of column stages.

The increasing concentration of solid particles influenced negatively values of gas holdup and  $k_L a_L$  and thus even the energy effectiveness of gas-liquid contacting. Higher power input has to be therefore supplied to the three-phase reactors to ensure a gas-liquid

mass transfer rate equal to that achieved at comparable working conditions in gas-liquid reactors.

The functional dependence of  $k_{LaL}$  on gas holdup was within the whole range of experimental conditions virtually independent of phases flow rates and solid phase concentration and varied only with the number of column stages. In cases where the suspension of solid particles can be treated as a pseudohomogeneous continuum (i.e. for small non-sedimenting particles), gas holdup ratio can thus be obviously regarded, in analogy with the gas-liquid systems, as a lumped parameter representing, for a particular reactor configuration, the effect of individual operating variables on the rate of gas-liquid mass transfer. Experimental data proved a favourable effect of secondary gas dispersion in sectionalised bubble columns on  $k_{LaL}$  values corresponding to given gas holdup in the reactor. Comparison with the dual-flow plates proved the suitability of the plate design tested in our work for the countercurrent flow arrangement, regarding both higher values of bubble bed voidage achieved and lower plates pressure drop.

## RECOMMENDATIONS FOR FUTURE WORK

While there seems to be no doubt that sectionalised bubble columns may offer distinct advantages to reaction processes in g-l-s systems, as compared with other types of multiphase contactors, further experimental work is still needed, aimed at clarifying particular aspects of their performance with slurry systems and ultimately at providing reliable, generally applicable design and scale-up recommendations. An outline of suggested research topics is given in the following.

Performance of multistage slurry reactors in the two basic flow arrangements, concurrent upflow and countercurrent flow, should be compared under different working conditions (gas and liquid flow rates, solids loading, particle size and density). Both dual flow plates and plates with downcomers should be tested in the countercurrent flow regime with the purpose of formulating general criteria for objective selection of flow arrangement and plate type for specific process demands. In comparison with the single-stage bubble columns, the multistage units exhibit significantly smaller operating flexibility, i.e. a much narrower region of gas and liquid (slurry) flow rates in which these reactors can be operated for a specific plate geometry. The selection of the optimum plate parameters for given working conditions thus represents an essential step of the multistage reactor design. The design rules proposed for dual flow plates in gas-liquid reactors (see e.g. Deckwer, 1985 or Kaštánek *et al.*, 1993) should be re-examined in the view of possible solid phase effect and, similarly, additional experiments should be devoted to testing plates with downcomers in a wide region of phases flow rates.

In analogy with the single-stage bubble columns, conditions of the homogeneous bubbling regime formation in multistage slurry reactors should be investigated. Generally, parameters governing the formation and stability of the homogeneous bubbling regime in g-l-s systems include plate and column geometry, liquid properties, solids loading and particle size and density (Pandit and Joshi, 1986; Gavroy *et al.*, 1995). The effect of such parameters and their mutual, possibly synergistic, coupling should be examined with due regard to the specific features of multistage units (e.g. gas redisposition in individual stages, lower bed height and  $H_{oi}/D_r$  ratio etc.), which could,

from the analogy with the g-l data, extend the region of the homogeneous regime stability. Subsequently, the performance of multistage slurry reactors in the homogeneous and the heterogeneous bubbling regimes should be compared, regarding the appropriate hydrodynamic, mixing and transport characteristics. Attention should be also paid to possible differences in the effect of solid particles on the values of such system characteristics, reflecting a different extent of micro-scale turbulence under the homogeneous and heterogeneous bubbling conditions.

In general, the flow pattern studies should be extended from the pseudohomogeneous slurries to those with particles possessing non-negligible slip speeds, i.e. to the systems exhibiting different flow patterns for the liquid and solid phases and/or solids concentration profiles in individual stages and along the reactor height. Both small particles with large density difference from the liquid phase and large particles with the density close to  $\rho_L$  should be employed in experiments to simulate conditions in the two most common industrial applications of g-l-s reactors—catalytic reactors and bioreactors.

Further attention should be paid to the effect of solids loading and particle size and density on the rate of gas-liquid mass transfer in g-l-s systems and on the values of respective parameters of three-phase beds (gas holdup, specific interfacial area, liquid-side volumetric mass transfer coefficient,  $k_{LaL}$ ). Analysis of related literature on single-stage bubble column reactors (Brück and Hammer, 1986; Pandit and Joshi, 1986; Kratochvíl and Kaštánek, 1989; Khare and Joshi, 1990; Wilkinson *et al.*, 1992) indicates the extreme complexity of this issue, as well as sometimes contradictory findings reported by various authors. Additional experiments are needed to allow reliable prediction of the solid phase effect under complex conditions of simultaneous influence of liquid phase properties and/or gas dispersion mode. While there seems to be a broad consensus in the literature on the positive effect of fine particles with adsorbing capacity (Alper *et al.*, 1980; Pal *et al.*, 1982; Pandit and Joshi, 1986; Kratochvíl and Kaštánek, 1989) and, on the other hand, of large particles with diameter above 1 mm (Ostergaard and Fosbol, 1972; Sittig, 1977; Khare and Joshi, 1990), contradictory information found in the literature on the effect of fine inert particles implies different possible mechanisms of their influence on bubble coalescence. To clarify this issue, coalescence studies should be performed in a coalescence cell (Zahradník *et al.*, 1995), ensuring clearly defined hydrodynamic conditions (contacting of two bubbles in a pseudoinfinite medium), in a wide range of liquid and solid phase properties and solids concentrations. In addition, experiments in multistage bubble columns should be aimed at linking the fundamental knowledge of the gas-liquid mass transfer in microparticle slurry systems with the specifics of sectionalised units (e.g. hindered establishing of equilibrium bubble size in coalescing systems due to gas redispersion by the internal plates and low bed height in individual stages).

Experimental programmes in the coalescence cell as well as in the slurry reactors should include measurements in non-aqueous media (alcohols, esters, hydrocarbons), as well as in viscous liquids (both Newtonian and non-Newtonian) and in aqueous solutions of surface active substances (alcohols, electrolytes).

Data on liquid-solid mass transfer are needed to allow complex modelling of reactions in g-l-s systems. The published information on particle—liquid mass transfer coefficient ( $k_{SL}$ ) is, however, far from complete and additional experiments within a wider region of particle sizes and solids loading are to be performed to verify general validity of

correlations proposed for  $k_{SL}$  in the literature (see, e.g., the generally recommended equation by Sänger and Deckwer, 1981).

Many industrial processes in g-l-s systems are carried out in high pressure, high temperature reactors (hydrogenation of industrial fats and fatty oils, hydroprocessing operations in petrochemistry, Fischer-Tropsch synthesis, etc.). Data on hydrodynamics, mixing and transport characteristics under these conditions, with real systems, should therefore be obtained.

Scale-up studies should be aimed at examining whether, and to what extent, the favourable features of multistage units observed in lab-scale experiments can be preserved in full-size industrial units and ultimately at providing the guidance for multistage reactors scale-up.

## NOMENCLATURE

$a_L$	gas-liquid interfacial area per unit liquid volume, $\text{m}^2\text{m}^{-3}$
c	concentration, wt.%
$D_r$	reactor diameter, m
$d_n$	plate orifice diameter, m
$E_d$	overall rate of energy dissipation, W
$E_{i+1,i}$	coefficient of liquid backflow
$e_d$	rate of energy dissipation per unit of bed mass, $\text{W kg}^{-1}$
g	gravity acceleration, $\text{m s}^{-2}$
$H_{oi}$	slurry height in a column stage, m
$k_L$	liquid-side mass transfer coefficient, $\text{m s}^{-1}$
N	number of column stages
$\Delta P_b$	bubble bed pressure drop, Pa
$\Delta P_w$	wetted plates pressure drop, Pa
Q	volumetric flow rate, $\text{m}^3 \text{s}^{-1}$
$u_o$	superficial velocity, $\text{m s}^{-1}$
$u_{bs}$	bubble swarm velocity, $\text{m s}^{-1}$
$We_n$	Weber number related to a plate orifice, $We_n = u_{nG}^2 \rho_G d_n / \sigma$
Y	y-coordinate of dimensionless RTD curves
$\varepsilon$	fractional holdup
$\theta$	dimensionless time
$\mu$	dynamic viscosity, $\text{mPa s}$
$\rho$	density, $\text{kg m}^{-3}$
$\sigma$	surface tension, $\text{N m}^{-1}$
$\Phi$	energy effectiveness criterion, $\text{kg J}^{-1}$

$\varphi$  free plate area ratio

### Subscripts

av	average
calc	calculated
crit	critical
exp	experimental
G	gas phase
L	liquid phase
S	solid phase
sl	slurry
2F	two-phase
3F	three-phase

### REFERENCES

- Alper, E., Wichtendahl, B. and Deckwer, W.-D. (1980) Gas absorption mechanism in catalytic slurry reactors. *Chem. Engng Sci.* **35**, 217–222.
- Brinkman, H.J. (1952) The viscosity of concentrated suspensions and solutions. *J. Chem. Phys.* **20**, 571.
- Brück, F.-J. and Hammer, H. (1986) Intensification of mass transfer in bubble column reactors by suspended solids. *Ger. Chem. Eng.* **9**, 382–390.
- Deckwer, W.-D. (1985) *Reaktionstechnik in Blasensaulen*, Salle+Sauerlander, Frankfurt a.M.
- Doraiswamy, L.K. and Sharma, M.M. (1984) *Heterogeneous Reactions: Analysis, Examples, and Reactor Design Vol.2, Fluid-Fluid-Solid Reactions*. J. Wiley and Sons, New York.
- Epstein, N. (1983) Hydrodynamics of three-phase fluidization. In *Handbook of Fluids in Motion* (Ed. Cheremisinoff, N.P. and Gupta, R.), Ann Arbor Science, Ann Arbor, Chap. **42**, p. 1175.
- Gavroy, D., Joly-Vuillemenin, C., Cordier, G. and Delmas, H. (1995) Gas hold-up, liquid circulation and gas-liquid mass transfer in slurry bubble columns. *Chem. Eng. Res. Des.* **73**, 637–642.
- Kaštánek, F. and Zahradník, J. (1973) The residence time distribution in multistage bubble column reactors. *Collect. Czech. Chem. Commun.* **38**, 3725–3741.
- Kaštánek, F., Zahradník, J. and Rylek, M. (1974) Backflow between stages in bubble column reactors, *Collect. Czech. Chem. Commun.* **39**, 1672–1685.
- Kaštánek, F. (1977) The volumetric mass transfer coefficient in bubble bed columns. *Collect. Czech. Chem. Commun.* **42**, 2491–2497.
- Kaštánek, F., Zahradník, J., Kratochvíl, J. and Ermák, J. (1993) *Chemical Reactors for Gas-Liquid Systems*. Ellis Horwood, New York.
- Kato, Y., Nishiwaki, A., Fukuda, T. And Tanaka, S. (1972) The behaviour of suspended solid particles and liquid in bubble columns. *J. Chem. Eng. Japan* **5**, 112–118.
- Khare, A.S. and Joshi, J.B. (1990) Effect of fine particles on gas holdup in three-phase sparged reactors. *Chem. Eng. J.* **44**, 11–25.
- Kratochvíl, J., Winkler, K. and Zahradník, J. (1985) Gas holdup and  $k_{L,a}$  in perforated-plate bubble columns in the presence of solid particles. *Collect. Czech. Chem. Commun.* **50**, 48–60.
- Kratochvíl, J. and Kaštánek, F., Mass transfer rate from gas bubbles into liquid in presence of solid particles with strong adsorbing properties. *Collect. Czech. Chem. Commun.* **54**, 3061–3068.

- Kürten, H. and Zehner, P. (1979) Slurry reactors. *Ger. Chem. Eng.* **2**, 220–227.
- Mashelkar, R.A. (1970) Bubble columns. *Brit. Chem. Eng.* **15**, 1297–1304.
- Mersmann, A., Schneider, G., Voit, H. and Wenzig, E. (1990) Selection and design of aerobic bioreactors. *Chem. Eng. Technol* **13**, 357–370.
- Ostergaard, K. and Fosbol, P. (1972) Transfer of oxygen across the gas-liquid interface in gas-liquid fluidized beds. *Chem. Eng. J.* **3**, 105–111.
- Pal, S.K., Sharma, M.M. and Juvekar, V.A. (1982) Fast reactions in slurry reactors: Catalyst particle size smaller than film thickness: Oxidation of aqueous sodium sulphide solutions with activated carbon particles as catalyst at elevated temperatures. *Chem. Engng Sci.* **37**, 327–336.
- Pandit, A.B. and Joshi, J.B. (1986) Mass and heat transfer characteristics of three phase sparged reactors. *Chem. Eng. Res. Des.* **64**, 125–157.
- Poncin, S., Midoux, N. and Laurent, A. (1990) Hydrodynamics and residence time distribution in a countercurrent gas-liquid bubble column partitioned with sieve plates. *10th International Congress of Chem. Eng., Chem. Equip. Des. and Automation, CHISA '90*, Prague.
- Prokop, A., Eriksson, L.E., Fernandez, J. and Humphrey, A.E. (1969) Design and physical characteristics of a multistage, continuous tower fermentor. *Biotechnol. Bioeng.* **11**, 945–966.
- Reith, T. and Beek, W.J. (1971) Gas hold-ups, interfacial areas abd mass transfer coefficients in gas-liquid contactors. *Proceedings of the 4th Europ. Symp. on Chem. React. Eng.*, pp. 191–202. Pergamon Press, Oxford.
- Roscoe, R. (1952) The viscosity of suspensions of rigid spheres. *Brit. J. Appl. Phys.* **3**, 267–269.
- Sada, E., Kumazawa, H. and Lee, H.C. (1986) Influence of suspended fine particles on gas holdup and mass transfer characteristics in a slurry bubble column. *AIChE J.* **32**, 853–856.
- Sänger, P. and Deckwer, W.-D. (1981) Liquid-solid mass transfer in aerated suspensions. *Chem. Eng. J.* **22**, 179–186.
- Schügerl, K., Lücke, J. and Oels, U. (1977) Bubble column bioreactors. In *Advances in Biochem. Eng. Vol.7* (Eds. Ghosh, T.K., Fiechter, A. and Blakeborough, N.), Springer Verlag, Berlin, pp. 1–84.
- Schügerl, K. (1980) Neue Bioreaktore für aerobe Prozesse. *Chem.-Ing.-Tech.* **52**, 951–965.
- Schügerl, K. (1983) Process design aspects and comparison of different bioreactors. In *Mass Transfer with Chemical Reaction in Multiphase Systems, Vol. 1 Two-phase systems* (Ed. E. Alper) pp. 525–552, Martinus Nijhoff Publishers, The Hague.
- Schügerl, K. (1983) Apparatechnische Aspekte der Kultivierung von Einzellern in Turmreaktoren. *Chem.-Ing.-Tech.* **55**, 123–134.
- Shah, Y.T., Stiegel, G.J. and Sharma, M.M. (1978) Backmixing in gas-liquid reactors. *AIChE J.* **24**, 369–400.
- Shah, Y.T. (1979) *Gas-Liquid-Solid Reactor Design*. McGraw-Hill, New York.
- Shah, Y.T., Kelkar, B.C., Godbole, S.P. and Deckwer, W.-D. (1982) Design parameters estimations for bubble column reactors. *AIChE J.* **28**, 353–379.
- Sittig, W. (1977) Untersuchungen zur Verbesserung des Stoffaustausches in Fermentern. *Verfahrenstechnik* **11**, 730–740.
- Sittig, W. And Heine H. (1977) Erfahrungen mit grosstechnisch eingesetzten Bioreaktoren. *Chem.-Ing.-Tech.* **49**, 595–605.
- Valentin, F.H.H. (1967) Absorption in Gas-Liquid Dispersions: *Some Aspects of Bubble Technology*. E. & F.N. Spon Ltd., London.
- Vlaev, S.D. and Zahradník, J. (1987) Energy effectiveness and working characteristics of different tower reactors for aerated slurry systems. *Collect. Czech. Chem. Commun.* **52**, 2624–2639.
- Westlake, R. (1986) Large-scale continuous production of single cell protein. *Chem.-Ing.-Tech.* **58**, 934–937.
- Wilkinson, P.M., Spek, A.P. and van Dierendonck, L.L. (1992) Design parameters estimation for scale-up of high-pressure bubble columns. *AIChE J.* **38**, 544–554.
- Zahradník, J. and Kaštánek, F. (1974) The effect of plates on some parameters of a heterogeneous bed in bubble-type flow reactors. *Collect. Czech. Chem. Commun.*, **39**, 1419–1425.

- Zahradník, J., Kratochvíl, J., Kaštánek, F. and Rylek, M. (1982a) Energy effectiveness of bubble column reactors with sieve-tray and ejector-type gas distributors. *Chem. Eng. Commun.* **15**, 27–40.
- Zahradník, J., Kaštánek, F. and Kratochvíl, J. (1982b) Hydrodynamics and mass transfer in uniformly aerated bubble column reactors. *Collect. Czech. Chem. Commun.* **50**, 48–60.
- Zahradník, J., Fialová, M., Kaštánek, F., Green, K.D. and Thomas, N.H. (1995) The effect of electrolytes on bubble coalescence and gas holdup in bubble column reactors. *Chem. Eng. Res. Des.* **73**, 341–346.



# **CHAPTER TWO**

## **NEW METHODOLOGIES FOR MULTIPHASE BIOREACTORS 2: IMAGE ANALYSIS AND MULTIPHASE BIOREACTORS**

EUGÉNIO C.FERREIRA<sup>1</sup>, MANUEL MOTA<sup>1</sup>, AND MARIE-NOËLLE PONS<sup>2</sup>

<sup>1</sup>*Department of Biological Engineering, Universidade do Minho, 4710–057 Braga, Portugal*

<sup>2</sup>*Laboratoire des Sciences du Génie Chimique, CNRS-ENSIC-INPL, 1 Rue Grandville BP 451, F-54001 Nancy Cedex, France*

### **ABSTRACT**

The applications of visualisation and image analysis to bioreactors can be found in two main areas: the characterisation of biomass (fungi, bacteria, yeasts, animal and plant cells, etc), in terms of size, morphology and physiology, and the less developed characterisation of the multiphase behaviour of the reactors (flow patterns, velocity fields, bubble size and shape distribution, foaming), which may require sophisticated visualisation techniques.

**Keywords:** Image Analysis, Morphology

### **INTRODUCTION**

Vision may be the only sense that provides holistic sensorial information. In a glance, we perceive a whole set of characteristics of an object: its distance, its motion, its colour, its shape, its size, its texture, its brightness and its transparency. Therefore, it is not surprising that the area of the brain cortex dedicated to vision is bigger than the areas allocated to the other senses.

Man has identified ten regions of the occipital lobe of the brain related to vision and, today, the functions of some are still unknown (Logothetis, 1999). And yet, Kandel, Schwartz and Jessel (1995) state: “We have learned that contrary to the intuitive analysis of our personal experience, perceptions are not precise and direct copies of the world around us. Sensation is an abstraction, not a replication of the real world. The brain does not simply record the external world like a three dimensional photograph. Rather, the brain constructs an internal representation of external physical events after first analysing them into component parts. In scanning the visual field the brain simultaneously but separately analyses the form of objects, their movement and their colour, all before

putting together an image according to the brains' own rules. How this reconstruction occurs—the binding problem—is one of the most pressing questions in cognitive neural science.”

Nevertheless, vision's holistic properties have obvious advantages in terms of information storage and interpretation.

Thus, according to the saying “an image speaks louder than a thousand words”, various areas of knowledge have used images to represent complex phenomena in a condensed manner. That is the case, for example, of medical imagiology, or of the process of making tri-dimensional computerized models in fluid dynamics (CFD), nowadays widely used in the design of aerodynamic surfaces or in the study of mixing phenomena in bioreactors.

The development of great capacity automatic systems, provided by the increase of the computer processing capacity on the one hand, and the acknowledgement of the importance of some unquantifiable parameters in the performance of some industrial processes—agglomeration, roughness, brightness and morphology among others—has been encouraging the development of another aspect of vision. This is the capacity of perceiving and comparing complex processes, allowing their control, without having to use complex model equations, which are sometimes impossible to develop.

This side of image acquisition and analysis has been raising interesting problems for the very research of the mechanisms involved in the human vision, namely in the area of robotic vision: matters as segmentation, perception, recognition and memory concern automatic vision, as well as human vision. Indeed, according to Hans Moravec (1999), the present velocity of microprocessors is still very slow. Moravec argues that “...from long experience working on robot vision systems, I know that similar edge (to retina) or motion detection, if performed by efficient software, requires the execution of at least a hundred computer instructions. Thus, to accomplish the retina's ten million detections per second would require at least a thousand MIPS (million instructions per second).” And he proceeds further on: “Perhaps by 2010 the process will have produced the first broadly competent ‘universal robots’, as big as people but with lizardlike 5000 MIPS minds that can be programmed for almost any simple chore.”

The methodology of image acquisition and analysis will, therefore, invade all areas where quick and condensed processing of information shows to be critical. This is one of the characteristics of biochemical engineering, where the control of biological processes occurring in a bioreactor, involves a very large number of variables interacting simultaneously.

This subject and its evolutions, will now be discussed.

## IMAGE PROCESSING

If an image can be immediately understood by a human being, the quantification of the information it contains is far more difficult especially on a large set of images. Automated image processing plays that role, but obviously the image treatment will depend upon the type and quality of the image and the goal of the final user of the quantification.

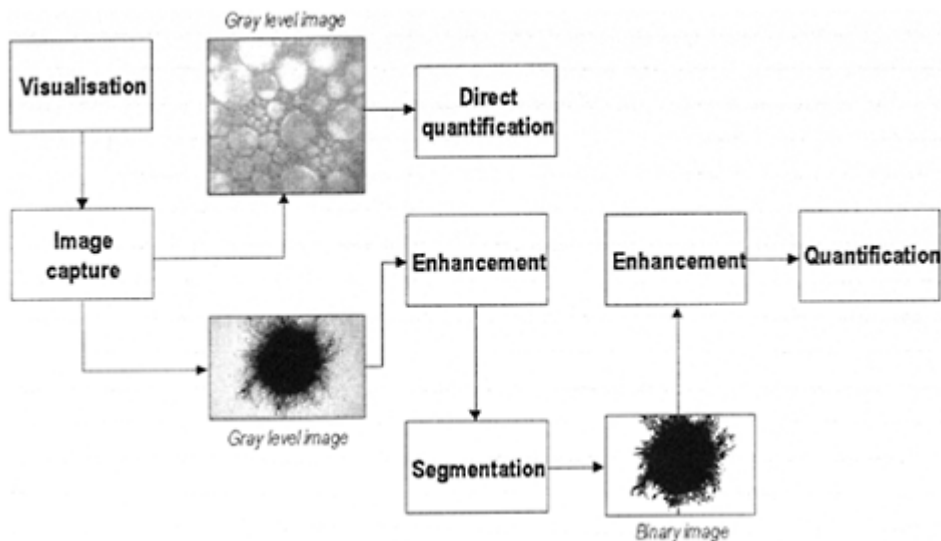


**Figure 2.1** Principle of image processing.

Nevertheless, it is possible to define a series of basic steps which can be found in any image analysis procedure (Figure 2.1).

The image processing starts with the visualisation step. Different devices can be used: for biomass characterisation optical microscopes are the most common tools but a large range of imaging methods can be used for the hydrodynamic behaviour characterisation. Generally an electronic eye (camera) is substituted to the human eye. The video signal is further processed into a digital one, the image, i.e. a set of picture elements (=pixels) arranged according to lines and columns. It is important to note that an image is a projection onto a plane of a reality, which is 3-dimensional. In most applications, especially for biomass characterisation, the quantification will be made on projections. It will be seen later that it is possible to obtain 3D information, especially for hydrodynamic applications, to the expense of more sophisticated imaging systems. Generally, for routine applications, the imaging process is less expensive for biomass characterisation.

The digital image which has been captured is a grey-level image: the value assigned to each pixel is directly connected to the amount of transmitted or reflected electromagnetic energy and is generally coded on 8 bits, giving 256 grey levels or sometimes, for applications related to fluorescence or luminescence, on 12 bits (4096 grey levels). A colour image is a combination of three images, each one corresponding to one of the primary colours: Red, Green and Blue (RGB colour system).

Some images will be directly used as grey level images: it is the case for densitometry studies (tomography and radiography) or characterisation of visual textures (foams). Generally however the amount of information contained in the grey level images is so large that a simplification is needed: a segmentation between the objects of interest and the background is performed leading to binary images with just two grey levels: 1 for the

objects, 0 for the background. Although the highest care should be taken in the visualisation step for getting good quality images, some enhancement of the grey level images may be necessary at this stage. However, this enhancement should be minimised, since most of those treatments will introduce some bias in the final results.

Many procedures exist for the segmentation: it is recommended to use an automated or at least semi-automated algorithm, to reduce the interference with the operator. It is possible to segment colour images by triple threshold on the three primary colours, although the transformation into the Hue-Saturation-Intensity (HSI) colour system, closer to the human vision, is recommended: on epifluorescence images the segmentation in the Intensity plane gives directly the background (black i.e. with a low brightness level) and the objects. The colour characterisation will be conducted by combining the obtained binary image with the information contained in the Hue plane. The binary image may require some cleaning: removal of debris, especially with complex culture media, of objects in contact with the image frame, hole filling, etc. Finally the image is prepared to proceed to the next step, quantification that will greatly depends upon the application.

## BIOMASS CHARACTERISATION

### **Filamentous Fungi and Filamentous Bacteria**

Fungi and filamentous bacteria have been used to produce a range of important metabolites such as antibiotics, organic acids, proteins, enzymes, food and other chemicals. In submerged cultures they may grow either as disperse form (dispersed hyphae and clumps in a free mycelium) or as pellets that are resulting from the entanglement and aggregation of filamentous mycelium. The morphology of filamentous microorganisms was reviewed by Nielsen (1996) and Thomas (1992).

The main objective is, in any application, the classification according to the morphological type (i.e. dispersed hyphae, clumps and pellets) with a more precise description of each individual within its class. Dispersed hyphae are characterised generally by the total hyphal length, the number of tips (apices) and branching points, the main hyphal length, and the mean branch length. The hyphal growth unit (HGU) is given by the ratio of the total hyphal length to the number of tips. Clumps are often described by the ratio of their projected surface to the surface of the convex bounding polygon. Pellets are characterised by their total projected areas and the projected area of the hairy crown or the core. Durant and co-workers (Durant *et al.*, 1994; Durant, Crawley and Formisyn, 1994) improved the discrimination between filamentous regions and compacted cores, by staining mycelial aggregates of *Basidiomycetes* with crystal violet.

Once again it has to be reminded that an image is a 2D projection of a 3D reality and that only a single projected surface can be obtained directly. Assumptions on the 3D shape have to be made to obtain volume-based information: this is typically the problem for pellets. In each morphological class, average values have to be calculated on a meaningful number of individuals. Tables 2.1 and 2.2 give examples of applications to fungi and filamentous bacteria.

Staining techniques associated to image analysis (IA) are becoming ubiquitous for the examination of active regions of hyphae and physiological characterisation. The first attempt to quantify the proportion of growing apices in *Penicillium chrysogenum* was

**Table 2.1** Applications to fungi

Microorganism	Comments	Reference
<i>Penicillium chrysogenum</i>	Morphology characterisation	Tucker <i>et al.</i> (1992)
	Rheology	Makagiansar <i>et al.</i> (1993)
		Tucker and Thomas (1993)
	Morphology kinetics in repeated fed-batch Mixing; rheology	Nielsen <i>et al</i> (1995)
<i>Penicillium roqueforti</i>		Nielsen & Krabben (1995)
		Jüsten <i>et al.</i> (1996)
	Morphology classification	Pichon, Vivier & Pons (1992a)
<i>Aspergillus niger</i>	Pellets	Cox & Thomas (1992)
	Rheology	Olsvik <i>et al.</i> (1993)
	Cyclone bioreactor	Kamilakis & Allen (1995)
	Carbon dioxide effect	McIntyre & McNeil (1997a)
		McIntyre & McNeil (1997b)
<i>Aspergillus oryzae</i>	Fractal dimension of pellets	Ryoo (1999)
	Rheology	Amanullah <i>et al.</i> (1999)
<i>Mortierella alpina</i>	Morphology classification; pilot-scale	Higashiyama <i>et al.</i> (1999)
<i>Fusarium moniliforme</i>	Mixing	Priede <i>et al.</i> (1995)

**Table 2.2** Applications to filamentous bacteria

Microorganism	Comments	Reference
<i>Streptomyces tendae</i>	Morphology classification	Reichl, King & Gilles (1992)
		Treskatis <i>et al.</i> (1997)
<i>Streptomyces virginiae</i>	Morphology classification	Yang <i>et al.</i> (1996)
<i>Streptomyces ambofaciens</i>	Filament characterisation	Pons <i>et al.</i> (1998)

<i>Streptomyces fradiae</i>	Rheology	Tamura et al. (1997) Choi, Park & Okabe (1998)
<i>Oscillatoria rubescens Anabaena flos-aquae</i>	Filament characterisation	Walsby & Avery (1996)

made by Paul, Kent and Thomas (1994) by using neutral red staining. A quantitative method was later developed (Vanhoutte *et al.*, 1995) for a more detailed characterisation of the physiology of *P. chrysogenum*. It was based on a differential staining procedure showing six physiological states: growing material, three differentiated states with an increasing granulation, a highly vacuolized state, and dead segments having lost their cytoplasm. More recently, Cox and Thomas (1999) used a fluorescent stain (Mag fura) to evaluate the active hyphal regions of two industrial strains of filamentous fungi (*P. chrysogenum* and *Aspergillus oryzae*).

*Streptomyces* hyphae are thinner than the fungal ones, and the magnification normally used in optical microscopy do not allow the cytoplasm visualisation. Nevertheless,

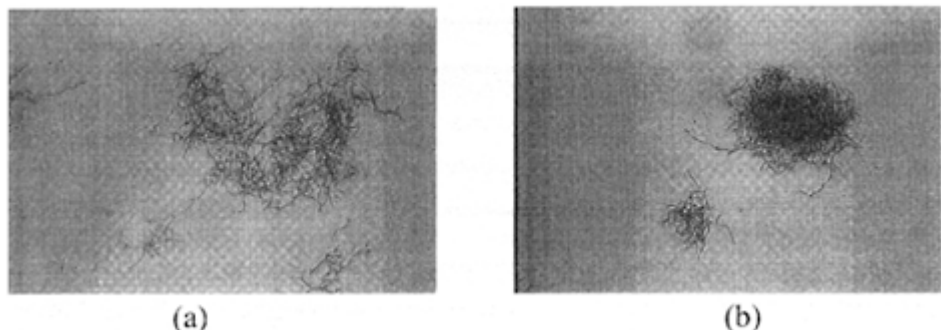


**Figure 2.2** *Streptomyces ambofaciens*:  
a) dispersed mycelia; b) pellet.

staining can bring valuable information for those bacteria strains. To understand relations between cellular differentiation of *Streptomyces ambofaciens* in submerged culture, (Figure 2.2) and spiramycin production, Drouin *et al.* (1997) used IA. Three parameters were measured: occurrence of empty zones in mycelium, number of septations, mycelium thickness. Previously, the same group used IA for localising the respiration sites based on the distribution of formazan crystals along the hyphae. Recently, Sebastine *et al.* (1999) developed an IA method to identify the different physiological states of *Streptomyces clavuligerus* using a fluorescent bacterial viability stain, a mixture of SYTO9 and propidium iodide.

### Non-filamentous Bacteria

Problem of non-filamentous bacteria imaging lays in the small size of the microorganisms. In spite of this , Dubuisson, Jain and Jain (1994) employed IA and

pattern recognition techniques to count and identify cultures of methanogens (*Methanospirillum hungatei* and *Methanosardna mazei*). In anaerobic wastewater digesters, flocs and granules are bacterial aggregates whose size (Dudley *et al.*, 1993) and roughness (Bellouti *et al.*, 1997) can be monitored by IA and related to the efficiency of the reactors. Settleability of activated sludge can be characterised by the fractal dimension of the flocs (Grijpspeerd and Verstraete, 1997).

The main routine applications are dealing with viability assessment using such vital stains as Orange Acridine, and epifluorescence microscopy (Singh, Pyle and McFeters, 1989).

The emergence of new fluorescent phylogenetic probes combined with microscopic techniques allows the assessment of the identities and activities of bacterial cells within complex microbial communities. Automated Confocal Laser Scanning Microscopy (CLSM) combined with image processing techniques allowed the assessment of 3D biofilm structures (see chapter "Biofilm Reactors" in this book) under *in situ* conditions (Kuehn *et al.*, 1998) and off line sampling from a rotating annular bioreactor (Lawrence, Nie and Swerhone, 1998).

When Fluorescence In Situ Hybridisation (FISH) was combined with CLSM this approach allowed visualising spatial organisations of microbes in methanogens granules (Sekiguchi *et al.*, 1999) of upflow anaerobic sludge blanket reactors. Properties of a synthetic biofilm (*Escherichia coli*) were examined by using CLSM in combination with fluorescent probes (Swope and Flicklinger, 1996). Combination of FISH and microautoradiography enabled the assessment of the structure and function of bacterial communities (Lee *et al.*, 1999), specially in activated sludge processes (Nielsen *et al.*, 1999; Kawaharasaki *et al.*, 1998).

## Yeasts

The yeast *Saccharomyces cerevisiae* is widely used in biopharmaceutical and food processes. Some authors have developed IA techniques for sizing and counting of *S. cerevisiae* (Vicente, Meinders and Teixeira, 1996; Yamashita *et al.*, 1993; Costello and Monk, 1985). Besides cell counting, morphological properties can be used to estimate physiological condition of yeast cultures especially related to cell budding and division (Hirano, 1990) and vacuolisation (Zalewski and Buchholz, 1996). A semiautomatic method was proposed by Pons *et al.* (1993) to characterise the morphology of yeast cells, (see Figure 2.3). Yeast size distributions and population kinetics (single and budding cells, cell clusters) were determined during alcoholic fermentations.

Walsh *et al.* (1996) determined geometric properties of immobilised *S. cerevisiae* microcolonies in alginate and carrageenan gel particles. IA provided measurements of the cross-sectional area and aspect ratio of each microcolony and the distance of the centroid of the microcolony from the centre of the cross-section.

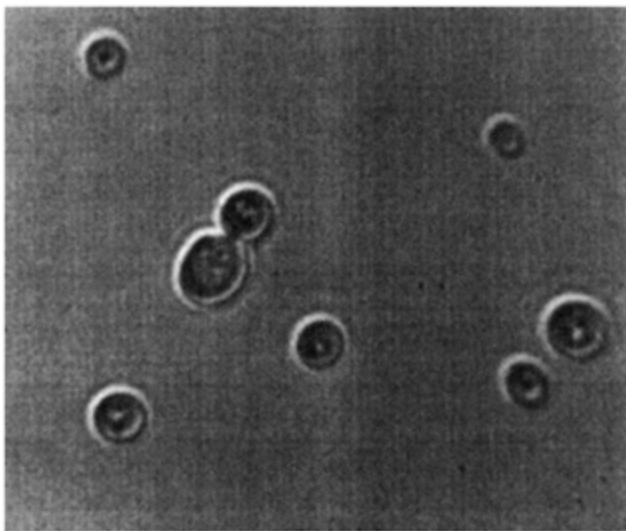


**Figure 2.3** *Saccharomyces cerevisiae* yeast cell.

O'Shea and Walsh (1996) applied IA to separate cells of the yeast *Kluyveromyces marxianus* into six defined categories (from ovoid cells to branched mycelial cells). These dimorphic yeast cells were used in an alcoholic fermentation of cheese whey permeate. This research was recently updated (McCarthy *et al.*, 1998) with the cell morphology characterisation and its effect on dead-end filtration.

IA techniques were utilised (Perrier-Cornet, Maréchal and Gervais, 1995) in a high-pressure optical micro-reactor to calculate cell volumes on individual cells of *Saccharomycopsis fibuligera*. Cells were assumed to be spherical and the projected area was accessed by IA on pictures taken on an inverted light microscope.

Machine vision microscopy systems have been proposed for yeast cell culture visualisation, usually employing an automatic sampling device for delivering the sample to the viewing stage of the microscope (Ren, Reid and Litchfield, 1994; Zalewski and Buchholz, 1996). In-situ microscopes were developed for on-line characterisation of *S. cerevisiae* (Suhr *et al.*, 1995; Bittner, Wehnert and Schepers, 1998). Cell concentration and cell size were estimated using a microscope mounted in a port of a bioreactor. Guterman and Shabtai (1996) proposed a machine vision system combined with neural networks and fuzzy logic techniques to recognise changes of population distribution of the yeast-like fungus *Aureobasidium pullulans*.

### Animal Cells

A real-time imaging system was presented by Konstantinov *et al.* (1994) for cell counting and sizing of animal-cell culture in a bioreactor. An *in situ* microscopic image analysis system was developed by Maruhashi, Murakami and Baba (1994) to automate

measurements of cell concentration and viability in a suspended animal cell culture (mouse-mouse hybridoma STK1).

At Novo Nordisk pilot plant an IA software was developed (Bonarius, Nielsen and Kongerslev, 1997) for monitoring the cell density in Chinese hamster ovary (CHO) cell cultures. Neural networks were used to distinguish stained nuclei from cell debris and other objects in the image. Ruaan, Tsai and Tsao (1993) reported the application of video IA for the on-line monitoring of CHO growth using an inverted microscope and a flow system. Local cell density, cell motility, and cell surface area were continuously estimated. Tucker *et al.* (1994) proposed an IA method for characterising the viability and morphology of hybridoma cells from suspension cultures. The total and viable cell counts and the percentage of dead cells present were found using the exclusion dye Trypan Blue.

IA was applied to the monitoring of cultures of human kidney tumour cells: procedures were developed to investigate microcarrier colonisation, cluster formation and cell size using scanning electron microscopy (Pons *et al.*, 1992) and optical microscopy (Pichon, Vivier and Pons, 1992b) as illustrated in Figure 2.4.

The total surface area occupied by a variety of mammalian cell lines, and the number of cells attached to fibronectin and a fusion protein (CBD/RGD) were evaluated using IA techniques (Wierzba *et al.*, 1995).

Chalmers and Bavarian (1991) presented a microscopic, high-speed video system to study the interactions of two suspended insect cells strains with bubble film and bubbles

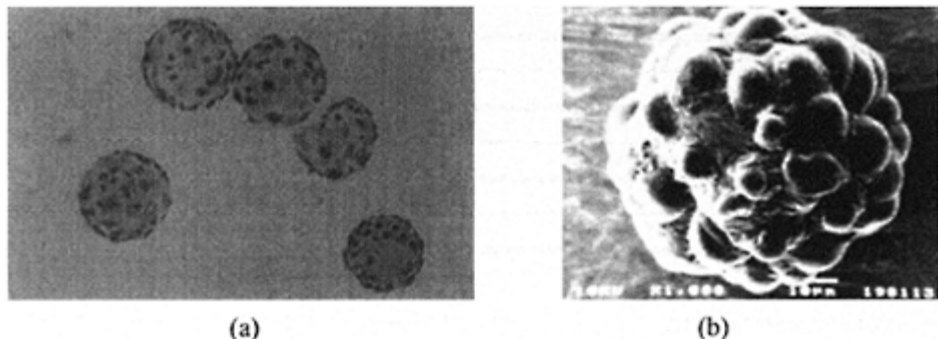


**Figure 2.4** Mammalian cells on microcarrier: a) optical microscopy; b) scanning electron microscopy.

rupturing. A fluorescence microscopy technique was used by Cowger *et al.* (1999) to characterise the distribution of necrotic and apoptotic insect cells in a rotating-wall vessel. The distribution was based on staining pattern and morphology.

### Plant Cells (and Suspended Somatic Embryos)

Bioreactor technology provides the potential for producing large numbers of plants more cheaply and efficiently (Cazzulino, Pedersen and Chin, 1991) than tissue culture on agar solidified medium or through the use of shake flask cultures. Diverse varying plant morphologies may be observed in cell cultures as illustrated in Figure 2.5: single cells, cell aggregates, and organised plant structures from different stages of embryogenesis, ranging from globular to torpedo. The heterogeneous mixture of cells needs to be quantified for evaluation of the conditions promoting good development of culture. IA technology provides one practical solution to the problem of characterising the morphology of somatic embryos in culture.

Recently, applications of image analysis in large scale plant micropropagation (during somatic embryogenesis) were reported: machine vision systems were used for the on-line growth monitoring of callus suspension cultures of *Ipomea batatas* in an airlift bioreactor (Harrell, Bieniek and Cantliffe, 1992) and of pigment-producing *Ajuga* cells (Smith, *et al.*, 1995). Uozumi *et al.* (1993) distinguished several morphological classes in liquid suspension cultures of celery through a pattern recognition technique based on neural networks; a similar approach was used by Chi *et al.* (1996) in liquid suspension cultures of carrot; Cazzulino, Pedersen and Chin (1991) developed IA procedures that enables the routine characterisation of carrot somatic embryos in a liquid culture. Shape recognition algorithms (multilevel simple statistical comparisons and classificatory discriminant analysis) were employed for microscopic observations of the different embryo stages. Honda *et al.* (1999) used the trichromatic colours (RGB) to distinguish between two kinds of sugarcane calli on solid media; Barciela and Vieitez (1993) determined morphological parameters on cultured cotyledon explants of *Camellia japonica*.

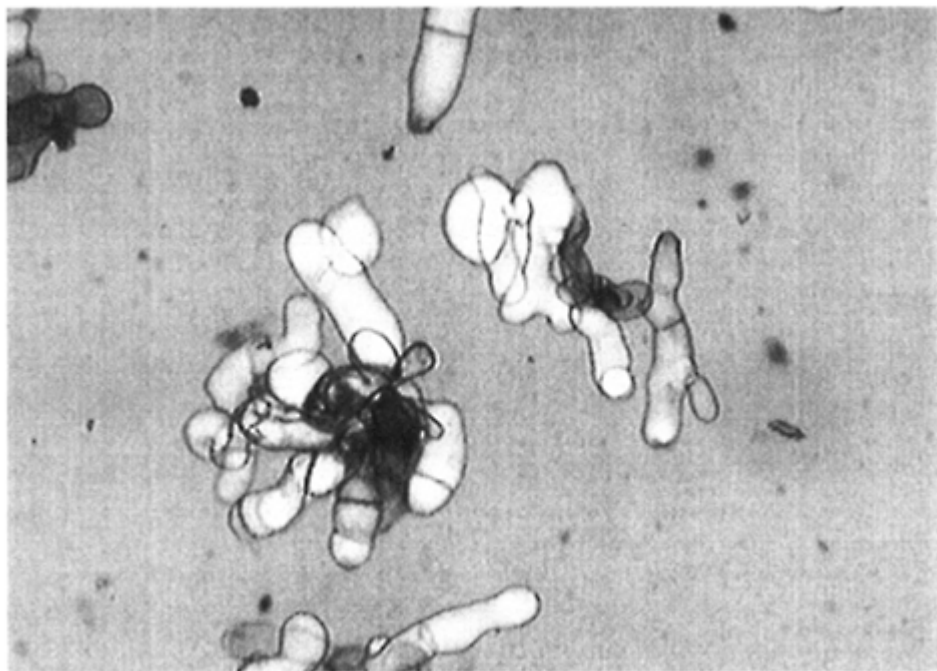


**Figure 2.5** Suspension of somatic embryos of *Pinnus pinaster* (courtesy of A. Dias).

Kieran, Malone and Macloughlin (1993) used IA to evaluate cell length, chain length and number of cells per chain in suspended cultures of *Morinda citrifolia* in batch and semi-continuous stirred tank reactor. Those properties were identified as useful indicators of the influence of stirrer speeds on the morphology of the cultures in the early exponential growth phase. These authors (Kieran *et al.*, 1995) also evaluate the effect of fluid shear susceptibility on the morphology.

### Protozoa and Other Higher Life Forms

Protozoa, rotifers and nematodes (see chapter on “Nematode Production”), etc. are microorganisms involved in the good operation of wastewater treatment plants by activated sludge (Jenkins, Richard and Daigger, 1993). This can be assessed by a Sludge Biotic Index (Madoni, 1994), which requires the counting, and recognition of the various members of the microfauna. Automation of this tedious task would be of great help for plant operators: some success in this direction has been obtained recently by Amaral *et al.* (1999). Figure 2.6 illustrates some examples of digitised images of protozoa species in wastewater activated sludge.

An IA system was developed by Kaneshiro *et al.* (1993) for the viability assessment of protozoa using a fluorescent staining technique.

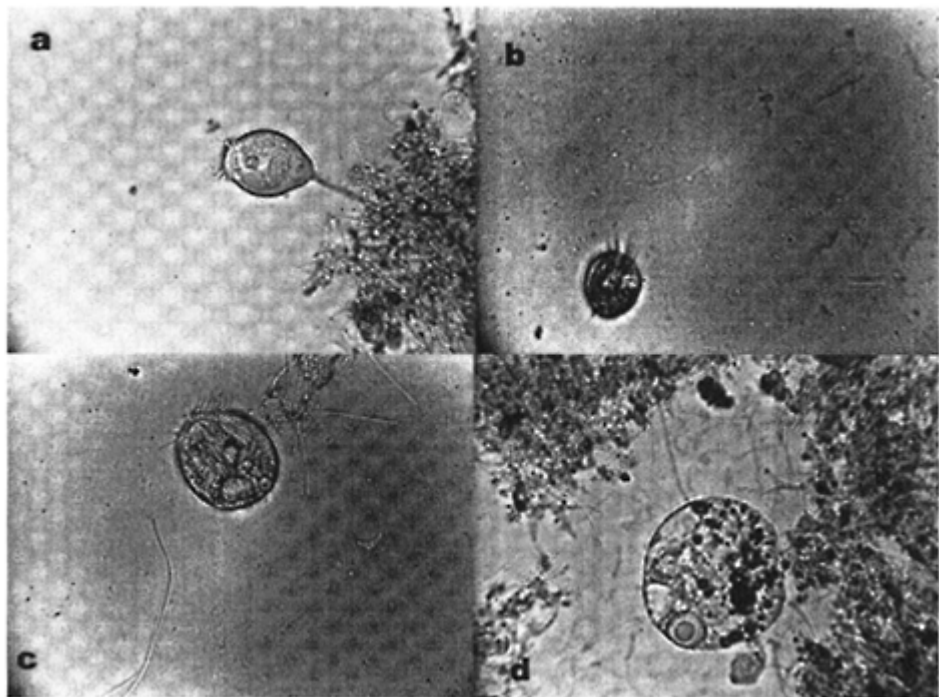


**Figure 2.6** Protozoa in activated sludge from a wastewater treatment reactor: a) *Vorticella microstoma*, b) *Euplotes*, c) *Glaucoma*, d) *Prorodon*.

#### BIOREACTOR IMAGING

Bioreactors are essentially multiphase systems in which the mass (and in some processes the heat) transfer is a key issue. The characterisation of mixing has received therefore a lot of attention. Traditionally residence time distributions obtained by inert tracer injection have been used for liquid, gas, and more seldom solid phases (Tatterson, 1991; Lumley and Horkeby, 1989).

Imaging methods have been developed, which provide two types of information:

- The global characterisation of the mixing, where the 2D or 3D distribution of at least one of the components of the multiphase system is given: the changes of a physical property with respect to the component concentration are monitored.
- The characterisation of flow patterns and velocity fields by tracking the motion of individual particles

Here the term of imaging has to be understood in its widest sense, meaning that light is not the only excitation beam.

Tomography and radiography enable non-invasive characterisation of multiphase flows. An excellent review is provided by Chaouki, Larachi and Dudukovic (1997). The selection of the excitation signal depends on the contrast of the chosen physical property between the different phases:

- Nuclear-based with ionising radiations, essentially and X rays. Neutron imaging is mostly used for reactive flows in consolidated porous media, therefore outside the scope of bioreactors.
- Nuclear-based with non-ionising radiations such as Nuclear Magnetic Resonance (NMR), which has been used for many years in medical applications. Proton NMR is particularly suited because water is abundant in biological systems, but other nuclei might be of interest, such as  $^{31}\text{P}$  and  $^{23}\text{Na}$ , to monitor biological activities (DiBiasio *et al.*, 1993; Sardonini and DiBiasio, 1993).
- Non nuclear-based: electrical capacitance, optical radiation, ultrasound, and microwave.

The difference between tomography and radiography lies in the detection system: the attenuation of the beam is registered by discrete detectors in the case of tomography when a sheet of film or a camera is used for radiography (Figure 2.7a). For tomography different arrangements have been proposed, with single or multiple, displaceable, sets of sources and detectors. The visualisation takes usually place in a plane.

In both methods the beam transmitted through the medium is attenuated depending upon the distribution of the sensitive physical property,  $f$ , along the path traversed by the beam. The collected signal,  $P$ , is a 2D projection of a 3D reality:

$$P(l, \theta) = \int_L f(x, y) ds$$

Different reconstruction algorithms (Kumar and Dudukovic, 1997; Godfroy *et al.*, 1997; Reinecke *et al.*, 1998) have been proposed to back-calculate  $f$  from  $P$  (Figure 2.7b).

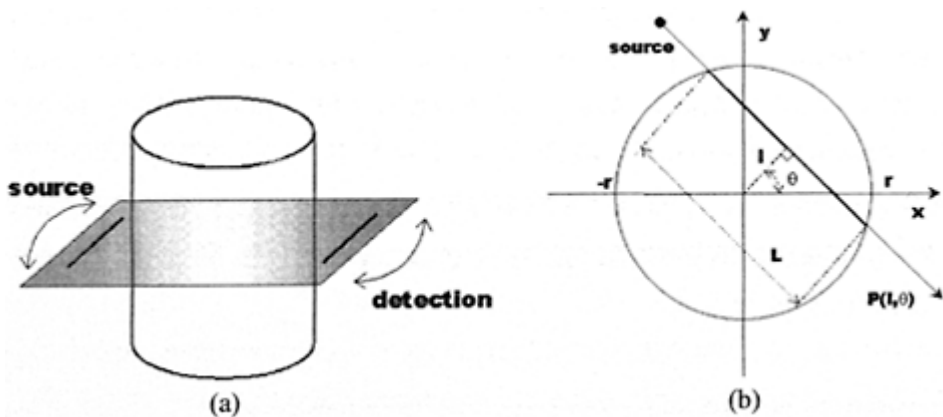


**Figure 2.7** (a) Principle of tomography and radiography; b) 3D reconstruction from a 2D projection.

The quality of the imaging is function of the spatial, temporal and density resolution. Spatial resolution is the minimum distance that two objects can be separated. With sets of detectors it depends upon their number, spacing and size: X-rays require smaller detectors than  $\gamma$ -rays. But the latter are more penetrating and can be used with larger test sections. With a camera, the spatial resolution depends upon the adequateness between the reactor size and the number of lines and pixels/line of the resulting image. With NMR the size of the bioreactor to be imaged is limited by the size of the magnet's bore. Temporal resolution is the basic limitation in X-rays and  $\gamma$ -rays tomography, due to the necessity to rotate the sources and/or the detectors to obtain the photon count rates for all the projections. Dynamic information can be obtained only when the flow characteristics change sufficiently slowly. This drawback does not exist with electrical capacitance or resistance tomography that is much faster (and safer!): however its spatial resolution is poorer although improvements have been made recently (Holden *et al.*, 1998). Density resolution refers to the smallest difference in the measured physical property that the system is able to distinguish. Optical methods require transparent media. Distortion effects are introduced by light diffraction phenomena: thin two-dimensional vessels are designed and cylindrical reactors are embedded in rectangular optical boxes. Hari-Prajitno *et al.*, (1998) have used a starch/iodine solution decolourised by injection of sodium thiosulfate to determine the mixing times in multi-impeller systems. Galindo and Nienow (1992, 1993) introduced methylene blue near the impeller to investigate the mixing characteristics of various devices in simulated xanthan gum broths. A similar technique is employed by Bujalski *et al.* (1999) to examine the suspension and liquid homogenisation in stirred tanks containing solids. In bioprocesses these solids could be microcarriers in cell cultures or sludge for wastewater treatment (Schaflinger, Acrivos

and Zhang, 1990). Figure 2.8a presents schematically a set-up to study the resuspension of sludge in sequencing batch bioreactors with surface aeration for wastewater treatment. The sludge is simulated by carboxymethylcellulose (CMC) solutions dyed with methylene blue. Clear water is poured above the CMC layer in the tank with care to avoid any mixing

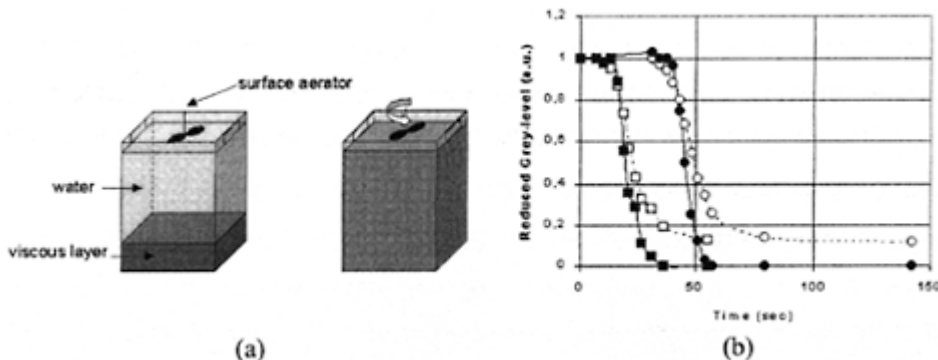


**Figure 2.8** (a) Experimental set-up of the simulated sludge resuspension test; (b) Comparison of the resuspension kinetics with a Rushton turbine. CMC concentration: 10 g/l (■, □) and 40 g/l (●, ○) Closed symbols for the area of interest (AOI) and open symbols for total field of view.

of the two layers. At time zero the impeller, here a Rushton turbine, is set into motion. After a lag phase, which is a function of the CMC concentration, i.e. the compactness of the sludge that may result from an extended settling period, the viscous layer is gradually mixed with the water layer. The mixing is monitored with a camera connected to a videotape recorder. The images are later digitised (Figure 2.9). The variation of the grey level within areas of interest enables to follow the progress of the mixing (Figure 2.8b).

Houcine *et al.* (1996) characterised the mixing in a plane defined as the cross section of the flow by a thin laser sheet, which excites the fluorescence of a non-reacting tracer (Figure 2.10a). The instantaneous field of dye concentration is obtained automatically from the digitised video images. Experiments in a continuous stirred tank have been run with two inlet sources: a contacting parameter which emphasises the average state of mixing and the field of temporal variance, which characterises the segregation of the investigated zone, are computed. This can be a useful technique to study the dispersion of highly concentrated nutrients or pH reagent streams in bioreactors. Other methods of data analysis such as 3D-wavelets have been proposed to help the comparison between systems (Li and Wei, 1999).

Velocimetry techniques use electromagnetically active particles, sensitive to nuclear radiations or visible or fluorescent light and which are able to mimic the motion of a flow particle. In positron emission trajectography (PET), particles are produced by direct irradiation of a particle in a cyclotron, by adsorption of a radioisotope on the tracer

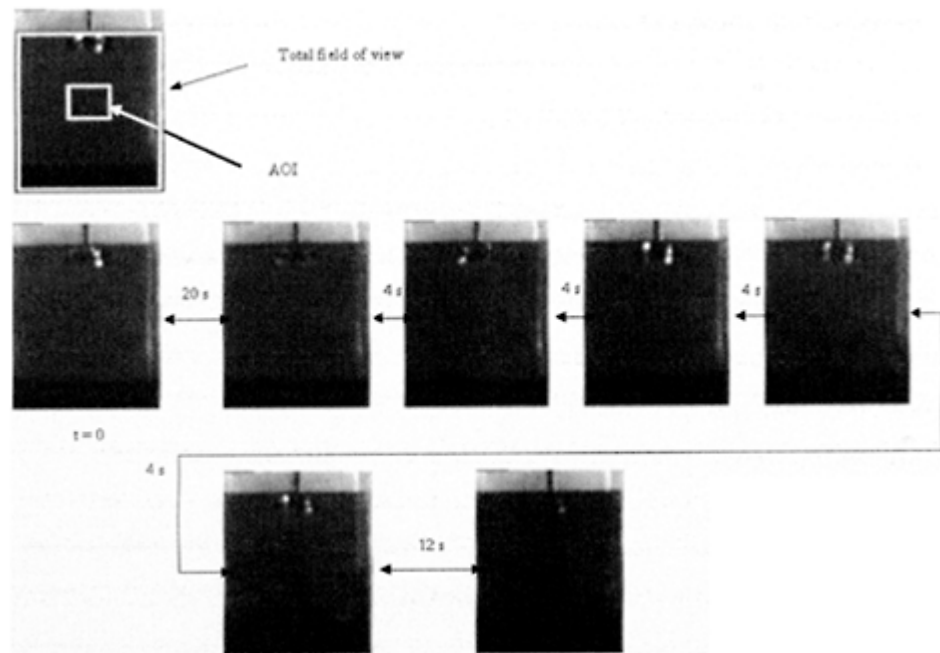


**Figure 2.9** Some frames of the experiment with a Rushton turbine and a CMC concentration in the viscous layer of 40 g/l.

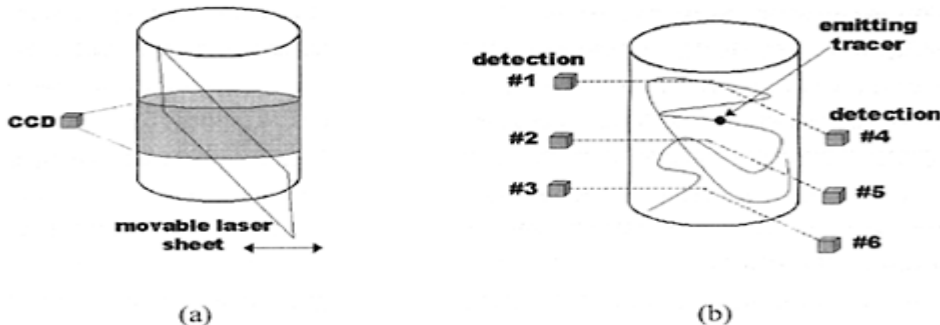


**Figure 2.10** (a) Visualisation by laser sheet illumination; (b) Radioactive particle tracking.

surface or by manufacturing a particle out of a radioactive material, but the detection systems able to reconstruct the trajectory of the particle are complex and expensive. A simpler radioactive particle tracking method makes use of  $\beta^-$  emitters produced by neutron capture. Different triangulation procedures have been developed to determine the 3D co-ordinates of the particles from the counts given by the detectors (Figure 2.10b).

In spite of distortion effects to be corrected, optical tracking of particles is more affordable. Different variants exist:

- Particle Imaging Velocimetry (PIV): the velocity of particles are calculated by correlating the displacements on a double exposure image
- Particle Streak Velocimetry (PSV): on a long-exposure image sections of the particles trajectory appear as streaks. However the particles should not leave the plane of focus and the particle density is much lower than with PIV.
- Particle Tracking Velocimetry (PTV): the motion of the particle is recorded by a video camera

A 3D-PTV system has been developed by Wittmer *et al.* (1995) and Pitiot, Falk and Vivier (1998) to study the mixing characteristics in mixed reactors with Newtonian and non-Newtonian fluids for different agitation systems (Figure 2.11). Two (or three) monochrome video cameras monitor the displacement of the particle, each camera being connected to one colour channel of an electronic encoder that delivers colour images (PAL format). This allows for a perfect synchronisation of the video signals. The colour images are digitised on a PC equipped with a special board for real-time image capture at the rate of 25 frames per second. One of the key problems is the quality of the particle, the buoyancy of which should be adapted with respect to the density of the fluid. Pitiot, Falk and Vivier (1998) manufacture their gelatine-based particle by micro-encapsulation: the particle self-adapts its buoyancy by diffusion of the bulk liquid phase through the particle

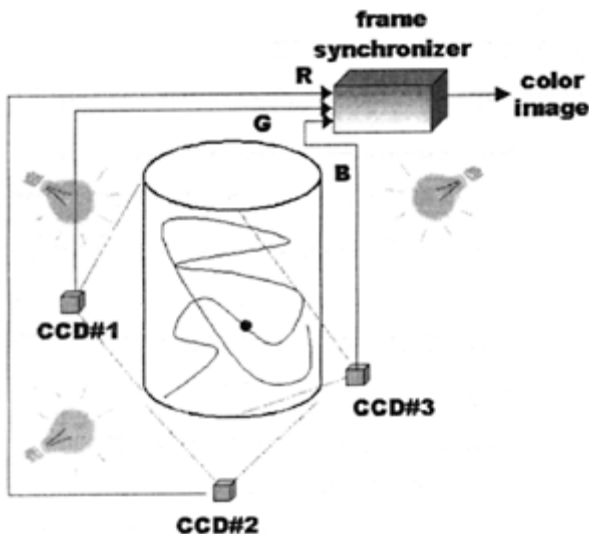


**Figure 2.11** 3D-PTV principle.

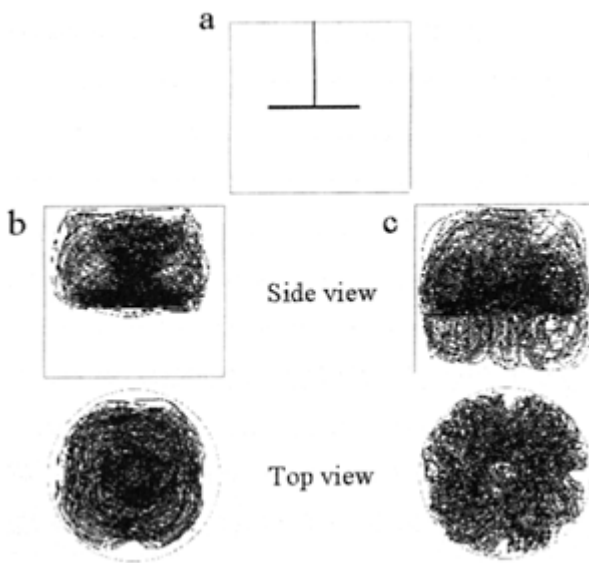


**Figure 2.12** 3D-trajectory of the particle with a Mixel mobile and a rotation speed of 110 rpm: (a) Schematic set up; Agitation Reynolds number: 5 (b) and 56 (c); Viscosity:

5.4 Pa.s (b) and 0.14 Pa.s (c). (By  
courtesy of P.Pitiot.)

wall. Figure 2.12 compares the effect of some Theological properties on the trajectory of the particle in a stirred tank equipped with a Mixel mobile. A single camera is used by Venkat *et al.* (1993) to track the motion of microcarriers in spinner vessels, but a suitable arrangement of mirrors enable a stereo-vision of the particles on a single image on a highspeed film (400 frames per sec). Another key issue is the spatial resolution: Pitiot's particles have a diameter of about 2 mm for a reactor diameter of 300 mm. Micro-carriers are smaller (about 200  $\mu\text{m}$ ) and the field of view is restricted to a portion of the spinner vessel.

Aerobic systems represent the largest group of commercial reactors. Bubbles transfer oxygen to microorganisms and remove carbon dioxide. The transfer is improved by high specific surfaces, corresponding to small bubble sizes. However liquid rheological properties and vessel geometry induce generally bubble size distributions. Large bubbles produced by coalescence are found near the surface, where gas disengages. Bubbles near walls are also larger than in the vicinity of impellers (Calderbank, 1958; Takahashi and Nienow, 1988). There is a need to characterise better the phenomena taking place around the bubbles to improve the scale-up of bioreactors, either mechanically agitated or flow contactors (air-lift, bubble columns).

When the bubble density is high, only the bubbles in the vicinity of the wall are considered. Some authors use two-dimensional column (de Swart, van Vliet and Khrisna, 1996; Atenas, Clark and Lazarova, 1998). To avoid blurring, a small shutter speed and flashlights are employed. When bubbles are almost spherical, their size distribution is obtained easily (Bouaifi and Roustan, 1998). But bubbles can deflect largely from spheres (de Swart, van Vliet and Khrisna, 1996) as seen in Figure 2.13. For rising bubbles, especially in viscous fluids like polysaccharide broths, the assumption of a vertical axis of symmetry enables to calculate their volume (Mouline, 1996; Margaritis, te Bokel and Karamanov, 1999). A Fourier analysis of the silhouette contour of bubbles was used by Atenas, Clark and Lazarova (1998) to investigate the shape of bubbles in a rectangular airlift bioreactor. Fourier analysis is usually rather cumbersome and more classical shape parameters, as those used to assess solid particle morphology (elongation, circularity, concavity index), may be useful in a first approach (Pons *et al.*, 1999).

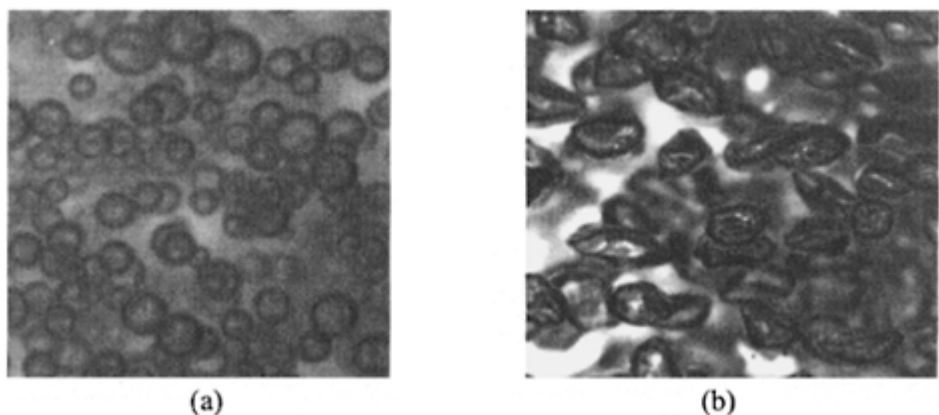


**Figure 2.13** Different shapes of bubbles in a bubble column: (a) with traces of a long-chain alcohol, (b) in pure water (*By courtesy of E.Camarasa and C.Vial*).

Bubbles shape and velocity can change with time. This has been studied by Benkrid (1999) in a 2D column using a high-speed camera (500 to 1000 i/s) and co-currents of gas and newtonian liquid. Gobal and Jepson (1997) work at a lower rate (30 i/s) but separate the two frames of each image, obtaining finally a rate of 60 f/s, in their study of velocity and void profiles in slug flow. Bubbles can break against various obstacles in the bioreactor, such as probes or immersed heat exchanger tubes (Pandit, Dodd and Davidson, 1993). Coalescence of bubbles in non-newtonian fluids has been investigated by Mouline (1996) and Li *et al.* (1997). The generation of bubbles at a sparger orifice (Figure 2.14) or at the surface of a membrane (Semmens *et al.*, 1999) can be studied with the same techniques.

To look in more detail at the mass transfer in the vicinity of a bubble, Schmidt and Lübbert (1993) immobilised a nitrogen bubble in a vertical conical tube through which water flowed downward. A pH-indicator, phenolphthalein, had been dissolved in the water. Ammonia was injected through the bubble by a thin capillary: ammonia was transferred to the liquid phase via the gas-liquid interface and the pH-indicator turned red. The reaction was monitored via a camera and took place in the wake of the bubble.

Bursting of bubbles has received a special attention in animal cell cultures, and to a smaller extent in plant cell cultures (Doran, 1999). These cells are susceptible to damage by mechanical agitation and/or gas sparging. Two phenomena are taking place: bubble coalescence and break-up at the free gas-liquid interface; shear stresses arising from high agitation speeds of the bulk liquid with Kolmogorov eddy sizes similar to or smaller than the cell sizes. Protective effect of serum and Pluronic F-68 has been noticed by many researchers (Tan *et al.*, 1993). The first visualisation of bursting bubbles has been reported by Rayleigh (1891). Bavarian, Fan and Chalmers (1991) and Chalmers and

Bavarian (1991) describe how insect cells get attached to bubbles and are killed by the rapid

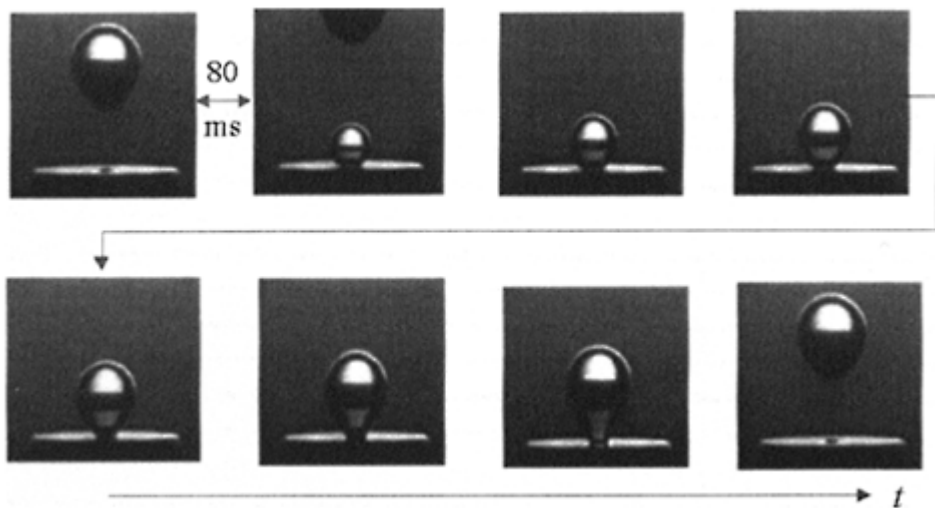


**Figure 2.14** Generation of bubble in a viscous fluid (*by permission from Dr H.Z. Li*).

acceleration of the bubble film after its rupture at the surface and by the high levels of shear stress in the boundary layer flow associated with the bubble jet formation. Furthermore the experimental shape of the jet can be compared to profiles given by simulation models and related to energy dissipation rates (Boulton-Stone and Blake, 1993; Garcia-Briones and Chalmers, 1993).

Fermentation media are usually prone to foaming, which causes problems of overflow and entrainment of liquid in the gas events. Foam control is usually done by addition of antifoams, which change the surface tension of the liquid and the coalescence behaviour of bubbles in the foam and in the liquid, affecting in that way the gas dispersion and the oxygen mass transfer coefficient. Furthermore antifoam can be poisonous for microorganisms. In an aerobic fermentation, the foam is produced continuously: if the foam height is constant, it means that the rate of bubble bursting at the top surface is equal to the rate of bubble formation at the layer base. Foams can be very different from their structure and bubble size distribution. Foams with bubbles of 2–3 mm in diameter or smaller, with a rather high liquid volume fraction (higher than 0.3) have bubbles that can be considered as spherical or slightly ellipsoidal. Foams with larger bubbles or small bubbles but with a low liquid volume fraction have polyhedral shapes.

The concept of foaminess characterises the foam forming properties of a solution. It is easily calculated from the height of the foam layer produced by a steady rate of gas in a column and monitored by a camera (Lee *et al.*, 1993). The structure of the foam is more difficult to characterise because the image represents a set of objects in contact. One way

to treat the problem is to appreciate quantitatively the visual texture: the challenge is to quantify the regularity, the fineness, the homogeneity, and the orientation of the textural patterns. This approach is extensively used in spatial and aerial imaging but applications can also be found in process engineering. The control of ore flotation can be automated by quantitative analysis of the visual texture of the froth (Moolman *et al.*, 1994). The analysis is directly conducted on the grey-level images. A very simple approach consists in classifying the images according to some properties of their grey-level histogram (mean, mode, standard deviation). Flow patterns (single phase, bubbly flow, slug flow, churn flow) in a circulation loop have been discriminated based on the simple examination of their histograms (Hsieh, Wang and Pan, 1997). But the methods which seem to be the most useful in that field are based on the analysis of the grey level run length (GLRL) matrices and the spatial grey level dependence (SOLD) matrices (Haralick, 1979; Conners, 1980) where the grey-level neighbourhood of each pixel is taken into consideration.

In the SLD method a co-occurrence grey-level matrix  $C(c_{ij})$  of dimension  $N_g \times N_g$ , where  $N_g$  is the maximal number of possible grey levels (usually 256) is defined as:

$c_{ij}$ =frequency of occurrence of having a pixel of grey level  $j$  at a distance  $d$  and angle of a pixel of grey level  $i$ . The  $C$  matrix is itself characterised by descriptors based on the  $c_{ij}$  such as inertia, entropy or energy. Generally it is useful to combine these techniques with a pattern recognition procedure, such as a principal component analysis of the descriptors (Einax, Zwanziger and Geiss, 1997). This enables a rapid comparison of the structures. The pattern recognition procedure consists in a training phase with reference textures and a validation phase. As an example several textures from Brodatz (1966) have been scanned. These textures have some visual similarities with foams. Foam images from a test column have also been obtained under various experimental conditions. All considered images have a size of 256×256 pixels. The co-occurrence matrices have been computed for  $d=5$  pixels and for  $\alpha=0^\circ, 45^\circ, 90^\circ$  and  $135^\circ$ . The descriptors have been averaged over the four values of  $\alpha$ . A map with the relative positions of the different textures, showing the similarities and dissimilarities can be found in Figure 2.15. Similarly Sarker *et al.* (1998) compare air-water foams prepared with different surfactants (proteins and emulsifiers) in a test column by combination of the GLRL method and a principal component analysis of the texture descriptors calculated on the GLRL matrices.

## CONCLUSION

The current applications of image analysis will be enlarged. For example, it does not belong to the field of Utopia to consider in the near future the utilisation of sophisticated morphometric techniques able to automatically identify and count the different kinds of microorganisms present in an optical microscopic field, or to determine the state of a sporulant culture.

On the other hand, IA will still be useful to condense information coming from different types of acquisition systems: 3-D NIR/FTIR spectra, confocal imaging, or simple optical “*in situ*” microscopy combined with adequately chosen chromophores or

fluorophores, which will enable in depth dynamic physiological studies of cellular phenomena.

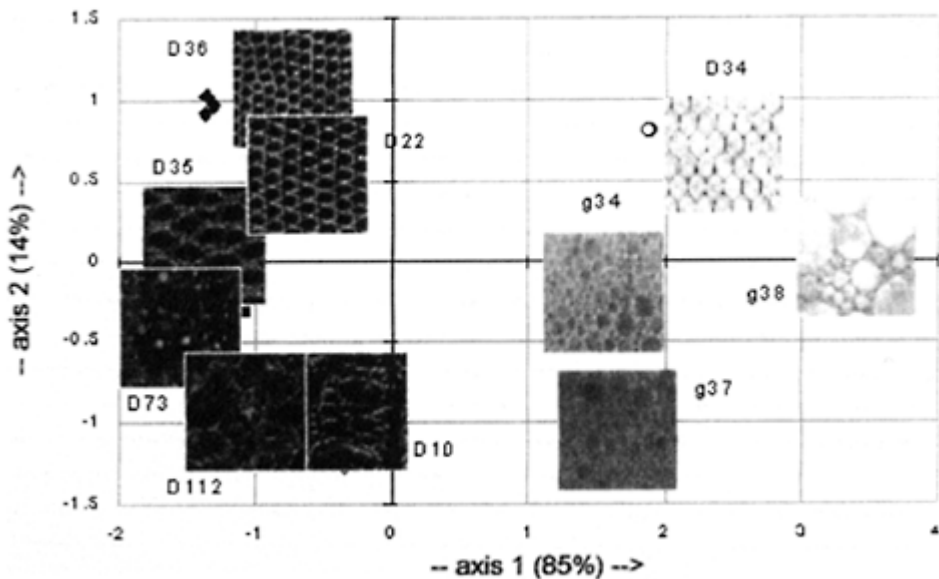


**Figure 2.15** Reference textures [Dxx from Brodatz (1966), gxx=experimental foams] for training.

Still, one may easily imagine more progresses in the years to come. Indeed, if, along life's evolution on Earth, several kinds of vision systems—eyespots, ocelli, compound eyes, camera-like eyes, among others—were retained following the implacable sieve of natural selection for millions of years, there will certainly be advantages and drawbacks in each vision system mother nature has finally adopted.

This line of research has not been deeply exploited so far, since the advantages of each vision system are not fully understood yet.

The mammalian vision system is organised in such a way that different image properties are processed in different brain areas (Kandel, Schwartz and Jessel, 1995). Since the neuronal responses are distributed among different cortex levels, neuroscience is currently investigating how the distinct levels relate themselves and interact to achieve the perceptual construction of an object. This is the well-known binding problem. Nowadays it is universally accepted that image perception in mammals comes from a sophisticated parallel processing of information. It is thus natural that parallel processing will also be a fertile field of research for new developments in image analysis (Leondes, 1998).

We may therefore conclude that Image Analysis will develop even further in the near future.

## REFERENCES

- Amanullah, A., Blair, R., Nienow, A.W. and Thomas C.R. (1999) Effects of Agitation Intensity on Mycelial Morphology and Protein-Production in Chemostat Cultures of Recombinant *Aspergillus-Oryzae*. *Biotechnology and Bioengineering*, **62**, 4, 434–446.
- Amaral, A.L., Baptiste, C., Pons, M.N., Nicolau, A., Lima, N., Ferreira, E.C., Mota, M. and Vivier H. (1999) Semiautomated Recognition of Protozoa by Image-Analysis. *Biotechnology Techniques*, **13**, 2, 111–118.
- Atenas, M., Clark, M. and Lazarova V. (1998) Characterization of bubbles in a rectangular air-lift bioreactor. *Particle and Particle Systems Characterization*, **15**, 191–199.
- Barciela, J. and Vieitez A.M. (1993) Anatomical Sequence and Morphometric Analysis During Somatic Embryogenesis on Cultured Cotyledon Expiants of *Camellia-Japonica L.* *Annals of Botany*, **71**, 5, 395–404.
- Bavarian, F., Fan, L.S. and Chalmers J.J. (1991) Microscopic visualization of insect cell-bubble interactions. I. Rising bubbles, air-medium interface and the foam layer. *Biotechnology Progress*, **7**, 140–150.
- Bellouti, M., Alves, M., Novais, J.M. and Mota M. (1997) Floes versus Granules: Differentiation by Fractal Dimension. *Water Research*, **31**, 5, 1227–1231.
- Benkrid, K. (1999) Etude globale et locale de l'hydrodynamique des écoulements gaz-liquide dans les réacteurs à lit fixe, PhD thesis, INPL, Nancy, France.
- Bittner, C., Wehnert, C. and Schepers T. (1998) In Situ Microscopy for On-line Determination of Biomass. *Biotechnology and Bioengineering*, **60**, 1, 24–35.
- Bonarius, H.P.J., Nielsen, N.P.V. and Kongerslev, L. Optimal Image-Analysis Software for Rapid and Reliable of Cultured-Mammalian-Cells. In *Abstracts of Papers of the American Chemical Society*, pp. 206-BIOT. Washington: American Chemical Society.
- Bouaifi, M. and Roustan M. (1998) Bubble size and mass transfer coefficients in dual-impeller agitated reactors. *Canadian Journal of Chemical Engineering*, **76**, 390–397.
- Boulton-Stone, J.M. and Blake J.R. (1993) Bursting bubbles at a free-surface. *Proc. 3rd Int. Conf. Bioreactor and Bioprocess Fluid Dynamics*, A.W. Nienow Ed., 163–173, London: MEP Ltd.
- Brodatz, P. (1966) *Textures*, New York: Dover Publications.
- Bujalski, W., Takenaka, K., Paolini, S., Jahoda, M., Paglianti, A., Takahashi, K., Nienow, A.W. and Etchells A.W. (1999) Suspension and liquid homogenization in high solids concentration stirred chemical reactors. *Transactions of the Institution of Chemical Engineers*, Part A, **77**, 241–247.
- Calderbank, P.H. (1958) The interfacial area in gas-liquid contacting with mechanical agitation. *Transactions of the Institution of Chemical Engineers*, **36**, 443–463.
- Cazzulino, D., Pedersen, H. and Chin C.-K. 1991, Bioreactors and Image Analysis for Scale-Up and Plant Propagation. In *Cell Culture and Somatic Cell*, vol. 8, pp. 147–177. San Diego: Academic Press.
- Chalmers, J.J. and Bavarian F. (1991) Microscopic visualization of insect cell-bubble interactions. II: the bubble film and bubble rupture. *Biotechnology Progress*, **7**, 151–158.
- Chaouki, J., Larachi, F. and Dudukovic M.P. (1997) Noninvasive tomographic and velocimetric monitoring of multiphase flows. *Industrial and Engineering Chemistry Research*, **36**, 4476–4503.
- Chi, C.M., Zhang, C., Staba, E.J., Cooke, T.J. and Hu W.S. (1996) An Advanced Image-Analysis System for Evaluation of Somatic Embryo Development. *Biotechnology and Bioengineering*, **50**, 1, 65–72.
- Choi, D.B., Park, E.Y. and Okabe M. (1998) Improvement of Tylosin Production from *Streptomyces-Fradiae* Culture by Decreasing the Apparent Viscosity in an Airlift Bioreactor. *Journal of Fermentation and Bioengineering*, **86**, 4, 413–417.

- Connors, R.W. (1980) A theoretical comparison of texture algorithms. *IEEE Transactions on Pattern Analysis and Machine Intelligence*, **3**, 204–222.
- Costello, P.J. and Monk P.R. (1985) Image Analysis Method for the Rapid Counting of *Saccharomyces cerevisiae* Cells. *Applied and Environmental Microbiology*, **49**, 4, 863–866.
- Cowger, N.L., O'Connor, K.C., Hammond, T.C., Lacks, D.J. and Navar C.L. (1999) Characterization of Bimodal Cell Death of Insect Cells in a Rotating-Wall Vessel and Shaker Flask. *Biotechnology and Bioengineering*, **64**, 1, 14–26.
- Cox, P.W. and Thomas C.R. (1992) Classification and Measurement of Fungal Pellets by Automated Image Analysis. *Biotechnology and Bioengineering*, **39**, 9, 945–952.
- Cox, P.W. and Thomas C.R. (1999) Assessment of the Activity of Filamentous Fungi Using *Mag fura*. *Mycological Research*, **103**, 6, 757–763.
- de Swart, J.W.A., van Vliet, R.E. and Krishna R. (1996) Size, structure and dynamics of “large” bubbles in a two-dimensional slurry bubble column. *Chemical Engineering Science*, **51**, 4619–4629.
- DiBiasio, D., Scott, J., Harris, P. and Moore S. (1993) The relationship between fluid flow and cell growth in hollow-fiber bioreactors: applications of magnetic resonance imaging. *Proc. 3rd Int. Conf. Bioreactor and Bioprocess Fluid Dynamics*, A.W. Nienow Ed., 457–471, London: MEP Ltd.
- Doran P. (1999) Design of mixing systems for plant cell suspensions in stirred reactors. *Biotechnology Progress*, **15**, 319–335.
- Drouin, J.F., Louvel, L., Vanhoutte, B., Vivier, H., Pons, M.N. and Germain P. (1997) Quantitative Characterization of Cellular Differentiation of Streptomyces ambofaciens in Submerged Culture by Image Analysis. *Biotechnology Techniques*, **11**, 11, 819–824.
- Dubuisson, M.P., Jain, A.K. and Jain M.K. (1994) Segmentation and Classification of Bacterial Culture Images. *Journal of Microbiological Methods*, **19**, 4, 279–295.
- Dudley, B.T., Howgrave-Graham, A.R., Bruton, A.C. and Wallis P.M. (1993) Image Analysis to Quantify and Measure UASB Digester Granules. *Biotechnology and Bio engineering*, **42**, 3, 279–283.
- Durant, C., Cox, P.W., Formisyn, P. and Thomas C.R. (1994) Improved Image Analysis Algorithm for the Characterization of Mycelial Aggregates after Staining. *Biotechnology Techniques*, **8**, 11, 759–764.
- Durant, G., Crawley, G. and Formisyn P. (1994) A Simple Staining Procedure for the Characterisation of Basidiomycetes Pellets by Image Analysis. *Biotechnology Techniques*, **8**, 6, 395–400.
- Einax, J.W., Zwanziger, H.W. and Geiss S. (1997) *Chemometrics in Environmental Analysis*, Weinheim: VCH.
- Galindo, E. and Nienow A.W. (1992) Mixing of highly viscous xanthan fermentation broths with Lightnin A315 impeller. *Biotechnology Progress*, **8**, 233–239.
- Galindo, E. and Nienow A.W. (1993) Performance of the SCAB A SRGT agitator in mixing of simulated xanthan gum broths. *Chemical Engineering and Technology*, **16**, 102–108.
- Garcia-Briones, M.A. and Chalmers J.J. (1993) Analysis of hydrodynamic information obtained from computer solutions of the rupture of a gas bubble in relation to animal cell damage in sparged bioreactors. *Proc. 3rd Int. Conf. Bioreactor and Bioprocess Fluid Dynamics*, A.W. Nienow Ed., 191–210, London: MEP Ltd.
- Gobal, M. and Jepson W. (1997) Development of digital image analysis techniques for the study of velocity and void profiles in slug flow. *International Journal of Multiphase Flow*, **23**, 945–965.
- Godfrey, L., Larachi, F., Kennedy, G., Grandjean, B.P.A. and Chaouki J. (1997) On-line flow visualization in multiphase reactors using neural networks. *Applied Radiation and Isotopes*, **48**, 225–235.
- Grijnspeerdt, K. and Verstraete W. (1997) Image Analysis to Estimate the Settleability and Concentration of Activated Sludge. *Water Research*, **31**, 5, 1126–1134.

- Guterman, H. and Shabtai Y. (1996) A Self-Tuning Vision System for Monitoring Biotechnological Processes. I. Application to Production of Pullulan by *Aureobasidium pullulans*. *Biotechnology and Bioengineering*, **51**, 501–510.
- Haralick R.M. (1979) Statistical and structural approaches to texture. *Proceedings of the IEEE*, **67**, 786–804.
- Hari-Prajitno D., Mishra V.P., Takenaka, K., Bujalski, W., Nienow, A.W. and McKemee J. (1998) Gas-liquid mixing studies with multiple up- and down-pumping hydrofoil impellers: power characteristics and mixing time. *Canadian Journal of Chemical Engineering*, **76**, 1056–1068.
- Harrell, R.C., Bieniek, M. and Cantliffe D.J. (1992) Noninvasive Evaluation of Somatic Embryogenesis. *Biotechnology and Bioengineering*, **39**, 4, 378–383.
- Higashiyama, K., Fujikawa, S., Park, E.Y. and Okabe M. (1999) Image Analysis of Morphological Change During Arachidonic Acid Production by *Mortierella alpina* 1S-4. *Journal of Bioscience and Bioengineering*, **87**, 4, 489–494.
- Hirano, T. (1990) Method for Measuring the Budding Index of Yeast Using an Image Processor. *ASBC Journal*, **48**, 2, 79–81.
- Holden, P.J., Wang, M., Mann, R., Pickin, F.J. and Edwards R.B. (1998) Imaging stirred-vessel macromixing using electrical resistance tomography. *AIChE Journal*, **44**, 780–790.
- Honda, H., Ito, T., Yamada, J., Hanai, T., Matsuoka, M. and Kobayashi T. (1999) Selection of Embryogénie Sugarcane Callus by Image Analysis. *Journal of Bioscience and Bioengineering*, **87**, 5, 700–702.
- Houcine, I., Vivier, H., Plasari, E., David, R. and Villermaux J. (1996) Planar laser induced fluorescence technique for measurements of concentration fields in continuous stirred tank reactors. *Experiments in Fluids*, **22**, 95–102.
- Hsieh, C.C., Wang, S.B. and Pan C. (1997) Dynamic visualization of two-phase flow patterns in a natural circulation loop. *International Journal of Multiphase Flow*, **6**, 1147–1170.
- Jenkins, D., Richard, M.C. and Daigger C.T. (1993) *Manual on the Causes and Control of Activated Sludge Bulking and Foaming*, 2nd edn. Chelsea: Lewis Publishers.
- Jüsten, P., Paul, C.C., Nienow, A.W. and Thomas C.R. (1996) Dependence of Mycelial Morphology on Impeller Type and Agitation Intensity. *Biotechnology and Bioengineering*, **52**, 6, 672–684.
- Kamilakis, E.G. and Allen D.G. (1995) Cultivating Filamentous Microorganisms in a Cyclone Bioreactor—The Influence of Pumping on Cell Morphology. *Process Biochemistry*
- Kandel, E.R., Schwartz, J.H. and Jessel T.M. (1995) *Essentials of Neural Science and Behaviour*, New Jersey: Prentice-Hall.
- Kaneshiro, E.S., Wyder, M.A., Wu, Y.P. and Cushion M.T. (1993) Reliability of Calcein Acetoxy Methyl-Ester and Ethidium Homodimer or Propidium Iodide for Viability Assessment of Microbes. *Journal of Microbiological Methods*, **17**, 1, 1–16.
- Kawaharasaki, M., Tanaka, H., Kanagawa, T. and Nakamura K. (1998) In Situ Identification of Polyphosphate-Accumulating bacteria in Activated Sludge by Dual Staining with rRNA-targeted Oligonucleotide Probes and 4,6-Diamidino-2-Phenylindol (DAPI) at a Polyphosphate-Probing Concentration. *Water Research*, **33**, 1, 527–265.
- Kieran, P.M., Malone, D.M. and Macloughlin P.P. (1993) Variation of Aggregate Size in Plant-Cell Suspension Batch and Semicontinuous Cultures. *Food and Bioproducts Processing*, **71**, Cl, 40–46.
- Kieran, P.M., Odonnell, H.J., Malone, D.M. and Macloughlin P.F. (1995) Fluid Shear Effects on Suspension-Cultures of Morinda-Citrifolia. *Biotechnology and Bioengineering*, **45**, 5, 415–425.
- Konstantinov, K., Chuppa, S., Sajan, E., Tsai, Y., Yoon, S. and Golini F. (1994) Real-time Biomass-concentration monitoring in Animal-cell Cultures. *Trends in Biotechnology*, **12**, 324–333.
- Kuehn, M., Hausner, M., Bungartz, H.J., Wagner, M., Wilderer, P.A. and Wuertz S. (1998) Automated Confocal Laser Scanning Microscopy and Semiautomated Image Processing for Analysis of Biofilms. *Applied and Environmental Microbiology*, **64**, 11, 4115–4127.

- Kumar, S.B. and Dudukovic M.P. (1997) Computer-assisted gamma and X-ray tomography: application to multiphase flow. In *Non-invasive Monitoring of Multiphase Flows*. Chaouki, J., Larachi, F., Dudukovic, M.P., Eds., Amsterdam: Elsevier.
- Lawrence, J.R., Nie, T.R. and Swerhone C.D.W. (1998) Application of Multiple Parameter Imaging for the Quantification of Algal, Bacterial and Exopolymer Components of Microbial Biofilms. *Journal of Microbiological Methods*, **32**, 3, 253–261.
- Lee, J.C., Salih, M.A., Sebai, N.N. and Withey A. (1993) Control of foam in bioreactors—action of antifoams. *Proc. 3rd Int. Conf. Bioreactor and Bioprocess Fluid Dynamics*, A.W.Nienow Ed., 275–287, London: MEP Ltd.
- Lee, N., Nielsen, P.H., Andreasen, K.H., Juretschko, S., Nielsen, J.L., Schleifer, K.H. and Wagner M. (1999) Combination of Fluorescent in-Situ Hybridization and Microautoradiography—A New Tool for Structure-Function Analyses in Microbial Ecology. *Applied and Environmental Microbiology*, **65**, 3, 1289–1297.
- Leondes, C.T. (1993) *Image Processing and Pattern Recognition*, San Diego: Academic Press.
- Li, H.Z., Mouline, Y., Choplis, L. and Midoux N. (1997) Chaotic bubble coalescence in nonnewtonian fluids. *International Journal of Multiphase Flow*, **23**, 713–723.
- Li, L. and Wei J. (1999) Three-dimensional image analysis of mixing in stirred vessels. *AIChE Journal*, **45**, 1855–1865.
- Logothetis, N.K. (1999) Vision: A Window on Consciousness, *Scientific American*, **281**, 5, 45–51.
- Lumley, D.J. and Horkeby, C. (1989) Retention time distribution of sludge in rectangular secondary settlers. *Water Science and Technology*, **21**, 1763–1766.
- Madoni, P. (1994) A Sludge Biotic Index (Sbi) for the Evaluation of the Biological Performance of Activated-Sludge Plants Based on the Microfauna Analysis. *Water Research*, **28**, 1, 67–75.
- Makagiansar, H.Y., Ayazi Shamlou, P., Thomas, C.R. and Lilly M.D. (1993) The Influence of Mechanical Forces on the Morphology and Penicillin Production of *Pénicillium chrysogenum*. *Bioprocess Engineering*, **9**, 83–90.
- Margaritis, A., te Bokkel D.W. and Karamanov D.C. (1999) Bubble rise velocities and drag coefficients in non-newtonian polysaccharide solutions. *Biotechnology and Bioengineering*, **64**, 257–266.
- Maruhashi, F., Murakami, S. and Baba K. (1994) Automated Monitoring of Cell Concentration and Viability Using an Image-Analysis System. *Cytotechnology*, **15**, 1–3, 281–289.
- McCarthy, A.A., O'Shea, D.G., Murray, N.T., Walsh, P.K. and Foley G. (1998) Effect of Cell Morphology on Dead-End Filtration of the Dimorphic Yeast Kluyveromyces-Marxianus Var. Marxianus NRRLy2415. *Biotechnology Progress*, **14**, 2, 279–285.
- McIntyre, M. and McNeil B. (1997a) Dissolved Carbon-Dioxide Effects on Morphology, Growth, and Citrate Production in Aspergillus-Niger A60. *Enzyme and Microbiology Technology*, **20**, 2, 135–142.
- McIntyre, M. and McNeil B. (1997b) Effect of Carbon-Dioxide on Morphology and Product Synthesis in Chemostat Cultures of Aspergillus-Niger A60. *Enzyme and Microbiology Technology*, **21**, 7, 479–83.
- Moolman, D.W., Aldrich, C, Van Deventer, J.S.J. and Stange W.W. (1994) Digital image processing as a tool for on-line monitoring of froth in flotation froths. *Minerals Engineering*, **7**, 9, 1149–1164.
- Moravec, H. (1999) Rise of Robots. *Scientific American*, **281**, 6, 86–93.
- Mouline, Y. (1996) Dynamique des bulles de gaz dans les fluides rhéologiquement complexes, PhD thesis, INPL, Nancy, France.
- Nielsen, J. and Krabben P. (1995) Hyphal Growth and Fragmentation of Penicillium-Chrysogenum in Submerged Cultures. *Biotechnology and Bioengineering*, **46**, 6, 588–598.
- Nielsen, J. (1996) Modeling the Morphology of Filamentous Microorganisms. *Trends in Biotechnology*, **14**, 11, 438–443.

- Nielsen, J., Johansen, C.L., Jacobsen, M., Krabben, P. and Villadsen J. (1995) Pellet Formation and Fragmentation in Submerged Cultures of *Penicillium-Chrysogenum* and Its Relation to Penicillin Production. *Biotechnology Progress*, **11**, 1, 93–98.
- Nielsen, P.H., Andreasen, K., Lee, N. and Wagner M. (1999) Use of Microautoradiography and Fluorescent in situ Hybridization for Characterization of Microbial Activity in Activated Sludge. *Water Science and Technology*, **39**, 1, 1–9.
- Olsvik, E., Tucker, K.G., Thomas C.R. and Kristiansen, B. (1993) Correlation of *Aspergillus niger* Broth Rheological Properties with Biomass Concentration and the Shape of Mycelial Aggregates. *Biotechnology and Bioengineering*, **42**, 9, 1046–1052.
- O’Shea, D.G. and Walsh P.K. (1996) Morphological Characterization of the Dimorphic Yeast Kluyveromyces-Marxianus Var Marxianus Nrrly2415 by Semiautomated Image-Analysis. *Biotechnology and Bioengineering*, **51**, 6, 679–690.
- Pandit, A.B., Dodd, P.W. and Davidson J.F. (1993) The effect of immersed tubes on bubble size in an air-lift fermenter. *Proc. 3rd Int. Conf. Bioreactor and Bioprocess Fluid Dynamics*, A.W.Nienow Ed., 213–232, London: MEP Ltd.
- Paul, C.C., Kent, C.A. and Thomas C.R. (1994) Image-Analysis for Characterizing Differentiation of *Penicillium chrysogenum*. *Transactions of the Institution of Chemical Engineers, Part C*, **72**, 2, 95–105.
- Perrier-Cornet, J.-M., Maréchal, P.-A. and Gervais P. (1995) A New Design Intended to Relate High Pressure Treatment to Yeast Cell Mass Transfer. *Journal of Biotechnology*, **41**, 49–58.
- Pichon, D., Vivier, H. and Pons M.N. (1992a) Growth Monitoring of Mammalian Cells on Microcarriers by Image Analysis. In *Modeling and Control of Biotechnical Processes*, edited by M.Nazmul Karim, C.Stephanopoulos, pp. 311- 314. Oxford: Pergamon Press.
- Pichon, D., Vivier, H. and Pons M.N. (1992b) Growth Monitoring of Filamentous Microorganisms by Image Analysis. In *Modeling and Control of Biotechnical Processes*, edited by M.Nazmul Karim, G.Stephanopoulos, pp. 307–310. Oxford: Pergamon Press.
- Pitiot, P., Falk, L. and Vivier H. (1998) Caractérisation, par trajectographie tridimensionnelle, du mélange dans un réacteur agité ouvert. *Récents Progrès en Génie des Procédés*, **12**, 61, 103–108.
- Pons, M.N., Drouin, J.F., Louvel, L., Vanhoutte, B., Vivier, H. and Germain P. (1998) Physiological Investigations by Image-Analysis. *Journal of Biotechnology*, **65**, 1, 3–14.
- Pons, M.N., Vivier, H., Rémy, J.F. and Dodds J.A. (1993) Morphological Characterization of Yeast by Image Analysis. *Biotechnology and Bioengineering*, **42**, 1352–1359.
- Pons, M.N., Wagner, A., Vivier, H. and Marc A. (1992) Application of Quantitative Image Analysis to a Mammalian Cell Line Grown on Microcarriers. *Biotechnology and Bioengineering*, **40**, 1, 187–193.
- Pons, M.N., Vivier, H., Belaroui, K., Bernard-Michel, B., Cordier, F., Oulhana, D. and Dodds J.A. (1999) Particle morphology: from visualisation to measurement. *Powder Technology*, **103**, 44–57.
- Priede, M.A., Vanags, J.J., Viesturs, U.E., Tucker, K.G., Bujalski, W. and Thomas C.R. (1995) Hydrodynamic, Physiological, and Morphological Characteristics of *Fusarium moniliforme* in Geometrically Dissimilar Stirred Bioreactors. *Biotechnology and Bioengineering*, **48**, 3, 266–277.
- Rayleigh, J.W. (1891) Some applications of photography, *Nature*, **44**, 249–254.
- Reichl, U, King, R. and Gilles E.D. (1992) Characterization of Pellet Morphology During Submerged Growth of *Streptomyces tendae* by Image Analysis. *Biotechnology and Bioengineering*, **39**, 2, 164–170.
- Reinecke, N., Petritsch, G., Boddem, M. and Mewes D. (1998) Tomographic imaging of the phase distribution in two-phase slug flow. *International Journal of Multiphase Flow*, **24**, 617–634.
- Ren, J., Reid, J.F. and Litchfield J.B. (1994) Knowledge-based Supervision and Control of Bioprocess with a Machine Vision-based Sensing System. *Journal of Biotechnology*, **36**, 1, 25–34.

- Ruaan, R.C., Tsai, G.J. and Tsao C.T. (1993) Monitoring and Modeling Density-Dependent Growth of Anchorage-Dependent Cells. *Biotechnology and Bioengineering*, **41**, 3, 380–389.
- Ryoo, D. (1999) Fungal Fractal Morphology of Pellet Formation in *Aspergillus niger*. *Biotechnology Techniques*, **13**, 1, 33–36.
- Sardonini, C.A. and DiBiaso D. (1993) Growth of animal cells around hollow fibers—Multifiber studies. *AICHE Journal*, **39**, 1415–1419.
- Sarker, D.K., Bertrand, D., Chtioui, Y. and Popineau Y. (1998) Characterisation of foam properties using image analysis. *Journal of Texture Studies*, **29**, 15–42.
- Schaflinger, U., Acrivos, A. and Zhang K. (1990) Viscous resuspension of a sediment within a laminar and stratified flow. *International Journal of Multiphase Flow*, **16**, 567–578.
- Schmidt, J. and Lübbert A. (1993). Detailed investigation of the mass transfer between bubbles and the continuous liquid phase. *Proc. 3rd Int. Conf. Bioreactor and Bioprocess Fluid Dynamics*, A.W.Nienow Ed., 231–239, London: MEP Ltd.
- Sebastine, I.M., Stocks, S.M., Cox, P.W. and Thomas C.R. (1999) Characterisation of Percentage Viability of *Streptomyces clavuligerus* Using Image Analysis. *Biotechnology Techniques*, **13**, 419–423.
- Sekiguchi, Y., Kamagata, Y., Nakamura, K., Ohashi, A. and Harada H. (1999) Fluorescence in-Situ Hybridization Using 16S Ribosomal-RNA-Targeted Oligonucleotides Reveals Localization of Methanogens and Selected Uncultured Bacteria in Mesophilic and Thermophilic Sludge Granules. *Applied and Environmental Microbiology*, **65**, 3, 1280–1288.
- Semmens, M.J., Gulliver, J.S. and Anderson A. (1999) An analysis of bubble formation using microporous hollow fiber membranes. *Water Environment Research*, **71**, 307–315.
- Singh, A., Pyle, B.H. and McFeters C.A. (1989) Rapid Enumeration of Viable Bacteria by Image Analysis. *Journal of Microbiological Methods*, **10**, 91–101.
- Smith, M.A.L., Reid, J.F., Hansen, A.C. and Madhavi D.L. (1995) Non-destructive Machine Vision Analysis of Pigment-Producing Cell Cultures. *Journal of Biotechnology*, **40**, 1–11.
- Suhr, H., Wehnert, G., Schneider, K., Geissler, P., Jahne, B. and Scheper T. (1995) In Situ Microscopy for On-line Characterization of Cell-Populations in Bioreactors, Including Cell-Concentration Measurements by Depth from Focus. *Biotechnology and Bioengineering*, **47**, 106–116.
- Swope, K.L. and Flicklinger M.C. (1996) The Use of Confocal Scanning Laser Microscopy and Other Tools to Characterize Escherichia-Coli in a High-Cell-Density Synthetic Biofilm. *Biotechnology and Bioengineering*, **52**, 2, 340–356.
- Takahashi, K. and Nienow A.W. (1988) Bubble sizes, gas hold-up and coalescence rates in aerated vessels agitated by a Rushton turbine: spatial variations. *Proc. 6th European Conf. On Mixing*, 285–293, Pavia, Italy.
- Tamura, S., Park, Y., Toriyama, M. and Okabe M. (1997) Change of Mycelial Morphology in Tylosin Production by Batch Culture of *Streptomyces-Fradiae* Under Various Shear Conditions. *Journal of Fermentation and Bioengineering*, **83**, 6, 523–528.
- Tan, W.S., Chen, Y.L. and Dai G.C. (1993) Growth and damage of continuous suspension cultured hybrydoma cells (2F7) in an agitated bioreactor with and without bubble entrainment or sparging. *Proc. 3rd Int. Conf. Bioreactor and Bioprocess Fluid Dynamics*, A.W. Nienow Ed., 153–161, London: MEP Ltd.
- Tatterson, G.B. (1991) Fluid mixing and gas dispersion in agitated tanks, New York: McGraw Hill.
- Thomas, C.R. (1992) Image-Analysis—Putting Filamentous Microorganisms in the Picture. *Trends in Biotechnology*, **10**, 10, 343–348.
- Treskatis, S.-K., Orgeldinger, V., Wolf, H. and Gilles E.D. (1997) Morphological Characterization of Filamentous Microorganisms in Submerged Cultures by On-Line Digital Image Analysis and Pattern Recognition. *Biotechnology and Bioengineering*, **53**, 2, 191–201.
- Tucker, K.C. and Thomas C.R. (1993) Effect of Biomass Concentration and Morphology on the Rheological Parameters of *Pénicillium chrysogenum* Fermentation Broths. *Transactions of the Institution of Chemical Engineers, Part C*, **71**, June, 111–117.

- Tucker, K.C., Chalder, S., Alrubeai, M. and Thomas C.R. (1994) Measurement of Hybridoma Cell Number, Viability, and Morphology Using Fully Automated Image-Analysis. *Enzyme and Microbial Technology*, **16**, 1, 29–35.
- Tucker, K.C., Kelly, T., Delgrazia, P. and Thomas C.R. (1992) Fully-Automatic Measurement of Mycelial Morphology by Image Analysis. *Biotechnology Progress*, **8**, 4, 353–359.
- Uozumi, N., Yoshino, T., Shiotani, S., Suehara, K.I., Arai, F., Fukuda, T. and Kobayashi T. (1993) Application of Image Analysis with Neural Network for Plant Somatic Embryo Culture. *Journal of Fermentation and Bioengineering*, **76**, 6, 505–509.
- Vanhoutte, B., Pons, M.N., Thomas, C.R., Louvel, L. and Vivier H. (1995) Characterization of *Pénicillium chrysogenum* Physiology in Submerged Cultures by Color and Monochrome Image Analysis. *Biotechnology and Bioengineering*, **48**, 1–11.
- Venkat, R.V., Brodkey R.S., Guezennec, Y.C. and Chalmers J.J. (1993) Experimental determination of local hydrodynamic information in microcarrier culture spinner vessels. *Proc. 3rd Int. Conf. Bioreactor and Bioprocess Fluid Dynamics*, A.W. Nienow Ed., 483–501, London: MEP Ltd.
- Vicente, A., Meinders, J.M. and Teixeira J.A. (1996) Sizing and Counting of *Saccharomyces cerevisiae* Floe Populations by Image Analysis, Using an Automatically Calculated Threshold. *Biotechnology and Bioengineering*, **51**, 6, 673–678.
- Walsby, A.E. and Avery, A. (1996) Measurement of Filamentous Cyanobacteria by Image Analysis. *Journal of Microbiological Methods*, **26**, 11–20.
- Walsh, P.K., Isdell, F.V., Noone, S.M., Odonovan, M.C. and Malone D.M. (1996) Growth-Patterns of *Saccharomyces-Cerevisiae* Microcolonies in Alginate and Carrageenan Gel Particles—Effect of Physical and Chemical-Properties of Gels. *Enzyme and Microbial Technology*, **18**, 5, 366–372.
- Wierzba, A., Reichl, U., Turner, R.F.B., Warren, R.A.J. and Kilburn D.C. (1995) Adhesion of Mammalian Cells to a Recombinant Attachment Factor, CBD/RGD, Analyzed by Image Analysis. *Biotechnology and Bioengineering*, **46**, 185–193.
- Wittmer, S., Vivier, H., Falk, L. and Villermaux J. (1995) Three-dimensional long-term particle tracking in a stirred tank. *Proc. 7th Int. Symposium on Flow Visualisation*, 623–633.
- Yamashita, Y., Kuwashima, M., Nonaka, T. and Suzuki M. (1993) On-line Measurement of Cell Size Distribution and Concentration of Yeast by Image Processing. *Journal of Chemical Engineering of Japan*, **26**, 6, 615–619.
- Yang, Y.K., Morikawa, M., Shimizu, H., Shioya, S., Suga, K.I., Nihira, T. and Yamada Y. (1996) Image Analysis of Mycelial Morphology in Virginiamycin Production by Batch Culture of *Streptomyces virginiae*. *Journal of Fermentation and Bioengineering*, **81**, 1, 7–12.
- Zalewski, K. and Buchholz R. (1996) Morphological Analysis of Yeast Cells Using an Automated Image Processing System. *Journal of Biotechnology*, **48**, 43–49.

# CHAPTER THREE

## NEW METHODOLOGIES FOR

### MULTIPHASE BIOREACTORS 3: DATA ACQUISITION, MODELLING AND CONTROL

SEBASTIÃO FEYO DE AZEVEDO<sup>1</sup>, RUI OLIVEIRA<sup>1</sup> AND  
BERNHARD SONNLEITNER<sup>2</sup>

<sup>1</sup>*Department of Chemical Engineering, Faculty of Engineering,  
Universidade do Porto, Rua Dr. Roberta Frias, 4200–465, Porto,  
Portugal*

<sup>2</sup>*Department of Chemistry, Zurich University of Applied Sciences, P.O.  
Box 805, CH-8401 Winterthur, Switzerland*

#### ABSTRACT

This chapter addresses several research topics concerning multiphase bioreactor operation, related to process monitoring, modelling and control. Latest advances in measurement and estimation techniques are reported, namely concerning non-invasive techniques, biosensors and on-line inferential methods for biological properties. Modelling methodologies are reviewed, focusing on hybrid modular solutions for knowledge integration. Issues concerning aspects of bioprocess automation and control are finally addressed. From classical and optimal open loop control to recent trends towards on-line optimising control, some solutions are discussed in terms of their potential industrial utilisation. Globally the paper emphasises the need for an integrated modular approach for process operation, requiring a co-operative work between all factors producing knowledge, i.e. scientists, process operators and technologists.

**Keywords:** bioreactors, instrumentation, monitoring, modelling, control

#### INTRODUCTION

Bioreactors are sterile containers in which biological reactions are performed under well monitored and controlled conditions. They are stepping-stones to achieve bioengineering objectives, namely 1) for the preparative production of products and 2) as a powerful tool for scientific research in many biological disciplines.

The domain of bioengineering, generally regarded as a central stage in a production process, is today playing an increasingly important role in the *in vivo* investigation of living systems (mono-and, hopefully in the future, more and more mixed cultures). The

fact that an increasing number of physico-chemical environmental factors can be monitored (quantitatively) and controlled opens the gateway for the natural sciences to study complex biological systems, including populations of a single species or of many distinct species without destruction or disturbance, i.e. *in vivo* and non-invasive. Quantitative studies of biological mechanisms on a higher organisational level than the molecular one are, in this way, possible and this corresponds to a highly valuable supplementation, not a substitution, of knowledge. Such achievable information about the regulation of primary and secondary metabolism, sequence control of cell cycle, interspecies signalling or survival strategies of cells is essential as the scientific basis for an economical and ecological optimisation of bioprocess operation and control.

Research topics in bioprocess operation and automation can be grouped in three main areas, viz.- 1) process monitoring; 2) process modelling; and 3) process control. These topics, which will be addressed in the present chapter, are sketched in Figure 3.1.

Modern bioprocesses are monitored by on-line sensing devices mounted either *in situ* or externally. Besides sensor probes, more and more analytical subsystems are being exploited to monitor the state of a bioprocess on-line and in real time.

What we can measure today routinely are operating and secondary variables such as the concentrations of metabolites, which fully depend on primary and operating variables. The cellular activities such as those of enzymes, DNA, RNA and other components are the primary variables determining the performance of microbial or cellular cultures. The development of specific analytical tools for measurement of these activities *in vivo* is therefore of essential importance in order to get direct analytical access to these primary variables.

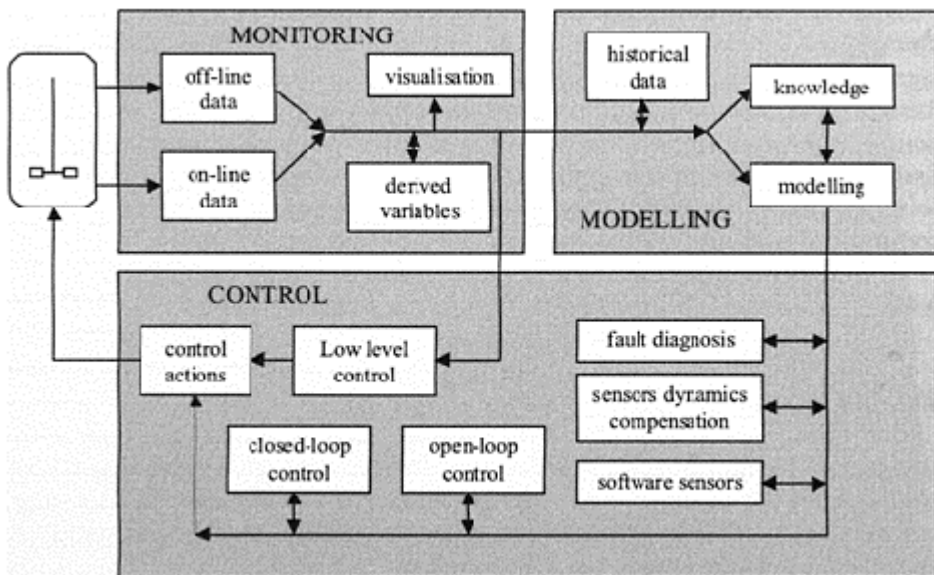


**Figure 3.1** Components in bioprocess monitoring and control.

In comparison to other disciplines such as physics or engineering, sensors useful for *in situ* monitoring of biotechnological processes are comparatively few and they measure physical and chemical variables rather than biological ones (Locher *et al.*, 1992). The reasons are manifold but, generally, biologically relevant variables are much more difficult and complex than others (e.g. temperature, pressure). Another important reason derives from restricting requirements, namely,

1. sterilisation procedures
2. stability and reliability over extended periods
3. application over an extended dynamic range
4. no interference with the sterile barrier
5. insensitivity towards protein adsorption and surface growth
6. resistance towards degradation or enzymatic break down.

Biomass concentration is of paramount importance both to scientists and engineers. It is a simple measure for the available quantity of a biocatalyst. It is definitely an important key variable because it determines—simplifying—the rates of growth and/or product formation. Almost all mathematical models used to describe growth or product formation contain biomass as a most important state variable. Many control strategies involve the objective of maximizing biomass concentration (though it remains to be discussed whether this is always wise).

The product is almost the only reason why a bioprocess is run. One is interested in maximising profit which depends directly on the concentration and/or volumetric productivity and/or on the purity of the product. It is therefore interesting to know these values. The classical methods to determine product concentrations are typically off-line laboratory methods and the above statements for substrate determinations are valid here, too.

The interest and pressure for developing new monitoring techniques, particularly non-invasive ones, come from both scientists and process engineers. The former aim mainly at a better understanding of physiology and its regulation. The latter search for robust and reliable forms of process operation in order to achieve high global quality: volumetric productivity, product purity and yield as well as high reproducibility.

More and more non-invasive techniques are invented and developed. Some are experimentally based, others are model based. Many of them are presently state of the art and not yet state of routine.

A binding link between measurement and control is modelling. Mechanistic (deterministic) models can promote the understanding of biological and physico-chemical process mechanisms. A sound and verified basis of experimental analysis is necessary to create this type of model. Very often they are not available. In many instances, only a few relevant variables are known (or measurable) and then simplified mechanistic models or black box-type models are employed. These simplified models, sometimes tailor-made, are useful in describing and predicting typical trajectories and patterns, and very importantly, in creating versatile and efficient control algorithms.

Modelling most effectively links theoretical and experimental knowledge, aiming at describing and improving the understanding of the process, namely,

- 1) the basic understanding of molecular or simply functional mechanisms of microbial and cellular physiology;

- 2) the relation between kinetics and dynamic behaviour of the bio-systems of interest; and
- 3) the behaviour of the physical systems in which the bio-processes take place.

A never-ending comment in bioprocess engineering is the following: “Due to the lack of appropriate monitoring techniques and due to the bad predictability of bioprocesses we need to...”. This is complemented by a final affirmative part which varies. It ranges from “...use fuzzy models and expert systems” over “...eliminate the anyhow too complex kinetics” to “...control the feed rate optimally”. Certainly, there is a large grain of truth in the first part of the statements. Those different closing comments indicate that there are no unique solutions. The issues related to measurement, modelling and control, of course, gives rise to many controversial discussions. Several of these issues will be discussed in the following sections of this paper.

## BIOREACTOR MONITORING

### Measuring Techniques

#### *pH*

pH is one of the variables often controlled in bioprocesses operated in bioreactors because enzymatic activities and, therefore, metabolism is very sensitive to pH changes. The acidification derives—in most cases—dominantly from the ammonia-uptake when ammonium ions are provided as nitrogen source: NHs is consumed and the proton left over from the  $\text{NH}_4^+$  contributes to the pH-drop.

pH of process suspensions is measured potentiometrically using electrodes filled with liquid or gel electrolytes. Glass electrodes develop a gel layer with mobile hydrogen ions when dipped into an aqueous solution. pH changes cause ion diffusion processes generating an electrode potential. Lithium rich glasses are well suited for this purpose. The potential is measured in comparison to a reference electrode which is usually a Ag/AgCl-system since kalomel would decompose during sterilisation (strictly speaking above 80°C). The electric circuit is closed via a diaphragm separating reference electrolyte from solution. Since the diaphragms are known to be prone to fouling, electrodes without diaphragm are currently under development.

#### *Pressure*

The direct dependence of micro-organisms on pressure changes is negligible provided they do not exceed many bars. But indirectly, the partial pressure of dissolved gases and their solubility is affected and must, therefore, be at least considered if not controlled. A data sampling frequency in the range of a few 100 ms is appropriate for direct digital pressure control (DDC) in laboratory scale bioreactors.

### **Oxygen**

Oxygen solubility is low in aqueous solutions, namely  $36 \text{ mg l}^{-1} \text{ bar}^{-1}$  at  $30^\circ\text{C}$  in pure water. Mass transfer is, therefore, determinant whether a culture suffers from oxygen limitation or not.

Several attempts to measure  $\text{pO}_2$  have been made in the past. Generally, oxygen is reduced by means of a cathode operated at a polarising potential of 600–750 mV which is generated either externally (polarographic method) or internally (galvanic method). A membrane separates the electrolyte from the medium to create some selectivity for diffusible substances rather than non-diffusible materials. The membrane is responsible for the dynamic sensor characteristics which are diffusion controlled.

Measurements of oxygen in the gas phase are based on its paramagnetic properties. Any change of the mass concentration of  $\text{O}_2$  affects the density of a magnetic field and thus the forces on any (dia- or para)magnetic material in this field. These forces on, for instance, an electro-balance, can be compensated electrically and the current can be converted into mass concentrations: further conversion into a molar ratio, e.g. %  $\text{O}_2$ , requires the knowledge of total pressure.

### **Carbon dioxide**

$\text{CO}_2$  affects microbial growth in various ways according to its appearance in catabolism as well as in anabolism. Morphological changes and variations of growth and metabolic rates in response to  $\text{pCO}_2$  have been demonstrated.

$\text{pCO}_2$  can be measured indirectly: the pH value of a bicarbonate buffer, separated from the medium by a gas-permeable membrane, drops whenever  $\text{CO}_2$  diffuses into this compartment and vice versa; pH depends on the logarithm of  $\text{pCO}_2$ . Either a glass electrode or optical principles can be used for pH determination.

$\text{CO}_2$  in the gas phase can be determined by means of its significant infrared absorbance at wave lengths  $\lambda < 15\mu\text{m}$ , particularly at  $4.3\mu\text{m}$ ; or by acoustic means. The integrated photoacoustic spectroscopy and magnetoacoustics (PAS/MA) technology for combined  $\text{CO}_2$  and  $\text{CO}$  analysis has a rapid response time and a small sample volume is sufficient. The acoustic methods are accurate, stable over long periods and very simple to use.

### **Redox potential**

Bioprocess media and culture liquids contain many different components which can exist in a reduced and an oxidised form as redox couples. The resulting redox potential, as measured by a redox electrode, is related to an “overall availability of electrons” rather than to a specific compound. The extracellular redox measurement is very instructive, specifically under micro aerobic conditions where the  $\text{pO}_2$  sensor signal becomes inaccurate. The signal generation is faster than that of  $\text{pO}_2$  because the diffusion step is omitted.

Redox potential is measured potentiometrically with electrodes made of noble metals (Pt, Au). The mechanical construction is similar to those of pH electrodes. Accordingly, the reference electrode must meet the same requirements.

### **Biomass**

Since an on-line generated signal for biomass concentration is decisive for control purposes a series of sensors and methods that can be automated have appeared in recent decades. Many of them rely on optical measuring principles, others exploit filtration characteristics, density changes of the suspension as a consequence of cells, or (di)electrical properties of suspended cells.

The nowadays commercially available OD-sensors are based on the determination of either transmission, reflection or scatter of light, or a combination thereof. The theoretical backgrounds why these OD measurements reflect the biomass concentration are rather manifold, complicated and would constrain the application tremendously if few simplifications could be reasonably applied. A direct *a priori* calculation of dry weight concentration from any OD measurement must not be expected as realistic, but the systems can be calibrated from case to case.

The measurement principle of the biomonitor (formerly called Bugmeter) relies on the fact that the capacitance of a suspension at low radio frequencies is correlated with the concentration of the suspended phase of fluid elements that are enclosed by a polarisable membrane, i.e. intact cells. The capacitance range covered is from 0.1 to 200 pF, the radio frequency some 200 kHz to 10 MHz. A severe limit to this principle is the maximally acceptable conductivity.

Bioreactions are exothermic. The net heat released during growth represents the sum of the many enzymatic reactions involved. A completely non-invasive method is to exploit the heat generated during growth and other metabolic activities of organisms which is also proportional to the amount of active cells in a reaction system (Boe and Lovrien, 1990). Under well defined conditions, calorimetry can be an excellent method for the estimation of total (active) biomass, even for such slow growing organisms as hybridoma cells or for anaerobic bacteria growing with an extremely low biomass yield. The method is so inherently sensitive that cell cycle dependent events can be analysed as well.

### **Interfacing to ex-situ measurements**

Samples removed from the reactor in some way can be analysed with devices that are not (yet) suitable or available to be mounted *in situ*, but this is a reasonable work-around. Depending on the analyte of interest, i.e. whether it is soluble or (in) the dispersed phase, one needs to sample either the entire culture liquid or just the supernatant. The latter can be acquired using, for instance, a filter. In this case, the filter is usually also the sterile barrier.

When the dispersed phase, usually but not necessarily the cells, is of interest, no separation of phases must take place during sampling. The system must be opened in a way that allows no infections to enter the reaction space neither during sampling nor between the sampling events.

Time of sampling is very critical. Cooling, heating, poisoning or separating phases may be a solution, but this cannot be generalised; it depends specifically on the actual intentions. If enzyme activities are to be determined, heating may be the worst choice, if just biomass-concentration is to be determined, immediate filtering may be the best choice.

### ***Flow injection analysis (FIA)***

FIA has been used for on-line determination of glucose or to estimate biomass directly or indirectly by means of an extended Kalman filter (Valero *et al.*, 1990). Chemical oxygen demand (COD) from a waste water stream was determined using an FIA in the range of 30 to 23,000 mg l<sup>-1</sup> within only 3 to 7 min. FIA is therefore useful in environmental sciences such as water monitoring and it is increasingly important in down stream processing. FIA has been applied to detect micro-organisms indirectly by measuring the concentration of a mediator which is reduced by the organisms. Amino acids, such as L-lysine were measured and even intracellular enzymes can be determined on-line. Rapid analyses of antibiotics have been realised by a combination of supracritical fluid extraction and FIA. DNA and RNA have been quantified in extracts. Metabolic studies of a lactic acid production based on glucose, lactose, galactose, lactate, and protein determinations after nutrient pulses were made. Also by-products such as acetate have been determined on-line with an FIA-technique. An important development is the combination with cytometry or the estimation of nucleic acids.

More and more are biosensors used as detectors in FIA-systems. The drawbacks of biosensors as direct *in situ* sensors, namely low dynamic range, inability to survive sterilisation, limited life time, etc. are no longer valid ex-situ because the FIA interfaces the biosensor which can be changed any time and the FIA can provide samples in optimal dilution. The need for chemicals and reagents can be drastically reduced when employing biosensors, in specific, when the entire system is miniaturised.

### ***Chromatography***

A review on chromatographic methods is beyond the scope of this contribution. Both, liquid chromatography (LC) and gas chromatography (GC) have been applied in numerous cases to off-line analyses of biotechnological samples but the on-line application is only recently developing.

The scope of chromatographic methods is the separation of the individual constituents of mixtures as they pass through columns filled with suitable stationary phases. The retention in the column is determined by the interaction between the individual constituents and the stationary phase. Miniaturised versions using micro machined instruments or array detectors have recently been reported. A filter as an interface is usually sufficient.

### ***Mass spectrometry***

MS has been applied mainly for the on-line detection and quantification of gases such as pO<sub>2</sub>, pCO<sub>2</sub>, pN<sub>2</sub>, pH<sub>2</sub>, pCH<sub>4</sub> and H<sub>2</sub>S or volatiles (alcohols, acetoin, butanediol). The

detection principle allows simultaneous monitoring and consequently control of important metabolites.

### ***Biosensors***

The rational for using biosensors is to combine the high specificity of biological components with the capabilities of electronic tools (i.e. “usual” sensors). Biosensors consist of a sensing biological module of either catalytic (e.g. enzymes, organism) or affinity reaction type (e.g. antibodies, cell receptors) in intimate contact with a physical transducer. The latter converts the chemical finally into an electric signal. Co-immobilisation of enzymes can be advantageous when compared to sequential operation. In general, the bio-part of the biosensor cannot be sterilised.

Electrochemical transducers work based on either an amperometric, potentiometric, or conductometric principle.

Optical biosensors typically consist of an optical fibre which is coated with the indicator chemistry for the material of interest at the distil tip. The quantity or concentration is derived from the intensity of absorbed, reflected, scattered, or re-emitted electromagnetic radiation (e.g. fluorescence, bio-and chemiluminescence). Usually, enzymatic reactions are exploited.

Another type of biosensors exploits the fact that enzymatic reactions are exothermic (5 to 100 kJ mol<sup>-1</sup>). The biogenic heat can be detected by thermistors or temperature sensitive semiconductor devices.

The piezo-electrical effect of deformations of quartz under alternating current (at frequency in the order of 10 MHz) is used by coating the crystal with a selectively binding substance, e.g. an antibody. When exposed to the antigen, the antibody-antigen complex will be formed on the surface and shift the resonance frequency of the crystal proportional to the mass increment which is some way, but not necessarily linearly proportional to the antigen concentration.

### ***Time aspects***

A notorious underestimation of the dynamic properties of microbial and cellular populations results from matching the duration of the respective batch cultivations to the relevant time constant of the biosystem under investigation. However, metabolic regulation of enzyme activities and fluxes often takes place in the time scale of seconds rather than days although the latter may be true as well.

The relaxation time concept of Harder and Roels (1982) maps typical time constants of microbial and cellular control on the level of modification of enzymes (activation, inhibition, dis/association of subunits, covalent modification or digestion) to the range of ms to s, on the level of regulation of gene expression (induction, repression or derepression of transcription) to min and on the level of population selection and evolution to d and larger units.

The dynamics of microbial cultures has important impacts on the characteristics of measurement and process control. The “typical time constant” in a bioprocess is often erroneously anticipated to be equivalent to the entire duration of a cultivation.

The quantitative investigation of substrate uptake requires a time resolution of several few 100 ms, otherwise, artifacts must result. One can stop glucose metabolism within 100 ms by spraying the cell suspension from the over-pressurized bioreactor into 60% methanol which was pre-chilled to -40°C. This procedure does not damage the integrity of the cells and the pre-treated sample remains liquid which is advantageous for further processing.

### ***Trends in sensor development***

Clearly, the development of reliable on-line estimation of intracellular components is a (the) major challenge for the future (e.g. Schuster, 1999 and other contributions in Sonnleitner, 1999).

### **Data Acquisition**

All stages in a data acquisition system are represented schematically in Figure 3.2. Transducers incorporated in measurement devices normally deliver a continuous electrical signal. This will generally undergo some form of conditioning (galvanic insulation, amplification, attenuation, etc.) depending on aspects related to transmission (continuous or digital transmission, distance of transmission, etc.). The final stage is normally local signal acquisition, corresponding to multiplexing, analog-to-digital conversion (ADC) and storage in the process computer or front-end-system. Data are stored in a computer in distinct time intervals resulting in discretisation with respect to time and concomitantly in a possible loss of information. A data reduction algorithm should therefore be applied which must account for this fact: raw data should be scanned with high frequency and the essential data (corresponding only to important changes) may be stored with the necessary frequency, i.e. variably or not equidistant with respect to time.

Automated measurement and control of bioprocesses, presently an art but a routine in the near future, generates a tremendous amount of data. This requires judging of the importance of these data for documentation in order to implement an effective data reduction method without loss of valuable information. The reduction algorithm must keep a true image of the real data. We adopted a simple algorithm to achieve this goal: all data—*independent of whether measured or calculated*—are treated as variables and kept in a circular buffer in the frequency with which they were generated. Values (data-points) of variables that change significantly with time are written to the archive. The significance of a change is judged by a reasonably defined window for each variable—including all intended culture parameters—the width of which is usually determined by the noise on the respective signal. At any instance, every “first” data-point (of an experiment) is archived, together with a time-stamp. A next entry to the archive is made only if the variable moves outside the respective window which had been centered around the last archived value;

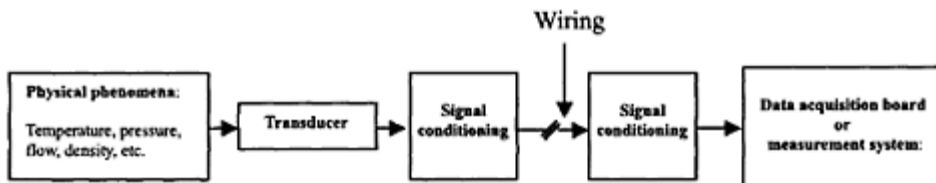


**Figure 3.2** Schematic representation of stages in a data acquisition system.

concomitantly, the window is re-centered around the new entry, and so on. This technique assures that all relevant changes—including those not intended—of any considered variable are trapped and that the dynamics of all signal trajectories are fully documented. The only inconveniences with this data treatment are that one needs to time-stamp every data entry individually and one ends up with non-equidistant data-vectors. The benefit is a data-to-archive reduction usually by between  $10^{-2}$  and  $10^{-4}$  and the assurance that no important data are lost.

### Derived Variables

Some very important process variables are not measured on-line but can be easily calculated from on-line measurements usually available in fermentation systems. They are typically dilution rate ( $D$ ), oxygen (OTR) and carbon dioxide (CTR) transfer rates, the respiratory quotient (RQ) and the volumetric mass transfer coefficient  $kLa$ . The calculation of OTR is particularly noise sensitive especially at low biomass concentrations due to the small differences in oxygen concentrations between inlet—and outlet-gas. Hence special care should be taken on noise filtering. As reported in the work of Locher *et al.* (1993), many times due to unaccounted effects, erroneous experimental procedures and sensor calibration problems, dramatic errors in the calculation of derived variables may occur. It was shown that neglecting changes in the atmospheric pressure may result in errors for RQ evaluation larger than 100%. Obviously, errors in derived variables are the direct consequence of errors attached to on-line measurements. Depending also on the way they are calculated, numerical error propagation may have significant effects. Many other derived variables may be monitored on-line. When some nutrients fed to the bioreactor are kept at constant concentrations by feedback control, the corresponding consumption rate  $r_i$  may be approximated by the relationship  $r_i = D(c_i - c_{Fi})$   $D$  being the dilution rate ( $D$ , the ratio of feed rate to volume, =  $F/V$ ),  $c_i$  the concentration in the medium and  $c_{Fi}$  the concentration in the input feed rate  $F$ . When two quantities are kept constant the corresponding yield is easily evaluated also from the ratio between the two rates. These variables may give important information about the micro-organism's metabolic state.

## BIOREACTOR MODELLING: A PROCESS CONTROL PERSPECTIVE

Several closed-loop control strategies are commonly implemented in fermentation systems regarding physico-chemical and environmental properties (temperature, pH, pressure, oxygen partial pressure). Classical control policies such as PID or on/off control are sufficient to solve successfully such control tasks. However, to progress into biological mechanisms control, models are required to establish the link between extracellular physico-chemical quantities (the quantities that we can manipulate) with intracellular phenomena. In several ways and variants, dynamic bioprocess models for control aim at establishing this link.

In spite of the undeniable potential that models may have in bioprocess control it should be stressed that modelling is not a current practice in the biotechnological industry. For such industrial applications we should probably ask ourselves why model-based developments are not sufficiently attractive rather than engaging on the task of developing all kinds of more and more complex models which at the end are not of practical utilisation.

Several reviews on bioprocess modelling have been published (Kneinstreuer, 1987; Thornhill and Royce, 1991; Nielsen and Villadsen, 1992; Bellgardt, 1993) and it is not intended to add much to these here. In addition to the traditional mathematical modelling in bioprocesses other modelling techniques based on artificial intelligence have been catching attention in recent years. These techniques will be briefly presented in relation to the potential application for process control.

Bioprocess models address two main systems: 1) the bioreactor system and 2) the cells system. Bioreactor models deal with transport processes, rheology, mass/heat/momentum transfer aspects and flow patterns. Cell models deal with the kinetics at the individual cell level and at the whole cell population level. The bioreactor system and the cell system have very complex interactions and cannot be analysed separately. Cells are continuously transforming the liquid phase by consuming several nutrients, which are metabolised into several products, some of them being excreted into the surrounding media.

### **Classical Mathematical Modelling**

#### ***Basic modelling concepts***

Having in mind model-based applications for bioprocess monitoring and control, when we develop a model we are mainly interested in the description of the dynamics of macroscopic quantities that influence the behaviour of the cell system, recognising that cells are ultimately the bioreaction promoters. These quantities are mainly concentrations in the biosuspension of several components such as biomass, substrates, and products, and also several other quantities such as temperature and pH.

Those variables which define the process state are termed state variables. A mathematical (mechanistic) dynamical description of the state variables, irrespective of

the type of bioreactor in study, is obtained by applying general mass, energy and momentum balances (Roels, 1983).

In practical applications the choice of a sub-set of state variables may be sufficient, this depending on the objectives of the model and on the operating conditions. When, for instance, the temperature is kept constant by means of an efficient control, there is no need to include the variable temperature in the state space vector. This avoids the need to employ macroscopic energy balances for describing and analysing the process state. The energy equations are however required if the objective of the model is the design of a temperature controller or, just to give another example, where cooling problems are likely to be found as is the case in large scale bioreactors (Humphrey, 1998).

A problematic issue concerns the rheological effects in bioreactors. In most cases modelling of flow patterns is too complex and much for this reason almost invariably the assumption is taken that both liquid and gas phases are well mixed, i.e. the medium is assumed to be homogeneous, in both industrial and research applications. From the mathematical and numerical point of view this introduces a significant simplification since, otherwise, a mathematically complex distributed parameter analysis would have to be performed (e.g. Reuss, 1996). Under this assumption, and by considering that temperature, pressure and pH are usually controlled quantities being kept at constant values, there is solely the necessity of applying mass balance principles to the relevant components. This leads to a set of ordinary differential equations that almost invariably are the backbone of simplified bioreactor models,

$$\frac{dx}{dt} = r + \frac{F}{V}(x_{in} - x) + q, \quad (1)$$

being  $x$  a vector of concentrations (the state space vector),  $r$  a vector of reaction kinetics,  $F$  the input feed rate into the bioreactor,  $V$  the working volume,  $x_{in}$  a vector of concentrations in the input feed with the feed rate  $F$ , and  $q$  a vector of flows associated with the gas phase (such as oxygen and carbon dioxide transfer rates).

Mass transfer and hydrodynamic issues are addressed in detail in Chapter 1 of this book. It is however worth stressing at this point that oxygen transfer limitations represent an important constraint in bioprocess optimisation and control. With the exception of cooling limitation problems usually found in large bioreactors (Kneinstreuer, 1987), the most frequent limitation to growth in aerobic fermentations is dissolved oxygen (Thornhill and Roy ce, 1991). Oxygen has a very low solubility in fermentation media in comparison to other typical substrates, thus needing to be continuously supplied, usually by aeration. The mass transfer capacity between gas and liquid phases, quantified by the volumetric mass transfer coefficient  $k_{La}$  is a central concern in aerobic bioprocesses design and operation. From a practical point of view, a very important issue in carbon limited bioprocesses is that the maximum  $k_{La}$  imposes the most important constraint in bioprocess optimisation. The correlation between  $k_{La}$ , stirrer speed and air flow (see Humphrey, 1998) is also important for designing control systems for dissolved oxygen.

### ***Cell Models***

The reaction term  $r$  in eqn. (1) is the result of a complex metabolic reactions network at both cell level and at the whole cell population level. In general cell models can be

classified as structured/unstructured or segregated/non-segregated. Cell models considering the existence of intracellular components are termed structured otherwise they are termed unstructured. They may also assume the existence of a morphological structure, being then termed segregated models, or may assume that all cells are identical (only one morphological form) being then termed non-segregated models.

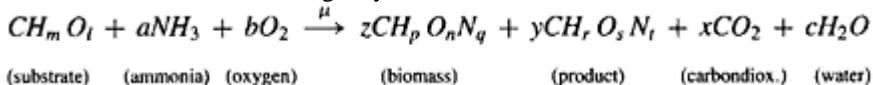
For bioprocess optimisation, control and supervision, unstructured and non-segregated models are the ones which have been applied in the past obviously for the sake of simplicity. The other side of the coin is that unstructured and non-segregated cell models are rough simplifications of the reality. As such parametric uncertainty is one of the frequently mentioned problems affecting robustness of underlying model-based closed-loop control and optimisation.

In developing unstructured and non-segregated cell models, principles of macroscopic stoichiometry and Monod-type kinetics (Table 3.1) are employed. The starting point of such an analysis is the establishment of a set of biochemical equations describing the most

**Table 3.1** Monod type kinetic models

according to Monod:	$\frac{q}{q_{\max}} = \frac{s}{s + K}$
according to Blackman:	$\frac{q}{q_{\max}} = \begin{cases} B \cdot s : & s \leq A \\ 1 : & s \geq A \end{cases}$
according to Moser:	$\frac{q}{q_{\max}} = \frac{s^n}{s^n + K}$
according to Contois:	$\frac{q}{q_{\max}} = \frac{s}{s + K \cdot x}$
according to Teissier:	$\frac{q}{q_{\max}} = 1 - e^{(k)} \cdot e^{-k \cdot s}$
according to Kargi & Shuler:	$\frac{d \left( \frac{q}{q_{\max}} \right)}{ds} = K \cdot \left( \frac{q}{q_{\max}} \right)^n \cdot \left( \frac{q_{\max} - q}{q_{\max}} \right)^n$
according to the logistic formula:	$\frac{q}{q_{\max}} = \left( 1 - \frac{x}{x_{\max}} \right)$
analogous to non-competitive inhibition (formally: $q_{\max}$ is affected)	$\frac{q}{q_{\max}} = \frac{s}{s + K_s \cdot \frac{K_i}{s + K_i}}$
analogous to competitive inhibition (formally: $K_s$ is affected)	$\frac{q}{q_{\max}} = \frac{s}{s + K_s \cdot \left( 1 + \frac{k}{K_s} \right)}$ or $\frac{q}{q_{\max}} = \frac{s}{s + K_s \cdot \left( 1 + \frac{s^2}{K_s} \right)}$
analogous to un-competitive inhibition (formally: both $q_{\max}$ and $K_s$ are affected)	$\frac{q}{q_{\max}} = \frac{s}{s + K_s \cdot \left( s + \frac{K_s}{s} \right)}$ or $\frac{q}{q_{\max}} = \frac{s}{s \cdot \left( 1 + \frac{s}{K_s} \right) + K_s}$

relevant mechanisms in the cell. In the most simple version of such an analysis, all metabolic reactions are lumped together in a single biochemical reaction describing the overall cell metabolism. For instance, a biochemical aerobic reaction where one substrate, ammonia and oxygen are consumed, producing biomass, one product, carbon dioxide and water is stated in the following way:



When the elemental composition of all species involved is known it is possible to evaluate the molar stoichiometric coefficients a, b, y z x and y by applying general mass and energy balance principles (Reels, 1978; Erickson *et al.*, 1978). The well-known yield coefficients in biotechnology are related to these stoichiometric coefficients by simple molar-to-massbase transformations. The consumption and production kinetics of all the species are linked together by the stoichiometry, and by the specific rates of growth,  $\mu$ , and of product formation,  $f_p$ .

The growing availability of more detailed models of basic cell growth mechanisms, in the form of structured and segregated models, poses a challenge to systems and control scientists and engineers in the search of new methods for bioreactor optimisation and control that can make use of such available models.

### ***Identification***

The use of kinetic models requires a previous identification of the parameters involved. For instance, when using the Monod model (or alternatives as compiled in Table 3.1) the maximum specific growth rate  $\mu_{\max}$ , and the yield coefficient  $Y_{X/S}$  (or  $Y_{P/S}$ ) must be identified for the actual cultivation conditions. Unfortunately even for such a simple kinetic relationship as the Monod model this identification is not straightforward, requiring a careful experimental planning (Baltes *et al.*, 1994; Munack, 1989). Additionally the coupling of Monod-type kinetic models with mass balance equations forms non-linear dynamical systems, which, depending on its structure, may not be identifiable.

### **A New Perspective: Knowledge Integration Modelling**

Modelling through knowledge integration is emerging as an alternative to the classical modelling approach (Schubert *et al.*, 1994a; Psichogios and Ungar, 1992; Thomson and Kramer, 1994; Feyo de Azevedo *et al.*, 1997, Simutis *et al.*, 1997). Modelling through knowledge integration aims at exploring all sources of *a priori* knowledge/information about the process that should be optimally expressed and incorporated in the process

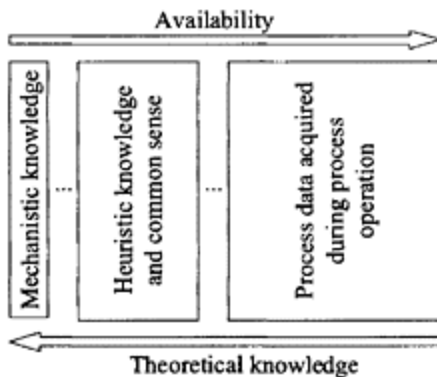


**Figure 3.3** Main sources of knowledge usually available for developing a bioprocess model.

model. This knowledge spectrum (Figure 3.3) ranges from mechanistic knowledge to information hidden in process data records. People in industry seem to be attracted by this methodology for the reason that heuristic knowledge and rules of thumb may be incorporated directly in the process model. It should however be stressed that these concepts face a certain criticism, mainly in that the substitution of mechanistic kinetic models by black-box models has obvious risks in affecting model robustness.

#### ***Knowledge and expression of knowledge***

A variety of information sources is normally available on biotechnological cultivation processes (Schubert *et al.*, 1994a; Lübbert and Simutis, 1994). Three main types of knowledge can be identified:

1. Mechanistic (phenomenological) knowledge: this kind of knowledge is usually represented by mathematical models. This is the classical approach followed by chemical and biochemical engineers for developing their process models mentioned previously. It has the highest level of sophistication, involving the understanding of the basic transport mechanisms and kinetics. These mechanisms are often poorly understood or even completely unknown. Therefore this kind of knowledge is usually the one available in minor quantities.
2. Heuristic knowledge and common sense: this kind of knowledge is more qualitative than the former, being usually available in larger quantities in the industrial environment. The Fuzzy theory is used to manipulate this type of information. It provides methods for quantifying qualitative knowledge. Heuristic knowledge is often stated in terms of rules of thumb. These can be readily represented by the so-called knowledge-based systems such as fuzzy inference systems and expert systems (e.g. Sugeno, 1985; Kosko, 1992; Wang, 1994).
3. Knowledge hidden in the process data acquired during process operation: in many situations the available mechanistic and/or heuristic knowledge is not sufficient to

develop a process model with the desirable accuracy. In this situation data-driven modelling can be used to improve the accuracy of the model. In many industrial plants the relevant cause/effect mechanisms have been registered for many years in the form of process input/output data. Some of these mechanisms have been at least observed by the people operating the plant, but many of them have been just recorded in process data files and passed completely unaware. The modelling of unknown parts of the process can be made using the so-called black box methods, namely time-series and artificial neural networks (ANN). A very complete survey of black-box modelling in system identification is given by Sjöberg *et al.* (1995). In particular ANNs have been getting a great deal of attention from researchers in the last years. They prove to be extremely flexible in representing complex non-linear relationships (e.g. Cybenko, 1989; Hornik *et al.*, 1989; Poggio and Girosi, 1990) without requiring any kind of knowledge concerning the structure of the underlying model. Several important results have been published concerning the application of ANNs for dynamical system identification and control (e.g. Hunt *et al.*, 1992; Pollard *et al.*, 1992; Narendra and Partha sarathy, 1990).

### ***Efficient knowledge fusion***

The preceding analysis leads naturally to the questions of knowledge utilisation, knowledge fusion and hybrid solutions. There are two types of hybrid modular structures:

- 1) modular complementary (Figure 3.4a), where different kinds of information for the sub-system complement themselves (Schubert *et al.*, 1994b); the case depicted in Figure 4a shows the combination of an Artificial Neural Network (ANN) kinetic model (black-box model) with a mechanistic mass balance equation (white-box model). and
- 2) modular competitive (Figure 3.4b) where different forms of information about the same sub-system are available for possible utilisation; in the example, a mechanistic/empirical-Monod type-kinetic model (white-box module), a fuzzy kinetic model (grey-box module) and an ANN kinetic model (black-box module).

In competitive hybrid model structures, a mechanism for dynamical weighting of each single model is necessary (Figure 3.4b). This mechanism should obey to the criterion that for the current set of inputs the best model should have a higher weight for the final output while the worst model should have the lowest weight.

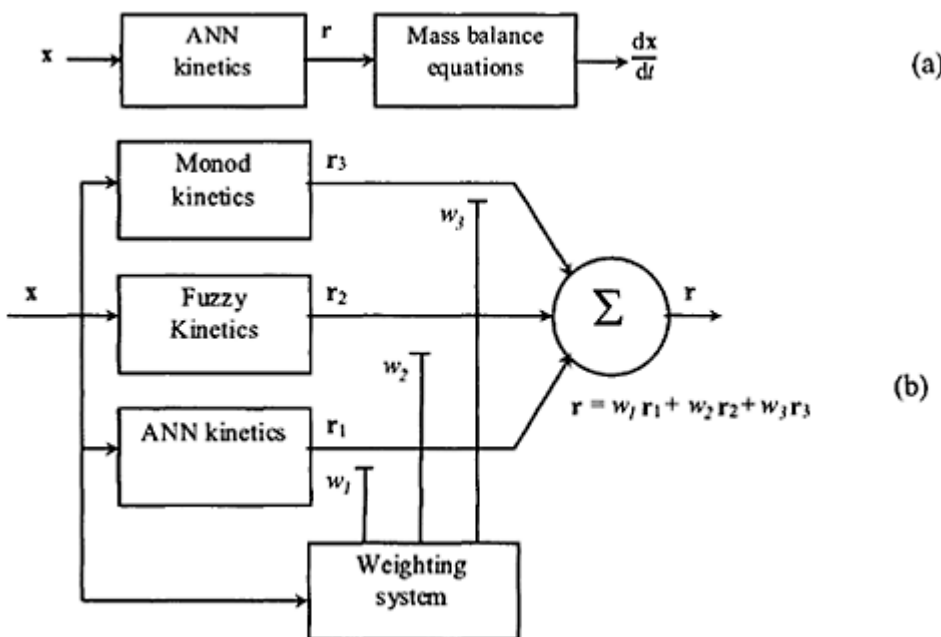


**Figure 3.4** Hybrid modular structures:  
 (a) modular complementary structure  
 (b) modular competitive structure.

While complementary hybrid structures have been frequently reported in the literature competitive structures are not so common. The main reason for this may be due to the lack of theoretical results in this area. A central question is: how should the weighting system be defined. Some examples of weighting methods have been reported in the literature, from which the most important are:

1. Weighting methods based on clustering techniques (e.g. Simutis *et al.*, 1995; Leonard *et al.*, 1992)
2. Weighting methods based on expert systems (e.g. Schubert *et al.*, 1994b)
3. Weighting methods based on gating networks (Peres *et al.*, 2000)

#### *Common hybrid model structures*

Several hybrid model structures have been reported in the literature. An important class of these structures are the neural-fuzzy systems. The neural-fuzzy systems combine artificial neural networks and fuzzy logic in one single model structure (e.g. Gupta and Rao, 1994; Werbos 1992; Shi and Shimizu, 1992; Lin and George Lee, 1991).

Another important approach for designing hybrid model structures is based on the division of the process in study in several modules according to the kind of knowledge available in different parts of the process. The result is expressed by a diagram of

interconnected modules. Each module is expressed by an input-output relationship based on a particular modelling technique.

Several authors have used the very simple complementary hybrid model structure represented in Figure 3.4a (e.g. Wilson and Zorzetto, 1997; Psichogios and Ungar, 1992; Montague and Morris, 1994; Feyo de Azevedo *et al.*, 1997) based on the use of artificial neural networks for describing the microorganism kinetics embedded into mass balance equations.

Feyo de Azevedo *et al.* (1997) analysed the practical advantages and disadvantages of such a structure in terms of model accuracy and robustness. Neural networks are powerful for kinetic modelling provided sufficient data is available covering the whole operating region. Model predictions are most significantly degraded whenever the neural network operates outside the input space used in the training phase. These aspects are illustrated in Figure 3.5.

To improve robustness of the above mentioned hybrid structure, Simutis *et al.* (1995) suggested to include a safety model which should be used whenever the ANN is operating in extrapolation conditions. In this way the global extrapolation properties of the model are improved. This type of approach is illustrated in Figure 3.6, where a Monod-type model and an ANN model compete for the modelling of a baker's yeast fermentation.

## BIOPROCESSES AUTOMATION AND CONTROL

One of the most important tasks for bioprocess automation and control is to force the process state to follow an optimal path defined according to a pre-established economic target. The economic performance of the production process is most often quantified by

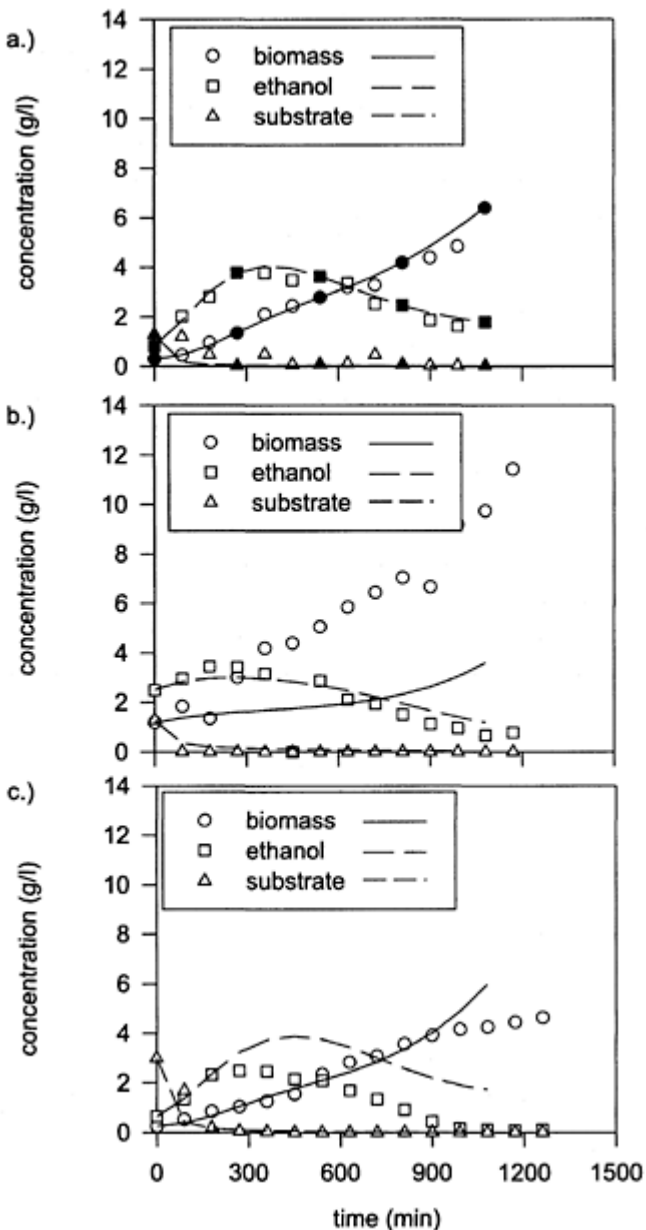


**Figure 3.5** Prediction ability of an hybrid model in a baker's yeast production process (kinetics module: feedforward network with one hidden

layer and 8 units in the hidden layer. Input data:  $t$ ,  $V$ ,  $F$ ,  $S_{\text{inlet}}$ ). (a) training data set. (b) validation data set. (c) test data set. Calculations: lines; experiments: symbols (solid symbols are training data).

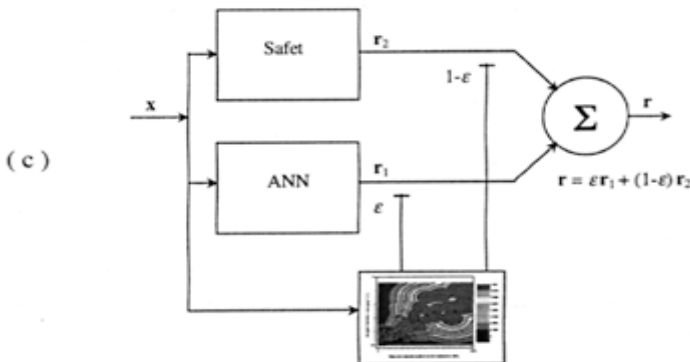
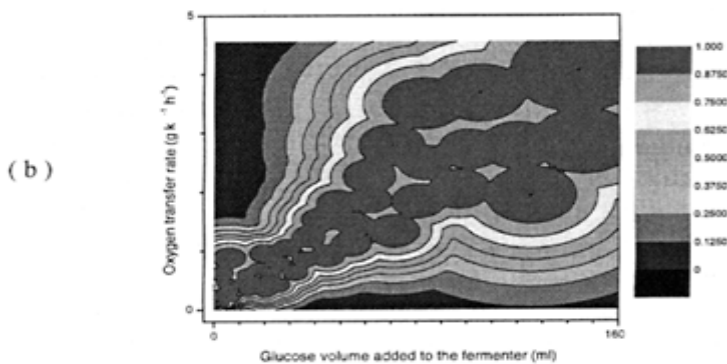
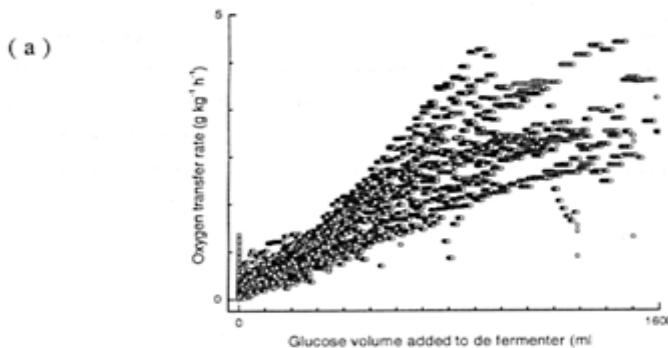


**Figure 3.6** Extrapolation measure weighting mechanism: (a) set of P discrete measured points used for training the ANN (in a two-dimensional input space); (b) continuous density function (extrapolation measure  $0 \leq \varepsilon \leq 1$ ) obtained by clustering the training patterns with a set of C«P hyperspherical clusters (k-mean algorithm); (c) Extrapolation measure weighting mechanism: competition between an ANN kinetic model and a safety (Monod type) kinetic model. When  $\varepsilon$  is high (ANN is not extrapolating) the ANN is used preferentially. When  $\varepsilon$  is low (ANN is extrapolating) the safety model is preferred.

the total amount of product, purity of final product (which is related to costs in downstream processing), and production costs. The economic goals of the process are dictated ultimately by the market dynamics. Unlike many chemical processes, security is usually not a major concern in bioprocess operation but sterility is. This is one of the main reasons why bioprocess automation and control did not develop as much as in the chemical industry. However the economic benefits could be considerable in many production plants if proper control were in operation.

As stressed by Roy ce (1993), whilst for the different types of biochemical processes and products different types of production costs are dominant, they all share the common interest of improving process yield as a major economic benefit. The straightforward way to improve process yield is investing in process control. Currently industrial production plants are controlled manually and empirically which leads to slow process improvement. Three major advantages should be expected from the implementation of automation and control:

1. Faster adapting and enforcing of new optimum whenever the process is changed (e.g., new strain or new media).
2. Faster adapting and enforcing of new optimum related to new market demands.
3. Releasing of staff that might concentrate on more relevant tasks.

It also is relevant to stress that strain development, medium optimisation and process control are all important issues contributing to economic benefits and that complement themselves. For instance, tests for comparing strain productivity in production conditions

require experiments at lab or pilot scale with extremely well controlled environmental conditions. In the same way a new strain might require different operating strategies in order to achieve a pre-established economic output.

One issue is the potential benefit of process control and the other is the practical benefit achievable with the current state of the-art in theory, practice and hardware. Process control has both benefits and costs associated. As mentioned by Royce (1993) the cost/benefit ratio did not justify up to now investments in advanced process control. In the present section we will go through some important concepts in bioprocess automation and control while trying to focus on the practical usability of the methods in terms of such ratio.

### **Optimal Open-loop Control**

In open-loop control optimal time profiles for manipulated and state variables are evaluated off-line according to some predefined economic profit function. The optimal trajectories for the manipulated variables are implemented on-line using for instance programmable controllers. No automatic corrective action is taken if the process deviates from the expected optimal path. The central task for open-loop control is hence to determine optimal trajectories for the most relevant process variables (relevant in respect to the process performance) using appropriate design procedures.

Two important points should be noticed. The first is that the model must be sufficiently detailed in order to describe the most important features of the process related to the economic profit function. The optimal C-source feeding rate profile is often evaluated in this manner in the industry. The second is that, considering that no on-line corrective actions are taken, this control leads almost inevitably to sub-optimal process operation due to process disturbances and parametric uncertainty. This question will be discussed further in the next section.

Traditionally, the open-loop control problem is solved by applying mathematical optimisation techniques based on Pontryagin's maximum principle (e.g. Modak, 1993). As pointed out by Simutis *et al.* (1996) this technique is difficult to apply and is subject to some practical limitations:

1. Only simple models can be worked with Pontryagin's maximum principle to keep the mathematical analysis workload at bearable costs. However sufficiently accurate process models are normally complex models.
2. Practical constraints in objective function and physical equipment hinders the application of the method.
3. High development times even for experienced scientists, and only a few specialists are able to properly apply this theory.

Some authors suggest the application of stochastic optimisation techniques that can be used successfully with today's availability in computing power (Montague and Ward 1994; Simutis and Lübbert 1997). In relation to classical optimisation techniques the advantages are clear: the method is more robust, much simpler to apply and no restrictions on model complexity and objective function constraints are imposed. The only serious constraint is computation time. In the work of Simutis *et al.* (1996) it was

shown that stochastic optimisation techniques may provide results of the same quality as Pontryagin's maximum technique with much less development cost.

Considering that stochastic approaches are not limited to simple models and that computing power is less and less a constraint, this represents an attractive solution for industrial applications of open-loop control.

### Closed-loop Control

In general terms closed-loop control aims at forcing the process state to follow some predetermined path (reference). This path may be defined heuristically or mathematically and can be kept unchanged along the operation or subject to periodic adaptation.

Going back to open-loop control discussion, an obvious application of closed-loop control is to enforce the optimal trajectories evaluated within the open-loop procedures.

The viability of closed-loop control is constrained by the availability and robustness of on-line measurement devices for the control quantities. This poses currently the most serious impediment for closed-loop control in the industrial environment. In many situations the problem can be circumvented by implementation of estimation models that provide on-line and real time estimates of the control quantities. Not surprisingly most of the many control studies reported in the literature rely on linear or non-linear estimation/predictive (adaptive) models. Several control strategies can be implemented ranging from classical PID control to non-linear control. In the present section we look to some of the most pertinent issues in bioprocess closed-loop control.

### *Compensation of measurement dynamics*

It is often the case in industrial installations that measurements are available but process conditions under which they are performed and/or the intrinsic sensor dynamics lead to distorted information on relevant process properties. Common practical situations are related to the design of the process production line, to sensor location and to specific operating conditions. As a simple practical example, process measurements, namely of quantities such as concentrations, may have to take place quite distant from the source of interest. In such cases, and merely for reasons of process layout and operating conditions, measurements are corrupted by a first order dynamics with a transportation lag, (e.g. Tham *et al.*, 1989). This limitation in the quality of these measurements may lead to unnecessary difficulties even in the simplest regulatory problem where control set-points are kept constant. Such difficulties are particularly meaningful for time varying reference-tracking control problems (with rapidly changing outputs) or in naturally unstable process operations where the precise knowledge of the output transient trajectory is essential for control purposes.

In general terms and whatever the causes, for those measurement systems where significant time constants and transportation lags are observed, sensor outputs will not (instantaneously) be representative for the real process. This may hinder the implementation of efficient operation control policies.

Recently, Georgieva and Feyo de Azevedo (2000) studied the application of neural networks (NN) for recovering process outputs from sensor signals, e., for modelling sensor inverse dynamics so that once the trained NN is placed in series with the

measurement device (Figure 3.7a) it results in an identity mapping which will lead to the recovery of real process output (RPO). They concluded that simple 3-layered feedforward neural networks may provide very accurate recovery of data distorted by first order dynamics, including time delay. Closed-loop control could subsequently be performed

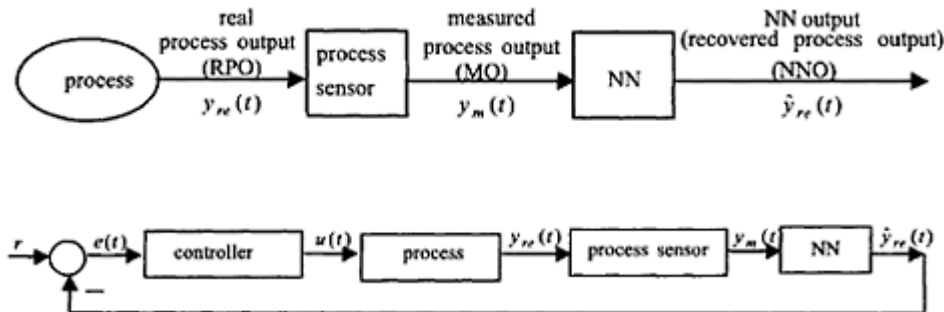


**Figure 3.7** (a) Neural network measurement dynamics compensation; (b) application to closed-loop control.

with the recovered signal (Figure 3.7b), without the difficulties experienced when feeding the controller with distorted measurements.

#### *Software sensors/Inferential measuring*

The design and implementation of software sensors provides a suitable answer to cope with the lack of instrumental sensors and have been widely reported in the literature. Software sensors are algorithms for the on-line estimation of those state variables and parameters, that are not measurable in real time, from more easily accessible related measurements. One of the most common industrial application is biomass estimation, using exhaust gas analysis by means of very simple empirical correlations.

The most serious problem regarding industrial application of software sensors is that they are based on process models that must be accurate and robust. With this respect, and as usual, kinetics present the most serious difficulty. For these reasons, in recent years many authors focused their work in developing algorithms for state observation and parameters estimation, avoiding the knowledge of the underlying kinetic model essentially by the application of systems theory.

Over the last 20 years, different approaches have been proposed for state and parameter estimation in fermentation processes. Extended Kalman filters have been widely reported. This and other stochastic algorithms have been preferred due to the problems posed by the large quantities of white noise attached to on-line measurements. However there are today several useful methods available for successful noise filtering. Many other works focused on the robustness of model-based estimators. Several applications using the general theoretical framework developed by Bastin and Dochain (1990) have been reported. Farza and co-authors (Farza *et al.*, (1997a), (1997b), (1998), (1999)) have proposed observerbased estimators derived from nonlinear systems theory.

In all these works, reaction rates are estimated from the measurement of state variables (i.e. concentrations). Some authors have used exit-gas analysis for the estimation of the growth rates (Estler, 1995; Lubenova, 1999; Rothen et al., 1998).

An illustrative example is given in the study of Oliveira *et al.* (2000a) on software sensors applications in a baker's yeast production process. An estimation scheme consisting of a Luenberger-type state estimator (Luenberger, 1971) and a second order dynamic kinetics estimator (Oliveira *et al.*, 1996) was developed with the major concern of keeping the number of required (and easily available) on-line measurements as low as possible. The overall estimation scheme allowed on-line tracking of 3 state variables (biomass, glucose and ethanol concentrations) and 3 rates (specific growth rates related to glucose oxidation, glucose fermentation, and ethanol oxidation), using on-line measurements of only 2 state variables (concentrations of dissolved oxygen and of dissolved carbon dioxide) and off-gas analysis. An interesting feature of this scheme is related to on-line kinetics estimation: the "true" process kinetics could be tracked with a second order dynamics convergence, as illustrated in Figure 3.8.

### **Classical control**

Classical control theory relies on linear time-invariant process dynamics. Bioprocesses are inherently non-linear and time-varying. Nevertheless, classic control strategies such as

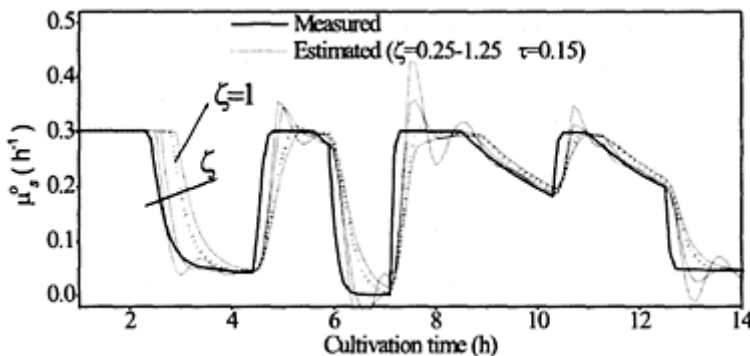


**Figure 3.8** Specific growth ( $\mu_s^0$ ) rate estimates (dotted lines) and "true" (full line) in a baker's yeast production process. The kinetics estimator imposes second order dynamics of convergence from estimates to true kinetics;  $\tau$  and  $\zeta$  are the natural period of oscillation and damping coefficient of the second order response.

PID control or even on/off control can be used successfully for controlling some environmental quantities in bioreactors. Temperature is usually controlled with a P(I(D)) controller. Pressure is normally controlled with an on/off control strategy. pH is normally controlled with P(ID)-control but can be controlled satisfactorily with on/off control as well. These are the simplest control loops normally found in bioreactor control. For other control loops it is difficult to implement PID control due to the non-linear and time-varying nature of the process. This essentially means that the problem is to find a set of PID parameters that guarantees stability and acceptable tracking properties for the entire operating range.

### ***Advanced model based control***

Model-based control can be classified as linear or non-linear depending on the type of model it is based on. Additionally, the control system may be adaptive if on-line measurements are used to tune the model (controller) parameters. They may also be predictive if the model is used to predict the process dynamic behaviour for a given time horizon. Many applications of all these control strategies were reported in the literature in recent years with predominance of linear adaptive and/or predictive control. An overview of many of these control strategies is given by Chattaway *et al.* (1993). For those cases where model uncertainty is a significant constraint, as it is the case of waste water treatment reactors, robust control is receiving increasing attention (e.g. Georgieva and Feyo de Azevedo, 1999). Within the non-linear control class black-box non-linear control using neural networks and Fuzzy control have been catching an enormous attention (e.g. Montague and Morris, 1994; Shi and Shimizu, 1992; Glassey *et al.*, 1997).

In many control problems more or less complex controller designs are required, however this is not always necessary. Sometimes the non-linear and time-varying characteristics of the process can be captured with sufficient accuracy by a mechanistic or hybrid model within the operating region. In this situation the application of a Direct Model Control

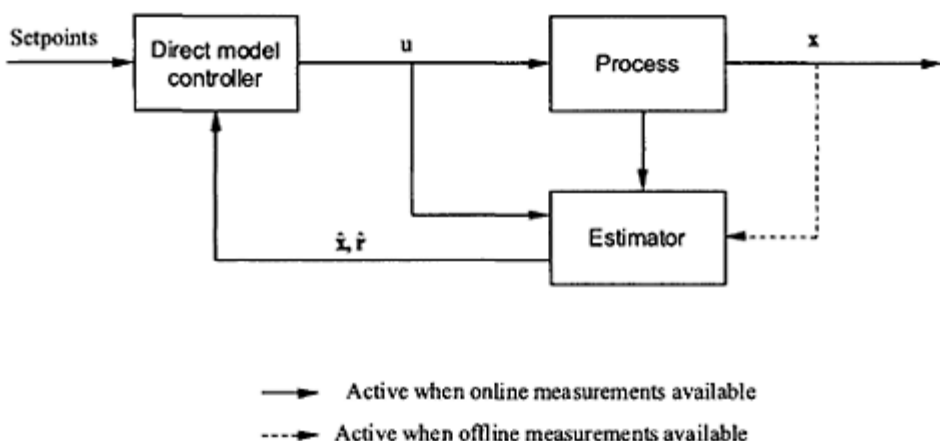


**Figure 3.9** Direct model control.

(DMC) strategy is rather simple. In a DMC strategy (Figure 3.9) the non-linear controller may be derived analytically from the process model and from a reference model. The reference model imposes desirable dynamics for the convergence of control variable to the corresponding setpoint profile, e.g. first order dynamics of convergence. This strategy was applied with good results for a penicillin production process (Oliveira *et al.*, 2000b).

### Trends in Bioreactor Control: On-line Optimising Control

The follow up of an open-loop control implementation is often the conclusion that the process is operated at sub-optimal conditions not coincident with the expected process performance evaluated by the off-line optimisation procedure. The natural conclusion to be made is that in order to improve further productivity and/or product yield and/or product quality, on-line optimising control should be implemented. There are two obvious explanations for this. First, open-loop control is not robust to disturbances in the process since no process data acquired on-line is used to take corrective actions. In practice, open-loop control is complemented by on-line corrective actions performed manually by process operators. When for instance viscosity increases above a threshold level the operator supersedes the open-loop set-point decreasing manually the sugar feed rate in order to prevent the process running into oxygen limitation. Second, open-loop control leads invariably to sub-optimal process trajectories due to inaccuracy of models, also commonly referred to in the literature as parametric uncertainty. The straightforward way to improve robustness in open-loop control is investing in on-line optimising control.

Basically, on-line optimisation control consists of the optimisation of a cost function on-line and in real-time using successively measurements acquired on-line and/or off-line for the current process run. A schematic representation for the tasks accomplished in on-line optimising control is depicted in Figure 3.10.

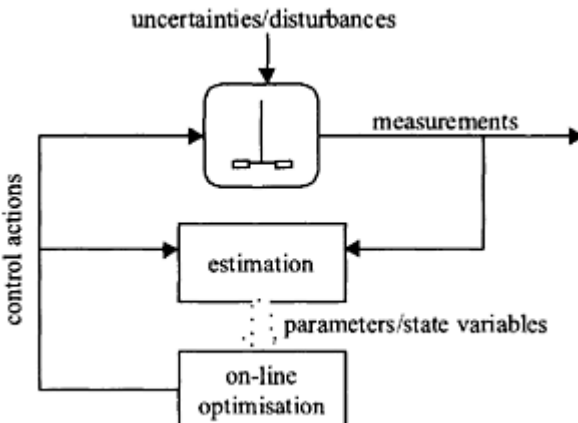


**Figure 3.10** General structure of an on-line optimisation control system.

In the work of Loeblein *et al.* (1999) a method is presented for evaluating the economic performance of the on-line optimisation control in batch reactors under parametric uncertainty. Since the integration of the dynamic process model is required in the optimisation, and since the integration may be time consuming and may preclude the on-line implementation, they suggested to approximate the set of algebraic differential equations in a set of algebraic equations by orthogonal collocation. In this way the dynamic optimisation problem reduces to a nonlinear programming (NLP) optimisation problem more easily solved on-line. The NLP optimisation problem can then be solved using standard techniques like Successive Linear Programming (SLP) and Successive Quadratic Programming (SQP).

### Software Support for an Integrated Approach

Advanced methodologies for bioprocess monitoring and control include an integrated utilisation of a multiplicity of tasks, as depicted in Figure 3.11. Such an approach can be brought into practice only through an appropriate software environment, which should make it easy to integrate all those tasks and methodologies. It is obviously difficult to develop such a support tool. This can be only achieved by classification of tasks and adoption of software engineering procedures suitable for programming such complex systems. Some important concepts are:

1. Object oriented modelling with object oriented programming.
2. Tree-like model hierarchies/Tree-like objects with object inheritance.
3. Standard interfacing of procedures like Single Input Single Output (SISO) and Multiple Input Multiple Output (MIMO) computation elements, optimisation procedures, adaptation schemes, etc...

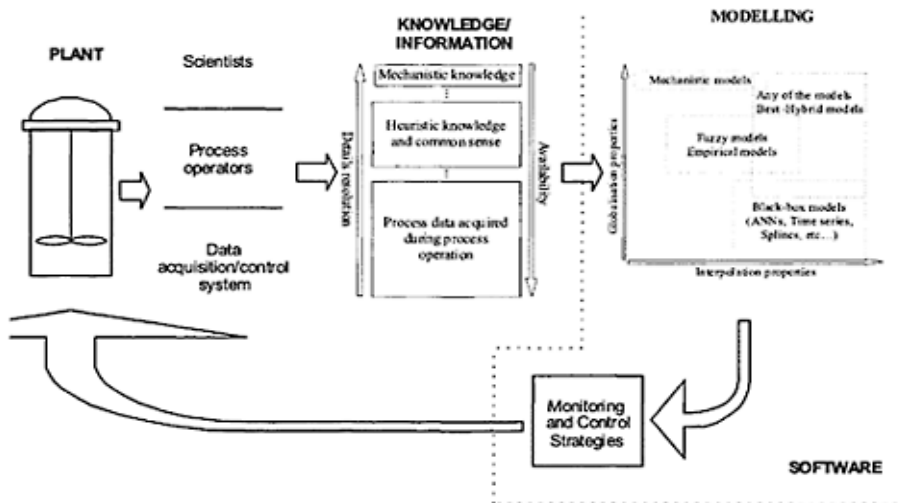


**Figure 3.11** An integrated approach for advanced bioprocess monitoring and control.

4. Requirements of real-time communication/needs for parallel processing.
5. Definition of priority of tasks with management of priority of software processes.

### CONCLUDING REMARKS

Improvement of bioprocess operation implies co-operative work between all factors producing knowledge, i.e. scientists, process operators, and technology (Figure 3.11). The more knowledge is available the more accurate can the process models be and the more efficient can the new model-based operating strategies be.

Modelling through knowledge integration is becoming an attractive methodology for industry people, mainly because it represents a straightforward way of linking all factors producing knowledge. More accurate models may be developed at lower costs since all different types of knowledge may be integrated in the process model.

A major constraint is the availability of suitable support software. Provided that this constraint is eliminated, the acceptance of model-based methodologies for improvement of industrial processes could increase considerably (in terms of both open-loop and closed-loop control).

Up to now most industrial plants did not progress into closed-loop automatic control at production scale even for some of the most basic environmental variables. Such steps could be achieved, in some cases, with low risks and minor investments even with a limited number of measuring devices. The extension of the front-end-system with a computer dedicated for closed-loop control is sometimes a reasonable solution for starting to investigate the benefits of closed-loop control at production scale.

### REFERENCES

- Baltes, M., Schneider, R., Sturm C. and Reuss M. (1994) Optimal Experimental Design for Parameter Estimation in Unstructured Growth Models. *Biotechnol. Prog.* **10**, pp. 480–488.
- Bastin, G. and Dochain D. (1990) On-Line Estimation and Adaptive Control of Bioreactors. Elsevier, Amsterdam.
- Bellgardt, K.-H. (1993) Cell Models. In Biotechnology, A multi-volume comprehensive treatise (Eds. H.-J.Rehm, G.Reed, A.Pühler and P.Stadler, 2nd Ed.), Volume 4 (Ed. K.Schügerl), pp. 267–298, VCH, Weinheim.
- Boe, I. and Lovrien R. (1990) Cell counting and carbon utilization velocities via microbial calorimetry. *Biotechnol Bioeng* **35** (1), pp. 1–7.
- Chattaway, T., Montague, C. and Morris A. (1993) Fermentation Monitoring and Control. In Biotechnology: A multi-volume comprehensive treatise (Eds. H.-J.Rehm, C.Reed, A.Pühler and P.Stadler, 2nd Ed.), Volume 3 (Ed. C.Stephanopoulos), Ch. 14, pp. 319–354, VCH, Weinheim.
- Cybenko, C. (1989) Approximation by Superpositions of a Sigmoidal Function, *Math. Control, Signals Sys.* **2**, pp. 303–314.
- Erickson, L.E., Minkevich, I.C. and Eroshin V.K. (1978) Application of Mass and Energy Balance -Regularities in Fermentation, *Biotechnol Bioeng*, Vol **XX**, pp. 1595–1621.

- Estler, M.U. (1995) Recursive On-Line Estimation of the Specific Growth Rate from Off-Gas Analysis for the Adaptive Control of Fed-Batch Processes, *Bioprocess Eng.*, **12**, pp. 205–207.
- Farza, M., Busawon, K. and Hammouri H. (1998) Simple: Nonlinear Observers for On-line Estimation of Kinetic rates in Bioreactors. *Automatica*, **34**(3), pp. 301–318.
- Farza, M., Hammouri, H., Jallut, C. and Lieto J. (1999) State Observation of a Nonlinear System: Application to (Bio)chemical Processes, *AICHE Journal*, **45**(1), pp. 93–106.
- Farza, M., Hammouri, H., Othman, S. and Busawon K. (1997b) Nonlinear Observers for Parameter Estimation in Bioprocesses, *Chemical Engineering Science*, **52**(23), pp. 4251–4267.
- Farza, M., Othman, S., Hammouri, H. and Biston J. (1997a) A Nonlinear Approach for the On-line Estimation of the Kinetic Rates in Bioreactors. Application to a Lactic Acid Production Process. *Bioprocess Eng.*, **17**, pp. 143–150.
- Feyo de Azevedo, S., Dham, B. and Oliveira F.R. (1997) Hybrid Modelling of Biochemical Processes: a comparison with the conventional approach, *Computers Chem. Engng.*, **21S**, pp. 751-S756.
- Georgieva, P. and Feyo de Azevedo S. (1999) Robust Control Design of an Activated Sludge Process, *Int. Journal of Robust and Non-linear Control*, **9**(13), pp. 949–967.
- Georgieva, P. and Feyo de Azevedo S. (2000) *A Neural Network Based Approach for Measurement Dynamics Compensation*, submitted for publication.
- Glassey, J., Ignova, M., Ward, A.C., Montague, G.A. and Morris A.J. (1997) Bioprocess supervision : neural networks and knowledge based systems. *Journal of Biotechnology*, **52**, pp. 201–205.
- Gupta, M.M. and Rao D.H. (1994) On the principles of fuzzy neural networks. *Fuzzy Sets and Systems*, **61**, pp. 1–18.
- Harder A, Roels J.A. (1982) Application of simple structured models in bioengineering. *Adv Biochem Eng*, **21**, pp. 56–107.
- Hornik, A.K., Stinchcombe, M. and White H. (1989) “Multi-Layer Feedforward Networks are Universal Approximators,” *Neural Networks*, **2**(5), pp. 359–366.
- Humphrey A. (1998) Shake Flask to Fermentor: What Have We Learned? *Biotechnol. Prog.*, **14**, pp. 3–7.
- Hunt, K.J., Sbarbaro, D., Zbikowski, R. and Gawthrop P.J. (1992) “Neural Networks for Control Systems-A Survey,” *Analitica*, **28**(6), pp. 1083–1112.
- Kneinstreuer C. (1987) Analysis of biological reactors. In *Advances in Biochemical Engineering*, H.Bungay and C.Belfont, eds., Wiley, New York, USA, pp. 33–78.
- Kosko, B. (1992) Neural networks and fuzzy systems: a dynamical systems approach to machine intelligence. Prentice-Hall, Englewood Cliffs, New Jersey.
- Leonard, J.A., Kramer, M.A. and Ungar L.H. (1992) A neural network that computes its own reliability. *Comp. Chem. Eng.*, **16**, pp. 819–835.
- Lin, C.-T. and George Lee C.S. (1991) Neural-Network-Based Fuzzy Logic Control and Decision System. *IEEE Transactions on computers*, **40**(12), pp. 1320–1336.
- Locher, C., Sonnleitner, B. and Fiechter A. (1992) On-line measurement in biotechnology: techniques. *J Biotechnol* **25**(1/2): (minireview) pp. 23–53.
- Locher, G., Hahnemann, U., Sonnleitner, B. and Fiechter A. (1993) Automatic bioprocess control. Biologically and technical caused effects during cultivation. *Journal of Biotechnology*, **29**, pp. 75–89.
- Loeblein, C., Perkins, J.D., Srinivasan, B. and Bonvin D. (1999) Economic performance analysis in the design of on-line batch optimisation systems, *J. Proc. Control*, **9**, pp. 61–78.
- Lübbert, A. and Simutis R. (1994) Adequate use of measuring data in bioprocess modeling and control, *Trends in Biotechnology*, **12**, pp. 304–311.
- Lubenova, V.N. (1999) Stable adaptive algorithm for simultaneous estimation of time-varying parameters and state variables in aerobic bioprocesses, *Bioprocess Eng.*, **21**(3), 219–226.
- Luenberger, D.C. (1971) An introduction to observers. *IEEE Trans. Automatic Control*, **AC-16**, 596–603.

- Modak, J.M. (1993) Choice of control variable for optimization of fed-batch fermentation, *Chem. Eng. J.*, **52**, pp. 59–69.
- Montague, G. and Morris J. (1994) Neural network contribution in biotechnology. *Trends Biotechnol.*, **12**, pp. 312–324.
- Montague, G.A. and Ward A.C. (1994) A sub-optimal solution to the optimisation of bioreactors using the chemotaxis algorithm, *Process Biochemistry*, **29**, pp. 489–496.
- Munack, A. (1989) A Optimal feeding strategy for identification of Monod-type models by fed batch experiments. In Reprints of the 4th International Congress on Computer Applications in Fermentation Technology, N.M. Fish, R.I. Fox, Eds., Ellis Hot-wood Limited: Chichester, U.K.
- Narendra, K.S. and Parthasarathy K. (1990) Identification and control of dynamical systems using neural networks. *IEEE Trans. Neural Networks*, **1**, pp. 252–262.
- Nielsen, J. and Villadsen J. (1992) Modelling of Microbial Kinetics, *Chemical Engineering Science*, **47** (17/18), pp. 4225–4270.
- Oliveira, R., Ferreira, E.C. and Feye de Azevedo S. (2000a) On-line State Observation and Reaction Rate Estimation in a Baker's Yeast Fermentation Process (submitted to the Journal of Process Control).
- Oliveira, R., Ferreira, E.C., Oliveira, F., Feye de Azevedo S. (1996) A Study on the Convergence of Observer-Based Kinetic Estimators in Fed-Batch Fermentations, *J. Process Control*, **6**(6), 367–371.
- Oliveira, R., Simutis, R., Smolders, G.J.F., Lübbert A. (2000b) Closed-loop Control Using an On-line Learning Hybrid Model Network (in preparation).
- Peres, M.J., Oliveira, R. and Feye de Azevedo S. (2000) *Knowledge Integration Methods for Improved Bioprocess Modelling*, Submitted.
- Poggio, A.T. and Girosi F. (1990) "Networks for Approximation and Learning," *Proc. IEEE*, **78**(9), pp. 1481.
- Pollard, J.F., Broussard, M.R., Garrison, D.B. and San K.Y. (1992) Process identification using neural networks. *Comp. Chem Eng.*, **16**, pp. 253–270.
- Psichogios, D.C. and Ungar L.H. (1992) A hybrid neural network-First principles approach to process modelling. *AICHE J.*, **38**, pp. 1499–1511.
- Reuss, M. (1996) Fermentation-the relation between intracellular metabolism and reactor dynamic. In Proceedings of the *1st European Symposium On Biochemical Engineering Science*, Dublin, Ireland, September 19–21, pp. 3.
- Roels, J. (1983) Energetics and Kinetics in biotechnology. Elsevier Biomedical Press, Amsterdam.
- Roels, J.A., Kossen N.W.F. (1978) On the modelling of microbial metabolism. *Prog. Ind. Microbiol.*, **14**, pp. 45–58.
- Rothen, S.A., Sauer, M., Sonnleitner, B. and Witholt B. (1998) Growth characteristics of *Escherichia coli* HB 101 [pGEc47] on defined medium. *Biotechnol Bioeng* **58**(1), pp. 92–100.
- Royce, P.N.C (1993) A discussion of recent developments in fermentation monitoring and control from a practical perspective, *Critical reviews in Biotechnology*, **13**(2), pp. 111–149.
- Schubert, J., Simutis, R., Dors, M., Havlik, I. and Lübbert A. (1994a) Hybrid Modelling of Yeast Production Processes-Combination of a priori knowledge on Different levels of Sophistication. *Chem Eng. Technol.*, **17**, pp. 10–20.
- Schubert, J., Simutis, R., Dors, M., Havlik, I. and Lübbert A. (1994b) Bioprocess optimization and control: Application of hybrid modelling. *J. Biotechnol.*, **35**, pp. 51–68.
- Shi, Z. and Shimizu K. (1992) Neuro-Fuzzy Control of Bioreactor Systems with Pattern Recognition, *J. Ferment. Bioeng.*, **74**(1), pp. 3945.
- Simutis, R., Havlik, I., Schneider, F., Dors, M. and Lübbert A. (1995). Artificial Neural Networks of Improved Reliability for Industrial Process Supervision. Preprints of the 6th Int. Conference on Computer Applications in Biotechnology, Garmisch-Partenkirchen, Germany, pp. 59–65, May 14–17, 1995.
- Simutis, R. and Lübbert A. (1997), A comparative study on random search algorithms for biotechnical process optimisation, *J. Biotechnol.*, **52**, pp. 245–256.

- Simutis, R., Oliveira, R. and Lübbert A. (1996) Hybrid modeling with neural networks and its utilization in bioprocess control. In: Bioreactor Engineering, EFB Working Party Bioreactor Performance Course Book (Eds), Larsson, G., Förberg, C., KTH Stockholm, pp. 380–406.
- Simutis, R., Oliveira, R., Manikowski, M., Feye de Azevedo, S., and Lübbert A. (1997) How to Increase the Performance of Models for Process Optimization and Control. *Journal of Biotechnology*, **59**, pp. 73–89.
- Sjöberg, J., Zhang, Q., Ljung, L., Benveniste, A., Delyon, B., Glorennec, P., Hjalmarsson, H. and Juditsky A. (1995) Nonlinear Black-box Modeling in System Identification: a Unified Overview. *Automatica*, **12**, pp. 1691–1724.
- Sonnleitner, B. (1999) Bioanalysis and biosensors for bioprocess monitoring. *Adv Biochem Eng Biotechnol* 66 (volume editor).
- Sugeno, M. (1985) Industrial applications of fuzzy control. *North-Holland, Holland*, Amsterdam.
- Tham, M.T., Morris, A.J., and Montague G.A. (1989) Soft-sensing: a solution to the problem of measurement delays. *Che. Eng. Res. Des.*, **67**, pp. 547–554.
- Thomson, M.L. and Kramer M.A. (1994) Modeling chemical processes using prior knowledge and neural networks, *AICHE J.*, **40**, pp. 1328–1340.
- Thornhill, N.F. and Royce P.N.C. (1991) Modelling Fermenters for Control. In *Measuring and Control in Bioprocessing*, K.C.Carr-Brion, ed., Elsevier, New York, USA, pp. 67–77.
- Valero, F., Lafuente, J., Poch, M., Sola, C. (1990) Biomass estimation using online glucose monitoring by flow-injection analysis: Application to *Candida rugosa* batch growth. *App Biochem Biotechnol*, **24–25**, pp. 591–602.
- Wang, L.-X. (1994) Adaptive fuzzy systems and control: design and stability analysis. Prentice-Hall, Englewood Cliffs, New Jersey.
- Werbos, P.J. (1992) Neurocontrol and Fuzzy Logic: Connections and Designs. *International Journal of Approximate Reasoning*, **6**(185), pp. 185–219.
- Wilson, J.A. and Zorzetto L.F.M. (1997) “A generalised approach to process state estimation using hybrid artificial networks/mechanistic models,” *Computers chem. Engng*, **21**(9), pp. 951–963.



# **CHAPTER FOUR**

## **DESIGN AND MODELLING OF**

## **IMMOBILISED BIOCATALYTIC**

## **REACTORS**

BRUNO S.FERREIRA<sup>1</sup>, PEDRO FERNANDES<sup>1,2</sup> AND JOAQUIM  
M.S.CABRAL<sup>1</sup>

<sup>1</sup> *Centre for Biological and Chemical Engineering, Institute Superior  
Técnico, Av. Rovisco Pais, 1049–001 Lisboa, Portugal*

<sup>2</sup> *Universidade Lusófona de Humanidades e Tecnologias, Av. do Campo  
Grande, 376, 1749–024 Lisboa, Portugal*

### **ABSTRACT**

Immobilised biocatalysts can be effectively employed in a wide variety of reactor configurations. High concentrations of the biocatalyst can be used, thus allowing high volumetric productivities. Furthermore, the biocatalyst is easily separated from other components in the reaction mixture, simplifying downstream processing. The process integration thus achieved can lead to lower production costs. However, in order to render the use of immobilised biocatalysts effective, an adequate understanding of the interrelationship between mass transfer and reaction kinetics is required to allow rational design of the bioreactor. In the first part of this chapter, expressions describing the effect of internal or external mass transfer effects and different kinetics on the overall reaction rate are presented. In the second part of the chapter, the main features of different reactor configurations are discussed and their design equations are presented.

### **BIOCATALYST IMMOBILISATION AND PERFORMANCE**

#### **Introduction**

The use of immobilised biocatalysts in laboratory studies, in analytical and medical applications and in large-scale industrial processes is presently a widespread technique. Immobilisation can be defined as the confinement of a biocatalyst inside a bioreaction system, with retention of its catalytic activity and stability, and which can be used repeatedly and continuously. Table 4.1 lists some advantages and limitations which can arise from the use of immobilised biocatalysts.

**Table 4.1** General aspects related to the use of immobilised biocatalysts.

General aspects	Specific aspects	
<i>Advantages</i>		
RETENTION OF THE BIOCATALYST IN THE BIOREACTOR	—possible biocatalyst reuse —product contamination avoided —high dilution rates allowed without biocatalyst wash-out	
HIGH BIOCATALYST CONCENTRATION	—increased volumetric productivity —rapid conversion of unstable substrates —minimised side-reactions	
CONTROL OF BIOCATALYST MICROENVIRONMENT	—manipulation of biocatalyst activity and specificity —stabilization of biocatalyst activity —protection of shear-sensitive biocatalysts	
FACILITATED SEPARATION OF THE BIOCATALYST FROM THE PRODUCT	—precise control of bioreaction time —minimisation of further product transformation	
<i>Limitations</i>		
INCREASED COSTS OF BIOCATALYST PRODUCTION	—increased requirements of materials and equipment —need for specific reactor configurations	
LOSS OF BIOCATALYST ACTIVITY DURING IMMOBILISATION	—biocatalyst-related —microenvironment related	<i>—exposure to pH and temperature extremes —exposure to toxic reactants —exposure to high shear or mechanical strain</i> <i>—exclusion of macromolecular substrates —blocking of the enzymatic active site —local pH shifts —mass transfer limitations</i>
LOSS OF BIOCATALYST ACTIVITY DURING BIOREACTOR OPERATION	—leakage of biocatalyst —matrix poisoning or fouling	<i>—matrix erosion or solubilisation —small support particles carried in the outflow —cell growth inside the matrix —broad pore-size range</i> <i>—build-up of inhibitors in the microenvironment —retention of suspended solids —growth of contaminating species (biofilms) —need for a stricter control of feed</i>

*composition*


---

EMPIRICISM	<ul style="list-style-type: none"> <li>—need for case specific, multi-parameter optimisation</li> <li>—difficult process modelling and control</li> </ul>
------------	---

---

The biocatalyst forms which can be immobilised range from purified enzymes to viable microbial cells and animal and plant tissues. Isolated enzymes can give high activity levels per unit mass or mole, high specificity, and minimum levels of side reactions. However they are often difficult and costly to prepare. They are, in addition, frequently unstable and in many cases require parallel cofactor regenerating systems. Due to their relatively simple chemical nature, as compared to organelles or whole cells, isolated or partially purified enzymes are the biocatalysts most extensively studied in relation to immobilisation. Such studies have led to most of the present knowledge of the nature of interactions between the biocatalysts and the attachment support or confinement barrier they have also contributed to an understanding of the origin of activity, specificity, or stability changes upon immobilisation, allowing the optimisation of process operating conditions. Immobilised, purified enzymes find suitable applications in developing biosensors and preparing high added-value substances, such as chiral compounds. In more crude forms, immobilised enzymes are also used in large scale applications in the carbohydrate, food and pharmaceutical industries.

Multienzyme systems, such as organelles, whole cells, or cell tissues, have some clear advantages over isolated enzymes, from the view point of immobilisation. Being already water-insoluble particles, they can be efficiently retained by mild, physical means, thus preserving, in adequate conditions, the enzyme synthesising and cofactor regenerating capabilities and providing a suitable microenvironment for single and multiple enzymatic activities. However, the efficient use of immobilised cells relies on the control of metabolic and physiological alterations throughout the retention procedure and the subsequent catalytic process. The major large-scale utilisations of immobilised cell systems take advantage of the natural tendency of many microbial species to flocculate or to adhere to solid surfaces. Other applications are restricted to single-enzyme transformations with non-growing cells in the manufacture of pharmaceuticals and amino acids.

### **Effect of Immobilisation on the Enzyme Kinetics and Properties**

Although enzyme immobilisation can be very useful, immobilisation may also change the kinetics and other properties of the enzyme, usually with a decrease of enzyme-specific activity. This may be ascribed to several factors:

- (i) Conformational and steric effects are present—even when the enzyme is bound without loss of activity—when conformational change of the enzyme molecule occurs by binding to a carrier or when the interaction of the substrate with the enzyme is affected by steric hindrance.

- (ii) Partitioning effects, related to the chemical nature of the support material, may arise from electrostatic or hydrophobic interactions between the matrix and low molecular weight species present in the solution, leading to a modified microenvironment.
- (iii) Mass transfer or diffusional effects arise from diffusional resistance to the translocation of substrate from the bulk solution to the catalytic sites and from the diffusion of products of the reaction back to the bulk solution. These diffusional resistances may be classified as internal or intraparticle mass transfer effects when the enzyme is located in a porous medium, and external or interparticle mass transfer effects when they occur between the bulk solution and the outer surface of the enzyme-matrix particle.

When the kinetic behaviour of immobilised enzyme can be controlled by one or more of the above effects, it is useful to distinguish among (i) intrinsic rate parameters, the kinetic parameters inherent in a particular immobilised enzyme and that are different from those of free enzyme (because of conformational change and steric effects); (ii) inherent rate parameters, the kinetic parameters that are observed in the absence of any diffusional effects; (iii) effective rate parameters, the kinetic parameters when mass transfer effects are present and in the presence or the absence of partition effects.

### *Conformational and steric effects*

The decrease of specific activity of enzymes, which occurs on their binding either to solid supports or upon intermolecular crosslinking, is usually attributed to conformational changes in the tertiary structure of the enzymes. For instance, co valent bonds between the enzyme and the matrix can stretch the enzyme molecule and thus the three-dimensional structure at the active site. The specific activity decrease may also be attributed to steric hindrance resulting in limits on the accessibility of the substrate. In these two cases the decrease in enzyme activity can be reduced or prevented by choosing suitable conditions for immobilisation. Thus the active center of the enzyme can be protected with a specific inhibitor, substrate, or product, and the shielding effect of the matrix that causes steric hindrances can be reduced by the introduction of "spacers" that keep the enzyme at a definite and certain distance from the matrix. In addition to these problems, denaturation of the enzyme can arise by the action of reagents used in entrapment methods.

In addition to their influence on the enzyme activity, any physical or chemical matrixenzyme interactions may additionally modify the selectivity and stability of the bound enzyme from that which it normally possesses in free solution.

### *Partition effects*

In the carrier binding method, when the support matrix is charged the kinetic behaviour of the immobilised enzyme may differ from that of the free enzyme even in the absence of mass transfer effects. This difference is commonly attributed to partition effects that cause different concentrations of charged species, substrates, products, hydrogen ions, hydroxyl ions, and so on, in the domain of the immobilised enzyme and in the domain of the bulk solution, owing to electrostatic interactions with fixed charges on the support.

These differences in the equilibrium concentrations of charged soluble compounds may be described by the partition coefficient,  $P$  given by

$$P = C_i/C_o \quad (1)$$

where  $C_i$  and  $C_o$  are the local and bulk concentrations, respectively.

The main consequences of these partition effects is a shift in the optimum pH, with a displacement of the pH-activity profile of the immobilised enzyme towards more alkaline or acidic pH values for negatively or positively charged carriers, respectively. Assuming the Boltzmann distribution, the partitioning of hydrogen ions between the local activity ( $a_i^{H+}$ ) and the bulk activity ( $a_o^{H+}$ ) is given by

$$P_{H^+} = a_i^{H+}/a_o^{H+} = \exp(-e\Psi/kT) \quad (2)$$

or by the definition of pH

$$\text{pH} = \text{pH}_i - \text{pH}_o = 0.43(-e\Psi/kT) \quad (3)$$

where  $e$  is the electronic charge,  $\psi$  is the electrostatic potential,  $k$  is the Boltzmann constant,  $T$  is the absolute temperature, and  $\text{pH}_i$  and  $\text{pH}_o$  are the local and the bulk pH values. This equation shows that the local pH is higher if the support is negatively charged.

By similar considerations, the partitioning of charged compounds, substrate or product, between a charged enzyme particle and the bulk solution can be represented in the following form:

$$S_i = S_o \exp(-Ze\Psi/kT) \quad (4)$$

where  $Ze$  is the substrate charge.

Thus for positively charged substrate, when using a negatively charged enzyme particle, a higher concentration of substrate is obtained in the local environment or microenvironment than in the bulk solution, and a higher value of relative activity is obtained than with a neutrally charge matrix. However, when effects other than partitioning are present, it is possible to have no shift of the enzyme's pH optimum on charged supports.

### ***External mass transfer effects***

When a biocatalyst is immobilised on or within a solid matrix, mass transfer effects may exist because the substrate must diffuse from the bulk solution to the active site of the immobilised biocatalyst. If the biocatalyst is attached to nonporous carriers there are only external mass transfer effects on the catalytically active outer surface; in the reaction solution, being surrounded by a stagnant film, substrate and product are transported across the Nernst layer by diffusion. The driving force for this diffusion is the

concentration difference between the surface and the bulk concentration of substrate and product.

For instance, the rate of flow of substrate  $r_{\text{dif}}$  from the bulk solution to the biocatalyst surface is given by

$$r_{\text{dif}} = k_L^S a (S_B - S_s) \quad (5)$$

where  $k_L^S$  is the substrate mass transfer coefficient;  $a$  is the particle surface area per unit volume, and  $S_B$  and  $S_s$  are the bulk and surface concentrations of the substrate respectively. In a surface reaction, the flow of substrate to the biocatalyst surface and the biocatalytic reaction take place consecutively. At steady state the rate of external mass transfer of substrate,  $r_{\text{dif}}$ , will be equal to its removal by reaction. Hence, the overall rate of reaction,  $r_{\text{obs}}$ , will be

$$r_{\text{obs}} = r_{\text{dif}} = r(S_s, P_s) \quad (6)$$

where  $r(S_s, P_s)$  is the reaction rate for the immobilised biocatalyst and  $P_s$  is the surface concentration of the product.

Consider the reaction  $S \rightarrow vP$ , where  $v$  is the stoichiometric coefficient relating substrate and product. In the case of steady state behaviour, no accumulation of substrate or product in the stagnant film occurs. Thus,

$$v k_L^S a (S_B - S_s) = k_L^P a (P_s - P_B) \quad (7)$$

where  $P_B$  is the bulk concentration of the product and  $k_L^P$  is the product mass transfer coefficient.

Rearranging this equation and defining a transport parameter as  $\xi = k_L^S/k_L^P$  results in an expression for the product concentration at the surface of the support:

$$P_s = P_B + v\xi (S_B - S_s) \quad (8)$$

which can be substituted in the expression for  $r(S_s, P_s)$  to obtain an equation with  $S_s$  as the only unknown.

The kinetics of biocatalytic irreversible reactions may include substrate inhibition, like the -carboxybenzylpenicillin towards the  $\beta$ -lactamase enzyme produced by *Pseudomonas aeruginosa* (Fullbrook 1983); competitive product inhibition, as L-DOPA inhibition of the tyrosinase ortho-hydroxylation of L-tyrosine (Pialis and Saville, 1998); non-competitive product inhibition like the cellobiose and glucose inhibition of cellulase (Fan and Lee, 1983); and simultaneous substrate and competitive product inhibition, as the case of sucrose hydrolysis by invertase (López-Santín *et al.*, 1982). All cases can be expressed by a Michaelis-Menten type equation and  $r(S_s, P_s)$  can be defined as

$$\frac{r(S_s, P_s)}{r_{\max}} = \frac{\beta_s}{\alpha_0 + \alpha_1 \beta_s + \alpha_2 \beta_s^2} \quad (9)$$

where  $r_{\max}$  is the maximum reaction rate,  $\beta_S$  is the dimensionless substrate surface concentration ( $\beta_S = S_S/K_m$ ) and  $\alpha_0$ ,  $\alpha_1$  and  $\alpha_2$  are kinetic constants, the expressions of which are given in Table 4.2.

Thus substituting equations (5) and (9) in equation (6) yields an expression for the overall rate of reaction,  $r_{\text{obs}}$ :

$$\frac{r_{\text{obs}}}{r_{\max}} = \frac{\beta_B - \beta_S}{\mu} = \frac{\beta_S}{\alpha + \alpha_1 \beta_S + \alpha_2 \beta_S^2} \quad (10)$$

where  $\mu$  is the dimensionless substrate modulus ( $\mu = r_{\max}/k_L^S a K_m$ ), from which the dimensionless substrate concentration at the support surface,  $\beta_S$ , can be calculated.

The dependence of  $r_{\text{obs}}/r_{\max}$  on  $\beta_B$  for different values of  $\mu$  is shown in Figure 4.1 for the case of Michaelis-Menten kinetics. Similar plots have been obtained by other authors (Horvath and Engasser, 1974).

When the kinetic constant  $\alpha_2$  is not equal to zero, equation (10) leads to a third-order polynomial. In the acceptable domain of  $0 < \beta_S < \beta_B$  three different values satisfy equation (10) at certain values of  $\beta_B$  and  $\mu$ . The possibility of multiple steady states is illustrated by Figure 4.2 where both the rate of surface reaction and the transport rate of the substrate are plotted against  $\beta_S$ . As the two rates are equal at steady state, the intersections of the two curves yield the possible substrate surface concentrations that comply with equation (10). For a Michaelis-Menten kinetics ( $\alpha_2=0$ ) there is only one solution in the acceptable domain, but for certain values of  $\alpha_2$ ,  $\mu$  and  $\beta_B$ , there can be up to three different mathematical solutions for  $\beta_S$ . Figure 4.2 shows a situation with three possible solutions  $\beta_{S1}$ ,  $\beta_{S2}$  and  $\beta_{S3}$ . The stability of the rate at  $\beta_{S1}$  can be established by considering a small increase in the surface concentration (Moo-Young and Kobayashi,

**Table 4.2** Expressions for reaction rates and coefficients  $\alpha_0$ ,  $\alpha_1$  and  $\alpha_2$  accounting for external or internal mass transfer effects. When accounting for external mass transfer effects the transport parameter is given by  $\xi = k_L^S/k_L^P$  and  $S_L=S_B$  and  $P_L=P_B$ . When accounting for internal mass transfer effects the transport parameter is given by  $\xi = D_e^S/D_e^P$  and  $S_L=S_S$  and  $P_L=P_S$ .  $K_S$  and  $K_P$  are the substrate and product inhibition constants, respectively.

*Michaelis-Menten kinetics:*

$$\frac{r(S)}{r_{\max}} = \frac{S}{K_m + S}$$

$$\alpha_0 = 1 \quad \alpha_1 = 1 \quad \alpha_2 = 0$$

*Substrate inhibition:*

$$\frac{r(S)}{r_{\max}} = \frac{S}{K_m + S + S^2/K_S}$$

$$\alpha_0 = 1 \quad \alpha_1 = 1 \quad \alpha_2 = K_m/K_S$$

Competitive product inhibition:

$$\frac{r(S, P)}{r_{\max}} = \frac{S}{K_m(1 + P/K_p) + S}$$

$$\alpha_0 = 1 + \frac{v}{K_p} \left( \frac{P_L}{v} + \xi S_L \right) \quad \alpha_1 = 1 - v\xi \frac{K_m}{K_p} \quad \alpha_2 = 0$$

Non-competitive product inhibition:

$$\frac{r(S, P)}{r_{\max}} = \frac{S}{(S + K_m)(1 + P/K_p)}$$

$$\alpha_0 = 1 + \frac{v}{K_p} \left( \frac{P_L}{v} + \xi S_L \right) \quad \alpha_1 = \alpha_0 + \alpha_2 \quad \alpha_2 = -v\xi \frac{K_m}{K_p}$$

Substrate inhibition and competitive product inhibition:

$$\frac{r(S, P)}{r_{\max}} = \frac{S}{K_m(1 + P/K_p) + S + S^2/K_S}$$

$$\alpha_0 = 1 + \frac{v}{K_p} \left( \frac{P_L}{v} + \xi S_L \right) \quad \alpha_1 = 1 - v\xi \frac{K_m}{K_p} \quad \alpha_2 = K_m/K_S$$

Reversible Michaelis-Menten Kinetics:

$$\frac{r(S, P)}{r_{\max}} = \frac{(S - S_{eq})}{K_m + (S - S_{eq})}, \quad S > S_{eq} = \frac{S + P}{1 + K_{eq}}$$

$$\alpha_0 = K_{eq} + \xi \quad \alpha_1 = \frac{P_L + \xi S_L}{K_m} \quad \alpha_2 = \alpha_1 - (1 + K_{eq})$$


---

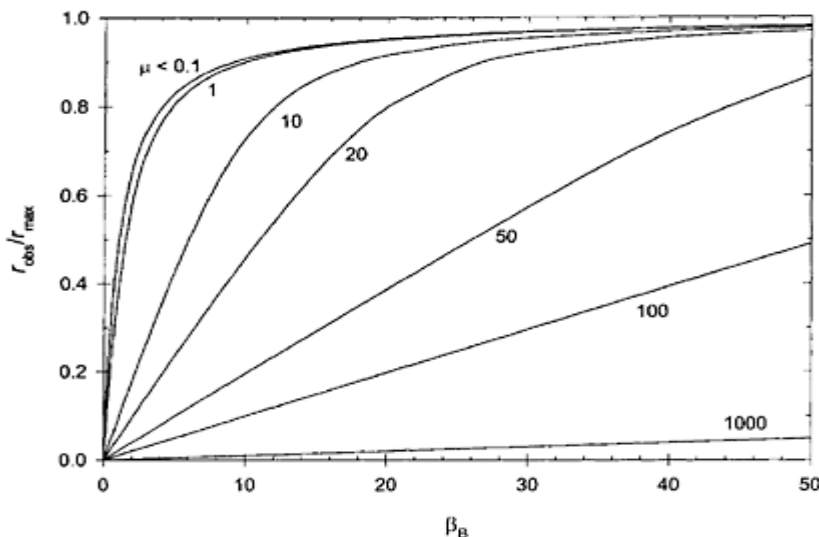


**Figure 4.1**  $r_{obs}/r_{\max}$  against the dimensionless bulk concentration  $\beta_B$

for different values of substrate modulus  $\mu$  for external diffusion.

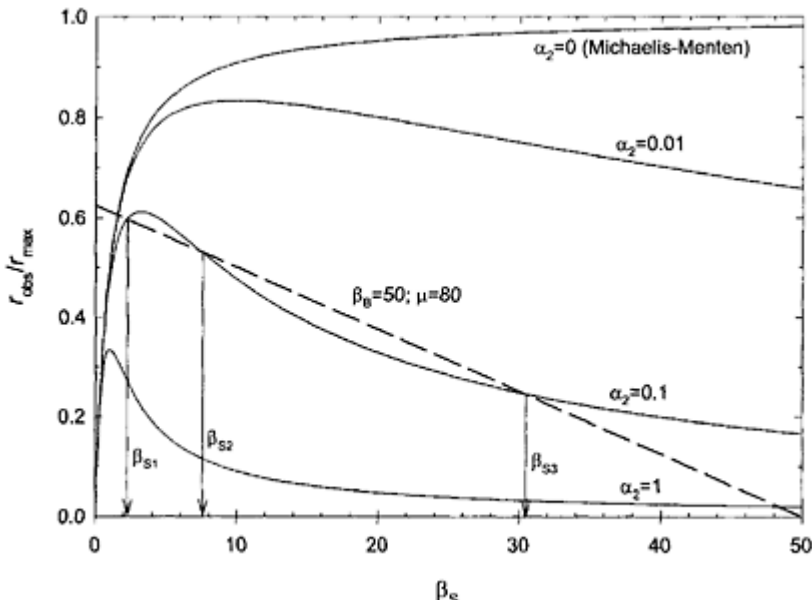


**Figure 4.2** Rate of the inhibited biocatalytic reaction, with  $\alpha_0=1$  and  $\alpha_1=1$ , (solid lines) and of the substrate transport (dashed line) as a function of the dimensionless substrate concentration at the biocatalyst surface for different  $\alpha_2$  values. Three steady-states of the overall reaction are possible for some values of  $\beta_B$ ,  $\mu$  and  $\alpha_2$  at  $\beta_{S1}$  and,  $\beta_{S2}$  and  $\beta_{S3}$ .

1972). The response of the system to this perturbation will be an increase of the substrate consumption rate while the diffusion rate, that is, the rate of substrate supply to the surface, decreases. Since both effects tend to decrease  $\beta_S$ , the surface concentration will return to  $\beta_{S1}$ . Therefore, the rate at  $\beta_{S1}$  is stable and can occur in practice. At  $\beta_{S2}$  both the diffusion and reaction rates decrease when  $s$  is slightly increased. However, the decrease in the reaction rate is greater than that in the diffusion rate resulting in a further increase of the surface concentration and the system does not return to  $\beta_{S2}$ , which is consequently unstable. Similar considerations show that the rate at  $\beta_{S3}$  is stable.

The rate of flow of substrate,  $r_{\text{dif}}$ , or the rate of biocatalytic reaction,  $r_{\text{kin}}$ , may play predominant roles, depending on their relative magnitudes, as the lower step will be the controlling step. As it can be seen from Figure 4.3 for a Michaelis-Menten kinetics, at high bulk substrate concentrations when the reaction is zero order,  $r_{\text{obs}}$  will always be equal to  $r_{\text{max}}$  and the reaction will be kinetically controlled. At lower bulk substrate concentrations the reaction can be both kinetically or diffusionaly controlled, depending on the substrate modulus,  $\mu$ . At low  $\mu$ , when  $k_L^S a \gg r_{\text{max}}/K_m$ , mass transfer is much faster than the biocatalytic reaction, but at high  $\mu$ , when  $k_L^S a \ll r_{\text{max}}/K_m$ , the biocatalytic reaction is much faster than the diffusion of substrate.

Figure 4.4 shows what happens for an inhibition kinetics. Again, the reaction can be both kinetically or diffusionaly controlled, depending on the substrate modulus,  $\mu$ . However, a major difference from Michaelis-Menten kinetics is that from a certain bulk

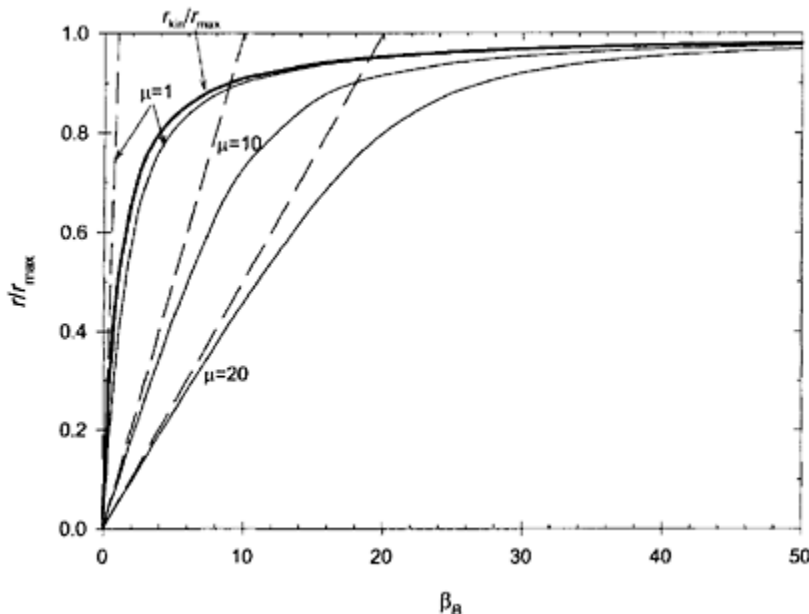


**Figure 4.3** Roles of the rate of flow of substrate,  $r_{\text{dif}}$ , and the rate of enzyme reaction,  $r_{\text{kin}}$ , on the observed reaction rate,  $r_{\text{obs}}$ , as function of the substrate modulus for a Michaelis-Menten kinetics. The heavy solid line refers to  $r_{\text{kin}}/r_{\text{max}}$ ; the light solid lines refer to  $r_{\text{obs}}/r_{\text{max}}$  and the broken lines refer to  $r_{\text{dif}}/r_{\text{max}}$ .

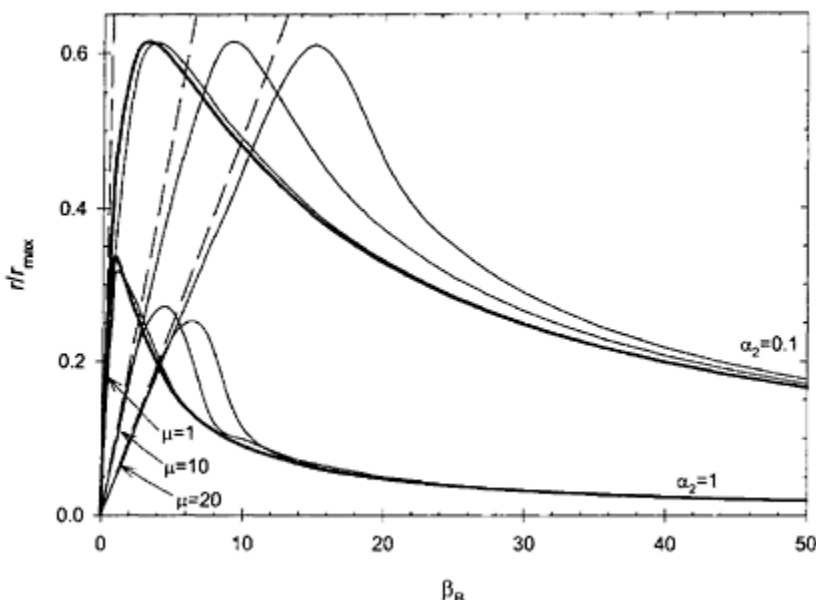


**Figure 4.4** Roles of the rate of flow of substrate,  $r_{\text{dif}}$ , and the rate of enzyme reaction,  $r_{\text{kin}}$ , on the observed reaction rate,  $r_{\text{obs}}$ , as function of the substrate modulus and  $\alpha_2$ , for an inhibition Michaelis-Menten kinetics where  $\alpha_0=1$  and  $\alpha_1=1$ . The heavy solid line refers to  $r_{\text{kin}}/r_{\text{max}}$ ; the light solid lines refer to  $r_{\text{obs}}/r_{\text{max}}$  and the broken lines refer to  $r_{\text{dif}}/r_{\text{max}}$ .

substrate concentration, the observed rate is higher than the expected rate of the biocatalytic reaction,  $r_{\text{kin}}$ . This happens since the surface substrate concentration is lower than the bulk substrate concentration, thus resulting in a smaller inhibition effect.

The enzymatic isomerization of glucose into fructose is probably the most successful industrial application of immobilised enzyme technology (Olsen, 1995). This reaction can be described by a reversible form of Michaelis-Menten kinetics (Lee *et al.*, 1976) which does not fit the general equation (9). Considering the reversible reaction  $S \leftrightarrow P$ , the rate expression will be

$$\frac{r(S, P)}{r_{\text{max}}} = \frac{(S - S_{\text{eq}})}{K_m + (S - S_{\text{eq}})} \quad (11)$$

where  $S_{\text{eq}}$  is the substrate concentration at equilibrium, given by

$$S_{\text{eq}} = \frac{S + P}{1 + K_{\text{eq}}} \quad (12)$$

where  $K_{\text{eq}}$  is the equilibrium constant for reversible Michaelis-Menten kinetics. Substituting (12) and (8) in (11) and considering  $v=1$ , the dimensionless balance for reaction and diffusion of substrate becomes

$$\frac{r(S, P)}{r_{\max}} = \frac{\alpha_0 \beta_S - \alpha_1}{\alpha_0 \beta_S - \alpha_2} \quad (13)$$

where  $\alpha_0, \alpha_1$  and  $\alpha_2$  are kinetic constants, the expressions of which are given in Table 4.2. The condition  $S > S_{\text{eq}}$  in dimensionless form is  $\beta > \alpha_1/\alpha_0$ . Thus, the expression for the overall rate of reaction,  $r_{\text{obs}}$ , for reversible Michaelis-Menten kinetics is

$$\frac{r_{\text{obs}}}{r_{\max}} = \frac{\beta_B - \beta_S}{\mu} = \frac{\alpha_0 \beta_S - \alpha_1}{\alpha_0 \beta_S - \alpha_2} \quad (14)$$

An adequate method to describe the influence of diffusional resistance on the observed reaction rate is to use the concept of effectiveness factors. The external mass transfer effects on the activity of an immobilized biocatalyst can be quantitatively expressed by the effectiveness factor  $\eta_{\text{ext}}$ , defined as the ratio of the observed reaction rate  $r_{\text{obs}}$  to the kinetic rate calculated with bulk concentrations  $r_{\text{kin}} = r(S_B, P_B)$

$$\eta_{\text{ext}} = \frac{r_{\text{obs}}}{r(S_B, P_B)} \quad (15)$$

Figure 4.5 shows the dependence of the effectiveness factor  $\eta_{\text{ext}}$  on  $\beta_B$  and  $\mu$  for Michaelis-Menten kinetics. For inhibition-type kinetics, the increase in rate caused by the decreasing substrate inhibition towards the center of the catalyst particle can be greater than the decrease in rate caused by the drop in concentration. This can cause the effectiveness factor to exceed unity, as shown by Figure 4.6.

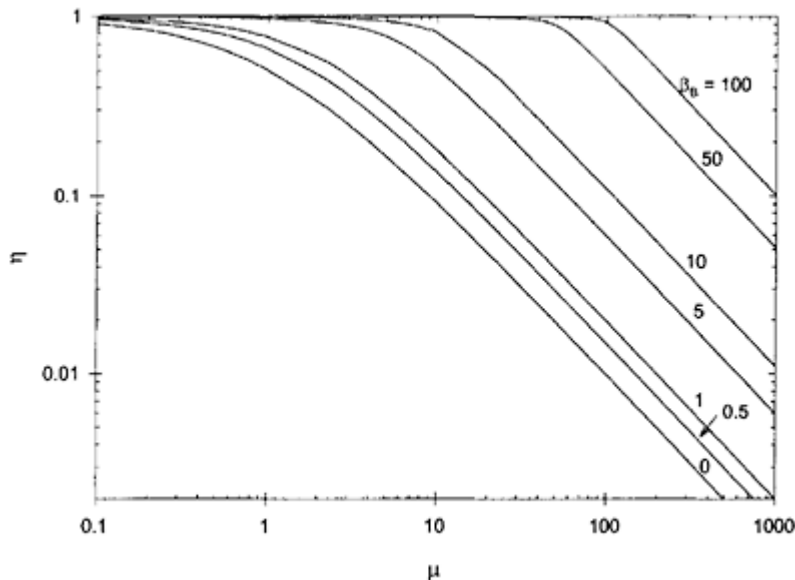


**Figure 4.5** Effectiveness factor  $\eta_{\text{ext}}$  against the substrate modulus  $\mu$  for external diffusion for different values of the dimensionless bulk concentration  $\beta_B$ .

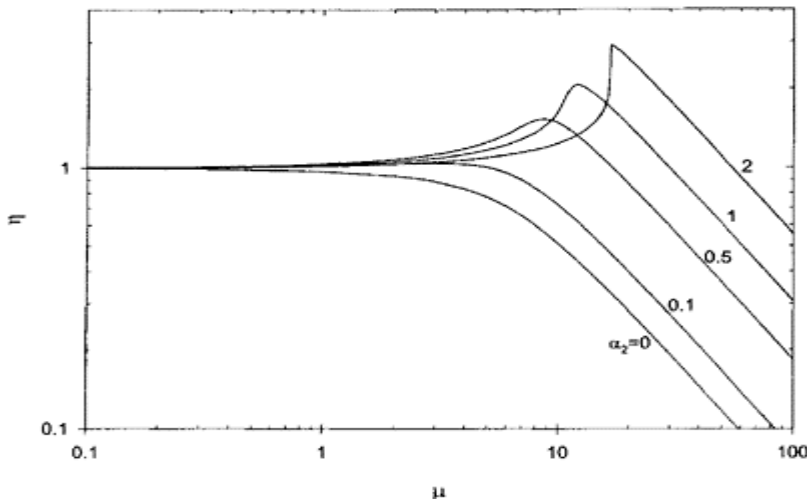


**Figure 4.6** Effectiveness factor  $\eta_{\text{ext}}$  against the substrate modulus  $\mu$  for

external diffusion with  $\beta_B=5$ ,  $\alpha_o=1=1$   
and for  $\alpha_1$  different of  $\alpha_2$ .

### ***Internal mass transfer effects***

When a biocatalyst is immobilized within a porous support, in addition to possible external mass transfer effects there could also exist resistances to internal diffusion of substrate, as this must diffuse through the pores in order to reach the biocatalyst, and product, as it must diffuse to the bulk solution. Consequently a substrate concentration gradient is established within the pores, resulting in a concentration decrease with increased distance (in depth) from the surface of immobilised biocatalyst preparation. A corresponding product concentration gradient is obtained in the opposite direction.

Unlike external diffusion, internal mass transfer proceeds in parallel with the biocatalytic reaction and takes into account the depletion of substrate within the pores with increasing distance from the surface of the biocatalyst support. The rate of reaction will also decrease, for the same reason. The overall reaction is dependent on the substrate concentration and the distance from the outside support surface.

The usual way to study this problem is by considering that there is a coupled reaction-diffusion process that can be solved, at the steady state, when the rates of internal diffusion and biocatalytic reaction are equal. Prior to modelling the immobilised biocatalyst system, the following assumptions are made:

1. The biocatalyst is uniformly immobilised inside the particle;
2. The reaction occurs at every position within the immobilised biocatalyst;
3. The reaction has one rate-limiting substrate;
4. The reaction is isothermal and intraparticle pressure gradients are negligible;
5. Mass transfer through the immobilised biocatalyst occurs via diffusion and is represented by Fick's law;
6. There is no partitioning of both substrate and product between the exterior and interior of the support;
7. There is no interaction between substrate and product;
8. There is no preferential adsorption of substrate or product on the immobilisation matrix.

The mass balance (Smith, 1981) obtained for various geometries is:

$$D_e^S \left( \frac{d^2 S}{dx^2} + \frac{p + 1 dS}{x dx} \right) = r(S, P) \quad (16)$$

where  $x$  is the distance from the outer surface;  $p$  is a geometrical factor with the values of +1 for spherical pellets, 0 for cylindrical pellets, and -1 for rectangular membranes;  $r(S, P)$  is the reaction rate; and  $D_e^S$  is the effective diffusivity of the substrate inside the support, given by:

$$D_e^S = D^S \varepsilon / \tau \quad (17)$$

where  $D^S$  is the substrate diffusivity;  $\varepsilon$  is the void fraction in the porous matrix; and  $\tau$  is a tortuosity factor that takes into account the pore geometry and by definition is larger than unity.

Considering, again, the reaction  $S \rightarrow vP$ , at steady state behaviour, no accumulation of substrate or product within the support occurs. Thus,

$$vD_e^S(S_S - S) = D_e^P(P - P_S) \quad (18)$$

Rearranging this equation and defining the transport parameter as  $\xi = D_e^S / D_e^P$  results in an expression for the local product concentration:

$$P = P_S + v\xi(S_S - S) \quad (19)$$

which can be substituted in the expression for  $r(S, P)$  in equation (13) to obtain an equation in terms of  $S$  only.

As for the case of external mass transfer limitation, the rate of Michaelis-Menten type reactions can be defined as:

$$\frac{r(S, P)}{r_{\max}} = \frac{\beta}{\alpha_0 + \alpha_1\beta + \alpha_2\beta^2} \quad (20)$$

where  $\beta$  is the dimensionless substrate concentration ( $\beta = S/K_m$ ) and  $\alpha_0$ ,  $\alpha_1$  and  $\alpha_2$  are kinetic constants, the expressions of which are given in Table 4.2.

The solution of equation (16) gives the concentration profile of the substrate, which allows the calculation of the overall reaction rate within the immobilisation support. The analytical solutions of these equations are easily obtained for first-order or zero order reactions, but numerical solutions are required for Michaelis-Menten type reactions. The above equations, in these cases, are usually rewritten in terms of dimensionless variables:

$$\frac{d^2\beta}{dz^2} + \frac{p+1}{z} \frac{d\beta}{dz} = \Phi^2 \frac{\beta}{\alpha_0 + \alpha_1\beta + \alpha_2\beta^2} \quad (21)$$

In this equation  $z$  is the dimensionless position in the porous support, given by  $z=x/L$  where  $L$  is the characteristic length of the support particle (the radius of a spherical or a cylindrical pellet or the thickness or half-thickness of a rectangular membrane for asymmetric and symmetric boundary conditions, respectively).  $\Phi$  is the Thiele modulus for the substrate defined by:

$$\Phi = L \sqrt{\frac{r_{\max}}{K_m D_e^S}} \quad (22)$$

Most authors use different definitions for the Thiele modulus depending on the geometry of the support leading to some confusion when interpreting and using the graphs thereby derived (Aris, 1957; Moo-Young and Kobayashi, 1972; Smith, 1981). For generalisation and clarification purposes we chose to use the definition above regardless the geometry of the support.

For reversible Michaelis-Menten kinetics, equation (21) becomes:

$$\frac{d^2\beta}{dz^2} + \frac{p+1}{z} \frac{d\beta}{dz} = \Phi^2 \frac{\alpha_0\beta - \alpha_1}{\alpha_0\beta - \alpha_2} \quad (23)$$

The boundary conditions for the solution of equations (21) and (23) are:

$$\beta = \beta_S \quad \text{for } z = 1 \quad (24)$$

$$\frac{d\beta}{dz} = 0 \quad \text{for } z = 0 \quad (25)$$

The effectiveness factor for internal mass transfer effects is defined as the ratio between the overall rate of substrate consumption inside the particle  $r_{\text{overall}}(S)$ , and the rate evaluated for the surface concentration of the substrate,  $r(S_S)$ . At steady state the substrate does not accumulate inside the support particle, thus:

$$r_{\text{overall}}(S) \cdot V_p = J \quad (26)$$

where  $V_p$  is the catalyst particle volume and  $J$  is the diffusive flow of substrate at the support surface given by Fick's law:

$$J = A \cdot D_e^S \left. \frac{dS}{dx} \right|_{z=L} \quad (27)$$

where  $A$  is the superficial area of the catalyst. Thus, the effectiveness factor will be given as:

$$\eta_{\text{int}} = \frac{A \cdot D_e^S \left. \frac{dS}{dx} \right|_{z=L}}{V_p \cdot r(S_S)} \quad (28)$$

or, in a dimensionless form:

$$\eta_{\text{int}} = \frac{\frac{A}{V_p} \cdot D_e^S \left. \frac{K_m}{L} \frac{d\beta}{dz} \right|_{z=1}}{r_{\max} \frac{\beta_S}{\alpha_0 + \alpha_1 \beta_S + \alpha_2 \beta_S^2}} \quad (29)$$

It can be easily shown that,

$$\frac{A}{V_p} = \frac{p+2}{L} \quad (30)$$

thus substituting this in equation (29) yields:

$$\eta_{\text{int}} = \frac{(p+2) \left. \frac{d\beta}{dz} \right|_{z=1}}{\Phi^2 \cdot \frac{\beta_S}{\alpha_0 + \alpha_1 \beta_S + \alpha_2 \beta_S^2}} \quad (31)$$

For reversible Michaelis-Menten kinetics the effectiveness factor expression becomes:

$$\eta_{\text{int}} = \frac{(p+2) \frac{d\beta}{dz} \Big|_{z=1}}{\Phi^2 \cdot \frac{\alpha_0 \beta_S - \alpha_1}{\alpha_0 \beta_S - \alpha_2}} \quad (32)$$

Figure 4.7 shows the normalised observed reaction rate as a function of the dimensionless surface concentration of the substrate,  $\beta_S$ , and the Thiele modulus for Michaelis-Menten kinetics and spherical particles. The dependence of the effectiveness factor  $\eta_{\text{int}}$  as a function of the dimensionless surface concentration of the substrate and the Thiele modulus is shown on Figure 4.8 for Michaelis-Menten kinetics and for spherical particles and rectangular membranes.

The mathematics involved in the numerical methods force many enzymologists to still use the charts derived from Horvath and Engasser's pioneer work (Horvath and Engasser, 1974). However, this often leads to inaccurate results.

More or less complex numerical integration techniques such as Runge-Kutta integration and orthogonal collocation have been suggested to solve equation (16) (Villadsen and Stewart 1967, Vos *et al.*, 1990). Furthermore, another problem arises when the numerical methods are applied with boundary condition (25) due to the 0/0 undetermination that occurs at the center of a spherical or cylindrical particle (Oliveira, 1999).

Following, the method of the finite differences is used to solve equation (21). The particle is divided into  $n$  layers and the first and second derivatives are replaced by their finite difference analogues:

$$\frac{d^2\beta}{dz^2} = \frac{\beta_{i-1} - 2\beta_i + \beta_{i+1}}{\Delta z^2} \quad (33)$$

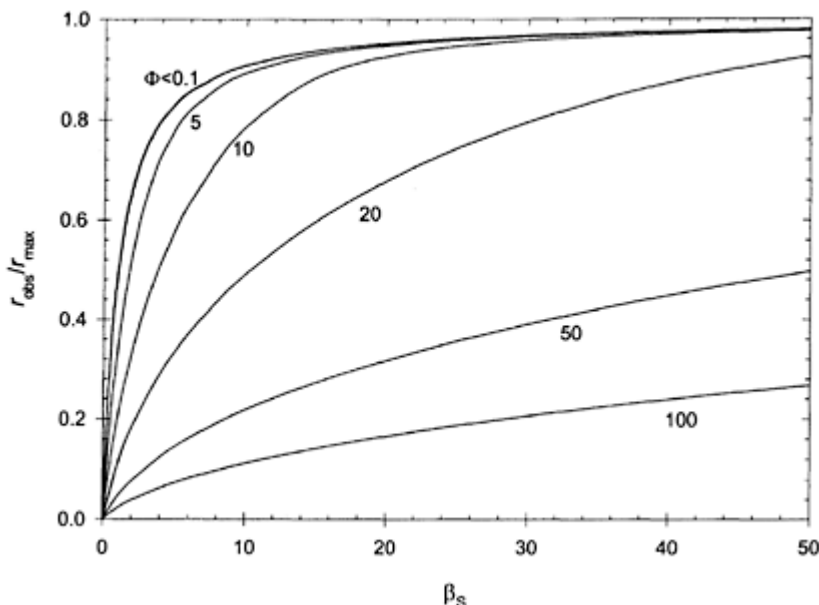


**Figure 4.7** Normalised  $r_{\text{obs}}$  as a function of the dimensionless surface concentration of the substrate  $\beta_s$  with the Thiele modulus  $\Phi$  for Michaelis-Menten kinetics and spherical particles.

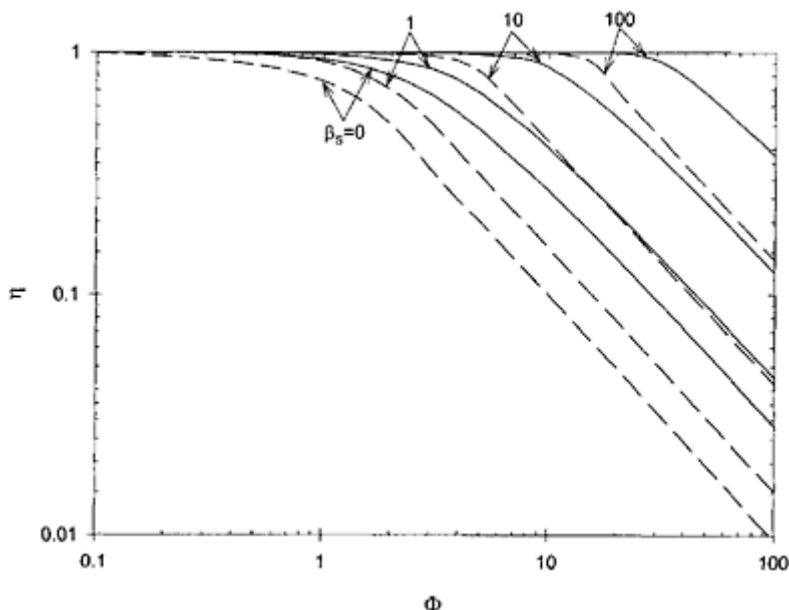


**Figure 4.8** Effectiveness factor  $\eta_{\text{int}}$  for Michaelis-Menten kinetics as a function of the Thiele modulus  $\Phi$  with the dimensionless surface concentration  $\beta_s$  as the parameter. The effectiveness factor for spherical particles and membranes is represented by solid and broken lines respectively.

$$\frac{d\beta}{dz} = \frac{\beta_{i+1} - \beta_{i-1}}{2\Delta z} \quad (34)$$

where  $\Delta z = 1/n$  and  $i$  is an index which varies from 1 to  $n-1$ . Substituting (33) and (34) in equation (21) yields:

$$\frac{\beta_{i-1} - 2\beta_i + \beta_{i+1}}{\Delta z^2} + \frac{p+1}{z_i} \frac{\beta_{i+1} - \beta_{i-1}}{2\Delta z} = \Phi^2 \frac{\beta_i}{\alpha_0 + \alpha_1 \beta_i + \alpha_2 \beta_i^2} \quad (35)$$

Noting that  $z_i = i \cdot \Delta z$ , equation (35) gives:

$$\beta_{i+1} = \left( \Phi^2 \frac{\Delta z^2}{\alpha_0 + \alpha_1 \beta_i + \alpha_2 \beta_i^2} + 2 \right) \left( \frac{2i}{p+1+2i} \right) \beta_i + \left( \frac{p+1-2i}{p+1+2i} \right) \beta_{i-1} \quad (36)$$

This simple transformation allowed elimination of the 0/0 undetermination.

Analogously, for the case of reversible Michaelis-Menten kinetics:

$$\beta_{i+1} = \left( \Phi^2 \Delta z^2 \frac{\alpha_0 \beta_i - \alpha_1}{\alpha_0 \beta_i - \alpha_2} + 2\beta_i \right) \left( \frac{2i}{p+1+2i} \right) + \left( \frac{p+1-2i}{p+1+2i} \right) \beta_{i-1} \quad (37)$$

To better understand this equation, we can think of a spherical catalyst particle made of  $n$  concentric layers, like an onion. Layer 0 is the core of the particle, while layer  $n$  is the surface layer of the catalyst particle.

Taking into account the boundary condition (25), it can be assumed that  $\beta_1 \approx \beta_0$  provided that  $\Delta z \rightarrow 0$ . Thus, from  $\beta_0$  and  $\beta_1$  it is possible to calculate  $\beta_2$ , and from this and  $\beta_1$ , we can compute  $\beta_3$ , and so forth, until reaching  $\beta_n$ . Since the substrate concentration at layer 0,  $\beta_0$ , is unknown, the method consists of guessing this concentration and then computing the successive  $\beta_i$  values until obtaining  $\beta_n$ , which must be equal to  $\beta_s$ , according to the boundary condition (24).

Such a procedure can be implemented in any spreadsheet software or easily programmed in any language.

The derivative term of equations (31) and (32) is computed from a finite difference and the boundary condition (24):

$$\left. \frac{d\beta}{dz} \right|_{z=1} = \frac{\beta_n - \beta_{n-1}}{\Delta z} = \frac{\beta_S - \beta_{n-1}}{\Delta z} \quad (38)$$

To test the accuracy of the proposed method we have used it with a first-order kinetics ( $\alpha_0=1$ ,  $\alpha_1=0$  and  $\alpha_2=0$ ) and compared the obtained results with the analytical solution to the problem. It was observed that the accuracy of the proposed method depends on both the number of “slices” in which we divide the catalyst particle and on the Thiele modulus, as shown on Figure 4.9.

### ***Combined external and internal mass transfer effects***

When external and internal diffusion resistances simultaneously affect the rate of the enzymic reaction, the relative contributions of each effect must be estimated separately and quantified by the corresponding effectiveness factors. Hence the total effectiveness factor is given by:

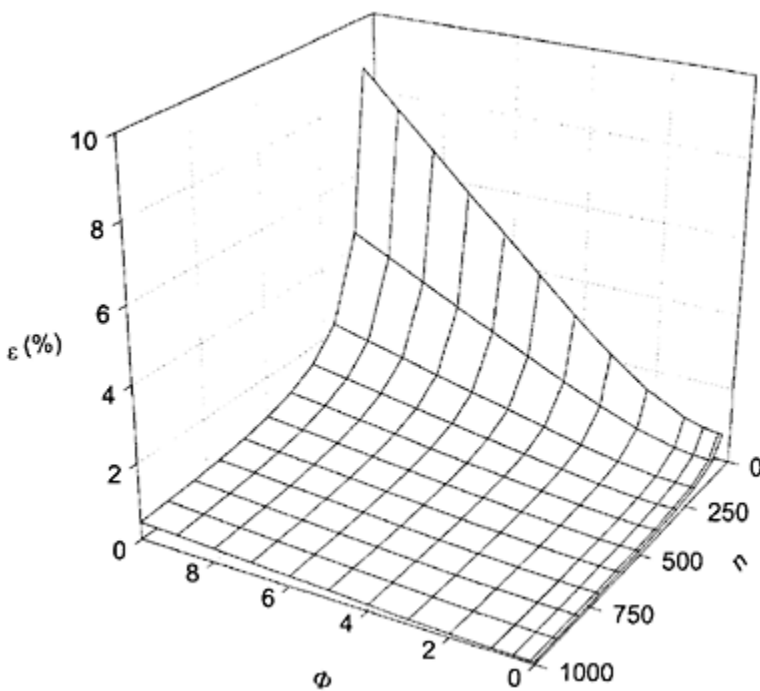


**Figure 4.9** Effects of  $v$  and  $\Phi$  on the accuracy of the proposed method for the calculation of the internal mass transfer effectiveness factor for a spherical catalyst and a 1st order kinetics.

$$\eta_T = \eta_{\text{ext}} \cdot \eta_{\text{int}} \quad (39)$$

where  $\eta_{\text{ext}}$  and  $\eta_{\text{int}}$  are the effectiveness factors when only external and internal diffusion resistances occur respectively.

Another way to calculate  $\eta_T$  is to use equation (21). However, the boundary condition (25) is no longer valid since the substrate concentration at the surface of the support is different from the bulk substrate concentration due to the external diffusional resistances. Under steady state conditions, the flux of substrate through the support surface per unit of support surface area equals that through the outer diffusion layer. Thus, the correct boundary condition is expressed as:

$$D_e^S \frac{dS}{dx} \Big|_{x=1} = k_L^S (S_B - S_S) \quad (40)$$

By using dimensionless variables, this equation yields:

$$\frac{d\beta}{dz} = Bi(\beta_B - \beta_S) \quad (41)$$

where  $Bi$  is the Biot number ( $Bi = k_L^s L / D_e^s$ ). The solution of equation (21) with (24) and (41) as boundary conditions gives the dimensionless concentration profile of the substrate, from which the total effectiveness factor can be calculated.

### ***Miscellaneous effects***

Apart from the influence of these factors on the activity of the enzyme, other properties of the enzyme can change. Thus substrate specificity alters, particularly when using a high molecular weight substrate, by effect of steric hindrance and diffusional resistances. The kinetic constants  $K_m$  and  $r_m$  of the immobilised enzyme are different from the free enzyme as a consequence of conformational changes of the immobilised form, which affect the affinity between enzyme and substrate. The increase of activity energy for some immobilised enzymes may be attributed to diffusional resistances, mainly in porous supports.

One of the major properties of the immobilised enzymes is their stability, especially the operational stability. This enhanced stability is particularly valuable in the continuous use of immobilised enzymes, in industrial operations.

Such increased stability has been observed in many cases, although a decreased stability has been observed in a few systems.

## **IMMOBILISED ENZYME REACTORS**

Among the applications of immobilised enzymes, their utilisation in industry is perhaps the most important and consequently the most frequently discussed.

The use of immobilised enzymes in industrial processes is performed in basic chemical reactors. A classification of enzyme reactor based on the mode of operation and the flow characteristics of substrate and product is presented in Table 4.3.

**Table 4.3** Classification of enzyme reactors

Mode of operation	Flow pattern	Type of reactor
Batch	Well mixed	Batch stirred tank reactor (BSTR)
	Plug flow	Total recycle reactor
Continuous	Well mixed	Continuous stirred tank reactor (CSTR) CSTR with continuous ultrafiltration membrane
	Plug flow	Packed bed reactor (PBR) Fluidized bed reactor (FBR) Tubular reactor (other) Hollow fiber reactor

## Batch Reactors

Batch reactors are the most commonly used type of reactor when soluble enzymes are used as catalysts. The soluble enzymes are not generally separated from the products and consequently are not recovered for reuse.

Since one of the main goals of immobilising an enzyme is to permit its reuse, the application of immobilised enzymes in batch reactors requires a separation (or an additional separation) to recover the enzyme preparation. During this recovery process, appreciable loss of immobilised enzyme material may occur as well as loss of enzyme activity, therefore the use of immobilised enzymes in a batch operation is generally limited to the production of rather small amounts of fine chemicals. Traditionally, the stirred tank reactor has been used for batchwise work. Composed of a reactor and a stirrer, it is the simplest type of reactor that allows good mixing and relative ease of temperature and pH control. However, some matrices, such as inorganic supports, are broken up by attrition in such vessels, and alternative designs have therefore been attempted. A possible laboratory alternative is the basket reactor, in which the catalyst is retained within a "basket" either forming the impeller "blades" or the baffles of the tank reactor.

Another alternative is to change the flow pattern, using a plug flow type of reactor: the total recycle reactor or batch recirculation reactor, which may be a packed bed or fluidised bed reactor, or even a coated tubular reactor.

This type of reactor may be useful where a single pass gives inadequate conversions. However, it has found greatest application in the laboratory for the acquisition of kinetic data, when the recycle rate is adjusted so that the conversion in the reactor is low and it can be considered as a differential reactor. One advantage of this type of reactor is that the external mass transfer effects can be reduced by the operational high fluid velocities.

## Continuous Reactors

The continuous operation of immobilised enzymes has some advantages when compared with batch processes, such as ease of automatic control, ease of operation, and quality control of products.

Continuous reactors can be divided into two basic types: the continuous feed stirred tank reactor (CSTR) and the plug flow reactor (PFR).

In the ideal CSTR the conversion degree is independent of the position in the vessel, as a complete mixing is obtained with stirring and the conditions within the CSTR are the same as the outlet stream, that is, low substrate and high product concentrations. With the ideal PFR the conversion degree is dependent on the length of the reactor as no mixing device at all exists and the condition, within the reactor are never uniform.

While a nearly ideal CSTR is readily obtained, since it is only necessary to have good stirring to obtain complete mixing, an ideal PFR is very difficult to obtain. Several adverse factors to obtaining an ideal PFR often occur, such as temperature and velocity gradients normal to the flow direction and axial dispersion of substrate.

Several considerations influence the type of continuous reactor to be chosen for a particular application. One of the most important criteria is based on kinetic

considerations. For Michaelis-Menten kinetics, the PFR is preferable to the CSTR as the CSTR requires more enzyme to obtain the same degree of conversion as a PFR. If product inhibition occurs, this problem is accentuated, as in a CSTR high product concentration is always in direct contact with all of the catalyst. There is only situation where a CSTR is more favorable kinetically than a PFR, namely, when substrate inhibition occurs.

The form and characteristics of the immobilised enzyme preparations also influence the choice of reactor type, and operational requirements are still another factor to be taken into account. Thus, when pH control is necessary, for instance with penicillin acylase, the CSTR or batch stirred tank reactor is more suitable than PFR reactors. Due to possible disintegration of support through mechanical shearing, only durable preparations of immobilised enzyme should be used in a CSTR. With very small immobilised enzyme particles, problems such as high pressure drop and plugging arise from the utilisation of this catalyst in packed bed reactors (the most commonly used type of PFR). To overcome these problems, a fluidised bed reactor, which provides a degree of mixing intermediate to the CSTR and the ideal PFR, can be used with low pressure drop.

Reactant characteristics can also influence the choice of reactor. Insoluble substrates and products and highly viscous fluids are preferably processed in fluidised bed reactors or CSTR, where no plugging of the reactor is likely to occur, as would be the case in a packed bed reactor.

As it can be deduced from this outline, there are no simple rules for choosing the reactor type and the different factors mentioned must be analysed individually for a specific case.

### Modelling of Immobilised Biocatalyst Reactors

The modelling of immobilised biocatalyst reactors should take into account the several factors which influence their performance. These factors are:

- (a) the immobilised enzyme (or biocatalyst) kinetics;
- (b) the external and internal mass transfer effects;
- (c) the dispersion (back mixing) effects;
- (d) the heat transfer effects;
- (e) the operational stability of the immobilised biocatalyst.

The design equations of immobilised enzyme (biocatalyst) reactors can be obtained from the basic chemical reactor equations and the rate of the biochemical reactions catalysed by immobilised biocatalysts.

The total mass balance is the basis for the design of any reactor. The component balances account for the mass of the individual chemical species which are transformed by biochemical reaction. The general form for a component  $i$ , is:

$$\left[ \begin{array}{l} \text{rate of accumulation} \\ \text{of component } i \text{ in} \\ \text{the reactor} \end{array} \right] = \left[ \begin{array}{l} \text{rate of} \\ \text{inflow of} \\ \text{component } i \end{array} \right] - \left[ \begin{array}{l} \text{rate of} \\ \text{outflow of} \\ \text{component } i \end{array} \right] + \left[ \begin{array}{l} \text{production rate} \\ \text{of component } i \\ \text{in the reactor} \end{array} \right] \quad (42)$$

This general balance can be written in terms of measurable quantities: concentrations  $C_i$ , reaction rate  $r_i$ , flow rate  $Q$ , and reactor volume  $V$ :

$$\frac{d(VC_i)}{dt} = (QC_i)_{in} - (QC_i)_{out} \pm (r_i V) \quad (43)$$

### **Ideal reactors**

Basically there are three types of ideal reactors:

- (a) the batch stirred tank reactor (BSTR);
- (b) the plug flow reactor (PFR);
- (c) the continuous stirred tank reactor (CSTR).

The reactor performance of these three main types of reactors, when the reactions are kinetically controlled, are described in the following sections.

#### *Batch stirred tank reactors*

A batch reactor has neither feed nor effluent streams. The substrate on the biocatalyst is introduced to start the reaction, and both the product concentration,  $P$ , and the conversion degree,  $X = [I(S_0 - S)/S_0]$ , increase within time,  $t$ , while the substrate concentration,  $S$ , decreases. Referring to the general balance equation (42), for a constant volume batch reactor, volume  $V$ , the balance becomes:

$$-\frac{dn_s}{dt} = r_i V \quad (44)$$

**accumulation = production**

For heterogeneous catalysis, the reaction takes place at the surface of the solid catalyst and:

$$-\frac{dn_s}{dt} = r_w W \quad (45)$$

where  $r_w$  is the reaction rate per weight unit of the solid and  $W$  is the solid weight. For immobilised biocatalyst systems:

$$r_w = r_{IME} \quad (46)$$

and:

$$W = W_{IME} \quad (47)$$

The following equation describes the reactor performance of an immobilised enzyme batch reactor:

$$n_{s_0} \frac{dX}{dt} = r_{IME} W_{IME} \quad (48)$$

This equation can be integrated for a particular kinetic expression. For the Michaelis-Menten kinetics,

$$r_{\text{IME}} = \frac{k_{2i} E_W S}{K_{mi} + S} \quad (49)$$

equation (48) is:

$$k_{2i} \frac{E_T t}{V} = S_0 X - K_{mi} \ln(1 - X) \quad (50)$$

where  $k_{2i}$  is the reaction rate constant,  $K_{mi}$  the Michaelis constant for the immobilised system, and  $E_T$  is the total enzyme activity in the reactor ( $E_T = E_W W_{\text{IME}}$  with  $E_W$  the enzyme activity per unit weight of solid support).

The term  $E_T t/V$  is defined as the normalised residence time,  $\tau$ . This is an important reactor parameter which allows the comparison of the different types of reactors.

When the enzymes are subjected to inhibition by substrate and/or product the reactor performance is significantly modified. Table 4.4 summarises the BSTR performance equations for Michaelis-Menten, substrate-inhibition and product-inhibition (competitive and non-competitive) and reversible equilibrium reactions kinetics.

#### *Plug flow reactors*

A plug flow reactor is characterised by a variation of component concentrations from the entrance to the exit. The substrate concentration decreases and the product concentration increases with the length of the reactor. Plug flow assumes radial mixing but no axial mixing. Making a mass balance to a fluid element, the following equation can be obtained:

$$S_0 Q dX = r_{\text{IME}} dW_{\text{IME}} \quad (51)$$

The equations for the design of plug flow immobilised enzyme reactors are shown in Table 4.4.

For continuous reactors it can be seen that the normalised residence time can be given by  $\tau = E_T/Q$ .

#### *Continuous stirred tank reactors*

In a continuous stirred tank reactor, assuming complete mixing, the component concentration in the reactor is the same as in the outlet stream. The composition of the liquid phase is independent of the position in the reactor.

The general design equation for an immobilised enzyme system is:

$$S_0 Q (X_f - X_i) = r_{\text{IME}} W_{\text{IME}} \quad (52)$$

where  $X_f$  and  $X_i$  are the final and initial conversion degrees, respectively.

Table 4.4 also shows the design equations for several kinetic types.

**Table 4.4** Reactor performance equations for immobilised biocatalysts

Kinetic form	Kinetic equation	Reactor performance equation	
		CSTR	PFR, BSTR
Michaelis-Menten	$r = \frac{k_2 E_W}{1 + (K_{mi}/S_0)}$	$k_2 t = S_0 X + K_{mi} \frac{X}{1 - X}$	$k_2 t = S_0 X + K_{mi} \ln(1 - X)$
Reversible Michaelis-Menten	$r = \frac{k_2 E_W}{\left( \frac{K_{mi}}{K_p} + S + P \frac{K_p}{K_t} \right) / \left( S + P \frac{K_p}{K_t} \right)}$	$k_2 t = \frac{X \cdot \left( K_{mi} + S_0 - S_0 X + \frac{K_p}{K_t} S_0 X^2 \right)}{X_t - X}$	$k_2 t = S_0 X \left[ 1 - \frac{K_{mi}}{K_p} \right] + \left[ \frac{K_{mi}}{S_0} + 1 - X_t + X_t \frac{K_{mi}}{K_p} \right] \cdot \ln \left( \frac{X_t}{X_t - X} \right)$
Substrate inhibition	$r = \frac{k_2 E_W}{1 + (K_{mi}/S) + (S/K_S)}$	$k_2 t = S_0 X + K_{mi} \frac{X}{1 - X} + \frac{S_0^2}{K_S} (X - X^2)$	$k_2 t = S_0 X - K_{mi} \ln(1 - X) + \frac{S_0^2}{2K_S} (2X - X^2)$
Product inhibition (competitive)	$r = \frac{k_2 E_W}{1/(K_{mi}/S) \cdot [1 + (P/K_p)]}$	$k_2 t = S_0 X + K_{mi} \frac{X}{1 - X} + \frac{K_{mi}}{K_p} \frac{S_0 X^2}{1 - X}$	$k_2 t = S_0 X \left[ 1 - \frac{K_{mi}}{K_p} \right] - K_{mi} \ln(1 - X) \left[ 1 + \frac{S_0}{K_p} \right]$

### Comparison of immobilised enzyme reactors

When the biochemical reactions are kinetically controlled, it can be seen that the BSTR and PFR are described by the same design equations and show a better performance than the CSTR in most cases, except for substrate inhibition kinetics. Figure 4.10 compares the substrate conversion degrees obtained in a PFR and a CSTR with the same normalised residence time in both types of reactors, for the Michaelis-Menten kinetics.

For zero order, both reactors show the same performance:

$$X_{\text{CSTR}} = X_{\text{PFR}} \quad (53)$$

For first-order reaction rates the PFR displays a higher performance than the CSTR:

$$\frac{X_{\text{CSTR}}}{1 - X_{\text{CSTR}}} = -\ln(1 - X_{\text{PFR}}) \quad (54)$$

### Effect of mass transfer on the performance of immobilised biocatalyst reactors

The design equations previously described are only valid when there are no factors which modify the kinetics of the immobilised biocatalyst (partition effects, heat and mass transfer effects and decay of biological activity) and the hydrodynamic characteristics of the reactor (back-mixing). Thus the kinetic constants,  $K_{mi}$  and  $k_2$  and the activity of the

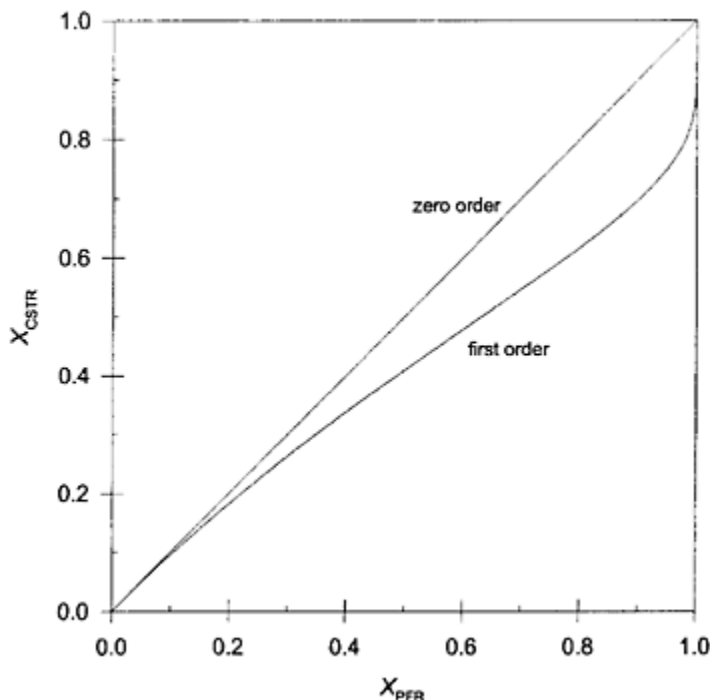


**Figure 4.10** Comparison of CSTR and PFR performance.

immobilised biocatalyst,  $E_W$ , used in those equations are intrinsic values obtained in the absence of those factors, being only dependent on the conformational and stereochemical effects inherent to the immobilisation procedure used.

When the mass transfer (diffusional) effects are significant, the design equations for immobilised biocatalyst reactor can be modified, by introducing the concept of the effectiveness factor,  $\eta$ , in the equation of the reaction rate:

$$r_{IME} = \eta \frac{k_{2i} E_W S}{K_{mi} + S} \quad (\text{for Michaelis-Menten kinetics}) \quad (55)$$

The following equations describe the reactor performance of the three main types of reactors in the presence of mass transfer effects (for Michaelis-Menten kinetics):

$$\bar{\eta} k_{2i} \tau = S_0 X - K_{mi} \ln(1 - X) \quad (\text{BSTR and PFR}) \quad (56)$$

$$\bar{\eta} k_{2i} \tau = S_0 X + K_{mi} \frac{X}{1 - X} \quad (\text{CSTR}) \quad (57)$$

where  $\eta$  is the overall effectiveness factor and  $\bar{\eta}$  is the average effectiveness factor.

For a CSTR, because the component concentrations are constants, the effectiveness factor does not change in the reactor. While for a BSTR or a PFR the component concentrations change with time or the length of the reactor, respectively, which influences the effectiveness factor, as this factor is dependent on the substrate concentration.

The average effectiveness factor,  $\bar{\eta}$ , can be obtained by the following equation:

$$\bar{\eta} = S_0 X - K_{mi} \ln(1 - X) \left( \int_{S_0}^S \frac{dS}{\eta S / (K_{mi} + S)} \right)^{-1} \quad (58)$$

### *Effect of back-mixing on the performance of immobilised biocatalyst reactors*

In real tubular (or column) reactors there is, usually, a back-mixing effect which influences the performance of the ideal plug flow reactor. This axial dispersion is higher for fluidised bed reactors than for packed-bed reactors, although comparatively lower than for continuous stirred tank reactors, where the mixing is complete.

The modelling of real immobilised enzyme column reactors, mainly the fluidised bed reactors, has been described by mathematical models based on the dispersion concept, by incorporating an additional term to account for back-mixing in the ideal plug flow reactor. This term describes the non-ideal effects in terms of a dispersion coefficient.

The design equation is:

$$\frac{D_u}{uL} \frac{d^2S}{dZ^2} - \frac{dS}{dZ} - \frac{W}{Q} r_{IME} = 0 \quad (59)$$

where  $D_u$  is the dispersion coefficient,  $u$  is the superficial fluid velocity,  $L$  the reactor length or bed height and  $Z$  the normalised distance along the reactor length ( $= Z/L$ ). When there are simultaneously dispersion and mass transfer effects, the equation (59) involves the effectiveness factor  $\eta$ :

$$\frac{D_u}{uL} \frac{d^2S}{dZ^2} - \frac{dS}{dZ} - \frac{W}{Q} \eta_{IME} = 0 \quad (60)$$

### *Effect of enzyme inactivation on the performance of immobilised biocatalyst reactors*

The performance of immobilised biocatalyst (enzyme) reactors is influenced by enzyme inactivation during operation, mainly due to the thermal denaturation, desorption of the biocatalyst from the solid support, disintegration or solubilisation of the support, and microbial attack.

The overall effect of these factors can be determined experimentally, and it is convenient to reduce them in order to increase the operational stability of the biocatalyst.

The prediction of the loss of the performance of an immobilised enzyme reactor due to thermal denaturation can be quantified taking into account enzyme inactivation kinetics models. The most used is the exponential decay model:

$$-\frac{dE}{dt} = k_d E \quad (61)$$

where  $E$  is the effective enzyme activity in the reactor at time  $t$  and  $k_d$  is the first-order decay constant.

Substituting this model in the reactor performance equation for Michaelis kinetics, the following equations can be obtained for the three main types of reactors:

$$\ln \left( \frac{S_0 X - K_{mi} \ln(1 - X_0)}{S_t X - K_{mi} \ln(1 - X_t)} \right) = k_d t \quad (\text{BSTR and PFR}) \quad (62)$$

and;

$$\ln \left( \frac{S_0 X - K_{mi}[X_0 / (1 - X_0)]}{S_t X - K_{mi}[X_t / (1 - X_t)]} \right) = k_d t \quad (\text{CFSTR}) \quad (63)$$

where  $X_0$  and  $X_t$  are the degrees of substrate conversion at  $t=0$  and when the reactor has been operating for time  $t$ .

From these equations it can be seen that the immobilised biocatalyst deactivates slower in a CSTR than in a BSTR or a PFR.

Other models of enzyme inactivation have also been proposed:

(a) substrate-dependent enzyme decay

$$-\frac{dE}{dt} = \frac{k_d}{S} E \quad (64)$$

(b) product-dependent enzyme decay

$$-\frac{dE}{dt} = \frac{k_d}{P} E \quad (65)$$

(c) inverted linear model:

$$-E = \frac{E_0}{1 + kt} \quad (66)$$

(d) time-dependent enzyme decay:

$$-\frac{dE}{dt} = k_d E t^n \quad (67)$$

With these models similar equations to (62) and (63) can be obtained.

### *Modelling of immobilised viable cell reactors*

When viable cells are immobilised on the surface of a support, the cells grow on the available surface area  $A(\text{m}^2\text{l}^{-1})$ , until the support-loading capacity  $X_s^{\max}$  (g dry cell weight  $\text{m}^{-2}$ ) is reached, and the bulk given by  $X_b(\text{g l}^{-1})$ .

It is assumed that the cells first grow on the surface with a specific growth rate,  $\mu_s$ , where:

$$\mu_s = \frac{1}{X_s} \frac{dX_s}{dt} = \frac{\mu_s^{\max} S}{K_s + S} \quad (68)$$

When the support is completely loaded the cells grow into the bulk solution with a specific growth rate,  $\mu_b$ , different (higher) from the surface growth rate  $\mu_s$ .

The total biomass ( $X_{\text{total}}$ ) is given by:

$$X_{\text{total}} = X + X_{\text{im}} \quad (69)$$

For a CSTR the following equation can be obtained:

$$\mu_s = \frac{\mu_s^{\max} S}{K_s + S} = \frac{DY_X(S_0 - S)}{Y_X(S_0 - S) + X_{\text{im}}} \quad (70)$$

where  $D(=Q/V)$  is the dilution rate and  $Y_X$  is the biomass yield coefficient.

When  $X_{\text{im}} \rightarrow 0$ , it can be seen that the typical continuous culture relationship  $\mu_s = D$  can be obtained.

For an immobilised viable cell process the relationship  $D > \mu_s$  is obtained at all values of  $D$ . This implies that for a given  $D$ , the exit cell concentration for the immobilised cell process is always higher than for the continuous culture system. Hence, the immobilised viable cell reactor is superior to continuous culture in terms of conversion efficiencies and the washout conditions in submerged continuous cultures are eliminated by using immobilised cells.

For metabolite production by immobilised viable cells the Luedeking-Piret model can be used:

$$\frac{dP}{dt} = K_1 X_{\text{total}} + K_2 \frac{dX_{\text{total}}}{dt} \quad (71)$$

where  $P$  is the metabolite concentration.

If  $K_2 > K_1$ , the rate of product formation (primary or growth-associated metabolite) is given by:

$$\frac{dP}{dt} = K_2 \frac{dX_{\text{total}}}{dt} = K_2 D X_{\text{total}} \quad (72)$$

Maximizing the primary metabolite productivity is the same as maximizing biomass productivity.

When  $K_1 > K_2$ , a secondary metabolite is obtained and is dependent primarily on the cell concentration:

$$\frac{dP}{dt} = K_1 X_{\text{total}} \quad (73)$$

or,

$$P = \frac{K_1}{D} X_{\text{total}} \quad (74)$$

When  $K_1$  and  $K_2$  are both significant, the product mass balance is given by the mixed growth model:

$$P = \frac{K_1 + K_{2,b}}{D} X_{\text{total}} \quad (75)$$

## REFERENCES

- Aris, R. (1957) On shape factors for irregular particles—I. The steady state problem. Diffusion and reaction. *Chem. Eng. Sci.*, **6**, 262–268.
- Fan, L.T. and Lee Y.-H. (1983) Kinetic studies of enzymatic hydrolysis of insoluble cellulose: derivation of a mechanistic kinetic model. *Biotechnol. Bioeng.*, **25**, 2707–2733.
- Fullbrook, P.D. (1983) Kinetics. In *Industrial Enzymology*, edited by T.Godfrey and J.Reicht, pp. 8–110. New York: The Nature Press.
- Horvath, C. and Engasser J.-M. (1974) External and internal diffusion in heterogeneous enzyme systems. *Biotechnol. Bioeng.*, **16**, 909–923.
- Lee, Y.Y., Fratzke, A.R., Wun, K. and Tsao G.T. (1976) Glucose isomerase immobilized on porous glass. *Biotechnol. Bioeng.*, **18**, 389–413.
- López-Sántin, J., Solà, C. and Lema J.M. (1982) Substrate and product inhibition significance in the kinetics of sucrose hydrolysis by invertase. *Biotechnol. Bioeng.*, **24**, 2721–2724.
- Moo-Young, M. and Kobayashi T. (1972) Effectiveness factors for immobilized-enzyme reactions. *Can. J. Chem. Eng.*, **50**, 162–167.
- Olsen, H.S. (1995) Enzymes in food processing. In *Biotechnology*, 2nd edn, edited by H.-J. Rehm, G.Reed, A.Püller and P.Stadler, Vol. 9, pp. 665–736. Weinheim: VCH.
- Pialis, P. and Saville B.A. (1998) Production of L-DOPA from tyrosinase immobilized on nylon 6,6: enzyme stability and scaleup. *Enzyme Microb. Technol.*, **22**, 261–268.
- Oliveira, S.C. (1999) Evaluation of effectiveness factor of immobilized enzymes using Runge-Kutta-Gill method: how to solve mathematical undetermination at particle center point?. *Bioprocess Eng.*, **20**, 185–187.
- Smith, J.M. (1981) *Chemical Engineering Kinetics*, 3rd edn. Singapore, McGraw-Hill Book Co.
- Villadsen, J.V. and Stewart W.E. (1967) Solution of boundary-value problems by orthogonal collocation. *Chem. Eng. Sci.*, **22**, 1483–1501.
- Vos, H.J., Heederik, P.J., Potters, J.J.M. and Luyben K.Ch.A.M. (1990) Effectiveness factor for spherical biofilm catalysts. *Bioprocess Eng.*, **5**, 63–72.

# **CHAPTER FIVE**

## **ADVANCES IN THE SELECTION AND DESIGN OF TWO-LIQUID PHASE BIOCATALYTIC REACTORS**

GARY J.LYE AND JOHN M.WOODLEY

*The Advanced Centre for Biochemical Engineering, University College London, Torrington Place, London WC1E 7JE, UK*

### **ABSTRACT**

The application of two-liquid phase biocatalysis presents some difficult biochemical engineering challenges including the selection of an appropriate reaction medium, reactor design and operating parameters. These selections also have critical implications for subsequent downstream processing operations such as phase separation and product recovery. In this Chapter each of these areas will be discussed in the light of progress made in recent years. With the advent of molecular biology techniques allowing, for example, the engineering of solvent-resistant biocatalysts, the application of two-liquid phase biocatalysis is set to become more widespread in the coming years. Environmental constraints may also lead to the development of alternatives to organic solvents as the second liquid phase, which including the possibility of using room temperature ionic liquids.

**Keywords:** Aqueous-organic media, multiphase biocatalysis, ionic liquids, scale-up

### **INTRODUCTION**

Biocatalysis offers some significant advantages over traditional chemical catalysis from the viewpoint of both the organic chemist and the process engineer. For example, stereo-, regio-and reaction-specific catalysts, operating under mild conditions, enable reactions difficult to perform chemically to be carried out effectively with minimum side reactions and by-products. In the past 30 years biocatalytic processes have come to find application in the pharmaceutical and fine chemical industries as an alternative to chemical synthesis for high value products (in particular optically pure compounds) and today over 100 processes are operating commercially throughout the world. However, the majority of these processes are hydrolytic resolutions of racemic compounds to produce chiral synthons or optically pure products. Recent developments in biocatalysis will now enable the application of biologically mediated carbon-carbon bond forming reactions and redox conversions which is where the real power of biocatalysis lies.

For each class of biocatalytic process the medium in which the conversion occurs is dependent on the properties of the reactants and products. In many cases the reaction components have relatively low water solubilities (less than 50 mM). Increasingly, the substrate(s), product(s), or both are novel compounds which may be aromatic, multicyclic or bulky molecules. These compounds bear little relationship in size, shape or hydrophilicity to the natural substrates of a given enzyme. This leads to biocatalytic conversions at low rates and, since most are poorly water-soluble, operation at low reactant concentrations. Consequently the process streams leaving the reactor frequently contain low product concentrations, making a difficult problem downstream (separation of structurally similar compounds in water) still more difficult.

The use of a two-liquid phase medium to effect bioconversions at higher overall concentrations has clear advantages for those reactions where one or more of the reaction components is poorly water-soluble (Lilly and Woodley, 1985; Lilly *et al.*, 1987). It has also been found to have particular benefits where these compounds are inhibitory and/or toxic to the biocatalyst by providing a reservoir for the molecules away from the vicinity of the biocatalyst. The use of a multiphasic liquid-liquid medium, however, also presents a number of unique problems for the biochemical engineer designing and scaling-up such a process. The potential advantages and disadvantages of two-liquid phase biocatalytic processes are summarised in Table 5.1. In this Chapter we will address the issues of when such a technology may be applied and the basis for the design of both the reactor and the downstream process.

## FUNDAMENTALS

In two-liquid phase biocatalytic processes a virtually water-immiscible organic solvent is added to an aqueous phase (at a concentration well above the aqueous phase saturation limit) containing the biocatalyst to create a biphasic reaction medium. Where the substrate is hydrophobic the organic phase will be initially rich in substrate which will then partition into the aqueous phase. Once in the aqueous phase the substrate will be acted upon by the biocatalyst which can only operate at concentrations up to the aqueous phase saturation

**Table 5.1** Potential advantages and disadvantages of two-liquid phase biocatalysis

Process feature	Advantages and disadvantages
Reactor Operation	<ul style="list-style-type: none"> <li>+Solubilisation of poorly water-soluble molecules</li> <li>+Reduced inhibition/toxicity</li> <li>+Excellent substrate/catalyst contact</li> <li>-Reduced activity per unit volume</li> <li>-Diffusional limitations</li> <li>-Liquid-liquid interfacial damage to biocatalyst</li> </ul>

## Downstream Processing

- Dissolved organic phase damage to biocatalyst
  - +Isolation of reactant from product
  - +Higher product concentration
  - Emulsification
- 

limit of the substrate. Due to the action of the biocatalyst more substrate will subsequently partition out of the organic phase in order to maintain a thermodynamic equilibrium. In this way a high concentration of product can be produced in a typical batch process. A second substrate may also be present, either preferentially present in the organic phase or alternatively supplied from another phase (for example oxygen from the gas phase or water from the aqueous phase). Depending upon its solubility, the product may either remain in the aqueous phase or partition into the organic phase. The basic mass transfer and biocatalytic reaction steps are summarised in Figure 5.1. This implies that the key to the design of two-phase biocatalytic reactors will be to match the rate of substrate supply to (or product removal from) the biocatalyst with the rate of the reaction itself such that the aqueous phase concentration of any inhibitory substrate (or product) is maintained below a

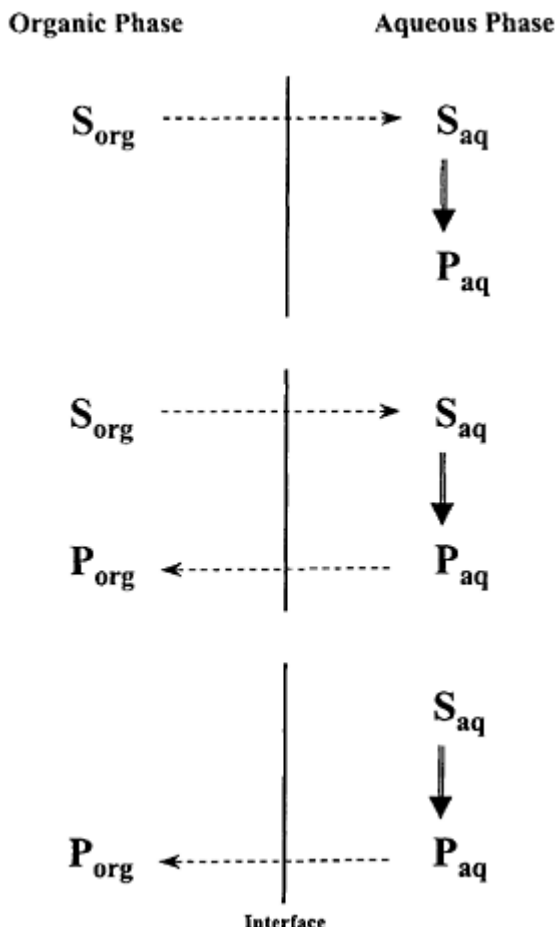


**Figure 5.1** Classification of two-liquid phase biocatalytic processes based on the solubility of both the substrate (S) and product (P) molecules. The biocatalyst may be a whole-cell or an immobilised enzyme and is assumed to be present in the aqueous phase. Dashed lines represent mass transfer processes.

critical level and maximum use is made of the available activity. Reactor designs and operating conditions to allow us to achieve these criteria will be discussed later.

Multiphasic systems thus allow high overall concentrations of all substrates in the reactor, regardless of preferential solubility, while concentrations local to the biocatalyst

may be limited to the aqueous phase saturation concentration of the components. This may also be used to limit exposure of the biocatalyst to poorly water-soluble inhibitory or toxic substrates/products. The high overall concentration of product produced, however, facilitates downstream processing. As stated previously the product may or may not be preferentially soluble in the same phase as the substrate and, where the latter situation is the case, separation of the phases enables a primary isolation of product from substrate.

## CLASSIFICATION

A number of different two-liquid phase systems can be identified and these have been discussed in detail elsewhere (Lilly and Woodley, 1985; Lilly *et al.*, 1987). Some are listed in Table 5.2. Initially a distinction can be drawn between those reactions where catalysis occurs at the interface between the liquid phases and those where catalysis occurs in the bulk of the aqueous phase. With the exception of lipases (which have a tertiary structure to enable them to work in an amphipathic environment) all other enzyme and microbial biocatalysts examined to date have been found to catalyse conversions in the bulk of the aqueous phase (*e.g.* Woodley *et al.*, 1991a; 1991b). Nevertheless the interface may still contribute to the reaction rate, or loss of catalytic activity over time, via direct contact between the cells or enzyme and the interface. It is well known that immobilisation to prevent damage to biocatalysts as a result of this direct interfacial contact has implications even for those reactions where conversion occurs in the bulk of the aqueous phase.

From the perspective of reactor and downstream process design two features are particularly critical:

- (a) Organic phase. Reactions may operate with an organic phase which is either the substrate itself or which has the substrate dissolved in it. The former case is of benefit where the substrate is not inhibitory or toxic. In this way direct transfer of substrate to catalyst via interfacial contact can help contribute to the reaction rate. In the latter case the organic solvent can be selected to act as a diluent for an inhibitory

**Table 5.2** Possible classes of two-liquid phase biocatalytic reactors

Feature	Option
Organic phase	Substrate or carrier solvent
	Light or dense phase
	Continuous or dispersed phase
Reaction	Substrate/product distribution
	Bulk phase or at interface
Catalyst	Whole-cell or immobilised enzyme

or toxic substrate, reducing the interfacial concentration and also that which partitions into the aqueous phase.

(b) Solubility of product. Theoretically it is possible to calculate that for systems of up to two substrates and two products, 25 combinations of preferential solubility exist with only four all aqueous and four all organic. This leaves 17 cases where two-liquid phase biocatalysis is appropriate. However the preferential distribution of substrate(s) and product(s) between the phases is difficult to manipulate. In many cases at least one substrate and the desired product are both preferentially distributed to the organic phase. Where the distribution is favourable it can be exploited downstream. For example the hydroxylation of aromatics by *Pseudomonas putida* gives a product of many fold higher aqueous solubility than the substrate to afford an easy product recovery by phase separation (Collins and Woodley, 1993). Even in such cases the poorly-soluble compound will be present in trace quantities in the product stream and will need to be removed.

## ORGANIC PHASE

### Organic Phase Selection

Enzymes and whole-cell catalysts usually operate in an aqueous environment. Hence organic solvents (whether dissolved in an aqueous phase or present as a discrete second liquid phase) have long been known to be harmful to biocatalytic activity. The search for an indicator characteristic of different organic solvents which could be used to predict biocatalyst tolerance has led to various proposals. One of the most comprehensive early studies examined the relationship between solvent molecular weight and the Hildebrand solubility parameter with the maintenance of biocatalytic activity (Brink and Tramper, 1985). More recently (Laane *et al.*, 1987) it was suggested that solvents with Log P values (logarithm of the partition coefficient of an organic solvent in a standard octanol-water system) greater than 4 were most suitable, while use of those with lower Log P values, especially less than 2, resulted in considerable loss of activity (Bruce and Daugulis, 1991).

However, further studies in our laboratory have revealed that while the trend of increased activity with increased Log P value appears universal, the solvent Log P-biocatalyst activity profile is specific to a particular biocatalyst and the extent of its contact with the organic phase. For example differences have been observed between two-liquid phase biotransformations carried out in shaken-flasks and stirred reactors and between the use of Gram-positive (*Arthrobacter simplex*) and Gram-negative (*Pseudomonas putida*) bacteria as catalysts as shown in Figure 5.2 (Harrop *et al.*, 1992). While immobilisation may protect Gram-positive bacteria from solvent damage this has not been conclusively observed for Gram-negative bacteria. Such observations underline the empirical nature of these rules and provide guidance for the further research required to understand the way in which different organic solvents damage different types of biocatalyst. These studies will almost certainly require examination of the precise role of the frequency and duration of interfacial contact with the biocatalyst.

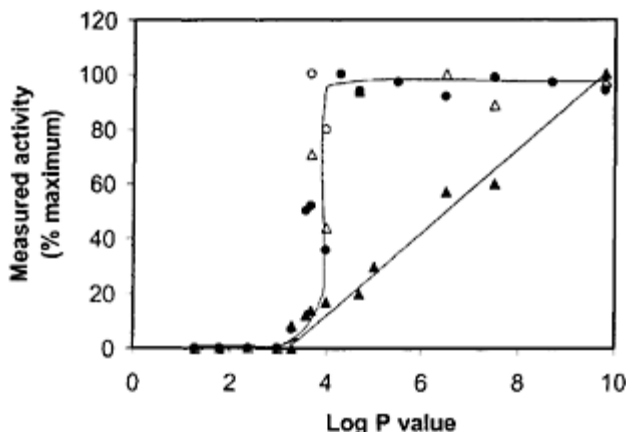


**Figure 5.2** Relationship between solvent Log P value and residual activity measured in aqueous-organic solvent reaction mixtures for steroid  $\Delta^1$ -dehydrogenation by free ( $\blacktriangle$ ) and immobilised ( $\triangle$ ) *Arthrobacter simplex* and for naphthalene oxidation by free ( $\bullet$ ) and immobilised ( $\circ$ ) *Pseudomonas putida*. Redrawn from Harrop *et al.* (1992).

At a fundamental level, a considerable amount of work has addressed the issue of how micro-organisms respond when exposed to an organic solvent and the features that characterise "solvent-tolerant" strains. The toxic effect of solvents is now known to be due to their interaction with the cytoplasmic membrane: the degree of toxicity being proportional to the solvent concentration in the membrane itself which, in turn, is proportional to the solvent Log P value. Solvent-resistant bacteria typically possess a number of physiological mechanisms to counteract the presence of solvents in the cytoplasmic membrane (de Bont, 1998). These mechanisms include the rapid synthesis of *trans*-unsaturated fatty acids to alter membrane fluidity and the active pumping of solvents out of the membrane.

#### Choice of Phase Ratio

The amount of organic phase present in the medium is commonly characterised by the phase volume ratio (organic volume/aqueous volume). The phase volume ratio affects both the reactor concentration of water-soluble and poorly water-soluble organic components and the degree of reduction or elimination of substrate or product inhibition. The ease or otherwise of pH control at different phase volume ratios is a particular issue

with regard to the activity of the biocatalyst and the chemical stability of the substrate and product molecules. Where the aqueous phase is not the continuous phase, “hot” spots of extreme pH may arise which can only be made homogeneous by continual coalescence and breakage with other droplets *i.e.* by inter-droplet mixing. An alternative approach, and the most common, is to operate with the aqueous phase as the continuous phase where the phase volume ratio is typically less than 0.3–0.4. The phase volume ratio also affects both the absolute and specific interfacial areas as will be discussed later.

**Table 5.3** Organic solvent and phase volume ratio selection criteria

Factors to consider	Phase volume ratio effects
Solubility limit of S and P in organic phase	Ease of pH control
S and P distribution coefficients	Nature of dispersed phase
Biocompatibility (e.g. Log P values)	Possibility of phase inversion
Aqueous solubility limit of solvent	Ease of phase separation
Emulsion formation	Interfacial area available for mass transfer
Toxicity and flammability	Inter-droplet mixing
Solvent recycling options	
Environmental impact	
Cost and availability	

Table 5.3 summarises the factors to be considered when screening a range of solvents and indicates effects which will be a function of the phase volume ratio used. A more detailed discussion of the phase volume ratio affects can be found in a review by Lilly and coworkers (1990).

## TWO-LIQUID PHASE REACTORS

### Types of Reactor

The two key requirements in selecting an appropriate reactor are (1) to establish sufficient interfacial area between the aqueous and organic phases to enable adequate substrate or product mass transfer, and (2) to be able to readily control the interfacial area. To date these requirements have been achieved in three types of reactor; stirred tanks, liquid-impelled loops and membrane reactors.

The stirred-tank reactor is by far the most popular since it enables excellent control of the interfacial area via agitator speed. It is also the design of reactor most readily available in both research laboratories and industrial facilities. For such reactors it has been shown that the rate of a particular biotransformation will be a function of the reactor geometry (Collins and Woodley, 1993) and the power input per unit volume (Woodley, 1990a). Based on the principles of the gas fluidised bed and the air-lift reactor an

equivalent two-liquid phase reactor has been proposed, known as the liquid-impelled loop reactor (van Sonsbeek *et al.*, 1993). Clearly such a reactor has the difficulty that the density difference between the two liquid phases is small relative to gas and liquid density differences and this makes the separation zone at the end of the reactor difficult to design. This problem is made worse by the presence of emulsifying agents, either secreted from cells or present in solution. Such reactors are also not available commercially.

Examples of membrane reactors used with two-liquid phase biocatalytic systems fall into two categories, those using microporous membranes and those using dense-phase membranes. In both cases the aqueous and organic phases are kept apart by the membrane in order to overcome problems of emulsion formation. With microporous membranes, breakthrough of either liquid phase is prevented by careful control of the transmembrane pressure (Prazeres and Cabral, 1994) and solute mass transfer coefficients are typically in the range  $0.17\text{--}1.67 \times 10^{-5} \text{ m s}^{-1}$  (Molinari *et al.*, 1997). Industrial installations of this type have emerged for the production of diltiazem with an installed membrane area of  $1440 \text{ m}^2$  and a productivity of  $75 \text{ kg yr}^{-1} \text{ m}^{-2}$  (Lopez and Matson, 1997). The use of nonporous, dense-phase membranes, such as silicon, has recently been explored in order to overcome the need to carefully control the transmembrane pressure (Doig *et al.*, 1998). Here solute transfer occurs by a solution-diffusion mechanism and overall mass transfer coefficients in the range  $0.1\text{--}2.1 \times 10^{-5} \text{ m s}^{-1}$  have been determined. The main disadvantages of both types of membrane reactor are the low solute mass transfer coefficients (and hence the large membrane areas required) and fouling of the membrane surface over extended periods of operation (Prazeres and Cabral, 1994; Westgate *et al.*, 1998).

### Mass Transfer and Reaction Kinetics

Clearly intimate contact of the aqueous and organic phases is necessary in order to effectively transfer reactants and/or products from one phase to the other. Considerable work has been done to examine these issues in the past and in the majority of systems studied mass transfer was not found to be limiting. In particular, whole-cell catalysed reactions are slow and therefore mass transfer is not likely to be a problem. Where solvents are used with a very high viscosity individual mass transfer coefficients will be reduced which may cause problems. In contrast, reactions catalysed by isolated enzymes (usually immobilised to assist with downstream processing) may display mass transfer limitations when the catalyst has a high specific activity. Such effects will be dependent on the Michaelis constant of the enzyme. If the Michaelis constant is very low relative to the aqueous phase saturation concentration of substrate then the effectiveness factor (i.e. the observed reaction rate in a two-phase system divided by the reaction rate in a single phase system) will still be high. It is interesting to note that in a number of cases examined to date we have found the Michaelis constant of the enzymes to be a fraction of the aqueous phase saturation concentration. Figure 5.3 illustrates typical data for three such systems.

Figure 5.4 shows a general mass transfer-reaction model for the case of a transformation occurring in the bulk of the aqueous phase and a biocatalyst which exhibits normal Michaelis-Menten kinetics. This describes the change in both substrate

and product concentrations in each of the organic and aqueous phases with time. Biocatalyst inhibition terms due to either specific substrate/product effects or the effect of biocatalyst exposure to the organic interface are not included. The advantage of such a model, even if numerical values of each parameter are not known, is that it highlights the important reactor operating parameters. These include substrate and product distribution coefficients, mass transfer coefficients, the interfacial area available for mass transfer and the concentration and kinetic constants of the biocatalyst. All of these need to be experimentally determined in relation to the design and operation of a two-liquid phase stirred-tank reactor. Similar models have been developed in the case of microporous (Molinari *et al.*, 1997) and dense-phase (Doig *et al.*, 1998) membrane reactors and the liquid-impelled loop reactor (Tramper *et al.*, 1987). Recent work has also shown that biosurfactants produced by some

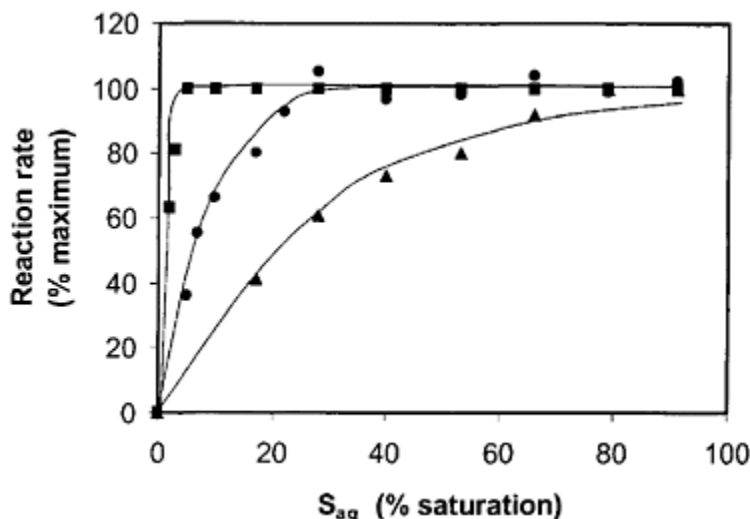


**Figure 5.3** The effect of aqueous phase substrate concentration on the initial reaction rate of toluene oxidation by *Pseudomonas putida* (■), benzyl acetate hydrolysis by pig liver esterase (●) and hydrocortisone  $\Delta^1$ -dehydrogenation by *Arthrobacter simplex* (▲). Redrawn from Woodley and Lilly (1994). Toxic effects of toluene not shown.

$$\frac{dS_{aq}}{dt} = \frac{k_s A}{V_{aq}} (S_{org} - m_s S_{aq}) - \frac{k_1 E_1 S_{aq}}{K_{M1} + S_{aq}}$$

$$\frac{dS_{org}}{dt} = -\frac{k_s A}{V_{org}} (S_{org} - m_s S_{aq})$$

$$\frac{dP_{aq}}{dt} = \frac{k_p A}{V_{aq}} (P_{org} - m_p P_{aq}) + \left( \frac{M_p}{M_s} \right) \frac{k_1 E_1 S_{aq}}{K_{M1} + S_{aq}}$$

$$\frac{dP_{org}}{dt} = -\frac{k_p A}{V_{org}} (P_{org} - m_p P_{aq})$$

**Figure 5.4** Mass transfer-reaction model for a reaction occurring in the aqueous phase and a biocatalyst exhibiting Michaelis-Menten kinetics. Nomenclature: A, interfacial area; E, enzyme concentration; K<sub>m</sub>, Michaelis constant; k, mass transfer coefficient; M, molecular mass; m, equilibrium distribution coefficient; P, product concentration, S, substrate concentration; t, time; V, volume.

organisms in two-liquid phase systems as a response to solvent exposure, will have a critical influence on a number of the model parameters such as the solute mass transfer coefficients and the interfacial area available for mass transfer (Schmid *et al.*, 1998b; Kollmer *et al.*, 1999).

### Reactor Operation

As previously indicated, knowledge of the location of the reaction within the biocatalytic medium is of key importance for reactor selection and design. One method for elucidating this is a set of experiments carried out in a defined, flat liquid-liquid interface apparatus known as a Lewis cell (Woodley, 1990b; Woodley *et al.*, 1991a). In such a device the rate of mass transfer of substrate from organic to aqueous phase under defined conditions can be measured and thus a mass transfer coefficient obtained. These data can be combined with measurements of aqueous phase biocatalyst kinetics (measured in all aqueous phase solution with dissolved levels of poorly water-soluble organic substrate

beneath the saturation concentration) to predict substrate and product concentration-time profiles in a Lewis cell with biocatalyst present. These can then be compared with those measured experimentally. This technique is valid both for microbial and enzymically catalysed biotransformations.

Figure 5.5 is a plot of data for the hydrolysis of benzyl acetate by pig liver esterase in a two-liquid phase system in a  $24.2 \text{ m}^{-1}$  (aqueous phase basis) specific interfacial area Lewis cell. The data show substrate and product concentration-time profiles with 0.01 g

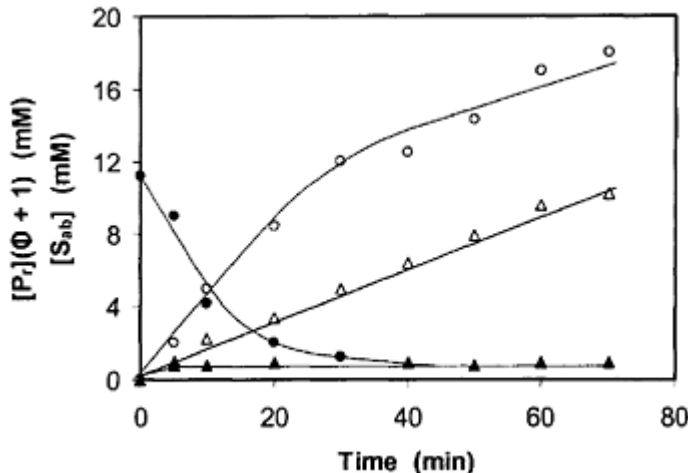


**Figure 5.5** Hydrolysis of benzyl acetate by pig liver esterase (0.01 g  $\text{m}^{-1}$ ) in a Lewis cell reactor showing the changes in the aqueous phase concentrations of benzyl acetate,  $[S_{ab}]$  ( $\blacktriangle$ ,  $\bullet$ ) and reactor concentrations of benzyl alcohol (on an aqueous phase basis),  $[P_r]$  ( $\Phi+1$ ) ( $\Delta$ ,  $\circ$ ) with time for two starting conditions,  $[S_{ab}]$  ( $\blacktriangle$ ,  $\Delta$ ) and  $[S_{ab}] = [S_{ab}^*]$  ( $\bullet$ ,  $\circ$ ). All points are the average of three determinations ( $\Phi = V_{\text{org}}/V_{\text{aq}}$ ). Redrawn from Woodley *et al.* (1991a).

$\text{l}^{-1}$  pig liver esterase in 200 ml of aqueous phase catalysing the hydrolysis of 300 ml of benzyl acetate (lower organic phase). Both phases were well mixed without disturbing the flat liquid-liquid interface using two turbine impellers each rotating at 120 rpm. The measured substrate mass transfer coefficient in the absence of any biotransformation was  $1.8 \times 10^{-8} \text{ s}^{-1}$ . Close agreement was observed between the steady-state aqueous phase

substrate concentration (0.6 mM) and the reaction rate ( $0.14 \mu\text{mol min}^{-1} \text{ ml}^{-1}$ ) predicted by the aqueous phase bulk reaction model and the measured values indicating that the reaction occurs in the bulk of the aqueous phase. The Lewis cell may also be used to measure the partitioning of substrates and products between phases. The generic use of the Lewis cell lies in the ability it gives to expose biocatalysts to defined amounts of interface and consequently the Lewis cell has a role in determining interfacial effects not only upon biocatalyst kinetics as illustrated here but also upon biocatalyst stability.

This Lewis cell-based design method gives an estimate of the reactant mass transfer coefficient required for a given reactor productivity which then enables a preliminary selection of reactor type. Liquid-liquid contacting equipment, suitable for biocatalytic reactions, may be characterised by the range of mass transfer duties (*i.e.* minimum and maximum mass transfer coefficients) achievable in that particular design (*e.g.* Doraiswamy and Sharma, 1984). Knowledge of the mass transfer coefficient required will therefore eliminate some of these possibilities.

## DOWNSTREAM PROCESSING

Reactor selection, design and operation all have an impact on subsequent product recovery and the potential to recycle either the biocatalyst or the organic phase. It is important therefore that design methods incorporate such reasoning. Figure 5.6 shows a schematic integrated process design strategy. Target productivity, together with preliminary selection of the biocatalyst form define the required mass transfer coefficient. This then sets guidelines for initial reactor selection which subsequently set operating parameters (for example, in a stirred-tank reactor: stirrer speed and phase volume ratio). The effects of these decisions on the rest of the process must then be considered and if there are problems for product recovery then either the catalyst selection or reactor selection or (operation or some combination of these) may need to be re-examined. The figure also shows that this is an iterative procedure and indicates where molecular genetic methods may be applied to overcome design constraints associated with the biocatalyst. Using graphical techniques (Woodley and Titchener-Hooker, 1996) many of the “what if” studies can be done prior to experimentation so as to guide the development effort. A number of experimental design tools can also be used here (Woodley and Lilly, 1992) and preliminary studies indicate that interfacial tension measurements can be used to predict the likelihood of emulsification.

To date only a limited number of authors have addressed the downstream processing issues of two-phase transformations carried out in stirred-tank reactors. Whole process flowsheets for the conversion of a poorly water-soluble substrate into either a poorly water-soluble product or a water-soluble product are shown in Figure 5.7 (options for recycling of the phases and the biocatalyst are also indicated). In both cases the key initial

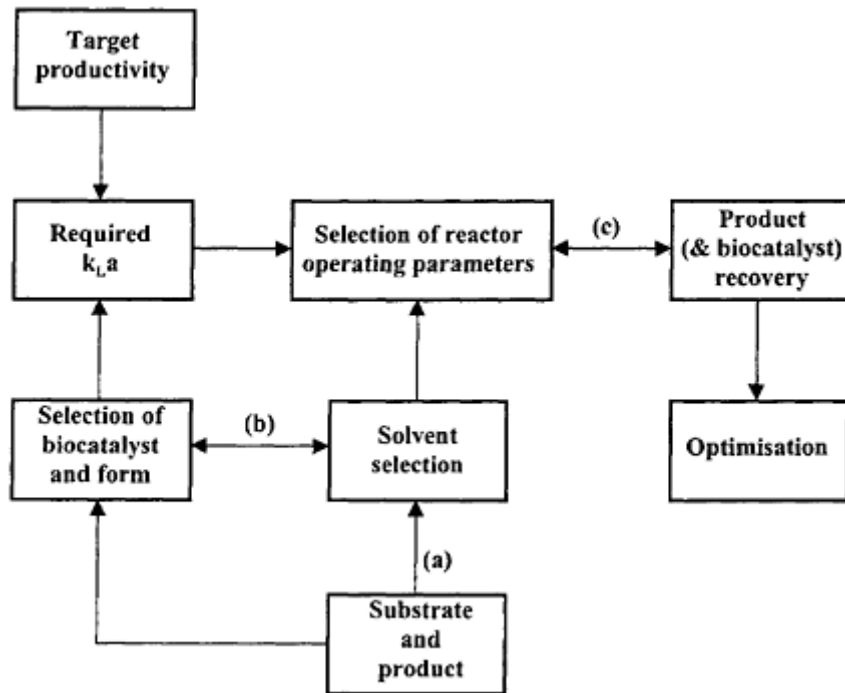


**Figure 5.6** Integrated design strategy for two-liquid phase biocatalytic processes: (a) may need to compromise on solvent selection to satisfy solubility constraints; (b) opportunities for protein/genetic engineering; (c) may need to compromise on reactor operation to satisfy downstream processing constraints.

downstream processing step is the separation of the product-containing phase from both the second phase and the biocatalyst. The favoured technique appears to be the use of microporous microfiltration membranes to aid dispersed phase coalescence which may be either ceramic (Conrad and Lee, 1998) or hydrophobic/hydrophilic polymer composites (Schroen and Woodley, 1997). In both cases it is important that the breakthrough pressure of the phase to be retained is not exceeded during operation. The use of centrifugation to directly separate the two bulk liquid phases is unlikely to be successful given the tendency to form stable emulsions, the low phase density difference and the small size of the dispersed phase droplets. Thermal pretreatment of the emulsified broth by either heating (autoclaving at 121°C) or cooling (freezing at -20°C) has been shown

to improve phase separation (Schmid *et al.*, 1998a) and may be applicable where the products are sufficiently stable.

As an alternative to the use of microporous membranes, dense phase membranes have also been investigated for the direct recovery of product from a two-phase, stirred-tank bioreactor by pervaporation (Mathys *et al.*, 1997). Data obtained from a wide range of polymeric membranes makes it clear that the design and operation of such units will involve a trade off between flux and selectivity. Following the phase separation step very

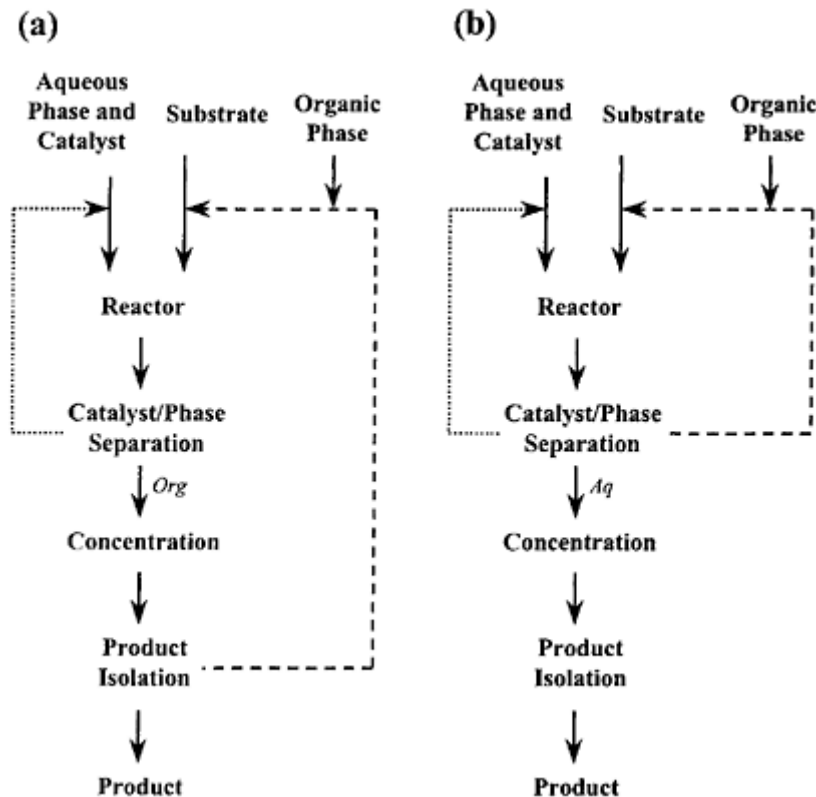


**Figure 5.7** Process flowsheets for (a) conversion of a poorly water-soluble substrate into a poorly water-soluble product, and (b) conversion of a poorly water-soluble substrate into a water-soluble product. Dashed lines represent options for organic phase recycle while dotted lines represent options for biocatalyst recycle.

little work has been carried out on the subsequent purification of the target solute from the phase in which it is contained. Given the nature of the phases and solutes used, distillation would appear to be a favoured operation (Mathys *et al.*, 1998a; 1998b). Here the influence of biological materials in the feed to the columns has, under certain conditions, led to colouring of the product stream and poor separations due to unfavourable gas-liquid hydrodynamics within the column. Clearly more research is required in this area.

## PROCESS SCALE-UP

### Considerations for Scale-up

The mass transfer-reaction model previously shown in Figure 5.4 provides some insight into the factors which might influence the performance of a stirred-tank reactor at various scales of operation. In order to reliably scale-up a two-phase process an understanding of how the individual parameters within the model will vary as a function of scale is required. Generally it would be expected that the kinetic constants of the biocatalyst and substrate/product partition coefficients would be scale independent. While the substrate/product mass transfer coefficients may vary somewhat, it would be expected that the most significant parameter with respect to scale-up would be the maintenance of a constant interfacial area per unit volume. This will be critical in determining solute mass transfer rates (flux being proportional to area per unit volume) and hence the maintenance of substrate/product concentrations in the vicinity of the biocatalyst below toxic levels. Rules for the scale-up of two-phase biocatalytic process are currently lacking. Current work in our laboratory is examining how the droplet size distribution in stirred-tank bioreactors changes as a function of scale (3–75 L vessels) in order to rationally specify a scale-up basis; either constant power per unit volume or constant impeller tip speed.

Scale-up will also require examination of several other factors. Figure 5.8 is a design chart (plot of agitation rate in a stirred-tank against biocatalyst concentration) for a two-liquid phase biocatalytic reaction. One operational limit occurs at high fractions of aqueous phase substrate saturation. Above this concentration (defined by a particular ratio of agitation rate to biocatalyst concentration) a loss of activity is observed over a period of time. This loss of catalyst stability may be explained by the high liquid-liquid interfacial area (relative to catalyst concentration) or by a time-dependent effect of a relatively high aqueous phase reactant concentration, both of which occur at a high operational agitation rate to biocatalyst concentration ratio. This, and the other bounds shown in Figure 5.8 therefore define a process operating window (Woodley and Titchener-Hooker, 1996). In scale-up, further bounds will be introduced

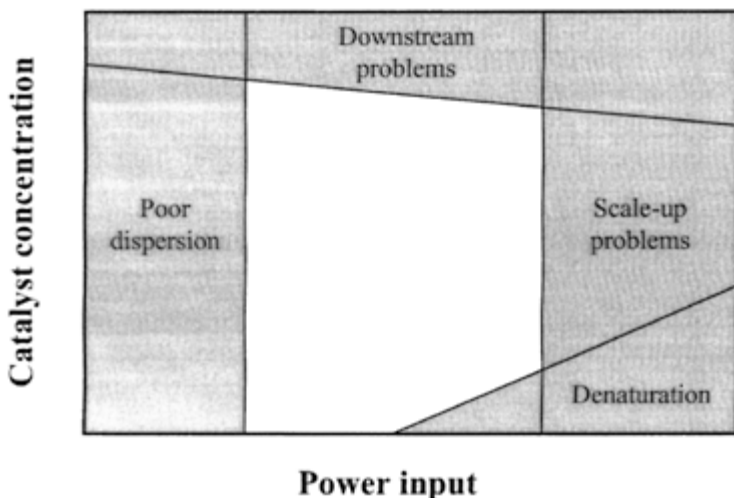


**Figure 5.8** Design chart showing the factors which determine the feasible operating window for a two-liquid phase biocatalytic process. Adapted from Woodley and Lilly (1994).

(e.g. limitations on the power input may mean that adequate mass transfer is difficult to achieve), thus reducing the size of the operating window as the process scale is increased. Hence it is possible to make laboratory scale measurements of mass transfer and reaction kinetics and use them to draw conclusions about larger scale operation. The rationale behind this argument is that the design method presented here is based on fundamental mass transfer-reaction concepts, which are therefore independent of scale. An added complication is that measurements made over a flat liquid-liquid interface (laboratory reactor) may not accurately simulate and be applicable to those made over a dispersed liquid-liquid interface (likely industrial reactor). However, preliminary results have indicated that this is not a problem (Woodley *et al.*, 1991b).

### Safety Considerations

In aerobic bioconversions, where volatile organic solvents are used, the potential to form an explosive atmosphere at large scales of operation raises serious safety issues. Clearly reactors for such processes must be housed in special facilities designed to comply with both explosion-proof and biological containment regulations. Schmid and coworkers (1998a) have identified several strategies to deal with explosion issues. First, high pressure reactors can be built capable of containing the pressure generated by an air-solvent vapour explosion. Secondly, the generation of an explosive atmosphere can be prevented by a range of operating strategies. These include the dissolution of volatile solvents in inert carrier solvents, reduction of the oxygen concentration in the inlet gas

and operation above critical pressures or below critical temperatures. The need to ensure the safe operation of two-phase biotransformations will lead to increased capital and operating costs compared to traditional fermentation processes.

## INDUSTRIAL EXAMPLES

Although a detailed understanding of the mass transfer and kinetic phenomena underlying the scale-up of two-liquid phase biocatalytic processes is only now beginning to emerge, a number of processes have been scaled-up on an empirical basis to either large-pilot or full process scale. Examples are summarised in Table 5.4. While a number of these processes have been operated commercially, there is little information in the literature regarding the economics of two-liquid phase processes. Such information is vital if biocatalytic processes are to be chosen over competing chemical alternatives. Mathys and coworkers (1999) recently published a detailed economic analysis for the production of alkanols from n-alkanes at a 10,000 tonne per year scale using a whole-cell biocatalyst. The downstream process sequence employed three phase separation stages and a two-stage distillation process for product isolation and solvent recycle. In contrast to many biological production processes the largest costs were associated with the upstream, rather than the downstream, processing due to the medium costs. For a fed-batch process the overall production cost for 1-octanol was estimated to be approximately 7 US\$ kg<sup>-1</sup>.

**Table 5.4** Industrial examples of two-phase biocatalytic processes

Reaction	Biocatalyst	Solvent	Company	References
1-octene epoxidation	<i>Nocardia corallina</i>	n-hexadecane	Nippon Mining	Furuhashi <i>et al.</i> (1986)
Phenol polymerisation	Horseradish peroxidase	Ethyl acetate	Mead	Pokora and Cyrus (1987)
Ester hydrolysis	Subtilisin (immobilised) Lipase	Various (reactant)	Bayer	Schutt <i>et al.</i> (1985)
			Sumitomo	Umemura and Hirohara (1989)
Steroid dehydrogenation	<i>Arthrobacter simplex</i>	Toluene	Upjohn	
Desulfurization	<i>Rhodococcus</i>	Oil (substrate)	Energy Biosy stems	Monticello (1993)

## FUTURE PERSPECTIVES

### Applications of Two-Phase Biocatalysis

After much initial interest in two-liquid phase biocatalysis it has become clear that there are three primary applications for this technology. These are for biotransformations involving:

- Poorly water-soluble reactants which are inhibitory or toxic to the biocatalyst.
- A difference in the water-solubility of reactant(s) and/or product(s).
- Poorly water-soluble reactants which are solids and inhibitory or toxic and therefore cannot be fed easily to the reactor.

Alternative reactor technologies do now exist in a number of cases. For example solid, poorly water-soluble reactants can be used in slurry reactors where the properties of the biocatalyst allow this (Kasche *et al.*, 1995; Michielsen *et al.*, 2000). Likewise in order to overcome downstream liquid-liquid emulsion separation problems the use of a solid hydrophobic adsorbent can be used as a reservoir for the reactant (Vicenzi *et al.*, 1997). Although limited by the capacity of the resin this is a very effective technique providing the biocatalyst can tolerate the reactor environment. In many examples however there remain very clear process advantages to using two-liquid phase biocatalysis. In these cases the productivity limitation frequently lies in the lack of tolerance of the biocatalyst to the dissolved levels of organic phase or the presence of the liquid-liquid interface. These are issues needing to be addressed in future research.

### **Designer Biocatalysts**

Developments in molecular biology now enable a number of possibilities for biocatalysis in two-liquid phase media. First, the identification of genes harbouring a particular activity, together with cheap expression systems (for use at scale) mean that cloning the enzymes from the natural host to another is now possible. The choice of host to date has largely been based on the knowledge of genetics and ability to overexpress effectively in the new host. It is clear that new opportunities are now possible to clone a desired enzyme activity into a more solvent tolerant host. Other properties to be cloned for might be a reduction in secreted or lysed material (implicated in mutiphasic media) or cell softening which leads to particular problems for downstream processing (*e.g.* via centrifugation). Directed evolution techniques (Arnold, 1996) will enable more solvent tolerant enzymes to be developed but more crucially high activities with non-natural substrates which will mean less catalyst is required. Difficulties in subsequent downstream separation often show a close correlation with the amount of catalyst present.

### **Designer Solvents**

Recent work in our laboratories has established the use of room temperature ionic liquids as direct replacements for organic solvents in two-phase biocatalytic processes (Cull *et al.*, 2000). Ionic liquids such as 1-butyl-3-methylimidazolium hexafluorophosphate, [bmim][PF<sub>6</sub>], are, as their name implies, solutions composed entirely of ions and have been shown to be non-toxic to a whole cell *Rhodococcus* biocatalyst. Ionic liquids have, among a unique set of chemical and physical properties (Seddon, 1997), effectively no measurable vapour pressure, which makes them ideal replacements for volatile,

conventional organic solvents. They also have the potential to act as “designer solvents” (Freemantle, 1998) as simple structural modifications to either the anion or cation will alter the physico-chemical properties of the liquid and offer the possibility to design an ionic liquid system optimised for a particular application. Although their use in biocatalytic processes is at an early stage, ionic liquids offer us the opportunity to operate two-phase processes more safely and with reduced environmental impact.

## CONCLUSIONS

There has been considerable development in the field of two-liquid phase biocatalysis in the last decade and some of the developments are outlined in Table 5.5. Two-liquid phase biocatalysis has matured into a technology with a particular niche in biocatalysis. Given the increasing interest in the use of biocatalysis to synthesise novel optically pure compounds it is clear that application of two-liquid phase processes will increase.

**Table 5.5** Recent developments in two-liquid phase biocatalysis

Process feature	Development	References
Biocatalyst	Solvent resistance	de Bont (1998)
	Increased activity with non-natural substrates	Affholter and Arnold (1999)
Organic phase	Ionic liquids as solvent replacements	Cull <i>et al.</i> (2000)
Reactor	Liquid-impelled loop reactor Dense phase membrane reactors	Tramper <i>et al.</i> (1987) Doig <i>et al.</i> (1998)
Downstream processing	Membrane-based phase coalescence	Conrad and Lee (1998)

Alternative technologies exist which may prove preferable in some cases. Most importantly the use of organic solvents which are environmentally compromising may now be replaced with ionic liquid media. Likewise the use of designer biocatalysts will create new opportunities.

## ACKNOWLEDGEMENTS

GJL would like to thank Esso and the Royal Academy of Engineering for the award of an Engineering Fellowship and the Nuffield Foundation for financial support (NUF-NAL).

## REFERENCES

- Affholter, J. and Arnold F.H. (1999) Engineering a revolution. *Chemtech*, **29**, 34–39.

- Arnold, F.H. (1996) Directed evolution: creating biocatalysts for the future. *Chemical Engineering Science*, **51**, 5091–5102.
- de Bont, J.A.M. (1998) Solvent-tolerant bacteria in biocatalysis. *Trends in Biotechnology*, **16**, 493–99.
- Brink, L.E.S. and Tramper J. (1985) Optimization of organic solvent in multiphase biocatalysis. *Biotechnology and Bioengineering*, **27**, 1258–1269.
- Bruce, L.J. and Daugulis A.J. (1991) Solvent selection strategies for extractive biocatalysis. *Biotechnology Progress*, **7**, 116–124.
- Collins, A.M. and Woodley J.M. (1993) The scale-up of two-liquid phase microbially catalysed aromatic oxidations. In *Proc 1993 IChemE Research Event*, pp. 179–181. Rugby: IChemE.
- Conrad, P.B. and Lee S.S. (1998) Two-phase bioconversion product recovery by microfiltration I. Steady state studies. *Biotechnology and Bioengineering*, **57**, 631–641.
- Cull, S.C., Holbrey, J.D., Vargas-Mora, V., Seddon, K.R. and Lye G.J. (2000) Room temperature ionic liquids as replacements for organic solvents in multiphase bioprocess operations. *Biotechnology and Bioengineering*, **69**, 227–233.
- Doig, S.D., Boam, A.T., Leak, D.J., Livingston, A.G. and Stuckey D.C. (1998) A membrane bioreactor for biotransformations of hydrophobic molecules. *Biotechnology and Bioengineering*, **58**, 587–594.
- Doraiswamy, L.K. and Sharma M.M. (1984) *Heterogeneous reactions: analysis, examples and reactor design. Vol. 2: Fluid-fluid-solid reactions*. New York: John Wiley.
- Freemantle, M. (1998) Designer solvents—Ionic liquids may boost clean technology development. *Chemical and Engineering News*, **76**, 32–37.
- Furuhashi, K., Shintani, M. and Takagi M. (1986) Effects of solvents on the production of epoxides by *Nocardia corallina* B-276. *Applied Microbiology and Biotechnology*, **23**, 218–223.
- Harrop, A.J., Woodley, J.M. and Lilly M.D. (1992) Production of naphthalene-cis-glycol by *Pseudomonas putida* in the presence of organic solvents. *Enzyme and Microbial Technology*, **14**, 725–730.
- Kasche, V. and Galunsky B. (1995) Enzyme catalysed biotransformations in aqueous two-phase systems with precipitated substrate and/or product. *Biotechnology and Bioengineering*, **45**, 261–267.
- Kollmer, A., Schmid, A., Rudolf von Rohr, Ph. and Sonnleitner B. (1999) On liquid-liquid mass transfer in two-liquid-phase fermentations. *Bioprocess Engineering*, **20**, 441–448.
- Laane, C., Boeren, S., Hilhorst, R. and Veeger C. (1987) Optimization of biocatalysis in organic media. In *Biocatalysis in Organic Media*, edited by C.Laane, J.Tramper and M.D.Lilly, pp. 3–17. Amsterdam: Elsevier.
- Lilly, M.D., Brazier, A.J., Hocknull, M.D., Williams, A.C. and Woodley J.M. (1987) Biological conversions involving water-insoluble organic compounds. In *Biocatalysis in Organic Media*, edited by C.Laane, J.Tramper and M.D.Lilly, pp. 3–17. Amsterdam: Elsevier.
- Lilly, M.D., Dervakos, C.A. and Woodley J.M. (1990) Two-liquid phase biocatalysis: choice of phase ratio. In *Opportunities in Biotransformations*, edited by L.C.Copping, R.E.Martin, J.A.Pickett, C.Bucke and A.W.Bunch, pp. 5–16. London: Elsevier.
- Lilly, M.D. and Woodley J.M. (1985) Biocatalytic reactions involving water-insoluble organic compounds. In *Biocatalysts in Organic Syntheses*, edited by J.Tramper, H.C.van der Plas and P.Linko, pp. 179–192. Amsterdam: Elsevier.
- Lopez, J.L. and Matson S.L. (1997) A multiphase/extractive enzyme membrane reactor for production of diltiazem chiral intermediate. *Journal of Membrane Science*, **125**, 189–211.
- Mathys, R.C., Heinzelmann, W. and Witholt B. (1997) Separation of higher molecular weight organic compounds by pervaporation. *Chemical Engineering Journal*, **67**, 191–197.
- Mathys, R.C., Kut, O.M. and Witholt, B. (1998a) Alkanol removal from the apolar phase of a two-liquid phase bioconversion system. Part 1 : comparison of a less volatile and a more volatile in-situ extraction solvent for the separation of 1-octanol by distillation. *Journal of Chemical Technology and Biotechnology*, **71**, 315–325.

- Mathys, R.C., Schmid, A., Kut, O.M. and Witholt, B. (1998b) Alkanol removal from the apolar phase of a two-liquid phase bioconversion system. Part 2: effect of fermentation medium on batch distillation. *Journal of Chemical Technology and Biotechnology*, **71**, 326–334.
- Mathys, R.C., Schmid, A. and Witholt B. (1999) Integrated two-liquid phase bioconversion and product recovery processes for the oxidation of alkanes: process design and economic evaluation. *Biotechnology and Bioengineering*, **64**, 459–477.
- Michielsen, M.J.F., Frieling, C., Wijffels, R.H., Tramper, J. and Beaufort H.H. (2000) D-malate production by permeabilized *Pseudomonas pseudoalcaligenes*; optimization of conversion and biocatalyst productivity. *Journal of Biotechnology*, **79**, 13–26.
- Molinari, F., Argozzini, F., Cabral, J.M.S. and Prazeres D.M.F. (1997) Continuous production of isovaleraldehyde through extractive bioconversion in a hollow-fiber membrane bioreactor. *Enzyme and Microbial Technology*, **20**, 604–611.
- Monticello, D.J. (1993) Biocatalytic desulfurization of petroleum and middle distillates. *Environmental Progress*, **12**, 1–4.
- Pokora, A.R. and Cyrus W.L. (1987) Phenolic developer resins. US Patent No **4**, 647,952.
- Prazeres, D.M.F. and Cabral J.M.S. (1994) Enzymatic membrane bioreactors and their applications. *Enzyme and Microbial Technology*, **16**, 738–750.
- Seddon K.R. (1997) Ionic liquids for clean technology. *Journal of Chemical Technology and Biotechnology*, **68**, 351–356.
- Schmid, A., Kollmer, A., Mathys, R.C. and Witholt, B. (1998a) Developments towards large-scale bacterial bioprocesses in the presence of bulk amounts of organic solvents. *Extremophiles*, **2**, 249–256.
- Schmid, A., Kollmer, A. and Witholt, B. (1998b) Effects of biosurfactant and emulsification on two-liquid phase *Pseudomonas oleovorans* cultures and cell-free emulsions containing n-decane. *Enzyme and Microbial Technology*, **22**, 487–493.
- Schroen, C.G.P.H. and Woodley J.M. (1997) Membrane separation for downstream processing of aqueous-organic bioconversions. *Biotechnology Progress*, **13**, 276–283.
- Shutt, H., Schmidt-Kastner, G., Arenus, A. and Preiss M. (1985) Preparation pf optically active D-arylglucines for use as side chains for semi-synthetic penicillins and cephalosporins using immobilized subtilisins in two-liquid phase systems. *Biotechnology and Biengineering*, **27**, 420–433.
- Tramper, J., Wolters, I. and Verlaan P. (1987) The liquid-impelled loop reactor: A new type of density-difference-mixed bioreactor. In *Biocatalysis in Organic Media*, edited by C.Laane, J.Tramper and M.D.Lilly, pp. 311–316. Amsterdam: Elsevier.
- Umemura, T. and Hirohara H. (1989) Preparation pf optically active pyrethroids via enzymatic resolution. In *Biocatalysis in Agricultural Biotechnology*, edited by J.R.Whitaker and P.E. Sonnet, pp. 371–384. Washington: American Chemical Society.
- Van Sonsbeek, H.M., Beaufort, H.H. and Tramper J. (1993) Two-liquid-phase bioreactors. *Enzyme and Microbial Technology*, **15**, 722–729.
- Vicenzi, J.T., Zmijewski, M.J., Reinhard, M.R., Landen, B.E., Muth, W.L. and Marier P.C. (1997) Large-scale stereoselective enzymatic ketone reduction with *in situ* product removal via polymeric adsorbent resins. *Enzyme and Microbial Technology*, **20**, 494–499.
- Westgate, S., Vaidya, A.M., Bell, C. and Hailing P.J. (1998) High specific activity of whole cells in an aqueous-organic two-phase membrane bioreactor. *Enzyme and Microbial Technology*, **22**, 575–577.
- Woodley, J.M. (1990a) Stirred tank power input data for the scale-up of two-liquid phase biotransformations. In *Opportunities in Biotransformations*, edited by L.G.Copping, R.E.Martin, J.A.Pickett, C.Bucke and A.W.Bunch, pp. 5–16. London: Elsevier.
- Woodley, J.M. (1990b) Two-liquid phase biocatalysis: reactor design. In *Biocatalysis*, edited by D.A.Abramowicz, pp. 337–355. New York: Van Nostrand Reinhold.
- Woodley, J.M. and Lilly M.D. (1992) Process engineering of two-liquid phase biocatalysis, *Progress on Biotechnology*, **8**, 147–154.

- Woodley, J.M. and Titchener-Hooker N.J. (1996) The use of windows of operation as a bioprocess design tool. *Bioprocess Engineering*, **14**, 263–268.
- Woodley, J.M., Brazier, A.J. and Lilly, M.D. (1991a) Lewis cell studies to determine reactor design data for two-liquid phase bacterial and enzymic reactions. *Biotechnology and Bioengineering*, **37**, 133–140.
- Woodley, J.M., Cunnah, P.J. and Lilly, M.D. (1991b) Stirred tank two-liquid phase biocatalytic reactor studies: kinetics, evaluation and modelling of substrate mass transfer. *Biocatalysis*, **5**, 1–12.

# CHAPTER SIX

## ENZYMATIC MEMBRANE REACTORS

DUARTE MIGUEL F.PRAZERES AND JOAQUIM M.S.CABRAL

*Centre for Biological and Chemical Engineering, Institute Superior  
Técnico, Av. Rovisco Pais, 1049–001 Lisboa, Portugal*

### ABSTRACT

Membrane bioreactors have been increasingly used in past years to perform numerous enzymatic catalysed transformations. The unique characteristics of these multi-functional reactors that integrate biocatalysis and membrane separation, have made them an alternative to more conventional reactors such as fixed or fluidised beds. The aim of this chapter is to provide an updated overview on the topic of enzymatic membrane bioreactors. The first sections review the basic concepts, classification, advantages and problems associated with enzymatic membrane reactors. Different applications that have been described in the scientific literature in the last 20 years are then presented and discussed. Finally, some comments on the current state of the art and future prospects of this area are outlined.

**Keywords:** Membrane Reactor, Ultrafiltration, Enzymatic Reactors, Process Integration, Process Intensification, Bioreactors

### INTRODUCTION

Process intensification has been defined by chemical engineers as "...the development of novel apparatuses and techniques that, compared to those commonly used today, are expected to bring dramatic improvements in manufacturing and processing, substantially decreasing equipment-size/production capacity ratio, energy consumption, or waste production, and ultimately resulting in cheaper, sustainable technologies" (Stankiewicz and Moulijn, 2000). This concept can be easily translated and applied to processes in Biochemical Engineering. This chapter describes a particular type of process-intensifying system, i.e. enzymatic membrane reactors that have been used for some years in the specific area of Enzymatic Engineering.

An enzyme catalysed transformation of substrates into products can be carried out either in homogeneous or heterogeneous systems. The separation of the final products from the unreacted reagents and, in homogeneous catalytic systems, the separation of the catalyst from the reaction mixture, is a necessary step that increases the general complexity and cost of the process. Furthermore, an efficient use of the biocatalyst usually demands the transformation to be carried out continuously. Membrane reactors are special units designed to meet these needs, constituting an attempt to integrate the

biocatalytic conversion, product separation and/or concentration and catalyst recovery into a single continuous operation.

It is well known that most of the enzymatic processes currently in industrial use are carried out in batch reactors (Cheryan & Mehaia, 1986; Siebel, 1992). However, this class of reactors suffers from a number of well-documented limitations, such as batch-to-batch oscillations, high labour costs, frequent start-up and shut-down procedures, and the need to recover the enzyme, or enzyme preparation, after each batch (Cheryan & Mehaia, 1986). The immobilisation of the enzyme in the reactor, with retention of its catalytic activity, has emerged as a practical solution to overcome some of those disadvantages that are associated to the use of free biocatalysts in solution. The technique not only enables the recovery and re-use of the enzyme but also offers the opportunity to carry out the process in a continuous mode if necessary. Further advantages of immobilisation include better enzyme stability and process control, better productivity, more uniform products and the integration of a purification step in the process (Cheryan & Mehaia, 1986; Cheryan, 1986).

The immobilisation of enzymes has been accomplished by chemical and physical attachment to porous or non-porous solid surfaces (Gekas, 1986; Gerhardt, 1990). A wide variety of surfaces with different geometry/morphology (beads, pellets, fibers) and chemical composition have been used in different types of reactors: fixed bed, fluidised bed, CSTR, expanded bed, etc. Rony (1972) first pointed out the advantages of using a membrane as this solid surface, leading to the development of the first membrane reactors. The unique features of membranes in these reactors enable them to accomplish additional tasks other than immobilisation which are not commonly carried out in conventional reactors: product separation, phase separation, enzyme compartmentalisation, etc. (Matson & Quinn, 1992). Membrane reactors can therefore complement and compete with other reactor types in the field of biotransformations.

## THE CONCEPT OF A MEMBRANE BIOREACTOR

The basic feature of a membrane reactor is the separation of enzyme, products and substrates by a semi-permeable membrane that creates a selective physical/chemical barrier. Permeable substrates and products can be selectively separated from the reaction mixture by the action of a driving force (chemical potential, pressure, electric field) present across the membrane that causes the movement (diffusion, convection, electrophoretic migration) of solutes. On the other hand, the enzyme is retained within the system by the membrane, allowing the establishment of a continuous operation with substrate feed and product withdrawal (Figure 6.1). The whole system can be set up by assembling and interconnecting vessels and membrane modules.

Membranes can be used in a bioreactor exclusively as a matrix for the immobilisation of the biocatalyst (*reactive membrane*), without any separation purposes (Furusaki & Asai,

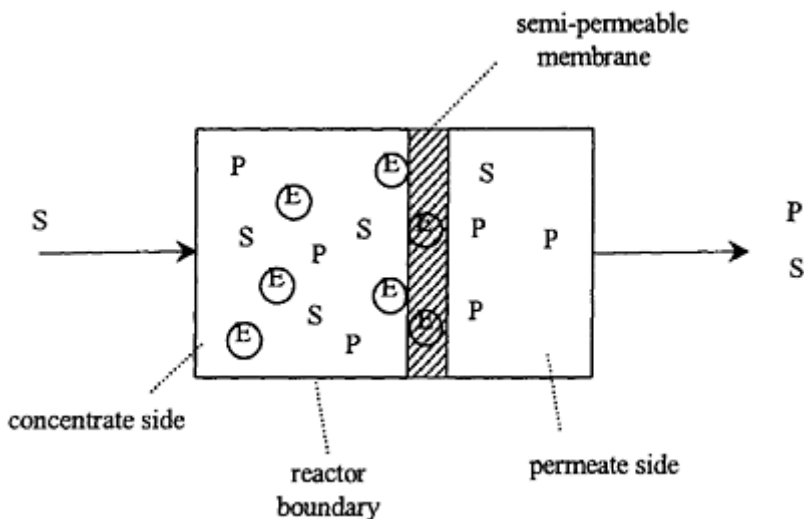


**Figure 6.1** Schematic diagram of a generic continuous enzymatic membrane reactor. Possible locations of the enzyme are shown (in solution, adsorbed or entrapped). E—enzyme, S—substrate, ~~P~~—product,—membrane.

**Table 6.1** The functions of a membrane in a membrane reactor

---

#### Membrane function

---

- enzyme retention and compartmentalisation
  - solute (substrate, product, cofactor) separation
  - immobilisation of liquid-liquid interfaces
- 

1983; Furusaki *et al.*, 1990; Bakken *et al.*, 1992; Garcia *et al.*, 1992; Maison & Quinn, 1992). However, and as suggested by Matson and Quinn (1992), the term membrane reactor should be reserved for those cases where the membrane is not merely a support for the enzyme, but rather adds its separating characteristics to the process (Table 6.1). Conventional separation processes usually involve the introduction of either an energy-separating agent (e.g. distillation) or a mass-separating agent (e.g. extraction). Membrane separations on the other hand are less complex and more energy efficient than other conventional separation processes (Gobina *et al.*, 1997).

The retention capability of a membrane towards a solute (enzyme, substrate or product) can be quantified by a parameter called the rejection coefficient,  $\sigma$ , which is defined as:

$$\sigma = 1 - \frac{C_p}{C_c} \quad (1)$$

where  $C_p$  is the solute concentration in the permeate side, and  $C_c$  the solute concentration in the concentrate side. A solute which is completely retained by a given membrane, will have a rejection coefficient of 1, while a solute which permeates freely across the membrane will have a rejection coefficient of 0.

In recent years, the functions of the membrane have extended with the systematic use of membrane reactors in two-phase bioconversions. In these situations, the membrane acts as a support for the interface between two distinct phases (liquid/liquid or liquid/gaseous). The membrane not only separates the phases, but also provides interfacial contact area and, together with the enzyme acts as an interfacial catalyst (Matson & Quinn, 1986; Lopez *et al.*, 1990, 1991; Matson & Lopez, 1991).

### **Enzyme Retention**

The complete retention of the enzyme in the system by the membrane is the first and most important requirement for the establishment of a successful continuous operation in a membrane reactor. This retention, which can be accomplished by different mechanisms, confines the enzyme to a specific region of the membrane reactor where reaction with substrate occurs. The enzyme is usually present in two forms; soluble or insolubilised at the surface or pores of the membrane matrix. If the enzyme is in solution, retention is achieved by confining the enzyme to one side of the membrane. As shown in Figure 6.2, this can be done by:

*Size exclusion:* enzyme molecules with sizes larger or close to the dimensions of the membrane pores are excluded (Ohlson *et al.*, 1984; Park *et al.*, 1985; Ishikawa *et al.*, 1989a; Fujii *et al.*, 1991; Bryjak *et al.*, 1996)

*Size exclusion via enlargement:* enzyme molecules enlarged through chemical/physical immobilisation onto an intermediate molecule—an inert protein (Alfani *et al.*, 1982), gels (Cantarella *et al.*, 1989) or liposomes (Chang *et al.*, 1991) are excluded.

*Electrostatic repulsion:* charged enzymes are repelled by membranes with charges of the same sign (Kulbe *et al.*, 1990; Rôthig *et al.*, 1990)

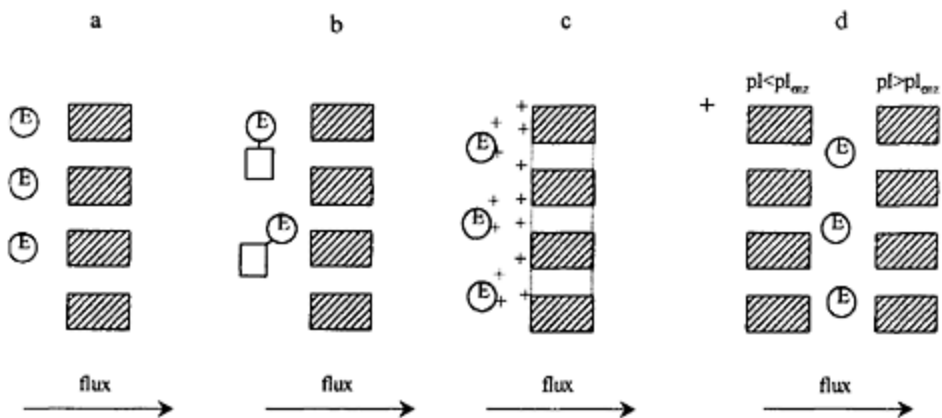


**Figure 6.2** Retention of soluble enzymes in membrane reactors by confinement through: a) size exclusion, b) size exclusion via enlargement, c) electrostatic repulsion and d) isoelectric trapping. (#—membrane)

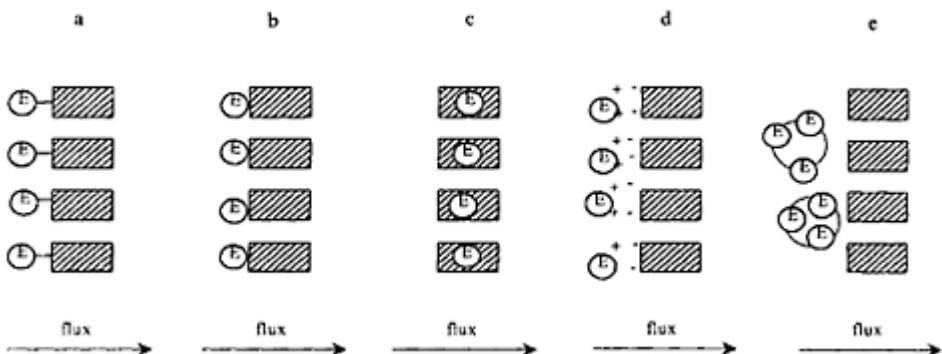


**Figure 6.3** Retention by direct immobilisation of enzymes in membrane reactors by: a) chemical coupling, b) adsorption, c) entrapment, d) electrostatic interactions and e) immobilisation on a macroscopic carrier. (#—membrane)

*Isoelectric trapping:* the enzyme is trapped between two isoelectric membranes with isoelectric point values far apart as to trap the enzyme by an isoelectric mechanism (Righetti *et al.*, 1997; Nembri *et al.*, 1997; Bossi *et al.*, 1999)

Alternatively the enzyme can be rendered insoluble by the direct immobilisation onto the surface and/or within the matrix of the membrane. This can be achieved in the following ways (Figure 6.3):

*Chemical coupling:* the enzyme is bound to membranes which carry reactive functional groups -OH, -COOH, -NH<sub>2</sub> (Nakajima *et al.*, 1989, 1993; Lozano *et al.*, 1990; Harrington, *et al.*, 1992; Hausser *et al.*, 1983; Okada *et al.*, 1994a; Ulbricht & Papra, 1997)

*Adsorption:* the enzyme adheres to the membrane surface via Van der Waals forces (Garcia *et al.*, 1992; Habulin, 1991; Malcata, 1991; Vaidya *et al.*, 1993; Prazeres *et al.*, 1992, 1994; Ulbricht & Papra, 1997)

*Entrapment:* the enzyme is entrapped within the matrix during membrane preparation by the phase inversion technique (Chen *et al.*, 1994)

*Electrostatic interactions:* charged enzymes are electrically bound to membranes with opposite charges (Furusaki & Asai, 1983; Furusaki *et al.*, 1990)

*Immobilisation on a macroscopic carrier:* enzyme molecules are immobilised (adsorption, covalent binding, electrostatic interaction) on a macroscopic carrier (beads, pellets) (Shefer *et al.*, 1993; 1995; Alfani *et al.*, 1998; Xin *et al.*, 2000).

### Substrate Retention and Product Separation

The presence of a membrane in a continuous membrane reactor, apart from enabling enzyme retention may allow for the retention of substrate molecules to a certain extent, thus increasing their concentration and residence time in the system. In such a situation, and for the case of enzyme kinetics without substrate inhibition, a membrane reactor operates at higher reaction rates than an equivalent CSTR (Prazeres, 1995). This situation

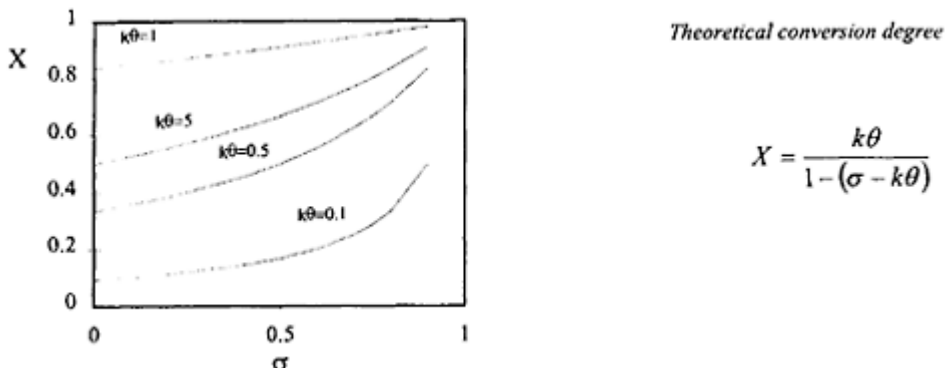


**Figure 6.4** Theoretical steady state conversion degree ( $X$ ) in a continuous enzymatic membrane reactor operating with first order kinetics (rate constant

$k$ ), as a function of the substrate rejection coefficient,  $\sigma$ . The reactor was modelled as a CSTR (see Prazeres, 1995 for further details).  $\theta$ —residence time.

is exemplified in Figure 6.4 which presents the theoretical, steady state conversion degree,  $X$ , obtained in a continuous enzyme membrane reactor operating with first order kinetics (rate constant  $k$ ), as a function of the substrate rejection coefficient,  $\sigma$ . As can be seen, the conversion degree is affected not only by the kinetics of the reaction, but also by the degree to which substrate molecules are retained by the membrane.

Furthermore, in those cases where chemical equilibrium affects the reaction yield, this substrate retention may contribute to a favourable shift of the equilibrium towards the product side (van der Padt *et al.*, 1991, 1996a; Prazeres, 1996). The extent of substrate retention depends mainly on the dimensions and/or chemical compatibility of the substrate molecules with the membrane material. Another way of promoting the retention of substrate molecules that are smaller than the membrane pores is by using charged membranes or by applying an electrical field across the membrane. The prerequisite necessary for this strategy to function is that the substrate can be rendered electrically charged. For instance, negatively charged membranes have been used to retain negatively charged cofactors [NAD(H), NADP(H)] inside reactors, thus preventing their leakage from the system (Ikemi *et al.*, 1990a; Kulbe *et al.*, 1990; Nidetzky *et al.*, 1996). Electrically charged membranes can also be used to attract substrate molecules in those cases where the enzyme is immobilised on the membrane (Chen *et al.*, 1994).

The products generated during the bioconversion should in principle permeate through the membrane, either by diffusion (induced by a concentration gradient) or convection (usually induced by a pressure gradient). An electric field may also be used to force charged products to migrate from the reactor and across the membrane into the permeate stream (Lee & Hong, 1988; Furusaki *et al.*, 1990; Righetti *et al.*, 1997; Nembri *et al.*, 1997; Bossi *et al.*, 1999).

Although the permeation of products through a membrane has been always regarded as an essential requirement for the successful operation of a membrane reactor, cases exist where the complete rejection of products might be desirable. For instance, if the target product has a low solubility in the media and precipitates or crystallises during reaction, the solid particles formed can be retained behind the membrane. The operation of a membrane reactor of this kind which enables the continuous synthesis of dipeptides (AcPheLeuNH<sub>2</sub>) by  $\alpha$ -chymotrypsin in reversed micellar media has been described (Serralheiro *et al.*, 1994; Prazeres *et al.*, 1995; Serralheiro *et al.*, 1999). Solid products formed upon reaction in a membrane reactor can also be collected during operation if a filtration unit is incorporated in the system (Furui *et al.*, 1996). This avoids the continued contact of solid particles with the membrane therefore preventing clogging and the consequent decrease in permeate flux.

## Membranes and Modules

The majority of enzymes (10,000–100,000 daltons), whether native or modified, can be retained in a membrane reactor with ultrafiltration (UF) membranes. Most of the commercial UF membranes are asymmetric, i.e., the pore size varies continuously in one direction. These membranes are formed by an ultra-thin layer deposited upon a sublayer of higher porosity. The ultra-thin layer is formed by a network of micropores with pore size distributions in the range 1–100 nm, corresponding to a nominal molecular weight cutoff of 500 to 100,000 daltons. During operation, fluids flow through the membrane due to a difference in hydrostatic pressure, and solutes are more or less retained by the thinner layer according to their size. Apart from this size discrimination, a steric exclusion process may be present for those molecules that have sizes inferior, but close to the dimensions of the pores. The selectivity is therefore most likely associated to the ratio of the molecule radius to the pore radius (Meireles *et al.*, 1992). The chemical nature of the membrane can also interfere with solute permeation due to non-specific interactions—electrostatic, hydrophobic, van der Waals, dipole-dipole, etc. (Prazeres *et al.*, 1993a)—which lead to the formation of a second layer (gel layer) that decreases the permeation (concentration polarisation phenomena). This is especially true if a chemical reaction occurs simultaneously with the membrane separation process.

The asymmetric structure of ultrafiltration membranes allows higher permeate flow rates and makes these membranes less susceptible to clogging and easier to clean (Hildebrandt, 1991a). The materials commonly used in the manufacturing of ultrafiltration membranes are synthetic polymers and ceramic materials (Santos *et al.*, 1991). Ceramic membranes when compared with polymeric ones are generally more resistant to high temperatures and chemicals and are mechanically stronger under pressure. The membranes used in the enzymatic reactors described in the literature have used materials such as nylon, polypropylene, polyamide, polyacrylonitrile, cellulose acetate, polysulfone, cellulose, polytetrafluoroethylene and carbon. The selection of a membrane for a particular enzymatic process should be carefully made since the membrane material can significantly affect the stability of the enzyme (Nakajima *et al.*, 1992; Alfani *et al.*, 1990). This choice is usually made tentatively and should consider characteristics such as morphology, molecular weight cutoff, porosity, pore size distribution, chemical resistance, temperature, pH and pressure tolerance and price (Hildebrandt, 1991a; Leuchtenberger *et al.*, 1984). In the particular case of multiphase reactors, the membrane material (wetting characteristics) and structure (pore size and asymmetry) should be carefully chosen in view of the need to maintain a stable interface between the two phases at the membrane (Vaidya *et al.*, 1992).

Nanofiltration membranes can also be used in a membrane reactor if the retention of small solutes ( $<200 \text{ g mol}^{-1}$ ) such as cofactors, substrates, products, and buffer compounds is desirable. The separation here is performed on the basis of size, and also charge (Lin *et al.*, 1997; Seelbach and Kragl, 1997).

The UF membrane material is usually in the form of a flat sheet, a tube or a hollow fibre. These are then assembled in modules with a determined geometry offering distinct flow zones and hydrodynamics for the feed and permeate streams (Santos *et al.*, 1991; Hildebrandt, 1991b). Different types of modules have been used in membrane reactors:

plate and frame, tubular, hollow fibres, spiral wound and ultrafiltration cells (Prazeres & Cabral, 1994). While the permeate flow is usually perpendicular to the membrane surface, the main flow in the concentrate side of these modules can be tangential or perpendicular, as in dead-end designs. The use of tangential flow is usually preferable since mass transfer and permeation flux are improved. Some module designs include turbulence promoters, such as spacers or screens, as a way of increasing permeation flux.

Improved filtration performance can be further obtained by coupling a controlled secondary flow to the main flow. This can be achieved for instance in devices where the membrane tubes or fibres are helically wrapped (Figure 6.5a), originating secondary flow structures named Dean vortices (Luque *et al.*, 1999; Kluge *et al.*, 1999). Another approach is to use two rotating concentric cylinders, one containing the membrane, in order to produce the secondary flow structures known as Taylor vortices (Figure 6.5b). In both cases, the vortices formed enhance back migration through increased wall shear rate and increased convective flow away from the membrane, increasing permeation flow rates (Luque *et al.*, 1999; Kluge *et al.*, 1999).

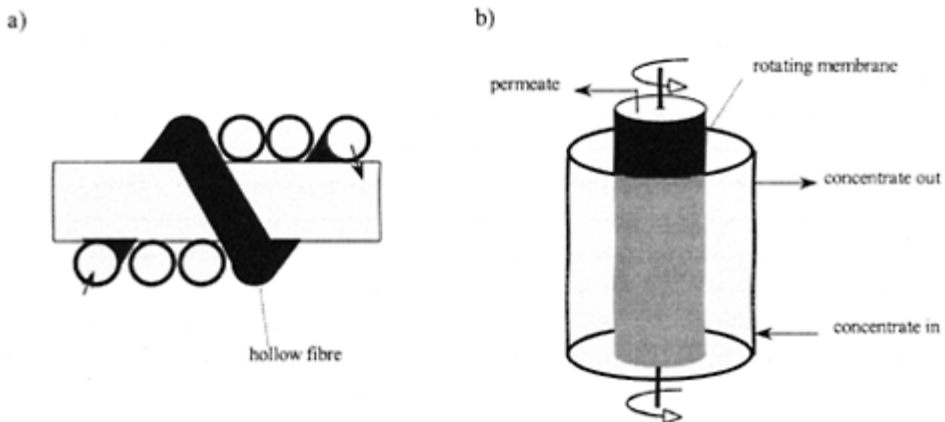


**Figure 6.5** Module designs that add secondary flow structures to the main flow: a) helically wound hollow fibre design: secondary flow- Dean vortices (adapted from Luque *et al.*, 1999) and b) rotating concentric cylinders: secondary flow-Taylor vortices.

#### CLASSIFICATION OF MEMBRANE REACTORS

Enzymatic membrane reactors can be broadly classified in three categories, according to the mechanism by which enzymes and substrates are brought into contact (Prazeres & Cabral, 1994).

### Direct Contact Membrane Reactors

In this type of membrane reactor, the substrates are added to the same compartment of the reactor that contains the enzyme. The enzyme, either in the soluble form or insolubilised at the membrane surface, can thus act directly on the substrate molecules as soon as they enter the system. This class of reactors can be further divided into recycle, dead-end and dialysis reactors.

*Recycle membrane reactors* are usually formed by a stirred vessel coupled to an ultrafiltration module in a semi-loop configuration (Figure 6.6). The substrate is added to the vessel and the reaction mixture is continuously recycled from and to the vessel through the UF unit. The reaction occurs both in the vessel and module if the enzyme is in the soluble form, or solely in the module if the enzyme is immobilised in the membrane. Products and excess solvent permeate through the membrane, being continuously removed from the system. The liquid volume is kept constant in the vessel as long as the inlet flow rate is equilibrated with the outlet permeate flow rate. If the enzyme is immobilised on the membrane surface, external mass transfer limitations can be reduced by increasing the recirculation flow rate (Lozano *et al.*, 1990). Tubular membranes and hollow fiber modules are the more used in this type of configuration. Studies on the residence time distribution in these recycle reactors indicate that the whole system behaves like an ideal CSTR (Deeslie & Cheryan, 1981; Bressolier *et al.*, 1988; Sims & Cheryan, 1992). This type of configuration is probably the most used and referred to in the literature (Prazeres & Cabral, 1994).

*Dead-end membrane reactors* are formed exclusively by an UF module. In this configuration, the reaction mixture is pressurised against the membrane and forced to flow

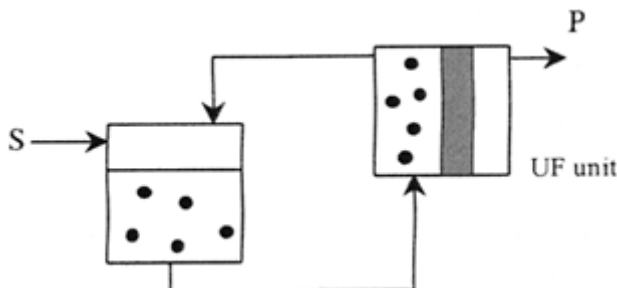


**Figure 6.6** Schematic diagram of a recycle membrane reactor (•—enzyme, S—substrate, P—product, —membrane)

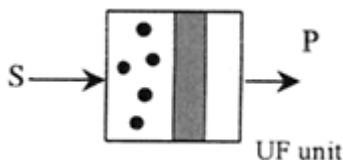


**Figure 6.7** Schematic diagram of a dead-end membrane reactor (•—enzyme, S—substrate, P—product, //—membrane)

across the micropores (Figure 6.7). This type of operation can be carried out in the wide spread ultrafiltration cells or, otherwise, in common ultrafiltration modules with the appropriate ends sealed (Harrington *et al.*, 1992).

In a continuous operation, the substrate should be added at a flow rate equal to the permeate flow. Ultrafiltration cells are essentially operated as CSTRs and the permeation of solutes is achieved by conventional filtration through a flat membrane placed perpendicularly to the reactor bottom. Despite a very low ratio of membrane area to reactor volume and low permeation fluxes caused by concentration polarisation, ultrafiltration cells are extensively used in laboratory-scale studies to test operation concepts and investigate kinetic mechanisms, probably due to their simplicity of operation (Prazeres & Cabral, 1994).

In *dialysis membrane reactors*, two process streams are circulated at approximately the same flow rate in each side of the membrane, thus minimising convective flow. The substrate is directly added to the stream that contains the enzyme. The products formed diffuse through the membrane towards the other stream as a consequence of the concentration gradient established (see Figure 6.8). The disadvantages of this type of configuration are mainly a consequence of a less efficient mass transport due to an operating mode based exclusively on diffusion. Few examples of this mode of operation have appeared in the literature (Chiang & Tsai, 1992a, b).

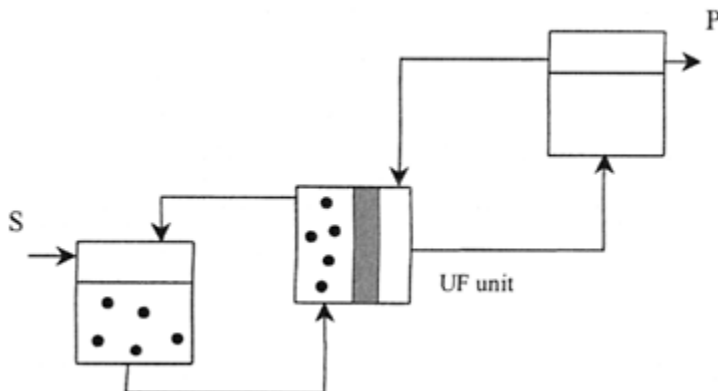


**Figure 6.8** Schematic diagram of a dialysis membrane reactor (•—enzyme, S—substrate, P—product, //—membrane)

### Diffusion Membrane Reactors

In the class of *diffusion membrane reactors*, unlike the previous one, the substrate is not added to the compartment that contains the enzyme. Instead, the contact between enzyme/ substrate is established only after diffusion of the substrate molecules through the membrane micropores to the other compartment where the enzyme is located (soluble or insolubilised). After reaction, the products back diffuse to the unreacted substrate stream that circulates by and leave the system (see Figure 6.9).

Hollow fibre modules are mostly used in this class of reactors, with the enzyme usually placed in the shell side of the module and the substrate stream passing through the fibre lumen. Closed tubings of dialysis membranes can also be used to contain the enzyme solution (Lüthi & Luisi, 1984; Bednarski *et al.*, 1987). The dialysis bag formed is then submerged in the reaction mixture that contains the substrate, which diffuses through the membrane. The product formed diffuses back to the bulk solution. Diffusion membrane reactors act essentially as dialysers as solutes are transferred through the membrane under a concentration driving force, rather than pressure. The majority of the disadvantages presented by this type of reactors are related to the fact that diffusion is the dominant transport mechanism. In many cases, the kinetic behaviour of enzymes in these reactors is inferior when compared with a free enzyme because the permeation of the substrates across the membrane is often the rate-limiting step. In addition, the control of the environmental conditions in the vicinity of the entrapped enzyme is also limited by the diffusion of chemical species in the media (Kitano & Ise, 1984; Kelsey *et al.*, 1990). The limited number of publications in the literature reporting the experimental operation of such types of membrane reactors (Park *et al.*, 1985; Bednarski *et al.*, 1987; Tegtemeir *et al.*, 1988; Ishikawa *et al.*, 1989a; Fujii *et al.*, 1991; Miyawaki *et al.*, 1990; Yonese *et al.*, 1990; Czermark & Bauer, 1991; Nakano *et al.*, 1999), is probably a reflection of transport limitations. Other arrangements can be implemented in this class of reactors such as the one shown in Figure 6.10, where the substrate-containing stream is recirculated from the module through an external vessel. This strategy provides one way of increasing the residence time of the substrate molecules inside the reactor and improves mixing. Furthermore, the presence of an external vessel is convenient in terms of the operation of

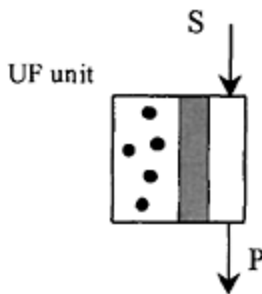


**Figure 6.9** Schematic diagram of a single-pass diffusion membrane reactor (•—enzyme, S—substrate, P—product, //—membrane)

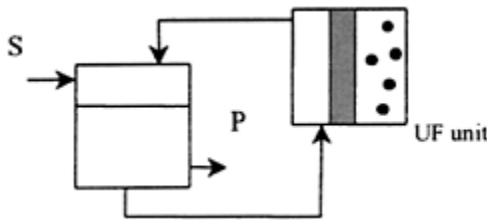


**Figure 6.10** Schematic diagram of a diffusion membrane reactor with recycle (•—enzyme, S—substrate, P—product, //—membrane)

the system, enabling measurement and control (pH, temperature, mixing, sampling, etc.). A recent publication describes a reactor of this type for the coupled transcription/translation from a PCR (polymerase chain reaction) product using T7 RNA polymerase and an *Escherichia coli* S30 extract with a hollow fibre module (Nakano *et al.*, 1999).

### Multiphase Membrane Reactors

*Multiphase membrane reactors* promote an interfacial contact between enzyme and substrates at the membrane matrix. The membrane usually acts as a support for the enzyme and for the interface between two immiscible liquid phases (hydrophilic and hydrophobic). These constitute reservoirs where substrates and products may be solubilised (Figure 6.11). Diffusion is again the dominant transport mechanism together with interfacial transport. If the membrane material/structure is carefully chosen, the hydraulic pressure caused by the circulation of the two phases is usually sufficient to maintain a good phase separation at the membrane (Pronk *et al.*, 1988). Eventually, a

slight positive pressure may have to be applied in order to keep the interface in the plane of the membrane and prevent the phases from mixing. In some cases the progressive

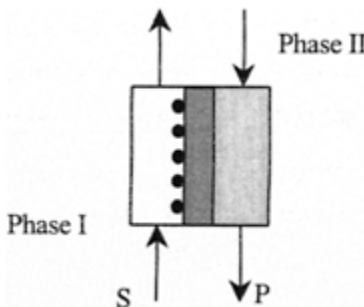


**Figure 6.11** Schematic diagram of a single pass multiphasic membrane reactor (•—enzyme, S—substrate, P—product,  $\text{---}$ —membrane)

adsorption/desorption of products/substrates (e.g. surface-active compounds) to the membrane may change the wetting characteristics of the material and cause a movement of the interface or even the breakthrough of one of the phases (Vaidya *et al.*, 1994). This will of course change the performance of the reactor.

The enzyme is usually placed in the aqueous side of the membrane in order to prevent contact with the hydrophobic phase—commonly an organic solvent—and to protect the enzyme from denaturation. In certain cases (e.g. lipases), immobilisation on the hydrophobic side is used (van der Padt *et al.*, 1990, 1992; Janssen *et al.*, 1991; Pronk *et al.*, 1992). Multiphase membrane reactors have been mostly used and seem specially indicated in those cases where the enzymes display interfacial activation, such as lipases and phospholipases. They are also especially suited for situations where substrates and products have distinct solubility characteristics.

Configurations with recycle of one or both phases through external vessels are also possible (Figure 6.12), with the advantages already mentioned in the previous section.

Although multiphase membrane reactors have exclusively used two phases, the construction of an appropriate module can enable a membrane reactor to operate with a higher number of phases. For instance, the installation of two independent bundles of fibres in a hollow fibre module would permit the operation of a three phase membrane reactor (Figure 6.13a). Phase I could serve as a substrate reservoir, phase II as a product collector and phase III, located in the shell side of the module could contain the enzyme. This type of module is commercialised by Hoechst (Liqui-Cel™ Contained Liquid Membrane—CLM module), and is used to perform two-step extraction processes. A similar process could also be implemented by coupling the shell side of two simple hollow fibre modules (Figure 6.13b).

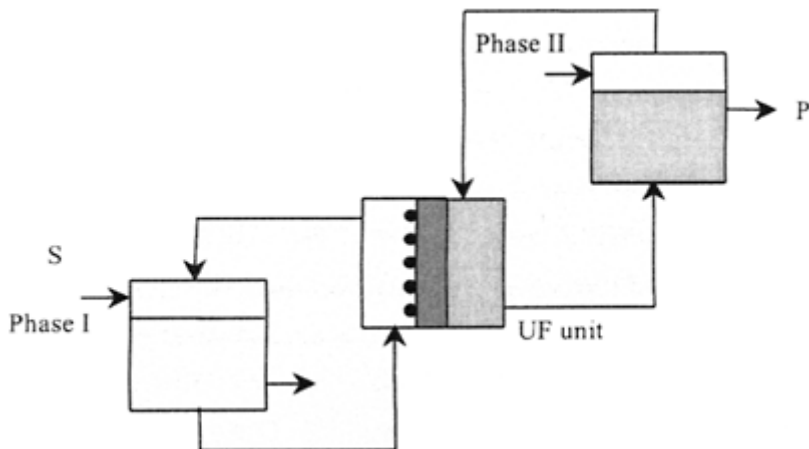


**Figure 6.12** Schematic diagram of a multiphasic membrane reactor with dual recycle (•—enzyme, S—substrate, P—product, //—membrane)

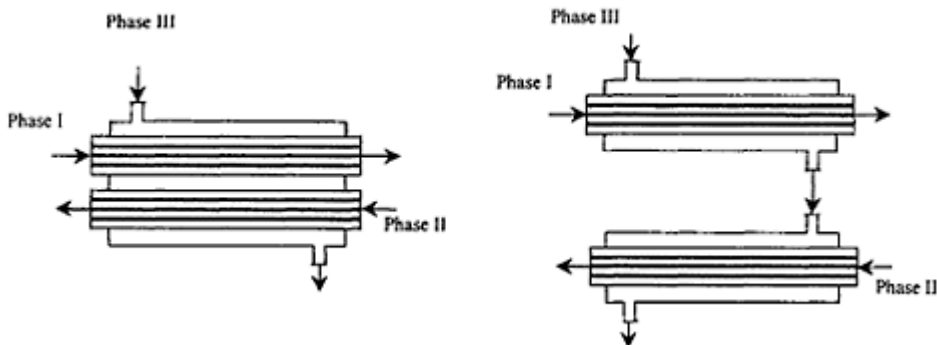


**Figure 6.13** Three phase membrane reactors: a) one module with two independent fibre bundles and b) two modules in parallel.

## ADVANTAGES AND DISADVANTAGES OF MEMBRANE REACTORS

### **Advantages**

Membrane reactors have several intrinsic advantages that make them an alternative system to more conventional enzymatic reactors (e.g. batch, fixed and fluidized beds) (Table 6.2). One of the great advantages of membrane reactors is certainly the possibility of a continuous and intensive use of enzymes. This contributes to an increase in productivity and possibly to the economical viability of the process. This aspect is common to all continuous reactors when compared to batch systems. However, the use of membranes instead of porous particles or beads as an immobilisation aid gives membrane reactors some competitive edge over conventional, continuous fixed or fluidised bed reactors.

**Table 6.2** Advantages and disadvantages of membrane reactors

Advantages	Disadvantages
Continuous operation possible	Unfavourable enzyme adsorption
Better control possibilities	Enzyme poisoning
Integration of unit operations	Deactivation of enzyme by shear effects
Higher reaction rates and productivity	Product/substrate inhibition at surface
Shift of chemical equilibrium	Loss of enzyme activators or cofactors
Concentration/enrichment of product streams	Concentration polarisation
Control of the MW of hydrolysates	Membrane fouling
Multiphase reactions possible	Enzyme leakage
Scale up is simple	High price of membranes and modules
Improved energy efficiency	Mechanical and thermal fragility
Reduction in equipment size	

(Belfort, 1989). Some of the advantages are related to the unique possibilities offered by a membrane reactor, that enables an integration of the enzymatic process with separation steps. Furthermore, the often occurring mass transfer limitations of conventional fixed or fluidised bed reactors due to external and pore diffusion effects, can be reduced in certain membrane reactor configurations, since in many cases it is possible to operate the system with convective mechanisms rather than diffusive ones. In this way, substrates and products can be readily transported to and swept away from the enzymes. This may be especially important in product inhibited reactions (Belfort, 1989). This enhancement of mass transfer could be responsible for increased productivities in membrane reactors.

when compared to traditional column reactors with enzymes immobilised on beads (Nakajima *et al.*, 1989, 1993).

Important advantages can also arise due to changes in the reaction rates caused by the presence of a membrane, as described earlier: retention of substrate molecules to a certain extent leads to higher reaction rates (Prazeres, 1995) and possibly to higher yields in equilibrium limited reactions (van der Padt *et al.*, 1991; Prazeres, 1996).

In the case of multi-product systems, the presence of a membrane may also be beneficial. In such a case, if the membrane exhibits some selectivity towards different products, an enrichment of the less rejected product is obtained in the outlet process stream (Matson & Quinn, 1986). On the other hand, the product that is more rejected can be concentrated inside the system. This may be disadvantageous if product inhibition is present.

One of the early-recognised advantages of membrane reactors was detected in the hydrolysis of macromolecules. In these cases, a membrane with the adequate *cut-off* usually enables some control of the molecular weight of the hydrolysates. This leads to an increase in lower molecular weight components in the permeate stream and to a concentration of the heavier products behind the membrane (Cheryan & Mehaia, 1986; Silva, 1990; Bouhallab *et al.*, 1992, 1993, 1995).

As already mentioned above, membrane reactors also offer the possibility to conduct two-phase reactions, without the emulsification problems; namely the inactivation of the enzyme caused by the intensive agitation necessary to make and maintain emulsions and the high power requirements (hence, energy costs).

### Disadvantages

The performance of membrane reactors during operation can be severely affected by losses in the catalytic and mass transfer efficiencies, which are inherent to the geometry and design of this particular type of reactor.

The stability of the enzyme during operation can be caused by several factors other than temperature related deactivation (Deeslie & Cheryan, 1981). For instance, a gradual decrease in activity may occur as a consequence of leakage of enzyme molecules through the membrane pores (Silva, 1990; Jones *et al.*, 1984). This may even occur in those cases where the molecular weight of the enzyme is higher than the membrane *cut-off*, since the shape of the enzyme molecules and the distribution of membrane pore sizes should be also taken into account. Cheryan & Mehaia (1986) suggested that in order to prevent this from occurring, a membrane with a *cut-off* at least 5–10 times lower than the enzyme molecular weight should be selected. Small enzyme activators such as metal ions or cofactors (Drioli *et al.*, 1993; Hayakawa *et al.*, 1985) may also cross the membrane, decreasing the enzyme activity (Deeslie & Cheryan, 1981). In such cases, supplementation of the leaking component is fundamental to ensure a successful operation.

When the enzyme is used in its soluble form, unfavourable adsorption to the membrane may occur. This contact with the membrane can lead to structural changes in the enzyme molecule and poisoning which can contribute to a decrease in activity. This means that the type of membrane material may influence the stability of the enzyme (Nakajima *et al.*, 1992; Alfani *et al.*, 1990).

Free enzyme molecules in membrane reactors are subjected to shear forces and frictions generated near the membrane walls. There is evidence that these shear fields and related secondary effects such as interfacial inactivation, adsorption, local heating and air entrapment can cause enzyme inactivation (Narendranathan & Dunnill, 1982; Virkar *et al.*, 1981; Thomas & Dunnill, 1979). Experimentally this effect is usually observed in the form of a correlation between the loss of activity with an increase in recirculating rates (Lozano *et al.*, 1990; Narendranathan and Dunnill, 1982). These effects may be significant in recycle reactors that usually operate with high recirculating flow rates. In the case of membrane reactors using stirrers, shearing-related effects associated with rotation may also contribute to deactivation (Alfani *et al.*, 1990). Whenever a decrease in operational kinetic stability caused by one of the factors described above occurs, fresh enzyme should be added to maintain a constant productivity in the reactor.

Decreases in the performance of membrane reactors can also be attributed to losses in mass transfer efficiency during the permeation process. Two distinct phenomena are usually responsible for the reduction in membrane permeation ability: concentration polarisation and fouling.

Concentration polarisation is the reversible build-up of dissolved and suspended solutes (including enzymes) at the boundary layer adjacent to the membrane, which leads to the formation of a concentration gradient. The gel layers formed at the interface act as a second membrane and originate a diffusion flux of solutes (products or substrates) from the membrane towards the bulk of the medium that decreases the net flux across the membrane. The solvent flow through the membrane is also restricted due to the presence of this additional hydrodynamic resistance that causes a decrease in the solvent filtration flux (Hildebrandt, 1991b). In many cases, concentration polarisation-related phenomena (adsorption, deposition, solute/membrane interactions) also contribute to an increase in the rejection capability of the membrane (Fane & Radovich, 1990). Concentration polarisation can be reduced and controlled by manipulating operating conditions such as temperature and pressure, and by increasing flow rates or by introducing cyclic backflushing or pulsatile flow (Park *et al.*, 1985). Another way of reducing this polarisation effect is by applying an electric current across the membrane. If the correct pH is chosen, some solutes and enzymes can be rendered charged and will migrate in the presence of the electric field (Lee & Hong, 1988). This strategy can be used to keep enzyme molecules from adsorbing to the membrane if the migration proceeds in a direction opposite to the permeate flow, and to accelerate the removal of electrically charged products from the reactor into the permeate stream (Furusaki *et al.*, 1990). Usually, a complete restoration of original permeation fluxes after operation is achieved by using efficient cleaning procedures.

The second limiting phenomenon most likely to occur during a filtration operation is fouling. This is associated with a modification in the filtration properties of a membrane as a result of the irreversible deposition or adsorption of solutes and particles at the surface or inside the pores. This process leads to a progressive reduction in the efficiency of a membrane, essentially due to a reduction in the solvent and solute permeate fluxes and to an increase in the rejection of solutes (Santos *et al.*, 1991; Hildebrandt 1991b). An adequate pre-treatment of the membrane and substrate feed can contribute to a minimisation of this effect, thus increasing the lifetime of the membranes.

A good control of both concentration polarisation and fouling effects is essential to maintain constant mass fluxes, and hence productivity, in membrane reactors.

Another factor that can have an impact in permeate flux is the viscosity of the reaction medium. Highly concentrated solutions of substrate/product (higher viscosity) will originate lower permeate fluxes and eventually a lower productivity of the membrane reactor (Nishizawa *et al.*, 2000).

## APPLICATIONS OF ENZYME MEMBRANE REACTORS

Membrane reactors can be used with any biocatalysed reaction with the aim of developing continuous integrated processes with high productivity. The applications found in a survey of the scientific literature over the past fifteen years were sorted out according to the type of reactions investigated, as shown in Table 6.3. Several research cases within each group are shortly described in Tables 6.4 to 6.10.

### Hydrolysis of Macromolecules

The majority of the first applications of membrane reactors described in the literature dealt with the enzymatic hydrolysis of macromolecules such as proteins and carbohydrates—starch and cellulose (Cheryan & Mehaia, 1986). Applications of the correspondent

**Table 6.3** General applications of membrane bioreactors

---

#### Applications

---

Hydrolysis of macromolecules

Biotransformation of lipids

Reactions with cofactors

Optical resolutions and synthesis of peptides

Biomédical and environmental applications

Conversion of oligosaccharides

other

---

products can be envisaged mainly in the food industry, with the use of the different hydrolisates in the supplementation of beverages and food products (Cheryan & Mehaia, 1986). One of the major functions played by the membrane of a reactor in these applications is the retention of the macromolecular substrates, with the concomitant increase in reaction rates during continuous operation. This type of reaction can only be promoted in direct contact membrane reactors (Figure 6.2), where there is no need for the substrate molecules to diffuse through the membrane in order to reach the enzyme. The membrane also plays an important role in the selective separation of low molecular

weight products. If size differences are significant, it is possible to continuously fractionate the reaction mixture, and obtain a permeate stream which is rich in low molecular weight products (Bouhallab *et al.*, 1992; Figure 6.14). These type of reactions continues to attract researchers as can be shown by the number of publications which have appeared in the literature in the past years dealing with the hydrolysis of different types of macromolecules in membrane reactors: proteins, peptides, cellulose, pectin, maltodextrins and starch (Table 6.4).

### Biotransformation of Lipids

A significant number of the applications of membrane enzyme reactors explore the lipase catalysed transformation of lipids such as bulk fats, oils, triglycerides, fatty acids and esters in one or two phase systems (Table 6.5). The majority of the examples listed in Table 6.5 deal either with the hydrolysis of lipids and fats for the production of fatty acids, mono and di-glycerides and glycerol or with the synthesis of esters including transesterification reactions. Although the large number of lipase applications might be a consequence of the large scientific and economic effort that has been devoted to these enzymes in the last few years, the particular structure and unusual mode of action of Upases is most likely responsible for this trend. The fact that Upases are activated by and act at interfaces probably makes them the perfect biocatalyst to use in membrane reactors,

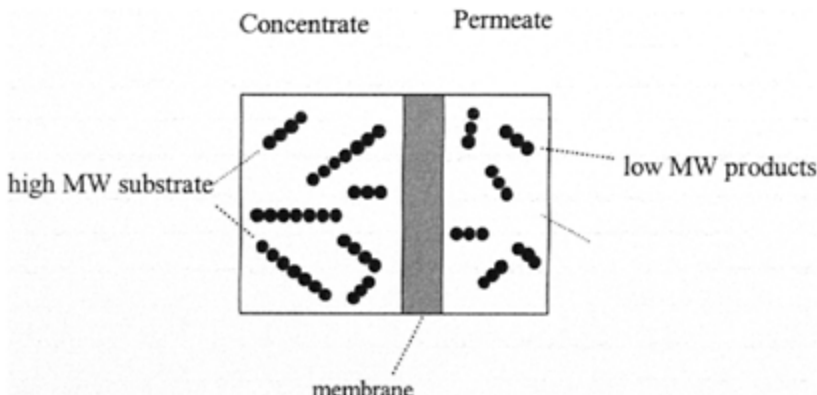


**Figure 6.14** Hydrolysis of macromolecules and selective separation of low MW products

**Table 6.4** Hydrolysis of macromolecules

Enzyme-reaction description	Reference
Hydrolysis of soy proteins catalysed by pronase	Deeslie & Cheryan, 1981, 1982
Production of maltose corn syrups by - amylase/glucoamylase	Hausser <i>et al.</i> , 1983

Hydrolysis of sodium-hydroxide-pretreated sallow catalysed by cellulase	Ohlson <i>et al.</i> , 1984; Frennesson <i>et al.</i> , 1985
Hydrolysis of vegetable proteins catalysed by a protease from <i>Penicillium dupontii</i>	Adu-Amankwa <i>et al.</i> , 1984
Hydrolysis of bovine plasma proteins catalysed by alcalase from <i>Bacillus licheniformis</i>	Bressollier <i>et al.</i> , 1988
Hydrolysis of cassava starch catalysed by glucoamylase	Darnoko <i>et al.</i> , 1989; Gaouar <i>et al.</i> , 1997; López-Ulibarri & Hall, 1997
Hydrolysis of starch catalysed by glucoamylase	Larsson & Mattiasson, 1984; Uttapap <i>et al.</i> , 1989
Pectin hydrolysis catalysed by pectolytic enzymes	Lozano <i>et al.</i> , 1987, 1990
Hydrolysis of maltodextrins by glucoamylase	Silva, 1990
Hydrolysis of cellulose catalysed by cellulases in an ultrafiltration cell	Alfani <i>et al.</i> , 1983; Kinoshita <i>et al.</i> , 1986; Lee & Kim, 1993; Ina & Kinoshita, 1993
Saccharification of liquefied corn starch catalysed by glucoamylase	Sims & Cheryan, 1992
Preparation of bioactive peptides by the hydrolysis of caseino-macropептиde and proteins catalysed	Bouhallab <i>et al.</i> , 1992, 1993, 1995 by trypsin
Hydrolysis of fish proteins catalysed by protease	Nakajima <i>et al.</i> , 1992
Hydrolysis of starch to maltose syrups by simultaneous use of -amylase and isoamylase	Houng <i>et al.</i> , 1992
Hydrolysis of starch by cyclodextrin glucanotransferase to produce cyclodextrin in a capillary MR	Okada <i>et al.</i> , 1994a
Hydrolysis of bovine hemoglobin by pepsin	Sannier <i>et al.</i> , 1994; Zhao <i>et al.</i> , 1995
Hydrolysis of starch into maltotetraose using maltotetraohydrolase from <i>Pseudomonas stutzeri</i>	Woo & McCord, 1994
Preparation of bioactive peptides by the hydrolysis of soyproteins using endopeptidases	Sonomoto <i>et al.</i> , 1995
Hydrolysis of proteins from the horn and hoof of cow and buffalo using a protease from <i>Bacillus subtilis</i>	Kida <i>et al.</i> , 1995
Hydrolysis of starch to glucose by glucoamylase and subsequent conversion to gluconic acid by	glucose oxidase Onda <i>et al.</i> , 1996
Depolimerization of dextran using endodextranase in an ultrafiltration cell	Mountzouris <i>et al.</i> , 1999

**Table 6.5** Hydrolysis, esterification and transesterification of lipids

Enzyme-reaction description	Reference
Production of glycerol and fatty acids by the	Hoi <i>et al.</i> 1985a, 1985c, 1986; Rélaifi-Bakó

hydrolysis of olive oil catalysed by lipase	<i>et al.</i> , 1994; Giorno <i>et al.</i> , 1995; Giorno & Drioli, 1997
Production of glycerol and fatty acids by the hydrolysis of lipids catalysed by lipase	Goto <i>et al.</i> , 1992; Pronk <i>et al.</i> , 1988, 1992
Phosphatidylglycerol synthesis catalysed by phospholipase D	Lee <i>et al.</i> , 1985
Synthesis of glycerides catalysed by lipase in a flat MR	Hoq <i>et al.</i> , 1985b
Production of glycerol and fatty acids by the hydrolysis of tallow catalysed by lipase	Taylor <i>et al.</i> , 1986; Taylor, 1996
Production of glycerol and fatty acids by the hydrolysis of triglycerides by lipase in emulsion	Molinari <i>et al.</i> , 1988
Hydrolysis of olive oil by lipase in an emulsion system	Brady <i>et al.</i> , 1988
Hydrolysis of the alkyl ester ethyl butyrate catalysed by porcine liver esterase	Maison & Lopez, 1990
Synthesis of n-butyl oleate catalysed by lipase in a hollow fibre MR	Habulin & Knez, 1991
Hydrolysis of triacetin catalysed by lipase in a hollow fibre MR	Guit <i>et al.</i> , 1991
Hydrolysis of butter oil catalysed by lipase and pregastric esterase	Malcata <i>et al.</i> , 1991, 1993; Garcia <i>et al.</i> , 1995, Garcia & Hill, 1995.
Esterification of sorbitol and fatty acids catalysed by lipase in a 2-phase MR	Janssen <i>et al.</i> , 1991
Synthesis of mono-, di-and tri-glycerides catalysed by lipase	van der Padt <i>et al.</i> , 1990, 1992, 1996a, 1996b
Transesterification of glycerol with olive oil by lipase in liposomes/AOT-isoctane reversed micelles	Chang & Rhee, 1991
Hydrolysis of soybean oil by lipase in a reactor with 2 different membranes	Tanigaki <i>et al.</i> , 1993
Hydrolysis of olive oil catalysed by lipase encapsulated in AOT/isoctane reversed micelles	Chiang & Tsai, 1992a, 1992b; Prazeres <i>et al.</i> , 1992, 1993a, 1993b, 1994; Hakoda <i>et al.</i> , 1996
Hydrolysis of milkfat triglycerides catalysed by lipase in an emulsion system with a spiral wound MR	Garcia <i>et al.</i> , 1992
Hydrolysis of ethyl laurate by lipase immobilised in a packed bed hollow fibre reactor	Vaidya <i>et al.</i> , 1994
Wax ester synthesis by lipase-surfactant complex in hexane using an ultrafiltration cell	Isono <i>et al.</i> , 1995

Hydrolysis of lecithin by phospholipase A2 encapsulated in lecithin/AOT/isoctane reversed micelles	Morgado <i>et al.</i> , 1996
Esterification of oleic acid and oleyl alcohol by a lipase-surfactant complex in an ultrafiltration cell	Isono <i>et al.</i> 1998
Hydrolysis of sunflower oil by lipase in an emulsion system	Can <i>et al.</i> , 1998
Hydrolysis of Menhaden oil by lipase in a hollow fibre reactor	Rice <i>et al.</i> , 1999
Interestesterification of butterfat with oleic acid by lipase in a hollow fibre reactor	Balcão & Malcata, 1997, 1998
Synthesis of short chain esters by cutinase encapsulated in AOT/isoctane reversed micelles	Carvalho <i>et al.</i> , 1998
Production of hexanal from linoleic acid by the action of lipoxygenase and hydroperoxide lyase in hollow fibre MR	Cass <i>et al.</i> , 2000

and particularly in multiphase membrane reactors. This class of reactors, especially when using membrane modules with a high specific area such as hollow fibres, is ideal to promote an interfacial contact between lipases and lipidic substrates.

In the typical multiphase membrane reactor application, the lipidic or organic phase is passed through one side of the membrane, while a buffer solution flows tangentially on the other side. The membrane becomes wetted by the lipidic phase if the membrane material is hydrophobic (Figure 6.15), or by the aqueous phase if it is hydrophilic, and the reaction takes place at the interface. The lipase is usually immobilised on the side of the membrane that faces the hydrophilic phase, or alternatively, inside the membrane. In certain cases the hydrophobic side can be used for immobilisation (van der Padt *et al.*, 1990, 1992; Janssen *et al.*, 1991; Pronk *et al.*, 1992). The substrates and products will distribute themselves between the two phases according to their solubility characteristics.

Tanigaki and co-workers (1993) developed a slightly different approach by using two different types of flat membranes in the reactor: hydrophilic and hydrophobic. The hydrolysis of soybean oil was carried out in an enzyme chamber separated by the two membranes with water permeating from one side through the hydrophilic membrane and oil permeating from the other through the hydrophobic membrane. The products formed, glycerol and fatty acids, back-diffused through the membranes to the recirculating aqueous and oil phases.

The contact between organic and aqueous phases needed for transforming lipids can also be promoted at a microscopic level but without phase separation at the macroscopic level, by using reversed micellar systems. Despite of several advantages, the applications of these systems have been mostly explored in batch reactors, at a laboratory scale. Nevertheless, continuous processes for the hydrolysis of lipids (Chang *et al.*, 1991; Chiang & Tsai, 1992a, 1992b; Prazeres *et al.*, 1992, 1993a, 1993b, 1994; Morgado *et al.*, 1996; Hakoda *et al.*, 1996), and synthesis of esters (Carvalho *et al.*, 1998) in reversed micellar systems have been investigated in membrane reactors. Despite the expectations,

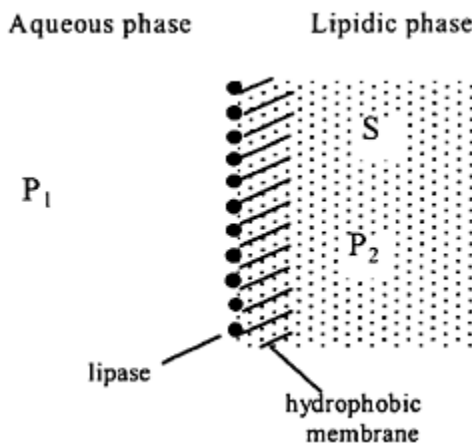


**Figure 6.15** Multiphase membrane (hydrophobic) reactor for the transformation of lipids (S—lipidic substrate, P<sub>1</sub> water soluble product, P<sub>2</sub> water insoluble product)

the membranes used in those cases were not capable of completely retaining the hydrated micelles, which had to be continuously supplemented to the reactor.

### Reactions with Cofactors

Many enzymes which are involved in useful reactions such as covalent bond synthesis, energy transfer, group transfer and redox reactions depend on the presence of freely dissociated cofactors or bound prosthetic groups to perform their catalytic tasks. These reactions are attractive from the point of view of industry because of the wide variety of products that can be synthesised (Cheryan & Mehaia, 1986). Among the enzymes used are for instance oxidoreductases, transferases and ligases which need cofactors such as nicotinamide adenine dinucleotide (NAD), nicotinamide adenine dinucleotide phosphate (NADP) and adenosine 5'-phosphate (ATP) or depend on prosthetic groups such as flavine adenine dinucleotide (FAD) or methoxantine (PQQ) for their catalytic activity (Miyawaki, 1993; Brielbeck *et al.*, 1994). The development of a bioprocess based on these reactions should consider the fact that cofactors and prosthetic groups are spent just like substrates after each turnover. Unfortunately, the cost of cofactors is most of the times so high that practical applications can only be developed if a regenerating system for those compounds is designed. The application of membrane reactors is presently considered the solution for this problem, constituting an interesting research topic and having originated a significant number of publications in the past years (Table 6.6).

Membrane reactors can offer the possibility of regenerating cofactors by using a coupled enzyme system or, alternatively coupled substrates approach (Kulbe *et al.*, 1990). In either case, the coenzyme is required only in catalytic amounts. The first

strategy requires the use of a cofactor regenerating enzyme and an inexpensive sacrificial substrate (Figure 6.16a).

This enzyme uses the extra substrate to catalyse the regeneration of the cofactor that was spent in the main reaction. The criteria used for the choice of the cofactor regenerating

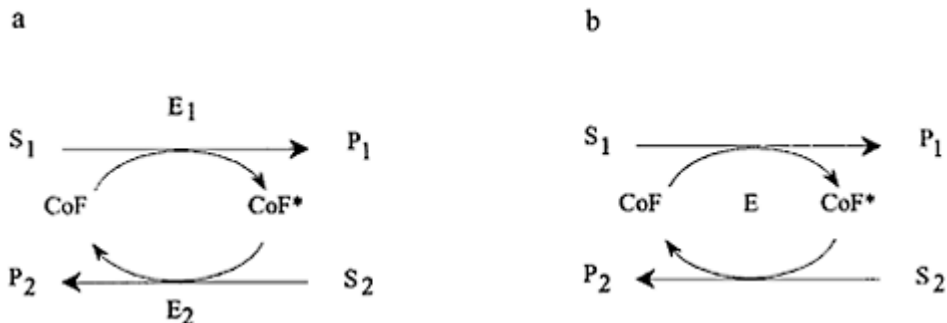


**Figure 6.16** Cofactor regeneration by:  
a) coupling of enzymes and b) coupled substrate approach ( $S_1$ —main substrate,  $S_2$ —auxiliary substrate,  $P_1$ —main product,  $P_2$ —secondary product, CoF—cofactor,  $CoF^*$ —spent cofactor,  $E_1$ ,  $E_2$  and  $E$ —enzymes).

**Table 6.6** Reactions with cofactors

Enzyme-reaction description	Reference
Synthesis of L-methionine and L-phenylalanine from the N-acetyl-DL-derivatives by acylase	Leuchtenberger <i>et al.</i> , 1984
Synthesis of L-malic acid by the fumarase stereoselective addition of water to fumaric acid	Leuchtenberger <i>et al.</i> , 1984
Synthesis of L-leucine with NADH (PEG bound) regeneration by leucine and formate dehydrogenases Leuchtenberger <i>et al.</i> , 1984; Ohshima <i>et al.</i> , 1985;	Kragl <i>et al.</i> , 1996a; Wichmann <i>et al.</i> , 2000
Transformation of LD-lactate via pyruvate to L-alanine with NADH (PEG bound) regeneration	Wandrey <i>et al.</i> , 1984
Synthesis of L-and D-2-hydroxyisocaproic acid by dehydrogenases with NADH (PEG bound) regeneration	Wichmann <i>et al.</i> , 1984
Synthesis of glucose 6-phosphate by hexokinase with ATP regeneration by acetate kinase	Berke <i>et al.</i> , 1984, 1988
Synthesis of L-lactate with NAD (PEG bound) regeneration by lactate and malate dehydrogenases	Hayakawa <i>et al.</i> , 1985

Production of -glutamyl-cysteine by -glutamyl-cysteine synthetase with ATP (PEG bound) regeneration kinase	Berke <i>et al.</i> , 1988
Synthesis of glucose 6-phosphate by glukokinase with ATP regeneration by acetatekinase	Ishikawa <i>et al.</i> , 1989a, 1989b
(R)-(-)-mandelic acid from benzoyl formate with NADH regeneration by formate dehydrogenase	Maeda <i>et al.</i> , 1990
Production of amino acids, hydroxyacids, alcohols, aldehydes and lactones with dehydrogenases	van Eikeren <i>et al.</i> , 1990
Production of sulcatol with simultaneous NADPH regeneration by alcohol dehydrogenase	Röthig <i>et al.</i> , 1990
Synthesis of mannitol by mannitol dehydrogenase with NADH regeneration by glucose dehydrogenase in a charged MR	Kulbe <i>et al.</i> , 1990
Coenzyme dependent reactions catalysed by dehydrogenases (production of propyl alcohol, lactate and 6-phosphogluconate)	Miyawaki <i>et al.</i> , 1990; Obón <i>et al.</i> , 1998
Synthesis of L-alanine by alanine dehydrogenase with NADH regeneration by lactate dehydrogenase	Fujii <i>et al.</i> , 1991
Production of sorbitol by aldose reductase with NADPH regeneration by glucose dehydrogenase in a charged MR	Ikemi <i>et al.</i> , 1990a, 1990b
Production of NADPH with alcohol dehydrogenase in an ultrafiltration cell	Peters & Kula, 1991
Synthesis of 12-ketoursodeoxycholic acid by dehydrogenases with NADH and NADPH regeneration	Carrea <i>et al.</i> , 1992
Synthesis of organic compounds by methylenehydroxilases with electrochemical enzyme reactivation using flavocytochromes	Brielbeck <i>et al.</i> , 1994
Synthesis of L-tert-Leucine by leucine dehydrogenase with NADH regeneration by formate dehydrogenase in 2 MR in series	Kragl <i>et al.</i> , 1996b
Production of (S)-l-acetoxy-2-alkanol with NADPH regeneration using bakers' yeast cell free extract	Ishihara <i>et al.</i> , 1996
Reduction of 2-ketoglutarate to L-glutamate by glutamate dehydrogenase with NADH regeneration by glucose dehydrogenase in a nonfiltration MR	Lin <i>et al.</i> , 1997
Production of L-carnitine by L-carnitine dehydrogenase with NADH regeneration by glucose dehydrogenase	Lin <i>et al.</i> , 1999
Production of xylitol by xylose reductase with NADH regeneration by glucose dehydrogenase in a charged MR	Nidetzky <i>et al.</i> , 1996b
Production and extraction of (S)-1-phenyl-2-propanol by alcohol dehydrogenase with NADH regeneration by formate dehydrogenase	Kragl <i>et al.</i> , 1996a
Resolution of l-phenyl-1, 2 ethanediol by glycerol dehydrogenase with NADH regeneration by lactate dehydrogenase	Liese <i>et al.</i> , 1996
Enantioselective reduction of 2-octanone by carbonyl reductase in an emulsion, two membrane reactor	Liese <i>et al.</i> , 1998 v

enzyme is based on the ease of removal of by-products and on equilibrium considerations. Dehydrogenases (alcohol, formate, glucose, lactate etc.) have been systematically used as regenerating enzymes.

In the second approach (Figure 6.16b), the enzyme that synthesises the product of interest also catalyses the regeneration of the cofactor by using another substrate (Kulbe *et al.*, 1990; Leuchtenberger *et al.*, 1984). For instances, in the synthesis of pheromone sulcatol catalysed by alcohol dehydrogenase, NADP<sup>+</sup> was regenerated by the same enzyme at the expense of isopropanol as a secondary substrate (Röthig *et al.*, 1990).

The membrane reactor, apart from immobilising the enzyme(s), should retain the cofactor, or at least increase its residence time in the system. This retention can be accomplished through size exclusion (Maeda *et al.*, 1990), electrostatic repulsion (Kulbe *et al.*, 1990; Röthig *et al.*, 1990; Drioli *et al.*, 1993; Nidetzky *et al.*, 1996a), or size exclusion via enlargement by covalent binding to polymers (e.g. PEG) (Röthig *et al.*, 1990; Leuchtenberger *et al.*, 1984; Hayakawa *et al.*, 1985; Wandrey *et al.*, 1984; Wichmann *et al.*, 1984; Ohshima *et al.*, 1985; Berke *et al.*, 1984, 1988; Kragl *et al.*, 1996b). The cofactor can also be used as a permeable solute by an immobilised enzyme (Ishikawa *et al.*, 1989a, 1989b; Fujii *et al.*, 1991; Miyawaki *et al.*, 1990).

These cofactor regenerating membrane reactors were used for the production of several different compounds: NADPH (Peters & Kula, 1991), amino acids (Fujii *et al.*, 1991; Leuchtenberger *et al.*, 1984; Wandrey *et al.*, 1984; van Eikeren *et al.*, 1990; Ohshima *et al.*, 1985; Kragl *et al.*, 1996), hydroxyacids (Wichmann *et al.*, 1984; van Eikeren *et al.*, 1990), alcohols (Kulbe *et al.*, 1990; Röthig *et al.*, 1990; Miyawaki *et al.*, 1990; van Eikeren *et al.*, 1990), acids (Leuchtenberger *et al.*, 1984; Carrea *et al.*, 1991; Maeda *et al.*, 1990), glucose-6 phosphate (Ishikawa *et al.*, 1989a, 1989b; Berke *et al.*, 1984), 6-phosphogluconate (Miyawaki *et al.*, 1990), lactate (Hayakawa *et al.*, 1985; Miyawaki *et al.*, 1990) and aldehydes and lactones (van Eikeren *et al.*, 1990). A large scale process was developed at DEGUSSA AG for the production of L-alanine from pyruvic acid catalysed by L-alanine dehydrogenase with NAD<sup>+</sup> being regenerated back to NADH by using formate dehydrogenase (Leuchtenberger *et al.*, 1984). In this case NADH was maintained in the system by increasing its molecular weight upon binding to polyethylene glycol. This use of membrane reactors as a process strategy for regenerating cofactors has enabled cycle numbers (defined as the number of product molecules per cofactor molecule) as high as 500,000 (reported by Wandrey, 1987).

Many of the membrane reactor systems developed for cofactor regeneration use two (e.g. Ishikawa *et al.*, 1989a; Maeda *et al.*, 1990; Fujii *et al.*, 1991) or even three (e.g. Wandrey *et al.*, 1984; Carrea *et al.*, 1991) enzymes acting synergistically. This possibility of easily immobilising different enzyme molecules is one of the particularly attractive features of membrane reactors that enable them to conduct enzyme catalysed sequential reactions. Some authors have described further applications (other than cofactor regenerating) of membrane reactors using the conjugated action of two enzymes. Kragl and co-workers (Kragl *et al.*, 1990b, 1990c) used an epimerase for the isomerisation of N-acetylglucosamine to N-acetylmannosamine that was then further converted to the final product, N-acetylneurameric acid, by the addition of pyruvic acid catalysed by a lyase. Other bi-enzyme membrane reactors investigated were:  $\beta$ -amylase/isoamylase (Hausser *et al.*, 1983) and  $\alpha$ -amylase/glucoamylase (Houng *et al.*, 1992) for the

production of maltose syrups from starch, and glucoamylase/glucose oxidase for the conversion of maltose into hydrogen peroxide (Bardeletti & Coulet, 1987).

### **Optical Resolutions and Synthesis of Peptides**

Other reactions that have been increasingly studied in membrane reactors are the production of optically pure compounds and the synthesis of oligopeptides for pharmaceutical and fine chemical uses (Table 6.7).

The ability of enzymes to discriminate between enantiomers in racemic substrates has made enzymatic synthesis an alternative to conventional chemical synthesis in the preparation of chiral pharmaceuticals (Margolin, 1993). Although the increasing use of enzymes (e.g. lipases) for the synthesis of optically pure drugs has not been accompanied by a comparable development of adequate enzyme reactors, membrane reactors have been emerging as one of the most appropriate configurations for large-scale optical resolutions. The majority of the applications described uses lipases as the biocatalyst in two-phase membrane reactors.

The Tanabe Seiyaku Company in cooperation with Sepracor Inc. (Tosa & Shibatani, 1995) industrialized one of the most successful processes developed. The process uses a lipase in a two-phase hollow fibre reactor, to perform the resolution of ( $\pm$ )-methoxyphenylglycidate methyl ester, an intermediate of the pharmaceutical diltiazem. The enzyme is immobilised by adsorption on the shell side of the module where toluene flows with the substrate and water is circulated in the lumen of the fibres. Biproducts of the reaction that inhibit the enzyme are extracted to the aqueous phase (Matsumae *et al.*, 1994; Tosa & Shibatani, 1995). One of the disadvantages of this reactor at the industrial level is the low level of productivity due to the use of substrate in the soluble form. An attempt to overcome this drawback was made by coupling a crystalUser to the membrane reactor at the lab scale. This unit was used as a reservoir for highly concentrated slurry of substrate and to recover product, which crystalUsed simultaneously during reaction (Furui *et al.*, 1996).

Other applications developed at Sepracor Inc. with two phase hollow fiber reactors were the racemic resolution of an ester (glycidyl butyrate) catalyzed by a lipase (López *et al.*, 1990) and the resolution of racemic amino acids by  $\beta$ -chymotrypsin (Matson & Quinn, 1986; Matson & López, 1990; López *et al.*, 1991).

The production of short chain peptides (2–32 amino acids) and their derivatives is of increasing importance in areas such as biomedical research, the development of pharmaceuticals and the food industry (Kelley, 1996). The interest in the protease catalysed synthesis of these compounds as opposed to traditional chemical synthesis, is due to the known advantages of the enzymatic approach: no racemisation, lower purification costs, higher yields, no need for side-chain protection and use of mild reaction conditions (pH, temperature, pressure) that lead to lower energy consumption. Membrane reactors have been used up to now especially to promote the synthesis of different dipeptides (Table 6.8). The literature describes for example the use of  $\alpha$ -chymotrypsin in the large scale synthesis of kyotorphin (Tyr-Arg) (Herrmann *et al.*, 1991) or the use of  $\alpha$ -chymotrypsin in reversed micelles to synthesise Phe-Leu, an intermediate of the pharmacological dipeptides enkephalin and dynorphin (Serralheiro *et al.*, 1994; 1999; Prazeres *et al.*, 1995).

**Table 6.7** Optical resolutions, enantioselective conversions and synthesis of peptides

Enzyme-reaction description	Reference
Resolution of a racemic mixture of N-benzoyl tyrosine ethyl ester by $\alpha$ -chymotrypsin in a 2-phase MR	López <i>et al.</i> , 1991; Matson & López, 1990
Synthesis of (R) glycidol by the lipase catalysed resolution of racemic glycidyl butyrate	López <i>et al.</i> , 1990
Resolution of a racemic mixture of N-acetyltyrosine ethyl ester by $\alpha$ -chymotrypsin in a 2-phase MR	Matson & Quinn, 1986
Resolution of ( $\pm$ )-trans-3-(4-methoxyphenyl) glycidic acid methyl ester by lipase from <i>Serratia marcescens</i> in a 2-phase MR	Matsumase <i>et al.</i> , 1994; Furui <i>et al.</i> , 1996
Resolution of ( $\pm$ )-methoxyphenylglycidate methyl ester by lipase in a 2-phase MR	Tosa & Shibatani, 1995
Resolution of racemic glycidyl butyrate by lipase in a 2-phase MR	Wu <i>et al.</i> , 1990, 1993
Resolution of racemic cyanomethyl [2-(4-isobutylphenyl) propionate] by lipase in a hollow fibre reactor	Giorno <i>et al.</i> , 1995
Resolution of 1-phenyl-L, 2 ethanediol by glycerol dehydrogenase with NADH regeneration by lactate dehydrogenase	Liese <i>et al.</i> , 1996
Resolution of (S)-(+)-2-(6-methoxy-2-naphthyl) propionic acid by lipase immobilised on solid particles in a 2-phase MR	Xin <i>et al.</i> , 2000
Enantioselective oxidation of methyl phenyl sulfid by chloroperoxidase in a UF cell	Pasta <i>et al.</i> , 1999
Peptide synthesis catalysed by $\alpha$ -chymotrypsin in reversed micelles	Lüthi & Luisi, 1984
Production of -glutamyl-cysteine by -glutamyl-cysteine synthetase with ATP (PEG bound) regeneration by acetate kinase	Berke <i>et al.</i> , 1988
Large scale synthesis of kyotorphin (Tyr-Arg) catalysed by $\alpha$ -chymotrypsin in a flat MR	Herrmann <i>et al.</i> , 1991
Dipeptide (Phe-Leu) synthesis catalysed by $\alpha$ -chymotrypsin in TTAB/octanol/heptane reversed micelles	Serralheiro <i>et al.</i> , 1994; 1999; Prazeres <i>et al.</i> , 1995
Continuous synthesis of kyotorphin (Tyr-Arg) catalysed by $\alpha$ -chymotrypsin in an ultrafiltration cell	Flörsheimer <i>et al.</i> , 1989; Fischer <i>et al.</i> , 1994

**Table 6.8** Biomedical applications

Enzyme-réaction description	Reference
Development of HF reactor with L-asparaginase for the deamidation of L-asparagine for the chemotherapy of cancer	Jackson <i>et al.</i> , 1979; Pedersen <i>et al.</i> , 1978a; Mazzola & Vecchio, 1980
Development of HF reactor with carboxypeptidase Cl for the conversion of folates for the chemotherapy of cancer	Pedersen <i>et al.</i> , 1978a

Development of HF reactor with L-phenylalanine amonialyase for the deamidation of L-phenylalanine and L-tyrosine for the chemotherapy of cancer	Pedersen <i>et al.</i> , 1978a, 1978b
Development of HF reactor with L-arginase for the cleavage of L-arginine to ornithine and urea	Rossi <i>et al.</i> , 1981
Extracorporeal removal of heparin from the blood stream by immobilised heparinase in hollow fibres	Comfort <i>et al.</i> , 1989a, 1989b, 1989c
Hydrolysis of urea by urease immobilised in an anion exchange membrane	Chen <i>et al.</i> , 1994
Extracorporeal removal of low density lipoproteins by phospholipase A2 immobilised in beads and confinée in hollow fibres	Shefer <i>et al.</i> , 1993, 1995
Extracorporeal removal of low density lipoproteins by phospholipase A2 in a combined packed bed/hollow fibre reactor	Labeque <i>et al.</i> , 1993

### Biomedical Applications

The application of immobilised enzymes as therapeutic agents for the treatment of cardiovascular, oncological, intestinal, viral and hereditary diseases is a promising technology that has been the subject of extensive laboratory and clinical investigation (Torchilin, 1987). One of the approaches that has been undertaken to immobilise the enzymes uses membrane bioreactors with hollow fibres or tubular modules as extracorporeal systems (Table 6.8). The therapeutic enzyme is usually located in the shell side of the module, while the blood stream (or other biological fluid) perfuses through the lumen of the fibres. The plasma is separated through the permeable walls of the fibres into the shell, leaving the cellular components behind. The separation of the enzyme from the whole blood not only increases its stability but also contributes to a decrease in immunological reactions (Pedersen *et al.*, 1978a). Typically, the enzyme possesses a specific degrading ability towards some diffusive low molecular weight metabolite of the plasma.

For instance, phospholipase A2 has been used immobilised in beads and confined in the shell of a hollow fibre module to modify low density lipoproteins (LDL) present in the blood of hypercholesterolemic rabbits (Labeque *et al.*, 1993; Shefer *et al.*, 1993, 1995). The plasma is separated through the permeable walls of the fibres leaving the blood cells behind (Figure 6.17). The immobilised enzyme is thus able to convert the plasma lipoprotein to a form that can be removed from the body at an enhanced rate. The reactor has two outlets, one carrying red blood cells from the lumen of the fibres and the other carrying treated plasma from the reactor shell. The treated plasma is then reconstituted with the blood cells before returning to the animal. The total plasma cholesterol concentration decreased up to 40% and the results of safety tests indicated that the treatment is safe. Therefore this technique offers a potential new approach for lowering serum cholesterol and LDL levels which are usually related with coronary heart disease (Shefer *et al.*, 1993).

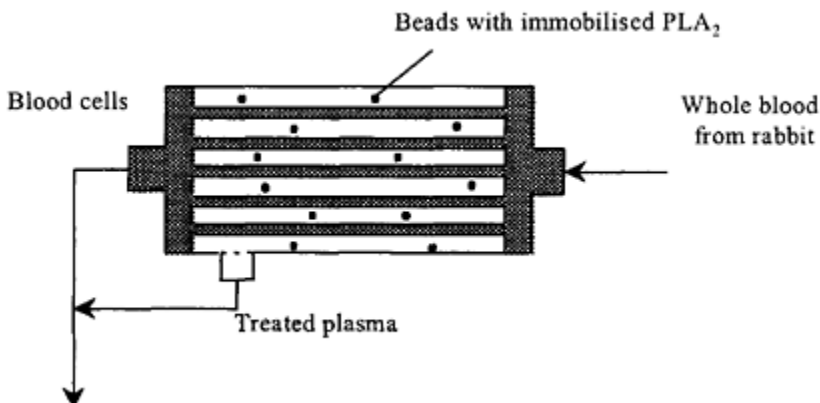


**Figure 6.17** Membrane reactor as an extracorporeal device for the treatment of hypercholesterolemia (adapted from Shefer *et al.*, 1993).

Enzymatic membrane reactors have also been used in the chemotherapy of cancer by exploiting the fact that malignant cells are more sensitive to some amino acids concentration (e.g. arginine, asparagine, phenylalanine) than normal cells. This suggested that the corresponding enzymes (arginase, asparaginase, phenylalanine ammonia-lyase) could be used for the depletion of those amino acids in the plasma with the consequent inhibition of the growth of malignant cells (Pedersen *et al.*, 1978; Rossi *et al.*, 1981; Mazzola & Vecchio, 1980; Jackson *et al.*, 1979). For instance, a hollow fibre module with covalently attached asparaginase to the outside of the fibres was successfully used as an extracorporeal device to reduce the level of asparagine in healthy dogs (Jackson *et al.*, 1979). This could contribute to the treatment of some acute lymphocytic leukaemias.

### Conversion of Oligosaccharides

A number of the applications of membrane reactors found in the literature deal with the transformation of oligosaccharides such as lactose, maltose, saccharose, cellobiose or cyclodextrins (Table 6.9). The products obtained via these reactions, whether being mono- or oligosaccharides, are usually sweet and may therefore find application in the food industry as sweeteners or dietary products (Belitz & Grosch, 1987). A number of references describes the continuous hydrolysis of lactose, an abundant disaccharide which is found in milk, whey and other dairy products (Jones *et al.*, 1984; Park *et al.*, 1985; Peterson *et al.*, 1989a, 1989b; Czernak & Bauer, 1991; Bakken *et al.*, 1992). In these applications  $\alpha$ -galactosidase was used to split lactose into its two component monosaccharides, glucose and galactose. The lactose-hydrolysed products thus obtained can be consumed in different forms (syrups, milk powders) by people that suffer from lactose intolerance with a concomitant decrease in symptoms (Bakken *et al.*, 1992).

The inversion (hydrolysis) of saccharose by invertase to produce an equimolecular mixture of fructose and glucose, has also been investigated (Cantarella *et al.*, 1989; Nakajima *et al.*, 1989, 1993). The product, known as invert sugar has sweetness comparable to saccharose and can be used, for instance, to produce artificial honey (Beltz & Grosch, 1987).

A more unusual reaction involving oligosaccharides has been recently described by Okada and coworkers (1994b). The authors used a cyclodextrin glucanotransferase covalently immobilised on the surface of a capillary membrane to catalyse the intermolecular transglycosylation of cyclodextrin with maltooligosaccharides, glucose and saccharose. The modified cyclodextrins thus obtained are potentially useful in various industrial fields such as food processing, medicine and cosmetics (Okada *et al.*, 1994b).

### Other Applications

Apart from the examples described above, other applications of membrane reactors have been investigated (Table 6.10). At DEGUSSA AG (Leuchtenberger *et al.*, 1984) a pilot scale (40 l) reactor coupled to 0.5 m<sup>2</sup> hollow fibre modules was used in a recycle configuration for the production of L-amino acids (L-methionine and L-phenylalanine) by enzymatic

**Table 6.9** Conversion of oligosaccharides

Enzyme-reaction description	Reference
Conversion of O-nitrophenyl- $\beta$ -D-galactopyranoside by - galactosidase	Kim & Chang, 1983b
Hydrolysis of maltose by amyloglucosidase immobilised by electrostatic forces in a MR	Furusaki & Asai, 1983
Hydrolysis of lactose catalysed by $\beta$ -galactosidase in a hollow fibre membrane reactor	Jones <i>et al.</i> , 1984
Hydrolysis of lactose catalysed by $\beta$ -galactosidase in a membrane reactor with pulsatile flow	Park <i>et al.</i> , 1985
Conversion of maltose into hydrogen peroxide by the sequential use of glucoamylase and glucose oxidase	Bardelletti & Coulet, 1987
Synthesis of 2-naphthol glucuronide by UDP-glucuronyltransferase with cofactor (UDPGA) addition	Tegtmeier <i>et al.</i> , 1988
Hydrolysis of lactose catalysed by $\beta$ -galactosidase in a capillary bed reactor	Peterson <i>et al.</i> , 1989a, 1989b
Study of product inhibition in the hydrolysis of cellobiose catalysed by $\beta$ -glucosidase from <i>Aspergillus niger</i>	Alfani <i>et al.</i> , 1990
Process optimisation of a membrane reactor for the lactose conversion catalysed by $\beta$ -galactosidase	Czermark <i>et al.</i> , 1991
Hydrolysis of lactose in skim milk catalysed by $\beta$ -galactosidase from <i>Bacillus subtilis</i>	Bakken <i>et al.</i> , 1992

*Bacillus circulans* in a spiral wound MR

Saccharose conversion into glucose and fructose catalysed by invertase	Cantarella <i>et al.</i> , 1989; Nakajima <i>et al.</i> , 1989, 1993
Intermolecular transglycosylation of cyclodextrin with maltooligosaccharides, glucose and sucrose by cyclodextrin glucanotransferase	Okada <i>et al.</i> , 1994b
Production of fructooligosaccharides by transfructosylation with $\beta$ -fructofuranosidase in a ceramic MR	Nishizawa <i>et al.</i> , 2000

**Table 6.10** Other applications

Enzyme-reaction description	Reference
Investigation of acid phosphatase activity over p-nitrophenyl phosphate in a tubular MR	Alfani <i>et al.</i> , 1982
Hydrolysis of urea catalysed by urease in an ultrafiltration cell	Gacesa <i>et al.</i> , 1983
Study of diffusion close to membrane containing glucose oxydase	Bardeletti <i>et al.</i> , 1985
Study of diffusion-reaction in the hydrolysis of urea catalysed by urease	Yonese <i>et al.</i> , 1990
Conversion of L-aspartate from L-fumarate by L-aspartase in a MR with simultaneous separation using electrophoresis	Furusaki <i>et al.</i> , 1990
Synthesis of optically pure (R)-mandelonitrile by (R)-oxynitrilase	Kragl <i>et al.</i> , 1990a
Synthesis of N-acetylneurameric acid by the conjugated action of epimerase and lyase	Kragl <i>et al.</i> , 1990b, 1990c
Investigation of penicillinase and lactate dehydrogenase activity	Harrington <i>et al.</i> , 1992
Production of peroxycarboxylic acids and epoxides by lipase in a 2-phase MR	Cuperus <i>et al.</i> , 1994
Degradation of phenols from model effluents by hydroxilases and oxygenases in an ultrafiltration cell	Bodzek <i>et al.</i> , 1994
Hydrolysis of penicillin C by penicillin acylase in a capillary membrane reactor	Bryjak <i>et al.</i> , 1996
Hydrolysis of p-nitrophenyl acetate by lipase immobilised in colloidal liquid aphrons in a hollow fibre reactor	Lye <i>et al.</i> , 1996
Oxidation of indole to oxindole by chloroperoxidase	Seelbach <i>et al.</i> , 1997
Oxidation of cephalosporin C by D-aminoacid oxidase immobilised on Duolite A365	Alfani <i>et al.</i> , 1998
Coupled transcription/translation using T7 RNA polymerase and <i>E. coli</i> extract in hollow fibre membrane reactor	Nakano <i>et al.</i> , 1999
Degradation of phenols from industrial effluents by phenol oxidase in a	Edwards <i>et al.</i>

(acylase) resolution of N-acetyl-D, L-derivatives. In a 1400 hour pilot plant experiment an approximate productivity of 10 kg of L-methionine per day was achieved (69% conversion), and in a combined 2300 hour experiment, 366 kg of L-methionine and 179 kg of L-phenylalanine were prepared consecutively (82–86% conversion). A production plant has even been conceived and constructed for the acylase-catalysed resolution of acetyl-D, L-amino acids with a capacity of 15–20 tons per month of L-amino acids (Leuchtenberger *et al.*, 1984). The fumarase catalyzed stereoselective production of L-malic acid from fumaric acid was also conducted in a similar 10 litre enzyme membrane reactor. In a 800 hour experiment, 300 kg of L-malic acid were produced with an approximately constant conversion of 70%, maintained by addition of fresh enzyme (Leuchtenberger *et al.*, 1984).

Two examples listed in Table 6.9 describe the use of enzymatic membrane reactors in environmental applications (Bodzek *et al.*, 1994; Edwards *et al.*, 1999). Both cases report on the degradation of phenols from model and industrial wastewaters. In one case bacterial hydroxilases and oxygenases isolated from microorganisms in activated sludge were used in an ultrafiltration cell (Bodzek *et al.*, 1994), while in the other a commercial polyphenol oxidase was used with a capillary membrane module (Edwards *et al.*, 1999).

The complexity that is possible to achieve in a membrane reactor is exemplified by a recent publication, which describes the synthesis of a protein, chloramphenicol acetyltransferase, by the direct *in vitro* expression from a PCR (polymerase chain reaction) template (Nakano *et al.*, 1999). The authors have used a diffusion type reactor, where the enzyme T7 RNA polymerase and an *Escherichia coli* S30 cell extract were placed in the shell side of an hollow fibre module. The PCR template was also trapped in the shell side. A substrate rich solution, containing the nucleotides ATP, CTP, GTP, UTP and 20 aminoacids, was recirculated through the fibres lumen. In this system, substrates diffuse to the shell side where the translation of the DNA template into messenger RNA is catalysed by T7 RNA polymerase. The transcription of mRNA into protein then occurs at the *E. coli* ribosomes from cell extract. The membrane reactor used thus mimics a living cell in its task of synthesising proteins.

Additional applications of membrane reactors include the hydrolysis of urea (Gacesa *et al.*, 1983; Yonese *et al.*, 1990), the synthesis of (R)-mandelonitrile (Kragl *et al.*, 1990a), the synthesis of N-acetylneuraminic acid (Kragl *et al.*, 1990b, 1990e), the production of peroxycarboxylic acids and epoxides by lipase (Cuperus *et al.*, 1994), the oxidation of indole to oxindole by chloroperoxidase (Seelbach *et al.*, 1997) and the oxidation of cephalosporin C by D-aminoacid oxidase immobilised on Duolite A365 (Alfani *et al.*, 1998).

## CONCLUSIONS AND FUTURE PROSPECTS

In recent years, membrane reactors have established themselves as an alternative configuration for enzymatic reactors. The unique advantages offered by these reactors together with the wide variety of membrane shapes, modules and materials commercially available, have made them an alternative to more conventional reactors such as fixed or

fluidised beds. Membrane reactors seem particularly suited to carry out complex enzymatic transformations, involving, for example, several enzymes, and cofactor regeneration. They also display unusual geometric characteristics that are particularly adequate for non-conventional types of media such as organic-aqueous two-phase systems and reversed micelles. And, the separation possibilities offered by these reactors open up new perspectives for the development of applications in enzyme engineering.

Considering that process integration and process intensification are becoming more and more a guiding philosophy in the development of new bioreactor configurations, membrane reactors constitute ideal systems for developing biotechnology applications with the coupling of bioconversion with separation process (extractive bioconversions). In general, membrane reactors represent a step forward in the development of bioreactors and constitute a new generation of enzymatic reactors. At this stage, however, membrane reactor possibilities have not been explored to their full extent. The future will probably bring the development of even more complex enzymatic systems and elaborate configurations based on these types of reactors, and hopefully the establishment of processes at the industrial scale. The following lines suggest some topics where research efforts in the area of membrane reactors may be concentrated in the coming years:

- Exploration of electric potential as a driving force for transport of solutes through membranes and eventually as an alternative cofactor regenerating technique in membrane reactors.
- Use of membrane reactors in reactions with insoluble substrates and/or products in order to explore the capability of ultrafiltration membranes to retain solid compounds.
- Investigation of membrane reactors in sequential reactions catalyzed by multi-enzymes acting synergistically.
- Improvement in efficiency of membrane reactors by using arrangements in series and parallel, and developing new module designs.
- Use of membrane reactors in the process development of enzymatic synthesis of chiral drugs.
- Development of highly selective membranes (e.g. affinity membranes, chiral membranes...).
- Developments in the field of materials engineering to improve membrane resistance (mechanical, thermal, chemical).
- Miniaturisation in order to develop micro membrane enzymatic reactors of extremely small dimensions. For instance, implantable devices could find applications in the biomedical area.

## REFERENCES

- Adu-Amankwa, B. and Constantinides, A. (1984) Mathematical Modelling of Diffusion and Reaction in the Hydrolysis of Vegetable Proteins in an Immobilized Enzyme Recycle Reactor. *Biotechnol. Bioeng.*, **6**, 156–166.
- Alfani, F., Albanesi, D., Cantarella, M. and Scardi, V. (1982) Effects of Temperature and Shear on the Activity of Acid Phosphatase in a Tubular Membrane Reactor. *Enzyme Microb. Technol.*, **4**, 181–184.

- Alfani, R., Cantarella, L., Gallifuoco, A. and Cantarella, M. (1990) Membrane Reactors for the Investigation of Product Inhibition of Enzyme Activity. *J. Membrane Sci.*, **52**, 339–350.
- Alfani, F., Cantarella, M. and Gallifuoco, A. (1998) Immobilized Enzyme Three- Phase Reactors for Oxidation of Cephalosporin C\*. *Biocatal. Biotrans.*, **16**, 395–409.
- Alfani, F., Cantarella, M. and Scardi, V. (1983) Use of a Membrane Reactor for Studying Enzymatic Hydrolysis of Cellulose. *J. Membrane Sci.*, **16**, 407–16.
- Bakken, A.P., Hill, C.G. and Amundson, L.H. (1992) Hydrolysis of Lactose in Skim Milk by Immobilized -Galactosidase (*Bacillus circulans*). *Biotechnol. Bioeng.*, **39**, 408–417.
- Balcão, V.M. and Malcata, F.X. (1997) Lipase Catalyzed Modification of Butterfat via Acidolysis with Oleic Acid. *J. Mol. Catalysis B: Enzymatic*, **3**, 161–169.
- Balcão, V.M. and Malcata, F.X. (1998) On the Performance of a Hollow-Fiber Bioreactor for Acidolysis Catalyzed by Immobilized Lipase. *Biotechnol. Bioeng.*, **60**, 114–123.
- Bardeletti, G. and Coulet, P.R. (1987) Sequential Bienzyme System Asymmetrically Immobilized on a Permeable Membrane: Final Product Compartmentalization. *Enzyme Microb. Technol.*, **9**, 652–657.
- Bardeletti, G., Maisterrena, B. and Coulet, P.R. (1985) Boundary Layer Effect on Product Flux-Splitting in an Immobilized Enzyme Membrane System. *J. Membrane Sci.*, **24**, 285–296.
- Bednarski, M.D., Chenault, H.K., Simon, E.S. and Whitesides, C.M. (1987) Membrane-Enclosed Enzymatic Catalysis (MEEC): A Useful, Practical New Method for the Manipulation of Enzymes in Organic Synthesis. *J. Am. Chem. Soc.*, **109**, 1283–1285.
- Bélafi-Bakó, K., Dombi, Á., Szábo, L. and Nagy, E. (1994) Triacylglycerol Hydrolysis by Lipase in a Flat Membrane Bioreactor. *Biotechnol. Techniques*, **8**, 671–674.
- Belfort, C. (1989) Membranes and Bioreactors: A Technical Challenge in Biotechnology. *Biotechnol. Bioeng.*, **33**, 1047–1066.
- Belitz, H.-D. and Grosch, W. (1987) Carbohydrates In: *Food Chemistry*. Springer Verlag, Berlin, pp. 201–256.
- Berke, W., Morr, M., Wandrey, C. and Kula, M.-R. (1984) Continuous Regeneration of ATP for Enzymatic Synthesis. *Ann. N.Y. Acad. Sci.*, **434**, 257–258.
- Berke, W., Schüz, H.-J., Wandrey, C., Morr, M., Denda, G. and Kula, M.-K. (1988) Continuous Regeneration of ATP in Enzyme Membrane Reactor for Enzymatic Synthesis. *Biotechnol. Bioeng.*, **32**, 130–139.
- Bodzek, M., Bohdziewicz and Kowalska, M. (1994) Preparation of Membrane- Immobilized Enzymes for Phenol Decomposition. *J. Chem. Tech. Biotechnol.*, **61**, 231–239.
- Bossi, A., Guerra, S. and Righetti, P.G., (1999) Electrically Immobilized Enzyme Reactors: Bioconversion of a Charged Substrate. Hydrolysis of Penicillin C by Penicillin C Acylase. *Biotechnol. Bioeng.*, **64**, 383–391.
- Bouhallab, S. and Henry, G. (1995) Enzymatic Hydrolysis of Sodium Casemate in a Continuous Ultrafiltration Reactor Using and Inorganic Membrane. *Appl. Microb. Biotechnol.*, **42**, 692–696.
- Bouhallab, S., Mollé, D. and Léonil, J. (1993) Continuous Hydrolysis of -casein in Membrane Reactor: Preparation of a Bioactive Peptide. *Biotechnol. Lett.*, **15**, 697–702.
- Bouhallab, S., Mollé, D. and Léonil, J. (1992) Tryptic Hydrolysis of Caseinomacropeptide in Membrane Reactor. *Biotechnol. Lett.*, **14**, 805–810.
- Brady, C., Metcalfe, L., Slaboszewski, D. and Frank, D. (1988) Lipase Immobilized on a Hydrophobic, Microporous Support for the Hydrolysis of Fats. *J. Am. Oil Chem. Soc.*, **65**, 917–921.
- Bressler, E. and Braun, E. (2000) Conversion of Citric Acid to Itaconic Acid in a Novel Liquid Membrane Bioreactor. *J. Chem. Technol. Biotechnol.*, **75**, 66–72.
- Bressollier, P., Petit, J.M. and Julien, R. (1988) Enzyme Hydrolysis of Plasma Proteins in a CSTR Ultrafiltration Reactor: Performance and Modeling. *Biotechnol. Bioeng.*, **31**, 650–658.
- Brielbeck, B., Frede, M. and Steckhan, E. (1994) Continuous Electroenzymatic Synthesis Employing the Electrochemical Enzyme Membrane Reactor, *Biocatalysis*, **10**, 49–64.

- Bryjak, J., Bryjak, M. and Noworyta, A. (1996) Membrane Reactor With Soluble Forms of Penicillin Acylase. *Enzyme Microb. Technol.*, **19**, 196–201.
- Cantarella, M., Cantarella, L., Cirielli, G., Gallifuoco, A. and Alfani, F. (1989) Sucrose Bioconversion in Membrane Reactors. *J. Membrane Sci.*, **41**, 225–236.
- Cantarella, M., Cantarella, L., Gallifuoco, A. and Alfani, F. (1990) Product Inhibition Studies in Membrane Reactors. *Ann. NY. Acad. Sci.*, **613**, 279–289.
- Carrea, G., Pilotti, A., Riva, S., Cani, E. and Ferrari, A. (1992) Enzymatic Synthesis of 12-ketourssodeoxycholic Acid from Dehydrocholic Acid in a Membrane Reactor. *Biotechnol. Lett.*, **14**, 1131–1135.
- Carvalho, C.M.L., Aires-Barros, M.R. and Cabral, J.M.S. (1998) A Membrane Bioreactor for Short Chain Esters Synthesis. In: Proc. 4nd European Symposium on Biochemical Engineering Science. (Feyo de Azevedo, S. Ferreira, E.C., Luyben, K.Ch.A.M. and Osseweijer, P. eds.), University of Porto, Porto, pp. 276.
- Cass, B.J., Schade, F., Robinson, C.W., Thompson, J.E. and Legge, R.L. (2000) Production of Tomato Flavor Volatiles from a Crude Enzyme Preparation Using a Hollow-Fiber Reactor. *Biotechnol. Bioeng.*, **67**, 372–377.
- Chang, P.S., Rhee, J.S. and Kim, J.J. (1991) Continuous Glycerolysis of Olive Oil by *Chromobacterium viscosum* Lipase Immobilized on Liposome in Reversed Micelles. *Biotechnol. Bioeng.*, **38**, 1159–1165.
- Chen, D.-H., Leu, J.-C. and Huang, T.-C. (1994) Transport and Hydrolysis of Urea in a Reactor-Separator Combining an Anion-Exchange Membrane and Immobilized Urease. *J. Chem. Tech. Biotechnol.*, **61**, 351–357.
- Cheryan, M. and Mehaia, M.A., (1986) Membrane Bioreactors In: Membrane Separations in Biotechnology. (McGregor, W.C., ed.). Marcel Dekker Inc., New York, pp. 255–302.
- Cheryan, M. (1986) Ultrafiltration Applications In: *Ultrafiltration Handbook* Technomic Publishing Company, Lancaster, PA, pp. 231–350.
- Chiang, C.L. and Tsai, S.W. (1992a) Application of a Recycle Dialysis System in a Reversed Micellar Reactor. *J. Chem. Tech. Biotechnol.*, **54**, 27–32.
- Chiang, C.L. and Tsai, S.W. (1992b) Mathematical Modelling and Simulation of a Recycle Dialysis Membrane Reactor in a Reversed Micellar System. *J. Chem. Tech. Biotechnol.*, **54**, 249–255.
- Comfort, A.R., Albert, E.C. and Langer, R. (1989a) Immobilized Enzyme Cellulose Hollow Fibers: I. Immobilization of Heparinase. *Biotechnol. Bioeng.*, **34**, 1366–1373.
- Comfort, A.R., Albert, E.C. and Langer, R. (1989b) Immobilized Enzyme Cellulose Hollow Fibers: II. Kinetic Analysis. *Biotechnol Bioeng.*, **34**, 1374–1382.
- Comfort, A.R., Albert, E.C. and Langer, R. (1989c) Immobilized Enzyme Cellulose Hollow Fibers: III. Physical Properties and In Vitro Biocompatibility. *Biotechnol Bioeng.*, **34**, 1383–1390.
- Cuperus, F.P., Bouwer, S.T., Kramer, G.F.H. and Derkx, J.T.P. (1994) Lipases Used for the Production of Peroxycarboxylic Acids. *Biocatalysis*, **9**, 89–96.
- Czernmark, P. and Bauer, W.J. (1991) Process Optimization of an Enzyme Membrane Reactor With Soluble Enzymes up to Industrial Scale. In *Effective Industrial Membrane Processes-Benefits and Opportunities*. (Turner, M. ed.). Elsevier Science Publishers Ltd., England, pp. 241–253.
- Darnoko, D., Cheryan, M. and Artz, W.E. (1989) Saccharification of Cassava Starch in an Ultrafiltration Reactor. *Enzyme Microb. Technol.*, **11**, 154–159.
- Deeslie, W.D. and Cheryan, M. (1981) A CSTR-Hollow-Fiber System for Continuous Hydrolysis of Proteins. Performance and Kinetics. *Biotechnol Bioeng.*, **23**, 2257–2271.
- Deeslie, W.D. and Cheryan, M. (1982) A CSTR-Hollow-Fiber System for Continuous Hydrolysis of Proteins. Factors Affecting Long-Term Stability of the Reactor. *Biotechnol Bioeng.*, **24**, 69–82.
- Doig, S.D., Boam, A.T., Leak, D.I., Livingston, A.C. and Stuckey, D.C. (1998) A Membrane Bioreactor for Biotransformations of Hydrophobic Molecules. *Biotechnol Bioeng.*, **58**, 587–594.

- Drioli, E., Molinari, R., Giorno, L., Bianchi, D. and Cesti, P. (1993) Use of Charged UF-Membrane Bioreactors for Retention of Cofactors. *Proc. 6th European Congress on Biotechnology*, WE268.
- Edwards, W., Bownes, R., Leukes, W.D., Jacobs, E.P., Sanderson, R., Rose, P.D. and Burton, S.G. (1999) A Capillary Membrane Bioreactor Using Immobilized Polyphenol Oxidase for the Removal of Phenols from Industrial Effluents. *Enzyme Microb. Technol.*, **24**, 209–217.
- Fane A.G. and Radovich, J.M. (1990) Membrane Systems In: *Separation Processes in Biotechnology*. (Asenjo, J.A., ed.). Marcel Dekker, New York, pp. 209–262.
- Fischer, A., Bommarius, A.S., Drauz, K. and Wandrey, C. (1994) A Novel Approach to Enzymatic Peptide Synthesis Using Highly Solubilizing N-Protecting Groups of Amino Acids. *Biocatalysis*, **8**, 289–307.
- Flörsheimer, A., Kula, M.-R., Schütz, H.-J. and Wandrey, C. (1989) Continuous Production of Kyotorphin. *Biotechnol Bioeng.*, **33**, 1400–1405.
- Frennesson, I., Trägårdh, O. and Hahn-Hägerdal, B. (1985) An Ultrafiltration Membrane Reactor for Obtaining Experimental Reaction Rates at Defined Concentrations of Inhibiting Sugars During Enzymatic Saccharification of Alkali-Pretreated Sallow: Formulation of a Simple Empirical Rate Equation. *Biotechnol. Bioeng.*, **28**, 1328–1334.
- Fujii, T., Miyawaki, O. and Yano, T. (1991) Modeling of Hollow-Fiber Capillary Reactor for the Production of L-Alanine With Coenzyme Regeneration. *Biotechnol. Bioeng.*, **38**, 1166–1172.
- Furui, M., Furutani, T., Shibatani, T., Nakamoto, Y. and Mori, T. (1996) A Membrane Bioreactor Combined With Crystallizer for Production of Optically Active (2R, 3S)-3-(4-Methoxyphenyl)-Glycidic Acid Methyl Ester. *J. Ferment. Bioeng.*, **81**, 21–25.
- Furusaki, S. and Asai, N. (1983) Enzyme Immobilization by the Coulomb Force. *Biotechnol. Bioeng.*, **25**, 2209–2219.
- Furusaki, S., Nozawa, T. and Nomura, S. (1990) Membrane Enzyme Reactor With Simultaneous Separation Using Electrophoresis. *Bioprocess Eng.*, **5**, 73–78.
- Gacesa, P., Eisenthal, R. and England, R. (1983) Immobilization of Urease Within a Thin Channel Ultrafiltration Cell. *Enzyme Microb. Technol.*, **5**, 191–195.
- Gan, Q., Rahmat, H. and Weatherley, L.R. (1998) Simultaneous Reaction and Separation in Enzymatic Hydrolysis of High Oleate Sunflower Oil—Evaluation of Ultrafiltration Performance and Process Synergy. *Chem. Eng. J.*, **71**, 87–96.
- Gaouar, O., Aymard, C., Zakhia, N. and Rios, G.M. (1997) Enzymatic Hydrolysis of Cassava Starch in a Continuous Membrane Reactor. *J. Chem. Tech. Biotechnol.*, **69**, 367–375.
- Garcia, H.S. and Hill, C.G. (1995) Improving the Continuous Production of Lipolyzed Butteroil With Pregastric Esterases Immobilized in a Hollow Fiber Reactor. *Biotechnol. Techniques*, **9**, 467–70.
- Garcia, H.S., Qureshi, A., Lessard, L., Ghannouchi, S. and Hill, C.G. (1995) Immobilization of Pregastric Esterases in a Hollow Fiber Reactor for Continuous Production of Lipolysed Butteroil. *Food Sci. Technol.*, **28**, 253–258.
- Garcia, H., Malcata, F.X., Hill, C.G. and Amundson, C.H. (1992) Use of *Candida rugosa* Lipase Immobilized in a Spiral Wound Membrane Reactor for the Hydrolysis of Milkfat. *Enzyme Microb. Technol.*, **14**, 535–545.
- Gekas, V.C. (1986) Artificial Membranes as Carriers for the Immobilization of Biocatalysts. *Enzyme Microb. Technol.*, **8**, 450–460.
- Gerhartz, W. (1990) General Production Methods. In: *Enzymes in Industry: Production and Applications*. VCH Verlagsgesellschaft, Weinheim, pp. 37–74.
- Giorno, L. and Drioli, E. (1997) Catalytic Behaviour of Lipase Free and Immobilized in Biphasic Membrane Reactor with Different Low Water-Soluble Substrates. *J. Chem. Tech. Biotechnol.*, **69**, 11–14.
- Giorno, L., Molinari, R., Drioli, E., Bianchi, D. and Cesti, P. (1995) Performance of a Biphasic Organic/Aqueous Hollow Fibre Reactor Using Immobilized Lipase. *J. Chem. Tech. Biotechnol.*, **64**, 345–352.

- Gobina, E., Hou, K. and Hughes, R. (1997) A Reactor-Separator Incorporating Porous and Dense Membrane Systems. *J. Chem. Tech. Biotechnol.*, **70**, 74–82.
- Goto, M., Goto, M., Nakashio, F., Yoshizuka, K. and Inoue, K. (1992) Hydrolysis of Triolein by Lipase in a Hollow Fiber Reactor. *J. Membrane Sci.*, **74**, 207–214.
- Guit, R.P.M., Kloosterman, M., Meindersma, G.W., Mayer, M. and Meijer, E.M. (1991) Lipase Kinetics: Hydrolysis of Triacetin by Lipase from *Candida cylindracea* in a Hollow-Fiber Membrane Reactor. *Biotechnol. Bioeng.*, **38**, 727–732.
- Habulin, M. and Knez, Z. (1991) Enzymatic Synthesis of n-Butyl Oleate in a Hollow Fiber Membrane Reactor. *J. Membrane Sci.*, **61**, 315–324.
- Hakoda, M., Enomoto, A., Hoshino, T. and Shiragami, N. (1996) Electro-Ultrafiltration Bioreactor for Enzymatic Reaction in Reversed Micelles. *J. Ferment. Bioeng.*, **82**, 361–365.
- Harrington, T.J., Gainer, J.L. and Kirwan, D.J. (1992) Ceramic Membrane Microfilter as an Immobilized Enzyme Reactor. *Enzyme Microb. Technol.*, **14**, 813–818.
- Hausser, A.C., Goldeberg, B.S. and Mertens, J.L. (1983) An Immobilized Two-Enzyme System (Fungal -Amilase/Glucoamilase) and Its Use in the Continuous Production of High Conversion Maltose-Containing Corn Syrups. *Biotechnol. Bioeng.*, **25**, 525–539.
- Hayakawa, K., Urable, I. and Okada, H. (1985) Operational Stability of a Continuous Enzyme Reactor Containing Poly(ethylene glycol)-bound NAD and Thermostable Dehydrogenases. *J. Ferment. Biotechnol.*, **63**, 245–250.
- Herrmann, C., Schwarz, A., Wandrey, C., Kula, M.-R., Knaup, G., Drauz, K.H. and Berndt, H. (1991) Scale-up of Enzymatic Peptide Synthesis in an Enzyme Membrane Reactor. *Biotechnol. Appl. Biochem.*, **13**, 346–353.
- Hildebrandt, J.R. (1991a) Membranes for Bioprocessing: Design Considerations. In *Chromatographic and Membrane Processes in Biotechnology*. (Costa, C.A. and Cabral, J.S. eds.). Kluwer Academic Publishers, The Netherlands, pp. 363–378.
- Hildebrandt, J.R. (1991b) Scale-Up and Optimization of Membrane Processes. In *Chromatographic and Membrane Processes in Biotechnology*. (Costa, C.A. and Cabral, J.S. eds.). Kluwer Academic Publishers, The Netherlands, pp. 415–28.
- Hoq, M.M., Koike, M., Yamane, T. and Shimizu, S. (1985a) Continuous Hydrolysis of Olive Oil by Lipase in Microporous Hydrophobic Hollow Fiber Bioreactor. *Agric. Biol. Chem.*, **49**, 3171–3178.
- Hoq, M.M., Tagami, H., Yamane, T. and Shimizu, S. (1985b) Some Characteristics of Continuous Glyceride Synthesis by Lipase in a Microporous Hydrophobic Membrane Bioreactor. *Agric. Biol. Chem.*, **49**, 335–342.
- Hoq, M.M., Yamane, T. and Shimizu, S. (1985c) Continuous Hydrolysis of Olive Oil by Lipase in Microporous Hydrophobic Membrane Bioreactor. *J. Am. Oil Chem. Soc.*, **62**, 1016–1021.
- Hoq, M.M., Yamane, T. and Shimizu, S. (1986) Role of Oleic Acid Solubilized in Buffer-Glycerol Solution on Adsorbed Lipase During Continuous Hydrolysis of Olive Oil in a Microporous Hydrophobic Membrane Bioreactor. *Enzyme Microb. Technol.*, **8**, 236–240.
- Houng, J.-Y., Chou, J.-Y. and Chen, K.-C. (1992) Production of High Maltose Syrup Using an Ultrafiltration Reactor. *Bioprocess Eng.*, **8**, 85–90.
- Ikemi, M., Koizumi, N. and Ishimatsu, Y. (1990a) Sorbitol Production in Charged Membrane Bioreactor With Coenzyme Regeneration System: I. Selective Retainment of NADP(H) in a Continuous Reaction. *Biotechnol. Bioeng.*, **36**, 149–154.
- Ikemi, M., Koizumi, N. and Ishimatsu, Y. (1990b) Sorbitol Production in Charged Membrane Bioreactor With Coenzyme Regeneration System: II. Theoretical Analysis of a Continuous Reaction With Retained and Regenerated NADPH. *Biotechnol. Bioeng.*, **36**, 155–165.
- Ina, H. and Kinoshita, S. (1993) Production of Cellobiose by an Ultra-Filter Membrane Reactor. *J. Ferment. Bioeng.*, **76**, 340–341.
- Ishihara, K., Higashi, Y., Nakajima, N., Utaka, M. and Nakamura, K. (1996) Enzymatic Production of (S)-l-Acetoxy-2-Alkanol With Bakers' Yeast Cell Free Extract in a Membrane Reactor. *J. Ferment. Bioeng.*, **811**, 266–268.

- Ishikawa, H., Tanaka, T., Takase, S. and Hikita, H. (1989b) Experimental Investigation of G6P Production and Simultaneous ATP Regeneration by Conjugated Enzymes in an Ultrafiltration Hollow-Fiber Reactor. *Biotechnol. Bioeng.*, **34**, 369–379.
- Ishikawa, H., Tanaka, T., Takase, S. and Hikita, H. (1989a) Theoretical Analysis of G6P Production and Simultaneous ATP Regeneration by Conjugated Enzymes in an Ultrafiltration Hollow-Fiber Reactor. *Biotechnol. Bioeng.*, **34**, 357–368.
- Isono, Y., Nabetani, H. and Nakajima, M. (1995) Wax Ester Synthesis in a Membrane Reactor With Lipase-Surfactant Complex in Hexane. *J. Am. Oil. Chem. Soc.*, **72**, 887–890.
- Isono, Y., Nakajima, M. and Nabetani, H. (1998) Solvent-Free Esterification of Oleic Acid and Oleyl Alcohol Using Membrane Reactor and Lipase-Surfactant Complex. *J. Ferment. Bioeng.*, **86**, 138–140.
- Jackson, J.A., Halvorson, H.R., Furlong, J.W., Lucast, K.D. and Dhore, J.A. (1979) A New Extracorporeal Reactor-Dialyzer for Enzyme Therapy Using Immobilized L-Asparaginase. *J. Pharm. Exp. Ther.*, **209**, 271–274.
- Janssen, A.E.M., Klabbers, C., Franssen, M.C.R. and van't Riet, K. (1991) Enzymatic Synthesis of Carbohydrate Esters in 2-pyrrolidone. *Enzyme Microb. Technol.*, **13**, 565–572.
- Jones, C.K.S., White, E.T. and Yang, R.Y.K. (1984) Enzymatic Hydrolysis of Lactose in a Hollow-Fiber Reactor. *Ann. N.Y. Acad. Sci.*, **434**, 119–122.
- Ju, Y.-H., Chen, W.-J. and Lee, C.-K. (1995) Starch Slurry Hydrolysis Using -amylase Immobilized on a Hollow-Fiber Reactor. *Enzyme Microb. Technol.*, **17**, 685–688.
- Kelley, W.S. (1996) Therapeutic Peptides: The Devil is in the Details. *Bio/Technology*, **14**, 28–31.
- Kelsey, L.J., Pillarella, M.R. and Zydny, A.L. (1990) Theoretical Analysis of Convective Flow Profiles in a Hollow-Fiber Membrane Bioreactor. *Chem. Eng. Sci.*, **45**, 3211–3220.
- Kida, K., Morimura, S., Noda, J., Nishida, Y., Imai, T. and Otagiri, M. (1995) Enzymatic Hydrolysis of the Horn and Hoof of Cow and Buffalo. *J. Ferment. Bioeng.*, **80**, 478–84.
- Kim, I.H. and Chang, H.N. (1983a) Variable Volume Enzyme Reactor With Ultrafiltration Swing: A Theoretical Study on CSTR Case. *AIChE J.*, **29**, 645–651.
- Kim, I.H. and Chang, H.N. (1983b) Variable-Volume Hollow Fiber Reactor with Pulsatile Flow. *AIChE J.*, **29**, 910–914.
- Kinoshita, S., Chua, J.W., Kato, N., Yoshida, T. and Taguchi, H. (1986) Hydrolysis of Cellulose by Cellulases of *Sporotrichum cellulophilum* in an Ultrafilter Membrane Reactor. *Enzyme Microb. Technol.*, **8**, 691–695.
- Kitano, H. and Ise, N. (1984) Hollow Fiber Enzyme Reactors. *Trends Biotechnol.*, **2**, 5–7.
- Kluge, T., Rezende, C., Wood, D. and Belfort, G. (1999) Protein Transmission During Dean Vortex Microfiltration of Yeast Suspensions. *Biotechnol. Bioeng.*, **65**, 649–658.
- Kragl, U., Gygax, D., Ghisalba, O. and Wandrey, C. (1990c) Large Scale Production of N-Acetyleneuraminic acid—Continuous Asymmetric C-C-Bond Formation in an Enzyme-Membrane-Reactor. In: *5th European Congress on Biotechnology, Abstract Book* (Christiansen, C., Munck, L. and Villadsen, J. eds.), Munksgaard International Publisher, Copenhagen, pp. 289.
- Kragl, U., Kruse, W., Hummel, W. and Wandrey, C. (1996a) Enzyme Engineering Aspects of Biocatalysis: Cofactor Regeneration as Example. *Biotechnol. Bioeng.*, **52**, 309–319.
- Kragl, U., Niedermeyer, U., Kula, M.-R. and Wandrey, C. (1990a) Engineering Aspects of Enzyme Engineering: Continuous Asymmetric C-C Bond Formation in an Enzyme Membrane Reactor. *Ann. NY Acad. Sci.*, **613**, 167–175.
- Kragl, U., Vasic-Racki, D. and Wandrey, C. (1996b) Continuous Production of L-tert-leucine in Series of Two Enzyme Membrane Reactors. *Bioprocess Eng.*, **14**, 291–297.
- Kragl, U., Wandrey, C., Ghisalba, O. and Gygax, D. (1990b) Enzymatic Process for Preparing N-Acetyleneuraminic acid. U.S. Patent N° 5071750.
- Kulbe, K.D., Howaldt, M.W., Schmidt, K., Rothig, T.R. and Chmiel, H. (1990) Rejection and Continuous Regeneration of the Native Coenzyme NAD(P)H in a Charged Ultrafiltration Membrane Enzyme Reactor. *Ann. NY Acad. Sci.*, **613**, 820–826.

- Labeque, R., Million, C.J.P., Ferreira, J.P.M., Lees, R.S. and Langer, R. (1993) Enzymatic Modification of Plasma Low Density Lipopoliproteins in Rabbits: A Potential Treatment for Hypercholesterolemia, *Proc. Natl. Acad. Sci. USA*, **90**, 3476–3480.
- Larsson, M. and Mattiasson, B. (1984) Continuous Conversion of Starch to Ethanol Using a Combination of an Aqueous Two-Phase System and an Ultrafiltration Unit. *Ann. NY Acad. Sci.*, **434**, 145–147.
- Lee, C.K. and Hong, J. (1988) Membrane Reactor Coupled with Electrophoresis for Enzymatic Production of Aspartic Acid. *Biotechnol. Bioeng.*, **32**, 647–654.
- Lee, S.G. and Kim, H.-S.- (1993) Optimal Operating Policy of the Ultrafiltration Membrane Bioreactor for Enzymatic Hydrolysis of Cellulose. *Biotechnol. Bioeng.*, **42**, 737–746.
- Lee, S.Y., Hibi, N., Yamané, T. and Shimizu, S. (1985) Phosphatidylglycerol Synthesis by Phospholipase D in a Microporous Membrane Bioreactor. *J. Ferment. Technol.*, **63**, 37–44.
- Leuchtenberger, W., Karrenbauer, M. and Plöcker, U. (1984) Scale-Up of an Enzyme Membrane Reactor Process for the Manufacture of L-Enantiomeric Compounds. *Ann. N.Y. Acad. Sci.*, **434**, 78–86.
- Liese, A., Karutz, M., Kamphuis, J., Wandrey, C. and Kragl, U. (1996) Enzymatic Resolution of 1-phenyl-1, 2-ethanediol by Enantioselective Oxidation: Overcoming Product Inhibition by Continuous Extraction. *Biotechnol. Bioeng.*, **51**, 544–550.
- Liese, A., Zelinski, T., Kula, M.-R., Kierkels, H., Karutz, M., Kragl, U. and Wandrey, C. (1998) A Novel Reactor Concept for the Enzymatic Reduction of Poorly Soluble Ketones. *J. Mol. Catalysis B: Enzymatic*, **4**, 91–99.
- Lin, S.-S., Harada, T., Hata, C., Miyawaki, O. and Nakamura, K. (1997) Nanofiltration Membrane Bioreactor for Continuous Asymmetric Reduction of 2-Ketoglutarate to Produce L-Glutamate With NADH Regeneration. *J. Ferment. Bioeng.*, **83**, 54–58.
- Lin, S.-S., Miyawaki, O. and Nakamura, K. (1999) Continuous Production of L-Carnitine With NADH Regeneration by a Nanofiltration Membrane Reactor With Coimmobilized L-Carnitine Dehydrogenase and Glucose Dehydrogenase. *J. Bioscience Bioeng.*, **87**, 361–364.
- Litjens, M.J.J., Sha, M., Straathof, A.J.J., Jongejan, J.A. and Heijnen, J.J. (1999) Competitive Lipase-Catalyzed Ester Hydrolysis and Ammoniolysis in Organic Solvents; Equilibrium Model of a Solid-Liquid-Vapor System. *Biotechnol. Bioeng.*, **65**, 347–356.
- López, J.L., Matson, S.L., Stanley, T.S. and Quinn, J.A. (1991) Liquid-Liquid Extractive Membrane Reactors. In: *Extractive Bioconversions*. (Mattiasson, B. and Hoist, O. eds.), Marcel Dekker Inc., New York, pp. 27–66.
- López, J.L., Wald, S.A., Matson, S.L. and Quinn, J.A. (1990) Multiphase Membrane Reactor for Separating Stereoisomers. *Ann. NY Acad. Sci.*, **613**, 155–166.
- López-Ulibarri, R. and Hall, G.M. (1997) Saccharification of Cassava Flour Starch in a Hollow-Fiber Membrane Reactor. *Enzyme Microb. Technol.*, **21**, 398–404.
- Lozano, P., Manjón, A., Iborra, J.L., Cánovas, M.e Romojaro, F. (1990) Kinetic and Operational Study of a Cross-Flow Reactor With Immobilized Pectolytic Enzymes. *Enzyme Microb. Technol.*, **12**, 499–505.
- Lozano, P., Manjón, A., Romojaro, F., Cánovas, M. and Iborra, J.L. (1987) A Cross Flow Reactor with Immobilized Pectolytic Enzymes for Juice Clarification. *Biotechnol. Lett.*, **19**, 875–880.
- Luque, S., Mallubhotla, H., Gehlert, G., Kuriyel, R., Dzengaleski, S., Pearl, S. and Belfort, G.A. (1999) New Coiled Hollow-Fiber Module Design for Enhanced Microfiltration Performance in Biotechnology. *Biotechnol Bioeng.*, **65**, 247–257.
- Lüthi, P. and Luisi, P.L. (1984) Enzymatic Synthesis of Hydrocarbon Soluble Peptides With Reversed Micelles. *J. Am. Chem. Soc.*, **106**, 7285–7286.
- Lye, G.J., Pavlou, O.P., Rosjidi, M. and Stuckey, D.C. (1996) Immobilization of *Candida cylindracea* Lipase on Colloidal Liquid Aphrons (CLAs) and Development of a Continuous CLA-Membrane Reactor. *Biotechnol. Bioeng.*, **51**, 69–78.
- Maeda H., Kajiwara, S., Yamazaki, Y., Hosong, K. and Livio, H.-L. (1990) Stabilization of the R-( $\beta$ )-Mandelic Acid Production Bioreactor and Scale-up. *Ann. NY Acad. Sci.*, **613**, 176–182.

- Malcata, F.X., Hill, C.G. and Amundson, C.H. (1993) Hydrolysis of Butteroil by Immobilized Lipase Using a Hollow Fiber Reactor: Part V. Effects of pH. *Biocatalysis*, **7**, 177–219.
- Malcata, F.X., Hill, C.G. and Amundson, C.H. (1991) Use of a Lipase Immobilized in a Membrane Reactor to Hydrolyze the Glycerides of Butteroil. *Biotechnol. Bioeng.*, **38**, 853–868.
- Margolin, A.L. (1993) Enzymes in the Synthesis of Chiral Drugs. *Enzyme Microb. Technol.*, **15**, 266–280.
- Matson, S.L. and Lopez, J.L. (1990) Multiphase Membrane Reactors for Enzymatic Resolution: Diffusional Effects on Stereoselectivity. In: *Frontiers in Bioprocessing*. (Sikdar, S.K., Bier, M. and Todd, P. eds.), CRC Press, Inc., Florida, pp. 391–403.
- Matson, S.L. and Quinn, J.A. (1986) Membrane Reactors in Bioprocessing. *Ann. N.Y. Acad. Sci.*, **469**, 152–165.
- Matson, S.L. and Quinn, J.A. (1992) Membrane Reactors. In: *Membrane Handbook*. (Ho, W.S. and Sirkar, K.K. eds.), van Nostrand Reinhold, New York, pp. 809–832.
- Matsumae, H., Furui, M., Shibatani, T. and Tosa, T. (1994) Production of Optically Active 3-Phenylglycidic Acid Ester by the Lipase from *Serratia marcescens* on a Hollow-Fiber Membrane Reactor. *J. Ferment. Bioeng.*, **78**, 59–63.
- Mazzola, G. and Vecchio, G. (1980) Immobilization and Characterization of L-Asparaginase on Hollow Fibers. *Int. J. Artif. Org.*, **4**, 120–123.
- Meireles, M., Aimar, P. and Sanchez, V. (1992) Les Techniques à Membranes: Micro et Ultrafiltration. *Le Technoscope de Biofutur*, **111**, cahier 52
- Miyawaki, O. (1993) Affinity Chromatographic Reactors. In: *Preparative and Production Scale Chromatography*. (Ganetsos, G. and Barker, P.E., eds.), Marcel Dekker, Inc., New York, pp. 607–615.
- Miyawaki, O., Yano, T. and Nakamura, K. (1990) Dynamic Immobilization of Dissociable Cofactors Through Enzyme-Coenzyme Affinity. *Ann. NY Acad. Sci.*, **613**, 816–819.
- Molinari, R., Drioli, E. and Barbieri, G. (1988) Membrane Reactor in Fatty Acid Production. *J. Memb. Sci.*, **36**, 525–534.
- Morgado, M.A.P., Cabral, J.M.S. and Prazeres, D.M.F. (1996) Phospholipase A<sub>2</sub>-Catalysed Hydrolysis of Lecithin in a Continuous Reversed Micellar Membrane Reactor. *J. Am. Oil. Chem. Soc.*, **73**, 337–348.
- Mountzouris, K.C., Gilmour, S.C., Grandison, A.S. and Rastall, R.A. (1999) Modeling of Oligodextran Production in an Ultrafiltration Stirred-Cell Membrane Reactor. *Enzyme Microb. Technol.*, **24**, 75–85.
- Nakajima, M., Nishizawa, K. and Nabetani, H. (1993) A Forced Flow Membrane Enzyme Reactor for Sucrose Inversion Using Molasses. *Bioprocess Eng.*, **9**, 31–35.
- Nakajima, M., Shoji, T. and Nabetani, H. (1992) Protease Hydrolysis of Water Soluble Fish Proteins Using a Free Enzyme Membrane Reactor. *Process Biochem.*, **27**, 155–160.
- Nakajima, M., Watanabe, A., Jimbo, N., Nishizawa, K. and Nakao, S. (1989) Forced-Flow Bioreactor for Sucrose Inversion Using Ceramic Membrane Activated by Silanization. *Biotechnol. Bioeng.*, **33**, 853–868.
- Nakano, H., Shinbata, T., Okumura, R., Sekiguchi, S., Fujishiro, M. and Yamane, T. (1999) Efficient Coupled Transcription/Translation from PCR Template by a Hollow-Fiber Membrane Bioreactor. *Biotechnol. Bioeng.*, **64**, 194–199.
- Narendranathan, T.J. and Dunnill, P. (1982) The Effect of Shear on Globular Proteins During Ultrafiltration: Studies on Alcohol Dehydrogenase. *Biotechnol. Bioeng.*, **24**, 2103–2107.
- Nembri, F., Bossi, A., Ermakov, S. and Righetti, P.C. (1997) Isoelectrically Trapped Enzymatic Bioreactors in a Multimembrane Cell Coupled to an Electric Field: Theoretical Modeling and Experimental Validation with Urease. *Biotechnol. Bioeng.*, **53**, 110–119.
- Nidetzky, B., Fürlinger, M., Gollhofer, D., Scopes, R.K., Haltrich, D. and Kulbe, K.D. (1997) Improved Operational Stability of Cell-Free Glucose-Fructose Oxidoreductase from *Zymomonas mobilis* for the Efficient Synthesis of Sorbitol and Gluconic Acid in a Continuous Ultrafiltration Membrane Reactor. *Biotechnol. Bioeng.*, **53**, 623–629.

- Nidetzky, B., Haltrich, D., Schmidt, K., Schmidt, H., Weber, A. and Kulbe, K.D. (1996a) Simultaneous Enzymatic Synthesis of Mannitol and Gluconic Acid: II. Development of a Continuous Process for a Coupled NAD(H)-Dependent Enzyme System. *Bicatal. Biotrans.*, **14**, 47–65.
- Nidetzky, B., Neuhauser, W., Haltrich, D. and Kulbe, K.D. (1996b) Continuous Enzymatic Production of Xylitol With Simultaneous Coenzyme Regeneration in a Charged Membrane Reactor. *Biotechnol Bioeng.*, **52**, 387–396.
- Nishizawa, K., Nakajima, M., and Nabetani, H. (2000) A Forced-Flow Membrane Reactor for Transfructosylation Using Ceramic Membrane. *Biotechnol. Bioeng.*, **68**, 92–97. Obón, J.M., Manjón, A. and Iborra, J.L. (1998) Retention and Regeneration of Native NAD(H) in Noncharged Ultrafiltration Membrane Reactors: Application to L-lactate and Gluconate Production. *Biotechnol. Bioeng.*, **57**, 510–517.
- Ohlson, I., Trägårdh, G. and Hahn-Hägerdal, B. (1984) Enzymatic Hydrolysis of Sodium Hydroxide Pretreated Sallow in an Ultrafiltration Membrane Reactor. *Biotechnol. Bioeng.*, **26**, 647–653.
- Ohshima, T., Wandrey, C., Kula, M.-R. and Soda, K. (1985) Improvement for L-Leucine Production in a Continuously Operated Enzyme Membrane Reactor. *Biotechnol. Bioeng.*, **27**, 1616–1618.
- Okada, T., Ito, M. and Hibino, K. (1994a) Immobilization of Cyclodextrin Glucanotransferase on Capillary Membrane. *J. Ferment. Bioeng.*, **77**, 259–263.
- Okada, T., Ito, M. and Hibino, K. (1994b) Intermolecular Transglycosylating Reaction of Cyclodextrin Glucanotransferase Immobilized on Capillary Membrane. *J. Ferment. Bioeng.*, **77**, 264–267.
- Onda, M., Lvov, Y., Ariga, K. and Kunitake, T. (1996) Sequential Reaction and Product Separation on Molecular Films of Glucoamylase and Glucose Oxidase Assembled on an Ultrafilter. *J. Ferment. Bioeng.*, **82**, 502–506.
- Orlich, B. and Schomaecker, R. (1999) Enzymatic Reduction of a Less Water-Soluble Ketone in Reverse Micelles With NADH Regeneration. *Biotechnol. Bioeng.*, **65**, 357–362.
- Park, T.H., Kim, I.H. and Chang, H.N. (1985) Recycle Hollow Fiber Enzyme Reactor With Flow Swing. *Biotechnol. Bioeng.*, **27**, 1185–1191.
- Pasta, P., Carrea, G., Monzani, E., Gaggero, N. and Colonna, S. (1999) Chloroperoxidase-Catalyzed Enantioselective Oxidation of Methyl Phenylsulfide With Dihydroxyfumaric Acid/Oxygen or Ascorbic Acid/Oxygen as Oxidants. *Biotechnol. Bioeng.*, **62**, 489–493.
- Pedersen, H., Horvath, C. and Ambrus, C.M. (1978b) Preparation of Immobilized L-Phenylalanine Ammonia Lyase in Tubular Form for Depletion of L-Phenylalanine. *Res. Commun. Chem. Pathol. and Pharmacol.*, **20**, 559–569.
- Pedersen, H., Horvath, C. and Bertino, J.R. (1978a) Immobilized Enzymes in Tubes and Hollow Fibers for Clinical Applications. In: *Enzyme Engineering*, Vol. 3. (Pye, E.K. and Weetall, H.H., eds.), Plenum Press, New York, pp. 397–408.
- Peters, J. and Kula, M.-R. (1991) Continuous Production of NADPH With Thermostable Secondary Alcohol Dehydrogenase in an Enzyme Membrane Reactor. *Biotechnol Appl. Biochem.*, **13**, 363–370.
- Peterson, R.S., Hill, C.G. and Amundson, C.H. (1989a) Effects of Temperature on the Hydrolysis of Lactose by Immobilized -galactosidase in Capillary Bed Reactor. *Biotechnol. Bioeng.*, **34**, 429–437.
- Peterson, R.S., Hill, C.G. and Amundson, C.H. (1989b) Lactose Hydrolysis by Immobilized -galactosidase in Capillary Bed Reactor. *Biotechnol. Bioeng.*, **34**, 438–446.
- Prazeres, D.M.F., Lemos, F., Garcia, F.A.P. and Cabral, J.M.S. (1993b) Modeling Lipolysis in a Reversed Micellar System. Part II:—Membrane Reactor. *Biotechnol. Bioeng.*, **42**, 765–771.
- Prazeres, D.M.F., Serralheiro, M.L.M., Feliciano, A.S. and Cabral, J.M.S. (1995) Process Integration in the Enzymatic Synthesis of Dipeptides in Organic Solvents. In: *Les Enzymes dans*

- L'Industrie Alimentaire/Enzymes for Food-EFF'95, CBB Développement, Rennes, pp. 223–230.
- Prazeres, D.M.F. (1996) Optimal Design of a Number of Membrane Reactors in Series Using Michaelis-Menten One-Substrate Reversible Kinetics. *Biotechnol. Technol.*, **10**, 313–318.
- Prazeres, D.M.F. (1995) Optimal Design of N Membrane Reactors in Series Using Michaelis-Menten Kinetics. *Can. J. Chem. Eng.*, **73**, 931–934.
- Prazeres, D.M.F. and Cabral, J.M.S. (1994) Enzymatic Membrane Bioreactors and Their Applications. *Enzyme Microb. Technol.*, **16**, 738–750.
- Prazeres, D.M.F., Garcia, F.A.P. and Cabral, J.M.S. (1993a) An Ultrafiltration Membrane Reactor for the Lipolysis of Olive Oil in Reversed Micellar Media. *Biotechnol. Bioeng.*, **41**, 761–770.
- Prazeres, D.M.F., Garcia, F.A.P. and Cabral, J.M.S. (1992) Batch and Continuous Lipolysis/Product Separation in a Reversed Micellar Membrane Bioreactor. In: *Biocatalysis in Non-Conventional Media*. (Tramper, J., Vermue, M.H., Beftink, H.H.e Stockar, U. eds.), Elsevier, Amsterdam, pp. 713–718.
- Prazeres, D.M.F., Garcia, F.A.P. and Cabral, J.M.S. (1994) Continuous Lipolysis in a Reversed Micellar Membrane Bioreactor. *Bioprocess Eng.*, **10**, 21–27.
- Pronk, M., Boswinkel, G. and Riet, K. (1992) Parameters Influencing Hydrolysis Kinetics of Lipase in a Hydrophilic Membrane Bioreactor. *Enzyme Microb. Technol.*, **14**, 214–220.
- Pronk, W., Kerkhof, P.J.A.M., van Helden, C. and van't Riet, K. (1988) The Hydrolysis of Triglycerides by Immobilized Lipase in a Hydrophilic Membrane Reactor. *Biotechnol. Bioeng.*, **32**, 512–518.
- Rice, K.E., Watkins, J. and Hill Jr., C.G. (1999) Hydrolysis of Menhaden Oil by a *Candida cylindracea* Lipase Immobilized in a Hollow-Fiber Reactor. *Biotechnol. Bioeng.*, **63**, 33–45.
- Righetti, P.C., Nembri, F., Bossi, A. and Mortarino, M. (1997) Continuous Enzymatic Hydrolysis of -Casein and Isoelectric Collection of Some of the Biologically Active Peptides in an Electric Field. *Biotechnol. Prog.*, **13**, 258–264.
- Rony, P.R. (1972) Hollow Fiber Enzyme Reactors. *J. Am. Chem. Soc.*, **94**, 8247–8248.
- Resell, C.M., Vaidya, A.M. and Hailing, P.J. (1996) Continuous *In Situ* Water Activity Control for Organic Phase Biocatalysis in a Packed Bed Hollow Fiber Reactor. *Biotechnol. Bioeng.*, **49**, 284–289.
- Rossi, V., Malinvernini, A. and Callegaro, L. (1981) Immobilization of Arginase on Hollow Fiber Hemodialyzer. *Int. J. Artif. Org.*, **4**, 102–107.
- Röthig, T.R., Kulbe, K.D., Buckmann, F. and Carrea, G. (1990) Continuous Coenzyme Dependent Stereoselective Synthesis of Sulcatol by Alcohol Dehydrogenase. *Biotechnol. Bioeng.*, **12**, 353–356.
- Sannier, F., Piot, J.-M., Dhuslter, P. and Guillochon, D. (1994) Stability of a Mineral Membrane Ultrafiltration Reactor for Peptic Hydrolysis of Hemoglobin. *J. Chem. Tech. Biotechnol.*, **61**, 43–47.
- Santos, J.A.L., Mateus, M. and Cabral, J.M.S. (1991) Pressure Driven Membrane Processes. In *Chromatographic and Membrane Processes in Biotechnology*. (Costa, C.A. and Cabral, J.S. eds.). Kluwer Academic Publishers, The Netherlands, pp. 177–205.
- Seelbach, K., van Deurzen, M.P.J., van Rantwijk, F., Sheldon, R.A. and Kragl, U. (1997) Improvement of the Total Turnover Number and Space-time Yield for Chloroperoxidase Catalyzed Oxidation. *Biotechnol. Bioeng.*, **55**, 283–288.
- Seelbach, K. and Kragl, U. (1997) Nanofiltration Membranes for Cofactor Retention in Continuous Enzymatic Synthesis, *Enzyme Microb. Technol.*, **20**, 389–392.
- Serralheiro, M.L.M., Prazeres, D.M.F. and Cabral, J.M.S. (1999) Continuous Production and Simultaneous Precipitation of a Dipeptide in a Reversed Micellar Membrane Reactor, *Enzyme Microb. Technol.*, **24**, 507–13.
- Serralheiro, M.L., Prazeres, D.M.F. and Cabral, J.M.S. (1994) Dipeptide Synthesis in a Reversed Micellar Membrane Reactor With Precipitation. *Enzyme Microb. Technol.*, **16**, 1064–1073.

- Shefer, S.D., Ferreira, J., Million, C.J.-P. and Langer, R. (1993) Extracorporeal Enzymatic Removal of Low Density Lipoproteins in Rabbits: Efficacy and Safety. *Int. J. Artif. Org.*, **16**, 218–228.
- Shefer, S.D., Rosenberger, V., Vahanian, G., Wong, W.T. and Langer, R. (1995) Implantable Hollow Fiber Bioreactor as a Potential Treatment for Hypercholesterolemia: Characterization of the Catalytic Unit. *Biotechnol. Bioeng.*, **48**, 36–41.
- Siebel, M.A. (1992) Batch Reactors. In: *Bioreactor Design and Product Yield*. Butterworth-Heinemann, Great Britain, pp. 103–112.
- Silva, M.C.B.M. (1990) Optimization of a Continuous Membrane Bioreactor for the Saccharification of Starch Using Temperature as a Control Variable: Experimental Study and Simulation Analysis. PhD Thesis, University of Reading.
- Sims, K.A. and Cheryan, M. (1992) Hydrolysis of Liquefied Corn Starch in a Membrane Reactor. *Biotechnol. Bioeng.*, **39**, 960–967.
- Sonomoto, K. and Okamoto, Y. (1995) An Integrated Bioreactor System for Biologically Active Peptides from Isolated Soybean Protein. *Ann. N.Y. Acad. Sci.*, **750**, 435–440.
- Stankiewicz, A.I. and Moulijn, J.A. (2000) Process Intensification: Transforming Chemical Engineering. *Chem. Eng. Prog.*, **January**, 22–34.
- Takagi, M., Oishi, K., Ishimura, F. and Fujimatsu, I. (1994) Production of S-(+)-Ibuprofen from a Nitrile Compound by Enzymatic Reaction Combined With Ultrafiltration. *J. Ferment. Bioeng.*, **78**, 54–58.
- Tanigaki, M., Sakata, M. and Wada, H. (1993) Hydrolysis of Soybean Oil by Lipase With a Bioreactor Having Two Different Membranes. *J. Ferment. Bioeng.*, **75**, 53–57.
- Taylor, F. (1996) Lipase Membrane Reactor for Continuous Hydrolysis of Tallow. In: *Engineering of/with Upases*. (Malcata, F.X. ed.). Kluwer Academic Publishers, The Netherlands, pp. 455–471.
- Taylor, F., Panzer, C.C., Craig, J.C. and O'Brien, D.J. (1986) Continuous Hydrolysis of Tallow With Immobilized Lipase in a Microporous Membrane. *Biotechnol. Bioeng.*, **28**, 1318–1322.
- Tegtmeier, F., Belsner, K. and Brunner, G. (1988) Enzymatic Synthesis of Glucoronides Using Lipophilic Hollow-Fiber Membranes. *Bioprocess Eng.*, **3**, 43–47.
- Thomas, C.R. and Dunnill, P. (1979) Action of Shear on Enzymes: Studies With Catalase and Urease. *Biotechnol. Bioeng.*, **21**, 2279–2302.
- Torchilin, V.P. (1987) Immobilised Enzymes as Drugs. *Adv. Drug. Deliv. Rev.*, **1**, 41–86.
- Tosa, T. and Shibatani, T. (1995) Industrial Applications of Immobilized Biocatalysts in Japan. *Ann. N.Y. Acad. Sci.*, **750**, 364–375.
- Ulbricht, M. and Papra, A. (1997) Polyacrylonitrile Enzyme Ultrafiltration Membranes Prepared by Adsorption, Cross-Linking, and Covalent Binding. *Enzyme Microb. Technol.*, **20**, 61–68.
- Uttapap, D., Koba, Y. and Ishizaki, A. (1989) Recycle Use of Immobilized Glucoamylase by Tangential Flow Filtration Unit. *Biotechnol. Bioeng.*, **33**, 542–549.
- Vaidya, A.M., Hailing, P.J. and Bell, C. (1993) Novel Reactor for Aqueous-Organic Two-Phase Biocatalysis: A Packed Bed Hollow Fiber Membrane Bioreactor. *Biotechnol. Techniques*, **7**, 441–46.
- Vaidya, A.M., Hailing, P.J. and Bell, C. (1994) Surfactant Induced Breakthrough Effects During the Operation of Two-Phase Biocatalytic Membrane Reactors. *Biotechnol. Bioeng.*, **44**, 765–771.
- Vaidya, A.M., Bell, G. and Hailing, P.J. (1992) Aqueous-Organic Membrane Bioreactors Part I. A Guide to Membrane Selection. *J. Membrane Sci.*, **71**, 139–149.
- van der Padt, A. and van't Riet, K. (1991) Membrane Bioreactors. In *Chromatographic and Membrane Processes in Biotechnology*. (Costa, C.A. and Cabral, J.S. eds.). Kluwer Academic Publishers, The Netherlands, pp. 443–448.
- van der Padt, A., Edema, M.J., Sewalt, J.J.W. and van't Riet, K. (1990) Enzymatic Acylglycerol Synthesis in a Membrane Bioreactor. *J. Am. Oil Chem. Soc.*, **67**, 347–352.

- van der Padt, A., Schroën, K. and van't Riet, K. (1996b) Scale up of Two-Phase Membrane Bioreactors: Use of Free and Immobilised Lipase. In: *Engineering of/with Lipases*. (Malcata, F.X. ed.). Kluwer Academic Publishers, The Netherlands, pp. 543–550.
- van der Padt, A., Sewalt, J.J.W. and van't Riet, K. (1996a) Membrane Bioreactor Design to Force Equilibrium Towards a Favourable Product Yield. In: *Engineering of/with Lipases*. (Malcata, F.X. ed.). Kluwer Academic Publishers, The Netherlands, pp. 473–481.
- van der Padt, A., Sewalt, J.J.W., Ágoston, S.M.I. and van't Riet, K. (1992) *Candida rugosa* Lipase Stability During Acylglycerol Synthesis. *Enzyme Microb. Technol.*, **14**, 805–812.
- van Eikeren, P., Brose, D.J., Muchmore, D.C. and West, J.B. (1990) Membrane Assisted Synthesis of Chiral Drugs and Fine Chemicals. *Ann. NY Acad. Sci.*, **613**, 796–801.
- Virkar, P.D., Narendranathan, T.J. and Dunnill, P. (1981) The Effect of Shear on Globular Proteins: Extension to High Shear Fields and to Pumps. *Biotechnol. Bioeng.*, **23**, 425–429.
- Vishwanath, S.K., Watson, C.R., Huang, W., Bachas, L.G. and Bhattacharyya, D. (1997) Kinetic Studies of Site-Specifically and Randomly Immobilized Alkaline Phosphatase on Functionalized Membranes. *J. Chem. Tech. Biotechnol.*, **68**, 294–302.
- Wandrey, C. (1987) Fine Chemicals. In: *Proc. 4th European Congress on Biotechnology*. (Neijssel, O.M., van der Meer, R.R. and Luyben, K. Ch. A.M. eds.), Elsevier Science Publishers, Amsterdam, pp. 171–188.
- Wandrey, C., Fiolitakis, E. and Wichmann, R. (1984) L-Amino Acids from a Racemic Mixture of  $\alpha$ -Hydroxy Acids. *Ann. N.Y. Acad. Sci.*, **434**, 91–94.
- Wichmann, R., Wandrey, C., Buckmann, A.F. and Kula, M.-R. (2000) Continuous Enzymatic Transformation in an Enzyme Membrane Reactor With Simultaneous NAD(H) Regeneration. *Biotechnol. Bioeng.*, **67**, 791–804.
- Wichmann, R., Wandrey, C., Hummel, W., Schutte, H., Buckmann, A.F. and Kula, M.-R. (1984) Enzymatic Production of Optically Active 2-Hydroxy Acids. *Ann. N.Y. Acad. Sci.*, **434**, 87–90.
- Woo, G.-J. and McCord, J.D. (1994) Bioconversion of Starches Into Maltotetraose Using *Pseudomonas stutzeri* Maltotetrahydrolase in a Membrane Recycle Bioreactor: Effect of Multiple Enzyme Systems and Mass Balance Study. *Enzyme Microb. Technol.*, **16**, 1016–1020.
- Wu, D.-P., Belfort, G. and Cramer, S.M. (1990) Enzymatic Resolution With a Multiphase Membrane Bioreactor: A Theoretical Analysis. *Ind. Eng. Chem. Res.*, **29**, 1612–1621.
- Wu, D.-R., Cramer, S.M. and Belfort, G. (1993) Kinetic Resolution of Racemic Glycidyl Butyrate Using a Multiphase Membrane Enzyme Reactor: Experiments and Model Verification. *Biotechnol. Bioeng.*, **41**, 979–990.
- Xin, J.-Y., Li, S.-B., Xu, Y. and Wang, L.-L. (2000) Enzymatic Resolution of (S)-(+)-Naproxen in a trapped Aqueous-organic Solvent Biphase Continuous Reactor. *Biotechnol. Bioeng.*, **68**, 78–83.
- Yang, V.C., Bernstein, H., Cooney, C.L. and Langer, R. (1988) The Development of an Immobilized Heparinase Reactor. In: *Bioreactor Immobilized Enzymes and Cells—Fundamentals and Applications* (Moo-Young, M. ed.). Elsevier Applied Science, London, pp. 83–94.
- Yonese, M., Murabayashi, H. and Kishimoto, H. (1990) Diffusion-Reaction of Urea Through Multimembrane Containing Urease—Effects of Microenvironments Around Urease and Asymmetry of the Membrane. *J. Membrane Sci.*, **54**, 145–162.
- Zhao, Q., Piot, J.-M., Sannier, F. and Guillochon, D. (1995) Peptic Hemoglobin Hydrolysis in an Ultrafiltration Reactor at Pilot Scale Generates Opioid Peptides. *Ann. N.Y. Acad. Sci.*, **750**, 452–458.

# **CHAPTER SEVEN**

## **REVERSED MICELLAR BIOREACTION SYSTEMS: PRINCIPLES AND OPERATION**

**CRISTINA M.L.CARVALHO<sup>1,2</sup> AND JOAQUIM M.S.CABRAL<sup>1</sup>**

<sup>1</sup> *Centre for Biological and Chemical Engineering, Institute Superior Técnico, Av. Rovisco Pais, 1049–001 Lisboa, Portugal*

<sup>2</sup> *Faculdade de Farmácia de Lisboa, Universidade de Lisboa, Av. Prof. Gama Pinto, 1649–003 Lisboa, Portugal*

### **ABSTRACT**

Reversed micelles have been used as a non-conventional medium to perform biocatalysis. Reversed micelles can be classified as a “microreactor” where the enzyme is sheltered and protected from solvent detrimental effects. This is a simplistic idea that led most researchers to ignore the specificities of this multiphasic system and especially what the enzyme experiences inside the reversed micelle. This chapter aims to analyse some of the fundamental aspects related to microencapsulation as well as to resume progress of the reversed micellar biosystems. The new trends where efforts should be focused to extend micellar technology to industrial processes, are also discussed.

The operation of micellar bioreactors (MBRs) is highlighted in terms of classification and definition of operational characteristics. The MBR operation is also analysed as batch and continuous reactors.

### **REVERSED MICELLAR PRINCIPLES**

#### **Definition**

Reversed micelles are microheterogeneous systems consisting of an aqueous micro-domain facing the polar heads of the surfactant that surrounds this core and interacts with the organic solvent, through the hydrophobic chains. The polar cores of the micelles have the ability to solubilise a significant amount of water, which depends on the reversed micellar system properties. When the enzymes are microencapsulated, usually, they are located in the interior aqueous phase of reverse micelles, although the degree of interaction with the surfactant interface is variable. This location is assumed to protect the enzyme from the adverse effects of organic solvent. However, the contact with surfactant may also be detrimental to the biocatalyst.

Reversed micelles are dynamic entities, which can exchange their constituents including water, surfactant, or other contents (Luisi and Magid, 1986). The exchange process may take place between two micelles or between each micelle and the bulk organic solvent. Upon collision of two micelles their coalescence occurs through a transient dimer, that permits a rapid exchange of material (Luisi, 1985).

The solutes such as enzymes, co-surfactants, substrates or products, may induce the structural change of the micelles, namely the size or water content affecting both the micelles and the microencapsulated biomolecules (Luisi and Magid, 1986).

### Surfactants

Surface active agents, commonly known as surfactants, are amphiphilic molecules containing non-polar and polar parts capable of interacting with interfaces. One of the most widely used parameters to evaluate surfactant activity is the critical micelle concentration (CMC). The CMC is the minimum surfactant concentration required to reach the lowest surface tension. Above the CMC, the surfactant molecules readily associate to form supramolecular structures, such as micelles, vesicles, bilayers or others.

Surfactants can be classified according to their ionic character in: anionic, cationic, amphotolytic or zwitterionic and non-ionic. The former group includes bis-(2-ethylhexyl) sulfosuccinate usually known as AOT as well as calcium dodecyl sulfate (CDS) and sodium dodecylsulphate (SDS). Cetyl trimethyl ammonium bromide or chloride (CTAB or CTAC), didodecyl dimethyl ammonium bromide (DDAB), tetradecyl trimethyl ammonium bromide (TTAB) and trioctyl methyl ammonium chloride (TOMAC) are examples of cationic surfactants. Amphotolytic surfactants include lecithin or phosphatidylcholine dérivátes with origin in egg yolk or soy bean. Finally, non-ionic surfactants include polyoxyethylene alcohols, esters and ethers.

The type of surfactant used to form the reversed micelles can largely influence enzyme activity (Patel *et al.*, 1996a). Rees *et al.* (1995a) compared the activity of five microbial lipases and verified that lactonisation activity was higher for the systems based on anionic surfactants (AOT), than for those based on cationic surfactants (CTAB). Lipase stability was higher in CTAB, but reached high levels in AOT reversed micelles with reduced water content (Rees *et al.*, 1995a).

A comparative study was carried out by Valis *et al.* (1992), in reversed micelles of anionic, cationic and nonionic surfactants, using *Rhizopus delemar* lipase. The assembling conditions of pH, Wo and temperature to reach the maximum enzyme activity, differ significantly in each reversed micellar system.

Cationic surfactants often need the presence of a co-surfactant to form reverse micelles. The same happens with most of the zwitterionic surfactants. Non-ionic and anionic surfactants yield reversed micellar systems in defined concentration regions.

The tailoring of surfactants to fulfill biocatalytic needs has been gaining interest. A new class of anionic surfactants (e.g. dioleyl phosphoric acid or DOLPA) was synthesised with long alkyl chains included in the hydrophobic moiety ensuring a high encapsulation ratio of proteins, such as hemoglobin, that could not be extracted with AOT (Goto *et al.*, 1997).

Concerns about the toxicity of surfactants led some authors to study alternatives and to suggest nontoxic microemulsions. Kahlweit *et al.* (1997) proposed the use of unsaturated

fatty acid alkyl esters together with 1, 2-diols as cosolvents. Other possibilities include the isopropyl myristate (saturated fatty acid ester) and essential oils, such as orange oil, or alternatively a mixture of long-chain soy bean lecithins (Epikuron 200) plus an alcohol or ( $\beta$ -D-alkyl polyglucoside (APG 600) (Kahlweit *et al.*, 1997). These alternatives also include biosurfactants, which are tolerated by living organisms. Some of the well known biosurfactants are rhamnolipid, mycolate, liposan, serra phobin, emulsan, dispersan, surfactin and cerilipid (Fletcher, 1992).

### Biocatalytic Advantages of Reversed Micelles as Organic Media

Traditionally, enzymes were used in an aqueous medium, but microemulsions became increasingly attractive, especially when substrates and/or products were lipophilic and a low water content was desired.

The advantages of reversed micellar systems are related to the following properties:

- Reversed micelles have a relatively ordered structure;
- Reversed micelles form spontaneously, reaching an equilibrium state in a short time;
- Normal and reversed micelles are recognized as models of biological structures (for a review see Martinek *et al.*, 1986);
- Solubilisation of both hydrophilic and hydrophobic substrates/products as well as inorganic salts overcome reagent incompatibility problems;
- Low reaction volumes are needed in comparison to two-phase systems;
- Synthetic processes are favored due to the shift of thermodynamic equilibrium;
- Side reactions such as reverse hydrolytic, polymerisation or others can be controlled;
- Microbial contamination is minimized;
- Increased interfacial area of contact (10–100 m<sup>2</sup>/ml);
- Intermicellar exchange processes are fast;
- Enzyme activity/stability are often improved;
- Regioselectivity enhancement as interface induces the orientation of reactants;
- Higher temperatures are possible as the thermal stability is often enhanced in low water media;
- High substrate (product) concentration is possible;
- Enzymatic aggregation is avoided;
- Solutions are isotropic (optically transparent) and this permits the use of several spectroscopic techniques for structural and monitoring (product formation or substrate consumption) purposes;
- Rigorous control of the amount of water present;
- The dimensions of the inner cavity may be easily changed (see hydration level and W<sub>0</sub> section); and
- Easy scale-up.

Furthermore, the dynamic character of reversed micelles gives them flexibility, which is profitable to reactivity, but in contrast affects the ordered structure of reversed micelles and consequently, the stability of biocatalysts. Originally, micelles were assumed not to be restricted by mass transfer limitations or product inhibition, although recent advances have raised some questions and this concept is not accepted as a rule any more as, will be discussed later. Regarding the system mixing, agitation is still required but not at high

rates, since in the micellar systems, biocatalysts are highly dispersed and the interfacial area of contact is enormous. This reduces the detrimental effect of shear stress forces on the enzyme structure.

The disadvantages are far fewer and include:

- Denaturing effects of surfactant; and
- Product recovery and enzyme re-use are still difficult.

### Applications

The early applications of microemulsions included their use in floor polishes, cutting oils and pesticide formulations. The actual applications are mainly in the industrial and household sectors. Three important applications of microemulsions were described by Holmberg (1998) and include enhanced oil recovery (EOR) and cleaning and reaction medium for organic reactions. The EOR application of microemulsions derives from its ability to reduce oil-water interfacial tension to very low values and is still at the research level. Finally, the biocatalytic applications are an emerging field and involve mainly w/o microemulsions.

The examples of enzymes studied in reversed micelles and catalysed reactions are numerous (for a review see Martinek, (1989); Martinek *et al.*, 1987); Oldfield, 1994). Among these processes some have potential industrial applications in areas such as foods, pharmaceuticals, chemicals and bioremediation (see Table 7.1).

Biotransformation in reversed micelles has not been exclusively performed by isolated enzymes. The inclusion of cells in reversed micellar aggregates functions as an immobilisation process, with the advantages of substrate/product solubility and protection against solvent effects. Furthermore, it avoids the time-consuming process of isolation/purification of enzymes and permits the use of the cell factory and respective resources such as co-factors. In spite of the fact that the process has these advantages, a few points still have to be investigated. One is the effect of surfactants on cell viability, since they can promote cell lysis. Another point to address is the structure of cell-encapsulated reversed micelles.

Some of the examples found in the literature on cell microencapsulation include: *Acinetobacter calcoaceticus* and a strain of *E. coli* (Haering *et al.*, 1985), *Mycobacterium sp.* strain M156 (Prichanont *et al.*, 1994) and *Saccharomyces cerevisiae* (Fadnavis *et al.*, 1989; 1990; Gajjar *et al.*, 1997). The possibility of maintaining bacterial cells in a viable state led Hochkoeppler and Luisi (1989) to study the microencapsulation of smaller organelles such as mitochondria opening new perspectives for the use of cellular machinery in reversed micellar biotransformations.

Reversed micellar technology has also been widespread in the antibodies field. A catalytic monoclonal antibody preparation (abzyme) was reported to retain its activity in

**Table 7.1** Areas of industrial application of biocatalysis performed in reversed micellar systems

Industry	Process	References
----------	---------	------------

Food industry	Esterification/Transesterification to obtain flavour and aroma components	(Carvalho <i>et al.</i> , 1997; Sebastião <i>et al.</i> , 1993)
	Production of mono-and di-glycerides (emulsifiers).	(Hayes and Gulari, 1991)
	Hydrolysis of complex long-chain oils	(Han and Rhee, 1986)
	Synthesis of triglycerides	(Morita <i>et al.</i> , 1984)
	Hydrolysis of proteins Peptide synthesis	(Luthi and Luisi, 1984; Pessina <i>et al.</i> , 1988)
	Hydrolysis of milk fat	(Chen and Chang, 1993; Patel <i>et al.</i> , 1996b)
	Oligosaccharide synthesis	(Bielecki and Idem-Somiari, 1998)
	Steroid conversions	(Hedström <i>et al.</i> , 1992; Larsson <i>et al.</i> , 1987)
Pharmaceutical industry	Enantioselective synthesis of ibuprofen	(Hedström <i>et al.</i> , 1993)
	Enhancement of (S)-naproxen prodrug production from racemic naproxen	(Chang and Tsai, 1997)
	Synthesis of prostanooids/prostaglandins	
	Oxidation/reduction of ketones and alcohols such as phenols	(Leaver <i>et al.</i> , 1987)
Chemical industry	Regioselective acylations of glycols and sugars	
	Asymmetric lipid transesterifications	(Rees <i>et al.</i> , 1995a)
	Synthesis of macrocyclic lactones	
Environmental applications	Removal of metal ions from aqueous streams	
	Degradation of pesticides like paraoxon by organophosphorous hydrolase	(Komives <i>et al.</i> , 1994)
	Coal desulphurisation using <i>Thiobacillus ferrooxidans</i> cell-free enzyme extract	(Lee and Yen, 1990)

reversed micelles despite the changes detected in  $K_m$  and  $k_{cat}$  constants, compared to the values attained in aqueous buffer (Durfor *et al.*, 1988). Abzymes have also been used in reverse micelles to catalyze enantiomeric resolutions (Janda, 1993). Abzyme 26D9 was the most stereoselective type tested, using only one enantiomer type in a highly unfavorable chemical process. Transesterification reactions have also been proven to be feasible (Janda, 1993).

### Determinant Factors for Biocatalysis in Reversed Micelles

This section focuses on the micellar reaction variables and their significance for the biocatalytic process as well as for enzyme stability.

**$W_0$  versus  $a_w$** *Hydration level and  $W_0$* 

The hydration degree of the reversed micelles is commonly given by the  $W_0$  parameter, which represents the molar ratio of water to surfactant concentrations. The optimum  $W_0$  value for catalysis depends on several aspects. A common feature is that normally the optimum  $W_0$  corresponds to a micellar size comparable to that of the protein. Martinek *et al.* (1989) found a direct relation between the effective radii of entrapped enzyme and the corresponding size of the micellar core (regulated by the  $W_0$  parameter). The optimal  $W_0$  also depends on the enzyme concentration and the higher the concentration the higher the  $W_0$  needed to attain maximal activity (Han *et al.*, 1990; Patel *et al.*, 1996a).

The study of the physical properties of water in the aqueous pool proved that they are quite different from the bulk water solutions, which reflects the enzymatic reactivity. As an example, at low  $W_0$ , water has a freezing temperature below zero, allowing cryoenzymology applications (Luisi *et al.*, 1990; Rees *et al.*, 1995b). The micellar solutions containing AOT were examined as a function of temperature by Douzou *et al.* (1979) to determine the range over which they remain homogeneous and it was verified that AOT microemulsions are feasible at temperatures as low as  $-45^\circ\text{C}$  and the presence of enzymes and electrolytes does not markedly affect the solubility of water.

Goto *et al.* (1995a) studied the solubilisation of water in AOT reversed micelles classifying the water as immobilised, hydration and free water. Below  $W_0$  2, only immobilised water exists whereas in the range 4–10 the water hydrates the AOT polar heads and finally the presence of free water is verified at  $W_0$  values above 10 (Figure 7.1).

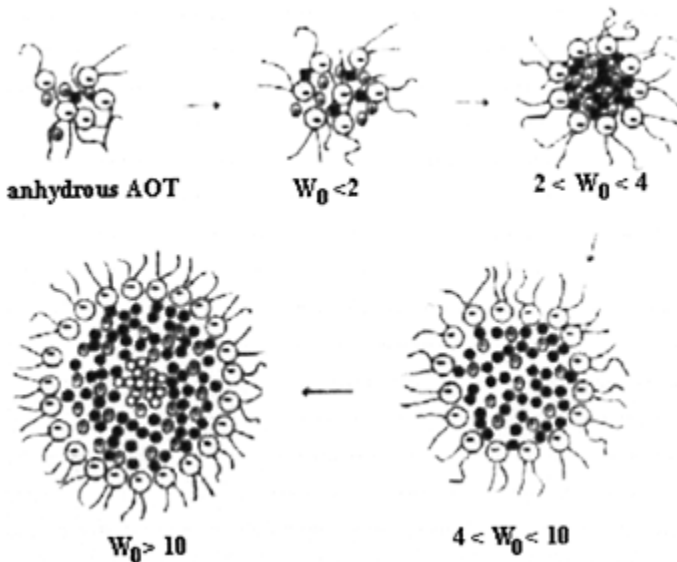


**Figure 7.1** Effect of adding increasing amounts of water to form AOT reversed micelles. Water molecules may be classified in three states: immobilised (■), hydration (●), or free (○) (adapted from Goto *et al.*, 1995).

Moreover, the microviscosity of the micellar water is higher than that of the bulk solutions (Andrade and Costa, 1996; Hasegawa and Kitahara, 1994), especially at low  $W_0$  values. In these conditions the activity is usually improved, possibly due to the elimination of spontaneous fluctuations of protein structure, which disturb the catalytic conformation in aqueous solution (Martinek *et al.*, 1989).

Another decisive factor in choosing the  $W_0$  value is the type of catalysed reaction. Hydrolytic or synthetic reactions have different water requirements and this also accounts for the overall reversed micellar catalytic system performance. By medium engineering it is possible to design systems with optimal enzyme activity, without detrimental effects on stability.

The thermal unfolding of small globular proteins was measured by Luisi *et al.* (1990) using differential scanning calorimetry (DSC), in the AOT/isoctane reversed micellar system. The authors verified that the thermal stability of the proteins hosted in reversed micelles depends on the water content, decreasing when the  $W_0$  value increases. The lowest  $W_0$  value used was 11, due to the limits of technique application, but it is possible that the use of lower values enhances the stability even more. Barbaric and Luisi (1981), studied enzymes in lower water content micelles (0.6–1% water) and verified a stability greater than in aqueous solutions.

Reversed micelles are capable of rearranging to accommodate a protein with dimensions higher than the water pool. Experimental evidence has shown that in some conditions 3 water-filled, but protein-free droplets, may be necessary to accommodate one molecule of protein (Gupte *et al.*, 1995a).

Since the use of very low  $W_0$  values is possible and this minimises the water molecules, which promote unfolding, the  $W_0$  is an important variable to take into account in stabilisation strategies.

Furthermore, substrate solubility in the aqueous sub-phase may also influence the choice of hydration level. The substrate concentration in the enzyme microenvironment is greatly influenced by this factor and for hydrophilic substrates it may be convenient to use higher  $W_0$  values. Additionally, there might be other variables such as the catalyst stability, which may influence the choice of  $W_0$ .

It should be emphasised that the  $W_0$  concept is usually associated only with the hydration level, although it is dependent on another variable—the concentration of surfactant. To establish their dependence it is very important to define the phase diagrams of each system by relating the phases with the concentrations of solvent, water and surfactant.

When the surfactant interacts with the enzyme accelerating the denaturing process, which often succeeds with anionic surfactants, e.g. SDS, AOT, the water content and

surfactant concentration have to be considered as independent variables, since the same Wo value can be obtained with different combinations of the two factors. Nevertheless, the restrictions in water content below certain levels dominate the interactions protecting the enzyme against denaturation. The lack of mobility may in this way be favorable.

The surfactant concentration also acts upon substrate distribution and catalysis itself. A model developed alongside the experimental work considers that a part of the overall substrate remains in close contact with the surfactant in the micellar sub-phase due to an adsorption effect. The increase in surfactant concentration will decrease the substrate accessed by the enzyme, explaining the reduction of  $k_{cat}$  by 2 to 4-fold in reversed micellar systems. Some changes in substrate specificity corroborate the partitioning explanation as the more hydrophilic substrates become preferred in reversed micellar catalysis. Brown *et al.* (1993) detected a decrease on *Rhizopus arrhizus* activity with an increase in AOT concentration that reflected the values of  $k_{cat}$ . Other authors explain the same phenomenon assuming a non-competitive inhibition by AOT (Marangoni, 1993; Tsai *et al.*, 1995).

#### Water activity

Another way to express the hydration level of reversed micelles is the use of the thermodynamic activity concept. Although the multiphase systems can be analysed in terms of concentrations, the use of water activity ( $a_w$ ) offers advantages (Hailing, 1994). In general, the reversed micellar systems are prepared with small amounts of water (although sufficient to attain the  $a_w$  value of 1) as a low water content does not warrant a low  $a_w$ . However, at very small Wo values  $a_w$  tends to decrease sharply.

Among the components of the reversed micellar system that can compete for the water are the organic solvent, protein, surfactant, substrates/products, buffer salts and co-surfactants such as alcohols (when present).

Competition between these components and the biocatalyst for available water may create "apparent" effects. For instance, high concentrations of a medium chain alcohol, used as substrate, may reduce the  $a_w$ , creating an apparent inhibitory effect if this water is necessary as a substrate of the reaction or if it integrates the "hydration shell" of the enzyme. The same may occur when raising the surfactant concentration.

Only very few papers (Hoppert *et al.*, 1994; Jorba *et al.*, 1992; Peng and Luisi, 1990; Stamatis *et al.*, 1995) report the control of  $a_w$  in reversed micellar systems and usually the methods used are the pre-equilibrating ones. This is probably a consequence of the constraints of the  $a_w$  determination, which exist in all systems but increase dramatically in reversed micelles due to the system components. One of the general problems in determining the  $a_w$  that applies to all systems is the handling of samples, due to the volatility and adsorption to materials which is even more complicated at higher temperatures.

Diagrams demonstrating the correspondence of Wo and  $a_w$  have been published by Luisi *et al.* (1988) (from the work of Higuchi and Misra, 1962) and more recently by Crooks *et al.* (1995). At  $W_0$  5 the  $a_w$  is 0.8 and increases to 0.9 at  $W_0$  10. Hailing and co-workers (unpublished data) also measured the  $a_w$  in reversed micelles containing enzyme and detected a sharp increase from Wo 0 to 10 and then a smooth evolution until  $a_w$  1.

### **pH**

The measurement of pH in the micellar environment has not been technically feasible, but the idea that a variation from the pH of the initial buffer solution occurs is widely spread. This accounts for the shift registered in the pH profile (1–2 units) of microencapsulated enzymes, in comparison with aqueous solutions (Menger and Yamada, 1979). Regardless of the pH measurement, the ionogenic groups of the enzyme will be affected by the microenvironment and their ionisation state severely influences the interaction with substrate(s) and the inhibition by products (Petersen *et al.*, 1998). In the case of AOT reversed micelles, the acidic impurities are, at least partially, responsible for the alkaline shift in the pH profile (Luisi and Magid, 1986).

Several methods for monitoring the pH of micellar solutions have been proposed. Luisi and Magid (1986) and Khmel'nitskii *et al.* (1984) suggested the use of (hydrophilic) indicators to monitor the pH.  $^{31}\text{P}$  NMR was also used with the same objective, using the  $^{31}\text{P}$  nucleus presence in the phosphate ion. Karpe and Ruckenstein (1990) made calculations of the pH variation with  $W_0$  in the first hydration shell of the reversed micelle (pHRM) and in the center of the micelle ( $\text{pH}_0$ ). In the two models presented (for phase transfer method and for injection method) the variations were more significant, up to  $W_0$  15–20, being the  $\text{pH}_0$  comparable to the pH of the stock solution and always higher than the  $\text{pH}_{\text{RM}}$ . This acidification may affect enzymes, which interact with the micellar interface.

The pH value for optimum activity greatly depends on the exposed residues of protein especially those close to the active site. The pH may also affect the microencapsulation of protein and the pH values below the isoelectric point and low ionic strength usually improve the uptake of protein.

### **Buffer molarity**

When solubilising biopolymers, buffer solutions are often used to constitute the aqueous phase forming the water pools. The presence of electrolytes in the water pools will alter the maximum  $W_0$  value, usually decreasing it (Luisi and Magid, 1986). This may be attributed to the increase of repulsion charges among the surfactant head groups. Another explanation for the decrease in droplet size and interdroplet attractive interaction with an increase in salinity was given by Hou *et al.* (1988). An increase in salinity decreases the interfacial area per mole head of surfactant molecule and makes the interface more rigid and less penetrable. This causes the decrease in strength of attractive interactions favouring a greater curvature of the interface (with consequent expulsion of water).

García-Río *et al.* (1994) noticed a reduction in the overall micellar viscosity caused by salts and also attributed this fact to a decrease in the attractive interactions among droplets by salt addition. All the electrolytes they used increased the temperature percolation threshold.

The effect of added salts may be understood within the more general framework of the effect of salts on the properties of surfactants in solution. The increase of salt concentration lessens the size of the polar effective area of the surfactants thereby increasing the curvature parameter of the surfactant. Hence, this explains the lower capacity of AOT to incorporate water molecules, since water solubilisation implies an increase of the micelles shortening the negative curvature of the interface. Another effect

of increasing the salt concentration is the salting-out of surfactant from the micelles to the organic phase due to the partial hydrophobic character of surfactant. Moreover, it also favors the undissociated form of the surfactant by the common ion effect (Wang *et al.*, 1994).

### **Additives and protecting compounds**

The mechanisms of stabilisation in reversed micelles or in other systems are normally associated with hydrogen bonding, dipole-dipole interactions and dispersion interactions (Luisi and Magid, 1986). It should be emphasized that the micellar properties previously referred to, such as low dielectric constant and higher microviscosity, can intensify hydrogen bonding in the protein thereby modifying its conformation.

A variety of additives are capable of improving these processes. The efficiency of an additive to preserve enzymatic activity depends on its chemical character and on the enzyme structure. Among the additives tested, alcohols, sugars and polyols have dominated prospective studies. This is mainly due to the fact that these compounds interact with the enzymes, strengthening hydrogen bonds and decreasing the water contact with protein unfolding, thereby preventing protein unfolding.

Some additives are used to improve the capacities of the micellar systems, namely their ability to form inverted micelles, as is the case with co-surfactants. Their effects on microencapsulated enzymes are variable, as some may be detrimental to activity/stability while others enhance enzymatic performance and the retention of activity. The addition of co-surfactants may increase or decrease the droplet size of microemulsions, depending on the chemical structure of the co-surfactant added.

The effects of increasing or decreasing the co-surfactant chain length are not straightforward. The most common situation when long chain co-surfactants are applied, is the hindrance of attractive interactions and the decrease of interfacial thickness, although, these co-surfactants may also increase the interfacial thickness when enhancement of interactions between the micellar interface and the bulk organic solvent occurs (Hayes and Gulari, 1995).

Freeman *et al.* (1998) reported an enhancement of chymotrypsin enzymatic activity in AOT reversed micelles by the addition of a bile salt cosurfactant, sodium taurocholate (NaTC), which modifies the interfacial properties increasing the water uptake, hence modifying the catalytic microenvironment. Additionally, this bile salt improves the aggregates organisation and may structurally alter the enzymes.

The addition of alcohols to micellar solutions of surfactants affects micellar properties such as CMC, ionisation degree, micellar molecular weight and micellar dynamics (Yiv *et al.*, 1981). Short chain alcohols usually increase the attractive interactions diminishing the degree of interpenetration of droplets whereas the interfacial fluidity is enhanced. The same happens with the addition of Arlacel-20 (non-ionic surfactant) to the ternary system AOT/dodecane/water (Hou *et al.*, 1988).

Hayes and Marchio (1998) studied the expulsion of water and protein from reversed micelles upon addition of different alcohols as co-surfactants. The addition of co-surfactant released ( $\alpha$ -chymotrypsin, pepsin, bovine serum albumin and catalase from reversed micelles and the release was enhanced with co-surfactant chain length (from 1-butanol to 1-dodecanol). The water was also co-expelled except on the addition of

butanol (Hayes and Marchio, 1998). The exclusion of water is likely to be a consequence of the increase in interfacial curvature. Moreover,  $W_0$  values lower than 10 improved protein expulsion whereas above 10, the  $W_0$  parameter did not influence the process.

Alcohols may also improve the enzyme's stability. According to Hayes and Gulari, (1994), their effect on stability is due to the strengthening of intermicellar attractive interactions (sometimes with clusters formation) and to a change in interface flexibility that hinders the enzyme-surfactant interactions (especially important when anionic denaturing surfactants are present).

Schübel and Ilgenfritz (1997) studied the influence of oligo and polyethylene glycols dissolved in AOT reversed micelles verifying a strong influence on the phase boundaries and on percolation of the system. The objective of the authors was the replacement of a portion of water by macromolecules, and they used PEG as a model polymer. In the stabilisation field this kind of work to surpass the unfolding process through the modification of the water pools microenvironment is welcomed.

Sorbitol has been reported to be a stabiliser of microencapsulated enzymes such as ( $\beta$ -D-fructofuranosidase (Subramani *et al.*, 1996), whereas glycerol has little effect. Glycerol is a water-miscible cosolvent that improves the aqueous ordering and the rigidification of proteins which enhances its stability. Rariy *et al.* (1998), verified this effect with ( $\alpha$ -chymotrypsin and Shah *et al.* (1997) with  $\alpha$ -amylase.

The addition of ethylene glycol and lauric acid on the behavior of AOT reversed micelles was investigated by Hayes and Gulari (1995). The former compound increased the solubilisation of water, whereas the later also improved the water solubilisation associated with ethylene glycol.

The effect of poly(oxyethylene) (POE) was analysed separately in reversed micelles of AOT and in reversed micelles of  $C_{12}E_5$  (Meir, 1996). In AOT reversed micelles, the attractive interactions between polymer and surfactant lead to the adsorption of the polymer at the interface, whereas in the case of the non-ionic surfactant the polymer molecules are repelled from the interface and forced into the droplet interior. In AOT the preferential location of POE in the interface may lead to the interconnection of droplets to form clusters which is supported by conductivity measurements (Meir, 1996).

Some substrates also induce stabilisation of enzymes. This is the case with acyl substrates (palmitic and oleic acids) which raise the stability of *Candida cylindracea* lipase in reversed micelles (Ayyagari and John, 1995).

### *Organic solvent*

The choice of solvent is normally determined by its compatibility with the surfactant and biocatalyst. Several correlations have been established between solvents and their properties affecting the enzymes' behavior and stability. Laane *et al.* (1987) related the stability of biocatalysts with the logarithm of partition coefficient of the organic solvent in the system octanol/water ( $\log P$ ), where solvents with high  $\log P$  were usually less detrimental to enzyme stability.

Gupte *et al.* (1995a) proposed a more detailed approach to the use of  $\log P$  in reverse micelles. The author uses the concept of  $\log P_b$ , which refers to the  $\log P$  of the microenvironment of the biocatalyst.  $\log P_b$  depends on  $\log P$  of surfactant, on the  $\log P$  of cosurfactant and on the molar ratio of the co-surfactant to the surfactant. This approach

highlights the attenuated effect of solvents in microencapsulated biocatalysts. Nevertheless, studies performed by Han and Rhee (1986) indicated large differences in the initial velocity of hydrolysis depending on the solvent. Isooctane produced the highest velocity of reaction followed by cyclohexane and octane (Han and Rhee, 1986).

Another aspect much less explored is the effect of the solvent on the reaction rate. The physical properties of the solvent are important in determining the substrate concentrations in the enzyme microenvironment. The development of models of substrate distribution explain how substrate concentrations can vary and the capacity of the organic solvent to solubilize the substrate(s) may be important to the process.

The droplet size and interdroplet interaction are also affected by the solvent and increase with the increment of the chain length of the oil, at a constant  $W_0$  (Hou *et al.*, 1988). Alkanes of small chain length are able to penetrate into the surfactant layer more effectively, by reducing the solubilisation of water (Hayes and Gulari, 1995).

### ***Temperature***

The influence of temperature on biocatalysis in reversed micelles is regulated by the same rules as in other aqueous or non-conventional media; here the activity is improved by raising the temperature up to a value dependent on the stability of the catalyst in the operating conditions. Nevertheless, the importance of temperature in the definition of the phase diagrams should be kept in mind, namely to keep the  $L_2$  phase correspondent to the reversed micelles.

High temperature and high droplet concentration lead to percolation, leading to changes in the electrical conductivity and eventually to the formation of bicontinuous structures (Almgren *et al.*, 1993). The electrical conductivity studies carried out by Suarez and Lang (1995) support this statement, as they verified that an increase in temperature strengthens the conductivity value above  $W_0$  10 (again when free water starts to exist in reversed micelles). The percolative behaviour appears to be consequence of the increase in attractive interdroplet interactions.

Zulauf and Eicke (1979) presented a study of the Stokes radii ( $r_h$ ) as a function of temperature and  $W_0$  that corroborates the importance of temperature to the physical properties of reversed micellar systems.

### **Kinetic Evaluation**

The kinetics of reactions catalysed by microencapsulated enzymes in reversed micelles usually obeys the classical Michaelis-Menten model. However, the kinetic constants determined for enzymes in these conditions differ significantly from those observed with the same enzyme in aqueous solution. Since the microencapsulated enzyme is subject to alterations in conformation, and micellar systems may have associated partition limitations, the enzyme kinetics in these systems is always inherent or even apparent depending on the role of diffusion (see chapter 5).

The consequences of the values determined reflect a general pattern. The most remarkable observation of kinetics in reversed micelles is the increment of  $K_m$  by 100 to 1000-fold and a simultaneous decrease in  $k_{cat}$  by a factor of 2–5 times (Gupte *et al.*, 1995b; Fletcher *et al.*, 1984).

The catalytic activities are dependent on the size of the micelles i.e. on the  $W_0$  parameter. Consequently, the optimally sized micelles allow the achievement of maximal  $k_{cat}$  values. A constant value of  $W_0$  corresponds to a distribution of various sizes of micelles, which transforms the  $k_{cat}$  by an average value (Kabanov *et al.*, 1988). At lower water content the enzymes often present a lower kinetic affinity for the substrate (Barbaric and Luisi, 1981). When water-insoluble substrates are used, these substrates' molecules are localised in the organic phase (oil phase) and to a great extent within the micellar phase.

### Distribution Models

The absence of specific and readily feasible techniques to determine directly the chemical species in contact with the enzyme imply different kinetic treatments for enzymes in different microenvironments. The models reported in the literature have the common objective of explaining the kinetic behavior of biocatalysts but they have very different approaches, including the distribution of enzymes, water, substrates, etc.

Eicke *et al.* (1976), proposed a model for solubilisates with limited solubility in iso-octane that is based on the collision of two micelles accomplished by a deformation during the compression phase. The compression of surfactant molecules induces an opening-channel through which each of the molecules of solubilisates has to diffuse from one micelle to the other.

Maestro and Walde (1992) developed a simple diffusion model to describe the ( $\alpha$ -chymotrypsin activity in reversed micelles. The authors considered two consecutive diffusion steps: the intermicellar diffusion (between micelles containing enzyme and micelles with substrate) and the intramicellar diffusion. However, this theoretical approach presented very low correlations with experimental data and did not consider the substrate partitioning.

Verhaert *et al.* (1990) combined features from two approaches to conceive their model. The first one is the diffusion and collision of substrate-filled and enzyme-filled reverse micelles. Sequentially, the exchange of components allows the enzymatic conversion in the reverse micelles. The authors raised the problem of real substrate concentrations for microencapsulated enzymes and distinguished between overall and water phase substrate concentrations to explain enzyme kinetics based on the pseudo micellar phases composition. In addition, they considered an exchange rate of substrates between filled and non-filled micelles. The deviations of kinetic parameters determined in reversed micelles from the aqueous phase values were shown to depend strongly on the concentration of reversed micelles, the intermicellar exchange rates and the volume fraction of water.

Other models were also developed to explain the differences verified for reversed micellar systems kinetics based on size distribution of reversed micelles (Kabanov *et al.*, 1988), partitioning of the enzyme between sub-phases (Bru *et al.*, 1989; Yang and Russel, 1995) and partitioning of substrates among micellar constituents (Khmelnitsky *et al.*, 1990b). These models helped to explain the catalysis in reversed micelles although only from the theoretical point of view since they do not advance to a quantitative definition of concentrations.

Recently, a model has been proposed to explain the distribution of hexanol in reversed micelles of AOT/isooctane (Carvalho *et al.*, 2000a). The distribution concentration of alcohols is of great importance in the micellar systems due to their properties as co-surfactants. Besides these properties, alcohols also act as substrates and stabilising agents, which give them further interest to model.

Cutinase is a suitable enzyme for examination of this issue, since it establishes a bridge between esterases and Lipases (Carvalho *et al.*, 1999c; Martinez *et al.*, 1992). Its activity and stability strongly depends on the presence of hexanol which plays a multiple role as substrate, as a co-surfactant and greatly improves cutinase stability (Carvalho *et al.*, 1997, 1999a; Sebastião *et al.*, 1993).

The non-homogeneity of microemulsions reflects on the analysis of kinetics performed, since the quantities of substrate accessed by the biocatalyst were not in straightforward relation to the substrate amount added to the reaction medium. Experimentally it was observed that the addition of hexanol up to 400–450 mM led to reaction velocities that do not follow the Michaelis-Menten kinetics. The deviation was overcome by calculating an effectiveness factor ( $\eta$ ), which was related to overall substrate concentration. Moreover, with low hexanol concentrations an analogous effect of substrate “deficiency” was observed while performing the thermostability assays, in spite of the fact that there was enough time for diffusion to occur, as hexanol stays in the system some hours or days before the activity evaluation. From the aforementioned results, it can be inferred that the lowest hexanol concentrations are comparatively less effective than would be expected. This suggests the substrate does not distribute equally in all the micellar components.

The experimental results discussed above were the start-point in developing a model to explain both kinetics and stability. This model encompasses three main processes: adsorption, partition and diffusion, and their relative importance is analysed.

In general, alcohols may distribute among the three main components of the micellar system, which are: the organic bulk phase ( $S_{org}$ ), the aqueous internal solution ( $S_w$ ) and the interface with the surfactant molecules ( $S_{aot,f}$  and  $S_{aot,ads}$ ).

The overall substrate concentration ( $ST$ ) is given by

$$ST = S_{org}^* + S_{aot}^* + S_{aot,ads}^* + S_w^* \quad (1)$$

The substrate concentrations are indicated as  $S^*$  as they refer to the overall concentration in the reversed micellar solution.

$S_{aot,f}^* + S_{aot,ads}^*$  represents the overall substrate concentration related to the AOT, either adsorbed ( $S_{aot,ads}^*$ ) and consequently unavailable to participate in the reaction or in the free form ( $S_{aot,f}^*$ ).

Henceforth,

$$S_{mic}^* = S_{aot,ads}^* + S_{aot,f}^* \quad (2)$$

The effective substrate concentration ( $S_{ef}^*$ ), which is available to reach the enzyme microenvironment, is given by:

$$S_{ef}^* = S_w^* + S_{aot,f}^* \quad (3)$$

It is assumed that hexanol will be accessed by cutinase if it is located in the water pool or in the surfactant (micellar) layer (as  $S_{aot,j}^*$ ), since the micelles are very small and re-size upon cutinase microencapsulation (Carvalho *et al.*, 1999a).

An adsorption process based on the Langmuir law was considered to define the concentrations of hexanol in the different micellar constituents. It is considered that the adsorption is a reversible process that takes place at the micellar interface, with the adsorbed alcohol molecules unavailable for reaction.

$$S_{aot,ads} = \frac{q_{max} \cdot K_L \cdot S_T}{1 + K_L \cdot S_T} \quad (4)$$

where  $q_{max}$  represents the monolayer capacity and  $K_L$  the adsorption equilibrium constant. The value of  $q$  is defined as the molar ratio of substrate (hexanol) to surfactant (AOT).

Partitioning has been mentioned as a key parameter to explain the varying behaviour of biocatalysts in reversed micelles (Fletcher, 1986; Fletcher *et al.*, 1985).

The partition coefficients (P1–P3) applied in the model are represented schematically in Figure 7.2 and their definitions as well as the values determined for hexanol are as follows (Khmelnitsky *et al.*, 1990b; Seeman, 1972):

$$P_1 = \frac{[S]_m}{[S]_w} = 13.0 \quad (5)$$

$$P_2 = \frac{[S]_{org}}{[S]_m} = 0.094 \quad (6)$$

$$P_3 = \frac{[S]_{org}}{[S]_w} = 1.22 \quad (7)$$

$$P_4 = \frac{\theta_w + P_1 \theta_m}{P_3(\theta_w + \theta_m)} = 4.8 \quad (8)$$

In Figure 7.2 the arrows originate in each of the phases and all the processes involved in substrate distribution are represented; the partition with coefficients  $P_1$ ,  $P_2$  and  $P_3$ , the adsorption ( $K_{ad}$ ) and the diffusion ( $K_{dif}$ ). The hexanol located in the micellar phase, but in strict contact with the AOT head groups (i.e. with the aqueous core) is considered accessible to the enzyme while the alcohol molecules interacting or adsorbing to the hydrophobic chains of the surfactant are not.

The volume fractions,  $\theta$ , were calculated for the experimental conditions ( $W_0$  2.7 with 150 mM AOT), using the partial specific volume for this  $W_0$ ,  $\rho=0.8831 \text{ cm}^3/\text{g}$  (estimated from Levashov *et al.*, 1982) and the concentrations of constituents AOT ( $C_{aot}$ ) and water ( $C_w$ ).

From eq. 1, it turns that the substrate mass balance is

$$S_T = S_{org} \times \theta_{org} + S_{mic} \times \theta_{mic} + S_w \times \theta_w \quad (9)$$

where  $S$  represents the local concentrations in each “compartment” and the respective volume fractions.

Since the partition phenomenon limits the substrate concentration in each sub-phase, the adsorbed substrate is conditioned by its initial concentration in the micellar phase, in the free form and eq. 5 transforms to:

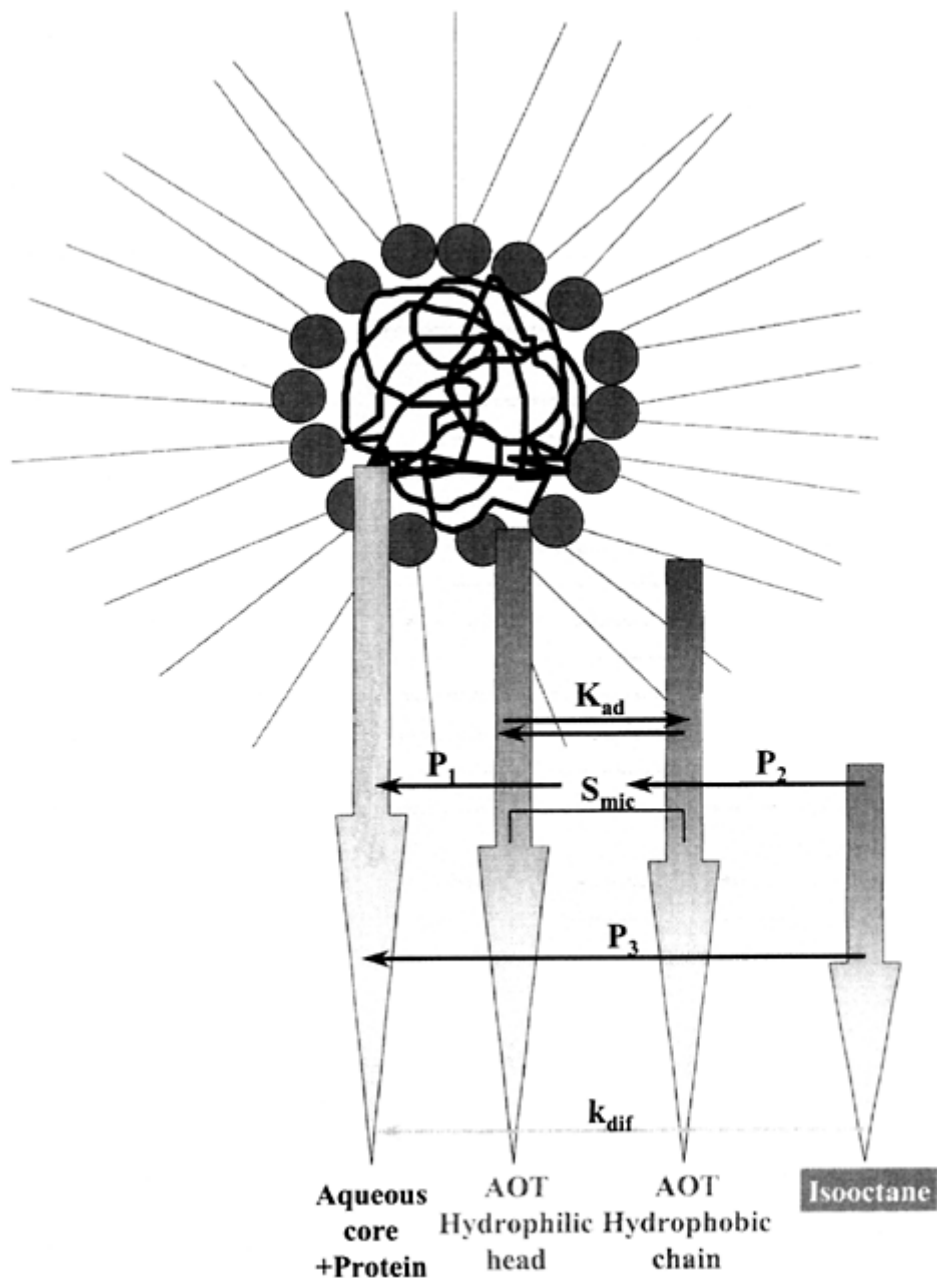


**Figure 7.2** General representation of a reverse micelle identifying the partitioning ( $P_1$ ,  $P_2$  and  $P_3$ ) adsorption ( $K_{ad}$ ) and diffusion ( $K_{dif}$ ) processes.

$$S_{aot,ads} = \frac{q_{\max} K_L S_{aot,f} [AOT]}{1 + K_L S_{aot,f}} \quad (10)$$

$S_w$  is obtained through the resolution of the second order equation:

$$(P_3 \theta_{org} + P_1 \theta_{aot} + \theta_w) K_L P_1 S^2_w + [(P_3 \theta_{org} + P_1 \theta_{aot} + \theta_w + q_{\max} K_L P_1 [AOT] \theta_{aot}) - K_L P_1 S_T] S_w - S_T = 0 \quad (11)$$

Similarly  $S_{org}$ ,  $S_{aot,f}$  and  $S_{aot,ads}$  are obtained respectively, from:

$$\left( \theta_{org} + \frac{P_1}{P_3} \theta_{aot} + \frac{\theta_w}{P_3} \right) K_L \frac{P_1}{P_3} S^2_{org} + \quad (12)$$

$$\left( \theta_{org} + \frac{P_1}{P_3} \theta_{aot} + \frac{\theta_w}{P_3} + q_{\max} K_L [AOT] \frac{P_1}{P_3} \theta_{aot} - K_L \frac{P_1}{P_3} S_T \right) S_{org} - S_T = 0$$

$$\left( \frac{P_3}{P_1} \theta_{org} + \theta_{aot} + \frac{\theta_w}{P_1} \right) K_L S^2_{aot,f} + \quad (13)$$

$$\left( \frac{P_3}{P_1} \theta_{org} + \theta_{aot} + \frac{\theta_w}{P_1} + q_{\max} K_L [AOT] \theta_{aot} - K_L S_T \right) S_{aot,f} - S_T = 0$$

$$(-K_L \theta_{aot}) S^2_{aot,ads} + \quad (14)$$

$$\left( \frac{P_3}{P_1} \theta_{org} + \theta_{aot} + \frac{\theta_w}{P_1} + K_{Lq} \max[AOT] \theta_{aot} + K_L S_T \right) S_{aot,ads} - K_{Lq} [AOT] S_T = 0$$

By applying the partition coefficients and the adsorption constants referred above, the concentrations of hexanol in the isoctane phase ( $S_{org}$ ), in the aqueous phase ( $S_w$ ) and in the AOT, either adsorbed ( $S_{aot,ads}$ ) or free ( $S_{aot,f}$ ) were calculated.

The analysis of different hypotheses enabled a point to be reached where the effective substrate concentrations coincide with the kinetic concentrations of substrate calculated through the effectiveness coefficients. In fact, considering  $K_H=0.0177 \text{ mol}^{-1}.\text{ml}$ , when  $q_{\max}=0.75$ , the estimation of effective substrate is very precise for the lower substrate concentrations (see Table 7.2) (Carvalho *et al.*, 2000a).

The model accurately estimates the effective substrate concentrations below the kinetic control. Above 300 mM hexanol, the  $S_{efMM}$  differs from  $S_{ef}$  due to the diffusion process. Diffusion does not control the process, but instead permits the rapid entry of substrate to replace the consumed molecules in the vicinity of the biocatalyst. Application of the model to calculate effective concentrations led to a linear relation between the hexanol accessed by cutinase and its thermostability (correlation coefficient ( $R$ ) was 0.994) (Carvalho *et al.*, 2000a).

The model identifies the micellar variables integrating the experimental data to predict consistent distribution values. A major point of the model is to stress the particular

behaviour of micellar systems and how dissimilar the substrates concentrations accessed by microencapsulated enzymes are. Therefore, reversed micellar systems should be regarded as complex systems instead of being classified as homogeneous systems since this definition causes detrimental effects to several aspects of their interpretation.

**Table 7.2** Concentration of hexanol in the micellar sub-phases (integrated model)

S <sub>T</sub>	S <sub>w</sub>	S <sub>aot,f</sub>	S <sub>aot,ads</sub>	S <sub>org</sub>	S <sub>ef</sub>	S <sub>efMM</sub>
<b>100</b>	0.077	8.01	79.8	12.1	8.01	8.60
<b>200</b>	0.370	38.3	103.6	57.8	38.6	34.1
<b>250</b>	0.551	57.0	106.4	86.1	57.6	52.5
<b>350</b>	0.925	95.7	108.8	144.5	96.7	201.2
<b>400</b>	1.114	115.3	109.4	174.1	116.5	376.5
<b>450</b>	1.304	135.0	109.8	203.8	136.3	273.2
<b>550</b>	1.686	174.5	110.4	263.4	176.1	516
<b>650</b>	2.068	214.0	110.8	323.0	216.1	650
<b>1000</b>	3.407	352.7	111.5	532.4	356.1	1000

## REVERSED MICELLAR BIOREACTORS

### State-of-the-Art

Reversed micelles have also been referred to as nanoreactors or microreactors due to their constitutional properties. Nevertheless, this does not ensure self-sufficiency to perform a continuous process. There are only very few examples of reactors applied to reversed micellar systems and all of them involve the use of membranes, usually membrane modules encompassing ceramic membranes.

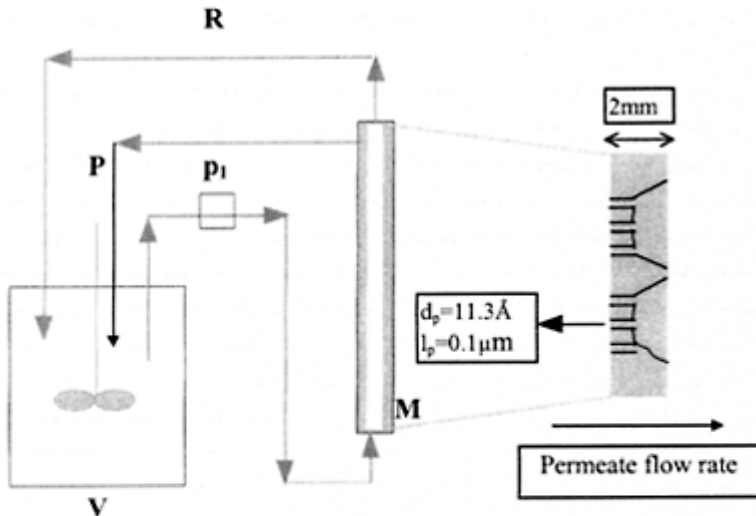
Ultrafiltration membrane reactors are one of the most appropriate type of reactors to achieve the confinement of microencapsulated enzymes, whilst simultaneously obtaining product separation, as they are based on a size exclusion pressure-driven process. One exception was the stirred tank reactor (STR)-plug flow reactor (PFR) used by Doddema *et al.* (1987). This reactor constituted of a STR made of glass and a stainless steel tube acting as a PFR, although this reactor also included an hollow fibre unit (Amicon polysulfonate) to separate the product in a counter-current mode. The STR-PFR reactor was designed to perform the enzymatic oxidation of steroids using isolated cholesterol-oxidase or *Nocardia rhodochrous* cells, both entrapped in reversed micelles.

The hydrolysis of olive oil (Hakoda *et al.*, 1996; Prazeres *et al.*, 1993, 1994a), peptide synthesis (Luisi and Laane, 1986; Serralheiro *et al.*, 1994, 1999), hydrolysis of lecithin (Morgado *et al.*, 1996), L-tryptophan production (Blanch, 1990; Eggers and Blanch, 1988) and degradation of pesticides (Komives *et al.*, 1994) are among the applications of the membrane bioreactors (MBR). Chang and Rhee (1991) also performed the continuous

glycerolysis of olive oil in a CSTR with an ultrafilter membrane (polysulfone) to retain the lipase immobilised on liposomes in reversed micelles. The half-life of the *Chromobacterium viscosum* was 7 weeks. Luthi and Luisi 1984 performed the enzymatic synthesis of hydrocarbon-soluble peptides in a micellar reactor where the ( $\alpha$ -chymotrypsin containing micelles were entrapped in semipermeable hollow fibers. Luisi and Laane (1986) used a flow hollow-fibre membrane reactor that was semi-permeable, retaining enzyme and micelles while the small molecules of substrate and products passed freely. Nevertheless, this type of reactor did not retain the surfactant molecules due to the dynamics of micelle formation that would inevitably contaminate the product solution (Khmelnistky *et al.*, 1988).

Cutinase performance was also evaluated in a MBR (Figure 7.3). Cutinase was microencapsulated in AOT reversed micelles following the optimisation of cutinase stability studies (Carvalho *et al.*, 1997, 1999a):  $W_0$  2.7 and 1M hexanol. A ceramic membrane of 15,000 Da MWCO was used. The MBR was continuously operated for five weeks maintaining the level of 60% conversion and leading to an estimated cutinase half life of 674 days, which represents an enhancement of 4.2 fold when compared with the thermostability of microencapsulated cutinase in the presence of 1 M hexanol (Carvalho *et al.*, 2000a, c, d).

The choice of membrane bioreactors is based on their capacity to retain the enzyme, and this confinement is mainly a function of the pore size of membranes—usually ultrafiltration membranes. The productivities achieved are usually high as are the enzymatic half-lives.



$p_1$ -recirculating pump

V-recirculation vessel

M-membrane module

F-feed solution

P-permeate

R-retentate

**Figure 7.3** Schematic of MBR operating in a total recirculation mode. A representation of the composite membrane characteristics is given on the right.

Furthermore, they are very suitable for performing a continuous operation and in some cases the process may be integrated with the downstream process in order to separate the target product(s). However, this is not so easy, due to one of the most interesting properties of reversed micelles: the interface flexibility. Indeed, the self-assembling capacity of the surfactant makes the micellar systems very versatile due to their capacity to change and adapt themselves to new circumstances. However, this advantage becomes a drawback when the objective is to confine the reversed micellar system inside a reactor that will be crossed by a feed stream with substrates to give rise to a permeate solution with concentrated products of the biocatalysis. Under these conditions the surfactant molecules suffer a rearrangement and cross the membrane in the form of small

aggregates or, more likely, as monomers. This leads to the presence of surfactant in the products' stream and makes the separation and purification of products extremely difficult, especially when they are to be used in foods, pharmaceuticals, cosmetics or other health areas.

An attempt to solve or minimise the surfactant contamination problem was made by Hakoda *et al.* (1996) and Nakamura and Hakoda (1992). The authors used the electro-ultrafiltration (EUF) method to decrease the gel formation in the membrane surface, improving the filtration flux, and achieving the separation of the AOT reverse micelles. The rejection of AOT was naturally influenced by the direction of applied voltage. The best solution occurred when the cathode (with negative charge) was installed in the permeate side—this can be explained by the repulsion of the AOT negative charge. The permeation flux increased with the electrical field strength. The rejection of AOT increased, but did not exceed 15%, while the rejection of water reached 30% (Nakamura and Hakoda, 1992). A drawback of the EUF was the deactivation of lipase caused by the application of voltage.

Other problems of the membrane reactors are the leakage of enzyme, adsorption and concentration polarisation leading to membrane fouling and enzyme deactivation promoted by shear forces.

One interesting work performed in a reversed micellar reactor was reported by Chiang and Tsai (1992). The reaction under study was the hydrolysis of olive oil by *Candida rugosa* lipase microencapsulated in reverse micelles of AOT/isooctane. The main portion of the reactor was a recycle dialysis stirred cell used to integrate the reaction and product recovery. The resistance of the dialysis membrane to reversed micelles was controlled by the water content and the rejection value after 24 hours was 95.9%. UV absorption was used to detect surfactant and the rejection coefficient was 97.3% after 24 hours (Chiang and Tsai, 1992). Despite the good results in micelle retention, further evaluation would be necessary to analyse the continuous operation of this type of reactor over time.

## Characterisation of Micellar Membrane Bioreactors

### *Membrane properties and characterisation*

The choice of a membrane for a specific enzyme process is determined by its nominal molecular weight cut-off (NMWCO), which depends on the average pore size and pore size distribution. Other properties of the membrane such as chemical resistance to organic solvents, temperature, pH and pressure should also be considered with respect to the operating conditions and the cleaning/sterilisation process (Hildebrandt, 1991). Ultrafiltration ceramic membranes, despite their cost, are highly resistant to chemicals and extreme operating conditions.

The membrane characterisation comprises the membrane porosity/morphology and also its surface properties. Recently, atomic force microscopy (AFM) has developed as a powerful tool for the characterisation of membranes (Bowen *et al.*, 1996).

MBR must be characterised in terms of filtration properties. The filtration flux rate,  $J$ , through a membrane is defined as:

$$J = \frac{Q}{A} \quad (15)$$

$Q$  being the flow rate and  $A$  the area of filtration.

The membrane permeability,  $L_p$ , can be obtained through the relation with the transmembrane pressure,  $\Delta PTM$ :

$$J = L_p \times \Delta PTM \quad (16)$$

The porosity of the membrane,  $\varepsilon_m$ , may also be estimated from:

$$\varepsilon_m = \frac{L_p 32 \eta l_p}{d_p^2} \quad (17)$$

where  $l_p$  is the pore length,  $\eta$  the viscosity and  $d_p$ , the pore diameter.

The number of membrane pores per unit area,  $n_p$ , can be obtained from:

$$\varepsilon_m = n_p \pi \frac{d_p^2}{4} \quad (18)$$

The internal area of each pore,  $A_p$  is:

$$A_p = \pi d_p l_p \quad (19)$$

and the total internal area of the pores is:

$$A_T = n_{p\ total} A_p \quad (20)$$

The volume of each pore,  $V_p$ , is given by:

$$V_p = \frac{\pi d_p^2}{4} l_p \quad (21)$$

In asymmetric or anisotropic membranes the pore length is usually  $1\text{--}2\mu\text{m}$  as determined by field emission scanning electron microscopy (FESEM) (Doyen *et al.*, 1996). However, the separation takes place in a layer of high density usually designated by “active surface of the membrane”, which is considerably thinner. According to Mulder (1992) this active layer has a thickness between 0.1 and  $0.5\ \mu\text{m}$  (see Figure 7.3).

### Membrane rejection coefficients

Transmission experiments have also to be performed to assess membrane rejection coefficients, ( $\sigma_{obs}$ ) for the different system components.

The NMWCO allows a prediction of membrane exclusion behaviour, although the dispersion of pore size, the hydrophobic/hydrophilic character of the membrane, orientation and conformation of the solutes and interactions may severely interfere with the final result which makes operational verification essential. The rejection coefficient is defined as:

$$\sigma_{obs} = \frac{C_r - C_p}{C_r} \quad (22)$$

where  $C_r$  is the concentration of a compound in the recirculated solution and  $C_p$  its concentration in the permeate solution. This coefficient quantifies the membrane capacity to retain a component of the reaction system, namely protein, substrates or products.

To determine the behavior of the membrane in the presence of enzyme and other components of the system including substrates and products, transmission experiments must be carried out, in the presence and absence of protein and of substrates and products.

### **Membrane resistance**

By knowing that,  $R_{memb}=1/L_p$ , the membrane resistance in the absence of protein ( $R_{memb}$ ) can be calculated from Eq. 16:

$$R_{memb} = \frac{\Delta PTM}{J} \quad (23)$$

Taking into account the resistance model, which considers the filtration flux controlled by several hydraulic resistances,

$$J = \frac{\Delta PTM}{R_{memb} + R_{prot}}, \quad (24)$$

it is possible to calculate the resistance yielded by the protein,  $R_{prot}$ , as:

$$R_{prot} = \frac{\Delta PTM}{J} - R_{memb} \quad (25)$$

Protein adsorption with ultrafiltration flux decline has been reported (Carvalho *et al.*, 2000b; Kulkarni *et al.*, 1992) (see Figure 7.4), being pointed out that the reduction in permeate flux is more pronounced near the protein isoelectric point (pI). Malmsten (1998) explained the role of protein charge as a driving force for adsorption, in relation to solvency effects, and also to the larger structural alterations verified in proteins well above or well below the pI. The decrease in protein net charge makes the protein-solvent interactions less favorable, which favors adsorption.

Figure 7.4 shows the evolution of permeate flow rate in different transmission experiments reported by Carvalho *et al.* (2000b). It can be observed that when using the reversed micellar system together with substrates and products, the permeate flow rate maintains its initial

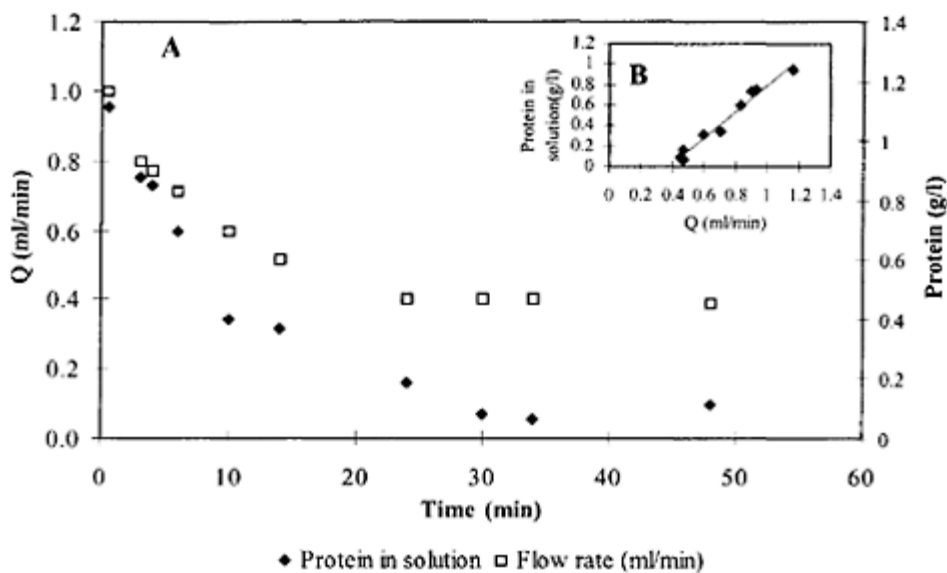


**Figure 7.4 A**—Time course of protein in solution and permeate flow rate.  
**B**—Correlation of protein adsorbed and permeate flow rate.

value. In the presence of protein, there is a significant decrease of permeate flow rate, especially during the first fifteen hours. The flow rate stabilises after 24 hours.

This behaviour correlates very well with the adsorption of protein, as the representation of adsorbed protein (on the basis of protein remaining in solution), as a function of permeate flow rate leads to a high correlation coefficient, ( $R^2=0.977$ ) (see Figure 7.4). This confirms that the reduction in the permeate flow rate is due to the presence of protein and not to an occlusion phenomenon caused by AOT film deposition on the membrane surface or inside its pores.

Based on the experimental data, namely on the permeate flow rate in the presence and in the absence of protein, the resistance due to the presence of protein can be estimated (see example in Table 7.4). From Table 7.4 it can be verified that the global resistance of the membrane increases 2.5 times after completion of the adsorption process and opposing the permeate flow rate variation.

The capacity of membrane filtration is reduced by two phenomena, concentration polarisation and membrane fouling, both leading to a decrease of flux across the membrane. As a result of solutes deposition, a gel layer could be formed on the membrane surface resulting in a higher feed side concentration as well as flux decline.

The polarisation effect can be observed in the transmission experiments (see Table 7.3). A solute concentration could be seen on the surface and inside the pores leading to a concentration gradient that hinders the course of products and substrates through the

membrane. As a consequence of this barrier, the permeate flow rate also decreases, although the situation reached an equilibrium.

**Table 7.3** Rejection coefficients after stabilisation of concentrations (24 h)

Solute	$\sigma_{obs} \times 100 (\%)$
protein	27 (or 94 if $\sigma_{real} \times 100 (\%)$ )*
water	17
Surfactant (AOT)	17
butanol	19
hexanol	17
butyl acetate	7
hexyl acetate	6

$$* \frac{[\text{Pr ot}]_p}{[\text{Pr ot}]_r + [\text{Pr ot}]_{memb}}$$

Enzyme membrane bioreactors can either be dead-end stirred cells (DESC) or crossflow systems. The latter is much more efficient to control the effects of flux reduction than the former.

### *Operation of enzyme micellar reactors in a batch mode*

#### *Modeling of a batch enzyme reactor*

The design equation of a batch enzyme reactor for a reversible reaction is

$$\frac{k_{cat} \cdot E \cdot t}{V} = S_o X_e \left\{ X \cdot \left( 1 - \frac{K_m}{K_p} \right) + \left( \frac{K_m}{S_o} + 1 - X_e + X_e \cdot \frac{K_m}{K_p} \right) \cdot \ln \left( \frac{X_e}{X_e - X} \right) \right\} \quad (26)$$

The kinetic parameters for both substrates and products are used to model the MBR with total recirculation as a batch reactor.

#### *Determination of the single-pass conversion in the MBR operating in a total recirculation operation mode*

The overall substrate conversion, X, is given by:

$$X = \frac{S_o - S}{S_o}, \quad (27)$$

and the substrate conversion per pass (corresponding to one passage through the membrane),  $X_n$ , in a recirculated reactor is:

$$X_n = \frac{S_{n-1} - S_n}{S_{n-1}}, \quad (28)$$

whereas the substrate concentration after a single-pass,  $S_n$ , is given by:

$$S_n = S_{n-1} - \frac{V}{Q_r} \left( -\frac{dS}{dt} \right) \quad (29)$$

$Q_r$  being the recirculation flow rate.

**Table 7.4** Relation of the protein adsorbed and the membrane resistance to the flux permeation

t(h)	Prot <sub>R</sub> (mg)	Prot <sub>p</sub> (mg)	Prot <sub>ads</sub> (mg)*	Q <sub>p</sub> (ml/min)	J (ml/min.cm <sup>2</sup> )	R <sub>memb</sub> (Kgm <sup>-2</sup> s <sup>-1</sup> .10 <sup>-4</sup> )	R <sub>prot</sub> (Kgm <sup>-2</sup> s <sup>-1</sup> .10 <sup>-4</sup> )	R <sub>total</sub>
<b>0.5</b>	10.9	3.15	—	1.167	0.0307	254		0 254
<b>3</b>	8.64	0.661	0.33	0.933	0.0246	254		63.0 317
<b>4</b>	8.38	0.956	0.59	0.900	0.0237	254		75.1 329
<b>6</b>	6.87	1.10	2.10	0.833	0.0219	254		102 356
<b>10</b>	3.91	0.965	5.06	0.700	0.0184	254		170 424
<b>14</b>	3.60	1.12	5.37	0.600	0.0158	254		240 494
<b>24</b>	1.85	1.35	7.12	0.467	0.0123	254		380 634
<b>30</b>	0.80	2.50	8.17**	0.467	0.0123	254		380 634
<b>34</b>	0.649	0	8.32**	0.467	0.0123	254		380 634
<b>48</b>	1.08	0.649	7.89**	0.450	0.0123	254		380 634

\*Prot<sub>ads</sub>=Prot<sub>inic</sub>-Prot<sub>r</sub>-Prot<sub>paverage</sub>, with Prot<sub>paverage</sub>=1.03 mg.

\*\*The average value of 8.13 mg of cutinase was used.

This leads to:

$$X_e = \frac{V}{Q_r} \frac{1}{S_{n-1}} \left( -\frac{dS}{dt} \right) \quad (30)$$

If the conversion obtained in a single-pass is lower than 1%, then the reactor has characteristics of a differential reactor where high recirculation velocities lead to low conversion rates. This permits classification of the membrane reactor as a differential reactor, which in a continuous operation would behave as a CSTR (continuous stirred tank reactor).

The number of cycles,  $N$ , in the total recirculation is defined as follows:

$$N = \frac{t \times Q_r}{V}. \quad (31)$$

### Continuous Operation of a Micellar Membrane Reactor

One of the current issues under investigation in reversed micellar technology is the development of reactors to perform continuous operation taking full advantage of this reaction medium. Continuous operation of this type of reactor is feasible as long as water-filled micelles are supplied to the reactor together with the substrates solution (Prazeres *et al.*, 1993).

The advantages of membrane bioreactors (MBRs) make them suitable for the operation of continuous processes. However, there are very few examples of exhaustive studies that attempt a full characterisation of membrane reactors from the hydrodynamic point of view (Deeslie and Cheryan, 1981; Sims and Cheryan, 1992).

#### *Analysis of the MBR set-up with differential and integral types of reactors*

The MBR can be broadly classified as a direct contact membrane recycle reactor, since the enzyme acts on the substrate molecules as soon as they enter the reaction system (Prazeres & Cabral, 1994). As a tubular reactor with partial recirculation, the MBR characterisation is based on a mass balance, the conversion per pass, the number of cycles and the hydraulic residence time.

An overall mass balance to the reactor system (see Figure 7.5) leads to:

$$Q_1 = Q_p + Q_r, \text{ with } Q_p = Q_o, \text{ as the liquid volume is constant} \quad (32)$$

where,  $Q_0$  is the feed flow rate;  $Q_1$  is the flow entering the ultrafiltration module;  $Q_p$  is the permeate flow rate and  $Q_r$  is the recirculation flow rate.

$$\text{Defining the recirculation ratio as } R = \frac{Q_r}{Q_o} \quad (33)$$

then;

$$Q_r = R.Q_o \quad (34)$$

$$Q_1 = R.Q_o + Q_o = (R + 1).Q_o \quad (35)$$

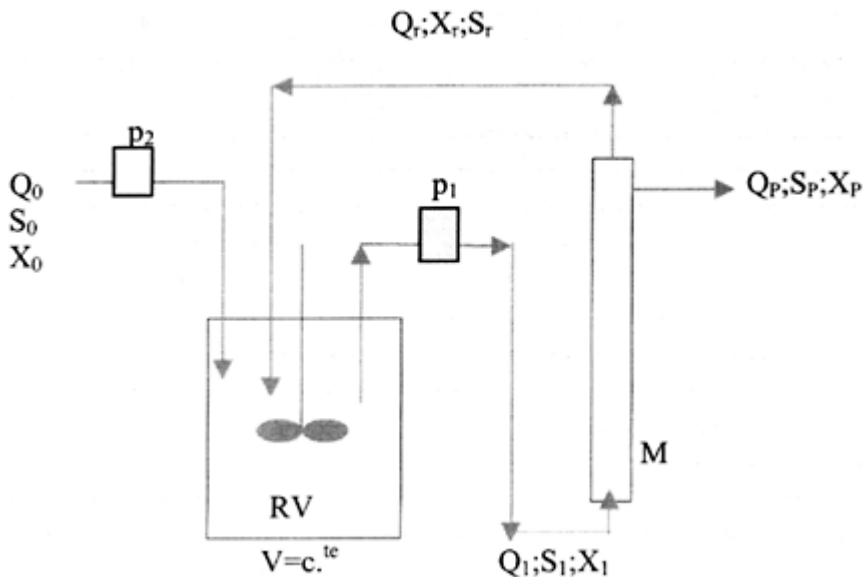


**Figure 7.5** Schematic of the membrane bioreactor for continuous operation.

Using the general design equation for a reactor:

$$\frac{V}{F_1} = \int_{x_e}^{x_i} \frac{dX}{v} \quad (36)$$

where the molar flow rate,  $F$ , is defined by:

$$F = S.Q \quad (37)$$

The overall molar balance to the reaction system leads to:

$$F_1 = F_0 + F_r = S_0 Q_0 + S_r Q_r = S_1 Q_1 \quad (38)$$

and taking into account the definition of conversion degree,  $X$ ,

$$X = \frac{S_o - S}{S_o} \quad (39)$$

From equation 40:

$$S_o(1 - X)(R + 1).Q_o = S_o Q_o + S_o(1 - X_r).R.Q_o \quad (40)$$

which divided by  $S_0 Q_0$ , yields:

$$(1 - X).(R + 1) = 1 + (1 - X_r).R \quad \text{hence;} \quad (41)$$

$$X_l = \left( \frac{R}{R + 1} \right) X_r \quad (42)$$

Equation 42 establishes the influence of the recirculation rate on the conversion degree. A recirculation rate, R, higher than 100, leads to differences between  $X_l$  and  $X_r$  that represent less than 1 % conversion, which is characteristic of a differential reactor. In addition, if  $X_l$  and  $X_r$  have a similar value, that suggests the reaction rate ( $v$ ) is approximately constant over the reactor.

For the start-up of the reaction it could be inferred that  $S_0 \cong S_1 \cong S_r$  and by substitution in Equation 40:

$$F_1 = S_0.Q_0 + S_r.R.Q_0 = S_0.Q_0.(R + 1) \quad (43)$$

Thus,

$$F_1 = F_0.(R + 1) \quad (44)$$

Replacing in Equation 36:

$$\frac{V}{(R + 1).F_0} = \int_{X_0}^{X_f} \frac{dX}{v} \quad (45)$$

Since the MBR acts like a tubular reactor with partial recirculation, assuming that the enzyme is all located in the membrane,  $X_l$  and  $X_r$  could be undertaken as the integration limits,

$$\frac{V}{(R + 1).F_0} = \int_{X_l}^{X_r} \frac{dX}{v} \quad (46)$$

Taking into account Equation 42, then;

$$\frac{V}{F_0} = (R + 1) \int_{\left( \frac{R}{R+1} \right) X_r}^X \frac{dX}{v} \quad (47)$$

If the two extreme cases of very high recirculation rate (A) and very low recirculation rate (B) are considered, the following equations are obtained:

(A)  $R \rightarrow \infty$  then  $X_l \cong X_r$ , the reaction rate will be approximately constant in the reactor and:

$$\frac{V}{F_0} = (R + 1) \cdot \frac{X_r - \left( \frac{R}{R+1} \right) X_r}{v} \quad (48)$$

which leads to;

$$\frac{V}{F_0} = \frac{X_r}{v} \quad \text{which is the design equation of a differential (mixed) reactor,} \quad (49)$$

(B)  $R \rightarrow 0$

$$\frac{V}{F_0} = \int_{X_i}^{X_r} \frac{dX}{v} \quad \text{which is the design equation of an integral (plug flow) reactor.} \quad (50)$$

### ***Determination of the single-pass conversion in the MBR***

The conversion per pass,  $X_n$ , is expressed by:

$$X_n = X_r - X_i \quad (51)$$

If  $R=10,000$ ;  $X_i=0.9999X_f$  and then  $X_n=0.0001X_f$

This clearly shows that the conversion per pass of the reaction mixture in the membrane module, where enzyme is confined, is very small. As an example when the conversion is 60%, the single pass conversion is only 0.006%. Since it is usually accepted that less than 1 % conversion is typical of differential reactors, this confirms the classification of MBR as a differential (mixed) reactor.

The number of cycles,  $N$ , with partial recirculation is defined as follows:

$$N = \frac{\theta Q_r}{V} \quad \theta \text{ being the hydraulic residence time,} \quad (52)$$

which is given by:

$$\theta = \frac{V}{Q_0} \quad (53)$$

From Equations 33, 52 and 53 it can be verified that  $N=R$ .

The hydraulic residence time corresponds in practice to the time needed for the total removal of the recirculating liquid. The fact that steady-state conditions can be reached within one reaction volume permeated through the system indicates a well mixed reactor type with no hindrance to the passage of products from the reactor to the permeate (Deeslie and Cheryan, 1981) in agreement with transmission experiments previously reported (Carvalho *et al.*, 2000b, 2001b).

### ***Modelling of the continuous MBR***

The comparison of the MBR with general types of reactors leads to similarities with a plug flow reactor (PFR) since no agitation device was employed. However, if the recirculation velocity becomes high enough that the conversion degree could be considered independent of the position in the reactor, then the reactor will assume a continuous stirred tank reactor (CSTR) behaviour.

*CSTR*

The design equation for an enzymatic CSTR for a reversible reaction at equilibrium is:

$$\frac{k_{cat} \cdot E}{Q} = \frac{X_e \cdot X \cdot \left( K_m + S_0 - S_0 \cdot X + \frac{K_m}{K_p} \cdot S_0 \cdot X \right)}{X_e - X} \quad (54)$$

$$k_{cat} = \frac{V_{max}}{[E]} \quad \text{with } k_{cat} = \frac{V_{max}}{[E]} \text{ (with mmol.min}^{-1}\text{g}^{-1} \text{ as units) and } X_e = \frac{K}{K+1}$$

For a first order kinetics, it can be considered that:

$$K_m \gg \left( S_0 - S_0 \cdot X + \frac{K_m}{K_p} \cdot S_0 \cdot X \right)$$

The equation that describes the conversion in a CSTR, in these conditions, is:

$$\frac{k_{cat} \cdot E}{Q} = K_m \cdot \frac{X_e \cdot X}{X_e - X} \quad (55)$$

### PFR

The design equation of a PFR for a reversible reaction at equilibrium is:

$$\frac{k_{cat} \cdot E}{Q} = S_0 \cdot X_e \left\{ X_e \left( 1 - \frac{K_m}{K_p} \right) + \left( \frac{K_m}{S_0} + 1 - X_e + X_e \cdot \frac{K_m}{K_p} \right) \cdot \ln \left( \frac{X_e}{X_e - X} \right) \right\} \quad (56)$$

For a first order kinetics, it can be considered that:

$$K_m \gg \left( S_0 - S_0 \cdot X_e + S_0 \cdot X_e \cdot \frac{K_m}{K_p} \right)$$

and,

$$K_m \cdot \ln \left( \frac{X_e}{X_e - X} \right) \gg S_0 \cdot X \left( 1 - \frac{K_m}{K_p} \right)$$

Therefore, the equation of a PFR for first order kinetics is:

$$\frac{k_{cat} \cdot E}{Q} = K_m \cdot X_e \cdot \ln \left( \frac{X_e}{X_e - X} \right) \quad (57)$$

### *Comparative performance of a CSTR and of a PFR for an equilibrium reaction*

For a first order equilibrium reaction, the performance of a CSTR and a PFR can be described as (adapted from Equations 55 and 57):

$$\text{CSTR} \quad \frac{k_{cat} \cdot E_{cstr}}{Q_{cstr}} = K_m \frac{X_e \cdot X_{cstr}}{X_e - X_{cstr}} \quad (58)$$

$$\text{PFR} \quad \frac{k_{cat} \cdot E_{pfr}}{Q_{pfr}} = K_m \cdot X_e \cdot \ln \left( \frac{X}{X_e - X_{pfr}} \right) \quad (59)$$

If the same normalised residence time is assumed in both reactors,  $\tau_{pfr} = \tau_{cstr}$ , then:

$$\frac{X_{cstr}}{X_e - X_{cstr}} = \ln \left( \frac{X_e}{X_e - X_{pfr}} \right) \quad (60)$$

The conversions obtained in both reactors are presented in Figure 7.6. It can be seen that the PFR leads to higher conversions being much more efficient, assuming the reactors are operated at ideal conditions.

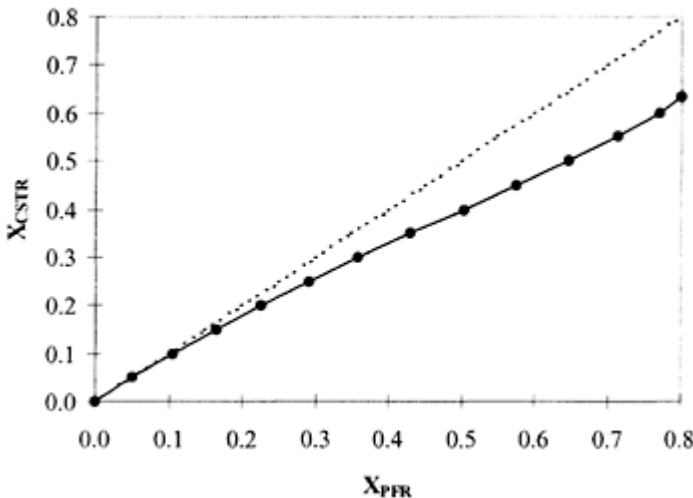


**Figure 7.6** Efficiency of the CSTR compared with PFR. The dotted line applies to a zero order reaction whereas the continuous line refers to a first order reaction.

#### *Operational stability*

To evaluate the enzymatic deactivation in MBR, and due to its similarities with a CSTR performing a first order reaction, Equation 55 was modified to include a deactivation constant, considering a first order activity decay:

$$\frac{k_{cat} \cdot E \cdot e^{-kdt}}{Q} K_m \frac{X_e \cdot X}{X_e - X} \quad (61)$$

The enzyme deactivation was evaluated using the relation of enzymatic activities ( $E/E_0$ ) at initial time ( $t_i$ ) and at final time ( $t_f$ ) after the steady-state conditions were reached in MBR. The activities were plotted against the time of operation (see Figure 7.7).

$$\frac{E}{E_0} = e^{-kd \cdot (t_f - t_i)} = \frac{X_f \cdot (X_e - X_i)}{X_i \cdot (X_e - X_f)} \quad (62)$$

The half-life time can be obtained from the deactivation constant,  $k_d$ , using the relation:

$$t_{\frac{1}{2}} = \frac{\ln 2}{k_d} \quad (63)$$

Continuous operation sometimes lessens the stability when compared with a batch reactor (Mukesh *et al.*, 1993). Nevertheless, in enzyme membrane reactors a deactivation of about 3% per day or less has been described (Kragl *et al.*, 1996). The enzyme stabilisation achieved may be a consequence of substrates presence. Supporting this hypothesis the

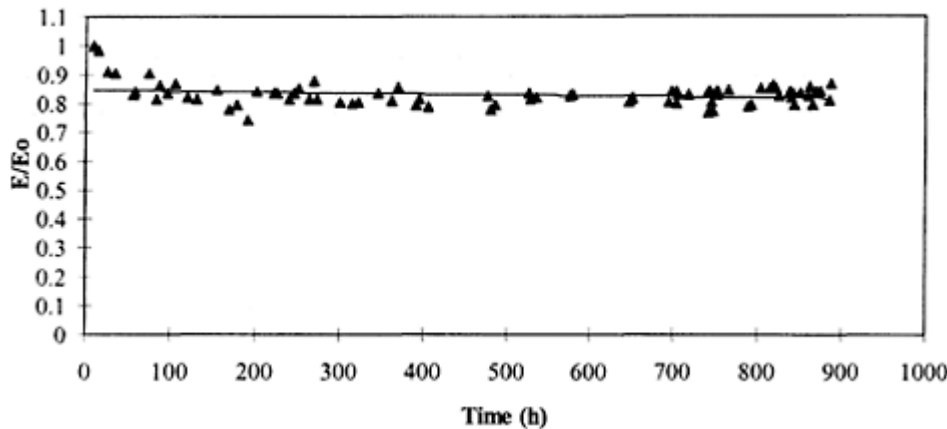


**Figure 7.7** Representation of relative cutinase activity against time during continuous operation using a flow rate of 0.1 ml/min. The correlation of the results was made using an exponential deactivation model (—). (From Carvalho *et al.*, 2001a)

reaction mechanism involves an acyl-enzyme complex in the first step, and this complex formation during reaction may account for cutinase stabilisation (Carvalho *et al.*, 2001a).

Leakage of enzyme through the membrane associated with the continuous start-up can be considered a common phenomenon in membrane reactors (Deeslie and Cheryan, 1981; Bressollier *et al.*, 1988). The consequence is an initial decrease in conversion.

#### *Linear velocity and flux regimen in the membrane module*

The linear recirculation velocity through the tubular membrane module is given by:

$$u_m = \frac{Q_r}{A_{cm}} \quad (64)$$

and the linear permeate velocity through the membrane pores, cross-flow velocity, is expressed by:

$$u_p = \frac{Q_p}{n_p \cdot A_{cp}} \quad (65)$$

Reynolds number,  $R_e$ , is also used to define the flux regimen:

$$R_e = \frac{\nu \cdot d_p \cdot \rho}{\eta} \quad (66)$$

#### *Analysis of reactor series*

The previous modeling clearly proves that the MBR acts globally as a CSTR. Nevertheless, the simultaneous analysis of permeate and recirculate samples (Figure 7.8) allows verification

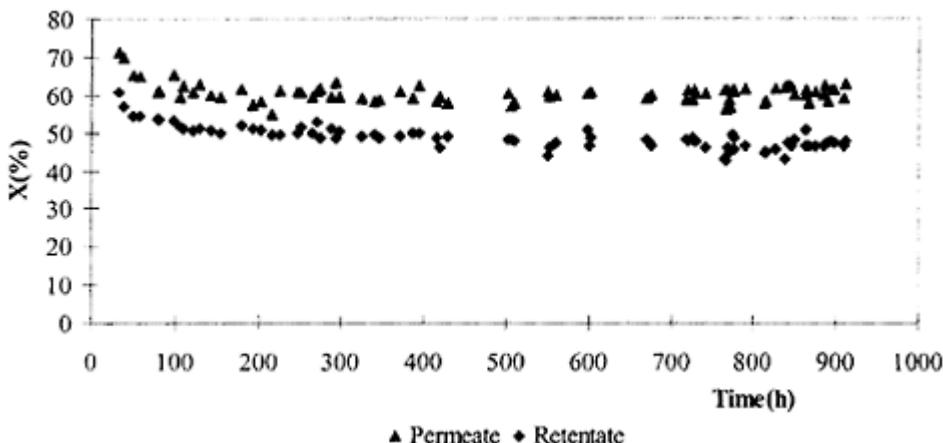


**Figure 7.8** Conversion degrees obtained for the 0.1 ml/min flow rate in permeate and recirculate solutions.  
(From Carvalho *et al.*, 2001b)

that the recirculate and permeate concentrations were different whatever the experimental conditions. The product concentration was always higher in permeate than in recirculate and the increase depended on the substrate ratio and on the flow rate selected.

In parallel with the global reactor analysis, it can be proposed that the membrane pores may act like a second CSTR, although with a higher residence time (there is no recirculation inside the membrane matrix). The main consequence will be the achievement of higher conversion degrees, when compared with one unique CSTR. Since the increment in permeate conversion was remarkable this may raise the possibility of having the inside of the membrane acting as a PFR.

Both hypotheses require enzyme to be retained in the pores of the membrane. In each series of reactors there is a distribution of cutinase on membrane surface and in the pores accounting for the conversions detected in the recirculate and in the permeate. The prediction of these amounts is based on Equations 55 and 57 (Carvalho *et al.*, 2001b).

The estimated enzyme quantities for each case, considering  $X_{in}=0$  and  $X_{out}=0.6$  for  $\frac{k_{cat}}{K_m}$  relation are given in Table 7.5. These values were used to model the different reactor series and the results are plotted in Figure 7.9. At low residence times the substrate remained at higher concentrations, causing the overlapping of the different models.

The two CSTRs model describe the results very well (Carvalho *et al.*, 2001b). When the flow rate is low, recirculation decreases, but by maintaining high recirculating flow rates, the MBR acts as a CSTR<sub>1</sub> on the hollow membrane side. The flux through the membrane pores is significantly lower, and the residence times become significantly different (by a 5000 fold factor), causing a deviation from CSTR<sub>1</sub> characteristics. Therefore, the inside (matrix) of the membrane is classified as a second CSTR<sub>2</sub>.

Besides this reactor sequence being a good model for the experimental behavior of MBR, it also upholds the fact that two CSTRs are more efficient than a unique CSTR.

**Table 7.5** Parameters used to model the conversion in MBR. (From Carvalho *et al.*, 2001b)

Reactor series	X <sub>e</sub>	K <sub>cat</sub> /K <sub>m</sub>	Enzyme distribution (g)
<b>PFR</b>	0.836	18.27	0.008175
<b>CSTR</b>	0.836	27.60	0.008175
<b>CSTR+ PFR</b>	0.836	22.16	0.005925+0.00225
<b>CSTR<sub>1</sub>+CSTR<sub>2</sub></b>	0.836	22.39	0.005494+0.002681

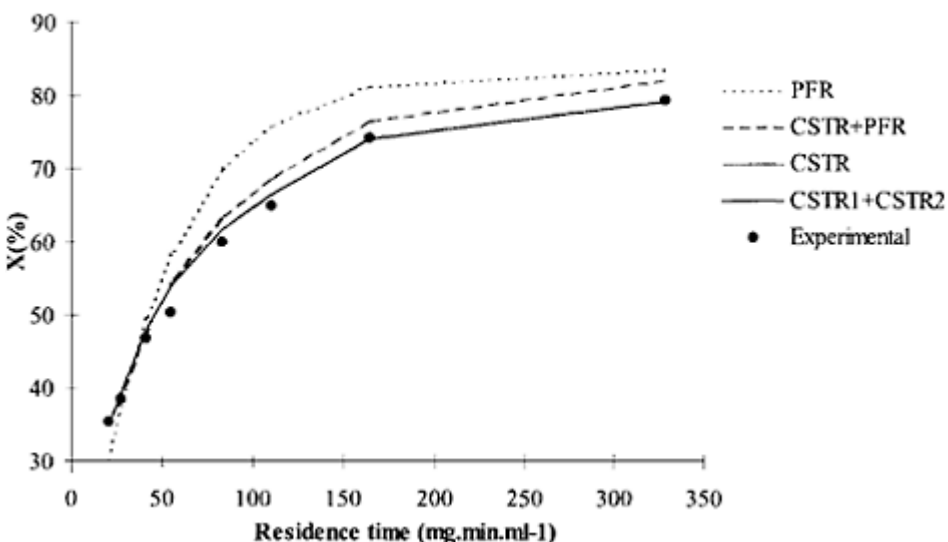


**Figure 7.9** Representation of different models and their correlation to the experimental results. (From Carvalho *et al.*, 2001b)

Accordingly, in the design and analysis of biological reactors for process optimisation, the sequence of reactors plays an important role. Most of the applications described in the literature are related to fermenters. To obtain high final cell concentrations, the best reactor combinations are always multiple fermenters connected in series (Lee, 1992). Bailey and Ollis (1977) and Levenspiel (1972) also discussed the efficiency of reactor sequences, and concluded that a CSTR-PFR sequence or a cascade of two CSTR maximise product yield and are suitable for a wide variety of process kinetics and design objectives.

#### *Analysis of stability on a series of two CSTRs*

From the aforementioned, the stability may be determined for the two CSTRs cascade. The determination of half-life time is again based on the conversion degree obtained in the retentate and permeate. The enzyme on the membrane surface (i.e. using the retentate conversion degree evolution) has a faster deactivation (4.3 times faster) than that observed for the enzyme entrapped in the pores (Carvalho *et al.*, 2001b). The explanation for this is based on the exposition conditions of the two portions of enzyme. The cutinase adsorbed onto the surface of the membrane supports high shear forces caused by the recirculated fluid, which accelerates the denaturing process. This may be better understood by the calculation of the linear velocity at the membrane surface and in the membrane pores (Equations 64 and 65).

The velocity on the surface of the membrane is  $10^5$  times higher than inside the membrane pores. These velocities have quite different effects on the properties of the fluid circulation in the reactor.

By employing Equation 66, the Reynolds number,  $R_e$ , for the reaction medium at the membrane surface and inside the membrane pores can be calculated. The ratio of the two values is in the order of magnitude of  $10^{12}$ , the  $R_{e_s}$  being characteristic of a turbulent regimen, whilst inside the pores the flux has a laminar or viscous property.

## CONCLUSIONS

We have now reached a point where we have extensive knowledge of the basic principles that rule the formation and properties of reversed micelles. Furthermore, a wide number of structural techniques are now available for the study of microstructure of these systems and in the near future they will provide more insight at this level. The numerous advantages of reversed micellar systems make them of special interest for technical purposes. Industrial application requires the scale-up of systems and the operation of reactors in a continuous mode. Moreover, it is desirable to define the characteristics of the reactor in order to control the final quality of products.

This chapter provides the analysis of a MBR both in terms of performance and hydrodynamics, describing in detail how the flow rate and the recirculation ratio affect the residence time of substrates and thus the reactor efficiency in continuous operation. Moreover, the comparison of conversions obtained in MBR when operating in a total recirculation mode and in continuous operation, as well as the conversion per pass, gave rise to the general classification of MBR as a global CSTR.

The properties of the membrane account significantly for the interactions with the biocatalyst. Thus, it is important to relate the differences in degree of permeate and retentate conversion to the prediction of enzyme distribution. The membrane pores may retain a fraction of enzyme that is responsible for the product increment in the permeate, especially with the higher residence time exhibited by this sequential reactor. The integration of all operating aspects together with the enhancement of product concentration on permeate and enzyme distribution in the membrane permits the identification of MBR with a cascade of two CSTRs.

The consequences for biocatalyst stability may be important since the deactivation is decreased when the enzyme is sheltered inside the membrane pores. Emphasis should be given to the fact that high shear stress forces, in a strong turbulent regimen, affect the operational stability whereas in a laminar regimen the half-life is largely improved.

## NOMENCLATURE

$\Delta PTM$	transmembrane pressure ( $ML^{-1}T^{-2}$ )
$\theta$	hydraulic residence time (T)
$\tau$	normalised residence time ( $ML^{-3}T$ )
$\eta$	viscosity ( $ML^{-1}T^{-1}$ )
$\rho$	volumetric mass ( $ML^{-3}$ )

[E]	overall enzyme concentration ( $\text{ML}^{-3}$ )
$\varepsilon_m$	porosity (dimensionless)
$\sigma_{\text{obs}}$	observed solute rejection (dimensionless)
$[\text{Prot}]_p$	concentration of protein in the permeate ( $\text{ML}^{-3}$ )
$[\text{Prot}]_r$	concentration of protein in the retentate ( $\text{ML}^{-3}$ )
$\sigma_{\text{real}}$	solute rejection taking into account the concentration polarisation process (dimensionless)
A	area ( $\text{L}^2$ )
$A_{\text{memb}}$	membrane area ( $\text{L}^2$ )
$A_p$	area of a pore ( $\text{L}^2$ )
$A_{\text{cm}}$	circular area of the membrane section ( $\text{L}^2$ )
$A_{\text{cp}}$	circular area of the pore section ( $\text{L}^2$ )
$A_T$	total porous area ( $\text{L}^2$ )
$C_p$	permeate concentration ( $\text{ML}^{-3}$ )
$C_r$	retentate or recirculate concentration ( $\text{ML}^{-3}$ )
$d_p$	pore diameter (L)
$E/E_0$	relative activity (dimensionless)
$E_T$	total amount of enzyme (M)
F	molar flow rate ( $\text{MT}^{-1}$ )
$F_0$	feed molar flow rate ( $\text{MT}^{-1}$ )
$F_1$	molar flow rate at the module entrance ( $\text{MT}^{-1}$ )
$F_r$	recirculated molar flow rate ( $\text{MT}^{-1}$ )
J	filtration flux ( $\text{LT}^{-1}$ )
K	equilibrium constant (dimensionless)
$k_{\text{cat}}$	catalytic constant ( $\text{T}^{-1}$ )
$K_d$	deactivation constant ( $\text{T}^{-1}$ )
$K_m$	Michaelis-Menten constant for the substrate ( $\text{ML}^{-3}$ )
$K_p$	Michaelis-Menten constant for the product ( $\text{ML}^{-3}$ )
$L_p$	membrane permeability ( $\text{L}^2\text{M}^{-1}\text{T}$ )
$l_p$	pore length (L)
N	number of cycles (dimensionless)
$n_p$	number of pores (dimensionless)
$n_p$	total total number of pores (dimensionless)
P	product concentration ( $\text{ML}^{-3}$ )
$P_e$	specific productivity ( $\text{L}^3\text{T}^{-1}$ )
$\text{Prot}_{\text{ads}}$	protein adsorbed onto the membrane (M)

$\text{Prot}_{\text{memb}}$	protein interacting with the membrane (M)
$\text{Prot}_p$	protein in the permeate (M)
$\text{Prot}_r$	protein in the retentate (M)
$P_v$	volumetric productivity ( $\text{MT}^{-1}$ )
$Q$	flow rate ( $\text{L}^3 \text{T}^{-1}$ )
$Q_0$	feed flow rate ( $\text{L}^3 \text{T}^{-1}$ )
$Q_1$	flow rate at the module entrance ( $\text{L}^3 \text{T}^{-1}$ )
$Q_p$	permeate flow rate ( $\text{L}^3 \text{T}^{-1}$ )
$Q_r$	recirculation flow rate ( $\text{L}^3 \text{T}^{-1}$ )
$R$	recirculation flow rate ratio (dimensionless)
$Re$	Reynolds number (dimensionless)
$R_{\text{memb}}$	membrane resistance ( $\text{ML}^{-2}\text{T}^{-1}$ )
$R_{\text{prot}}$	resistance of protein gel on the membrane ( $\text{ML}^{-2}\text{T}^{-1}$ )
$R_{\text{total}}$	sum of resistances ( $\text{ML}^{-2}\text{T}^{-1}$ )
$S$	substrate concentration ( $\text{ML}^{-3}$ )
$S_0$	initial substrate concentration ( $\text{ML}^{-3}$ )
$S_1$	substrate concentration at the module entrance ( $\text{ML}^{-3}$ )
$S_n$	substrate concentration after each single-pass ( $\text{ML}^{-3}$ )
$S_p$	permeate substrate concentration ( $\text{ML}^{-3}$ )
$S_r$	recirculated substrate concentration ( $\text{ML}^{-3}$ )
$t$	time (T)
$t_{1/2}$	half-life time of biocatalyst (T)
$t_f$	final time of operation during a deactivation process (T)
$t_i$	initial time of operation during a deactivation process (T)
$u$	linear velocity or cross flow velocity ( $\text{LT}^{-1}$ )
$v$	velocity or rate of reaction ( $\text{ML}^{-3}\text{T}^{-1}$ )
$V$	volume ( $\text{L}^3$ )
$V_{\text{max}}$	maximum enzyme velocity ( $\text{ML}^{-3}\text{T}^{-1}$ )
$v_p$	pore volume ( $\text{L}^3$ )
$V_p$	volume of a membrane pore ( $\text{L}^3$ )
$V_{\text{total}}$	total reaction volume ( $\text{L}^3$ )
$W_0$	water to surfactant molar ratio (dimensionless)
$X$	conversion degree (dimensionless)
$X_0$	feed conversion degree (dimensionless)
$X_1$	conversion degree at module entrance (dimensionless)
$X_e$	equilibrium conversion degree or steady state conversion

	degree in the permeate stream (dimensionless)
$X_f$	conversion degree at final time (dimensionless)
$X_i$	conversion degree at initial time (dimensionless)
$X_n$	conversion degree in a single-pass (dimensionless)
$X_p$	permeate conversion degree (dimensionless)
$X_r$	recirculated conversion degree (dimensionless)
$X_{R1}$	conversion degree after the first single-pass (dimensionless)

## REFERENCES

- Almgren, M., Jóhannsson, R. and Eriksson, J.C. (1993) Polydispersity of AOT droplets measured by time-resolved fluorescence quenching. *J. Phys. Chem.*, **97**, 8590–8594.
- Andrade, S.M. and Costa, S.M.B. (1996) Fluorescence studies of the drug piroxicam in reverse micelles of AOT and microemulsions of Triton X-100. *Prog. Colloid Polym. Sci.*, **100**, 195–200.
- Ayyagari, M.S. and John, V.T. (1995) Substrate-induced stability of the lipase from *Candida cylindracea* in reversed micelles. *Biotechnol. Lett.*, **17**, 177–182.
- Barbaric, S. and Luisi, P.L. (1981) Micellar solubilization of biopolymers in organic solvents. S. Activity and conformation of  $\alpha$ -chymotrypsin in isoctane-AOT reverse micelles. *J. Am. Chem. Soc.*, **103**, 4239–4244.
- Bielecki, S. and Idem-Somiari, R. (1998) Oligosaccharide synthesis by invertase in organic media containing SDS. *Biotechnol. Lett.*, **20**, 287–290.
- Blanch, H.W. (1990) Bioreactor development: from enzymes to animal cells. *Ferment. Technol. Ind. Appl.*, 329–336.
- Bowen, W.R., Hilal, N., Lovitt, R.W. and Williams, P.M. (1996) Visualisation of an ultrafiltration membrane by non-contact atomic force microscopy at single pore resolution. *J. Memb. Sci.*, **110**, 229–232.
- Bressollier, P., Petit, J.M. and Julien, R. (1988) Enzyme hydrolysis of plasma in a CSTR ultrafiltration reactor: performances and modeling. *Biotechnol. Bioeng.*, **31**, 650–658.
- Brown, E.D., Yada, R.Y. and Marangoni, A.G. (1993) The dependence of the lipolytic activity of *Rhizopus arrhizus* lipase on surfactant concentration in Aerosol-OT/isoctane reverse micelles and its relationship to enzyme structure. *Biochim. Biophys. Acta*, **1161**, 66–72.
- Bru, R., Sanchez-Ferrer, A. and Garcia-Carmona, F. (1989) A theoretical study on the expression of enzymic activity in reverse micelles. *Biochem. J.*, **259**, 355–361.
- Carvalho, C.M.L., Serralheiro, M.L.M., Cabral, J.M.S. and Aires-Barros, M.R. (1997) Application of factorial design to the study of transesterification reactions using cutinase in AOT-reversed micelles. *Enzyme Microb. Technol.*, **21**, 117–123.
- Carvalho, C.M.L., Cabral, J.M.S. and Aires-Barros, M.R. (1999a) Cutinase stability in AOT reversed micelles: system optimization using the factorial design methodology. *Enzyme Microb. Technol.*, **24**, 569–576.
- Carvalho, C.M.L., Aires-Barros, M.R. and Cabral, J.M.S. (1999b) Cutinase: from molecular level to bioprocess development. *Biotechnol. Bioeng.*, **66**, 17–34.
- Carvalho, C.M.L., Aires-Barros, M.R. and Cabral, J.M.S. (2000a) An integrated model for enzymatic reactions in reversed micellar system: nominal and effective substrate concentrations *Langmuir*, **16**, 3082–3092.

- Carvalho, C.M.L., Aires-Barros, M.R. and Cabral, J.M.S. (2000b) Performance of a membrane reactor for enzymatic transesterification: characterization and comparison with a batch stirred tank reactor. *Biocatal Biotrans.*, **18**, 31–57.
- Carvalho, C.M.L., Aires-Barros, M.R. and Cabral, J.M.S. (2001a) A continuous membrane bioreactor for ester synthesis in organic media: I-Operational characterization and stability. *Biotechnol. Bioeng.*, **72**, 127–135.
- Carvalho, C.M.L., Aires-Barros, M.R. and Cabral, J.M.S. (2001b) A continuous membrane bioreactor for ester synthesis in organic media: II-modelling of MBR continuous operation. *Biotechnol Bioeng.*, **72**, 136–143.
- Chang, P.S., Rhee, J.S. and Kim J.-J. (1991) Continuous glycerolysis of olive oil by *Chromobacterium viscosum* lipase immobilized on liposome in reversed micelles. *Biotechnol Bioeng.*, **38**, 1159–1165.
- Chang, C.S. and Tsai, S.W. (1997) Surfactant effects on enhancing (S)-naproxen prodrug production from racemic naproxen by lipase. *AppL Biochem. Biotechnol.*, **68**, 135–142.
- Chen, J.P. and Chang, K.C. (1993) Lipase-catalyzed hydrolysis of milk fat in lecithin reverse micelles. *J. Ferment. Bioeng.*, **76**, 98–104.
- Chiang, C.L. and Tsai, S.W. (1992) Application of a recycle dialysis system in a reversed micellar reactor. *J. Chem. Technol. Biotechnol.*, **54**, 27–32.
- Crooks, C.E., Rees, C.D., Robinson, B.H., Svensson, M. and Stephenson, C.R. (1995) Comparison of hydrolysis and esterification behavior of *Humicola lanuginosa* and *Rhizomucor miehei* lipases in AOT-stabilized water-in-oil microemulsions: I. Effect of pH and water content on reaction kinetics. *Biotechnol Bioeng.*, **48**, 78–88.
- Deeslie, W.D. and Cheryan, M. (1981) A CSTR-hollow fiber system for continuous hydrolysis of proteins, performance and kinetics. *Biotechnol. Bioeng.*, **23**, 2257–2271.
- Douzou, P., Keh, E. and Balny, C. (1979) Cryoenzymology in aqueous media: micellar solubilized water clusters. *Proc. Natl. Acad. Sci. USA*, **76**, 681–684.
- Doyen, W., Adriansens, W., Molenberghs, B. and Leysen, R. (1996) A comparison between polysulfone, zirconia and organo-mineral membranes for use in ultrafiltration. *J. Memb. Sci.*, **113**, 247–258.
- Durfor, C.N., Bolin, R.J., Sugasawara, R.J., Massey, R.J., Jacobs, J.W. and Schultz, P.G. (1988) Antibody catalysis in reverse micelles. *J. Am. Chem. Soc.*, **110**, 9713–9714.
- Eggers, D.K. and Blanch, H.W. (1988) Enzymatic production of L-tryptophan in a reverse micelle reactor. *Bioprocess Eng.*, **3**, 83–91.
- Eicke, H.-F. and Rehak, J. (1976) On the formation of water/oil microemulsions. *Helv. Chim. Acta*, **59**, 2883–2891.
- Fadnavis, N.W., Prabhakar-Reddy, N. and Bhalerao, U.T. (1989) Reverse micelles, an alternative to aqueous medium for microbial reactions: yeast-mediated resolution of  $\alpha$ -amino acids in reverse micelles. *J. Org. Chem.*, **54**, 3218–3221.
- Fadnavis, N.W., Deshpande, A., Chauhan, S. and Bhalerao, U.T. (1990) Peptide synthesis mediated by immobilized and viable baker's yeast in reverse micelles: synthesis of leucine-enkephalin analogs. *J. Chem. Soc. Chem. Commun.*, **21**, 1548–1550.
- Fiechter, A. (1992) Biosurfactants: moving towards industrial application. *TIBTECH*, **10**, 208–217.
- Fletcher, P.D.I., Freedman, R.B., Mead, J., Oldfield, C. and Robinson, B.H. (1984) Reactivity of  $\alpha$ -chymotrypsin in water-in-oil microemulsions. *Coll. Surf.*, **10**, 193–203.
- Fletcher, P.D.I., Rees, C.D., Robinson, B.H. and Freedman, R.B. (1985) Kinetic properties of  $\alpha$ -chymotrypsin in water-in-oil microemulsions: studies with a variety of substrates and microemulsion systems. *Biochim. Biophys. Acta*, **832**, 204–214.
- Fletcher, P.D.I. (1986) The partitioning of solutes between water-in-oil microemulsions and conjugate aqueous phases. *J. Chem. Soc., Faraday Trans. I*, **82**, 2651–2664.
- Freeman, K.S., Lee, S.S., Kiserow, D.J. and McGown, L.B. (1998) Increased chymotrypsin activity in AOT/bile salt reversed micelles. *J. Coll. Inter. Sci.*, **207**, 344–348.

- Gajjar, L., Singh, A., Dubey, R.S. and Srivastava, R.C. (1997) Enzymatic activity of whole cells entrapped in reversed micelles. Studies on or-amylase and invertase in the entrapped yeast cells. *Appl. Biochem. Biotechnol.*, **66**, 159–172.
- García-Rio, L., Leis, J.R., Mejuto, J.C. and Peña, M.E. (1994) Effects of additives on the internal dynamics and properties of water/AOT/isooctane microemulsions. *Langmuir*, **10**, 1676–1683.
- Goto, A., Yoshioka, H., Manabe, M. and Goto, R. (1995) NMR spectroscopic study on the dissolution of water in sodium bis(2-ethylhexyl) sulfosuccinate/toluene solution. *Langmuir*, **11**, 4873–875.
- Goto, M., Ono, T., Nakashio, F. and Hatton, T.A. (1997) Design of surfactants suitable for protein extraction by reversed micelles. *Biotechnol. Bioeng.*, **54**, 26–32.
- Gupte, A., Nagarajan, R. and Kilara, A. (1995a) Enzyme reactions in reverse micelles. In *Food Flavours: Generation, analysis and process influence* (Charalambous, G. ed.), Elsevier, Amsterdam, pp. 1–74.
- Gupte, A., Nagarajan, R. and Kilara, A. (1995b) Enzymatic oxidation in reversed micelles. *Ind. Eng. Chem. Res.*, **34**, 2910–2922.
- Haering, G., Luisi, P.L. and Meussdoerffer, F. (1985) Solubilization of bacterial cells in organic solvents via reverse micelles. *Biochem. Biophys. Res. Commun.*, **127**, 911–915.
- Hakoda, M., Enomoto, A., Hoshino, T. and Shiragami, N. (1996) Electro-ultrafiltration bioreactor for enzymatic reaction in reversed micelles. *J. Ferment. Bioeng.*, **82**, 361–365.
- Hailing, P.J. (1994) Thermodynamic predictions for biocatalysis in nonconventional media: theory, tests, and recommendations for experimental design and analysis. *Enzyme Microb. Technol.*, **16**, 178–206.
- Han, D. and Rhee, J.S. (1986) Characteristics of lipase-catalyzed hydrolysis of olive oil in AOT-isoctane reversed micelles. *Biotechnol. Bioeng.*, **28**, 1250–1255.
- Han, D., Walde, P. and Luisi, P.L. (1990) Dependence of lipase activity on water content and enzyme concentration in reverse micelles. *Biocatalysis*, **4**, 153–161.
- Hasegawa, M. and Kitahara, A. (1994) Micro viscosity in water pool of Aerosol-OT reversed micelle determined with viscosity-sensitive fluorescence probe, auramine O, and fluorescence depolarization of xanthene dyes. *J. Phys. Chem.*, **98**, 2120–2124.
- Hayes, D.G. (1991) Esterification reactions catalyzed by Lipases in reverse micellar media. Ph.D thesis. University of Michigan, USA
- Hayes, D.G. and Gulari, E. (1994) Improvement of enzyme activity and stability for reverse micellar-encapsulated lipases in the presence of short-chain and polar alcohols. *Biocatalysis*, **11**, 223–231.
- Hayes, D.G. and Gulari, E. (1995) Ethylene glycol and fatty acid have a profound impact on the behavior of water-in-oil microemulsions formed by the surfactant Aerosol-OT. *Langmuir*, **11**, 4695–4702.
- Hayes, D.G. and Marchio, C. (1998) Expulsion of proteins from water-in-oil microemulsions by treatment with cosurfactant. *Biotechnol. Bioeng.*, **59**, 557–566.
- Hedström, G., Slotte, J.P., Molander, O. and Rosenholm, J.B. (1992) Enzyme-catalyzed oxidation of cholesterol on physically characterized water-in-oil microemulsions. *Biotechnol. Bioeng.*, **39**, 218–224.
- Hedström, G., Backlund, M. and Slotte, J.P. (1993) Enantioselective synthesis of ibuprofen esters in AOT/isooctane microemulsions by *Candida cylindracea* lipase. *Biotechnol. Bioeng.*, **42**, 618–624.
- Higuchi, W.I. and Misra, J. (1962) *J. Pharm. Sci.*, **51**, 455.
- Hildebrandt, J.R. (1991) Membranes for bioprocessing: design considerations. In *Chromatographic and Membrane Processes in Biotechnology* (Costa, C.A. and Cabral, J.M.S. eds.), Kluwer Academic Publishers, Dordrecht, pp. 363–378.
- Hochkoeppler, A. and Luisi, P.L. (1989) Solubilization of soybean mitochondria in AOT/isooctane water-in-oil microemulsions. *Biotechnol. Bioeng.*, **33**, 1477–1481.

- Holmberg, K. (1998) Quarter century progress and new horizons in microemulsions. In: *Micelles, microemulsions and monolayers: science and technology*, Shah, D.O. (ed.), Marcel Dekker, Inc., New York, USA.
- Hoppert, M., Braks, I. and Mayer, F. (1994) Stability and activity of hydrogenases of *Methanobacterium thermoautotrophicum* and *Alcaligenes eutrophus* in reversed micellar systems. *FEMS-Microb. Lett.*, **118**, 249–254.
- Hou, M.J., Kim, M. and Shah, D.O. (1988) A light scattering study on the droplet size and interdroplet interaction in microemulsions of AOT-oil-water system. *J. Coll. Interf. Sci.*, **123**, 398–412.
- Janda, K.D. (1993) Catalytic antibodies: the rerouting of chemical reactions. *Biochem. Soc. Trans.*, **21**, 1090–1095.
- Jorba, X., Clapes, P., Xaus, N., Calvet, S., Torres, J.L. and Valencia, G. (1992) Optimization and kinetic studies of the enzymatic synthesis of Ac-Phe-Leu-NH<sub>2</sub> in reversed micelles. *Enzyme Microb. Technol.*, **15**, 117–124.
- Kabanov, A.V., Levashov, A.V., Klyachko, Namyotkin, S.N. and Pshezhetsky, A.V. (1988) Enzymes entrapped in reversed micelles of surfactants in organic solvents: a theoretical treatment of the catalytic activity regulation. *J. Theor. Biol.*, **133**, 327–343.
- Kahlweit, M., Busse, G. and Faulhaber, B. (1997) Preparing nontoxic microemulsions. 2. *Langmuir*, **13**, 5249–5251.
- Karpe, P. and Ruckenstein, E. (1990) Effect of the hydration ratio on the degree of counterion binding and pH distribution in reverse micelles with aqueous core. *J. Coll. Inter. Sci.*, **137**, 408–424.
- Khmel'nitskii, Y.L., Levashov, A.V., Klyachko, N.L. and Martinek, K. (1984) A microheterogeneous medium for chemical (enzymic) reactions based on a colloidal solution of water in an organic solvent. *Russ. Chem. Rev.*, **53**, 319–331.
- Khmelnitsky, Y.L., Levashov, A.V., Klyachko, N.L. and Martinek, K. (1988) Engineering biocatalytic systems in organic media with low water content. *Enzyme Microb. TechnoL*, **10**, 710–724.
- Khmelnitsky, Y.L., Neverova, I.N., Polyakov, V.I., Grineberg, V.Y., Levashov, A.V. and Martinek, K. (1990) Kinetic theory of enzymatic reactions in reversed micellar systems. Application of pseudophase approach for partitioning substrates. *Eur. J. Biochem.*, **190**, 155–159.
- Komives, C., Osborae, D. and Russel, A.J. (1994) Degradation of pesticides in a continuous-flow two-phase microemulsion reactor. *Biotechnol. Prog.*, **10**, 340–343.
- Kragl, U., Kruse, W., Hummel, W. and Wandrey, C. (1996) Enzyme engineering aspects of biocatalysis: cofactor regeneration as example. *Biotechnol. Bioeng.*, **52**, 309–319.
- Kulkarni, S.S., Funk, E.W. and Li, N.N. (1992) VII Ultrafiltration. In *Membrane Handbook* (Ho, W.S.W. and Sirkar, K.K. eds.), Van Nostrand Reinhold, New York, pp. 393–07.
- Laane, C., Boeren, S., Hilhorst, R. and Veeger, C. (1987) Optimization of biocatalysis in organic media. In *Biocatalysis in Organic Media* (Laane, C., Tramper, J. and Lilly, M.D. eds.), Elsevier Science Publishers, B.V., Amsterdam.
- Larsson, K.M., Adlercreutz, P. and Mattiasson, B. (1987) Study of horse liver alcohohydrogenase (HLADH) in AOT-cyclohexane reverse micelles. *Stud. Org. Chem.*, **29**, 355–360.
- Leaver, J., Gaternmann, T.C.C., Roberts, S.M. and Turner, M.K. (1987) Stereospecific reductions of bicycloheptenones catalyzed by 3- $\alpha$ , 20- $\beta$ -hydroxysteroid-dehydrogenase in one, two and three phase systems. *Stud. Org. Chem.*, **29**, 411–418.
- Lee, J.M. (1992) *Biochemical Engineering*, Prentice Hall, New Jersey.
- Lee, K.I. and Yen, T.F. (1990) Sulfur removal from coal though multiphase media containing biocatalysts. *J. Chem. TechnoL Biotechnol.*, **48**, 71–79.
- Levashov, A.V., Khmelnitsky, Y.L., Klyachko, N.L., Chernyak, V.Y. and Martinek, K. (1982) Enzymes entrapped into reversed micelles in organic solvents. Sedimentation analysis of the protein-aerosol OT-H<sub>2</sub>O-Octane system. *J. Coll Inter. Sci.*, **88**, 444–457.

- Levenspiel, O. (1972) *Chemical Reaction Engineering*, John Wiley & Sons, New York.
- Luisi, P.L. (1985) Enzymes hosted in reverse micelles in hydrocarbon solution. *Angew. Chem. Int. Ed. Engl.*, **24**, 439–450.
- Luisi, P.L. and Laane, C. (1986) Solubilization of enzymes in apolar solvents via reverse micelles. *Trends Biotechnol.*, **4**, 153–161.
- Luisi, P.L. and Magid, L.J. (1986) Solubilization of enzymes and nucleic acids in hydrocarbon micellar solutions. *Crit. Rev. Biochem.*, **20**, 409–475.
- Luisi, P.L., Giomini, M., Pilani, M.P. and Robinson, B.H. (1988) Reverse micelles as hosts for proteins and small molecules. *Biochim. Biophys. Acta*, **947**, 209–246.
- Luisi, P.L., Haring, G., Maestro, M. and Rialdi, G. (1990) Proteins solubilized in organic solvents via reverse micelles: thermodynamic studies. *Thermochim. Acta*, **162**, 1–16.
- Luthi, P. and Luisi, P.L. (1984) Enzymatic synthesis of hydrocarbon-soluble peptides with reverse micelles. *J. Am. Chem. Soc.*, **106**, 7285–7286.
- Maestro, M. and Walde, P. (1992) Application of a simple diffusion model for the enzymatic activity of  $\alpha$ -chymotrypsin in reverse micelles. *J. Coll Inter. Sci.*, **154**, 298–302.
- Malmsten, M. (1998) Formation of adsorbed protein layers. *J. Coll. Inter. Sci.*, **207**, 186–199.
- Marangoni, A.G. (1993) Effects of the interaction of porcine pancreatic lipase with AOT/isooctane reversed micelles on enzyme structure and function follow predictable patterns. *Enzyme Microb. Technol.*, **15**, 944–949.
- Martinek, K. (1989) Micellar enzymology: potentialities in fundamental and applied areas. *Biochem. Int.*, **18**, 871–893.
- Martinek, K., Levashov, A.V., Klyachko, N.L., Khmelnitsky, Y.L. and Berezin, I.V. (1986) Micellar enzimology (review). *Eur. J. Biochem.*, **155**, 453–468.
- Martinek, K., Berezin, I.V., Khmelnitsky, Y.L. Klyachko, N.L. and Levashov, A.V. (1987) Enzymes entrapped into reversed micelles of surfactants in organic solvents: key trends in applied enzymology (biotechnology). *Biocatalysis*, **1**, 9–15.
- Martinek, K., Klyachko, N.L., Kabanov, A.V., Khmelnitsky, Y.L. and Levashov, A.V. (1989) Micellar enzimology: its relation to membranology. *Biochim. Biophys. Acta*, **981**, 161–172.
- Martinez, C., Geus, P., Lauwereys, M., MatthysSENS, G. and Cambillau, C. (1992) *Fusarium solani* cutinase is a lipolytic enzyme with a catalytic serine accessible to solvent. *Nature*, **356**, 615–618.
- Meir, W. (1996) Poly(oxyethylene) adsorption in water/oil microemulsions: a conductivity study. *Langmuir*, **12**, 1188–1192.
- Menger, F.M. and Yamada, K. (1979) Enzyme catalysis in water pools. *J. Am. Chem. Soc.*, **101**, 6731–6734.
- Morgado, M.A.P., Cabral, J.M.S. and Prazeres, D.M.F. (1996) Phospholipase A2-catalysed hydrolysis of lecithin in a continuous reversed-micellar membrane bioreactor. *J. Am. Oil Chem. Soc.*, **73**, 337–346.
- Morita, S., Narita, H., Matoba, T. and Kito, M. (1984) Synthesis of triacylglycerol by lipase in phosphatidylcholine reverse micellar system. *J. Am. Oil Chem. Soc.*, **61**, 1571–1574.
- Mukesh, D., Banerji, A.A., Newadkar, R. and Bevinakatti, H.S. (1993) Lipase catalysed transesterification of vegetable oils—a comparative study in batch and tubular reactors. *Biotechnol. Lett.*, **15**, 77–82.
- Mulder, M. (1992) Characterization of membranes. In *Basic Principles for Membrane Technology* (Mulder M. ed.), Kluwer Academic Publishers, Dordrecht, pp. 110–144.
- Nakamura, K. and Hakoda, H. (1992) Electro-ultrafiltration bioreactor for enzymatic reaction in reverse micelles. In *Proceedings of Asia-Pacific Biochemical Engineering Conference 1992, Biochemical Engineering for 2001* (Furusaki, S., Endo, I. and Matsuno, R. eds.) Springer-Verlag, Tokyo, pp. 433–436.
- Oldfield, C. (1994) Enzymes in water-in-oil microemulsions (reversed micelles): principles and applications. *Biotechnol. Genet. Eng. Rev.*, **12**, 255–327.

- Patel, M.T., Nagarajan, R. and Kilara, A. (1996a) Lipase-catalysed biochemical reactions in novel media: a review. *Chem. Eng. Comm.*, **152–153**, 365–404.
- Patel, M.T., Nagarajan, R. and Kilara, A. (1996b) Hydrolysis of milk fat by lipase in solvent-free phospholipid reverse micellar media. *J. Food Sci.*, **61**, 33–38.
- Peng, Q. and Luisi, P.L. (1990) The behavior of proteases in lecithin reverse micelles. *Eur. J. Biochem.*, **188**, 471–80.
- Pessina, A., Luethi, P., Luisi, P.L., Prenosil, J. and Zhang, Y.S. (1988) Amide-bond syntheses catalyzed by penicillin-acylase. *Helv. Chim. Acta*, **71**, 631–641.
- Petersen, S.B., Jonson, P.H., Fojan, P., Petersen, E.I., Petersen, M.T.N., Hansen, S., Ishak, R.J. and Hough, E. (1998) Protein engineering the surface of enzymes. *J. Biotechnol.*, **66**, 11–26.
- Prazeres, D.M.F., Garcia, F.A.P. and Cabral, J.M.S. (1993) An ultrafiltration membrane bioreactor for the lipolysis of olive oil in reversed micellar media. *Biotechnol. Bioeng.*, **41**, 761–770.
- Prazeres, D.M.F., Garcia, F.A.P. and Cabral, J.M.S. (1994) Continuous lipolysis in a reversed micellar membrane bioreactor. *Bioprocess Eng.*, **10**, 21–27.
- Prazeres, D.M.F. and Cabral, J.M.S. (1994) Enzymatic membrane bioreactors and their applications. *Enzyme Microb. Technol.*, **16**, 738–750.
- Prichanont, S., Stuckey, D.C. and Leak, D.J. (1994) Whole cell biotransformations in reversed micelles. *Biotechnol. 94, Applied Biocatalysis*, Brighton, U.K.
- Rariy, R.V., Bec, N., Klyachko, N.L., Levashov, A.V. and Balny, C. (1998) Thermobarostability of  $\alpha$ -chymotrypsin in reversed micelles of aerosol OT in octane solvated by water-glycerol mixtures. *Biotechnol. Bioeng.*, **57**, 552–556.
- Rees, G.D., Robinson, B.H. and Stephenson, G.R. (1995) Macroyclic lactone synthesis by Lipases in water-in-oil microemulsions. *Biochim. Biophys. Acta*, **1257**, 239–248.
- Rees, G.D., Robinson, B.H. and Stephenson, G.R. (1995b) Preparative-scale kinetic resolutions catalysed by microbial lipases immobilised in AOT-stabilised microemulsion-based organogels: cryoenzymology as a tool for improving enantioselectivity. *Biochim. Biophys. Acta*, **1259**, 73–81.
- Schübel, D. and Ilgenfritz, G. (1997) Influence of polyethylene glycols on the percolation behavior of anionic and nonionic water-in-oil microemulsions. *Langmuir*, **13**, 4246–4250.
- Sebastião, M.J., Cabral, J.M.S. and Aires-Barros, M.R. (1993) Synthesis of fatty acid esters by a recombinant cutinase in reversed micelles. *Biotechnol. Bioeng.*, **42**, 326–332.
- Seeman, P. (1972) The membrane actions of anesthetics and tranquilizers. *Pharmacol. Rev.*, **24**, 583–655.
- Serralheiro, M.L.M., Prazeres, D.M.F. and Cabral, J.M.S. (1994) Di peptide synthesis and separation in a reversed micellar membrane reactor. *Enzyme Microb. Technol.*, **16**, 1064–1073.
- Serralheiro, M.L.M., Prazeres, D.M.F. and Cabral, J.M.S. (1999) Continuous production and simultaneous precipitation of a di peptide in a reversed micellar membrane reactor. *Enzyme Microb. Technol.*, **24**, 507–513.
- Shah, C., Sellappan, S. and Madamwar, D. (1997) Role of environment on activity and stability of  $\alpha$ -amylase incorporated in reverse micelles. *Appl. Biochem. Biotechnol.*, **62**, 183–189.
- Sims, K.A. and Cheryan, M. (1992) Hydrolysis of liquified corn starch in a membrane reactor. *Biotechnol. Bioeng.*, **39**, 960–967.
- Stamatis, H., Xenakis, A., Dimitriadis, E. and Kolisis, F.N. (1995) Catalytic behavior of *Pseudomonas cepacia* lipase in w/o microemulsions. *Biotechnol. Bioeng.*, **45**, 33–41.
- Suarez, M.J. and Lang, J. (1995) Effect of addition of water-soluble polymers in water-in-oil microemulsions made with anionic and cationic surfactants. *J. Phys. Chem.*, **99**, 4626–4631.
- Subramani, S., Shah, C. and Madamwar, D. (1996) Stability of invertase in reversed micelles. *Appl. Biochem. Biotechnol.*, **60**, 33–39.
- Tsai, S.W., Lee, K.P. and Chiang, C.L. (1995) Surfactant effects on lipase-catalyzed hydrolysis of olive oil in AOT/isooctane reverse micelles. *Biocatal. Biotrans.*, **13**, 89–98.
- Valis, T.P., Xenakis, A. and Kolisis, F.N. (1992) Comparative studies of lipase from *Rhizopus delemar* in various microemulsion systems. *Biocatalysis*, **6**, 267–279.

- Verhaert, R.M.D., Hilhorst, R., Vermuë, M., Schaafsma, T. and Veeger, C. (1990) Description of enzyme kinetics in reversed micelles. 1. Theory. *Eur. J. Biochem.*, **187**, 59–72.
- Wang, W., Weber, M.E. and Vera, J.H. (1994) Effect of alcohol and salt on water uptake of reverse micelles formed by dioctyldimethyl ammonium chloride (DODMAC) in isoctane. *J. Coll Inter. Sci.*, **168**, 422–27.
- Yang, F. and Russel, A.J. (1995) A comparison of lipase-catalysed ester hydrolysis in reverse micelles, organic solvents, and biphasic systems. *Biotechol. Bioeng.*, **47**, 60–70.
- Yiv, S., Zana, R., Ulbricht, W. and Hoffman, H. (1981) Effect of alcohol on the properties of micellar systems. *J. Coll. Inter. Sci.*, **80**, 224–236.
- Zulauf, M. and Eicke, H-F. (1979) Inverted micelles and microemulsions in the ternary system H<sub>2</sub>O/Aerosol-OT/Isooctane as studied by photon correlation spectroscopy. *J. Phys. Chem.*, **83**, 480–486.



# CHAPTER EIGHT

## SOLID-TO-SOLID BIOCONVERSIONS: BATCH OR CONTINUOUS?

M.J.F.MICHELSSEN, RENE H.WIJFFELS, JOHANNES TRAMPER  
AND H.H.BEEFTINK

*Food and Bioprocess Engineering Group, Wageningen University, P.O.  
Box 8129, 6700 EV Wageningen, The Netherlands*

### ABSTRACT

Studies of solid-to-solid bioconversions in the last decade have mainly focused on attaining a high conversion at a large scale in batch systems. Lately, attention has shifted towards batch systems with very high amounts of solid substrate, thus featuring a small liquid phase. Further development of these batch systems as well as the development of continuous systems has been hampered by the lack of mechanistic models, featuring the kinetics of dissolution, bioconversion, and crystallisation. Recently, such a model has been developed, giving a new impulse to this technology.

Based on the current status of biocatalyst immobilisation and of continuous reaction crystallisation, proposals for continuous systems for solid-to-solid bioconversions are given. Assuming that such continuous systems are feasible, a general procedure is developed to determine whether a batch or continuous mode of operation is most profitable for a spécifie solid-to-solid bioconversion.

**Keywords:** Solid-to-solid biocatalysis, batch systems, continuous systems, costs comparison

### INTRODUCTION

In aqueous media, biocatalysts often show low overall volumetric productivities due to limited substrate solubility and/or inhibition by substrate and/or product (Michielsen *et al.*, 1999a). Multi-phase systems are generally applied to increase overall substrate solubility and to reduce substrate and/or product inhibition; a second (or third) phase serves as a substrate reservoir or product sink. Other advantages of such systems are that biocatalytic production and downstream processing are integrated, and that high product concentrations can be gained as the product accumulates (mainly) in one phase.

For extraction of hydrophobic compounds, an organic solvent is often used as the water-immiscible second phase. However, use of an organic phase may cause loss in specificity and selectivity of the biocatalyst, product contamination, and it makes the process less cost efficient and less environmentally friendly.

For extraction of hydrophilic substrates and/or products, like proteins, a second aqueous phase may be suitable (Hustedt *et al.*, 1988; Zijlstra *et al.*, 1998). However, widespread industrial application of aqueous two-phase systems is hampered by the high costs of the polymers involved, and by the complexity of aqueous two-phase systems (Andersson and Hahn-Hägerdal, 1990).

It is obvious that in the case of two dissimilar substrates (both hydrophobic and hydrophilic), selection of a suitable solvent that is not deleterious to the enzyme and that solubilises high concentrations of both substrates equally well becomes even more difficult. For some specific bioconversions, solutions are reported that rely on substrate modification (e.g. by making it more hydrophobic; Adelhorst *et al.*, 1990; Fregapane *et al.*, 1991; Scheckermann *et al.*, 1995), or on cosolvent addition (Wolf *et al.*, 1999). However, a general approach for biocatalytic synthesis at high substrate concentrations and at low costs remains to be formulated.

### BIOCATALYSIS IN MULTI-PHASE SYSTEMS WITH SOLID SUBSTRATE AND/ OR PRODUCT

An attractive alternative for the multi-phase systems described above, is the use of solid substrate and product phases as water-immiscible reservoir and sink phases. In these systems, the solid substrate dissolves, is converted in the liquid phase by the biocatalyst, and if the product concentration exceeds the solubility limit, the product crystallises. These liquid-solid-solid three-phase systems have the following advantages: 1) extremely high overall substrate concentrations can be used (Erbeldinger *et al.*, 1998a); note that at least a part of the reactor volume must be liquid, as López-Fandiño *et al.* (1994a) and Kuhl *et al.* (1995) found that the biocatalytic conversion takes place in the liquid phase; 2) high conversions and rates can be attained (see below); 3) the formation of product crystals facilitates downstream processing (centrifugation or filtration followed by drying). The advantages of not needing an organic solvent or expensive polymers are obvious. All of these advantages give rise to lower overall production costs than in conventional multi-phase systems.

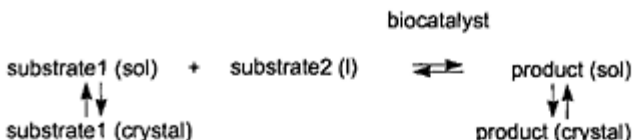
These findings have increased the interest in multi-phase systems with solid phases of substrate and/or product; this is reflected by the increased number of applications (Bornscheuer and Yamane, 1994; Cao *et al.*, 1996; Gill and Vulfson, 1994; Kasche, 1986; Michielsen *et al.*, 1999a; Petkov and Stoineva, 1984; Wolf *et al.*, 1997).

In the present paper, a short review on the latest developments in batch solid-to-solid bioconversions is given. These developments indicate that, for a specific solid-to-solid bioconversion, two systems may be commercially attractive: batch systems with high concentrations of undissolved substrate, and continuous systems. Since continuous systems for solid-to-solid bioconversions have not been developed yet, proposals for such systems are given. Finally, a general method is presented for selecting the most attractive kind of system for a specific solid-to-solid bioconversion.

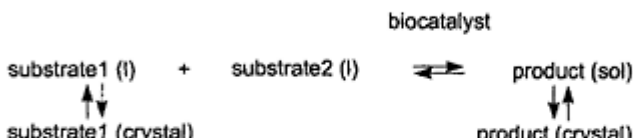
### BATCH SOLID-TO-SOLID BIOCONVERSIONS

The majority of studies on solid-to-solid bioconversions have been executed in batch systems. From these studies, we first derived a classification of batch solid-to-solid bioconversions in four types (Figure 8.1). Based on the characteristics of the four types, rules of thumb were developed that may be useful for selecting the most appropriate type for a specific solid-to-solid bioconversion. As for commercial application the conversion, scale-up, and kinetics of the process are important, each of these types is then characterised with respect to these features.

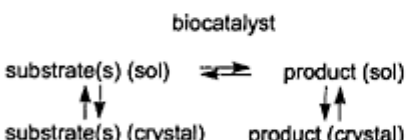
**Type 1:**



**Type 2:**



**Type 3:**



**Type 4:**

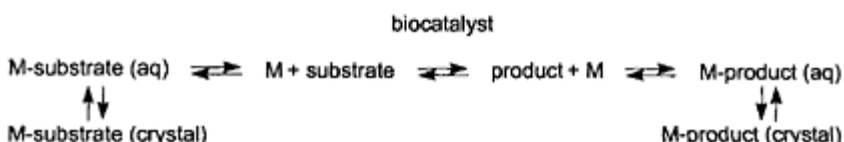


**Figure 8.1** Types of solid-to-solid bioconversions; M in type 4 refers to a métal ion.

### Classification

The classification of batch solid-to-solid bioconversions shown in Figure 8.1 is based on the preparation of each of these reaction mixtures. Types 1 and 2 in Figure 8.1 are systems in which no solvent is present, apart from the reactant(s). In systems of type 1, one of the substrates is added as a liquid phase. In systems of type 2, so-called semi-liquid eutectics, a liquid phase is formed on mixing of two solid substrates. Formation of the latter systems is based on the principle that the melting temperature of a mixture of two compounds can display a minimum as a function of mixture composition, the so-called eutectic temperature (TE, see Figure 8.2); such a mixture is called a eutectic. Below the eutectic temperature, an entirely solid mixture of the constituent components is present (Figure 8.2). Above the melting line (above the solid line in Figure 8.2), an entirely liquid phase exists at every composition of the mixture. At the remaining combinations of temperature and mixture composition, semi-liquid eutectic mixtures are formed. For a binary eutectic mixture, this means that a solid phase of only one of the components and a liquid phase consisting of both components are present (Figure 8.2).

The third type in Figure 8.1 are those systems in which all substrates are in part solid, but also dissolved in a separate, non-reacting solvent phase.

The last type of systems (type 4 in Figure 8.1) comprises bioconversions of a solid salt into another solid salt. The systems of this type are formed by salt addition to an aqueous solution. In contrast to the systems of types 1, 2, and 3, the substrate and product concentrations in the aqueous phase of these systems can be regulated by the amount of salt added. Note that, in addition to the bioconversion, dissociation and complexation reactions occur in the aqueous phase of these systems.

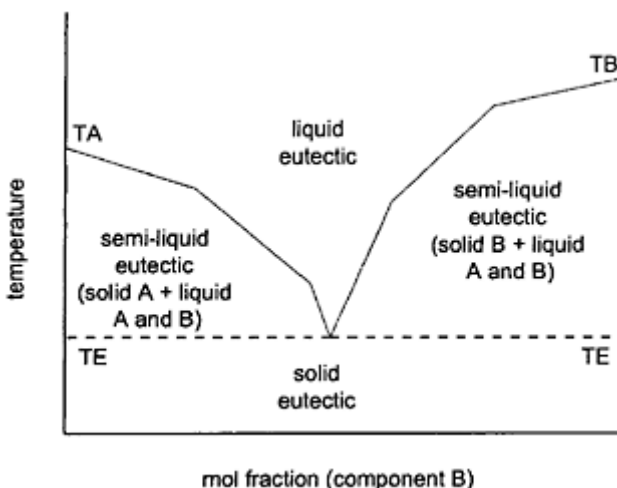


**Figure 8.2** Phase diagram for a model binary eutectic system; TA is the melting point of component A, TB is the melting point of component B, and

TE is the eutectic temperature (adapted from Gill and Vulfson, 1994).

In order to make an appropriate choice, if possible, between the four types of systems for a specific bioconversion, the following rules of thumb can be given:

- When the biocatalyst shows a high activity and stability in the liquid phase consisting of either one (type 1) or both substrates (type 2) at the reaction temperature, systems of types 1 and 2 are to be preferred, as the number of components in the final product suspension is minimal. The latter facilitates downstream processing.
- When the biocatalyst limits the use of systems of types 1 and 2, a solvent should be selected in which the biocatalyst shows a high activity and stability, and systems of type 3 should be created. Preferably the solubility of the product in the solvent should be low, as in case of equilibrium reactions the conversion increases, and in case of irreversible reactions the amount of solid product increases with decreasing product solubility.
- When the substrate(s) and/or the product(s) inhibit the biocatalyst, systems of type 3 or of type 4 should be created. For systems of type 3, the solvent should be selected on the basis of the same criteria as described above. Only when (also) substrate inhibition occurs, the substrate solubility in the solvent should be low as well. In systems of type 4, solubility and thus inhibition can be minimised by addition of an appropriate counter-ion to the aqueous solution. The extent to which the substrate and product concentrations (in the liquid phase) are lowered can be controlled by the amount of salt added.

### Conversion And Scale

Table 8.1 gives for every type of solid-to-solid bioconversions the reported range of the conversion and of the scale. For every type, examples exist in which conversions of 80–100% were obtained (Table 8.1). So far, most of the solid-to-solid bioconversions have been executed on the mmol-scale. Eichhorn *et al.* (1997) have done the first scale-up of solid-to-solid bioconversions for the production of Z-His-Phe-NH<sub>2</sub> and Z-Aspartame from the usual mmol-scale to a mol-scale in a stirred-tank reactor. Table 8.1 shows that,

**Table 8.1** Comparison of the conversion and scale of the four types of solid-to-solid bioconversions according to Figure 8.1

Type	Application area	Conversion (%)	Scale (mol)	Sources
1	peptide synthesis	36–83	$1.10^{-3}$ – $3.10^{-3}$	Gill and Vulfson (1993)
2	peptide synthesis	21–84	$0.3.10^{-4}$ – $6.8.10^{-2}$	Gill and Vulfson (1993) López-Fandino <i>et al.</i> (1994a, b)

	synthesis of sugar fatty acids	34–100	$0.5 \cdot 10^{-3}$ – $5.0 \cdot 10^{-3}$	Cao <i>et al.</i> (1996)
3	peptide synthesis	56–97	$0.5 \cdot 10^{-4}$ –2.7	Eichhorn <i>et al.</i> (1995, 1997) Erbeldinger <i>et al.</i> (1998b)
4	optically pure acids	85–100	$6.3 \cdot 10^{-2}$ –0.4	Kitahara <i>et al.</i> (1960) Van der Werf <i>et al.</i> (1995) Michielsen <i>et al.</i> (1999a)

besides the main application in peptide synthesis, solid-to-solid bioconversions are also applicable to the synthesis of sugar fatty acids and optically pure acids.

### Kinetics

By definition, the overall rate of a multi-process conversion is determined by the slowest process, also called the rate-limiting process. In solid-to-solid bioconversions, the rate-limiting process can be either dissolution, bioconversion, or crystallisation, depending on process conditions like temperature, biocatalyst concentration, solid substrate and product amounts (per cubic meter of suspension), stirring speed, etc. Erbeldinger *et al.* (1998a) reported one of the first kinetic studies of enzymatic solid-to-solid conversions. They investigated the effect of water (from 0 to 600 ml per mol substrates) on the initial rate of thermolysin-catalysed dipeptide synthesis with equimolar amounts of solid carbobenzoxy-L-glutamine (Z-Gln-OH) and solid L-leucamide (H-Leu-NH<sub>2</sub>) in a closed system without mixing. It appeared that the initial rate per mass unit of enzyme increased rapidly from almost zero until a maximum was reached at about 50 ml of water per mol substrates. The authors explain this with the finding of Kuhl *et al.* (1995), that water is necessary to maintain enzyme activity. However, Jakubke *et al.* (1996) reported that biocatalytic rates may decrease with increasing medium viscosity due to reduced protein mobility. Since high substrate concentrations are often accompanied by raised viscosity, this means that the increase in initial rate per mass unit of enzyme with increasing water amount could also be due to increased protein mobility. At higher amounts of water, the initial rate per mass unit of enzyme first decreased rapidly (between about 50 and 100 ml of water per mol substrates), and then levelled at higher amounts of water per mol substrates. This effect was explained by mass-transfer limitation, and emphasises that, besides the amount of water, mixing is also a key parameter. The maximum rate per mass unit of enzyme was attained at 20 mol of substrate per kg of water. The latter is promising in terms of industrial application, as in combination with a high conversion this can result in high overall product concentrations.

Improved solids mixing in solid-to-solid bioconversions can be obtained by rotary homogenisation (Čeřovský, 1992), (ultra)sonication (Kuhl *et al.*, 1992, 1995), and stirring (Kuhl *et al.*, 1992; Eichhorn *et al.*, 1997). Kuhl *et al.* (1995) have reported on the application of two different types of fluidized-bed batch reactors for the chymotrypsin-catalysed synthesis of Z-Phe-Leu-NH<sub>2</sub> and for the thermolysin-catalysed synthesis of Z-Ala-Phe-Leu-NH<sub>2</sub> and Boc-Ala-Phe-Leu-NH<sub>2</sub>. The solid substrate and enzyme particles were suspended and mixed by an upward moisturized air stream. However, low conversions of 10–40% were achieved, probably due to sticking of enzyme and substrate

particles to the reactor wall. Vibrating the whole reactor could not elucidate this. This indicates that further improvements of the mixing process in reactors for solid-to-solid bioconversions are thus still necessary.

With respect to the kinetics of solid-to-solid bioconversions, hardly any literature is available that goes beyond data on the biokinetics. However, for appropriate design, optimisation, and control of a batch or continuous system for solid-to-solid bioconversions, mechanistic models should also include the kinetics of dissolution and crystallisation. Only recently, we have reported the first mechanistic model for the conversion of a solid substrate salt to a solid product salt (type 4 conversion) in a batch stirred bioreactor seeded with product crystals (Michielsen *et al.*, 1999a). This model accounts for the kinetics of salt dissolution, the biokinetics (both the kinetics of conversion and of biocatalyst inactivation), and the salt crystal growth kinetics; salt dissociation and complexation of ions in the liquid phase were assumed to be at equilibrium. The model gave a good quantitative prediction of the conversion of solid Ca-maleate to solid Ca-D-malate by permeabilised *Pseudomonas pseudoalcaligenes* in a batch stirred bioreactor seeded with Ca-D-malate crystals (see Figure 8.3). As the parameters in the model were determined as a function of relevant process conditions, like temperature, the model could be used to predict the rate (and the conversion) as a function of these process conditions. It should be noted that the model can only be applied for well-mixed suspensions, as the effect of mixing was not incorporated.

From these kinetic studies we can conclude on the one hand that in batch systems with very high concentrations of undissolved substrate, and thus with a very small liquid phase, high rates per mass unit of enzyme are possible, if appropriate solids mixing can be provided. Since this can be combined with a high conversion and easy scale-up (see Table 8.1), these systems become attractive for commercial application. On the other hand, our kinetic model for one type of solid-to-solid bioconversions offers possibilities for good control of such conversions. Since the latter is an important prerequisite for reliable and stable operation of continuous systems (see below), a further development of these systems is quite opportune. Proposals for such developments are given below.

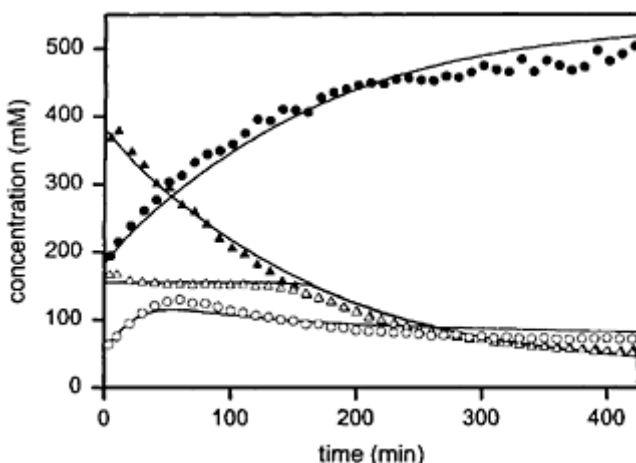


**Figure 8.3** Conversion of solid Ca-maleate to solid Ca-D-malate by permeabilized *P. pseudoalcaligenes* at 30°C and 250 rpm in a batch stirred bioreactor seeded with Ca-D-malate crystals; dissolved maleate (Ca-maleate and maleate<sup>2-</sup>; Δ), total maleate (in liquid and solid phase; ▲), dissolved D-malate (D-malate<sup>2-</sup> and Ca-D-malate; ) and total D-malate (in liquid and solid phase; ●) (adapted from Michielsen *et al.*, 1999a).

### CONTINUOUS SOLID-TO-SOLID BIOCONVERSIONS

The design of a continuous reactor for solid-to-solid bioconversions is governed by the following demands: 1) a high stability and appropriate retention of the biocatalyst; 2) reliable and stable operation for a long period of time, and 3) a large product crystal size for efficient downstream recovery (see below). The first demand is generally satisfied by immobilisation. The last two demands are related; for reliable and stable operation, product crystallisation by nucleation is usually minimised, which implies the formation of large crystals at certain process conditions. To illustrate this, the fundamentals of crystallisation are outlined shortly.

By definition, crystallisation consists of two processes, the formation of new crystals, called nucleation, and crystal growth. These two processes occur if the solubility ( $C^*$ ) is exceeded, resulting in supersaturation ( $\Delta C = C - C^*$ ). If super-saturation is the result of a (biocatalytic) reaction and the reaction substrate originates from another phase, the process of crystal formation is called heterogeneous reaction crystallisation. New crystals (nuclei) are mainly formed at high supersaturation (by so-called primary nucleation), or originate from attrition of existing crystals e.g. by collision or shear stress (so-called secondary nucleation). Secondary nucleation dominates over primary nucleation at intermediate and low supersaturation. At such a (lower) supersaturation in the presence of product crystals, crystal growth also takes place. This results in polydisperse crystals, which may be characterised by a crystal-size distribution. The crystal-size distribution is often summarised by the median crystal size and its coefficient of variation.

For reliable and stable operation of a continuous reaction crystalliser over a long period of time, nucleation phenomena are generally minimised, as a good prediction of nucleation rates is still not possible (Rohani, 1995). Besides, by minimising (primary) nucleation the median crystal size increases (Mersmann and Kind, 1989), which is advantageous for downstream processing. This can be achieved by seeding the crystalliser with an increasing number of product crystals, so that the total crystal area and hold-up in the crystalliser increases, assuming that the seed crystals have a constant (small) size; by increasing the hold-up, the growth rate (per unit of crystalliser volume)

increases too, which means that the crystalliser is operated at a lower supersaturation. Increasing the hold-up also implicates that the size increase of the seed crystals becomes smaller at constant residence time in the crystalliser. However, for appropriate downstream processing, a large product crystal size is required. The latter demand limits the increase in the crystal hold-up. So, an optimum crystal hold-up, and corresponding optimum supersaturation ( $\Delta C_{\text{opt}}$ ), exist in the crystalliser. The optimum supersaturation must be determined experimentally. In selecting the optimum supersaturation not only the desired median crystal size, but also other desired product characteristics (that depend more or less on the supersaturation) must be taken into account, like a small coefficient of variation of the crystal size, a regular and compact shape, and a high purity.

The main advantage of continuously operated crystallisers is that they are superior to batch crystallisers with respect to maintaining a constant optimal supersaturation and low nucleation rate (Mersmann, 1995a). As a result, more homogeneous product crystals are formed than in a batch crystalliser, which makes downstream processing cheaper (see below).

The current status of biocatalyst immobilisation and of continuous reaction crystallisation is reported shortly in relation to its relevance for solid-to-solid bioconversions. This is used as a basis for a reactor design. Note that some features are also applicable to batch systems. Finally, downstream processing of solids is discussed in order to emphasize the need for a large crystal size. It should be stressed that this work only focuses on systems in which dissolution, bioconversion, and crystallisation are coupled directly, in order to fully profit from the benefits of multi-phase systems.

### **Biocatalyst Immobilisation**

For continuous operation, biocatalysts are often immobilised, because immobilisation is generally associated with increased efficiency and it makes different system configurations possible; note, however, that with these profits the costs of immobilisation must be earned back.

Kasche and Galunsky (1995) pointed out that, in reaction crystallisations involving immobilised enzymes, small crystalline particles may be formed in the pores of the support of the enzyme. If so, the accessibility of the immobilised enzyme decreases, resulting in decreased reaction rates and in limited reuse of the immobilised enzyme. Their study revealed that it is essential to use supports with small pores in order to avoid intraparticle crystallisation; they reported a critical pore size range of 10–100 nm. The latter implicates that in their experiments the critical cluster size—the size a cluster of molecules in solution must have to grow spontaneously, so that a crystal is formed—was larger than 10–100 nm.

For application in a continuous reaction crystalliser, the support materials for immobilisation should have other characteristics too: insolubility, high mechanical stability, high diffusivity, simple immobilisation procedure, high biocatalyst retention, well separable from the product crystals, and preferably a low price. Leenen *et al.* (1996) studied the characteristics of natural gels as carrageenan, Ca-alginate, and Ba-Ca-alginate, and gels as polyvinyl alcohol (PVA), polycarbamoylsulphonate (PCS), and polyethylene glycol (PEG), for application in wastewater-treatment systems, and found that PVA, PCS, and PEG were more promising materials than natural gels. These

materials have good mechanical properties, which is especially important in draft-tube baffled stirred crystallisers (see below, Figure 8.4). However, the immobilisation procedures are more harsh and difficult than for natural supports, resulting in much biocatalyst inactivation; in PCS the diffusivity is lower. These characteristics indicate that optimisation is still necessary (Leenen *et al.*, 1996).

### Equipment Design

The design of the equipment is determined mainly by the desired product characteristics. It can affect the product characteristics by its influence on the process variables. For control and downstream-processing purposes, a large product crystal is generally aimed for. In order to achieve this, Mersmann and Rennie (1995) recommend the mean and especially the maximum (local) supersaturation to be limited by: a) excellent mixing of the entire vessel contents, so that gradients in the supersaturation are absent; this can be achieved by using a large ratio of stirrer to tank diameter, as such stirrers distribute power more evenly; b) low concentrations of the reactant(s), which are here the substrate(s), and of the biocatalyst; c) vigorous seeding especially at the feed point(s), and d) high circulation rates of slurry with a high suspension density. Note that by the latter two (c and d), the crystal hold-up, and thus the total crystal surface area that is available for crystal growth, can be regulated.

Objectives a) to d) can best be met in a continuous-flow, stirred-tank reactor (CSTR). Since both biocatalysts and crystals are sensitive to shear, axial flow impellers are frequently used, as they produce more flow and less shear rate than radial flow impellers at comparable power levels (Oldshue, 1993). A schematic view of a draft-tube baffled continuous crystalliser for solid-to-solid bioconversions is shown in Figure 8.4. By pumping the fluid down in the draft tube, an upward flow of (supersaturated) solution is created in the annulus. This flow fluidises a bed of substrate and product crystals and of solid support particles with immobilised biocatalyst; it will be desupersaturated during passage through the annular fluidised bed. When the product crystals have grown large enough, they settle from the bed to the bottom of the crystalliser. The solid substrate particles (and product seeds) can be fed to the draft-tube baffled crystalliser either by dropping them from a belt conveyor (Bennett, 1993), or by a suspension flow.

Another configuration that is often applied in continuous reaction crystallisation is a fluidised-bed crystalliser (or Oslo growth-type crystalliser). A schematic view of an fluidised-bed continuous crystalliser for solid-to-solid bioconversions is shown in Figure 8.5. This crystalliser works according to the same principles as described for the draft-tube baffled crystalliser of Figure 8.4, and mainly differs from it by its fluid

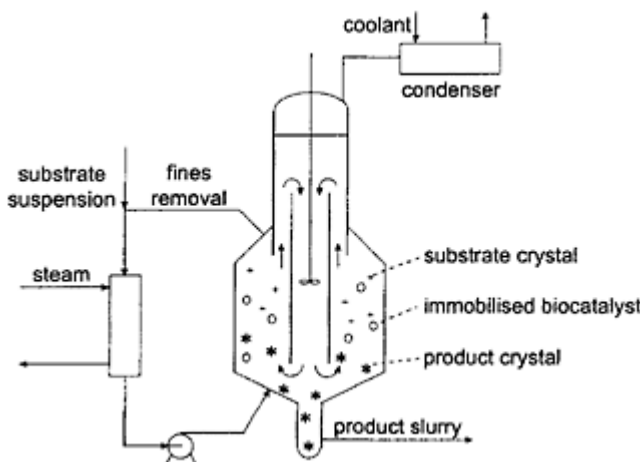


**Figure 8.4** Draft-tube baffled continuous crystalliser (adapted from Rohani, 1995) for solid-to-solid bioconversions.

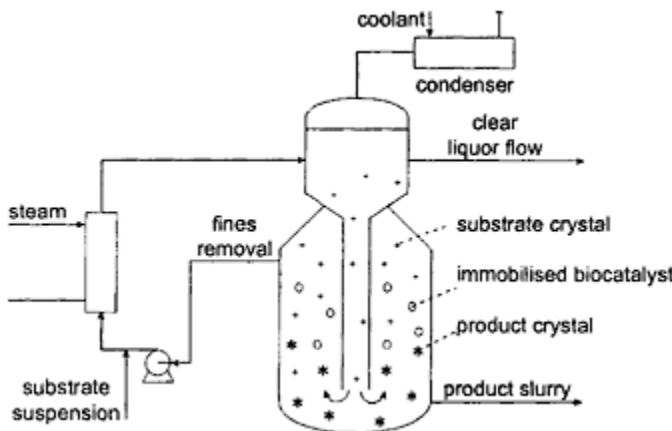


**Figure 8.5** Fluidised-bed continuous crystalliser (adapted from Rohani, 1995) for solid-to-solid bioconversions; this configuration is also known as an Oslo growth-type continuous crystalliser.

circulation device. The draft-tube baffled and fluidised-bed crystallisers of Figures 8.4 and 8.5, respectively, are especially suited for the production of large crystals, as secondary nucleation is reduced by fluidising the crystals.

### Process Control

The two main objectives for control of a dissolution-reaction-crystallisation process are to meet: 1) the product specifications, and 2) the manufacturer's requirements for economic and trouble-free operation. In large-scale continuous industrial crystallisers, this generally means that control is focused on preventing excessive nucleation by making sufficient crystal surface area available in the bulk of the suspension. For appropriate control, a model predicting the concentrations and crystal sizes of all components at any place in the vessel as a function of measurable process variables and other relevant processes, must be available.

In general, a model for a heterogeneous reaction crystalliser can be obtained by integrating a kinetic model, containing the dissolution, reaction, and crystallisation kinetics, and a hydrodynamic model, as mixing could cause dissolution, reaction, or crystallisation to be rate limiting. Our kinetic model for solid salt-to-solid salt bioconversions in a batch stirred bioreactor seeded with product crystals (Michielsen *et al.*, 1999a) can in principle also be applied for continuous solid-to-solid bioconversions. For that, the model should be extended with an expression for the secondary nucleation rate. Application of our crystal growth model (Michielsen *et al.*, 1999b), which is based on an exponential rate law derived by Nielsen and Toft (1984), revealed that it fails at low supersaturation, predicting a lower growth rate than is observed experimentally (Michielsen *et al.*, 1999a). Such a shortcoming of exponential growth rate models was also reported by Myerson and Ginde (1993). Our experimental data (Michielsen *et al.*, 1999a) could be predicted well by assuming that mixing was not rate limiting (see Figure 8.3). For that reason, it was unnecessary to develop a hydrodynamic model.

The measurable process variables used in the control of continuous crystallisers might be temperature, flow rate, pressure, the residence time of different size ranges of crystals, the total volume of the suspension in the crystalliser, and the volumetric ratio of the clear liquor flow and the product removal rate. The relevance of processes like mixing and reactants and seed addition with respect to appropriate control of a crystalliser is described above. With respect to seeding, a narrow distribution of prewashed product crystals is recommended. By prewashing the product crystals with supersaturated product solution (comparable with the solution in the crystalliser), breeding due to the adherence of small crystals to the surface of seed crystals can be avoided completely. Other processes often applied in the control of the crystal-size distribution of continuous crystallisers are classified product removal and fines dissolution. Classification relies on the relative settling of crystals of different sizes. The classifying device may be a hydrocyclone, a wet screen, a fluidised bed, or a centrifuge. It separates the suspension flow withdrawn from the crystalliser in at least two fractions, containing crystals smaller or larger than the separation size; the former fraction is generally recycled to the crystalliser (Mersmann, 1995b). Formation of some fines by nucleation is almost inevitable. These fines can serve as nucleation sites. For that, they are commonly

withdrawn from a quiescent zone of the crystalliser, and dissolved by the supply of either solvent or heat; the resulting solution is recycled.

Control schemes for effective control of continuous crystallisers require on-line measurements of crystal properties like crystal-size distribution, supersaturation, and crystal purity. As with the existing sensors, measurements are either not feasible or extremely difficult, significant progress can be made by the development of new robust on-line measurement techniques. Besides, measurement of secondary variables such as turbidity and the density of the liquor solution, which are related to the fines suspension density and supersaturation, offer potential for the control of crystallisation processes (Rohani, 1995).

### **Downstream Processing**

As a rule in solids production processes, downstream processing consists of solid-liquid separation by centrifuges or filters, followed by drying of the wet crystals. With respect to centrifugation, Mersmann (1995a) reported that for obtaining a low mass ratio of residual liquid to crystals (kg solution/kg crystals) the median crystal size is very important; the mass ratio decreases with increasing median crystal size and decreasing coefficient of variation of the crystal size. After centrifugation or filtration, the crystals with adherent liquor are dried by flowing a preheated agent (hot air) through the solid material. In this process, the need for a large median crystal size becomes even more pronounced, as the specific energy consumption per mass unit of crystals increases with increasing mass ratio of residual liquid to separated crystals. However, at a median crystal size larger than 500 µm, and thus at a low mass ratio, the energy consumption remains almost constant (Mersmann, 1995a).

### **BATCH OR CONTINUOUS?**

Assuming that the proposed continuous systems for solid-to-solid bioconversions (Figures 8.4 and 8.5) can be applied, the question arises which mode of operation to choose for a specific solid-to-solid bioconversion. Now that the first batch systems have been reported in which very high amounts of solid product per reactor volume can be attained at high rates (Erbeldinger *et al.*, 1998a), a shift to complex continuous operation should be carefully thought over.

Process optimisation is generally focussed on minimisation of the costs per kg of product. In a bioreactor the cost factors are: 1) the substrate, 2) the biocatalyst, 3) investments and operation, and 4) downstream processing. For commercial applications, the choice between batch or continuous operation is often based on a comparison of the costs per kg of product for the two systems. For each of the systems, therefore, the process conditions yielding minimum overall costs per kg of product should be determined first. Selection of these conditions is highly case specific, as they depend on the substrate and equipment used, the product produced, and the desired final purity of the product. In this section, a general method is presented that can be used to calculate the overall costs in both batch and continuous systems. If this method is coupled to an

optimisation routine, the optimum process conditions and corresponding minimum costs can be found. In the next treatment, mixing is assumed not to be rate limiting.

To illustrate this method, the overall costs are calculated in (1) a batch heterogeneous reaction crystalliser with immobilised biocatalyst and a high amount of undissolved substrate, and (2) in a continuous heterogeneous reaction crystalliser (draft-tube baffled or fluidised-bed) with immobilised biocatalyst and a substrate suspension as feed. In both calculations, the volume of the suspension, the initial biocatalyst concentration, and the biocatalyst inactivation rate are equal. For simplicity, diffusion limitation is assumed not to occur.

### **Rate-limiting Bioconversion**

At the optimum conditions in both systems, the bioconversion is most likely the rate-limiting process. For control of the crystallisation process, a rate-limiting bioconversion is advantageous, as this implies a low supersaturation and a minimal nucleation. In batch reaction crystallisers with a large amount of undissolved substrate, the surface area of the substrate particles will be large and the dissolution rate will exceed the bioconversion rate. Since a substrate conversion of 100% is generally aimed at, at some point dissolution will become rate limiting due to depletion of solid substrate (Michielsen *et al.*, 1999a). For that reason, use of a complete model for calculation of the amount of product produced in a batch reaction crystalliser is to be preferred, as this gives more accurate values. However, for gross calculation, as in this section, the assumption of one process being rate limiting, i.e. the bioconversion, can be justified. Though in the continuous reaction crystallisers proposed in this work (Figures 8.4 and 8.5), substrate dissolution or the bioconversion can be rate limiting, a rate-limiting bioconversion is favourable, as this would mean that the biocatalyst is operated at a high substrate concentration (near saturation). If the substrate saturation concentration is high as compared to the Michaelis constant  $K_m$ , the latter results in high conversion rates. Since the biocatalyst is often expensive in comparison with the reactants, such an efficient use of the biocatalyst should be aimed at. If efficient use of the biocatalyst can be combined with a high substrate conversion, the sum of the biocatalyst and substrate costs per kg of product approaches its minimum (Michielsen *et al.*, 1999c). In a continuous liquid-solid-solid three-phase system with a rate-limiting bioconversion, such a combination can be attained at low biocatalyst concentrations and long residence times (of substrate(s) and biocatalyst).

One reason for the fact that the bioconversion often is (or becomes) rate limiting is a high biocatalyst inactivation rate. In bioconversions, the biocatalyst inactivation rate is a crucial parameter, as it determines the operational time and thereby the amount of product produced per kg of biocatalyst. For that reason, the effect of biocatalyst inactivation on the overall costs in both batch and continuous reaction crystallisers is shown in this section.

### **Overall Costs Per Kg Of Product**

Box 8.1 shows how the amount of product in both batch and continuous reaction crystallisers with the bioconversion as rate-limiting process can be calculated. Thereby, it

is assumed that the bioconversion obeys zero-order kinetics, and that the biocatalyst inactivates according to first-order kinetics. In the continuous reaction crystalliser, biocatalyst losses due to wash-out are assumed to be negligible. This means that the bioconversion rate, and consequently the product supersaturation, can be kept constant by decreasing the feed flow in accordance with the biocatalyst inactivation rate; in this manner, the system is operated at pseudo steady-state. The densities of the substrate and the product are assumed to be equal, so that the volume of the initial substrate suspension equals the volume of the resulting product suspension.

Box 8.2 shows the calculation of the overall costs per kg of product produced in these batch and continuous reaction crystallisers with bioconversion as the rate-limiting process. Although the investment and operating costs are composed of a multitude of components like depreciation, labour, energy, cooling water, etc., the costs of these components were all lumped in the hourly price for handling 1 m<sup>3</sup> of suspension in the crystalliser ( $p_{io}$ ). According to Van 't Riet (1986),  $p_{io}$  is in the order of 10–100 \$·m<sup>-3</sup>·h<sup>-1</sup> for small-scale fermenters (1–3 m<sup>3</sup>), whereas for large-scale fermenters (100–300 m<sup>3</sup>)  $p_{io}$  is in the order of 1 \$·m<sup>-3</sup>·h<sup>-1</sup>. Above 100–300 m<sup>3</sup> the sensitivity decreases and therewith the need to increase the fermenter volume (Van 't Riet, 1986). For a reaction crystalliser,  $p_{io}$  is assumed to be of the same order of magnitude. The two downstream-processing operations, centrifugation and drying, are “volume-dependent” processes; the scale and related costs are, to a great extent, determined by the volume of the flow to be processed; and the concentration of the product is less relevant. For that reason, the downstream-processing price ( $p_{dp}$ ) is defined on the basis of the hourly costs to process 1 m<sup>3</sup> of product suspension from the crystalliser. In order to reduce the downstream—processing costs per kg of product (\$<sub>dp</sub>), probably more than one crystalliser ( $n$ ) will be coupled to one centrifugation and drying unit (see Box 8.2). Finally, during downstream processing, some

**Box 8.1** The amount of product in batch and continuous heterogeneous reaction crystallisers with the bioconversion as rate-limiting process; in the continuous reaction crystalliser, biocatalyst losses due to wash-out are assumed to be negligible, and the volume is assumed to be constant and well-mixed, with equal inflow and outflow rates.

In case of first-order biocatalyst inactivation, the active biocatalyst concentration  $C_e$  (in kg·m<sup>-3</sup>) decreases with time  $t$  (in h) and can be expressed as a function of the initial biocatalyst concentration  $C_e(0)$ , the first-order rate constant for biocatalyst inactivation  $k_d$  (h<sup>-1</sup>), and time  $t$ :

$$C_e(t) = C_e(0) \cdot e^{-k_d t}$$

Assume that production is stopped when 1% of the initial active biocatalyst concentration is left ( $C_e(t)0=0.01 \cdot C_e(0)$ ). For the stop moments  $t_b$  and  $t_c$  (in the batch and the continuous system, respectively) can now be derived:

$$t_b = t_c = -\frac{\ln 0.01}{k_d}$$

In case of zero-order bioconversion kinetics and assuming that in the batch reaction crystalliser the maximum attainable product concentration  $C_p(t_b)$  (see below) has not been reached, the amount of product produced (in  $\text{kg}\cdot\text{m}^{-3}$ ) in the batch reaction crystalliser and in the continuous reaction crystalliser without biocatalyst losses due to wash-out and with a feed flow decreasing in accordance with the biocatalyst inactivation rate, can now be expressed as (with  $q_p$  is the specific production rate, in  $\text{kg}\cdot\text{kg}^{-1}\cdot\text{h}^{-1}$ ):

$$\text{product produced} = q_p \cdot C_e(0) \int_0^{t_b} e^{-k_d t} dt = q_p \cdot C_e(0) \cdot \frac{0.99}{k_d}$$

Note that the product concentration in the continuous reaction crystalliser  $C_p$  (in  $\text{kg}\cdot\text{m}^{-3}$ ) is constant and can be calculated from the pseudo steady-state mass balance; in case of no product seeding,  $C_p$  can be expressed as a function of  $q_p$ ,  $C_e(0)$ , the volume of the suspension in the reactor  $V$  (in  $\text{m}^3$ ), and the initial flow  $F(0)$  (in  $\text{m}^3\text{h}^{-1}$ ):

$$C_p = \frac{q_p \cdot C_e(0) \cdot V}{F(0)}$$

In a batch reaction crystalliser, the maximum attainable product volume at  $t=t_b$ ,  $V_p(t_b)$  (in  $\text{m}^3$ ), is restricted by the volume of the liquid phase  $V_l$  (in  $\text{m}^3$ ), the volume occupied by the biocatalyst  $V_e$  (in  $\text{m}^3$ ), and the volume of the substrate left at  $t=t_b$ ,  $V_s(t_b)$  (in  $\text{m}^3$ ), according to (with  $Y_{ps}^{\text{ov}}$  is the overall yield of product on substrate (in  $\text{m}^3\cdot\text{m}^{-3}$ ),  $x_{\max}$  is the maximum attainable conversion (-), and assuming that the densities (in  $\text{kg}\cdot\text{m}^{-3}$ ) of the substrate  $\sigma_s$  and the product  $\sigma_p$  are equal):

$$V_p^{\max}(t_b) = V - V_l - V_e - V_s(t_b), \text{ with: } V_s(t_b) = V_s(0) - Y_{ps}^{\text{ov}} \cdot X_{\max} \cdot V_s(0) \geq 0$$

The amount of product produced in a batch reaction crystalliser  $C_p(t_b)$  (in  $\text{kg}\cdot\text{m}^{-3}$ ) can now be expressed as:

$$q_p \cdot C_e(0) \cdot \frac{0.99}{k_d} \leq C_p(t_b) \leq \frac{V_p^{\max}(t_b) \cdot \rho_p}{V}$$

**Box 8.2** The overall costs per kg of product in batch and continuous heterogeneous reaction crystallisers with the bioconversion as rate-limiting process; in the continuous reaction crystalliser, biocatalyst losses due to wash-out are assumed to be negligible, and the volume is assumed to be constant and well-mixed, with equal inflow and outflow rates.

In a batch reaction crystalliser, the substrate costs per kg of product  $\$/\text{kg}$  (in  $\$/\text{kg}$ ) equal the initial substrate concentration  $C_s(0)$  (in  $\text{kg}\cdot\text{m}^{-3}$ ) multiplied with the substrate price  $p_s$  (in  $\$/\text{kg}$ ) divided by the amount of product produced (in  $\text{kg}\cdot\text{m}^{-3}$ ). In a continuous reaction crystalliser without biocatalyst losses due to wash-out and with a feed flow decreasing in accordance with the biocatalyst inactivation rate, the bioconversion rate, and consequently the product concentration in the reactor  $C_p$  (in  $\text{kg}\cdot\text{m}^{-3}$ ), is constant and

the substrate costs per kg of product  $\$_s$  equal the substrate concentration in the inflow  $C_{si}$  (in  $\text{kg}\cdot\text{m}^{-3}$ ) multiplied with the substrate price  $p_s$  divided by the product concentration  $C_p$ :

$$\text{batch : } \$_s = \frac{C_{si}(0)}{C_p(t_b)} \cdot p_s \quad \text{continuous : } \$_s = \frac{C_{si}}{C_p} \cdot p_s = \frac{F(0) \cdot C_{si}}{q_p \cdot C_e(0) \cdot V} \cdot p_s$$

The biocatalyst costs per kg of product  $\$_e$  (in  $\text{\$}\cdot\text{kg}^{-1}$ ) equal the initial amount of active biocatalyst  $C_e(0)$  (in  $\text{kg}\cdot\text{m}^{-3}$ ) multiplied with the biocatalyst price  $p_e$  (in  $\text{\$}\cdot\text{kg}^{-1}$ ) divided by the amount of product produced (in  $\text{kg}\cdot\text{m}^{-3}$ ):

$$\text{batch : } \$_e = \frac{C_e(0)}{C_p(t_b)} \cdot p_e \quad \text{continuous : } \$_e = \frac{C_e(0)}{q_p \cdot C_s(0)^{0.99} \cdot k_d} \cdot p_e = \frac{k_d}{q_p \cdot 0.99} \cdot p_e$$

The investment and operating costs per kg of product  $\$_{io}$  (in  $\text{\$}\cdot\text{kg}^{-1}$ ) equal the investment and operating price  $p_{io}$  (in  $\text{\$}\cdot\text{m}^{-3}\cdot\text{h}^{-1}$ ) multiplied with the operational time  $t_b$  or  $t_c$  (in h) divided by the amount of product produced (in  $\text{kg}\cdot\text{m}^{-3}$ ):

$$\text{batch : } \$_{io} = \frac{p_{io} \cdot t_b}{C_p(t_b) \cdot k_d} = -\frac{\ln 0.01 \cdot p_{io}}{C_p(t_b) \cdot k_d} \quad \text{continuous : } \$_{io} = \frac{k_d \cdot p_{io} \cdot t_c}{q_p \cdot C_e(0) \cdot 0.99} = \frac{-\ln 0.01 \cdot p_{io}}{q_p \cdot C_e(0) \cdot 0.99}$$

In case that  $n$  reaction crystallisers are coupled to one downstream-processing plant, the downstream-processing costs per kg of product  $\$_{dp}$  (in  $\text{\$}\cdot\text{kg}^{-1}$ ) equal the downstream-processing price  $p_{dp}$  (in  $\text{\$}\cdot\text{m}^{-3}\text{h}^{-1}$ ) multiplied with the downstream-processing time, which is assumed to be equal to the operational time of the reaction crystalliser  $t_b$  or  $t_c$  (in h), divided by the amount of product produced (in  $\text{kg}\cdot\text{m}^{-3}$ ) in  $n$  reactors:

$$\text{batch : } \$_{dp} = \frac{p_{dp} \cdot t_b}{n \cdot C_p(t_b) \cdot k_d} \quad \text{continuous : } \$_{dp} = \frac{k_d \cdot p_{dp} \cdot t_c}{n \cdot q_p \cdot C_e(0) \cdot 0.99} = \frac{-\ln 0.01 \cdot p_{dp}}{n \cdot q_p \cdot C_e(0) \cdot 0.99}$$

Since the recovery yield will probably be smaller than one, the overall costs per kg of product  $\$_{ov}$  (in  $\text{\$}\cdot\text{kg}^{-1}$ ) equal the sum of the substrate, biocatalyst, investment and operating, and downstream-processing costs per kg of product, divided by the recovery yield  $Y_r$ :

$$\$_{ov} = \frac{\$_s + \$_e + \$_{io} + \$_{dp}}{Y_r}$$

product losses will always occur; in other words, the recovery yield ( $Y_r$ ) will be  $<1$ . For that reason, the overall costs in Box 8.2 are calculated by dividing the sum of all costs by  $Y_r$ . The recovery yield is generally known to decrease with the number of unit operations needed for downstream processing.

### Costs Comparison Between Batch and Continuous Operation

Figure 8.6 shows the overall costs ( $\$_{ov}$ ) in a batch reaction crystalliser and in a continuous reaction crystalliser with a feed flow decreasing in accordance with the biocatalyst inactivation rate, as a function of the first-order rate constant for biocatalyst inactivation  $k_d$ . The investment and operating costs ( $p_{io}$ ) and the downstream-processing costs ( $p_{dp}$ ) of both systems are assumed to be equal.

Figure 8.6a shows that at  $k_d \leq 4 \cdot 10^{-4} \text{ h}^{-1}$  (or  $t_b \geq 1.2 \cdot 10^4 \text{ h}$ ; see Box 8.1) in a batch system, constant substrate and biocatalyst costs were found. This can only result from the fact that the maximum attainable product concentration is reached (see Box 8.2). The latter implicates that at  $k_d \leq 4 \cdot 10^{-4} \text{ h}^{-1}$  the substrate conversion  $x$  is maximal; note that at  $k_d < 4 \cdot 10^{-4} \text{ h}^{-1}$ , maximal substrate conversion is obtained before the stop moment, at  $t=t_b$ , is reached. At  $k_d \leq 4 \cdot 10^{-4} \text{ h}^{-1}$ , biocatalyst productivity  $Pr$  (in kg of product per kg

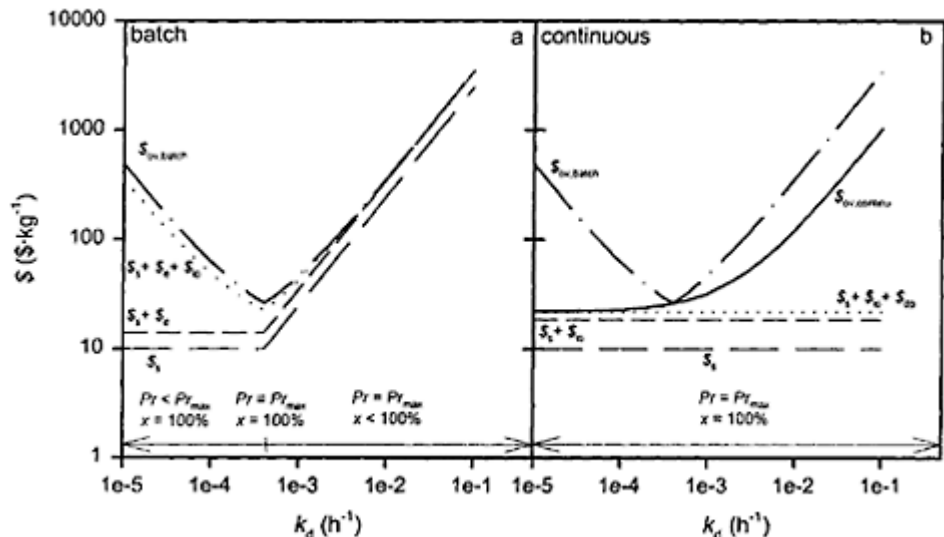


**Figure 8.6** The substrate, biocatalyst, investment and operating, downstream-processing, and overall costs per kg of product ( $\$_s$ ,  $\$_c$ ,  $\$_{dp}$ ,  $\$_{ov}$  respectively) as a function of the first-order rate constant for biocatalyst inactivation ( $k_d$ ) in a batch reaction crystalliser (a) and in a continuous reaction crystalliser without biocatalyst losses due to wash-out and with a feed flow decreasing in accordance with the biocatalyst inactivation rate

$$(b): q_p = 1 \cdot 10^{-2} \text{ kg} \cdot \text{kg}^{-1} \cdot \text{h}^{-1}, V = 200 \text{ m}^3,$$

$$V_1 = 10 \text{ m}^3, V_c = 10 \text{ m}^3, \rho_c = 1100 \text{ kg} \cdot \text{m}^{-3}, V_s = 180 \text{ m}^3, \rho_s = \rho_p = 1500 \text{ kg} \cdot \text{m}^{-3}$$

$$Y_f = 1, p_s = 10 \text{ \$} \cdot \text{kg}^{-1}, p_c = 100 \text{ \$} \cdot \text{kg}^{-1}, p_{dp} = 1 \text{ \$} \cdot \text{m}^{-3} \cdot \text{h}^{-1}, p_{ov} = 2 \text{ \$}$$

$$C_{ci} = 2.2 \text{ kg} \cdot \text{m}^{-3}, \text{ and } F(0) = 50 \text{ m}^3 \cdot \text{h}^{-1}.$$

of biocatalyst) increases with increasing  $k_d$ , as the amount of biocatalyst, not being used up as soon as  $x=100\%$ , decreases. At  $k_d > 4 \cdot 10^{-4} \text{ h}^{-1}$ , both the substrate and biocatalyst costs increase with increasing  $k_d$ . This is caused by the decrease in the amount of product produced due to the fact that (almost) complete biocatalyst inactivation is reached earlier with increasing  $k_d$ . The latter implicates that at  $k_d > 4 \cdot 10^{-4} \text{ h}^{-1}$ ,  $Pr = Pr_{max}$ , and that the conversion  $x$  decreases with increasing  $k_d$ . The investment and operating costs ( $\$_{io}$ ) and the downstream-processing costs ( $\$_{dp}$ ) are generally not affected by an increase in  $k_d$ , as the decrease in  $t_b$  is balanced by the decrease in the amount of product produced (see Box 8.2). However, at  $k_d \leq 4 \cdot 10^{-4} \text{ h}^{-1}$  these costs decrease with increasing  $k_d$ , as despite the decrease in  $t_b$ , the maximum attainable product concentration still can be reached.

The continuous system described in this work only differs from the batch system in that the substrate availability is not limited. As expected (see Box 8.2), Figure 8.6b shows that in such a continuous system the substrate, investment and operating, and downstream-processing costs per kg of product produced ( $\$, \$_{io}$  and  $\$_{dp}$ , respectively) are unaffected by  $k_d$ . However, the overall costs ( $\$_{ov}$ ) increase with increasing  $k_d$  due to the increase of the biocatalyst costs ( $\$_e$ ) with increasing  $k_d$  (Figure 8.6b). The latter is caused by the fact that the amount of product produced decreases with increasing  $k_d$ , whereas the initial active biocatalyst concentration is a constant (see Box 8.2). Note that in such a continuous system, the productivity of the biocatalyst is maximal at any biocatalyst inactivation rate, and the conversion  $x (= C_p/C_{si})$  depends on  $F(0)$  (assuming  $q_p$ ,  $C_e(0)$ , and  $V$  to be constant; see Box 8.1). By setting  $F(0)$  at  $50 \text{ m}^3 \cdot \text{h}^{-1}$ , a conversion of 100% is also obtained in the continuous system, so that a proper comparison of both systems is possible. Figure 8.6b also shows that only at  $k_d = 4 \cdot 10^{-4} \text{ h}^{-1}$ , the batch system can compete with the continuous system; at  $k_d = 4 \cdot 10^{-4} \text{ h}^{-1}$ , both the substrate conversion  $x$  is 100% and the biocatalyst productivity  $Pr$  is maximal (see Figure 8.6a).

In practice however, the biocatalyst inactivation rate is often a given constant at certain conditions, and the initial biocatalyst and substrate concentrations are variables. The optimum initial biocatalyst and substrate concentrations for batch operation can be determined by plotting the overall costs ( $\$_{ov}$ ) versus  $C_e(0)/C_s(0)$  (see Figure 8.7). With e.g.  $k_d = 1 \cdot 10^{-3} \text{ h}^{-1}$ , the minimum overall costs ( $\$_{ov,batch}$ ) were found at  $C_e(0)/C_s(0) = 0.10$  (Figure 8.7). Since at this ratio  $x = 100\%$  and  $Pr = Pr_{max}$  (Figure 8.7), these minimum overall costs correspond to the costs that would be obtained in the continuous system described in this section.

In this section it is shown that by introducing a number of assumptions, batch operation at high concentrations of undissolved substrate can compete with continuous operation, if both the conversion is 100% and the productivity of the biocatalyst is maximal, unless mixing becomes rate limiting in batch reaction crystallisers.

## CONCLUSIONS

Solid-to-solid bioconversions appear to offer interesting possibilities for biocatalysis at high substrate concentrations and at low costs in different application areas. Based on the preparation, the solid-to-solid bioconversions reported in the literature were classified into four types. To select the most appropriate type for a specific bioconversion, rules of thumb

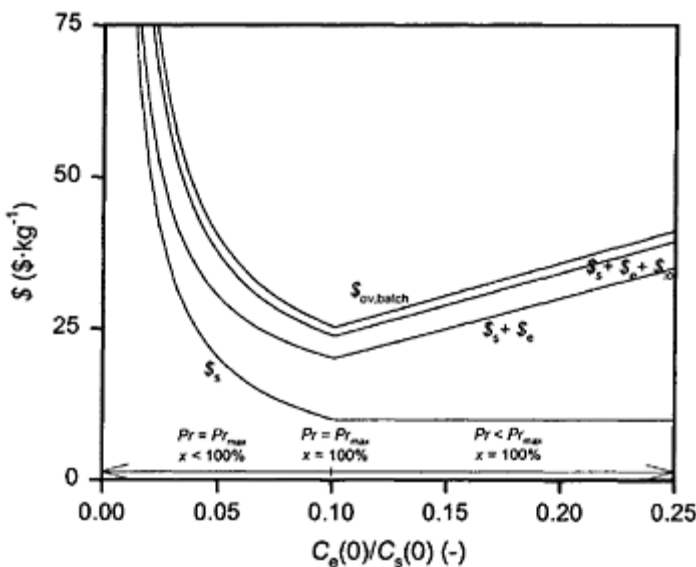


**Figure 8.7** The substrate, biocatalyst, investment and operating, downstream-processing, and overall costs per kg of product ( $\$_s$ ,  $\$_e$ ,  $\$_{dp}$ , and  $\$_{ov}$ , respectively) as a function of the ratio of the initial biocatalyst concentration ( $C_e(0)$ ) and the initial substrate concentration ( $C_s(0)$ ) in a batch reaction crystallizer;

$$q_p = 1 \cdot 10^{-2} \text{ kg} \cdot \text{kg}^{-1} \cdot \text{h}^{-1}, k_d = 1 \cdot 10^{-3} \text{ h}^{-1}, V = 200 \text{ m}^3, V_1 = 10 \text{ m}^3, \rho_c = 1100 \text{ kg} \cdot \text{m}^{-3}, \rho_b = \rho_p = 1500 \text{ kg} \cdot \text{m}^{-3}, x_{\max} = 1, Y_{\text{ov}} = 1, Y_r = 1, p_e = 100 \$ \cdot \text{kg}^{-1}, p_{\text{io}} = 1 \$ \cdot \text{m}^{-3} \cdot \text{h}^{-1}, p_{\text{dp}} = 2 \$ \cdot \text{m}^{-3} \cdot \text{h}^{-1}, \text{ and } n = 5.$$

were formulated. In batch systems, conversions of 80–100% are reported for every type of solid-to-solid bioconversion, even when hardly any liquid phase is present, and it seems that these systems can easily be scaled-up. Kinetic studies of these solid-to-solid bioconversions give rise to further development of two kinds of systems in the future: 1) batch systems with very high concentrations of undissolved substrate, and 2) continuous systems for solid-to-solid bioconversions. In continuous systems an optimum supersaturation ( $\Delta C_{\text{opt}}$ ) exists. The main advantage of continuous systems over batch systems is that they are able to maintain a constant (optimal) supersaturation, resulting in more homogeneous product crystals, and thus lower downstream-processing costs. In this work, two continuous systems for solid-to-solid bioconversions are proposed: a draft-tube baffled continuous crystalliser and a fluidised-bed continuous crystalliser, both with immobilised biocatalyst. Crystallisation in the pores of the support of the immobilised

biocatalyst can be avoided by making the pores sufficiently small, i.e. smaller than the critical cluster size.

Selection of the mode of operation for a specific solid-to-solid bioconversion, batch at high concentrations of undissolved substrate or continuous, is often based on the costs (per kg of product produced). By assuming that in both batch and continuous solid-to-solid bioconversions the bioconversion is rate limiting, and by introducing a number of simplifications, the costs of batch operation were compared with the costs of continuous operation. This revealed that a batch system can only compete with a continuous system if both the conversion is 100% and the productivity of the biocatalyst is maximal.

### ACKNOWLEDGEMENTS

This work was financially supported by the Ministry of Economic Affairs, the Ministry of Education, Culture and Science, the Ministry of Agriculture, Nature Management and Fishery in the framework of an industrially relevant research programme of the Netherlands Association of Biotechnology Centres in the Netherlands (ABON).

### REFERENCES

- Adelhorst, K., Björkling, F., Godtfredsen, S.E., Kirk, O. (1990) Enzyme catalysed preparation of 6-*O*-acyl-glucopyranosides. *Synthesis* **2**, 112–115.
- Andersson, E., Hahn-Hägerdal, B. (1990) Bioconversions in aqueous two-phase systems. *Enzyme Microb Technol* **12**, 242–253.
- Bennett, R.C. (1993) Crystallizer selection and design. In: Myerson A.S., editor. *Handbook of industrial crystallization*. Boston: Butterworth-Heinemann. p. 103–130.
- Bornscheuer, U.T., Yamane, Y. (1994) Activity and stability of lipase in the solid phase glycerolysis of triolein. *Enzyme Microb Technol* **16**, 864–869.
- Cao, L., Bornscheuer, U.T., Schmid, R.D. (1996) Lipase-catalysed solid phase synthesis of sugar esters. *Fett/Lipid* **98**, 332–335.
- Čeřovský, V. (1992) Protease-catalysed peptide synthesis in solvent-free system. *Biotechnol Tech* **6**, 155–160.
- Eichhorn, U., Bommarius, A.S., Drauz, K., Jakubke, H-D. (1995) Environmentally acceptable synthesis of peptides in high yields by suspension-to-suspension conversion via protease catalysis. In: Maia HLS, editor. *Peptides 1994*. Leiden, The Netherlands: ESCOM. p. 226–227.
- Eichhorn, U., Bommarius, A.S., Drauz, K., Jakubke, H-D. (1997) Synthesis of dipeptides by suspension-to-suspension conversion via thermolysin catalysis: from analytical to preparative scale. *J Pep Sci* **3**, 254–251.
- Erbeldinger, M., Xiongwei, N., Hailing, P.J. (1998a) Effect of water and enzyme concentration on thermolysin-catalysed solid-to-solid peptide synthesis. *Biotechnol Bioeng* **59**, 68–72.
- Erbeldinger, M., Xiongwei, N., Hailing, P.J. (1998b) Enzymatic synthesis with mainly undissolved substrates at very high concentrations. *Enzyme Microb Technol* **23**, 141–148.
- Fregapane, G., Sarney, D.B., Vulfson, E.N. (1991) Enzymic solvent-free synthesis of sugar acetal fatty acid esters. *Enzyme Microb Technol* **13**, 796–800.
- Gill, I., Vulfson, E.N. (1993) Enzymatic synthesis of short peptides in heterogeneous mixtures of substrates. *J Am Chem Soc* **115**, 3348–3349.
- Gill, I., Vulfson, E.N. (1994) Enzymatic catalysis in heterogeneous eutectic mixtures of substrates. *Trends Biotechnol* **12**, 118–122.

- Hustedt, H., Kroner, K.H., Papamichael, N. (1988) Continuous cross-current aqueous two-phase extraction of enzymes from biomass: automated recovery in production scale. *Proc Biochem* **23**, 129–137.
- Jakubke, H-D., Eichhorn, U., Hänsler, M., Ullmann, D. (1996) Non-conventional enzyme catalysis: application of proteases and zymogens in biotransformations. *Biol Chem* **377**, 455–464.
- Kasche, V. (1986) Mechanisms and yields in enzyme catalysed equilibrium and kinetically controlled synthesis of  $\beta$ -lactam antibiotics and other condensation products. *Enzyme Microb Technol* **8**, 4–16.
- Kasche, V., Galunsky, B. (1995) Enzyme catalysed biotransformations in aqueous two-phase systems with precipitated substrate and/or products. *Biotechnol Bioeng* **45**, 261–279.
- Kitahara, K., Fukui, S., Misawa, M. (1960) Preparation of L-malate from fumarate by a new process “enzymatic transcrystallization”. *J Gen Appl Microbiol* **6**, 108–116.
- Kuhl, P., Eichhorn, U., Jakubke, H-D. (1992) Thermolysin-and chymotrypsin-catalysed peptide synthesis in the presence of salt hydrates. In: Tramper, J., Vermé, M.H., Beeftink, H.H. and von Stockar, U., editors. *Biocatalysis in non-conventional media*. Amsterdam: Elsevier Science. pp. 513–518.
- Kuhl, P., Eichhorn, U., Jakubke, H-D. (1995) Enzymic peptide synthesis in microaqueous, solvent-free systems. *Biotechnol Bioeng* **45**, 276–278.
- Leenen, E.J.T.M., Martins dos Santos, V.A.P., Grolle, K.C.F., Tramper, J., Wijffels, R.H. (1996) Characteristics of and selection criteria for support materials for cell immobilization in wastewater treatment. *Wat Res* **30**, 2895–2996.
- López-Fandino, R., Gill, I., Vulfson, E.N. (1994a) Enzymatic catalysis in heterogenous mixtures of substrates: the role of the liquid phase and the effects of “adjuvants”. *Biotechnol Bioeng* **43**, 1016–1023.
- López-Fandino, R., Gill, I., Vulfson, E.N. (1994b) Protease-catalysed synthesis of oligopeptides in heterogenous substrate mixtures. *Biotechnol Bioeng* **43**, 1024–1030.
- Mersmann, A. (1995a) Thermal analysis and economics of processes. In: Mersmann A, editor. *Crystallization technology handbook*. New York: Marcel Dekker, Inc. p. 539–561.
- Mersmann, A. (1995b) Interaction between balances, processes, and product quality. In: Mersmann A, editor. *Crystallization technology handbook*. New York: Marcel Dekker, Inc. p. 79–213.
- Mersmann, A., Kind, M. (1989) Parameters influencing the mean particle size of a crystalline product. *Chem Eng Technol* **12**, 414–419.
- Mersmann, A., Rennie, F.W. (1995) Design of crystallizers and crystallization processes. In: Mersmann A, editor. *Crystallization technology handbook*. New York: Marcel Dekker, Inc. p. 215–325.
- Michielsen, M.J.F., Frielinck, C., Wijffels, R.H., Tramper, J., Beeftink, H.H. (1999a) Modeling solid-to-solid biocatalysis: integration of six consecutive steps. Submitted for publication.
- Michielsen, M.J.F., Frielinck, C., Wijffels, R.H., Tramper, J., Beeftink, H.H. (1999b) Growth of Ca-D-malate crystals in a bioreactor. Submitted for publication.
- Michielsen, M.J.F., Frielinck, C., Wijffels, R.H., Tramper, J., Beeftink, H.H. (1999c) D-malate production by permeabilized *Pseudomonas pseudoalcaligenes*; optimization of conversion and biocatalyst productivity. Submitted for publication.
- Myerson, A.S., Ginde, R. (1993) Crystals, crystal growth, and nucleation. In: Myerson, A.S., editor. *Handbook of industrial crystallization*. Boston: Butterworth-Heinemann. p. 33–63.
- Nielsen, A.E., Toft, J.M. (1984) Electrolyte crystal growth kinetics. *J Cryst Growth* **67**, 278–288.
- Oldshue, J.Y. (1993) Agitation and mixing. In: Myerson, A.S., editor. *Handbook of industrial crystallization*. Boston: Butterworth-Heinemann. p. 165–177.
- Petkov, D.D., Stoineva, I.E. (1984) Enzyme peptide synthesis by iterative procedure in a nucleophile pool. *Tetrahedron Lett* **25**, 3751–3754.
- Rohani, S. (1995) Control of crystallizers. In: Mersmann, A., editor. *Crystallization technology handbook*. New York: Marcel Dekker, Inc. p. 327–357.

- Scheckermann, C., Schlotterbeck, A., Schmidt, M., Wary, M., Lang, S. (1995) Enzymatic monoacylation of fructose by two procedures. *Enzyme Microb Technol* **17**, 157–162.
- Van der Werf, M.J., Hartmans, S., Van den Tweel, W.J.J. (1995) Effect of maleate counter-ion on malease activity: production of D-malate in a crystal-liquid two-phase system. *Enzyme Microb Technol* **17**, 430–436.
- Van't Riet, K. (1986) The selection of research targets based on forecasted production costs. *Trends Biotechnol* **4**, 236–241.
- Wolff, A., Zhu, L., Kielland, V., Straathof, A.J.J., Jongejan, J.A., Heijnen, J.J. (1997) Simple dissolution-reaction model for enzymatic conversion of suspension of solid substrate. *Biotechnol Bioeng* **56**, 433–40.
- Wolff, A., Zhu, L., Wong, Y.W., Straathof, A.J.J., Jongejan, J.A., Heijnen, J.J. (1999) Understanding the influence of temperature change and cosolvent addition on conversion rate of enzymatic suspension reactions based on regime analysis. *Biotechnol Bioeng* **62**, 125–134.
- Zijlstra, G.M., Michelsen, M.J.F., De Gooijer, C.D., Tramper, J. (1998) IgG and hybridoma partitioning in aqueous two-phase systems containing a dye-ligand. *Bioseparation* **7**, 117–126.

# **CHAPTER NINE**

## **SOLID/GAS SYSTEMS, THEORY AND APPLICATIONS**

**SYLVAIN LAMARE, T.MAUGARD AND MARIE D.LEGOY**

*Laboratoire du Génie Proéique et Cellulaire, Université de La Rochelle,  
Avenue Marillac, 17042 La Rochelle, Cedex 1, France*

### **ABSTRACT**

Non conventional enzymology cannot only be applied to the use of enzymes in monophasic organic systems. During the last few decades forever, new technologies in the field of enzymatic catalysis have been developed, such as multiphasic systems, micro emulsions and micellar systems. More recently, new techniques such as supercritical fluids or solid/gas catalysis have been tested and implemented for new biotechnological processes.

Solid/gas catalysis presents many advantages compared to other systems (*i.e.* liquid, mono or biphasic ones). Its strength derives from the possibility of obtaining very high conversion yields compatible with a high productivity for a minimal plant scale, and minimizing greatly the downstream processes when they exist, considering that:1) mass transfers are more efficient at the solid/gas interface;2) enzymes and cofactors are more stable in systems with restricted water availability; 3) problems of solubility of substrates and products do not exist, and 4) the use of solvent can be avoided. Moreover, because solid/gas catalysis is synonymous with the use of higher temperatures, microbial contamination of the bioreactor can be avoided.

Finally, the downstream process is simplified due to the absence of a solvent phase and the scale-up operation for such a process is simpler due to the use of a gaseous circulating phase. This research field led to the development of new continuous cleaner processes. Such biotechnological processes can be an alternative solution for producing naturally labeled molecules, minimising the constraints encountered in natural extraction, and offering closer economical costs compared to those the chemical processes.

**Keywords:** Solid, gas, bioprocess, enzyme, cell.

RAPID REVIEW OF SOLID GAS BIOREACTORS

The potentials of systems where biocatalysts are suspended in mixtures of substrates and water vapour are relatively unexplored in contrast to those where enzymes are placed directly in aqueous or non aqueous solvents. One of the major results of initial studies on such systems was to prove that biocatalysts, traditionally functioning in liquid systems, were able to bind and to transform molecules present in a gaseous phase, since there was only one example of an enzyme acting on gaseous substrates reported in the literature at that time.

Hydrogenase is a unique enzyme whose substrate is gaseous hydrogen. Yagi and collaborators (1969) have clearly demonstrated that hydrogenase in the dry state binds the hydrogen molecule and renders it activated, resulting in parahydrogen-orthohydrogen conversion, whereas aqueous protons do not participate in the reaction mechanism.

In a subsequent paper Kimura *et al.* (1979) have proven that, using purified hydrogenase, it was possible to obtain not only the conversion and exchange reactions, but also the reversible oxido-reduction of the electron carrier, cytochrome c<sub>3</sub> with H<sub>2</sub>.

Nevertheless, some other examples of utilisation of the gas/solid system using either entire cells or isolated enzymes can now be found in the literature (Kim and Rhee, 1992; Uchiyama *et al.*, 1992; Zilli *et al.*, 1992; Yang and Russell, 1996) and were reviewed a few years ago (Lamare and Legoy, 1993).

Some systems have already been developed for the use of enzymes where the natural substrates are non gaseous, such as the horse liver dehydrogenase (Pulvin *et al.*, 1986), the *Sulfolobus solfataricus* dehydrogenase (Pulvin *et al.*, 1988) the *Pischia pastoris* alcohol oxidase (Barzana *et al.*, 1987, 1989a, 1989b) and finally lipolytic enzymes (Parvaresh *et al.*, 1992; Robert *et al.*, 1992; Lamare and Legoy, 1995, 1997, 1999; Lamare, 1996).

Enzymatic solid/gas bioreactors described in the literature are mainly used for single-step biotransformations, but some examples have been described which use entire cells for multi-step biotransformations. Two main classes can thus be defined, the enzyme solid/gas bioreactors and the microbial solid/gas bioreactors.

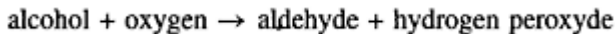
### **Enzyme solid/gas reactors**

Ethanol oxidation in the gaseous phase has been studied in batch reactors using *Pichia pastoris* alcohol oxidase (Barzana *et al.*, 1987, 1989).

Dehydrated enzyme immobilised on DEAE cellulose or on controlled pore glass beads has been shown to oxidise methanol and ethanol vapors at elevated temperatures, in the absence of water in the gas phase. Nevertheless, the study on the effect of water activity showed that enzyme activity in the gas phase increases by several orders of magnitude, whereas the thermostability decreases drastically when *a<sub>w</sub>* is increased from 0.11 to 0.97.

These studies yielded two important results. Firstly, the enzyme is active on gaseous substrates even at hydration levels below the full hydration of the protein. Secondly, there exists an antagonistic effect concerning the water activity. The higher the water activity, the higher the reaction rate, but the stability is lowered at elevated temperatures.

Considering the reaction scheme of alcohol oxidase:



it is possible to increase efficiently the half-life of the enzyme by the addition of enzymes that decompose H<sub>2</sub>O<sub>2</sub> (catalase or peroxidase) to the biocatalyst preparation (Barzana *et al.*, 1989). According to the authors, the reaction seems to occur by direct interaction of the gaseous substrate with the enzyme.

The use of alcohol dehydrogenases in solution has already received attention but serious limitations still exist:

- the operational instability of enzymes and cofactors (NAD<sup>+</sup> or NADH, H<sup>+</sup>);
- the insolubility of most of the substrates and products in water which requires working in emulsions or organic solvents;
- the product inhibition of the enzyme;
- the lack of stability of some substrates and products in aqueous solutions.

In order to overcome these problems, a solid-gas bioreactor has been used for alcohol and/or aldehyde production (Pulvin *et al.*, 1986, 1988). A methodology has been elaborated using alcohol dehydrogenase and NAD<sup>+</sup> (or NADH, H<sup>+</sup>) co-immobilised into albumin-glutaraldehyde porous particles in batch and continuous fed column reactors. An aldehyde reduction was coupled to a second alcohol oxidation in order to regenerate the cofactor.

Other types of enzymes have been tested in solid-gas reactions such as lipases, which are known to need interfacial activation. *Candida rugosa* lipase and other esterolytic enzymes have been coated on glass beads and suspended in mixtures of substrates and water vapors over a relative humidity range of 56 to 100% (Ross and Schneider, 1991). Since the relative humidities of the system were quite high, the enzyme was in a thin liquid film of concentrated buffer on the surface of the glass beads. Under these conditions, the extent of reaction can be classified in the following order, for decreasing a<sub>w</sub> values:

**hydrolysis > alcoholysis > ester exchange > esterification.**

With this system it has been possible to obtain hydrolysis of a wide variety of substrates even at 30°C with substrate vapor pressures as low as 0.08 mm Hg and with substrate boiling points as high as 206°C. This has served to demonstrate that it is possible to work in the gas phase with such compounds.

In all cases, what influences the activity and the stability of a gas/solid system is the combination between water activity and the applied temperature. When the water activity is high, that is to say, when free solvent water is present in the system, it cannot be considered a solid-gas biphasic medium but rather a solid-liquid medium. Solid-gas biocatalysis exists only when the biocatalyst has no free solvent surrounding the protein. This has to be determined by the isotherm sorption curve of the catalytic preparation.

More research concerning the kinetics of gas/solid systems is needed in order to understand precisely the catalysis in the gas phase. Nevertheless, for a single step biotransformation, the gas/solid system appears to be an interesting field for the development of new biotechnological purposes. The use of alcohol oxidases and dehydrogenases for the synthesis of aldehydes could be a novel approach for the production of precursors of flavours or fragrances, as well as the synthesis or the modification of esters with esterolytic enzymes. Furthermore, compounds obtained with

such technology could be labeled ‘natural’, because of the absence of organic solvents traditionally used in classical liquid systems.

### **Microbial solid/gas reactors**

Such solid-gas bioreactors have been tested for transformations involving more than one step. In this field, the studies are essentially devoted to the removal of toxic products. Nevertheless, the epoxidation of alkenes by bacteria has received some attention, in view of the possible production of certain epoxides using a biotechnological process. Some methods using immobilised enzymes have been developed, but the use of immobilised micro-organisms is more promising. The major problem in this transformation is the toxicity of the reaction product (ethylene or propylene oxide depending on the substrate used) towards the biocatalyst. To avoid epoxide accumulation in the microenvironment of the biocatalyst and thus inactivation, rapid removal of this product is essential. Ethylene oxide is very soluble in water and no suitable extractant, immiscible with water, is available. A solid-gas bioreactor has been used to promote a rapid and continuous removal of the toxic ethylene oxide from the environment of the immobilised cells. *Mycobacterium Py 1* immobilised in alginate beads and on sand has been used. The conversion of propylene or ethylene to the corresponding oxide is done by a mono-oxygenase system requiring molecular oxygen and NADH or NADPH. The cofactor regeneration is possible through endogenous respiration.

The same group has further studied the influence of immobilisation and reduced water activity from the fundamental point of view, on gaseous-alkene oxidation by the same type of bacteria in the solid-gas bioreactor (Hamstra *et al.*, 1986).

Continuous production of propylene oxide has been successfully demonstrated using a simple solid-gas heterogeneous bioreactor with *Methylosinus sp* CRL 31 coated onto porous glass beads (Hou, 1984).

Trichloroethylene, one of the contaminants frequently detected in groundwater, has been shown to be degraded by immobilised resting cells of *Methylocystis sp M* in the same kind of reactor (Uchyama *et al.*, 1992).

The alcohol oxidase enzyme of extruded pellets of *Pichia pastoris* has been tested for aqueous, organic and vapor phase oxidations showing the feasibility of all the reaction systems used (Duff and Murray, 1990). Again, the authors noted that the degree of conversion and the catalyst longevity was influenced by the moisture of the biocatalyst.

### **OPERATING SOLID GAS BIOREACTORS**

As noted in the case of enzyme gas/solid reactor uses, different parameters such as water activity, temperature, and nature of the substrate are crucial for optimising the performance of microbial solid-gas reactors or fermenters.

When dealing with reactors which contain growing cells, the moisture in the system has to be carefully controlled in order to obtain a correct growth of the cells without having the appearance of a well defined liquid phase. This type of bioreactor is very close to gas-liquid-solid systems, where the liquid phase constitutes an interface between the solid phase and the gaseous one, thus minimising greatly the external mass transfers and

lowering the productivity of these systems. Thus, a rational approach was developed for controlling proper operation of true solid/gas systems, involving a thermodynamic control of the different molecular species present in the gaseous phase thus insuring the true solid/gas characteristics.

### Controlling the thermodynamic parameters of a gaseous phase

If one considers a solid gas bioreactor based on a packed bed, the following representation can be made, as depicted on Figure 9.1. This allows very simple parameters controlling the thermodynamic activity of each compound to be easily identified.

The inlet gas will be characterised by its molar composition, the inlet temperature and the total pressure of the system. For poorly charged gas, if one assumes that it can be considered an ideal gas, these few parameters allow a complete definition of the thermodynamics of the gas entering the reactor.

While the molar composition of the inlet gas and the total pressure are known, it is possible to calculate easily the partial pressure of each compound ( $P_{p_x}$ ), resulting from the following equation:

$$P_{p_x} = \frac{n_x}{n_{total}} Pa = \frac{Q_x}{Q_{total}} Pa$$

assuming that  $n_x$  is equal to the number of moles of X in a finite gas volume containing a total of  $n_{total}$  moles at the absolute pressure of  $Pa$ . For continuous systems, the molar flow  $Q$  can be used instead of  $n$ . Then, the thermodynamic activity ( $a_x$ ) can be calculated using

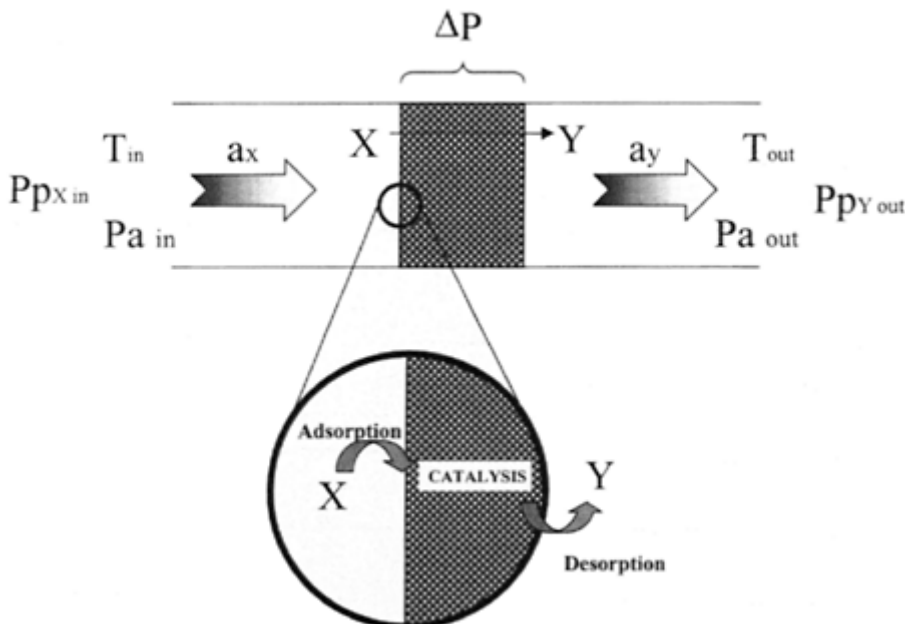


**Figure 9.1** Schematic diagram of solid gas catalysis in a packed bed reactor.

the saturation pressure of the pure compound, obtained from the saturation curves at the temperature of the gas stream ( $T_{in}$ ) as described in Figure 9.2 and using the following equation:

$$a_x = \frac{Pp_x}{Ppsat_x}$$

Then, the key parameter for the development of solid gas bioreactor is the thermodynamic activity of each species present in the gas phase. This thermodynamic parameter corresponds to a measure of the "availability" of each compound and strongly depends on two physical parameters; temperature and absolute pressure.

#### Atmospheric and reduced pressure reactors

Two main strategies are used for creating a gas for solid/gas biocatalysis system, based either on saturation by an organic molecule of a carrier gas or by vaporisation of liquid molecules using a liquid gas flash operation in a carrier flow. Most reactors described in the literature use the first approach, and simple calculations and controls allow a precise control of all the operating parameters of solid/gas systems.

If one considers the following bioreactor depicted in Figure 9.3 in which different saturated gases are mixed to produce the final gas, the control of operational parameters can be realised as indicated below.

One can assume that a carrier gas, after bubbling in a substrate solution at a controlled temperature, is in equilibrium with the liquid phase and so the partial pressure of the substrate in the gas leaving the saturation apparatus is equal to the vapor pressure

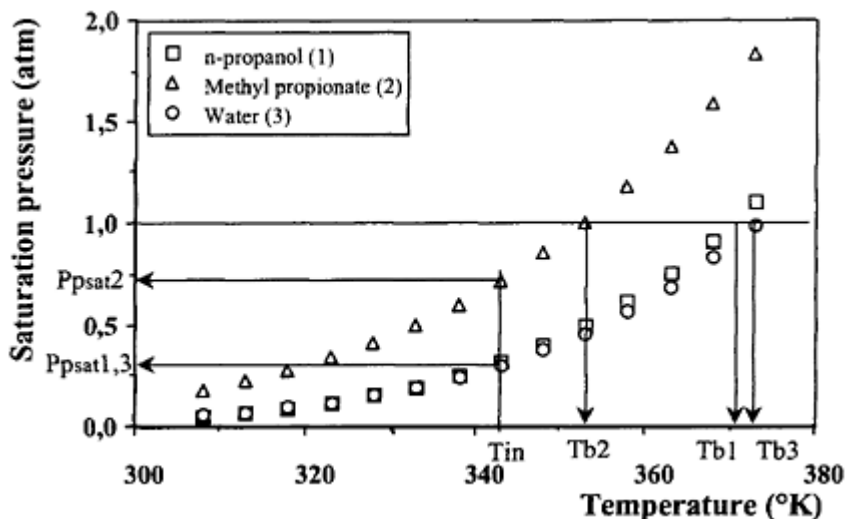


**Figure 9.2** Example of partial pressure saturation curves.

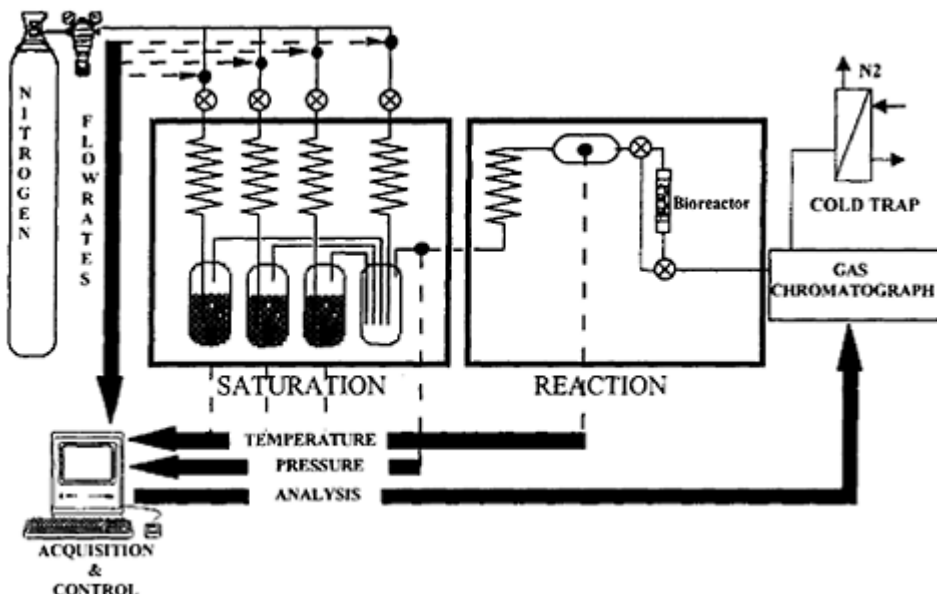


**Figure 9.3** Schematic diagram of a packed bed solid gas bioreactor working at atmospheric pressure.

corresponding to the saturation pressure above the pure compound. In order to calculate the composition of the gas, the different molar flows for each compound (carrier+substrates+water) have to be known. The molar carrier flow in each line is calculated using the volumetric normalised flows of carrier gas used for saturation:

$$Q_{N_2}^n = \frac{Qv_{N_2}^n \text{ normalized}}{R.T} \quad (\text{mol/h } T = 273.15 \text{ K})$$

Then, knowing the molar flow of the carrier gas it is possible to calculate the different molar flows leaving the saturation flasks by the formula using the saturation pressure:

$$Q_x^n = Q_{N_2}^n \frac{Ppsat_x^n}{(P_a - Ppsat_x^n)} \quad (\text{mol/h})$$

with  $Ppsat_x^n$  determined at the temperature of saturation.

After mixing the different lines, the partial pressure of each compound in the gas entering the bioreactor is determined using:

$$Pp_X^n = \frac{Q_X^n}{\sum_1^n (Q_{N_2}^n + Q_X^n)} Pa \text{ (atm)}$$

and the activity of each compound in the reactor stage is calculated as follows:

$$a_x = \frac{Pp_x^n}{Ppsat_X^n}$$

with  $Ppsat_X^n$  determined at the temperature of the bioreactor.

Assuming that the applied conditions are far from the critical temperature and critical pressure for each compound, and by applying the ideal gas law  $P.V=n.R.T$ , one can obtain a good estimate of the total volumetric flow and the residence time in the bioreactor.

$$Qv_{total} = \frac{RT \sum_1^n (Q_{N_2}^n + Q_X^n)}{Pa} \quad (1/h \text{ at the temperature of the bioreactor in K})$$

When a liquid/gas flash vaporisation technique is chosen, then precise control of the different molar flows of each molecule entering in the composition of the gas must be exerted. Figure 9.4 describes a solid/gas setup in which liquid substrates, water and nitrogen are injected into a flashing unit for the realisation of the gas (Lamare and Legoy, 1999).

Thermodynamic control is then realised by calculating the different partial pressures based on the different molar flows. When  $Q_{N_2}$  and  $Q_X^n$  are well known,  $Q_{total} = Q_{N_2} + \sum_1^n Q_X^n$  can be determined and partial pressures can be calculated easily by the following equation:

$$Pp_X^n = \frac{Q_X^n}{Q_{total} \cdot Pa}$$

and thermodynamic activities are calculated according to equations previously described.

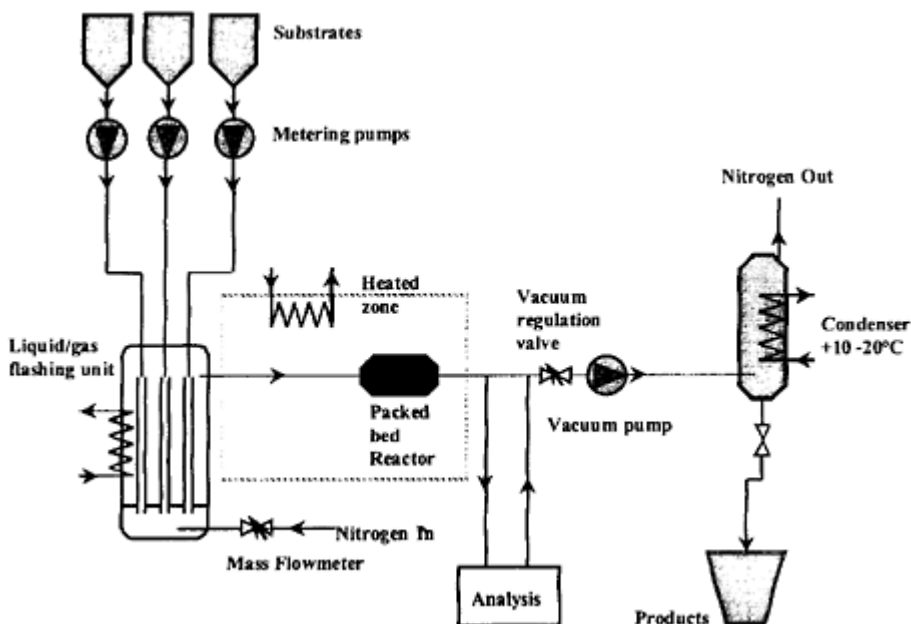


**Figure 9.4** Schematic diagram of a packed bed solid gas bioreactor working at reduced pressure.

Although the system allows a better control of the molar flow of substrates compared to the previous system described, care must be taken in order to insure a complete vaporisation of the different molecules injected into the system. To this end, saturation pressure curves are necessary for defining the minimal temperature that has to be used at the flash level. As a result, temperature must be chosen with regard to maximising the boiling point of the compound at working pressure. This point can be considered as a bottleneck, since in some cases, the use of very high temperatures can represent a serious constraint.

Nevertheless, this problem can be solved by performing solid/gas catalysis under reduced pressure. This strategy offers multiple advantages for the use of longer chain compounds or for the improvement of productivity. Moreover, according to the saturation pressure curves it is possible to minimise the temperature of the flash operation, and this allows an important enrichment of the gaseous phase in reactants while minimising greatly the quantity of carrier gas needed.

As an example, one can compare the effect of pressure on a simple theoretical transformation. The transformation of X to Y will be carried out at 100°C and  $a_x = a_w = 0.1$ . The saturation pressure of X at 100°C is 0.2 atm and partial pressure of water is 1 atm. The boiling point of X is 200°C at 1 atm.  $P_{p_x}$  is set to 0.02 atm and  $P_{p_{H2O}}$  thus will be 0.1 atm in the inlet gas. The total molar flow will be 100 moles/h, and the reaction will be carried out at two absolute pressures, 0.2 atm and 1 atm.

The characteristics of the two gases are summarised in Table 9.1.

The benefit of a reduced absolute pressure is clearly established, since the gas at 0.2 atm is highly charged in X molecules, while the nitrogen consumption is divided by a factor of 2.2 for a productivity increased by a factor of 5 compared to the system functioning at atmospheric pressure. Flashing temperature is also lowered by the use of reduced pressure, thus greatly minimising the power required for this operation.

Nevertheless, if one compares the two systems at the same productivity level, the advantages of reduced pressure are still significant. While total volumetric flow and molar flows for X and water will be the same in both cases, the required amount of nitrogen will be now 5 times lower at reduced pressure. Thus, nitrogen consumption is divided by a factor of 11 compared to a system at atmospheric pressure at the same productivity.

Moreover, the use of solid/gas systems functioning at reduced pressure is of great importance, considering the step following catalysis that allows recovery of the products.

**Table 9.1** Compositions of two different gases for the same reaction in term of thermodynamic activity performed at two different absolute pressures

Absolute working pressure	0.2 atm	1.0 atm
$Q_x$ (mole/h)	10	2
$Q_{H_2O}$ (mole/h)	50	10
$Q_{N_2}$ (mole/h)	40	88
Minimal flash temp. ( $^{\circ}C$ )	100	200
Condensable fraction of the gas	60%	10%
$Q_y$ total (m <sup>3</sup> /h)	15.3	3.06

If one considers now that after catalysis, the gas stream is injected onto a heat exchanger for the recovery of the product Y at a temperature of  $10^{\circ}C$  and that saturation pressure of Y at  $10^{\circ}C$  is 0.01 atm, then the system depicted in Figure 9.4 allows a more complete recovery of Y, which it is impossible for the system depicted in Figure 9.3.

If all X is transformed into Y, then in both systems the gas at the outlet of the reactor will have the following characteristics at the steady state:  $P_{pH_2O}=0.1$  atm,  $P_{p_x}=0$  atm,  $P_{p_y}=0.02$  atm.

Prior to the cooling operation, the gas on system described in Figure 9.4 will have an absolute pressure at the outlet of the vacuum pump of 1 atm. In this case, the characteristics prior the inlet of the condenser will be:  $P_{pH_2O}=0.5$  atm,  $P_{p_x}=0$  atm,  $P_{p_y}=0.10$  atm since  $P_a$  is multiplied by 5.

Once cooled at  $10^{\circ}C$ , condensation will take place, while the partial pressure of Y is higher than the saturation pressure of Y at  $10^{\circ}C$ . Thus, the efficiency will be completely different in the two cases. For the reactor working at atmospheric pressure, only 50% of

Y will be condensed while 90% of Y will be condensed for the system working at 0.2 atm.

$$\frac{P_{p_Y} - P_{psat_Y}}{P_{p_Y}} = \frac{0.02 - 0.01}{0.02} = 0.5$$

$$\frac{P_{p_Y} - P_{psat_Y}}{P_{p_Y}} = \frac{0.1 - 0.01}{0.1} = 0.9$$

Absolute pressure then appears a crucial parameter for optimising such processes. Moreover, the use of carrier gas can be avoided by working at an absolute pressure equal to the sum of the partial pressures of the different condensable molecules present in the gas phase.

As a result of these examples, it appears clear that the use of systems derived from the one presented in Figure 9.4 is more suitable for industrial purposes. But systems working under reduced pressure have their own constraints. Since temperature is also a key parameter, heat exchanges under partial vacuum are less effective, thus leading to oversized thermal exchange surfaces.

Nevertheless, in all cases special care must be taken to very accurately control physical parameters such as temperature and absolute pressure when one wants to work at controlled thermodynamic conditions.

### APPLICATION OF SOLID GAS CATALYSIS: REACTIONS USING LIPOLYTIC ENZYMES

As described previously, what influences the activity and the stability of a gas/solid biocatalytic system is the combination between the hydration level and the applied temperature. When the water activity is too high, denaturation phenomena are more important and when free solvent water is present in the system, serious diffusional limitations exist since the system cannot be considered as solid/gas biphasic media but rather as solid/liquid/gas system. Solid-gas biocatalysis exists only when the biocatalyst has no free solvent surrounding the protein as mentioned previously. When one wants to use solid/gas systems involving biocatalysts, one has to first study the sorption and desorption isotherms of the catalytic preparation.

When using enzymes in low water media, the most important question is: what is the minimal amount of water needed to obtain a stable and fully catalytic protein?

Experiments performed by Yang and Rupley (1979) related to the hydration of proteins shed much light on the processes involved. The main result was to show that the hydration of lysozyme was a sequential process, with a controlled distribution of water molecules onto the protein.

In order to characterize the hydration state of solid phases, one needs to characterise the isotherm sorption curve, the variation of water content versus the water activity. These curves allow the determination of the different states of water (Drapron, 1985). Different methods can be used for determination of the water content; gravimetric, or for more sensitivity, iodometric and coulometric methods (Macleod, 1991; Bernetti *et al.*, 1984). Typically, isotherms present two characteristic break points (A and B) corresponding to two important states of water as shown in Figure 9.5.

Before point A, the water is highly structured. Water molecules are located in ionic groups and polar groups. They constitute the first hydration "layer". Point O corresponds to the tightly bound water (buried water).

Between A and B, the water content changes in a linear way while increasing the  $a_w$ . It corresponds to the formation of new hydration layers. The protein dissolves molecules of water, thus forming a solid solution.

Point B corresponds to the appearance of free water. Once the water activity is higher than the abscissa value of point B, an aqueous phase exists, with many water molecules having no interaction with the protein. Point C corresponds to the total quantity of non solvent water, *i.e.* structured by the solid sample.

Realisation of the isotherms of the different components of the system allows a more accurate prediction concerning the behavior of an enzyme placed in solid/gas systems.

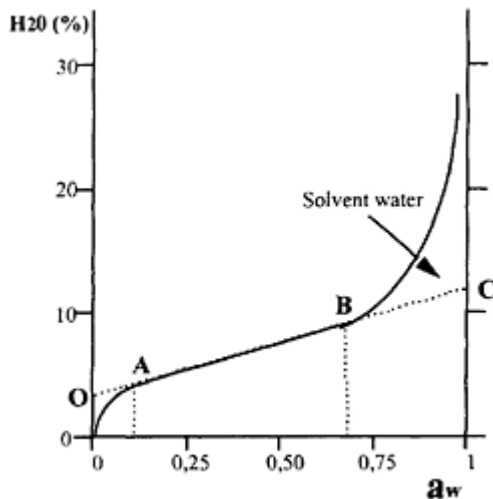


**Figure 9.5** Schematic diagram of an isotherm sorption curve. (From Drapron R. (1985), see details in text)

Nevertheless, one must be aware that because water activity is an equilibrium parameter, the exchanges of water between different phases have to be in a steady state.

As an example of the effect of water activity on the catalytic rate of a *F. solani pisi* cutinase, the following reported experiments (Lamare and Legoy, 1995, 1997) highlight the importance of controlling all the thermodynamic activities. In the first experiment, 1 mg of enzyme adsorbed on 15 mg of Chromosorb P was placed at 60°C or 70°C in the reactor described in Figure 9.1. The total flow passing through the bioreactor was set to 500 or 470 µmoles/min giving a volumetric flow of 12.5 ml/min and a residence time close to 0.4 s under both temperature conditions. The effect of water activity was studied on transesterification between n-propanol and propionic acid methyl ester, because water does not participate in the reaction scheme. a<sub>propionic acid methyl ester</sub> (a<sub>ester</sub>) and a<sub>n-propanol</sub> (a<sub>alcohol</sub>) were set to 0.200 giving partial pressures equal to 0.100 and 0.051 at 60°C and

0.143 and 0.064 atm at 70°C. The effect of water activity was monitored by scanning from 0 to 0.8 using plateaus of 2 h at a given  $a_w$  value. The same enzymatic preparation was used for the complete run due to its excellent stability. The partial pressures of water ranged from 0 to 0.160 atm at 60°C and from 0 to 0.250 at 70°C.

As depicted in Figure 9.6, it is clear that the correct parameter to use with a gas/solid process is the thermodynamic activity of water and not its volumetric concentration or its partial pressure. If the results are plotted against the partial pressure of water, the two curves obtained at 60 and 70°C exhibit different optima and some misunderstanding can arise from using this parameter.

When the two sets of data are plotted against water activity, the two curves obtained at 60 and 70°C are well superimposed, and present the same optimum at  $a_w=0.6$ . Furthermore, the catalytic activities measured at 60 and 70°C are very close, indicating also the necessity to use the thermodynamic activity of the other compounds present in the system (*i.e.* substrates).

This was confirmed using thermodynamic activities when studying the kinetics of two reactions, transesterification and hydrolysis, and the same results were observed (Lamare and Legoy, 1997).

Moreover, kinetic studies showed that an interaction exists between all the components of the gaseous phase, since organic compounds were found to solvate, thereby enhancing catalytic activity when using restricted water conditions.

Since it was possible to carry out reactions involving lipolytic enzymes at the solid/gas interface, it was also important to check the stability of enzymatic preparations in systems requiring relatively high temperatures for non-thermostable enzymes.

For these experiments the reactors used previously for 24 hours at the different water activities were reused at a fixed water activity corresponding to the maximal hydration state before appearance of free water (see isotherm on Figure 9.7).

The experimental conditions were as follows:  $a_{n\text{-propanol}}=a_{\text{methyl propionate}}=0.2$ . Fixed  $a_w$ , total molar flow set at 500  $\mu\text{moles}/\text{min}$ , and a temperature of 70°C.

The activity was measured for 4 hrs. Figure 9.7 shows that 80% of the maximal activity observed during the first run at  $a_w=0.6$  could be restored in all cases, once the reactor was used between  $a_w=0$  and  $a_w=0.6$ . Figure 9.8 compares the thermal stability of the solid/gas and liquid system of a *C. rugosa* lipase for a transesterification reaction. Whilst the thermodynamic activities are controlled, biocatalyst stability in solid/gas systems is excellent.

Hydrolysis (Lamare and Legoy, 1997) and esterification reactions were also studied, and the competitiveness of solid/gas catalysis led to the development of an industrial platform for the production of natural esters using a commercial enzymatic preparation. Results of this are presented in the conclusion.

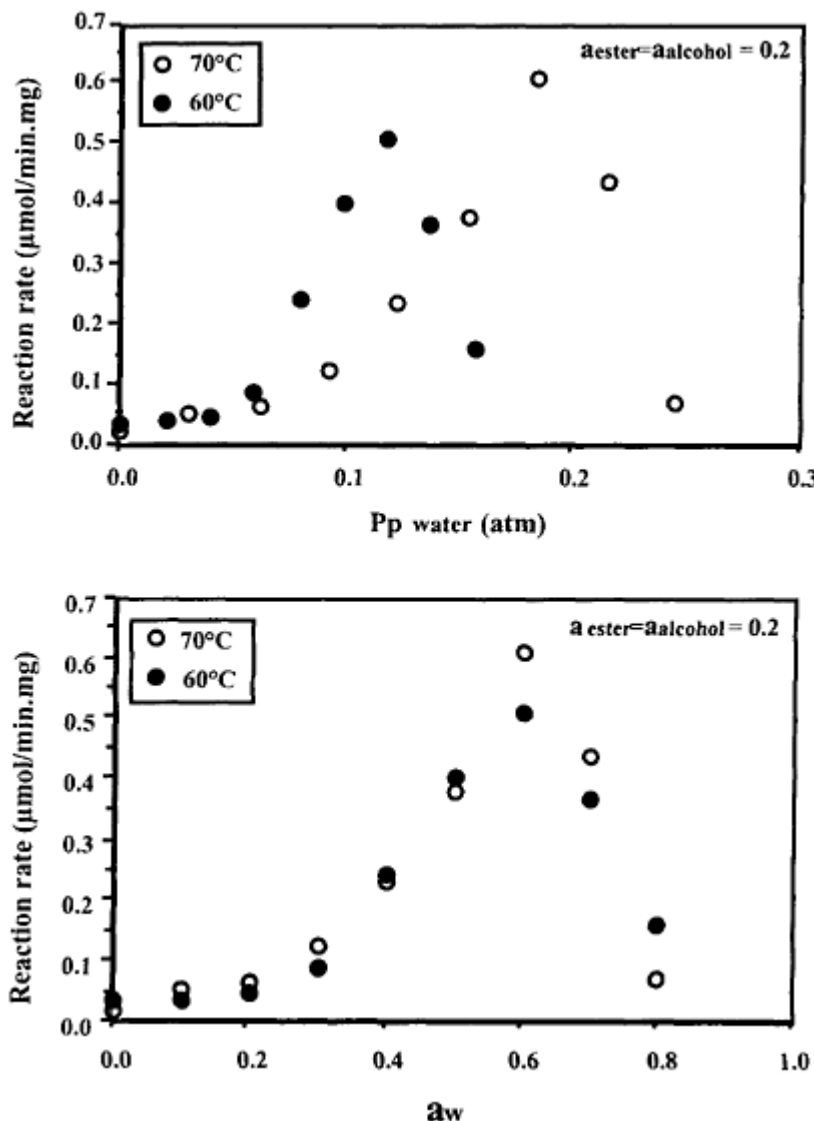


**Figure 9.6** Effect of the hydration level of the gaseous phase on the catalytic activity for transesterification between propionic acid methyl ester and n-propanol. Results are expressed as a function of partial pressure (P<sub>p</sub>) or thermodynamic activity (a).

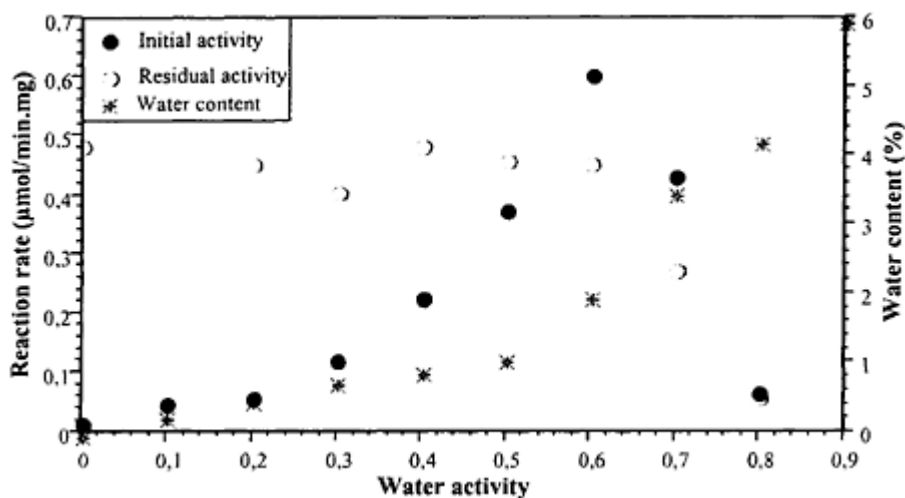


**Figure 9.7** Effect of water activity on the transesterification reaction rate for free cutinase used as freeze-dried powder at 70°C (●). The residual activities after 24 h of continuous use at the x value of aw, and measured at the optimal water activity determined by the filled circles ( $a_w=0.6$ ) are plotted (○). On the same graph are plotted the sorption isotherms determined at 30°C (\*). 1 mg of enzyme is placed in the bioreactor.

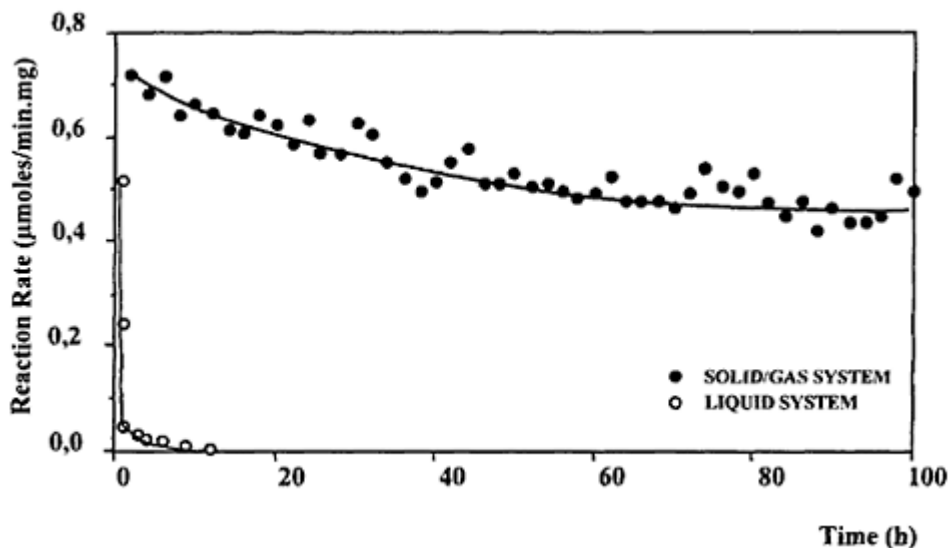


**Figure 9.8** Comparison of thermal stability of *C. rugosa* lipase adsorbed onto Chromosorb P for a transesterification between n-propanol and methyl propionate in gas/solid system and in liquid system at 70°C. Alcohol and ester were at the same molar ration in both systems and liquid system was previously prequilibrated at the same  $a_w$  (0.7 in this case).

#### APPLICATION OF SOLID/GAS CATALYSIS: THE ALCOHOL DEHYDROGENASE OF BAKER'S YEAST DEAD CELLS

Many aldehydes and alcohols are used in the agro-industries for their flavouring properties. The majority of flavours are produced by chemical means or by extraction from a natural product. For these reasons, an alternative approach was chosen for producing such compounds, but because purified alcohol dehydrogenase immobilised or co-immobilised with its cofactor was not economically viable for industrial application, the ability of whole baker's yeast dead cells to reduce aldehyde and oxidise alcohol vapors was already being studied (Hwang and Trantolo, 1993; Hwang and Park, 1994). In the following example, the reduction of hexanal with baker's yeast to prepare hexanol was chosen as the reaction model. In addition, cofactor NADH,  $H^+$  was regenerated with a second substrate, ethanol. The oxidized NAD is reduced back to NADH,  $H^+$  by baker's

yeast-catalysed conversion of ethanol to acetaldehyde. The coupled-substrate reaction in solid/gas system is illustrated in Figure 9.9.

As described previously, the same behaviour was observed with lipolytic enzymes regarding the dependence of stability and enzymatic activity on the hydration level of the system. As indicated on Figure 9.10, alcohol dehydrogenase was responsible for the conversion of hexanal to hexanol and the cofactor regeneration was effective. In this experiment, 200 mg of baker's yeast was placed at 65°C in the solid/gas bioreactor depicted in Figure 9.3. The total flow passing into the bioreactor was 680  $\mu$ moles/min. The hexanal activity was fixed at 0.05 (5  $\mu$ moles/min), the ethanol activity at 0.1 (73  $\mu$ moles/min), and

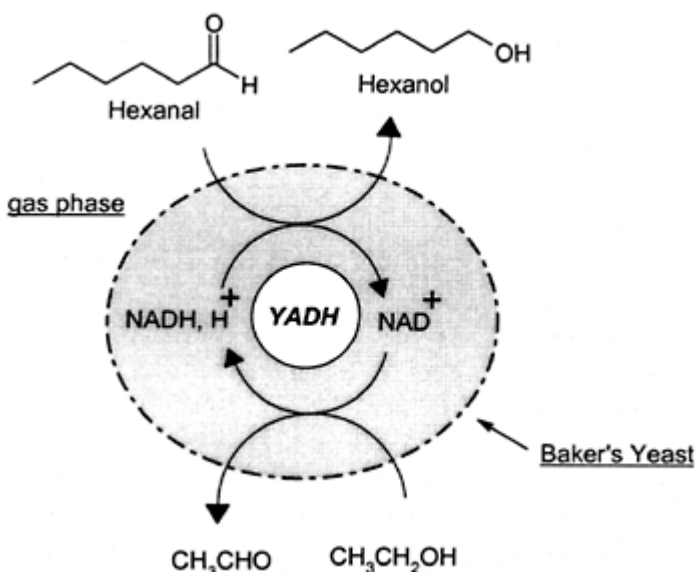


**Figure 9.9** Model for hexanal reduction by YADH of baker's yeast with an  $NAD^+$  regenerating system with ethanol.

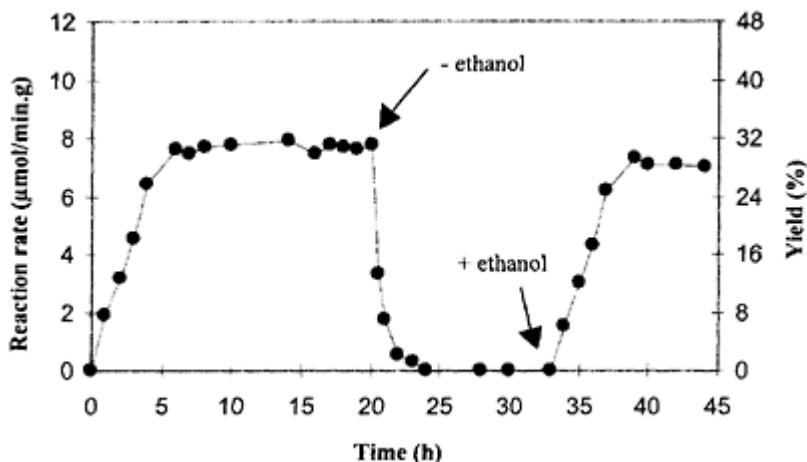


**Figure 9.10** Initial reaction rate of the reduction of hexanal catalysed by baker's yeast. The reaction was carried out at 65°C with 200 mg of yeast. The total flow passing into the bioreactor was 680  $\mu\text{moles}/\text{min}$ . The hexanal activity was fixed at 0.05, the ethanol activity at 0.1 and the water activity at 0.57.

the water activity at 0.57 (93  $\mu\text{moles}/\text{min}$ ). The initial rate of hexanol formation increases up to a maximum rate equal to 8  $\mu\text{moles}/\text{min.g}$  of yeast, corresponding to 32% hexanal conversion. The steady state is obtained after 8 hours. Since hexanal conversion is dependent on both the amount of available NADH,  $\text{H}^+$  and its turnover when regenerated using ethanol, the ethanol activity was fixed to 0 (0  $\mu\text{moles}/\text{min}$ ) after 20 hours of reaction. Consequently, the regeneration of NADH,  $\text{H}^+$  becomes impossible and the initial rate of hexanol formation decreases rapidly and tends towards zero. If ethanol is added, the conversion of hexanal is stimulated and the initial rate of hexanol formation increases again. This stimulation is the result of the conversion of ethanol by ADH leading to NADH,  $\text{H}^+$  production. Note also that the stability of ADH in this system is important, since, after addition of ethanol in the inlet gas, the restored reaction rate is almost equal to what was observed at the beginning under steady state conditions.

Water activity was also found to play a very important role. In a second experiment the same conditions as before were applied, except that the catalytic activity was assayed under different hydration conditions. As shown in Figure 9.11, the initial rate of hexanol formation is strongly influenced by water activity. A critical water activity of 0.4 is necessary for the yeast to become active. Then, the initial rate of bio-transformation increases with water activity to reach maximum initial rate equal to 12  $\mu\text{moles}/\text{min.g}$  of yeast, obtained for a water activity near to 0.7. For higher water activity a dramatic effect

is seen, the initial rate of hexanol formation decreasing rapidly and tending towards zero. Nevertheless, while it was clear when using isolated enzymes that deactivation was due to a thermal denaturation of the proteic material, it remains unclear in this system. The decrease in initial rate at high water activity can be related to limitations of diffusion caused by the presence of a distinct liquid phase, thus limiting mass transfers due to the

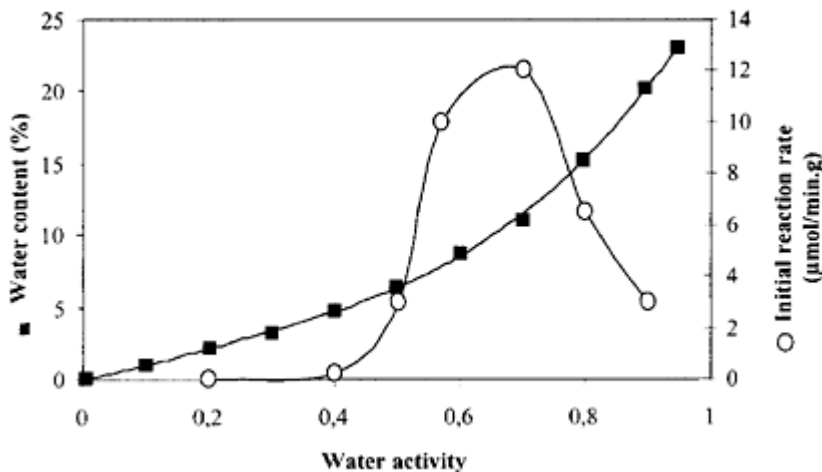


**Figure 9.11** Effect of water activity on initial reaction rate of the reduction of hexanal catalysed by baker's yeast (○). Isotherm sorption curve of the baker's yeast (◆). The reaction was carried out at 65°C with 200 mg of yeast. The total flow passing into the bioreactor was 680  $\mu$ moles/min. The hexanal activity was fixed at 0.05 and the ethanol activity at 0.2.

appearance of free water on the catalytic material as indicated on the sorption isotherm curve of the preparation. Nevertheless, while high hydration levels resulted in dramatic modifications at the macroscopic level to the dried cells, a reproducible measurement of the remaining activity was impossible.

Concerning possible diffusional limitations in the system, it was also important to check the effect of yeast quantity on the initial rate. The results presented in Figure 9.12 show

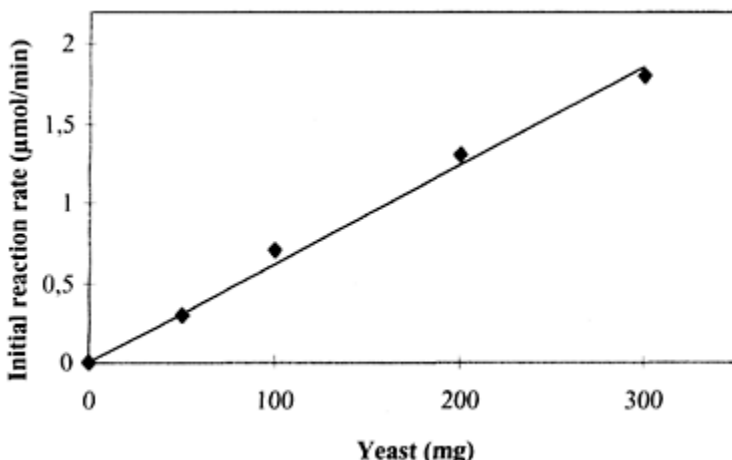


**Figure 9.12** Initial reaction rate of the reduction of hexanal as a function of amount of baker's yeast. The reaction was carried out at 65°C. The total flow passing into the bioreactor was 680  $\mu$ moles/min. The hexanal activity was fixed at 0.05, the ethanol activity at 0.2 and the water activity at 0.57.

that initial reaction rate increases linearly for the range investigated. This linearity proves that initial rate is under kinetic control and that internal diffusion rate of substrates is higher than transformation rate.

Thus, the key point of this system is to optimise hydration conditions without allowing any possible re-condensation on the catalytic material that would lead to a gas/liquid/solid system with poor performance and poor stability.

## CONCLUSIONS

Solid/gas catalysis appears to be highly interesting from the industrial point of view since it competes strongly with other bio-processes. To date, a pre-industrial platform has been developed for the production of esters sharing the “natural” label by solid/gas biocatalysis, fulfilling many objectives governed by economical constraints such as productivity from 2 to 5 kg of ester per hour, a condensation unit working at positive temperature, and no consumption of carrier gas.

To this end, the process was developed as a closed nitrogen loop, in which one part was placed under vacuum and heated for the vaporisation of substrates and the catalytic step, while the other part was pressurised and cooled, allowing product recovery and the recycling of clean nitrogen.

Figure 9.13 and 9.14 give an overview of the overall plant and the process control room. Rapid optimisation of different esterification reactions catalysed by Novozym 435 was performed using a thermodynamic approach to the system. The first step was the determination of the  $\Delta G^\circ$  of each targeted reaction. Rapid kinetic experiments and stability tests were subsequently performed in order to determine the limits of important parameters such as acid and alcohol thermodynamic activities, operating temperature and pressure, and initial water requirement. In the second step, optimisation of the operating parameters within the possible range of each parameter was realized, using calculation predictive sheets developed for this purpose. When theoretical optimisation was performed, a sample test production began based on the production of 200 g of ester on a lab scale experimental setup at 1/1000 scale of the platform. These sample productions were carried out over a minimum period of 24 to 100 hours in order to check the stability of the enzymatic activity concurrently. Figure 9.15 gives an example of stability under optimised conditions and half life time was found to be around 2000 hrs. Once the sample test was performed, large-scale production was engaged at the level of 100 to 200 kg of ester.

While it was unproven ten years ago, the technological feasibility of solid/gas bioprocesses at the pre-industrial level has now been demonstrated, and economical studies have shown that they are competitive.

Test productions of large quantities of product by solid/gas catalysis have been performed, and the gas/solid system technology proved its ability to efficiently perform esterification reactions while at the same time greatly simplifying the downstream process



**Figure 9.13** Continuous pre-industrial scale solid/gas bioreactor (LGPC, Université de La Rochelle, France).



**Figure 9.14** Process control room with sampling system and on-line monitoring of the pre-industrial

platform. (LGPC, Université de La Rochelle, France).

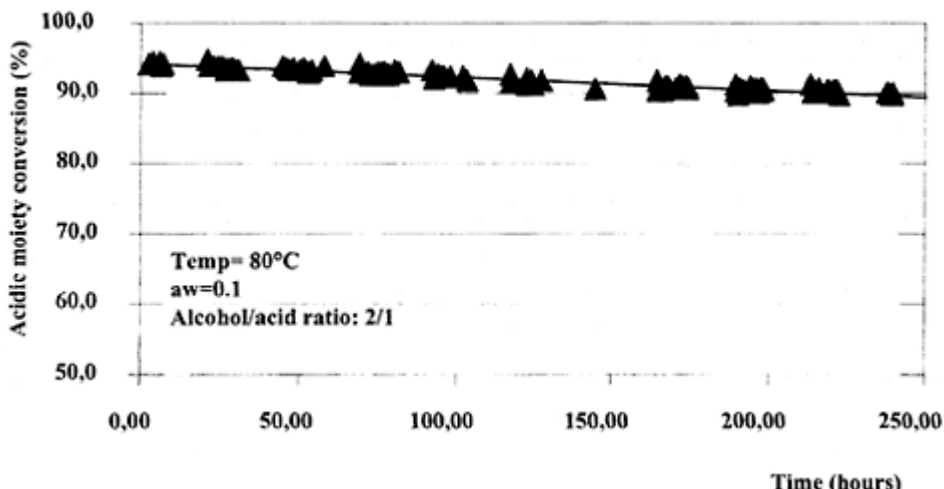


**Figure 9.15** Stability test realised at 80°C of Novozym 435 after optimisation of operational parameters for a propionic acid alkyl ester synthesis under reduced pressure.

by a considerable reduction of the volumes that have to be treated compared to liquid organic systems.

Numerous applications should benefit from this technology. The on line bio-treatment of waste gases for toxic removal or modification (Uchiyama *et al.*, 1992; Zilli *et al.*, 1992; Davison and Thompson, 1993) is already envisaged, since it is clear that high catalytic efficiency is possible with very short residence time in the solid/gas reactor. However, this step represents the next bottleneck to overcome, since it implies the maintenance of multiple enzymatic activity and cofactor regeneration systems.

#### ACKNOWLEDGMENTS

The authors wish to thank the E.U. for their financial support within the framework of a demonstration project (BIO4-CT98-0390).

#### REFERENCES

- Barzana, E., Klibanov, A. and Karel, M. (1987) Enzyme-catalysed gas-phase reactions, *Appl. Biochem. Biotechnol.* **15**, 25–34.
- Barzana, E., Klibanov, A. and Karel, M. (1989a) Enzymatic oxidation of ethanol in the gaseous phase, *Biotechnol. Bioeng.*, **34**, 1178–1185.
- Barzana, E., Klibanov, A. and Karel, M. (1989b) A colorimetric method for the enzymatic analysis of gases: the determination of ethanol and formaldehyde vapors using solid alcohol oxydase *Anal Biochem.*, **182**, 109–115.
- Bernetti, R., Kochan, S. and Pienkowski, J. (1984) Karl-Fischer determinations of water in oil and fats: International collaborative study. *J. Assoc. Off. Anal. Chem.*, **67**, 299–301.
- Davison, B. and Thompson, J. (1993) Sustained degradation of n-pentane and isobutane in a gas-phase bioreactor. *Biotechnol. Lett.*, **15**, 633–636.
- Drapron, R. (1985) Enzyme activity as a function of water activity in Properties of water in foods, Simatos, D. and Multon, J. (Eds), Martinus Nijhoff Publishers. *Dordrecht. Pays bas.* 171–182.
- Duff, S. and Murray, W. (1990) Extruded Pellets of *Pichia pastoris*: a practical biocatalyst for use in aqueous, organic and vapor phase oxydations. *Process Biochemistry*, April, 40–42.
- Hamstra, R., Murris, M. et Tramper, J. (1986) The influence of immobilization and reduced water activity on gaseous alkenes oxydation by mycobacterium PY1 and Xanthobacter PY2 in a gas-solid bioreactor. *Biotechnol. Bioeng.*, **29**, 884–891.
- Hou, C. (1984) Propylene oxyde production from propylene by immobilized whole cells of *Methylosinus* sp. CRL31 in a gas-solid bioreactor. *Appl Microbiol Biotechnol.*, **19**, 1–4.
- Hwang, S.O., Trantolo, D.J., Wise, D.L. (1993) Gas phase acetaldehyde production in a continuous bioreactor. *Biotechnol. Bioeng.*, **42**, 667–673.
- Hwang, S.O., Park, Y.H. (1994) Ethyl acetate production in the gas phase. *Biotechnol. Lett.*, **16**, 379–384.
- Kim, C. and Rhee S-K. (1992) Enzymatic conversion of ethanol into acetaldehyde in a gas-solid bioreactor, *Biotechnol. Lett.*, **14**, 1059–1064
- Kimura, K., Suzuki, A., Inokuchi, H. and Yagi, T. (1979) Hydrogenase activity in the dry state: isotope exchange and reversible oxidoreduction of cytochrom c3. *Biochim. Biophys. Acta b*, **567**, 96–105.
- Lamare, S. and Legoy, M.D. (1993) Biocatalysis in the gas phase. *Trends in Biotechnol.*, **11**, **10**, (117), 413–418.
- Lamare, S. and Legoy, M.D. (1995) Working at controlled water activity in a continuous process: the gas/solid system as a solution, *Biotechnol. Bioeng.*, **45**, 387–397.
- Lamare, S. and Legoy, M.D. (1995). Solid/Gas biocatalysis: How to fully define the system? *Biotechnol. Techniques.*, **9**, 127–132.
- Lamare, S. (1996) Engineering of/with lipases: importance of water in new biocatalytic processes: the solid/gas catalysis example, in Engineering of/with lipases, F.X Malcata Editor, NATO ASI series, Serie: E: Applied Sciences **317**, 357–390.
- Lamare, S. and Legoy, M.D. (1997) Kinetic studies of a *Fusarium solani* pisii cutinase used in a gas/ solid system. Hydrolysis and transesterification reactions, *Biotechnol Bioeng.*, **57**, 1–8.
- Lamare, S. et Legoy, M.D (1999) Procédé réactionnel par catalyse solide/gaz en milieu non-conventionnel, réacteur correspondant et utilisation de ce réacteur. *International Patent WO 99/04894*.
- Macleod, S. (1991) Moisture determination using Karl-Fischer titrations. *Anal. Chem.*, **63**, 557–566.
- Parvaresh, F., Robert, H., Thomas, D. and Legoy, M.D. (1992) Gas phase transesterification reactions catalyzed by lipolytic enzymes. *Biotechnol Bioeng.*, **39**, 467–473.
- Pulvin, S., Legoy, M.D., Lortie, R., Pensa, M. and Thomas, D. (1986) Enzyme technology and gas phase catalysis: alcohol dehydrogenase example. *Biotechnol. Lett.*, **8**, 11, 783–784.
- Pulvin, S., Parvaresh, F., Thomas, D. and Legoy, M.D. (1988) Solid-Gas reactors. A comparison between horse liver and the thermostable *sulfolobus solfataricus* ADH. *Ann. NY Acad. Sci.*, **545**, 434–439.

- Robert, H., Lamare, S., Parvaresh, F. and Legoy, M.D. (1992) The role of water in gaseous biocatalysis. *Prog. Biotechnol.*, **8**, 23–29.
- Ross, N. et Schneider, H. (1991) Activities of *Candida rugosa* lipase and other esterolytic enzymes coated on glass beads and suspended in substrate and water vapors: enzymes in thin liquid films. *Enzyme Microb. Technol.*, **13**, 370–377.
- Uchiyama, H., Oguri, K., Yagi, O. and Kokufuta, E. (1992) Trichloroethylene degradation by immobilized resting-cells of *Methylocystis* sp. M in a gas-solid bioreactor, *Biotechnol. Lett.*, **14**, 619–622.
- Yagi, T., Tsuda, M., Mori, Y. and Inokuchi, H. (1969) Hydrogenase Activity in the dry state. *J. Am. Chem. Soc.*, **91**, 2801.
- Yang, F.X. and Russell, A.J. (1996) The role of hydration in enzyme activity and stability:I.Water sorption by alcohol dehydrogenase in a continuous gas phase reactor. *Biotechnol. Bioeng.*, **49**, 700–708.
- Yang, P.-H. and Rupley, J. (1979) Proteins-water interactions. Heat capacity of the lysozyme-water system. *Biochemistry*, **18**, 2654–2661.
- Zilli, M., Converti, A., Lodi, A., Del Borghi, M. and Ferraiolo, C. (1992) Phenol removal from wate gases with a biological filter by *Pseudomonas putida*. *Biotechnol. Bioeng.*, **41**, 693–699.



# CHAPTER TEN

## BIOFILM REACTORS

LUIS F.MELO<sup>1</sup> AND ROSÁRIO OLIVEIRA<sup>2</sup>

<sup>1</sup> *Department of Chemical Engineering, University of Porto, Rua D.Roberto Frias, 4200–465 Porto, Portugal*

<sup>2</sup> *Department of Biological Engineering, Universidade do Minho, 4710–057 Braga, Portugal*

### ABSTRACT

After presenting the concept of biofilms, reference is made to their importance in industry and health. Although biofilms are also well known for their deleterious effects (biofouling), emphasis is here given to the beneficial use of biofilms in wastewater treatment. The main types of biofilm reactors are briefly described and the rôle of support material in the adhesion and stability of biofilms is explained, taking into account the mechanisms involved in biofilm attachment. Practical procedures for the start-up of biofilm reactors are also mentioned.

Biofilm growth processes are described together with their properties, structure and performance. The advantages and disadvantages of biofilm reactors *versus* suspended biomass systems are discussed.

The main equations of the diffusion-reaction model are developed from engineering science principles. Equations derived from the diffusion-reaction model to calculate the reactor volume are presented, together with experimental values of the kinetic parameters. Practical empirical expressions or rules-of-thumb used in the design of fixed biomass reactors are also given. An overall model to predict the growth rate of biofilms and their final thickness or mass is established. The main problems concerning biofilm reactor modelling are discussed and the “missing links” for an optimised design are identified.

### INTRODUCTION

Micro-organisms, like the vast majority of living creatures, tend to live in communities and form their own specific habitats. It has been estimated that up to 90% of microbial cells in nature grow within agglomerates (Costerton *et al.*, 1987). Microbial films, frequently designated as biofilms, are one of the types of biological agglomerates (together with flocs and granules). They are communities of microorganisms attached to surfaces, forming a porous matrix which contains the cells, the extracellular polymeric substances (EPS) they produce, and a substantial amount of water (Characklis and Marshall, 1990; Melo *et al.*, 1992). In nature and industry, this biofilm concept is

obviously too simple and should be extended to include organic debris and small inorganic particles (clays, metallic oxides, etc.) captured by the polymeric network, as well as adsorbed compounds. Microbial cells in biofilms are often bacteria, but living algae and fungi often appear in significant quantity in such matrices. In some cases, macro-organisms such as mussels and barnacles may attach to the microbial layer. Micro-organisms in biofilms can survive in extreme conditions, with pH ranging from 0 to more than 13, temperatures from -10°C to 120°C or higher, and even in ultra-pure water (Flemming, 1991).

The immobilisation of cells on supports without the formation of an extracellular polymeric matrix will not be considered here as a biofilm process.

Microbial films can be detrimental not only to health (infections on teeth, prosthetic implants, urinary catheters, etc.), but also to engineered systems such as pipes, pumps, valves, reverse osmosis membranes, heat exchangers and ship hulls (Characklis and Marshall, 1990; Flemming and Geesey, 1991; Melo *et al.*, 1992; Bott, 1995; Lapin-Scott and Costerton, 1995). Furthermore, since they grow on almost any surface immersed in aqueous environments offering a minimum availability of nutrients, they can inconveniently develop on the walls of biological reactors as well as on other surfaces existing inside fermenters, such as agitator blades, pH probes, etc. The purpose of the present chapter is, however, to focus on the beneficial aspects of biofilms in reactors, where the microbial layers can be used to degrade unwanted compounds or to obtain desired products. The most common examples in the literature are wastewater treatment facilities containing attached biomass (Harremöes, 1978), but there are also other industrial processes using biofilm technology, such as the recovery of metals through bacterial leaching of ores or the production of vinegar, ethanol (Dempsey, 1990) and citric acid (Briffaud and Engasser, 1979).

## BIOFILM REACTORS—TECHNOLOGICAL FEATURES

### Types of Biofilm Reactors

A biofilm reactor is a biological reactor with fixed biomass. It is usually filled with particles of a carrier material—the “support”—where the microbial film is attached. If the particles are porous, the film forms not only on the surface but also within their pores. A limiting case of a very simple biofilm reactor is a duct where the biomass develops on the walls: such a situation actually occurs in sewers, where the adhered biomass may act as an additional wastewater treatment biological reactor, although in some cases it also contributes to the deterioration of the wall material. Another example is the case of biofilms formed on rocks in contact with mountain streams that help to purify these waters.

In industrial microbial film reactors, the fluid flows in contact with the biofilm particles promoting the exchange of nutrients and metabolic products between the fixed biomass and the surrounding fluid. There is also exchange of mechanical energy between the two media: on one hand, the liquid exerts hydrodynamic forces on the biofilm enhancing both the detachment of biomass and the compactness of biofilms (these effects are particularly important in turbulent flow systems); on the other hand, the roughness

and viscoelasticity of the microbial film increase the pressure drop of the fluid along the reactor.

The tendency for cells to attach to supports in a reactor is determined not only by the physical-chemical properties of the surfaces, but also by the relative values of the specific microbial growth rate and the hydraulic residence time. When the residence time of the fluid in the reactor is small compared to the replication time of the cells, attachment becomes particularly relevant in avoiding the washout of the micro-organisms. The cells will then tend to adhere to the supports if the physical-chemical surface interactions are favourable.

Invariably, suspended biomass may also grow in microbial film reactors, although, if needed, this phenomenon can be minimised in many cases through proper design and operating procedures. Anyhow, since biofilms are dynamic structures, biologically speaking, a part of the biomass that is continuously building up on the supports has to be periodically purged from the system. This can be achieved through proper washing cycles (often, back-washing) in conjunction with external solid-liquid separation or through sedimentation of the detached biomass on the bottom zones of the reactor.

One of the oldest examples of artificial biofilm reactors was promoted by Frederich II of Prussia (Schlegel, 1985) who had lime walls built and put in contact with flowing liquid manure. The presence of ammonium compounds and bacteria in the liquid waste resulted in the development of nitrifying biofilms inside and on the lime stone, which converted ammonium to nitrate and contributed to the formation of calcium nitrate by reaction with the calcium of the lime walls. The purpose was to obtain potassium nitrate for gunpowder production.

In terms of particle-fluid dynamics, microbial film reactors are often classified as fixed bed or expanded bed reactors. The latter include classical fluidised beds (Cooper and Atkinson, 1981; Dempsey, 1990; Trinet *et al.*, 1991; Heijnen *et al.*, 1994; Nguyen and Shieh, 1995; Tavares *et al.*, 1995) where particles move up and down in the bed while the expanded bed as a whole is kept within a well defined zone of the reactor, and the so-called moving beds where the whole expanded bed circulates throughout the equipment together with the fluid, such as in air-lift reactor, moving bed or circulating bed reactors (Heijnen *et al.*, 1990; Tijhuis *et al.*, 1994; Ulonska *et al.*, 1994; Lazarova and Manem, 1997; Rusten *et al.*, 1997; Nogueira *et al.*, 1998). In those reactors, the bed is usually expanded by the liquid, sometimes containing gas bubbles, flowing upwards with a sufficiently high velocity to lift the bed. Recently, biofilm support particles made of low density material, which tend to float in water, have been used in reactors where the bed is expanded by circulating the liquid downwards; this is the so-called inverse fluidised bed (Nikolov *et al.*, 1990; Nikov and Karamanov 1991; Karamanov and Nikolov, 1992, 1996).

Fixed beds can be divided into: i) submerged beds (Hamoda and ABD-E1 Bary 1987), where the biofilm particles are completely immersed in the liquid (up-flow or down flow circulation); ii) trickling filters (Metcalf and Eddy, Inc. 1987; Briffaud and Engasser, 1979), where the liquid flows downwards split in small isolated streams as it percolates through the biofilm bed, while the gas usually flows upwards, and iii) rotating disk reactors, where the biofilm develops on the surface of vertical disks that rotate within the liquid. In aerobic processes, the lower part of each rotating disk is periodically submerged in the liquid and the upper zone is in contact with air; in anaerobic or anoxic

processes, the disk is (almost) completely submerged at any time, in order to avoid contact of the biofilm with the air. Trickling filter reactors were also adapted to the degradation of volatile organic compounds (VOC) in gaseous effluents (Pederson and Arvin, 1996, 1999; Peixoto, 1998), the biofilm being slightly humidified by water or another liquid.

Membrane biofilm reactors, where the microbial layer is attached to a porous gas permeable membrane, are a promising technology in some situations, including in VOC removal, since they provide a more efficient method of supplying gas to the base of the biofilm (Suzuki *et al.*, 1993; Wilderer, 1995; Freitas dos Santos and Livingston, 1995).

Detailed descriptions and comparative analysis of the advantages and disadvantages of the various types of biofilm reactors, as well as their performances *vis a vis* the conventional activated sludge systems can be found in a number of text books and research papers (e.g., Metcalf and Eddy, Inc. 1987; Eckenfelder *et al.*, 1989; Lazarova and Manem, 1994; Cabral and Tramper, 1994; Willaert *et al.*, 1996).

Table 10.1 summarises the characteristic types of biofilm reactors and some are schematically presented in Figure 10.1.

Most biofilm reactors operate in a continuous mode. An exception is the Sequencing Biofilm Batch Reactor (SBBR), where the tank containing biofilm particles is periodically filled with the feed liquid and discharged (Wilderer, 1995). The latter remains in the reactor during the "reaction period", after which it is drained out. This operation mode is particularly favourable when consecutive processes are involved: for example, in a nitrogen removal process, the biological nitrification (with aeration) and denitrification (without aeration) steps can be carried out in the same unit provided it contains biomass with nitrifying and denitrifying abilities. The operational flexibility of such reactors has been demonstrated to be advantageous in certain processes.

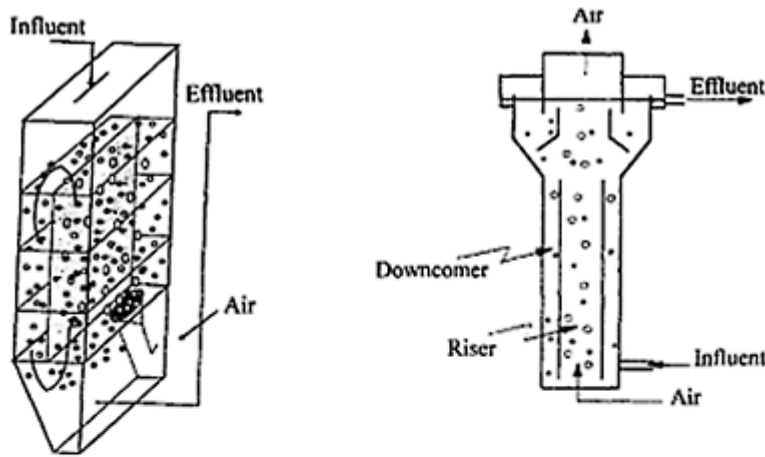
Sometimes, reactors containing microbial granules without support, such as the Up-flow Anaerobic Sludge Blanket reactor (UASB) are also treated as biofilm reactors, mainly as regards the kinetics of substrate consumption (Lettinga and Hulshoff-Pol, 1992; Alphenaar *et al.*, 1993; Brito and Melo, 1997a); aerobic granules have also been developed and tested in nitrification processes (Tijhuis *et al.*, 1995). The granules can be considered to be dense flocs composed by microbes and extracellular polymers, and in fact the problems they pose to the modelling of substrate diffusion and reaction are similar to those

**Table 10.1** Characteristic types of biofilm reactors

Fixed bed biofilm reactors	Expanded bed biofilm reactors
-Trickling filter	-Fluidised bed reactor (& inverse fluidis.)
-Submerged filter (downflow or upflow)	-Moving bed reactors:
-Rotating disk reactor	-air lift reactor
-Membrane biofilm reactor	-circulating bed reactor
	-Sequencing batch biofilm reactor (SBBR)

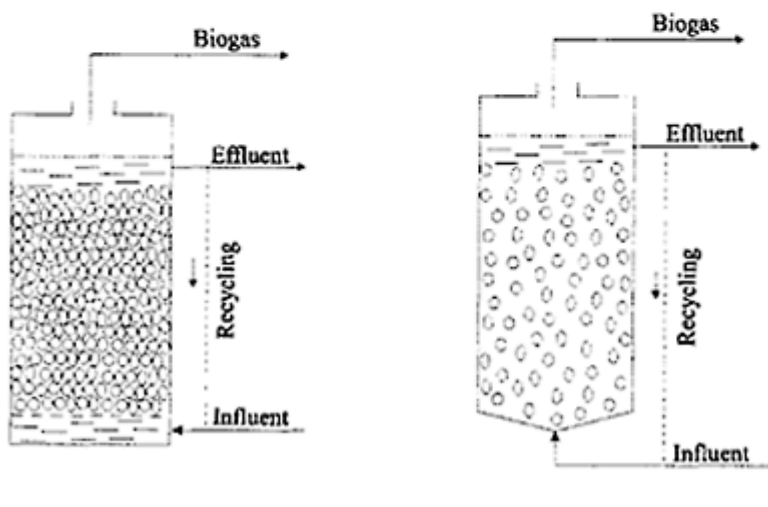
Reactors containing dense microbial granules not attached to solid supports:

Up-flow anaerobic blanket reactor (UASB)  
Expanded granular sludge blanket (EGSB)



(A)

(B)



(C)

(D)

**Figure 10.1** Schematic representation of a circulating bed reactor (A); air-lift reactor (B); anaerobic filter (C) and anaerobic fluidised bed (D).

of biofilms attached to a solid surface. Granules have a lower polymeric content, are usually more compact than microbial films and their formation follows specific distinct steps (Brito and Melo, 1997b).

A great variety (in shape, dimensions and materials) of supports is used in biofilm reactors, including: rough and rather large pieces of stones and gravel as the ones employed in the first generation of trickling filters (Metcalf and Eddy, Inc. 1987); small particles of sand, basalt or clay in fluidised bed and airlift reactors; particles with complex artificial geometries made of light plastic material used in circulating bed systems and agitated batch reactors; simple flat surfaces such as plastic disks in rotating biological

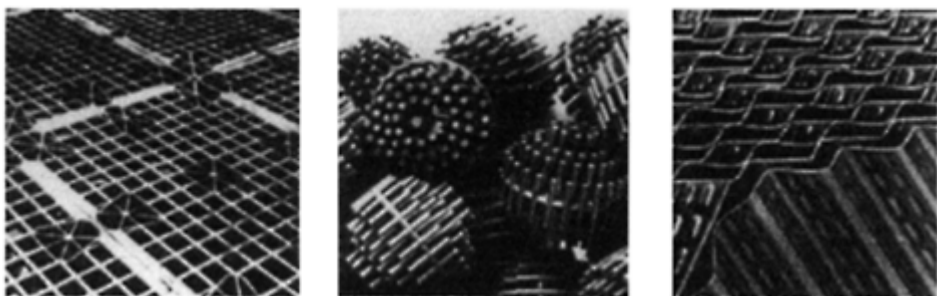


**Figure 10.2** Illustrative example of plastic supports used in trickling filters.

contactors. The specific area of the supports has been increasing over the last decades (Figure 10.2) in order to improve the efficiency and compactness of the reactors: initially, low specific surface areas of  $100 \text{ m}^2/\text{m}^3$  were available in trickling filters with rock supports and in biological disks; nowadays, fine granular and porous supports with  $500 \text{ m}^2/\text{m}^3$  or more are in use in many submerged, fluidised or moving bed reactors.

### The Importance of the Support

The prerequisite for the formation of a biofilm is the adhesion of the microbial cells to the support surface. Therefore, much effort has been put into investigating adhesion mechanisms (Busscher *et al.*, 1995, Teixeira and Oliveira, 1999, Azeredo *et al.*, 1999). However, in the more recent generation of biofilm-on-carrier reactors other processes might have a greater influence on biofilm formation. The carriers are subjected not only to higher turbulence and liquid shear than most fixed-support biofilms but also to the erosion and abrasion promoted by particle collisions (Gjaltema *et al.*, 1997). This means that the selection of the supports for biomass immobilisation is of great importance to obtain a stable biofilm leading to high reactor efficiency. In this way, the support must favour bacterial adhesion, must have a high mechanical resistance, a low cost and a great availability. To accomplish the first requirement, parameters like surface charge,

hydrophobicity, porosity, roughness, particle diameter, density and concentration can be of great importance.

An irreversible initial adhesion is the key factor for the development of a stable biofilm, but the support ability for microbial colonisation is also of crucial importance. This determines the colonisation velocity and ultimately the start-up rate of the reactor. For many years the adhesion mechanism was tentatively interpreted in terms of DLVO theory, with microbial cells considered as colloidal particles (Marshall *et al.*, 1971, van Loosdrecht *et al.*, 1988). Accordingly, the net force of interaction arises from the balance between the Lifshitz-van der Waals forces of attraction and the generally repulsive forces generated during the approach of the electrical double-layers of the interacting species (Oliveira, 1992). This repulsive character is due to the fact that most of the existing solid materials display a net negative charge when immersed in aqueous solutions with pH near neutrality. Bacterial cells are an example of negatively charged surfaces, especially because in most cases they are only able to survive in mild pH conditions. Therefore, the possibility for generating an electrostatic attraction is to utilise a positively charged support. However, as was said before, in nature only very few materials, like some metallic hydroxides, are able to display such behaviour. Other materials can be engineered in order to be positively charged; this is feasible for laboratory purposes, but it is not economically compatible with large-scale operation.

More recently it was demonstrated that the wettability, or in a reverse sense the hydrophobicity, of solid surfaces strongly influences adhesion either of bacteria, eukariotic cells or proteins (Margel *et al.*, 1993, Prime and Whitsides, 1993, Wiencek and Fletcher, 1997, Taylor *et al.*, 1997, Teixeira and Oliveira, 1999). According to van Oss (1997), hydrophobic interactions are usually the strongest of all long-range non-covalent interactions in biological systems and can be defined as the attraction between apolar or slightly polar entities (molecules, particles or cells) when immersed in water. It must be noted that hydrophobic attraction can prevail between one hydrophobic and one hydrophilic entity immersed in water, as well as between two hydrophobic surfaces (van Oss, 1995). The interaction between two hydrophobic surfaces is favoured in aqueous medium because they can establish a closer contact by squeezing the water in between. In other words, an increasing degree of hydrophobicity enhances adhesion. This has been confirmed by recent studies on the selection of supports for different types of biofilm reactors and using different bacterial strains. One example is the relation found between the higher degree of hydrophobicity of some polymeric materials and the increased biofilm activity of a consortium of autotrophic nitrifying bacteria (Sousa *et al.*, 1997). A more direct relation was established between the number of initially adhered cells of *Alcaligenes denitrificans* and the hydrophobicity of polymeric supports: the number of adhered cells increased linearly with the increase in hydrophobicity (Teixeira and Oliveira, 1999). A linear correlation was also obtained between the amount of attached biomass of an anaerobic consortium and the hydrophobicity of the supports: foam glass, pozzolana, clay and sepiolite (Pereira *et al.*, 1999).

The newest generation of suspended carriers biofilm reactors were designed to have a high biofilm area, which allows for higher loading rates and smaller space requirements. The smaller the diameter of the carrier particles the higher the surface area available for biofilm development. Particles with diameters as small as 0.2 mm have been used in airlift reactors (Heijnen *et al.*, 1992). It is interesting to note that even in fluidised bed

reactors it is possible to use dense particles (e.g. basalt) with small diameters without having high pumping power requirements because there is a drastic decrease in density when the particles become covered by the biofilm. Another means to provide more area for biomass attachment is to use rough and/or porous surfaces. Moreover, this is also a way to provide niches to retain micro-colonies, shielding them from the effects of shear forces (Bryers, 1987). For the purpose of colonisation, some authors consider surface roughness as one of the most important parameters (Gjaltema *et al.*, 1997), even more important than internal surface area (Petrozzi *et al.*, 1991). In order to accumulate large quantities of biomass, the porosity must be suitably sized. According to Messing and Opperman (1979 (a) and (b)), the adequacy of the pore size depends upon the cell dimensions and its mode of reproduction: fission, budding or spores (with mycelial growth). For instance, for microbes reproducing by fission at least 70% of the pores should have diameters up to five times the largest major dimension of the microbial cell. Other authors (Shimp and Pfaender, 1982) also confirmed that surface colonisation is favoured when crevices are microbially sized.

However, micro-organisms retained in pores or niches can be subjected to diffusional resistance to the flux of substrates and products. This is exemplified in a study already mentioned (Pereira *et al.*, 1999), where foam glass, pozzolana, clay and sepiolite were compared as supports for an anaerobic consortium. Sepiolite, although having the highest biomass retention, showed the lowest specific biological activity. This is a consequence of the combined effect of the small pore size of sepiolite and the high amount of attached biomass, promoting a deficient nutrient transport to the cells in the inner zones. Another point to be considered is the accumulation of gaseous metabolites inside porous carriers because this can induce the carriers washout, with a negative effect in the overall performance. This problem is overcome if the carriers have large pores with large internal porous volume because this enables the transport to be mediated also by convective flow.

The carrier concentration determines the available surface area for microbial attachment, but at the same time acts as a controlling factor of biofilm formation. Biofilm formation is balanced by biofilm detachment. In suspended bed reactors, where shear and abrasion is considerable, the detachment is mainly caused by particle-particle collisions (Heijnen *et al.*, 1992). The collision frequency depends on the size, the relative velocity and concentration of particles. In an airlift reactor, the rate of biomass detachment was found to be linear with the concentration of particles up to a solids hold-up of 30% (v/v) (Gjaltema, 1996).

### Reactor Start-Up

In biofilm reactors there will always exist a competition between organisms growing in suspension and organisms growing in the biofilm. Significant biofilm formation only occurs under conditions where suspended cells are quickly washed-out (Heijnen *et al.*, 1992). Generally this is accomplished by starting the reactor in batch mode until a significant amount of biomass is reached and then gradually increasing the dilution rate (lowering the hydraulic retention time) until the maximum growth rate of the culture is surpassed. From laboratory experience, in reactors with high shears (namely air-lift, circulating bed and fluidised bed), it is advisable to pre-colonise the supports outside the reactor in a sort of fed-batch mode, especially if the micro-organisms are slow growing.

That is to say, the culture medium must be periodically replaced by fresh medium, according to the microbial growth rate (Teixeira and Oliveira, 1998). Otherwise, if directly inserted in the reactor, a great number of carriers will remain bare. In the case of methanogenic bacteria, one method to encourage their growth is to supply a substrate that may be directly metabolised such as methanol (Balaguer *et al.*, 1992). The start-up period of anaerobic reactors can also be reduced with the adaptation of the inoculum to the specific substrate properties. It is preferable therefore to use a mix of several sources of active biomass instead of an inoculum from one source only.

When the biofilms are formed by heterotrophs producing large amounts of exopolymers it is common for thick biofilms to develop in the quieter parts of the reactors, as reported by Gjaltema *et al.* (1997). In extreme cases this can lead to the clogging of the reactor. Those situations become worse when working with high C/N ratios, which enhance the production of exopolymers. So, the C/N ratio must be controlled to avoid such undesirable biofilm formation.

## BIOFILM PROPERTIES, FORMATION AND PERFORMANCE

### Composition and Structure

The following characteristics may be considered typical of microbial films:

- they are slimy layers with gel-like consistency and viscoelastic rheological behaviour;
- their colours vary from translucent white or yellowish to dark brown or black, depending on the type of prevailing micro-organisms and substrates;
- they can have thicknesses that go from a few micra (films formed in liquids with low substrate concentration) to some millimetres or even centimetres (e.g., in the so-called “white waters” of pulp and paper mills);
- most of the wet biofilm mass is water (frequently, more than 90%);
- the mass of extracellular polymers, typically containing polysaccharides and glycoproteins, may represent 70% or more of the dry weight of the biofilm;
- the fraction of micro-organisms in biofilms depends on the metabolic characteristics of the microbial populations and on the substrate concentration, and it may correspond to 10% to 50% of the dry biomass.

The biofilm matrix is a natural structure built by the micro-organisms in what seems to be a way of protecting themselves from external aggressions—either physical, chemical or biological—and of finding suitable sites where nutrients can be more easily available. The extracellular polymers contribute both to the initial adhesion of the microbial cells to the surface and to the internal cohesion of the matrix due to the links established between the polymeric chains. This network tends to offer some resistance to the diffusion of components, be they toxic compounds or nutrients, and it can favour the adsorption of molecules as well as the capture and accumulation of external particles within the biofilm.

Biofilm structure has been a matter of considerable discussion in recent years (Lappin-Scott and Costerton, 1995; de Beer and Stoodley, 1995; van Loosdrecht *et al.*, 1995). The surface of most biofilms is wavy, sometimes with protruding visco-elastic filaments that

penetrate into the water. Microbial biofilms are not homogeneous matrices, showing regions with different concentrations of cells and polymers, together with water containing "voids". There is some controversy over whether the distribution of biomass is based only on randomly localised "clusters" of cells plus biopolymers, separated by water channels (de Beer and Stoodley, 1995), or based on superimposed porous layers of biomass with different densities and compositions (Christensen and Characklis, 1990). Both concepts seem to coexist in practical situations. Each cluster of biomass (cells and biopolymers) may include different layers, containing either distinct microbial populations, or similar populations in different metabolic states, or even just

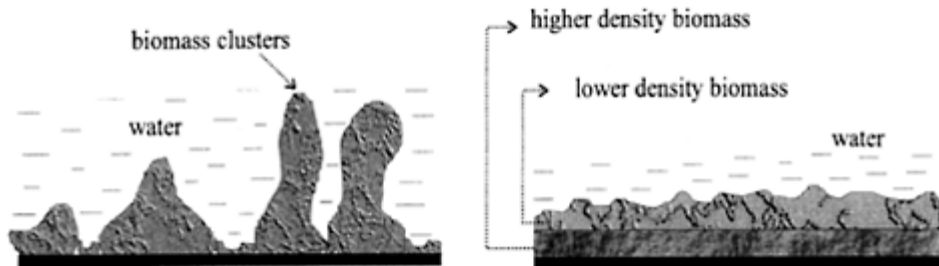


**Figure 10.3** Two conceptual models of biofilm structure.

different concentrations of cells and non-living biomass. It may happen that the cluster structure approaches the layer model as the biofilm grows older and the "void" spaces (water channels) are filled with more biopolymers and cells, as well as with organic and inorganic debris. This statement is supported by data showing the increase of biofilm density with time (Trulear, 1983). The two structural models are schematically presented in Figure 10.3.

### Dynamics of Biofilm Formation

The build up of microbial films is usually preceded by the adsorption of a thin layer of organic macromolecules to the adhesion surface, sometimes comprising also metallic hydroxides or oxides and very fine mineral powders (Chamberlain, 1992). The effect of organic films in promoting the biofouling of surfaces submerged in sea water had also been reported long time ago by Zobell and Allen (1935).

Micro-organisms suspended in the liquid are transported by diffusion, convection or self motility to the initially clean surface. Once at the solid surface, irreversible adhesion is favoured by the formation of "polymer bridges" between the adsorbed layer of macromolecules and the biopolymers excreted by the microbes (Characklis and Marshall, 1990). The "induction or lag period" of the biofilm development includes the adsorption of the organic conditioning film plus the first phase of microbial attachment before exponential growth of the biofilm begins.

Mass transfer mechanisms play an important role in the transport of dissolved nutrients and substrates (oxygen, sugars, organic acids, etc.) to the micro-organisms on

the solid surface, providing them with the essential elements for their metabolism. As a result, the biofilm mass increases by means of the growth and multiplication of microbes together with the production of the polymeric matrix. Above a certain thickness, the microbial metabolism inside the biological layer can become limited by the internal resistance to mass transfer of substrates, and also by the fact that the micro-organisms located near the biomass-liquid interface will tend to consume most of the substrate before it reaches the inner zones of the biofilm. At the same time, products from microbial metabolism are carried away from the biofilm. Apart from the initial period of surface inoculation, the transport and adhesion of new micro-organisms to the biofilm seems to have a minor role in the build up process, as compared to the growth processes that depend on substrate availability (Bott, 1995).

The processes described above contribute to the growth of the biological layer. Simultaneously, detachment processes occur, often promoted by the hydrodynamic forces of the fluid flowing over the biofilm surface, resulting in its erosion or even in the disruption ("sloughing off") of portions of the attached biomass. Even in the absence of fluid shear forces thicker biofilms may also slough off on account of their weaker internal cohesion and lack of nutrients in the inner zones. The competition between the biological growth and the detachment phenomena leads to a final balance where a maximum average thickness (subject to fluctuations due to the periodic detachment) of the biofilm is reached, which is sometimes considered a pseudo-steady state.

The structure and biological activity of microbial films depend on the history of their formation, including not only the specificities of the microbial populations involved in this process, but also the effects of environmental parameters such as the liquid velocity, temperature and pH, the nature and concentration of the substrate(s) and the surface properties (Bott, 1995; Characklis and Marshall, 1990; Messing and Oppermann, 1979a; Mott and Bott 1991; Vieira *et al.*, 1993). Biofilm development is favoured when the temperature and pH approach the optimum values for microbial growth, although it should be stressed that the conditions inside the biofilm are different from those in the surrounding liquid. The pH is particularly affected by the metabolic products excreted by the micro-organisms in the attached layer. A well documented example is the nitrogen biological removal process, which includes the nitrification and denitrification steps. While the pH inside nitrifying biofilms tends to decrease due to the production of H when  $\text{NH}_4^+$  is oxidised to  $\text{NO}_3^-$ , the opposite occurs in biofilms containing denitrifying micro-organisms (Harremoes, 1978).

The composition of the liquid, particularly the nature and concentration of nutrients and substrates, has a direct influence on biofilm development. A higher carbon/nitrogen ratio seems to favour bacterial attachment and the production of biopolymers (Veiga *et al.*, 1992), leading to an increase in biomass concentration in the reactor. Experiments were carried out where the substrate was suppressed from the liquid (Bott, 1995; Vieira and Melo, 1995) and, as a result, part of the microbial film detached from the surface within a few hours or, at the most, one day. This period of time was remarkably increased when small clay particles (around 10  $\mu\text{m}$ ) were incorporated in the biofilm during its development (Vieira and Melo, 1995).

The liquid velocity in contact with the biofilm is a major parameter that affects the dynamics of its development and its structure. In turbulent flow, higher velocities tend to originate thinner biofilms: although nutrient mass transfer to the biofilm surface increases

with velocity at an almost linear rate, hydrodynamic detachment forces have a stronger impact, since they are proportional to the square of the velocity. However, some experiments carried out with water at velocities below  $1\text{ m.s}^{-1}$  showed an increase of the biofilm thickness with the velocity, meaning that in those cases substrate mass transfer was the process controlling the biofilm growth rate (Bott, 1995). Such situations are usually favoured by low bulk substrate concentrations.

Additionally, the liquid velocity has also a significant effect on the structure of the microbial layer: Christensen and Characklis (1990) reported a linear increase in biofilm density (dry mass per unit wet volume) with shear stress; Vieira *et al.* (1993) measured densities of  $14\text{ kg.m}^{-3}$  and  $21\text{ kg.m}^{-3}$  for water velocities of  $0.34\text{ m.s}^{-1}$  and  $0.54\text{ m.s}^{-1}$ , respectively.

Biofilms formed under low velocities, particularly in non-turbulent conditions such as those occurring in many waste water treatment bioreactors, can be very thick—sometimes preventing substrates from reaching the inner zones—and/or have a very “loose” and “fluffy” consistence. In such cases, there is a high probability of occurring the detachment of biomass lumps (“sloughing off”) resulting in an unstable operation of the bio-reactor.

Hermanowicz (1999), using two-dimensional modelling, predicted that higher shear stresses and substrate concentrations lead to more compact layers and that a decrease in the liquid velocity results in a more open biofilm structure with protuberances extending from the biomass into the flowing liquid.

### **Biological Activity**

Here, biological activity is considered as the rate at which biofilms metabolise substrates and nutrients. Basically, it depends on the nature and concentration of the microbial species present in the biofilm, on the chemical composition and mass transfer properties of the surrounding fluid and on the physical structure of the attached biomass. The latter is also affected by the environmental conditions, including the hydrodynamics and the surface properties and morphology, as discussed before.

The distribution and metabolic state of the micro-organisms within a biofilm is a most sensitive aspect in terms of its performance. If the consumption of substrate in the upper part of the biofilm and/or the mass transfer resistance offered by the polymeric network lead to substrate depletion in the inner zones, the latter will remain fairly inactive as regards that substrate; this means that the bacteria in those zones will either be able to survive with residual nutrients or change their metabolism and start consuming other compounds existing in the liquid (which may correspond to the development of new species or strains). It has been shown by different authors (e.g., Trulcar, 1980; Capdeville *et al.*, 1992) that in thicker biofilms only a small portion of its mass is in fact active in metabolising a given substrate: for example, Trulcar (1980) found that a mono-species biofilm fed with  $2\text{ mg/m}^2.\text{min}$  of glucose had the same substrate consumption rate when its thickness was  $25\text{ }\mu\text{m}$  as when its thickness was  $100\text{ }\mu\text{m}$ , a few days later. Capdeville *et al.* (1992) showed that the active biomass in aerobic biofilms formed under different substrate concentrations was the same (around  $0.1\text{ mg/cm}^2$ ), in spite of the total mass of the several biofilms being quite different. Hamdi (1995) defined a critical diameter for flocs and biofilms, above which there will be inactive zones within the biomass.

There are cases where the activity of biofilms is dependent on the relative concentrations of different substances in the liquid. For instance, in an ammonia oxidation process carried out in rotating disk systems, it was found that if the ratio of bulk oxygen to ammonia is below  $2.5 \text{ gO}_2/\text{gN-NH}_4^+$  the ammonia consumption rate will be limited by the oxygen concentration (Gönenç and Harremoes, 1985). Other authors (Nogueira *et al.*, 1999), working with thinner nitrifying biofilms in a circulating bed reactor, under turbulent flow, obtained a lower critical value of  $1.5 \text{ gO}_2/\text{gN-NH}_4^+$ , which could be explained by the reduced resistance to oxygen transport within the thinner biofilms.

The following is an interesting example (Mendez *et al.*, 1989) of the effect that the history of a biofilm has on its performance: two anaerobic biofilm reactors using clay particles as supports for the fixed biomass were fed with the same carbon source, but with different carbon/nitrogen ratios (250/7.5 and 250/1.5). The reactor with less nitrogen content presented a higher concentration of the attached biomass than the other, although the suspended biomass concentration was the same in both. The conversion rate and the methane production rate obtained in the two reactors were also similar. However, significant differences appeared when pulses of volatile fatty acids were introduced: the nitrogen deficient reactor showed a lower conversion rate of these fatty acids, meaning that its biofilm had less active bacteria (and probably much more polymers) than the other. In fact, the specific activity of the nitrogen deficient microbial layer was one third of the biofilm fed with a greater amount of nitrogen compounds. It can then be said that thicker biofilms do not necessarily correspond to more active ones, mainly if their mass is essentially composed of extracellular polymers. Much depends on the amount of active bacteria they contain.

### Biofilms versus Suspended Biomass

The basic advantage of biofilm reactors over suspended biomass systems (either with dispersed cells or with flocs) is that the former are able to retain much more biomass—5 to 10 times more, per unit volume of the reactor—substantially reducing its wash out and allowing for a more stable operation with a higher biomass concentration. As a consequence, the investment in downstream liquid-solid separation equipment is much smaller, the reactors are more compact and offer a greater flexibility in terms of the hydrodynamic operating conditions (different flow rates or hydraulic residence time can be chosen without the risk of washing out the biomass). The structure of the biofilm matrix favours the resistance of its microbial cells not only to hydraulic shocks but also to toxic substances that can unexpectedly get into the reactor with the liquid stream.

A further advantage of biofilms is that they offer enhanced possibilities of transferring metabolites from one species to another, due to their spatial proximity. A study on an anaerobic fixed bed reactor carried out by Miyhara and Noike (1995) demonstrated that the degradation of long chain fatty acids was more easily accomplished in the biofilm than in the suspended biomass, because the lipolytic bacteria that produce hydrogen are surrounded by hydrogen consuming bacteria (methanogenic). This spatial arrangement is possible in an aggregated biomass and not in dispersed biomass, and it favours the interspecies exchange of hydrogen, which is determinant for the success of the anaerobic process.

However, fixed biomass does not necessarily have higher biological activity per unit of organic dry mass than the suspended cells or flocs, in terms of substrate consumption rate, partly on account of the internal diffusional limitations caused by the polymeric matrix. For example, in nitrification experiments (Wiesmann, 1994), values around 0.2 g of  $\text{N-NH}_4^+$  per gram of dry biomass and per day were obtained for both activated sludges and biofilms. Since the total biomass concentration was significantly higher in the fixed biomass systems, it seems that either there were less active nitrifying bacteria in the biofilm than in the activated sludge, or each cell in the biofilm had, in average, a lower biological activity than one cell in the suspended biomass.

This raises a very important question about the metabolic state of the cells in biofilms: are their yield coefficients, maximum specific growth rates, saturation constants, etc., the same as when they are in suspension? Biofilm modelling has been developed by considering that the main differences in biological activity result from the fact that the substrate diffusional limitations are more severe in a biofilm than in a suspended biomass system. However, it does not seem correct to assume that the cells in the biofilm act in every other aspect as if they were freely dispersed, because the microenvironment around them can be totally different; not only the substrate concentrations can be lower than in suspended cultures, but also the distances between cells are much smaller. Additionally, there are increasing evidences of phenotypic changes in cells when they go from a planktonic growth mode to biofilms (Costerton and Lappin-Scott, 1995).

## BIOFILM REACTOR MODELLING

Biofilm reactors are usually calculated on the basis of lumped empirical parameters, the values of which are assumed to be known from previous experience. An example of such parameters is the so-called "eliminated load" (mass of substrate consumed per unit time and unit volume of the reactor), frequently referred to in the design of wastewater treatment plants (Harremoes and Henze, 1995). Hence, there are no generalised relationships between the lump parameters and operational or design variables like substrate concentration, liquid velocity, hydraulic residence time, biofilm thickness, support characteristics, etc.

As yet, not even the existing unstructured mathematical models based on a phenomenological approach of mass transfer and biological reaction rates (e.g., AQUASIM, see: Reichert 1994, 1995; Wanner and Reichert, 1996) are commonly used by the practical designers, on account of the lack of sound estimates of the kinetic and diffusion coefficients. In this section, a simple diffusion-reaction model, applied to a biofilm system, will be presented with the aim of estimating the bio-reactor volume and of offering the reader a basis for a quantitative analysis of the underlying mechanisms that affect the reactor performance. This can also be helpful in terms of the understanding of further developments of more sophisticated mathematical tools available for the design of bio-reactors.

### Diffusion-Reaction Model: Calculation of Substrate Consumption Rate for a Single Substrate and a Single Microbial Species in Steady-state Biofilms

The model will be described for the case of single limiting substrate and single microbial species in the biofilm, and the latter will be supposed to be in “steady state conditions”. By this, it is meant that the amount of attached biomass, its thickness and the rate of substrate consumption in the biofilm are constant with respect to time. Moreover, the equations will be applied to describe the case of a flat biofilm, that is, a microbial layer attached to one side of a flat particle or thin biofilms attached to particles of other shapes; here, the meaning of “thin” depends on the relative dimensions of the biolayer and the support particle: a biofilm may be considered “thin” if its thickness is smaller than roughly 30–50% of the radius of the support particle (supposing the latter is spherical). The model is derived from the well-known heterogeneous catalysis approach in chemical engineering (Froment and Bischoff, 1979), and its application to enzyme reactors and wastewater treatment biofilm reactors has been fully reported by several authors in the last decades (Harremöes, 1978; Cabral and Tramper, 1994; Harremöes and Henze, 1995).

Let  $r_f$  be the reaction rate inside the biofilm, that is, the substrate consumption rate per unit volume of wet biofilm ( $\text{kg} \cdot \text{m}^{-3} \cdot \text{s}^{-1}$ ),  $y$  the distance inside the biofilm, measured from the liquid-biofilm interface, and  $J$  the substrate flux through the biofilm, referred to the unit area of a microbial layer attached to a supposedly flat surface ( $\text{kg} \cdot \text{m}^{-2} \cdot \text{s}^{-1}$ ). A mass balance to the substrate across an element of thickness  $dy$  inside the biofilm results in:

$$\frac{dJ}{dy} = -r_f \quad (1)$$

Assuming unidimensional mass transfer in the biofilm, Fick's law will be written as:

$$J = -D_f \frac{dS_f}{dy} \quad (2)$$

where  $S_f$  is the substrate concentration inside the biofilm at a distance  $y$  from the biofilm-liquid interface, and  $D_f$  is the effective diffusion coefficient (also called “effective diffusivity”) of the substrate in the microbial layer. This coefficient may not be equal to the molecular diffusivity of the same compound in the liquid phase, on account of the tortuosity and porosity of the biofilm and of the fact that convective flow (and not only molecular diffusion) may also take part in the transport of substrates inside the microbial matrix (Stoodley *et al*, 1994).

The steady-state diffusion-reaction differential equation is obtained from Equations (1) and (2):

$$D_f \frac{d^2S_f}{dy^2} = r_f \quad (3)$$

Once the expression for the biological reaction rate ( $r_f$ ) is known, the next problem is the integration of Equation (3). In the present case, an equivalent of the traditional Monod formula will be used to describe the kinetics of biomass production and substrate consumption in the biofilm. It should be stressed that the Monod model was developed

only for describing the specific growth rate of suspended cells in simple situations (e.g., without substrate or product inhibition, in dilute solutions). Therefore, the application of such a model to a system where cells are entrapped within a polymeric matrix built by themselves, should be carried out with extreme caution, since the environment around the cells can be totally different from the one encountered by dispersed cells in solution.

The original Monod equation is:

$$\mu = \mu_{\max} \frac{S}{K_s + S} \quad (4)$$

where  $K_s$  is the affinity (or “saturation”) constant of the suspended cell culture; it can be interpreted as the substrate concentration for which the specific growth rate ( $\mu$ ) will be equal to half the maximum specific growth rate ( $\mu_{\max}$ ) and the higher is its value, the lower is the affinity of the micro-organism with the substrate. The specific growth rate is defined as the mass of new cells produced per unit mass of existing cells and per unit time ( $\text{kg} \cdot \text{kg}^{-1} \cdot \text{s}^{-1}$ ).  $S$  is the bulk substrate concentration in the solution.

The adaptation of the Monod concept to biofilms implies the introduction of a few modifications. Since the active cells in a biofilm produce not only new cells but also a substantial amount of exopolymers, a new variable, called “specific biofilm production rate” ( $\mu_p$ ), should be defined: it represents the mass of cells and exopolymers (dry biofilm) produced per unit time and per unit mass of the biofilm. Then, the Monod equation will be transformed into:

$$\mu_p = (\mu_p)_{\max} \frac{S_f}{K_s + S_f}, \quad (5)$$

$(\mu_p)_{\max}$  being the maximum value of the specific biofilm production rate and  $S_f$  the substrate concentration inside the biofilm. Note that the value of  $K_s$  in a biofilm is not necessarily the same as in a suspended culture.

If  $(X_f)_a$  is the active cell density in the microbial film (that is, the mass of active cells per unit volume of wet biofilm,  $\text{kg} \cdot \text{m}^{-3}$ ), and  $Y_{f/S}$  is the mass of dry biofilm (cells plus exopolymers) produced per unit mass of substrate consumed in the biofilm (kg of dry biofilm/kg substrate), the following relationship applies:

$$r_f = (\mu_p)_a \frac{(X_f)_a}{Y_{f/S}} \quad (6)$$

where  $(\mu_p)_a$  is the mass of dry biofilm produced per unit time and per unit mass of active cells in the biofilm. If the whole biofilm is biologically active, then  $(\mu_p)_a = \mu_p$ .

The biofilm reaction rate equation will then be given by:

$$r_f = (r_f)_{\max} \frac{S_f}{K_s + S_f} \quad (7)$$

In this equation,  $(r_f)_{\max}$  is the maximum substrate consumption rate per unit volume of wet biofilm. Substitution of Equation (7) into Equation (1) results in the following equation, which has to be integrated to obtain  $r_f$ :

$$D_f \frac{d^2 S_f}{dy^2} = (r_f)_{\max} \frac{S_f}{K_s + S_f} \quad (8)$$

Solutions of this equation are generally obtained by numerical methods. The analytical integration of the equation is however possible in particular situations, such as in the case of intrinsic first order (low substrate concentrations,  $S_f$  substantially lower than  $K_s$ ) and zero order reactions (high substrate concentrations,  $S_f$  substantially higher than  $K_s$ ). In those cases, as indicated in Figure 10.4, Equation (8) will be reduced to:

$$D_f \frac{d^2 S_f}{dy^2} = (r_f)_{\max} S_f \quad (\text{first order reaction}) \quad (9)$$

or to;

$$D_f \frac{d^2 S_f}{dy^2} = (r_f)_{\max} \quad (\text{zero order reaction}) \quad (10)$$

As shown in Figure 10.4, the reaction rate constants for the two limiting cases are:

$$\text{First order biofilm reaction (s}^{-1}\text{)} : \quad k_{lf} = \frac{(r_f)_{\max}}{K_s} \quad (11)$$

$$\text{Zero order biofilm reaction (kg.m}^{-3}.s^{-1}\text{)} : \quad k_{of} = (r_f)_{\max} \quad (12)$$

So far, we have only described the reaction and diffusion phenomena inside the microbial layer. In the more general case, where the external mass transfer (in the liquid medium) may also control the consumption rate, the mass transfer resistance in the liquid film next to the biofilm surface should be incorporated in the model. In steady state conditions, the rate of external mass transfer will be equal to the overall rate of diffusion and reaction in the biofilm. Therefore, if  $J_e$  is the external mass transfer rate of substrate in the liquid:

$$J_e = k_m(S - S_i) \quad (13)$$

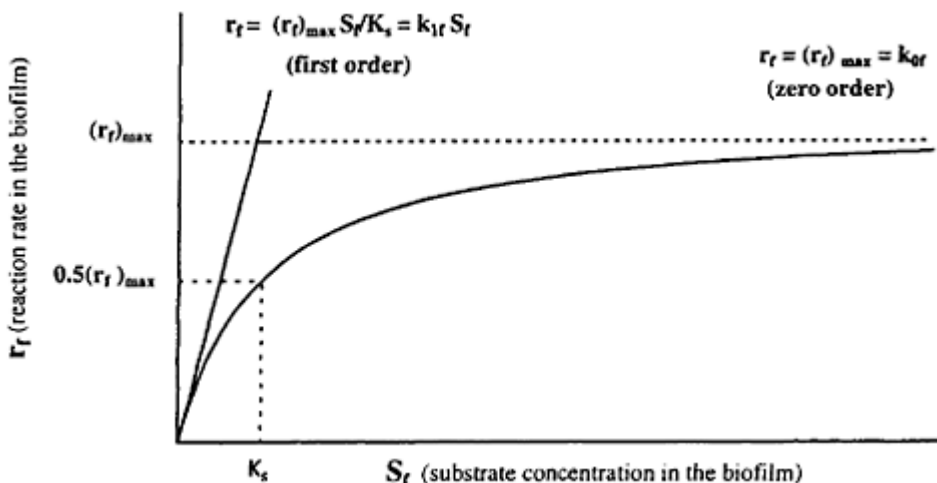


**Figure 10.4** Graphic representation of the Monod type reaction rate model and its two limiting cases (first order and zero order).

where  $k_m$  is the external mass transfer coefficient, and  $S$  and  $S_i$  are the substrate concentrations in the bulk liquid and at the biofilm-liquid interface, respectively, then:

$$J_e = r_f \quad (14)$$

In biofilm reactors, it is more common to calculate the “surface reaction rate”,  $r_A$  ( $\text{kg}_{\text{substrate}} \cdot \text{m}^{-2} \cdot \text{s}^{-1}$ ), that is the substrate consumption rate per unit area of biofilm. This variable is related to  $r_f$  through:

$$r_A = r_f L_f \eta \quad (15)$$

where  $L_f$  is the thickness of the microbial layer and  $\eta$  is the overall efficiency of the biofilm (see below).

The following integrated expressions may be obtained to estimate the substrate consumption rate per unit surface area of biofilm:

a) First order intrinsic reaction:

$$r_A = \frac{S}{\frac{1}{k_m} + \frac{1}{\eta_i k_{lf} L_f}} \quad (16)$$

The “biofilm internal efficiency” ( $\eta_i$ ) represents the ratio between the actual substrate consumption rate and the substrate consumption rate that the biofilm would display if there were no internal diffusional limitations. This parameter is given by:

$$\eta_i = \frac{\tanh \phi}{\phi} \quad (17)$$

and  $\phi$  is the Thiele modulus for a first order reaction for a flat plate:

$$\phi = \sqrt{\frac{k_{lf} L_f^2}{D_f}} \quad (18)$$

The Thiele modulus represents the ratio between the reaction rate and the internal diffusion rate. When the Thiele modulus has a small value, the biological reaction will be the rate limiting step. For high values of  $\phi$ , internal diffusion will control the rate of substrate consumption. The more general expression of the Thiele modulus, which can be applied to reactions of any order "n" is:

$$\phi = \phi \sqrt{\frac{(n+1)k_{nf}L_f^2S_i^{n-1}}{2D_f}} \quad (19)$$

$k_{nf}$  is the rate constant for a reaction of order "n".

The concentration profile in the biofilm (Figure 10.5), in the case of first order kinetics, is:

$$\frac{S_f}{S_i} = \frac{\cosh[\phi(1 - \frac{y}{L_f})]}{\cosh(\phi)} \quad (20)$$

where  $y$  is the distance inside the biofilm (measured from the liquid-biofilm interface) corresponding to the concentration  $S_f$ .

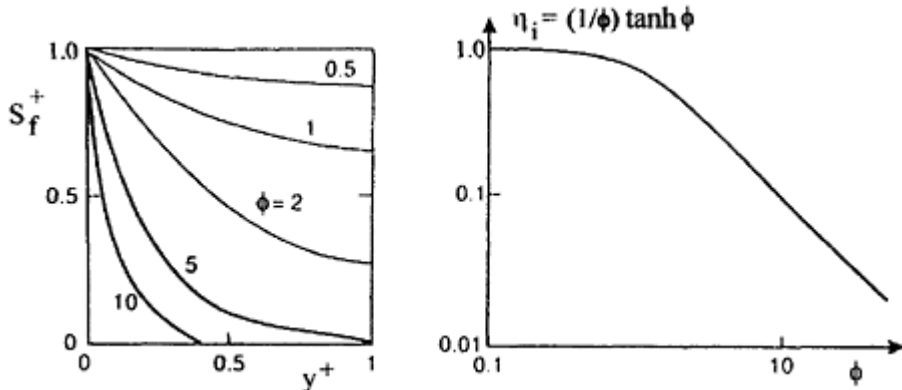


**Figure 10.5** Dimensionless concentration ( $S_f^+ = S_f/S_i$ ) as a function of the dimensionless distance inside

the biofilm ( $y^+ = y/L_f$ ) for a flat biofilm with first order kinetics at several values of the Thiele modulus ( $\phi$ ) and efficiency factor ( $\eta_i$ ).

Sometimes, the observed reaction rate per unit area of biofilm ( $r_A$ ) is written as:

$$r_A = \eta k_{lf} L_f S \quad (21)$$

where  $\eta$  is the overall biofilm efficiency for a flat plate:

$$\frac{1}{\eta} = \frac{1}{\eta_i} + \frac{k_{lf} L_f}{k_m} = \frac{1}{\eta_i} + \frac{\phi^2}{Bi} \quad (22)$$

$Bi$  is the mass transfer Biot number which represents the ratio between the maximum external mass transfer rate and the maximum internal mass transfer rate:

$$Bi = \frac{k_m L_f}{D_f} \quad (23)$$

Equations (16) and (21) are simply two different forms of the same expression,

b) Zero order intrinsic reaction:

$$r_A = \frac{k_m S}{2\lambda^2} \left[ \sqrt{1 + 4\lambda^2} - 1 \right] \quad (24)$$

where;

$$\lambda = \frac{k_m \sqrt{S}}{\sqrt{2k_{of} D_f}} \quad (25)$$

$\lambda$  is a dimensionless variable that represents the ratio between the external mass transfer rate and the internal coupled diffusion-reaction rate.

If the external mass transfer is the limiting step of the overall process, then:

$$r_A = k_m S \quad (26)$$

If the internal phenomena of diffusion and reaction are much slower than the external mass transfer (consumption rate limited by internal processes), then:

$$r_A = \sqrt{2k_{of} D_f S} \quad (27)$$

When applying the equations for zero order kinetics, two extreme situations can be easily identified: either the biofilm is fully penetrated by the substrate or not. A new parameter  $\beta$ , which represents the degree of substrate penetration in the biofilm, is related to the reciprocal of the Thiele modulus for zero order intrinsic reactions:

$$\beta = \frac{\sqrt{2}}{\phi} = \sqrt{\frac{2D_f S_i}{k_{of} L_f^2}} \quad (28)$$

Here,  $\beta$  corresponds to the biofilm internal efficiency ( $\eta_i$ ) for a flat plate geometry and zero order reaction.

- bi) If the substrate fully penetrates through the whole microbial film ( $\beta > 1$ ), the surface reaction rate will be given by:

**no external mass transfer limitations :**  $r_A = k_{of} L_f$  (29)

or by;

**control by external mass transfer :**  $r_A = k_m S$  (26)

and the concentration profile will be:

$$\frac{S_f}{S_i} = \frac{\left(\frac{y}{L_f}\right)^2}{(\beta)^2} - 2\frac{\left(\frac{y}{L_f}\right)}{(\beta)^2} + 1 \quad (30)$$

In a fully penetrated biofilm, the reaction is of zero order throughout the whole biological layer.

- bi) When the substrate cannot fully penetrate the microbial film ( $\beta < 1$ ), then the surface reaction rate is given by Equation (27), above (no external mass transfer control):

$$r_A = \sqrt{2k_{of} D_f S} = k_{of} L_f \beta \quad (27)$$

In this case, the overall process (also named as the “apparent” or “observable” reaction) has a half-order dependency on the bulk substrate concentration. The concentration profile (Figure 10.6) inside the biofilm in the partially penetrated film is then:

$$\frac{S_f}{S_i} = \frac{\left(\frac{y}{L_f}\right)^2}{(\beta)^2} - 2\frac{\left(\frac{y}{L_f}\right)}{\beta} + 1 \quad (31)$$

The reaction rate constants for the first and zero orders are related by:

$$k_{of} = k_{if} K_s \quad (32)$$

where  $K_s$  is the affinity constant of the Monod model.

It can be shown (Harremoes and Henze 1995) that, by defining parameter as:

$$\alpha = \sqrt{\frac{k_{of} L_f^2}{K_s D_f}} \quad (33)$$

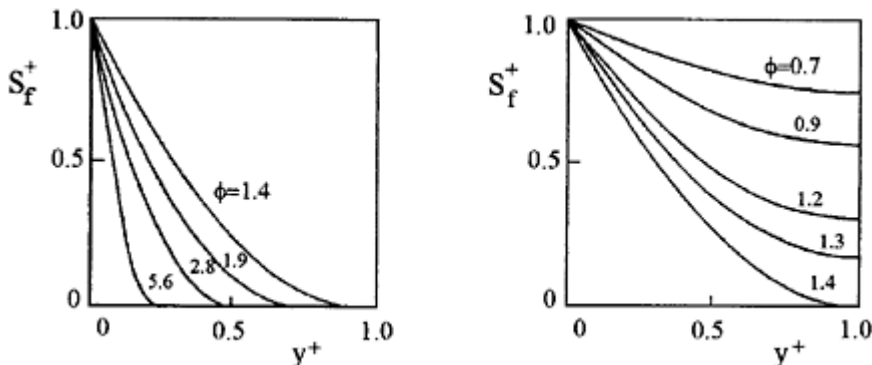


**Figure 10.6** Dimensionless concentration ( $S_f^+ = S_f/S_i$ ) as a function of the dimensionless distance inside the biofilm ( $y^+ = y/L_f$ ) for a flat biofilm with zero order kinetics at several values of the Thiele modulus ( $\phi$ ): (A) biofilm partially penetrated by the substrate; (B) biofilm fully penetrated by the substrate.

only first order or zero order reactions (and no half-order apparent reaction) can exist when  $\alpha < 2$ . If the concentration is low and the biofilm is thin (1st order process) or if the concentration is very high and the biofilm is totally penetrated (zero order process), diffusional limitations will not affect the order of the overall process; that is, an intrinsic zero order reaction in the biofilm will yield an apparent overall zero order reaction (process), and an intrinsic first order reaction will yield an apparent first order reaction.

For  $\alpha > 2$ , the apparent (or observable) “half-order” process will predominate for intermediate values of the substrate concentration, although the intrinsic order is zero. The half-order case emphasises the existence of strong diffusional limitations inside the biofilm.

Figure 10.7 shows the internal efficiency factor as a function of a “dimensionless observable modulus” ( $\psi$ ) for two different geometries, spheres and slabs. The new modulus  $\psi$  is defined as:

$$\Psi = \frac{r_A L_f}{D_f S_i} \quad (34)$$

#### *Limiting substrate*

Many biological degradation processes involve at least two nutrients or, more precisely, a nutrient/substrate and an electron acceptor: they are of the oxidation-reduction (redox) type. In order to use the diffusion-reaction model described above, it is essential to

identify the limiting substrate (substance), that is, the first one to reach zero concentration (that is, to be completely consumed) within the biofilm. This depends on the mass transfer and the reaction rates of the two components in the microbial layer. For the case of intrinsic zero order kinetics, and taking into account the penetration depths ( $\beta$ ), it can be easily shown (Harremoes and Henze 1995) that:

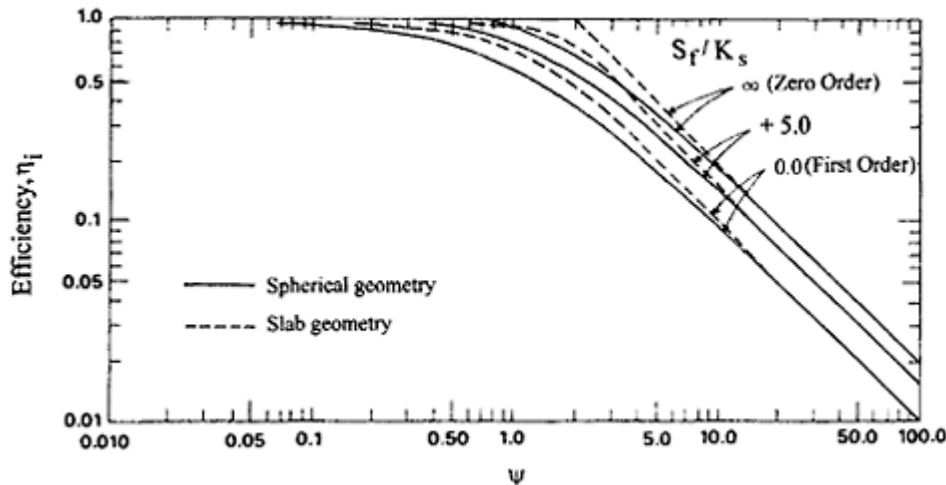


**Figure 10.7** Biofilm internal efficiency as a function of the “dimensionless observable modulus”  $\psi$  (equation 34).

i) the oxidant will be the limiting factor if:

$$\frac{S_{\text{ox}}}{S_{\text{red}}} < \frac{(D_f)_{\text{red}}}{(D_f)_{\text{ox}} N_{\text{ox/red}}} \quad (35a)$$

where the subscripts “ox” and “red” refer to the oxidant and reductant substance, respectively, and  $N_{\text{ox/red}}$  is the stoichiometric ratio between the two reactants;

ii) the reductant will be the limiting factor if:

$$\frac{S_{\text{ox}}}{S_{\text{red}}} > \frac{(D_f)_{\text{red}}}{(D_f)_{\text{ox}} N_{\text{ox/red}}} \quad (35b)$$

The previous equations apply to a flat biofilm. They can also be used when the biofilm is formed around a particle, provided that the microbial layer is thin. In the case of thick biofilms around small spherical supports or of microbial granules without any support surface, a spherical geometry should be considered in the derivation of the model, and the variable  $L_f$  in the Thiele modulus should be replaced by  $r_{pf}/3$  ( $r_{pf}$  is the radius of the spherical biofilm-particle). The reader should look in specialised textbooks on heterogeneous catalysis for further modifications to the model equations when using spherical or cylindrical particles.

### Calculation of Reactor Volume

Let  $\mathbf{Q}$  be the volumetric flow rate of the liquid through the system,  $S_1$  the inlet substrate concentration and  $S_2$  the substrate concentration at the reactor outlet. A simple mass balance to the substrate, from the inlet to the outlet of the reactor, results in:

$$\mathbf{Q}(S_1 - S_2) = r_A A_f \quad (36a)$$

In the case where the substrate concentration varies continuously along the reactor, it is advisable to write a differential balance:

$$QdS = -r_A dA_f \quad (36b)$$

$A_f$  is the surface area of the biofilm (the external mass transfer area), which will be here supposed to be smooth, that is, without filaments or protuberances. The case of spherical support (or carrier) particles will be considered below, although the biofilm can be modelled as a flat geometry.

#### *Ideal continuous stirred tank reactor*

Let  $r_p$  be the radius of the bare carrier particles (i.e., without biofilm) and  $L_f$  the thickness of the microbial layer. The surface area of the biofilm can then be related to the reactor volume ( $V_R$ ) through:

$$A_f = \frac{3V_R(1 - \varepsilon)}{L_f + r_p} \quad (37)$$

where  $\varepsilon$  is the porosity of the reactor (liquid volume over reactor volume, the latter containing liquid and particles with biofilm). Therefore, the reactor volume will be given by:

$$V_R = \frac{Q(L_f + r_p)}{3(1 - \varepsilon)k_{lf}L_f\eta} \cdot \ln \left( \frac{S_1}{S_2} \right) \quad (38)$$

In an ideal stirred tank reactor, the substrate concentration in the liquid will be the same in every point and equal to the outlet concentration. Therefore, the observed reaction rate  $r_A$  (per unit surface area of biofilm) will be given by equations (16) to (18) in the case of intrinsic first order reaction, with  $S=S_2$ , and by Equations (24) and (25) in the case of intrinsic zero order reaction, also with  $S=S_2$ .

If the biofilm is thin,  $(L_f+r_p)$  can be replaced by  $r_p$ .

#### *Ideal plug flow reactor*

In this case, the following simplified expressions can be used (Harremoes, 1978; Harremoes and Henze, 1995), assuming pseudo-homogeneity in the reactor (i.e., uniform substrate concentration along the cross section area of the reactor):

- i) First order reaction:

$$V_R = \frac{Q(L_f + r_p)}{3(1-\varepsilon)k_{if}L_f\eta} \cdot \ln \left( \frac{S_1}{S_2} \right) \quad (39)$$

- ii) Zero order reaction with full substrate penetration ( $\beta > 1$ ) and no external mass transfer limitations:

$$V_R = \frac{Q(L_f + r_p)}{3(1-\varepsilon)k_{of}L_f} (S_1 - S_2) \quad (40)$$

- iii) Zero order reaction with partial substrate penetration ( $\beta < 1$ ) and no external mass transfer limitations:

$$V_R = \frac{\sqrt{2S_1}(L_f + r_p)Q}{3(1-\varepsilon)\sqrt{k_{of}D_f}} \left( 1 - \sqrt{\frac{S_2}{S_1}} \right) \quad (41)$$

### ***Transition between different reaction orders***

Biofilms may be subject to different operating conditions within the same reactor, particularly in plug flow systems. Near the reactor outlet, a substantial amount of substrate will have been consumed and its concentration will be low, giving rise to a first order reaction in the biofilm. Near the reactor inlet, if the concentration is large enough, the biofilm may be completely penetrated (zero order overall process) or partially penetrated (half order overall process). Therefore, when calculating bioreactors, it is useful to have a way of detecting which reaction order will prevail in the biofilm system at each zone of the reactor. The following simple criteria can be applied:

- i) Transition from zero order to half order overall process:

The critical substrate concentration will be defined, by considering  $\beta=1$ , as:

$$S_{crit} = \frac{L_f^2 k_{of}}{2D_f} \quad (42)$$

Therefore, if  $S > S_{crit}$ , the overall process (apparent reaction) will be of zero order. On the other hand, if  $S < S_{crit}$ , the overall process will be of half-order.

- ii) Transition from half order to first order overall process:

In this case, the transition point will be defined in relation to the Monod saturation constant. When  $S > 2K_s$ , the apparent reaction will be of half-order. In the case of  $S < 2K_s$ , the process will be of first order.

### ***Values of the diffusion-reaction parameters: illustrative examples***

In spite of the limitations of the diffusion-reaction model, mainly those related to the supposed homogeneous distribution of the active biomass in the microbial layer, many reports have been published on its application to different substrates and different biofilm reactors. The purpose of such studies was often to obtain values of the biofilm kinetic

parameters by fitting the model to experimental data on substrate consumption rates in laboratory or larger scale reactors. Most of the time, the external mass transfer resistances were not taken into account, and only the *apparent* kinetic constants were estimated. Since it is considered that in wastewater treatment processes using biofilms the apparent kinetic order is in most cases 1/2 (Harremöes, 1978), Table 10.2 indicates typical values of the apparent half order constant ( $k_{1/2ap}$ ), which, from Equation (27), is:

$$k_{1/2ap} = \sqrt{2k_{of}D_f} \quad (43)$$

Although the data in Table 10.2 display some scattering, the order of magnitude of the  $k_{1/2ap}$  values is the same and there are no large inconsistencies in aerobic heterotrophic and autotrophic systems. This is somehow remarkable in view of the considerable differences between the cases studied (different reactors, different substrates, etc.), often without a real accurate control of the measured variables. Anyhow, design

**Table 10.2** Apparent half order kinetic constants in wastewater treatment ( $k_{1/2ap}$ .)

Biological process and Limiting metabolic factor	Reactor type	$K_{1/2ap} \cdot 10^5$ ( $\text{kg}^{1/2} \cdot \text{m}^{-1/2} \cdot \text{s}^{-1}$ )	Reference
Aerobic, heterotrophic biomass Oxygen	Fixed bed	0.12	Grasmick <i>et al.</i> (1982)
Aerobic, heterotrophic biomass Oxygen	Rotating drum	0.12–0.15	Harremöes <i>et al.</i> (1980)
Aerobic, heterotrophic biomass Glucose	Rotating drum	0.12	Harremöes (1978) Harremöes <i>et al.</i> (1980)
Aerobic, heterotrophic biomass Toluene	Waste gas trickling filter	0.07–0.11	Pederson and Arvin (1996)
Nitrification, autotrophic biomass Oxygen	Rotating disk	0.075–0.14	Gönenç and Harremöes (1985)
Nitrification, autotrophic biomass Oxygen	Submerged filter	0.05–0.10	Çeçen and Gönenç (1994)
Nitrification, autotrophic biomass Oxygen	Circulating bed reactor	0.15	Nogueira <i>et al.</i> (1998)
Nitrification, autotrophic biomass Ammonium	Rotating disk	0.06	Gönenç and Harremöes (1985)
Anaerobic, methanogenic biomass Acetate	Downflow filter	0.12	Hamoda and Kennedy (1987)
Anaerobic, methanogenic biomass Acetate	UASB	0.05	Brito and Melo (1997)
Anaerobic, methanogenic biomass Molasses	Upflow filter	0.04–0.48	Gönenç <i>et al.</i> (1991)

Anoxic, denitrifying biomass Methanol	Rotating drum	0.10–0.20	Jansen and Kristensen (1980) Jansen (1982)
Anoxic, denitrifying biomass Nitrate	Rotating drum	0.02–0.14	Jansen and Kristensen (1980) Jansen (1982)
Anoxic, denitrifying biomass Nitrate	Rotating disk	0.11	Watanabe (1978)

engineers do not seem yet to rely on such values for the efficient design of biofilm reactors.

So far, there are no widely acceptable values for other model parameters, such as the effective diffusion coefficient (Harremoes 1978; Henze and Harremoes 1995) and the Monod saturation constant, which may be quite different from the values obtained in suspended cell cultures, both of them having strong effects on the results yielded by the model.

Some authors advocate that the diffusion coefficient in biofilms should be taken approximately as 80% of the value in water, but there is much disagreement on the experimental values published in different sources (for example, some values are even larger than the coefficient in water). Table 10.3 presents only a few illustrative values of the diffusion coefficients in different biofilm systems.

Such large differences in diffusivities may be due to a variety of factors (Fan *et al.*, 1990, de Beer *et al.*, 1997) related to the nature of diffusing substance, the microbial species present and the physical structure of the biofilms. The latter is in turn very much dependent on the conditions under which the microbial layer was developed, among others the nature and concentration of the substrate, the hydrodynamic parameters (fluid velocity, turbulence), the presence of toxic substances, etc. Information about the precise chemical, microbiological and hydrodynamic parameters that affected the history of formation of the biofilm are missing in many of the publications reporting diffusivity values. Some authors have tried, with a certain degree of success, to correlate the diffusivity with biofilm properties such as the cell or biomass density in the attached layer. Fan *et al.* (1990) presented the following correlation based on the experimental data of a significant number of authors:

$$\frac{D_f}{D_w} = 1 - \frac{0.43 D_v^{0.92}}{11.19 + 0.27 X_v^{0.99}} \quad (44)$$

which shows that the diffusion coefficient decreases with the increase in the cell density ( $X_v$ ,  $\text{kg.m}^{-3}$ ) within the biofilm.  $D_w$  is the diffusion coefficient in water (variable  $X_v$  seems to represent biomass dry density and not only cell density, in spite of the authors having used this last name). Although this type of correlation is a step forward in the estimation of diffusivities, relationships between the biomass density in biofilms and the

**Table 10.3** Measured or estimated effective diffusion coefficients in biofilms

Diffusing component	Diffusion coefficient $\times 10^9$ (m <sup>2</sup> /s)	$D_f$ (biofilm)/ $D_f$ (water) (%)	References
Oxygen	2.2 (20°C)	105%	Kissel <i>et al.</i> (1984)
Oxygen	2.55 (20°C)	120%	Williamson and McCarty (1976)
Oxygen	1.75 (29°C)	66%	Nogueira <i>et al.</i> (1998)
Lithium chloride	0.33 (35°C)	33%	Nilsson and Karlsson (1989)
Glucose	0.08–0.63 (20°C)	15%–117%	Onuma and Omura (1982)

reactor operating conditions are needed to predict diffusion coefficients for proper reactor design.

The Monod saturation constant in biofilms is often considered similar to the one in cell suspensions, but this may be quite erroneous on account of the microenvironment surrounding the micro-organisms being quite different in a biological layer from that in a dispersed cell culture, leading to distinct metabolic states (Fletcher 1992a, 1992b).

### Mathematical Models for Multisubstrate and Multispecies Biofilms

The diffusion-reaction model presented above applies to simple situations where only one microbial species and one substrate are present. Sometimes, for the sake of simplicity, while incurring possible errors, the model has been applied to mixed cultures where one or more substrates are involved in the biochemical reactions. Empirical parameters can be obtained to describe the consumption of substrates in that specific situation, but it will not be advisable to try to apply those values to any other case. More complex models were published and tested for the cases where multisubstrate and/or multispecies are present, as well as when inhibiting factors or particulate material affect the biological process. A limited number of references is given below, for the reader interested in more specialised models or in further developments of the above model: Wanner and Reichert, 1996; Reichert, 1994, 1995; Coelhoso and Rodrigues, 1995; Bryers, 1993; van Ede *et al.*, 1993; San *et al.*, 1993; Droste and Kennedy, 1986; Wanner and Gujer, 1986.

Comparison of the behaviour of plug flow and continuous stirred reactors may be found in several published sources (Moser 1988; Rodrigues *et al.*, 1983).

The recent investigations on the composition and spatial distribution of biomass and void spaces within biofilms, using microelectrodes, confocal laser microscopy and molecular probes, led to the development of new multidimensional modelling strategies and techniques which may contribute to a better understanding and quantification of the activity, population dynamics, stability, morphology of microbial films, as well as of the dynamics of their transient growth processes (Wanner 1995; Ritmann *et al.*, 1999; Picioreanu *et al.*, 1999; Noguera *et al.*, 1999; Hermanowics, 1999).

### Practical Design Procedures for Reactor Calculation

For practical design purposes, empirical equations are still the most common method to calculate biofilm reactors in wastewater treatment processes. Trickling filters, the classical technology, have received more attention from the designers. One of the well known mathematical formulae for this case is (Metcalf and Eddy, Inc., 1987):

$$\frac{C_2}{C_1} = \exp \left[ -K_T Z A_v \frac{A_s}{Q} \right] \quad (45)$$

$C_2$  and  $C_1$  are the substrate concentrations at the outlet and the inlet of the reactor, respectively, expressed as  $\text{mg.L}^{-1}$  of soluble  $\text{BOD}_5$  (5-day biological oxygen demand, that is the dissolved oxygen used by the micro-organisms in the biochemical oxidation of soluble organic matter during an incubation period of 5 days).  $Z$  is the depth of the filter (m),  $A_v$  is the specific area of support per unit volume of reactor ( $\text{m}^2.\text{m}^{-3}$ ),  $A_s$  is the cross sectional area of the filter ( $\text{m}^2$ ) and  $Q$  the volumetric flow rate of the wastewater to be treated ( $\text{m}^3.\text{s}^{-1}$ ).  $K_T$  is the observed removal rate constant ( $\text{m.s}^{-1}$ ) at temperature  $T$ , which has been correlated with temperature through:

$$K_T = K_{20^\circ\text{C}} 1.08^{(T-20)} \quad (46)$$

For municipal wastewater, an approximate value of  $K_{20^\circ\text{C}}=0.10 \text{ m.day}^{-1}$  was suggested. For industrial wastewaters, values of  $K_T$  should be determined experimentally in pilot-plant studies using the same wastewater and support particles as the ones in the real case.

Practical rules recommended by different sources for the design of biological disk reactors show large differences (Harremöes and Henze 1995; McGhee 1991); values from 5 to 60  $\text{kg BOD.m}^{-2}.\text{day}^{-1}$  have been reported for domestic wastewater. Rotating speed at the tip of the disks should be around  $20 \text{ m.min}^{-1}$ .

### Overall Model for Biofilm Transient Development

The diffusion-reaction model was established for biofilms in steady state and does not allow calculations of the transient development of the microbial layer. The value of the steady-state biofilm thickness should be known in order to apply the model to reactor design. To predict the final biofilm thickness and mass or the time needed to reach steady state, biofilm growth models are needed. A simple overall model (Melo and Vieira, 1999) is presented below giving biofilm mass as a function of time.

Let  $m_f$  be the mass of attached biofilm per unit surface area, at a given time  $t$ . The change in  $m_f$  with time is the result of two competitive parallel phenomena; the production of biomass by the micro-organisms in the biofilm and the removal of attached biomass (biofilm detachment) caused by the hydrodynamic forces:

$$\frac{dm_f}{dt} = M_p - M_d \quad (47)$$

$M_p$ —“biofilm production flux” (increase in biofilm mass per unit time and unit surface area, associated to the production of biomass—cells plus extracellular polymers—as the result of the microbial activity within the biofilm),  $\text{kg m}^{-2} \text{ s}^{-1}$ .

**M<sub>d</sub>**—“biofilm detachment flux” (decrease in biofilm mass per unit time and per unit surface area, associated to the detachment of parts of the biological deposit caused by the fluid forces), kg m<sup>-2</sup> s<sup>-1</sup>.

The “biofilm detachment flux” is assumed to be proportional to the amount of biomass attached to the surface, since the probability of existing “weak zones” in a thick biofilm is higher than in a thinner one. Therefore:

$$M_d = b m_f \quad (48)$$

where **b** is proportional to the hydrodynamic forces acting upon the biofilm surface and varies inversely with the cohesiveness of the biofilm (i.e., **1/b** represents the “mechanical strength” or the “resistance to detachment” of the biofilm).

As regards the “production flux” ( $M_p$ ), the colonisation of the clean surface by bacteria coming from the fluid is an essential feature only in the first hours of biofilm formation. Experimental results have shown that the subsequent growth of the biolayer is mainly due to the activity of the micro-organisms located in the attached film and not to the transport of new bacteria from the liquid to the biofilm surface (Bott and Miller, 1983; Melo and Vieira, 1999). Due to this biological activity and to diffusional limitations, the substrate concentration may in some cases decrease down to zero within the biofilm before reaching the surface of the support. Thus, modelling of the “biofilm production flux” ( $M_p$ ) must take into account two different situations (named below as *i* and *ii*) during the build up of the biofilm layer. A mono-species biofilm will be considered here.

### *i) Thick biofilm, partially penetrated by the substrate*

In this case, there is an “active layer” located in the outer part of the biofilm, and a “non-active” layer that occupies the inner part of the biofilm, close to the support. The latter contains microbial species with residual activity as regards the main substrate, plus polymeric substances and, possibly, other microbial species that do not use that substrate. If the biofilm is partially penetrated, then the active layer will have a constant thickness along the time, equal to the maximum depth of substrate penetration. On the contrary, the thickness of the inner layer can increase with time due, for instance, to the production of polymeric material by the micro-organisms in the active layer, which will result in an overall increase of the total amount of attached biomass.

As indicated before, let  $\mu_p$  be the “biofilm specific production rate”, that is, the mass of biofilm produced by the active layer per unit time and per unit mass of biofilm. Thus, at a given time t:

$$\mu_p = (\mu_p)_a \frac{(m_f)_a}{m_f} \quad (49)$$

where  $(\mu_p)_a$  is the (constant) biomass specific production rate of the active zone, i.e., the mass of biofilm produced per unit time and per unit mass of active layer, and  $(m_f)_a$  is the mass of active layer per unit surface area (constant with time). Therefore:

$$M_p = \mu_p m_f = (\mu_p)_a (m_f)_a = \text{constant} \quad (50)$$

### *ii) Thin biofilm, completely penetrated by the substrate*

In this case, the biofilm is biologically active (as regards the main substrate) throughout its entire depth, i.e.:

$$\mu_p = (\mu_p)_a \quad (51)$$

The mass of this active layer increases with time as the biofilm builds up, until its thickness reaches the maximum penetration depth. From this point on, case *i*) applies. It should be stressed, however, that the number of micro-organisms in the biofilm does not increase proportionally to the biofilm mass, because the result of their activity is not only the production of new microbial cells but also of extra cellular substances (biopolymers). The latter, although not biologically active, can be a major fraction of the biofilm mass. As a consequence, the rate of biomass produced per unit mass of biofilm will decrease with time, meaning that the *specific* activity (i.e., per unit mass) of the active layer will get lower as its mass builds up. Therefore, in a completely penetrated biofilm, it does not seem unreasonable to assume that  $\mu_p$  is inversely proportional to the mass of active layer at each instant of time:

$$\mu_p = (\mu_p)_a \propto \frac{1}{(m_f)_a} \quad (52)$$

where the symbol indicates proportionality. Since all the biofilm is active ( $m_f = m_{fa}$ ), the following equation may be applied to case ii):

$$M_p = (\mu_p)_a (m_f)_a = \text{constant} \quad (53)$$

### *Biofilm growth equation*

In both cases, *i*) and *ii*),  $M_p$  is constant. Replacing  $M_r$  in Equation (47) by Eq. (48):

$$\frac{dm_f}{dt} = M_p - bm_f \quad (54)$$

which, upon integration, results in the final equation of the overall model:

$$m_f = m_f^* [1 - \exp(-bt)] \quad (55)$$

where  $m_f^* = (M_p/b)$  is the maximum mass of biofilm, at steady state. Graphically, Equation (55) represents a curve that tends to an asymptotic value of  $m_f$  for  $t=\infty$ .

$M_p$  can be modelled in more detail by using the concepts and equations of heterogeneous catalysis summarised in the preceding sections (Vieira and Melo, 1999). Assuming that the biomass yield in the biofilm (that is, the mass of cells plus polymers produced per unit mass of substrate consumed by the active cells in the biofilm) is known, the substrate consumption rate, i.e., the overall apparent reaction rate ( $r_A$ ), can be calculated according to:

$$r_A = \frac{M_p}{Y_{f/s}} \quad (56)$$

By experimentally monitoring the growth curves of biofilms produced by a given microbial culture under different operating conditions, values of the parameters  $m^*$  and  $b$  can be correlated with variables such as substrate concentration, liquid velocity, temperature, pH, etc. This will enable the prediction of the steady-state biofilm mass for any set of operating conditions within the range of applicability of those parameters.

### CONCLUDING REMARKS

Microbial film reactors are still calculated by means of practical design criteria that are not based upon sound phenomenological equations such as the diffusion-reaction models. Those procedures have been used for many years in designing wastewater biofilm reactors but, although many processes are operating in quite acceptable conditions, some design errors and, most probably, over-design are the natural consequence of the lack of more reliable and precise calculation methods (Harremoes and Henze, 1995). Over-designed reactors imply excessive capital costs, and can also result in operational problems such as the instability of the bio-reactor due to the formation of thick biofilms that tend to detach or slough off, causing periodic poor performances. Efficient control of the microbial layer thickness has been discussed by several authors in the last decade (Capdeville *et al.*, 1992; Lazarova and Manem, 1994, 1997; Tijhuis *et al.*, 1994) as a way of achieving an enhanced reactor stability.

The major problems in biofilm modelling are not the unavailability of more or less sophisticated mathematical tools. They result from the lack of correlations able to produce values of the diffusion coefficients, the biological kinetic parameters and the biofilm thickness as a function of the operating conditions and reactor characteristics; from the lack of capacity to relate the composition and structure of the microbial film, particularly the density and spatial distribution of active cells, to the conditions under which the biofilm was formed; and from the lack of accurate information on the biomass yield in the biofilm. Obviously, all this implies a deeper knowledge of the microbial metabolism inside the biological matrix, including a better understanding of the physiological state of the micro-organisms and their kinetics in the specific micro-environment that surrounds them in a biofilm. The concurrent efforts of both engineering science (to develop semi-empirical models that relate intrinsic parameters to external operating and design variables) and biological science (to shed light on the behaviour of micro-organisms in attached biomass systems) are clearly needed.

### NOMENCLATURE

$A_f$	surface area of biofilm ( $\text{m}^2$ )
$A_s$	cross sectional area of the filter ( $\text{m}^2$ )
$A_v$	specific area of support per volume of reactor ( $\text{m}^2 \cdot \text{m}^{-3}$ )

$b$	reciprocal of the resistance to detachment
$Bi$	Biot number
$C_1$	substrate concentration at reactor inlet, as soluble BOD <sub>5</sub> (mg.L <sup>-1</sup> )
$C_2$	substrate concentration at reactor outlet, as soluble BOD <sub>5</sub> (mg.L <sup>-1</sup> )
$D_f$	effective diffusion coefficient or effective diffusivity (m <sup>2</sup> .s <sup>-1</sup> )
$(D_f)_{ox}$	effective diffusivity of the oxidant (m <sup>2</sup> .s <sup>-1</sup> )
$(D_f)_{red}$	effective diffusivity of the reductant (m <sup>2</sup> .s <sup>-1</sup> )
$D_w$	diffusion coefficient in water (m <sup>2</sup> .s <sup>-1</sup> )
$dy$	element of thickness (m)
$J$	substrate flux through the biofilm (kg.m <sup>-2</sup> .s <sup>-1</sup> )
$J_e$	external substrate flux (kg.m <sup>-2</sup> .s <sup>-1</sup> )
$k_m$	external mass transfer coefficient (m.s <sup>-1</sup> )
$K_s$	affinity (or saturation) constant of a suspended cell culture (kg.m <sup>-3</sup> )
$k_{nf}$	rate constant for a reaction of order n.
$K_T$	observed removal rate constant at temperature T (m.s <sup>-1</sup> )
$k_{0f}$	zero order biofilm reaction rate (kg.m <sup>-3</sup> .s <sup>-1</sup> )
$k_{1f}$	first order biofilm reaction rate (s <sup>-1</sup> )
$k_{1/2ap}$	apparent half order constant (kg <sup>1/2</sup> .m <sup>-1/2</sup> .s <sup>-1</sup> )
$L_f$	thickness of the microbial layer (m)
$M_d$	biofilm detachment flux (kg.m <sup>-2</sup> .s <sup>-1</sup> )
$m_f$	mass of attached biofilm per surface area (kg.m <sup>-2</sup> .s <sup>-1</sup> )
$m_f^*$	maximum mass of biofilm at steady state
$M_p$	biofilm production flux (kg.m <sup>-2</sup> .s <sup>-1</sup> )
$n$	order of reaction
$N_{ox/red}$	stoichiometric ratio between the oxidant and reductant
$Q$	volumetric flow rate (m <sup>-3</sup> .s <sup>-1</sup> )
$r_A$	reaction rate per unit area of biofilm or surface reaction rate (kg.m <sup>-2</sup> .s <sup>-1</sup> )
$r_f$	reaction rate inside the biofilm (kg.m <sup>-3</sup> .s <sup>-1</sup> )
$(r_f)_{max}$	maximum reaction rate per unit volume of wet biofilm (kg.m <sup>-3</sup> .s <sup>-1</sup> )
$r_p$	radius of the bare carrier particles (m)
$r_{pf}$	radius of the biofilm-particles (m)
$S$	bulk substrate concentration in the solution (kg.m <sup>-3</sup> )

$S_{\text{crit}}$	critical substrate concentration ( $\text{kg} \cdot \text{m}^{-3}$ )
$S_f$	substrate concentration inside the biofilm ( $\text{kg} \cdot \text{m}^{-3}$ )
$S_f^+$	dimensionless concentration inside the biofilm ( $S_f/S_i$ )
$S_i$	substrate concentration at the biofilm-liquid interface
$S_{\text{ox}}$	concentration of oxidant substance ( $\text{kg} \cdot \text{m}^{-3}$ )
$S_{\text{red}}$	concentration of reductant substance ( $\text{kg} \cdot \text{m}^{-3}$ )
$S_1$	substrate concentration at reactor inlet ( $\text{kg} \cdot \text{m}^{-3}$ )
$S_2$	substrate concentration at reactor outlet ( $\text{kg} \cdot \text{m}^{-3}$ )
$t$	time (s)
$T$	temperature ( $^{\circ}\text{C}$ )
$V_R$	reactor volume
$(X_p)_a$	active cell density in the biofilm ( $\text{kg} \cdot \text{m}^{-3}$ )
$X_v$	cell density within the biofilm ( $\text{kg} \cdot \text{m}^{-3}$ )
$y$	distance inside the biofilm measured from the liquid-biofilm interface (m)
$y^+$	dimensionless distance in the biofilm ( $y/L_f$ )
$Y_{\text{f/s}}$	mass of dry biofilm (kg)
$Z$	depth of the trickling filter (m)

### Greek Symbols

$\alpha$	parameter defined by equation (33)
$\beta$	degree of substrate penetration in the biofilm
$\epsilon$	reactor porosity
$\phi$	Thiele modulus
$\eta_i$	biofilm internal efficiency
$\eta$	biofilm efficiency based on external substrate concentration
$\lambda$	external mass transfer rate/internal coupled diffusion-reaction rate
$\mu$	specific growth rate ( $\text{s}^{-1}$ )
$\mu_{\text{max}}$	maximum specific growth rate ( $\text{s}^{-1}$ )
$\mu_p$	dry biofilm production rate per unit mass of biomass ( $\text{s}^{-1}$ )
$(\mu_p)_a$	specific dry biofilm production rate per unit mass of active biomass ( $\text{s}^{-1}$ )
$(\mu_p)_{\text{max}}$	maximum specific biofilm production rate ( $\text{s}^{-1}$ )
$\psi$	dimensionless observable modulus, defined in equation (34)

## REFERENCES

- Alphenaar, P.A., Perez, C. and Lettinga, C. (1993) The influence of substrate transport on porosity and methanogenic activity of anaerobic sludge granules. *Appl. Microb. Biotechnol.*, **39**, 276–280.
- Azeredo, J., Visser, J. and Oliveira, R. (1999) Exopolymers in bacterial adhesion: interpretation in terms of DLVO and XDLVO theories. *Colloids and Surfaces B: Biointerfaces*, **14**, 141–148.
- Balaguer, M.D., Vincent, M.T. and Paris, J.M. (1992) Anaerobic fluidized bed reactor with sepiolite as support for anaerobic treatment of vinasse. *Biotechnology Techniques*, **14**, 433–438.
- Bott, T.R. (1995) Biological growth on heat exchanger surfaces. In Bott, T.R. *Fouling of Heat Exchangers*, chapt. 12, pp. 223–267, Elsevier, Amsterdam.
- Briffaud, J. and Engasser, J.M. (1979) Citric acid production from glucose. II-Growth and excretion kinetics in a trickle-flow fermenter. *Biotechnol. Bioeng.*, **XXI**, 2093–2111.
- Brito, A.G. and Melo, L.F. (1997a) A simplified analysis of reaction and mass transfer in UASB and EGSB reactors. *Environmental Technology*, **18**, 35–44.
- Brito, A.G. and Melo, L.F. (1997b) Granulation during the start up of a UASB reactor used in the treatment of low strength wastewaters. *Biotechnol. Letters*, **19** (4), 363–367.
- Bryers, J.D. (1987) Biologically active surfaces: processes governing the formation and persistence of biofilms. *Biotechnology Progress*, **3**, 57–68.
- Bryers, J. (1993) Evaluation of the effectiveness factor for a multiple species biofilm. *Biofouling*, **6**, 363–380.
- Busscher, H.J., Bos, R. and van der Mei, H.C. (1995) Initial microbial adhesion is determinant for the strength of biofilm adhesion. Hypothesis. *FEMS Microbiology Letters*, **128**, 229–234.
- Cabral, J.M.S. and Tramper, J. (1994) Bioreactor design. In *Applied Biocatalysis*, edited by Cabral, J.M.S., Best, D., Boross, L. and Tramper, J., pp. 333–370, Harwood Academic Publishers, Switzerland.
- Çeçen, F. and Gönenç, I.E. (1994) Nitrogen removal characteristics of nitrification and denitrification filters. *Water Sci. Technol.*, **29**, 409–416.
- Capdeville, B., Nguyen, K.M. and Rols, J.L. (1992) Biofilm modelling: structural, reactional and diffusional aspects. In *Biofilms-Science and Technology*, edited by Melo, L.F., Bott, T.R., Fletcher, M. and Capdeville, B., pp. 251–276, Kluwer Academic Publishers, Dordrecht.
- Chamberlain, A.H.L. (1992) The role of adsorbed layers in bacterial adhesion. In *Biofilms-Science and Technology*, edited by Melo, L.F., Bott, T.R., Fletcher, M. and Capdeville, B., pp. 59–67, Kluwer Academic Publishers, Dordrecht.
- Characklis, W.G. and Marshall, K.C. (1990) *Biofilms*, John Wiley and Sons, New York.
- Christensen, B.E. and Characklis, W.G. (1990) Physical and chemical properties of biofilms. In *Biofilms*, edited by Characklis, W.G. and Marshall, K.C., pp. 93–130, John Wiley and Sons, New York.
- Costerton, J.W., Cheng, K.J., Geesey, G.G., Ladd, T.J., Nickel, J.C., Dasgupta, M. and Marrie, T. (1987) Bacterial biofilms in nature and disease. *Ann. Rev. Microbiol.*, **41**, 435–464.
- de Beer, D. and Stoodley, P. (1995) Relation between the structure of an aerobic biofilm and transport phenomena. *Water Sci. Technol.*, **32**, 11–18.
- de Beer, Stoodley, P. and Lewandowski, Z. (1997) Measurement of local diffusion coefficients in biofilms by microinjection and confocal microscopy. *Biotechnol. Bioeng.*, **53**, 151–158.
- Dempsey, M. (1990) Ethanol production by *Zymomonas mobilis* in a fluidised bed fermenter. In *Physiology of Immobilized Cells*, edited by de Bont, J.A.M., Visser, J., Matiasson, B. and Tramper, J., pp. 137–148, Elsevier Science Publishers B.V., Amsterdam.
- Droste, R.L. and Kennedy, K.J. (1986) Sequential substrate utilization and effectiveness factor in fixed biofilms. *Biotechnol. Bioeng.*, **XXVIII**, 1713–1720.
- Ecknenfelder, W.W., Argaman, Y. and Miller, E. (1989) Process selection criteria for the biological treatment of industrial wastewaters. *Environmental Progress*, **8** (1), 40–45.

- Fan, L.-S., Leyva-Ramos, R., Wisecarver, K.D. and Zehner, B.J. (1990) Diffusion of phenol through a biofilm grown on activated carbon particles in a draft-tube three-phase fluidized-bed bioreactor. *Biotechnol Bioeng.*, **35**, 279–286.
- Fletcher, M. (1992a) Bacterial metabolism in biofilms. In *Biofilms-Science and Technology*, edited by Melo, L.F., Bott, T.R., Fletcher, M. and Capdeville, B., pp. 113–124, Kluwer Academic Publishers, Dordrecht.
- Fletcher, M. (1992b) Metabolism and adhesion: report on workshop discussion. In *Biofilms-Science and Technology*, edited by Melo, L.F., Bott, T.R., Fletcher, M. and Capdeville, B., pp. 673–675, Kluwer Academic Publishers, Dordrecht.
- Flemming, H.-C. (1991) Introduction: biofilms as a particular form of microbial life. In *Biofouling and Biocorrosion in Industrial Water Systems*, edited by Flemming, H.-C. and Geesey, G.G., pp. 1–6, Springer-Verlag: Berlin, Heidelberg, New York.
- Freitas dos Santos, L.M. and Livingston, A.G. (1995) Membrane-attached biofilms for VOC wastewater treatment. I: novel in situ technique. *Biotechnol. Bioeng.*, **47**, 82–89.
- Froment, G.F and Bischoff, K.B. (1979) *Chemical Reactor Analysis and Design*, New York: John Wiley & Sons.
- Gjaltema, A. (1996) Biofilm development: growth versus detachment. PhD Thesis, Biochemical Engineering Department, Technical University of Delft, Delft, The Netherlands.
- Gjaltema, A., van der Marel, N., van Loosdrecht, M.C.M. and Heijnen, J.J. (1997) Adhesion and biofilm development on suspended carriers in air-lift reactors: hydrodynamic conditions versus surface characteristics. *Biotechnology, and Bioengineering*, **55**, 880–889.
- Gönenç, I.E. and Harremöes, P. (1985) Nitrification in rotating disk systems- I, Criteria for transition from oxygen to ammonia rate limitation. *Water Research*, **19**, 1119–1127.
- Gönenç, I.E., Orhon, D and Baikal, B.B. (1991) Application of biofilm kinetics to anaerobic fixed bed reactors. *Water Sci. Technol.*, **23**, 1319–1326.
- Grasmick, A., Elmaleh, S. and Ben Aim, R. (1980) *Water Research*, **14**, 613.
- Hamdi, M. (1995) Biofilm thickness effect on the diffusion limitation in the bioprocess reaction: biofloc critical diameter significance. *Bioprocess Engineering*, **12**, 193–197.
- Hamoda, M.F. and ABD-El Bary, M.F. (1987) Operating characteristics of the aerated submerged fixed-film (ASFF) bioreactor. *Water Research*, **21** (8), 939–947.
- Hamoda, M.F. and Kennedy, K.J. (1987) Biomass retention and performance in anaerobic fixed-film reactors treating acetic acid wastewater. *Biotechnol. Bioeng.*, **30**, 272–281.
- Harremöes, P. (1978) Biofilm kinetics. In *Water Pollution Microbiology*, Vol. 2, edited by Mitchell, R., pp. 82–109, John Wiley and Sons, New York.
- Harremöes, P. and Henze, M. (1995) Biofilters. In *Wastewater Treatment: Biological and Chemical Processes*, edited by Henze, M., Harremöes, P., Jansen, J. la Cour and Arvin, E., pp. 143–193, Springer-Verlag, Berlin.
- Harremöes, P., Jansen, J. la Cour and Kristensen, G.H. (1980) Practical problems related to nitrogen bubble formation in fixed film reactors. *Progr. Water Technol.*, **12**(6), 253–269.
- Heijnen, J.J., Mulder, A., Weltvrede, R., Hols, J., van Leeuwen, H.L.J.M. (1990) Large scale anaerobic/arerobic treatment of complex industrial wastewater using immobilized biomass in fluidized and air-lift suspension reactors. *Chem. Eng. Tech.*, **13**, 145–220.
- Heijnen, J.J., van Loosdrecht, M.C.M., Mulder, A. and Tijhuis L. (1992) Formation of biofilms in a biofilm air-lift suspension reactor. *Water Sci. Technol.*, **26**, 647–654.
- Hermanowics, S.W. (1999) Two-dimensional simulations of biofilm development: effects of external environmental conditions. *Water Sci. Technol.*, **39**, 107–114.
- Jansen, J. la Cour (1982) Fixed film kinetics- kinetics of soluble substrates. *PhD Thesis*, Department of Environmental Engineering, Technical University of Denmark, Lyngby.
- Jansen, J. la Cour and Kristensen, G.H. (1980) Fixed film kinetics- denitrification in fixed films. *Report 80–59*, Department of Environmental Engineering, Technical University of Denmark, Lyngby.

- Karamanov, D.G. and Nikolov, L.N. (1992) Bed expansion of liquid-solid inverse fluidization. *AIChE Journal*, **38** (12), 1916–1922.
- Karamanov, D.G. and Nikolov, L.N. (1996) Application of inverse fluidization in wastewater treatment: from laboratory to full-scale reactors. *Environmental Progress*, **15** (3), 194–196.
- Kissel, J.C., McCarty, P.L. and Street, R.L. (1984) Numerical solution of mixed-culture biofilm. *J. Environ. Eng. Div. ASCE*, **110**, 393–411.
- Lappin-Scott, H.M. and Costerton, J.W. (1995) *Microbial Films*, Cambridge University Press, Cambridge.
- Lazarova, V. and Manem, J. (1994) Advances in biofilm aerobic reactors ensuring effective biofilm activity control. *Water Sci. Technol.*, **29**, 319–327.
- Lazarova, V. and Manem, J. (1997) An innovative process for waste water treatment: the circulating floating bed reactor. *Water Sci. Technol.*, **34**, 89–99.
- Lettinga, C. and Hulshoff-Pol, L.W. (1992) UASB-process design for various types os wastewaters. In *Design of anaerobic processes for the treatment of industrial and municipal wastes*, edited by Malina, J. and Pohland, F., pp. 119–145, Technomic Pub., Lancaster.
- Margel, S., Vogel, E.A., Firment, L., Watt, T., Haynie, S. and Sogah, D.Y. (1993) Peptide, protein and cellular interactions with self-assembled monolayer model surfaces. *J Biomed. Mater. Res.*, **27**, 1463–1476.
- Marshall, K.C., Stout, R. and Mitchell, R. (1971) Mechanisms of the initial events in the sorption of marine bacteria to surfaces. *J. Gen. Microbiol.*, **68**, 337–348.
- McGhee, T.J. (1991) *Water Supply and Sewerage*, 6th Edition, McGraw-Hill, Inc., Singapore.
- Melo, L.F., Bott, T.R., Fletcher, M. and Capdeville, B. (1992) *Biofilms- Science and Technology*, Kluwer Academic Publishers, Dordrecht.
- Melo, L.F. and Vieira, M.J. (1999) Physical stability and biological activity of biofilms under turbulent flow and low substrate concentration. *Bioprocessing Engineering*, **20**, 363–368.
- Mendez, R., Pan, M. and Lema, J.M. (1989) Effect of C/N/P ratio on the performance of a DSFFR working at low organic loading rates. *Water Sci. Technol.*, **21**, 1673–1676.
- Messing, R.A. and Opperman, R.A. (1979a) Pore dimensions for accumulating biomass. I. Microbes that reproduce by fission or by budding. *Biotechnology and Bioengineering*, **XXI**, 49–58.
- Messing, R.A. and Opperman, R.A. (1979b) Pore dimensions for accumulating biomass. II. Microbes that form spores and exhibit mycelial growth. *Biotechnology and Bioengineering*, **XXI**, 59–67.
- Metcalf & Eddy, Inc. (1987) *Wastewater Engineering: Treatment and Disposal*, 2nd ed., Tata McGraw-Hill Publishing Company, New Dehli.
- Miyahara, T. and Noike, T. (1995) Behavior of suspended solids and anaerobic bacteria in an anaerobic fixed bed reactor. *Water Sci. Technol.*, **30**, 75–86.
- Mott, I.E.C. and Bott, T.R. (1991) The Adhesion of Biofilms to Selected Materials of Construction for Heat Exchangers. *9th Intern. Heat Transf. Conf.*, Jerusalem, **5**, 21–26.
- Nguyen, V.T. and Shieh, W.K. (1995) Evaluation of intrinsic and inhibition kinetics in biological fluidized bed reactors. *Water Research*, **29** (11), 2520–2524.
- Nikolov, L.N. and Karamanov, D.G. (1990) The inverse fluidized bed reactor; a new laboratory scale apparatus for biofilm research. *J. Ferment. Bioeng.*, **69** (4), 265–267.
- Nikov, I. and Karamanov, D. (1991) Liquid-solid mass transfer in inverse fluidized bed. *AIChE Journal*, **37** (5), 781–784.
- Nilsson, B.K. and Karlsson, H.T. (1989) Diffusion rates in a dense matrix of methane-producing microorganisms. *J. Chem. Technol. Biotechnol.*, **44**, 255–260.
- Noguera, D.R., Pizarro, G., Stahl, D.A. and Ritmann, B.E. (1999) Simulation of multispecies biofilm development in three dimensions. *Water Sci. Techn.*, **39**, 123–130.
- Nogueira, R., Lazarova, V., Manem, J. and Mélo, L.F. (1998) Influence of dissolved oxygen on the nitrification kinetics in a circulating bed biofilm reactor. *Bioprocess Engineering*, **19**, 441–449.

- Oliveira, R. (1992) Physico-chemical aspects of adhesion. In *Biofilms- Science and Technology* edited by Melo L.F., Bott T.R., Fletcher M. and Capdeville B., pp. 45–58. Dordrecht, Boston, London: Kluwer Academic Publishers.
- Onuma, M. and Omura, T. (1982) Mass transfer characteristics within microbial systems. *Water Sci. Technol.*, **14**, 553–568.
- Pederson, A.R. and Arvin, E. (1996) Toluene removal in a biofilm reactor from waste gas treatment. *3rd International IAWQ Special Conference on Biofilm Systems*, Copenhagen.
- Pederson, A.R. and Arvin, E. (1999) The function of a toluene-degrading bacterial community in a waste gas trickling filter. *Water Sci. Technol.*, **39**, 131–137.
- Peixoto, J. and Mota, M. (1998) Biodegradation of Toluene in a Trickling Filter. *Bioprocess Engineering*, **19** (5), 393–397.
- Pereira, M.A., Alves, M.M., Azereedo, J., Mota, M. and Oliveira, R. (1999) Physico-chemical properties of porous microcarriers in relation with the adhesion of an anaerobic consortium. *Journal of Industrial Microbiology*, in press.
- Petrozzi, S., Kut, O.M. and Dunn, I.J. (1993) Protection of biofilms against toxic shocks by the adsorption and desorption capacity of carriers in anaerobic fluidized bed reactors. *Bioprocess Engineering*, **9**, 47–59.
- Picioreanu, C., van Loosdrecht, M.C.M. and Heijnen, J.J. (1999) Discrete- differential modelling of biofilm structure. *Water Sci. Technol.*, **39**, 115–122.
- Prime, K.L. and Whitside, G.M. (1993) Adsorption of proteins onto surfaces containing end- attached oligo(ethylene oxide): a model system using self- assembled monolayers. *Journal of American Chemical Society*, **115**, 10714–10721.
- Reichert, P. AQUASIM-A tool for simulation and data analysis of aquatic systems. *Water Sci. Technol.*, **30**, 21–30.
- Reichert, P. Design techniques of a computer program for the identification of processes and the simulation of water quality in aquatic systems. *Environmental Software*, **10** (3), 199–210.
- Ritmann, B.E., Pettis, M., Reeves, H.W. and Stahl, D.A. (1999) How biofilm clusters affect substrate flux and ecological selection. *Water Sci. Technol.*, **39**, 99–105.
- Rusten, B., Kolkin, Odegaard, H. (1997) Moving bed biofilm reactors and chemical precipitation for high efficiency treatment of wastewater from small communities. *Water Sci. Technol.*, **35**, 71–79.
- San, H.A., Tanik, A. and Orhon, D. (1993) Micro-scale modelling of substrate removal kinetics in multicomponent fixed-film systems. *J. Chem. Tech. Biotechnol.*, **58**, 39–48.
- Schlegel, H.G. (1985) *Allgemeine Mikrobiologie*, Thieme, Stuttgart.
- Shimp, R.J. and Pfaender, F.K. (1982) Effect of surface area and flow rate on marine bacterial growth on activated carbon columns. *Applied and Environmental Microbiology*, **44**, 2, 471–476.
- Sousa, M., Azereedo, J., Feijó, J. and Oliveira, R. (1997) Polymeric supports for the adhesion of a consortium of autotrophic nitrifying bacteria. *Biotechnology Techniques*, **11**, 751–754.
- Stoodley, P., de Beer, D., Lewandowski, Z. (1994) Liquid flow in biofilm systems. *Appl. Environm. Microbiol.* 2711–2716.
- Suzuki, Y., Miyahara, S. and Takeishi, K. (1993) Oxygen supply method using gas permeable film for wastewater treatment. *Water Sci. Technol.*, **28**, 243–250.
- Tavares, C.R.C., Sant'Anna, J.R., C.L. and Capdeville, B. (1995) The effect of air superficial velocity on biofilm accumulation in a three phase fluidized- bed reactor. *Water Research*, **29** (10), 2293–2298.
- Taylor, G.T., Zheng, D., Lee, M., Troy, P.J., Gyanamaht, G. and Sharma, S.K. (1997) Influence of surface properties on accumulation of conditioning films and marine bacteria on substrata exposed to oligotrophic waters. *Biofouling*, **11**, 31–57.
- Teixeira, P. and Oliveira, R. (1998) The importance of surface properties in the selection of supports for nitrification in airlift bioreactors. *Bioprocess Engineering*, **19**, 143–147.

- Teixeira, P. and Oliveira, R. (1999) Influence of surface characteristics on the adhesion of *Alcaligenes denitrificans* to polymeric substrates. *J. of Adhesion Science and Technology*, **13**, 1287–1294.
- Tijhuis, L., Huisman, J.L., Hekkelman, H.D., van Loosdrecht, M.C.M. and Heijnen, J.J. (1995) Formation of nitrifying biofilms on small suspended particles in airlift reactors. *Biotechnol. Bioeng.*, **47**, 585–595.
- Tijhuis, L., van Loosdrecht, M.C.M. and Heijnen, J.J. (1994) Formation and growth of heterotrophic aerobic biofilms on small suspended particles in airlift reactors. *Biotechnol. Bioeng.*, **44**, 595–608.
- Trulear, M.G. (1980) Dynamics of biofilm processes in an annular reactor. *MSc Thesis*, Rice University, Texas, USA.
- Trulear, M.G. (1983) Cellular reproduction and extracellular polymer formation in the development of biofilms. *PhD Thesis*, Montana State University, Bozeman, USA.
- Ulonska, A., Deckwer, W.D. and Hecht, V. (1994) Degradation of quinoline by immobilized *Comamonas acidovorans* in a three-phase airlift reactor. *Biotechnol. Bioeng.*, **46**, 80–87.
- van Ede, C.J., Bollen, A.M. and Beenackers, A.A.C.M. (1993) Analytical effectiveness factor calculations concerning product-inhibited fermentations associated with biofilm growth and maintenance. *Can. J. Chem. Eng.*, **71**, 901–910.
- van Loosdrecht, M.C.M., Eikelboom, D., Gjaltema, A., Mulder, A., Tijhuis, L. and Heijnen, J.J. (1995) Biofilm structures. *Water Sci. Technol.*, **32**, 35–43.
- van Loosdrecht, M.C.M., Lyklema, J., Norde, W. and Zhender, A.B (1988) Bacterial adhesion: a physico chemical approach. *J. Gen. Microbiol.*, **68**, 337–348.
- van Oss, C.J. (1995) Hydrophobicity of biosurfaces—origin, quantitative determination and interaction energies. *Colloids and Surfaces B: Biointerfaces*, **5**, 91–110.
- van Oss, C.J. (1997) Hydrophobicity and hydrophilicity of biosurfaces. *Current Opinion in Colloid Interface Science*, **2**, 503–512.
- Veiga, M.C., Mendez, R. and Lema, J.M. (1992) Development and stability of biofilms in bioreactors. In *Biofilms—Science and Technology*, edited by Melo, L.F., Bott, T.R., Fletcher, M. and Capdeville, B., pp. 421–434, Kluwer Academic Publishers, Dordrecht.
- Vieira, M.J. and Melo, L.F. (1995) Effect of Clay particles on the behaviour of biofilms formed by *Pseudomonas fluorescens*. *Wat. Sci. Tech.*, **32** (8), 45–52.
- Vieira, M.J. and Melo, L.F. (1999) Intrinsic kinetics of biofilms formed under turbulent flow and low substrate concentration. *Bioprocessing Engineering*, **20**, 369–375.
- Vieira, M.J., Melo, L.F. and Pinheiro, M.M. (1993) Biofilm Formation: Hydrodynamic Effects on Internal Diffusion and Structure. *Biofouling*, **7**, 67–80.
- Vieira, M.J., Oliveira, R., Melo, L.F., Pinheiro, M.M. and Martins, V. (1993) Effect of Metallic Ions on the Adhesion of Biofilms Formed by *Pseudomonas fluorescens*. *Colloids and Surfaces B: Biointerfaces*, **1**, pp. 119–124.
- Wanner, O. (1995) New experimental findings and biofilm modelling concepts. *Water Sci. Technol.*, **32**, 133–140.
- Wanner, O. and Gujer, W. (1986) A multispecies biofilm model. *Biotechnol. Bioeng.*, **XXVIII**, 314–328.
- Wanner, O. and Reichert, P. (1996) Mathematical modeling of mixed-culture biofilms. *Biotechnol. Bioeng.*, **49**, 172–184.
- Watanabe, Y. and Ishiguro, M. (1978) Denitrification kinetics in a submerged rotating biological disk unit. *Progr. Water Technol.*, **5**, 187–195.
- Wiesmann, U. (1994) Biological nitrogen removal from wastewater. *Advances in Biochemical Engineering/Biotechnology*, **51**, 113–154.
- Wilderer, P. (1995) Technology of membrane biofilm reactors operated under periodically changing process conditions. *Water Sci. Technol.*, **31**, 173–183.
- Willaert, R.G., Baron, G.V. and de Backer, L. (1996) *Immobilised Living Cell Systems: Modelling and Experimental Methods*, Chapter 3, John Wiley and Sons, Chichester, England.

- Williamson, K. and McCarty, P.L. (1976) A model of substrate utilization by bacterial biofilms. *J. Water Poll. Contr. Fed.*, **48**, 9–24.
- Wienczek, K.M. and Fletcher, M. (1997) Effects of substratum wettability and molecular topography on initial adhesion of bacteria to chemically defined substrata. *Biofouling*, **11**, 293–311.
- Zobell, C.E. and Allen, E.C. (1935) The significance of marine bacteria in the fouling of submerged surfaces. *J. Bacteriol.*, **20**, 239–251.

# CHAPTER ELEVEN

## PULSING BIOREACTORS

JUAN M.LEMA, ENRIQUE ROCA, ANGELES SANROMÁN, M.JOSÉ NÚÑEZ, M.Teresa MOREIRA AND GUMERSINDO FEIJOO

*Department of Chemical Engineering, Institute of Technology, University of Santiago de Compostela, Av. das Ciencias s/n, E-15706 Santiago de Compostela, Spain*

### ABSTRACT

The application of external energy in the pulsing form has for a long time been a common practice to improve mass transfer rates in chemical engineering units. This chapter reviews the different types and applications of pulsed bioreactors, pointing out most especially the use of the elastic membrane pulsator (EMP). Considering the hydrodynamic behaviour, pulsed bioreactors coupled with an EMP display a lower axial dispersion than non-pulsed ones. Besides, pulsation overcomes a series of problems usually associated with the use of packed-bed bioreactors: difficulty of gas supply (aeration); retention of the gas produced in fermentation processes within the bed; and clogging of the bed by excessive microorganism growth. Examples concerning the enzymatic hydrolysis of starch solutions, the alcoholic fermentation by immobilised cells and the continuous production of ligninolytic enzymes by filamentous fungi are presented.

**Keywords:** Pulsation; Packed-bed; Starch hydrolysis; Alcoholic fermentation; Immobilised cells; Filamentous fungi; Ligninolytic enzymes; Bioreactor

### TYPES AND APPLICATIONS OF PULSING DEVICES

The application of external energy in the pulsing form has, for a long time, been a common practice to improve mass transfer rates in chemical engineering units. The general principles about pulsing columns were established by Van Dijk (1935), who developed several systems to improve the efficiency of solid-liquid extraction processes at the Royal Dutch/Shell Laboratory in Amsterdam, in the 1930's. Since then, a number of techniques, based on several principles, have been developed and adapted for their application to very different fields.

#### Types of Pulsing Devices

In general, pulsing equipment may be classified into two different types:

- a) The first one involves the alternating motion of some intrinsic elements of the column. It may be worth mentioning the pulsing plates column (Figure 11.1-a), in which the pulsation is generated by means of an upwards-downwards motion of plates (Baird and Rao, 1988; Skala and Veljkovic, 1988) and the columns with a piston pulsator (Figure 11.1-b), where a plug is coupled to the bottom of the column (Harrison and Mackley, 1992).
- b) In the second type, pulsation is generated by the hydraulic transmission of a perturbation to the liquid contained in the column. The systems using positive displacement pumps (plug or membrane) to introduce the feed into the column (Mak *et al.*, 1992) and the pneumatic pulsation systems (Figure 11.1-c) are characteristic of this type. In the latter, the pulsation is generated by means of a pressurised gas, which propels the liquid contained in a parallel branch to the column (Murthy *et al.*, 1987). The self-propelled pulsators, shown in Figure 11.1-d, are based on a different

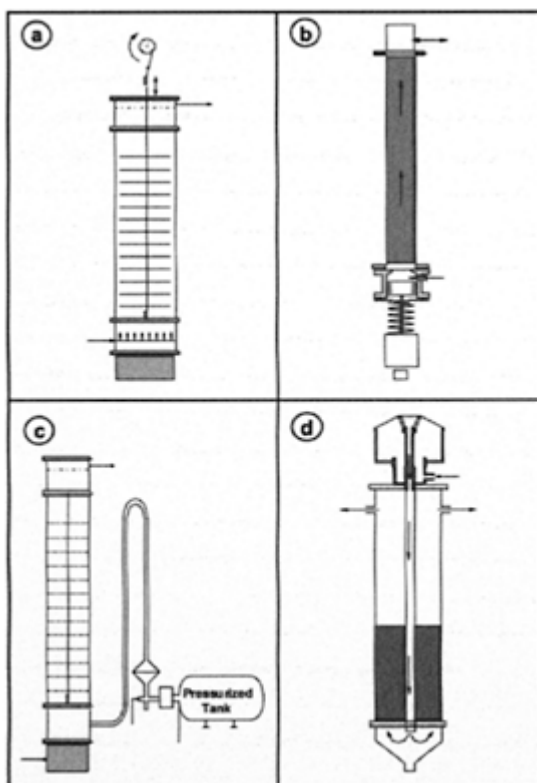


**Figure 11.1** Types of pulsing devices,  
a. Pulsing plates column. b. Piston  
pulsator. c. Pneumatic pulsator. d.  
Self-propelled pulsator.

concept. In this case, pulsation is the result of the liquid entering the columns, through the pulsation chamber. Once the pressure in the chamber is high enough, the membrane covering the feeding tube injects the liquid into the column; the membrane then closes the inlet tube again, which creates a cyclical feed system. In contrast with the previous pulsators, in this system, the motion of the liquid in the column is always upwards (Baltar, 1972).

### Uses of Pulsing Systems

Pulsation was firstly used in several separation processes in order to enhance the contact between the phases and, consequently mass transfer rate improved. Pulsation has been applied to a number of systems, including chemical and biochemical reactors. Table 11.1 shows a summary of the different pulsators coupled to several types of unit operations and processes.

#### *Separation processes*

One of the most extended and useful applications of pulsation is to liquid-liquid extraction. In this process, pulsation generates higher degrees of turbulence, which increases the interfacial area and, accordingly, enhances mass transfer rate (Bailes *et al.*, 1976). An electric motor connected, *via* an acetalical and a crank-rod to the central rod,

**Table 11.1** Some equipment and process to which different pulsing systems have been applied.

Equipment of pulsation	Unit type	Process	Reference
Pulsing plates column	Column of perforated plates	Absortion	Skala and Veljkovic 1988
	Packed-bed column with perforated plates	Anaerobic treatment of waste-water	Brauer and Sucker 1979
Membrane pulsator	Column of perforated plates	L-L Extraction	Golding and Lee 1981
	Anaerobic filter	Anaerobic treatment of waste-waters	Etzold and Stadlbauer 1990
Alternating motion pumps	Packed-bed column	S-L Extraction	Göebel and Fortuin 1986
Pulsing pump	Ultrafiltration unit	Clarification of juices	Finnigan and Howell 1989
Plug pulsator	Column of perforated plates	Obtention of SCP	Serieys <i>et al.</i> 1978
	Batch bioreactor	Production of biodegradable plastic	Harrison and Mackley 1992
Pneumatic pulsator	Packed-bed column with	Alcoholic fermentation	Navarro and Goma

which links the pile of plates, causes them to rise and fall, and thus generates the pulsation. The efficiency of such equipment depends on the geometry of the plate, its amplitude, the speed at which the plates move and the flow velocity of each phase, factors which also control the intensity of the axial mixing.

Mass transfer is improved when the agitation speed increases and, for a given frequency, both an increase in the amplitude of the pulsation and a decrease in the diameter of the plate holes improve extraction efficiency (Baird *et al.*, 1989). Besides, these systems present other advantages, such as limited energy demand, smaller risk of preferential ways in the dispersed phase, reliability of scale-up and the possibility of working with phases of similar density. It is also possible to achieve an effect similar to that of the light phase by introducing an inert gas in pulsed flow (Miñana *et al.*, 1985).

The application of pulsation in hydrometallurgy (for mineral, metallurgical and nuclear industries), in which the speed required for extraction is high, allows an increase in the overall mass transfer coefficients to be obtained, especially when operating at large pulsation amplitudes (Golding and Lee, 1981). Göebel and Fortuin (1986) used a pulsed packed-bed column to improve the contact between a dispersed solid phase, fed at the top of the column, and a pulsed liquid phase, using a system of reciprocating pumps. Mak *et al.* (1992) determined the relation between the solid phase flow and the axial dispersion coefficient of the liquid phase. Pulsation must take place at a relatively high speed for a good distribution of the liquid phase.

The use of pulsing perforated plates columns is also of interest in processes involving a contact between gas and liquid phases (absorption). The overall mass transfer coefficient increases with the intensity of the pulsation and the average velocity of the gas due to the better contact between the phases (Yang *et al.*, 1986). Baird and Garstang (1972) indicated that the mass transfer rate always improves, either as a result of a vibration or a pulsation.

In filtering processes through membranes, efficiency diminishes because of clogging, caused by polarisation of the filtered particles on the membrane surface. Until now, the devices commonly used to minimise this problem caused strong turbulence at the surface of the membrane. In this context, Finnigan and Howell (1989) determined that pulsation in an ultrafiltration system, used for the clarification of juices of high solid contents, increases the filtration capacity.

### **Biochemical reactors**

In aerobic transformations carried out in fixed-bed bioreactors by immobilised microorganisms, the limited availability of dissolved oxygen in the fermenting medium is a major obstacle. Pulsing flow helps to diminish external resistance to the oxygen transfer. Ghommath *et al.* (1982) studied the production of acetic acid in a pulsing reactor by *Acetobacter acetii* immobilised on a ceramic support, the pulsation being generated through a piston pump installed at the bottom of the reactor (similar to Figure 11.1-b). For SCP production, where the requirements of oxygen are also high, a mechanical pulsation system (similar to the piston) joined to a column of perforated plates, has been used successfully. This system presents an oxygen transfer effectiveness as high as air-lift

or stirred tank reactors with a Rushton turbine, which represents a considerable saving in agitation-aeration energy (Serieys *et al.*, 1978).

A piston pulsator was coupled to an extractive fermentation system for alcoholic fermentation, where liquid-liquid extraction permits the continuous separation of ethanol. Pulsation was shown useful to increase the contact between aqueous and organic phases, thus improving ethanol extraction, and also minimising gas hold-up (Minier and Goma, 1982). Good results were also obtained in ethanol fermentation employing a pneumatic pulsator, shown in Figure 11.1-c (Navarro and Goma, 1980). The use of a perforated plates column with a pneumatic pulsing system also improved the effectiveness of the aeration and, additionally, it was responsible for a reduction of gas hold-up and the enhancement of the mass transfer coefficients (Dondé *et al.*, 1987).

The reciprocating jet bioreactor consists of a cylindrical vessel with a height/diameter ratio of 4 to 8 and contains an assembly of sieve plates attached to a vertical rod (similar to Figure 11.1-a). The reciprocating motion is achieved by an electric motor and a special crank gear connected to the package of sieve plates by means of a central axis. The turbulence generated, due to the movement of the plates, causes the dispersion of the gas bubbles and reduces the pellet size, which implies an increase of the interfacial area between bubbles and pellets, this enhancing mass transfer.

This reactor was successfully applied to the anaerobic wastewater treatment (Brauer and Sucker, 1979). A system of three reciprocating jet bioreactors provided with settlers for biomass retention, was effectively applied to remove carbon and nitrogen from highly polluted wastewaters (Brauer and Annachhatre, 1992a,b). Reciprocating bioreactors have also been employed for the production of antibiotics (by *Cyathus striatus*), citric acid (by *Aspergillus niger*) and ethanol (by *Zymomonas mobilis*) (Brauer, 1991).

One important point in wastewater treatment in fixed-bed systems based on anaerobic (associated to the production of  $\text{CH}_4$  and  $\text{CO}_2$ ) or aerobic processes (in which apart from the air which is introduced, there is production of  $\text{CO}_2$ ) is degassing. The gas retained between the bioparticles reduces the effective reactor volume and, also, impedes an efficient contact between the dissolved organic matter and cells. Pulsation helps degassing due to shearing off the gas bubbles and favours their evacuation outside the reactor. Furthermore, it facilitates the generation of a large interfacial surface, as well as the periodical renewal of the interphase and the uniform distribution of the air bubbles.

Other types of pulsing devices (membrane pumps) have been applied to anaerobic wastewater treatment aiming to minimise the formation of preferential pathways and clogging at the exit of the reactor in anaerobic filters, fluidised-bed reactors and loop reactors. Pulsation improves degassing and increases stability of the pH, mainly because of an improvement in the distribution of substrate and of the slow movements of the bed, which generates new exchange surfaces (Etzold and Stadlbauer, 1990).

Each type of the above mentioned pulsators is particularly suitable to the resolution of particular problems, although all of them attempt to increase mixing inside the system, this being undesirable in the cases of processes inhibited by product. In order to make the concepts of plug flow and pulsed flow compatible, a device, the "elastic membrane pulsator" (EMP), was proposed (Lema *et al.*, 1995).

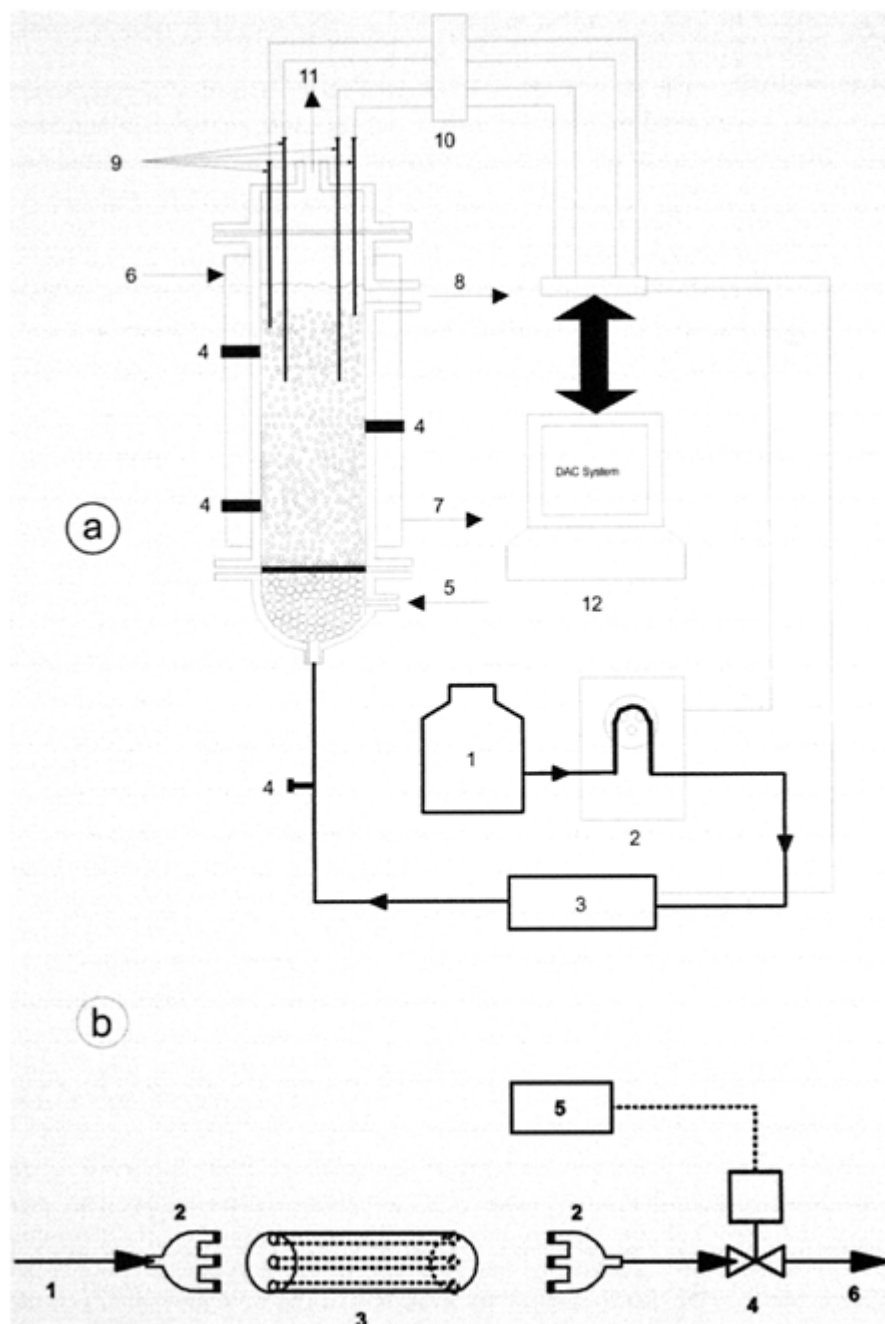


**Figure 11.2** Diagram of bioreactor and pulsing device. 2a) *Bioreactor:* 1.

Feeding tank; 2. Pump; 3. Elastic membrane pulsator; 4. Sampling ports; S. Air difusor; 6, 7. Inlet, outlet of thermostated water; 8. Liquid outlet; 9. Sensors (T, pH, etc); 10. Meters; 11. Gas exit; 12. Data Acquisition and Control Unit. 2b) *Pulsing device*: 1. Inlet stream; 2. Heads; 3. Elastic rubber tubes; 4. Electrovalve; 5. Connection to the control loop; 6. Outlet stream.

### ELASTIC MEMBRANE PULSATORT

The elastic membrane pulsator (EMP) consists of a system formed by one or more elastic tubes connected in parallel by means of two heads with defined internal diameters, wall thickness and length, which are coupled to an electrovalve which is opened and closed by a timer or a computerised system (DAC system). A diagram of a packed-bed bioreactor coupled to the pulsing device is presented in Figure 11.2.

The pulsation is produced when the gas or liquid retained within the elastic tubes (when the valve is closed), is impelled into the reactor once the valve opens. According to the flow provided by the feeding pump, the volume of the fluid retained is regulated by the shutting time of the electrovalve, which therefore determines the volume of pulsed fluid and, accordingly, the amplitude of pulsation.

The pulsation frequency  $f$  and the amplitude  $a$  in the bioreactor are expressed through the following equations:

$$f = \frac{1}{t_o + t_s} \quad (1)$$

$$a = 3.54 \cdot 10^{-5} \cdot \frac{F \cdot t_s}{\varepsilon \cdot D^2} \quad (2)$$

where  $t_o$ ,  $t_s$ ,  $F$ ,  $\varepsilon$  and  $D$  are the opening and shutting times, liquid flowrate, void fraction and column diameter, respectively. The electrovalve opening time is fixed in a determined value and therefore the pulsation frequency and amplitude are regulated by varying the electrovalve shutting time.

### HYDRODYNAMIC BEHAVIOUR OF A PULSED PACKED-BED REACTOR

The effects of pulsation on the modification of hydrodynamics of packed-bed reactors were studied in different sets of conditions (Roca *et al.*, 1994) (different feed flowrates,

particle diameters and fluid viscosities) in a column of L/D=34 (length/diameter) with an inert bed (glass beads) to which the fluid phase is fed with or without pulsation.

A stimulus-response technique has been used to obtain the Residence Time Distribution (RTD) of the fluid inside the reactor (Levenspiel, 1988). To do that, a small volume (one mL) of a tracer (HC1) was injected into the inlet stream of the column in order to get an almost ideal pulse ( $\delta$  function of Dirac) and this moment is considered the beginning of the experiment.

Figure 11.3 shows, as an example, the RTD's curves obtained in the same operating conditions ( $Re_p=95$ , a particle diameter of 6 mm and water as liquid) with an EMP, a pneumatic pulsator, a self-propelled pulsator and without pulsation. For this set of curves, the values of the Peclet module are always within the limits of the Minimum Dispersion model (Levenspiel, 1988). As can be seen, the axial dispersion in the reactor coupled with the self-propelled pulsator and the EMP are lower than that corresponding to the system without pulsation. However, the pulsation carried out with the pneumatic equipment produces greater dispersion, and considerably smaller Peclet modules are obtained. The lowest degree of dispersion and, consequently, the flow model closest to the plug flow reactor is achieved by applying the EMP pulsator.

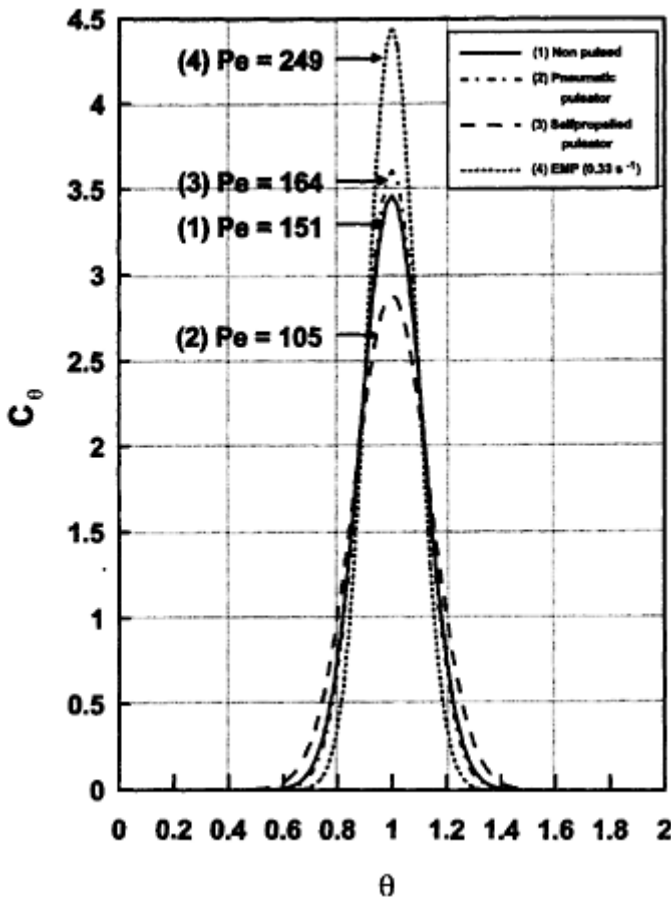


**Figure 11.3** Residence Time

Distribution (RTD) curves obtained at  $Re_p=95$ , in a packed bed reactor with particles of 6 mm diameter and water as fluid.

Figure 11.4 shows the dependency of the axial dispersion coefficient ( $D_A$ ) on the feed flowrate, when operating at different pulsation frequencies with two fluids of different viscosities. The results are compared with those from the equipment without pulsation. As is predictable, the fluid flowrate increases  $D_A$  independently of the pulsation frequency, a phenomenon which also occurs in the experiments without pulsation. When pulsation is applied at low frequencies and high flowrates (higher amplitudes) the effect of pulsation on  $D_A$  is more significant.

20% sucrose-water solutions (2 cP), with viscosity characteristics similar to those of many fermentation broths, were used to quantify the effects of viscosity on the dispersion

generated by the pulsing system. As the solutions exhibit a Newtonian behaviour (viscosity only depending on the temperature), the effects of pulsation can be determined at different flowrates. The increase in  $D_A$  at higher linear velocity is remarkable even in the cases of high viscosity fluids, the axial dispersion coefficients being, on average, approximately twice as high as those obtained with water (Figure 11.4).

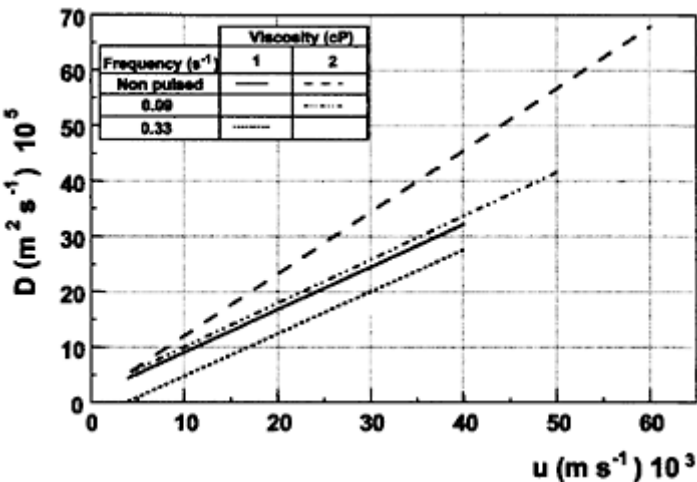


**Figure 11.4** Effect of linear velocity on axial dispersion for a packing of 6 mm of particle diameter using two fluids of different viscosities (water and a sucrose solution of a viscosity of 2 cP).

Finally, the effects of the packing size were analysed by evaluated columns with particles of three different diameters (4.5, 6 and 8 mm). In all cases,  $D_A$  decreases with the particle diameter, this tendency being noticeable when operating at higher feed flowrates (data not shown).

#### APPLICATION OF PULSING BIOREACTORS TO BIOTECHNOLOGICAL PROCESSES

The development of high efficiency bioreactors has been an important research objective in the field of bioprocesses. Appropriate selection and design could greatly improve the efficiency of the overall process. Several bioreactor configurations (fixed/fluidised-bed, gas-lift, membrane fermentors, reciprocating bioreactors) have been considered (Brauer, 1988; Chamy *et al.*, 1990; Chisti, 1989; Mehaia and Cheryan, 1984). In many cases, gas-

lift, fluidised or reciprocating bioreactors seemed better suited to particular applications (Brauer, 1991; Fontana *et al.*, 1992; Gilson and Thomas, 1993).

Several different fermentation and enzymatic processes in which pulsation may prevent operational problems, facilitating the improvement of efficiency and control of multiphase bioreactors, are presented. The pulsed phase was gas or liquid depending on the particular application.

### Liquid-phase Pulsing Bioreactors

Fixed and expanded bed bioreactors, using immobilised enzymes or microorganisms have been widely applied because of their simple design and operation (Tyagi *et al.*, 1992). However, these systems present some drawbacks (mass transfer limitation, gas retention, dead volumes), which have proved difficult to solve. The application of a pulse to the bioreactor has been assayed as an useful partial solution to the above mentioned problems.

#### *Enzymatic hydrolysis of starch by immobilised glucoamylase on chitin slabs*

The hydrolysis of starch by immobilised glucoamylase is the first step in industrial HFCS production. When processing high viscosity solutions in packed-bed bioreactors, the diffusion of the substrate can represent the limiting factor of the overall reaction rate. In the hydrolysis of starch, viscosity plays a definitive role, which in some cases led authors to confuse this effect with an apparent inhibition by substrate (Miranda *et al.*, 1991). In order to overcome this difficulty, a pulsing flow was applied to the reaction bed. Experiments were conducted in two equal glass upflow continuous packed-bed reactors ( $L/D=2.3$ ), with and without pulsation, operated at residence times ( $\tau$ ) of 0.33–1.8 h (Sanromán *et al.*, 1991).

Since the reaction rate corresponds well with the Michaelis-Menten model (Miranda *et al.*, 1991) and that, after determining RTD curves, the flow model corresponds to an almost ideal plug flow reactor, equation 3 describes properly the behaviour of the system.

$$\left( \frac{V_{max}}{K_M} \right) \cdot \tau = -\ln \left( \frac{S}{S_o} \right) + \frac{(S_o - S)}{K_M} \quad (3)$$

The kinetic parameters obtained are presented in Table 11.2 and as can be observed, an increase in the maximum hydrolysis rate ( $V_{max}$ ) and a slight reduction in  $K_M$  are obtained when a pulsing reactor is used, thus improving the final efficiency of the process.

Figure 11.5 shows a comparison between the substrate consumption rate obtained in a packed bed bioreactor, pulsed and non-pulsed, both operated at a HRT of one hour for three substrate concentration in the feeding stream. As can be seen, in all cases a higher substrate consumption rate is obtained with the pulsed system, the effect of pulsation being more significant at higher substrate concentration, when liquid viscosity is eight times higher than the corresponding to  $50 \text{ g L}^{-1}$ .

***Alcoholic fermentation of glucose by Ca-alginate immobilised  
Saccharomyces cerevisiae***

Alcoholic fermentation is a process often affected by the presence of the product, which causes a progressive decrease in the production rate until a threshold value is reached at

**Table 11.2** Kinetic parameters of the enzymatic hydrolysis of starch operating in packed-bed bioreactor with and without pulsation

Packed-bed reactor	Without pulsation		With pulsation	
	V <sub>max</sub>	K <sub>M</sub>	V <sub>max</sub>	K <sub>M</sub>
50	0.099	12.44	0.110	12.42
100	0.097	13.02	0.123	12.50
150	0.102	13.36	0.144	12.53

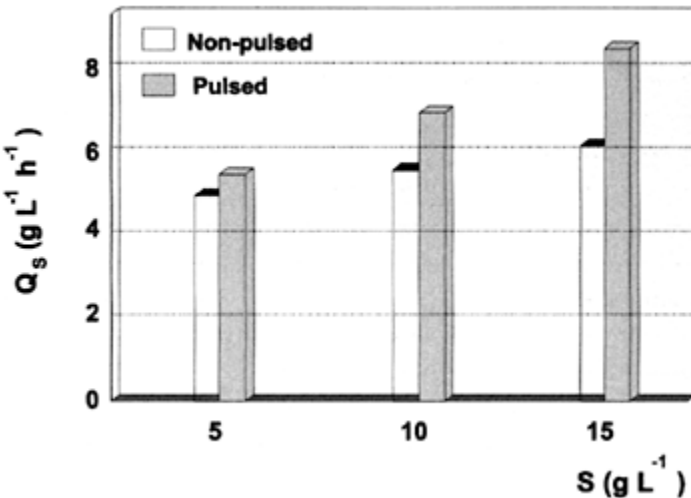


**Figure 11.5** Effects of pulsation on enzymatic hydrolysis of starch in pulsed and non-pulsed packed-bed bioreactors for different substrate concentrations at a hydraulic retention time of 1 h.

which it stops. Accordingly, for this process, a hydraulic behaviour such as plug flow is desirable.

Plug flow may be achieved using packed-bed systems, in which the yeast is immobilised in or on a particular support. However, packed-bed reactors have a number of drawbacks: a) Mass transfer limitations, especially in the end zone, when the concentration of substrate is the lowest; b) Inter and intra-particular accumulation in the lower zone of the gas produced ( $\text{CO}_2$ ), which occurs when the bed is not sufficiently porous; c) The formation of preferential paths which reduce the effective working volume; and d) The compacting of the bed due to the partial disintegration of the bioparticles (because of shear stress or the intraparticulate accumulation of gas) (Núñez and Lema, 1987).

In order to overcome these problems, the application of a pulsation in the liquid entering the bioreactor has been proposed (Sanromán *et al.*, 1994a,b). The EMP system was selected as it offers operational advantages, the most important being the maintenance of the plug flow hydrodynamics (Roca *et al.*, 1994).

### *i) Effects of pulsation on bioreactor performance*

The effects of pulsation on the bioreactor ( $V=2.1 \text{ L}$ ;  $H/D=2.7$ ) performance were analysed at three hydraulic residence times of 3, 1.4 and 0.7 h, pulsation frequencies between 0.008 and  $0.024 \text{ s}^{-1}$ , glucose concentrations of 100 and  $200 \text{ g L}^{-1}$ , their efficiency always being compared with the results obtained during the operation without pulsation (Roca *et al.*, 1996a).

More stable operation was obtained for longer periods when a pulsation was applied to the feed stream, which prevented bubble gas occlusions, bed fragmentation and bed slug formation, problems that frequently arise when operating without pulsation. At higher glucose concentrations, higher amounts of gas are produced, and therefore pulsing at a higher frequency facilitates more efficient gas removal. Thus, the selection of an appropriate frequency to synchronise the pulses with gas production could help to improve the performance of the bioreactor (Figure 11.6). The explanation of this effect is complex as pulsation controls two different factors; mass transfer resistance and degasification of the bed. The mechanical effect, which improves mass transfer, increases with the amplitude of the pulse for a particular flow rate. The effect of pulsation on degasification is more complex because it also depends on the gas production rate during the fermentation process.

The selection of the optimum amplitude and frequency of pulsation is quite difficult because there are many contradictory effects (Roca *et al.*, 1996b). Higher substrate concentrations imply the evacuation of greater volumes of gas and therefore the optimum pulsation frequency should be higher. On the other hand, operation at higher hydraulic residence times should imply a decrease in the optimum pulsation frequency, in order to keep the mechanical effect of pulsation. To determine the best pulsing conditions, a control-supervision system based on the knowledge of the process, including an optimum search algorithm for the determination of the best frequency for each particular operation (residence time and substrate concentration), was implemented.

### *ii) Efficiency*

In Figure 11.7, the performance of the pulsing system is compared with that of the nonpulsed one. As can be seen, the differences in efficiency are more evident in the second half of the bioreactor, as it is predictable.

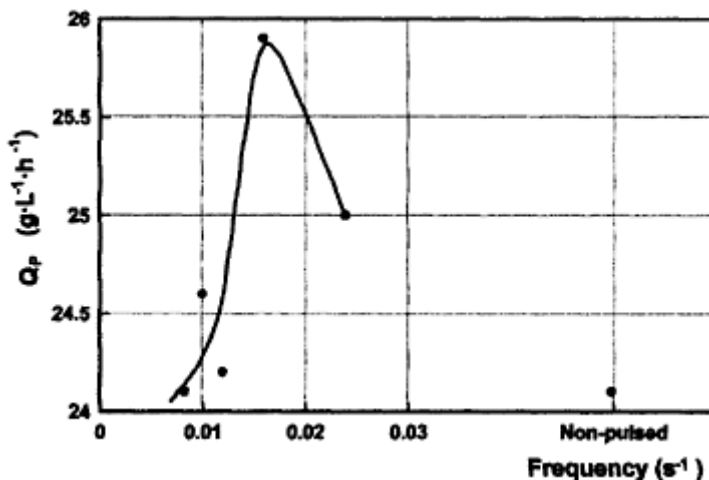


**Figure 11.6** Influence of pulsation frequency on overall productivity ( $Q_p$ ) obtained for an alcoholic fermentation by *S. cerevisiae* immobilised on alginate with  $S_0=100 \text{ g L}^{-1}$  and at a hydraulic residence time of 1.4 h in a packed bed bioreactor.

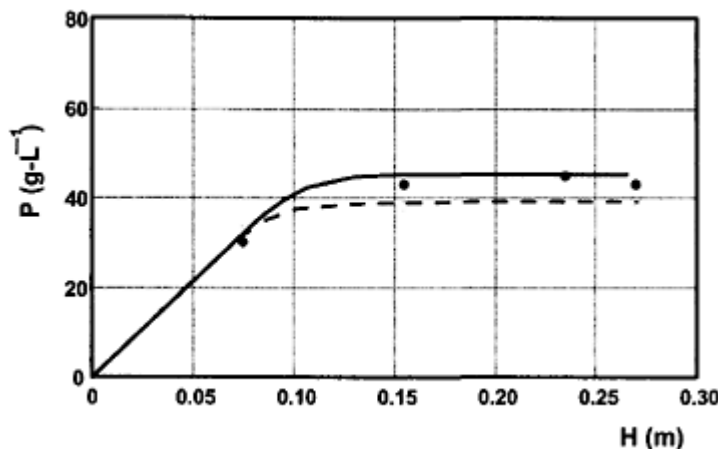


**Figure 11.7** Performance of the pulsed and non-pulsed packed bed bioreactor for the production of ethanol by immobilised *S. cerevisiae*, at a HRT of 3 h by using 100 g L<sup>-1</sup> of glucose as substrate. Symbols: Non pulsed and (●) Pulsed with a frequency of 0.008 s<sup>-1</sup>.

When the residence time was high enough for pulsation to exert limited mechanical effects, the ethanol concentration in the bioreactor reached its maximum value at a bed height of 0.15 m, where the substrate was completely consumed. Pulsation enables hydrodynamic behaviour to follow that of plug flow model quite closely, and partially impedes the backmixing observed in non-pulsed operation. As a complete substrate conversion is achieved in both cases, the difference in the results is explained not by possible differences in external mass transfer and internal effective diffusion but by differences in free yeast growth caused by the wash out obtained through the application of the pulses.

Operation in a pulsed mode increases productivity significantly in the upper part of the fermentor, when appropriate pulsations are applied. The same behaviour was observed when working with smaller bioreactors (Sanromán *et al.*, 1994a,b).

### Gas-phase Pulsing Bioreactors

The physiological and morphological growth characteristics of many filamentous fungi require the introduction of large amounts of gas to maintain the levels of dissolved oxygen desirable for metabolite production. Besides, after a very short period of time, the excessive growth of fungi gives rise to technical difficulties such as fouling of the fermenter probes, bed spouting and bioreactor clogging due to the interconnection of conglomerates of pellets or immobilised bioparticles (Presser and Tough, 1991). An example of this is shown in Figure 11.8, which corresponds to the formation of conglomerates of *Phanerochaete chrysosporium* pellets after a 3-day operational period, in an expanded-bed bioreactor. As a consequence, a low productivity of metabolites and a short bioreactor performance in stable conditions are common.

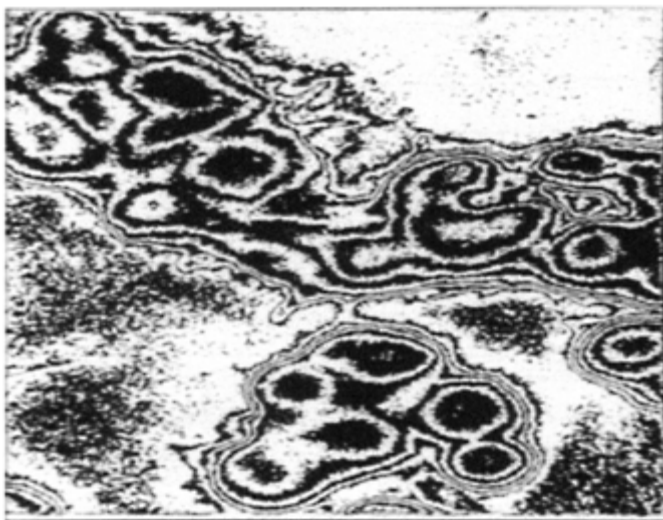


**Figure 11.8** Digitalised image of conglomérates of *P. chrysosporium*. Dark bioparticles correspond to nucleus of original pellets.

The application of the liquid-phase pulsation might be considered a useful tool to increase mass transfer rate, and consequently the oxygen availability; however the high aerobic requirements associated with these bioprocesses constrain the use of this alternative. Considering these facts, we proposed the so-called gas-phase pulsing bioreactors. In this bioreactor scheme, the pulsing flow is generated by means of the hydraulic transmission of a perturbation in the form of pulsed gas (air or oxygen) to the culture medium in the bioreactor. A design for the pulsed bioreactor corresponding to a fixed-bed bioreactor is shown in Figure 11.9. A few modifications should be considered in the case of other bioreactor configurations such as expanded or fluidised-bed ones. In this case, the scheme of the bioreactor is almost identical, except for the existence of a settler in the upper part, which allows gas/liquid/pellet separation. Besides, a continuous supply of air is introduced to maintain proper fluidisation. The two important objectives of the introduction of gas in a pulsing form are: i) the maintenance of high oxygen tension and ii) the control and regulation of hyphal extension and pellet size by a shearing stress associated with the pulsation.

#### *Control of pellet morphology*

Although pulsation was found to regulate different filamentous fungi growth by controlling pellet size efficiently (Moreira *et al.*, 1996), here we present results corresponding to the production of citric acid from *A. niger* in a pulsed fluidised bioreactor.

The effects of pulsation on pellet morphology were analysed by varying the pulsation frequency between 0.5 and 0.05 s<sup>-1</sup> for *A. niger* and compared with the corresponding

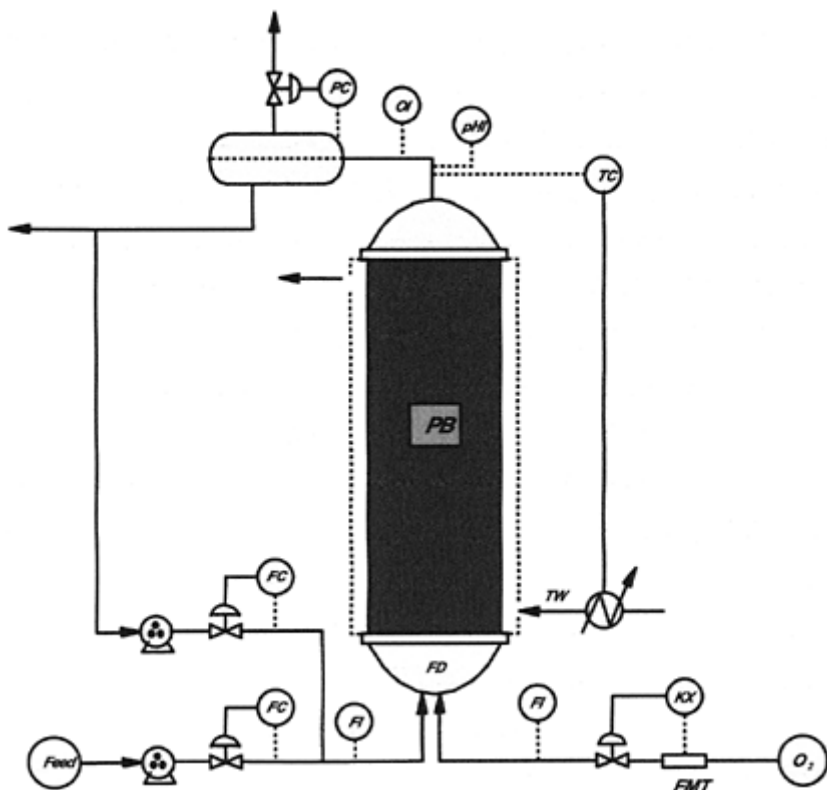


**Figure 11.9** Pulsed bioreactors used for the culture of filamentous fungi. Abbreviations: PB: Packed bed; TW: Thermostated water; FD: Feed distributor; FI: Flow indicator; pHI: pH indicator; OI: Oxygen indicator; TC: Temperature controller; FC: Flow controller; PC: Pressure controller; FMT: flexible membrane tube, KX: Timer.

results from the operation without pulsation. As can be seen in Figure 11.10, the pulsation frequency exerted a remarkable effect on pellet diameter and pellet size distribution. The minimum pellet diameter ( $3.3 \pm 0.1$  mm after 20 days) corresponded to the pulsed system operated at 0.35 s<sup>-1</sup>. On the other hand, the system without pulsation

presented great conglomerates of mycelia with sizes ranging from 3 to 7 cm, producing bed compacting after a few days and disabling a longer operation.

As far as external morphology is concerned, the appearance of the pellets of *A. niger* corresponding to air pulsation is compact, with negligible peripheral growth of mycelium around the pellet. In contrast, the pellets from the system without pulsation have a greater radius because of hyphal extension and branching (Figure 11.11). This phenomenon displaces the growth mechanism to dispersed mycelia by shifting the pellet distribution to the formation of conglomerates of pellets, which are constantly being increased by the linking of free hyphal fragments.

Gas pulsation implies not only the control of hyphal extension but also an improved efficiency of metabolite production, in this case citric acid (Table 11.3). The optimum

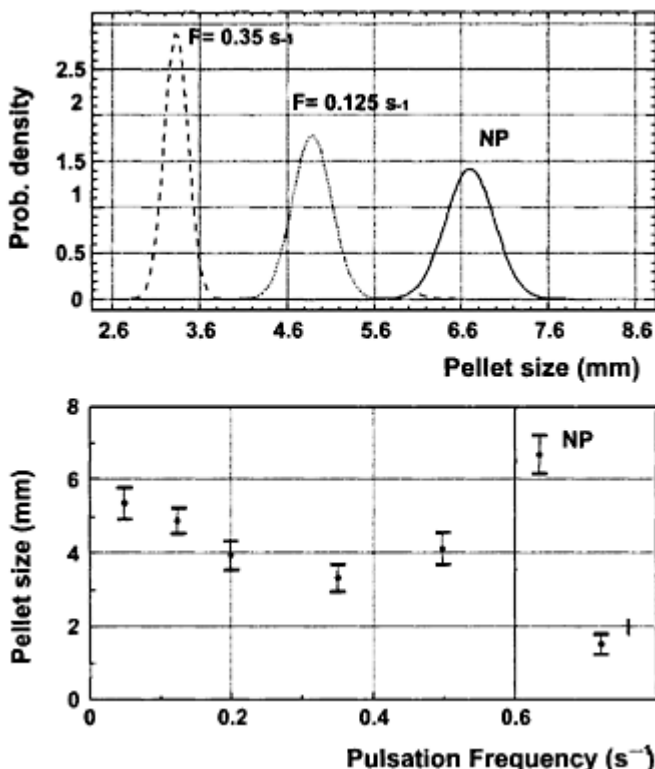


**Figure 11.10** Distribution of *A. niger* pellet size after 22 days of operation for the different pulsation frequencies. Pulsation frequency F; inoculum I; nonpulsed bioreactor NP.

frequency is considered as that which gives a higher productivity as well as an increased stability in continuous production. These beneficial effects may be explained by the fact that the control of pellet size increases the active surface of mycelia and increases nutrient availability. Moreover, it prevents bed compacting and consequently, improves overall mass transfer and substrate conversion.

### ***Continuous production of Manganese Peroxidase (MnP)***

The production of a ligninolytic enzyme, MnP, is associated with nutrient nitrogen limitation. This fact implies that MnP is typically produced during a very short period of time, after which the enzyme is rapidly deactivated by extracellular protease secretion and cell lysis due to the extreme nutritional conditions. In accordance with this, the extent of the ligninolytic activity is rather limited and only achieved in batch cultures. The low amount of enzyme obtained in such conditions makes its application for biotechnological purposes rather impractical. Hence, it seems logical to develop an efficient production system for these enzymes. Continuous operation appears to be a good choice, since it would lead to the continuous production of the enzyme. However, this possibility needs an additional requirement to displace batch fermentations; production has to be kept stable,

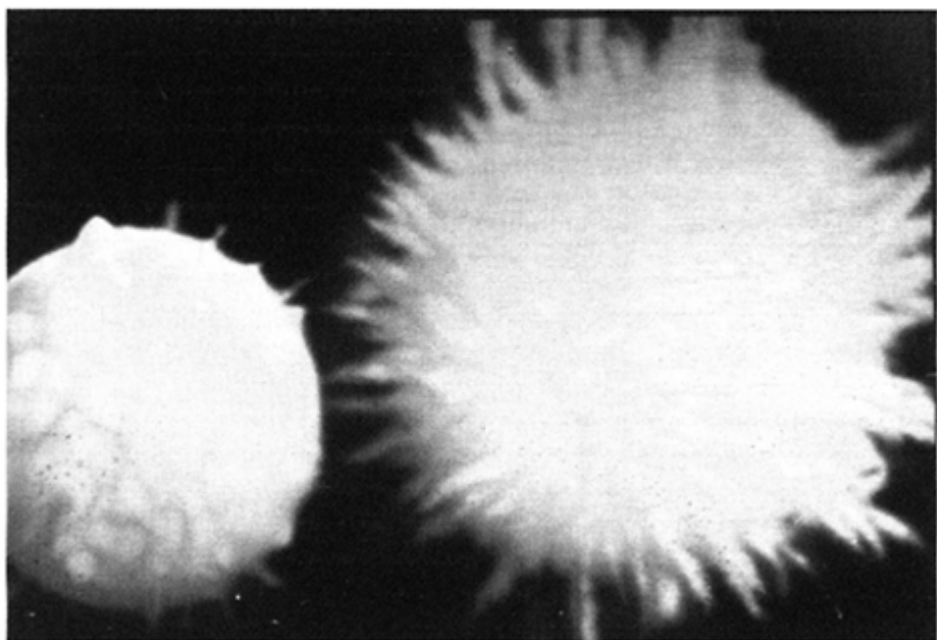


**Figure 11.11** Pellets of *A. niger* corresponding to the bioreactor operated with (left) and without (right) pulsation.

**Table 11.3** Citric acid production by *A. niger* in a continuous fluidised bed reactor with different air pulsation frequency

Time	Frequency ( $s^{-1}$ )					
	0.50	0.35	0.20	0.125	0.050	Non-Pulsed
0	0	0	0	0	0	0
3	1.06	1.22	1.78	0.78	0.78	0.89
7	5.11	6.58	5.53	0.61	5.44	5.31
9	8.03	9.85	8.15	7.95	7.06	7.56
13	11.02	14.62	11.85	9.53	7.97	NA
16	16.55	19.55	16.72	13.79	10.86	NA
20	16.83	18.98	17.88	17.38	13.64	NA

NA: Not applicable.

with high levels of activity, comparable with the batch process. The success of the process depends on its ability to maintain stable secondary metabolism conditions and control fungal growth. The combination of a proper feed rate and the application of a pulsation in a packed-bed bioreactor were fundamental in the enhancement and prolongation of MnP production by *P. chrysosporium* (Moreira *et al.*, 1998). For this work, two different configurations were considered: expanded-bed bioreactor operated with pellets or fixed-bed bioreactor packed with *P. chrysosporium* BKM-F-1767 immobilised in cubes of polyurethane foam, both bioreactors coupled with oxygen pulsation.

The comparison of the effect of pulsation on MnP production in pulsed and non-pulsed bioreactors is highlighted in Figure 11.12. A clear difference is observed when comparing the operation with and without pulsation. In both pulsed bioreactors, continuous production of MnP is maintained for a long period (more than 30 days). In the case of the non-pulsed bioreactor, MnP production is comparatively low and maintained for a shorter period.

Just as pulsation modifies the morphology of mycelial pellets, the application of the gas pulsation to the immobilised bioparticle efficiently limits hyphal extension between foam blocks, and avoids interconnection and aggregation.

#### *Application of the fungal pulsed bioreactor to the decolourisation of synthetic dyes*

Conventional biological technologies have been applied extensively in the treatment and detoxification of many industrial effluents. However, these treatment alternatives present specific limitations, especially when applied to the decolourisation of recalcitrant compounds. The following example seeks to describe another possible application of gas-

phase pulsing bioreactors in decolourisation and detoxification of highly coloured wastewaters, based on the oxidative capability of MnP towards xenobiotic degradation.

The decolourisation of an industrial dye, Poly R-478 by *P. chrysosporium*, is shown in Figure 11.13. The proposed system is effective and achieves a high degree of

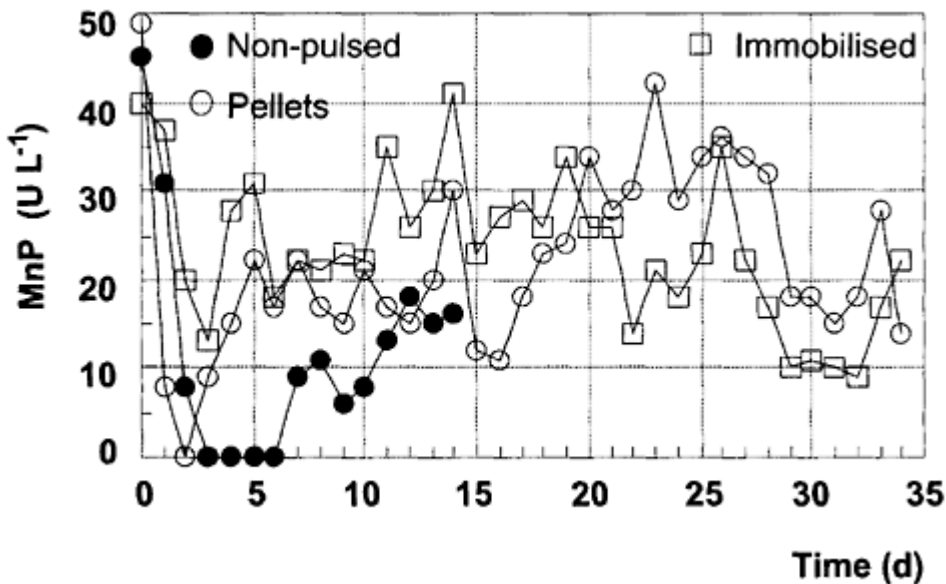


**Figure 11.12** Continuous production of MnP by free and immobilised *P. chrysosporium* in fixed-bed bioreactors with (open symbols) and without (close symbols) oxygen pulsation.

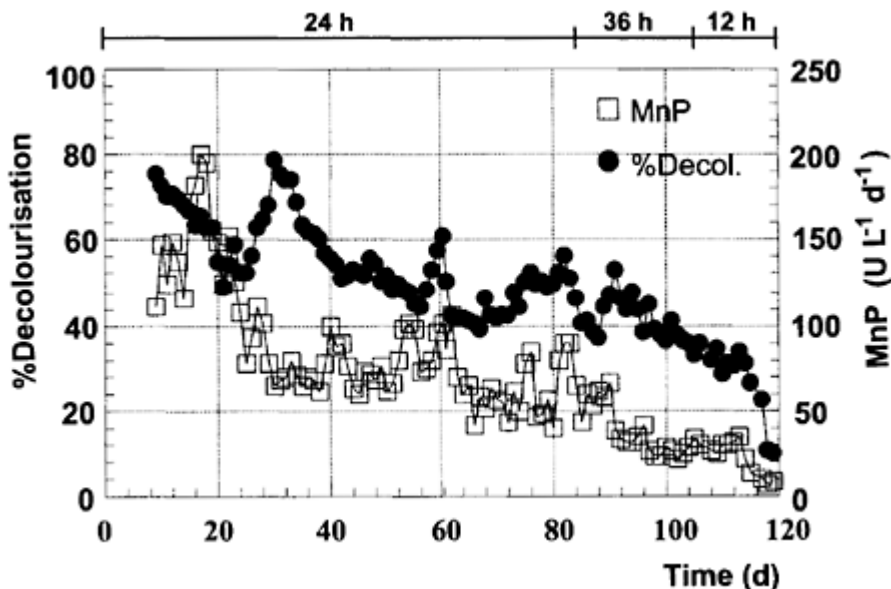


**Figure 11.13** Poly R-478 decolourisation efficiency and MnP productivity (referred to reactor volume and flow rate) in a packed bed bioreactor operating at HRT of 24, 36 and 12 h.

decolourisation of the dye, which is degraded to percentages exceeding 70% at variable HRT of 12, 24 and 32 h. Moreover, stable operation is maintained for an extended period of time (more than 100 days) (Palma *et al.*, 1999). It is advisable for the fungal bioreactor to be used as a pretreatment step in an integrated treatment system, combining the use of fungi and anaerobic bacteria.

## REFERENCES

- Bailes, P.J., Hanson, C. and Hughes, M.A. (1976) Liquid-liquid extraction: The process and the equipment. *Chem. Eng.*, **83**, 86–100.
- Baird, M.H.I. and Garstang, J.H. (1972) Gas absorption in a pulsed bubble column. *Chem. Eng. Sci.*, **27**, 823–833.
- Baird, M.H.I. and Rao, N.V.R. (1988) Characteristic of a counter current reciprocating plate bubble column. II. Axial mixing and mass transfer. *Can. J. Chem. Eng.*, **66**, 222–231.
- Baird, M.H.I., Vijayan, S., Rao, N.V.R. and Rohatgi, A. (1989) Extraction and absorption with a vibrating perforating plate. *Can. J. Chem. Eng.*, **67**, 787–800.
- Baltar, C. (1972) Device for the generation of pulsing phenomena in fluids. Spanish Patent N° 44 3893.

- Brauer, H. (1988) Development and efficiency of a new generation of bioreactors. Part 2. *Bioprocess Eng.*, **3**, 11–21.
- Brauer, H. (1991) Growth of fungi and bacteria in the reciprocating jet bioreactor. *Bioprocess Eng.*, **6**, 1–15.
- Brauer, H. and Annachhatre, A.P. (1992a) Nitrification and denitrification in a system of reciprocating jet bioreactor. *Bioprocess Eng.*, **7**, 269–275.
- Brauer, H. and Annachhatre, A.P. (1992b) Wastewater nitrification kinetics using reciprocating jet bioreactor. *Bioprocess Eng.*, **7**, 277–286.
- Brauer, H. and Sucker, D. (1979) Biological waste water treatment in a high efficiency reactor. *Ger. Chem. Eng.*, **2**, 77–86.
- Chamy, R., Núñez, M.J. and Lema, J.M. (1990) Optimization of the hardening treatment of *Saccharomyces cerevisiae* bioparticles. *Enzyme Microb. Technol.*, **12**, 749–754.
- Chisti, M.Y. (1989) Airlift reactors: Current Technology. In: *Air-lift bioreactors*. Elsevier Sci. Pub. Ltd., pp. 33–86, Barking, U.K.
- Dondé, M., Goma, C. and Durand, C. (1987) Transfer oxygen potential of an air-pulsed continuous fermentor. *Biotechnol. Process*, **4**, 135–141.
- Etzold, M. and Stadlbauer, E.A. (1990) Design and operation of pulsed anaerobic digesters. *Bioprocess Eng.*, **5**, 7–12.
- Finnigan, S.M. and Howell, J.A. (1989) The effect of pulsatile flow on ultrafiltration fluxes. *Chem. Eng. Res. Des.*, **67**, 278–282.
- Fontana, A., Ghommidh, C., Guiraud, J.P. and Navarro, J.M. (1992) Continuous alcoholic fermentation of sucrose using flocculating yeast. The limits of invertase activity. *Biotechnol. Lett.*, **14**, 505–510.
- Gilson, C.D. and Thomas, A. (1993) A novel fluidised bed bioreactor for fermentation of glucose to ethanol using alginate immobilized yeast. *Biotechnol. Tech.*, **7**, 397–400.
- Göebel, J.C. and Fortuin, J.M.H. (1986) Solids hold-up in a pulsed packed column used for solid-liquid contacting. *Chem. Eng. Sci.*, **41**, 2531–2539.
- Golding, J.A. and Lee, J. (1981) Recovery and separation of Cobalt and Nickel in a pulsed sieve-plate extraction column. *Ind. Eng. Chem. Process. Des. Dev.*, **20**, 256–261.
- Harrison, S.T.L. and Mackley, M.R. (1992) A pulsatile flow bioreactor. *Chem. Eng. Sci.*, **47**, 490–493.
- Lema, J.M., Núñez, M.J., Sanromán, A. and Roca, E. (1995) Pulsing device to be coupled to fermentation equipments, enzymatic reactors or chemical reactors. Spanish Patent N°2059228.
- Levenspiel, O. (1988) Nonideal Flow. In: *Chemical Reactor Engineering*. Wiley and Sons, Inc. pp. 277–346, New York, USA.
- Mak, A.N.S., Hamersma, P.J. and Fortuin, J.M.H. (1992) Solids hold-up and axial dispersion during countercurrent solid-liquid contacting in a pulsed packed column containing structured packing. *Chem. Eng. Sci.*, **47**, 565–577.
- Mehaia, M.A. and Cheryan, M. (1984) Hollow fiber bioreactor for ethanol production: Application to the conversion of lactose by *Kluyveromyces fragilis*. *Enzyme Microb. Technol.*, **6**, 117–120.
- Minier, M. and Goma, G. (1982) Ethanol production by extractive fermentation. *Biotechnol. Bioeng.*, **24**, 1565–1579.
- Miñana, A., Rubio, M. and Albentosa, J. (1985) Aplicación de pulsación neumática y flujo de aire a una columna de extracción líquido-líquido. *Afinidad*, **42**, 407–415.
- Miranda, M., Murado, M.A., Sanromán, A. and Lema, J.M. (1991) Mass transfer effects in the enzymatic hydrolysis of polysaccharides by glucoamylase. *Enzyme Microb. Technol.*, **13**, 142–147.
- Moreira, M.T., Sanromán, A., Feijoo, C. and Lema, J.M. (1996) Control of pellet morphology of filamentous fungi in fluidized bed bioreactors by means of a pulsing flow. Application to *Aspergillus niger* and *Phanerochaete chrysosporium*. *Enzyme Microb. Technol.*, **19**, 261–266.

- Moreira, M.T., Feijoo, G., Palma, C. and Lema, J.M. (1998) Strategies for the optimization of continuous production of Manganese Peroxidase by *Phanerochaete chrysosporium* immobilized on polyurethane foam. *J.Biotechnol.*, **66**, 27–39.
- Murthy, V.V.P.S., Ramachandran, K.B. and Ghose, T.K. (1987) Gas hold-up and power consumption in an air-pulsed column bioreactor. *Process Biochem.*, **22**, 3–8.
- Navarro, J.M. and Goma, G. (1980) Nouveau dispositif de mise en oeuvre des microorganismes. Paténté Française N° 78 28572. Institut National de la Propriété Industrielle, Paris.
- Núñez, M.J. and Lema, J.M. (1987) Cell immobilization: Application to alcohol production. *Enzyme Microb. Technol.*, **9**, 642–651.
- Palma, C., Moreira, M.T., Mielgo, I., Feijoo, G. and Lema, J.M. (1999) Use of a fungal bioreactor as a pretreatment or post-treatment step for continuous decolourisation. *Water Sci. Technol* (in press)
- Prosser, J.I. and Tough, A.J. (1991) Growth mechanisms and growth kinetics of filamentous microorganisms. *Crit. Rev. Biotechnol.*, **10**, 253–274.
- Roca, E., Flores, J., Núñez, M.J. and Lema, J.M. (1996a) Ethanolic fermentation by immobilized *Saccharomyces cerevisiae* in a semipilot pulsing packed-bed bioreactor. *Enzyme Microb. Technol.*, **19**, 132–139.
- Roca, E., Flores, J., Rodríguez, I., Cameselle, C., Núñez, M.J. and Lema, J.M. (1996b) Knowledge based control applied to fixed-bed pulsed bioreactors. *Bioprocess Eng.*, **14**, 113–118.
- Roca, E., Sanromán, A., Núñez, M.J. and Lema, J.M. (1994) A pulsing device for packed-bed bioreactors: I.-Hydrodynamic behaviour. *Bioprocess Eng.*, **10**, 61–74.
- Sanromán, A., Chamy R., Núñez M.J. and Lema J.M. (1991) Enzymatic hydrolysis of starch in a fixed-bed pulsed-flow bioreactor. *Applied Biochem. Biotech.*, **28/29**, 527–538.
- Sanromán, A., Chamy, R., Núñez, M.J. and Lema, J.M. (1994a) Alcoholic fermentation of xylose by immobilized *Pichia stipitis* in a fixed-bed pulsed bioreactor. *Enzyme Microb. Technol.*, **16**, 72–78.
- Sanromán, A., Roca, E., Núñez, M.J. and Lema, J.M. (1994b) A pulsing device for packed-bed bioreactors: II.-Application to alcoholic fermentation. *Bioprocess Eng.*, **10**, 75–82.
- Serieys, M., Goma, G. and Durand, G. (1978) Design and oxygen-transfer potential of a pulsed continuous tubular fermentor. *Biotechnol. Bioeng.*, **20**, 1393–1406.
- Skala, D. and Veljkovic, V. (1988) Mass transfer characteristics in a gas-liquid reciprocating plate column. I. Liquid phase volumetric mass transfer coefficient. *Can. J. Chem. Eng.*, **66**, 192–199.
- Tyagi, R.D., Gupta, S.K. and Chand, S. (1992) Process engineering studies on continuous ethanol production by immobilized *Saccharomyces cerevisiae*. *Process Biochem.*, **27**, 23–32.
- Van Dijk, W.J.D. (1935) Tower with internal perforated plates suitable for extracting liquid by treatment with other liquids and for similar countercurrent contact processes. U.S. Patent 2,011,186, Aug. 13.
- Yang, N.S., Chen, B.H. and McMillan, A.F. (1986) Axial mixing and mass transfer in gas-liquid Karr columns. *Ind. Eng. Chem. Process Des. Dev.*, **25**, 776–780.



# **CHAPTER TWELVE**

## **DESIGN OF LIQUID-LIQUID-SOLID**

### **FLUIDISED-BED BIOREACTORS**

ERIK VAN ZESSEN, ARJEN RINZEMA AND JOHANNES  
TRAMPER

*Food and Bioprocess Engineering Group, Wageningen University, P.O.  
Box 8129, 6700 EV Wageningen, The Netherlands*

#### **ABSTRACT**

A liquid-liquid-solid three-phase system is automatically formed, when in one apparatus an immobilised biocatalyst is used for a biotransformation and an organic solvent is used for extraction. The aim of this paper is to show that the application of such a three-phase reactor system for biotransformations strongly inhibited by the product will result in a higher degree of conversion, compared to a conventional reactor system. Thus, different reactor configurations are discussed. These include a simple three-phase fluidised bed, but also more elaborate options, such as variations of a loop reactor. It is concluded that building and operating a three-phase system is nothing more than a minor extension of conventional bioreactors. In the second part of this paper a simple reactor model is developed for a three-phase liquid-liquid-solid fluidised-bed bioreactor. The influence of different parameters is discussed, e.g. the distribution coefficient of product over medium/ organic solvent, the toxic product concentration, and the flux of the organic solvent. In the last part of this paper conditions have been established under which this three-phase reactor performs better than a conventional two-phase fluidised bed. At a given maximum substrate conversion rate, the distribution coefficient is determined for which the three-phase fluidised bed performs equally well as the two-phase fluidised bed. It appears already that a low distribution coefficient (larger than 1 but less than 2) suffices for a better operation. If *in situ* extraction is needed for such a biotransformation, a three-phase fluidised bed, or less simple three-phase bioreactors, are a good choice.

#### **INTRODUCTION**

Advantages of using a liquid-liquid two-phase system in biotransformations have been discussed (van Sonsbeek *et al.*, 1993; Vermüe and Tramper, 1995a; Tramper *et al.*, 1992; Adlercreutz, 2000). Depending on the nature of the biotransformations, the reason for applying a liquid-liquid two-phase system varies. Examples of different

biotransformations carried out in a two-phase system and the advantages of using such a system are given by Vermuë and Tramper (1995a). In general one can chose a liquid-liquid two-phase system when:

- the substrate dissolves poorly in the medium; the organic solvent acts as a reservoir;
- there is product inhibition; by using an organic solvent the product concentration in the medium is lowered;
- the reaction equilibrium is unfavourable; the equilibrium products dissolve in the organic solvent and the degree of conversion can be enhanced.

Another reason for using *in situ* extraction, the combination of bioconversion with the first unit operation in the downstream processing, might be a facilitated product recovery.

Obviously, using an organic solvent in bioconversions also leads to disadvantages. For example, the toxicity of the solvent might reduce the biocatalytic activity and stability (Vermuë *et al.*, 1995b). Furthermore, in any bioconversion with micro-organisms involved, surface active agents are present, whether excreted by the micro-organism, or present due to cell lysis. This can result in non-desirable, stable emulsions that are difficult to separate (Vermuë *et al.*, 1995b).

Inhibition due to direct contact between micro-organisms and the organic solvent can be reduced by immobilising the micro-organism. Immobilisation may also reduce the amount of surface-active agents, and consequently prevent a stable emulsion (Vermuë *et al.*, 1995b). Immobilisation of micro-organisms has been studied extensively (Wijffels *et al.*, 1996), and a particularly elegant way of immobilising micro-organisms is a method that uses a natural gel solution (e.g.  $\kappa$ -carrageenan, alginate). Broth is mixed with the gel solution and gel beads are made as described by, for instance, Hunik and Tramper (1993). Obviously, immobilisation will only work when there is hardly any outgrowth of the micro-organisms, and little excretion of proteins.

In operating an extractive bioconversion one should decide whether to use a bioreactor with bioconversion and extraction integrated, or use a plant set-up with both processes separated. In the latter case the medium has to be circulated between both apparatus at a high velocity (see the section on loop reactors for more detail). Using, in one apparatus, immobilised cells for a bioconversion and an organic solvent for extraction, a three-phase system is automatically formed. As apparatus, stirred tank reactors, although favourable for good mixing and a high interfacial area between medium and organic solvent, are not very useful; the harsh conditions in the tank will destroy the gel beads. A stronger immobilisation matrix would be required than the natural gels mentioned above. Another option is using column reactors. For this purpose a liquid analogue of the air-lift loop reactor, the liquid-impelled loop reactor, was designed (Tramper *et al.*, 1987) and hydrodynamically characterised by van Sonsbeek (1992a). Different biotransformations have been executed in this type of reactor (Vermuë *et al.*, 1995; Buitelaar *et al.*, 1991; van den Tweel *et al.*, 1987; Mateus *et al.*, 1996). The application of this type of reactor is discussed in the section on loop reactors. Another simple bioreactor is the liquid-liquid-solid three-phase fluidised bed. The reactor is almost identical to a liquid-impelled loop reactor, but the water flow is controlled with a pump and not induced by a density difference. The hydrodynamics of this reactor have been studied: the hold-up of the different phases as a function of the fluxes of both phases (van Zessen *et al.*, 2000a), as well as the mixing of the medium phase (van Zessen *et al.*, 2000b). This type of reactor

has good mixing characteristics, and seems promising for application in an *in situ* extraction bioprocess.

The aim of this chapter is to show that the application of a three-phase reactor system for bioconversions strongly inhibited by product, will result in a higher degree of conversion, compared to a conventional reactor system. Not all conditions favour a three-phase system, but it will be shown that with the right combination of operating conditions (fluxes of both liquids), and physical parameters (distribution coefficient and inhibition constant), a three-phase system is always favourable.

Figure 12.1 summarises different aspects looked upon in this paper. First, possible process lay-outs and different reactor configurations for a liquid-liquid-solid three-phase system are discussed. Next, the focus is on one of the reactor configurations: a three-phase fluidised-bed bioreactor. Then, a reactor model is developed, and characteristics of this model are discussed. Thereafter, the conditions for which a three-phase fluidised-bed gives a better performance than a liquid-solid fluidised bed are demonstrated.

- *Reactor Configuration*

- 1 Three phase liquid-liquid-solid fluidised-beds, both liquids flow co-currently
- 2 Three phase liquid-liquid-solid fluidised-beds, water flow counter-currently
- 3 Liquid-impelled loop reactors

- *Model derivation for reactor configuration 1*

Simulations for a batch operation

- Profiles inside a gel bead
- Different distribution coefficients
- Different toxic product concentrations
- Different fluxes of organic solvent

- *Comparison between conventional reactor and reactor configuration 1*

Evaluation of the distribution coefficient for which reactor configuration 1 performs equally well

Batch operation is studied extensively

Continuous operation is briefly discussed

**Figure 12.1** Short overview of different aspects looked upon

## PROCESS LAY-OUT AND OPERATION

A schematic presentation of a possible plant is shown in Figure 12.2. The core of the plant is the bioreactor, i.e. a three-phase fluidised bed. This column is fed by a continuous medium flow, introduced at the bottom of this column. This up-flowing stream is also

used for fluidising the biocatalytic particles. An immiscible solvent is pumped through a sparger, and the droplets formed rise through the fluidised bed. If coalescence of the droplets is easily achieved, which might be a prerequisite for good operation, both liquids are separated at the top of the column and sent back to their respective storage vessels. If separation between both liquids is not achieved by a simple one-stage gravity settler, the two-phase mixture can be separated outside the column.

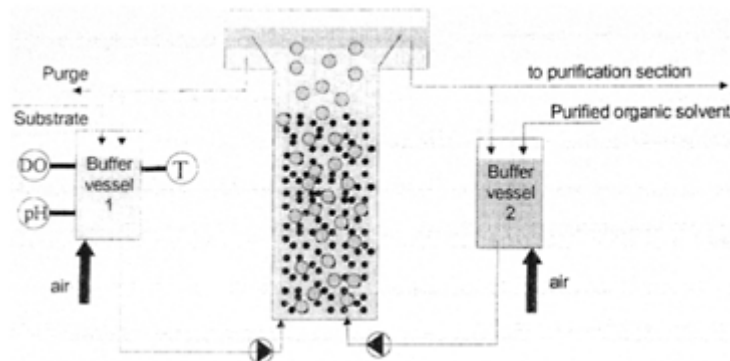


**Figure 12.2** Process lay-out for three-phase fluidised-bed bioreactor

If the biocatalyst requires oxygen, than aeration of one or both storage vessels will be an adequate method. Temperature control of the bioreactor can be done by keeping the temperature of both storage vessels constant. pH is controlled by keeping the pH of the substrate storage vessel constant.

Operating the bioreactor in this manner is a batch operation; accumulation of the product in the organic phase and depletion of the substrate will occur. A continuous operation with respect to the substrate phase can be achieved by adding a high substrate concentration to the storage vessel, keeping the substrate concentration constant. To prevent overflow of the storage vessel part of the circulating medium flow has to be purged, see also Figure 12.2.

Operating the bioreactor with a continuous supply of substrate will still result in the accumulation of the product in the organic phase. Operating the organic phase continuously is easily done by sending the total out-flowing organic phase to the recovery section, and pumping purified organic phase into the column. This strategy will be disadvantageous when the product concentration in the organic phase is low; a large volume of organic solvent has to be clarified. A better strategy would be to allow accumulation of the product to a certain concentration, below the equilibrium concentration, and to send part of the out-flowing organic phase to the recovery section, see Figure 12.2.

In the above discussion of a plant lay-out and a process operation for a three-phase fluidised-bed bioreactor, it is assumed that both liquid phases flow upward co-currently. This is true when the organic phase has a smaller density than the medium phase. When

the organic phase density is larger, this liquid has to be introduced at the top of the column, and both liquids have to be separated at the bottom of the column.

Another assumption is that the three-phase fluidised-bed bioreactor is stable, which means that the fluidised bed is in a hydrodynamic equilibrium; particles remain in the column and the droplets do not coalesce in the fluidised bed. Experiments with different kinds of gel beads have shown that a stable fluidised bed exists, at least, for gel beads with a density of  $1060 \text{ kg/m}^3$  and a diameter of 2.3 mm. Applying gel beads with a density of  $1010 \text{ kg/m}^3$  and a diameter of 2 mm in a three-phase fluidised bed resulted in the wash out of the beads at any organic flow rate larger than  $10^{-4} \text{ m}^3/(\text{m}^2 \text{ s})$ . It can be concluded that a stable three-phase fluidised bed is possible for particles with a settling velocity larger than 5.0 cm/s. Coalescence of droplets can be prevented by carefully adjusting both flows.

### Alternatives

Below two different alternatives are given for operating a three-phase liquid-liquid-solid system, see also Figure 12.1.

#### *Counter-current water flow*

A three-phase fluidised bed with both liquids flowing co-currently is not possible for each type of particle. For particles with a terminal settling velocity larger than 5.0 cm/s a stable bed is possible, but for particles with a velocity smaller than 2 cm/s a stable bed could not be obtained (van Zessen, unpublished). We do not know whether a stable fluidised bed is possible for particles with a terminal settling velocity between 2 and 5.0 cm/s.

A stable three-phase fluidised bed is possible for those particles with a settling velocity smaller than 2 cm/s, if a different strategy is followed. In operating this strategy, droplets rise from bottom to top and medium flows counter-currently, i.e. from top to bottom, see Figure 12.3. A limited version of this strategy would be a case in which there is no medium flow.

For bubble columns, it is known that gel beads can be fluidised—kept in suspension—by the rising gas bubbles. As a liquid-liquid-solid three-phase fluidised bed is the liquid analogue of a gas-liquid-solid three-phase fluidised bed, it should be possible to create a droplet column with solids kept in suspension. Indeed, it has been possible to keep two different kinds of K-carrageenan gel beads in suspension in a droplet column (van Zessen, unpublished). These gel beads had a density of  $1007.4 \text{ kg/m}^3$  and  $1005.4 \text{ kg/m}^3$  and a diameter of 1.97 mm and 3.12 mm. However, to maintain the gel beads in suspension a minimal solvent flux was required. Experimental data on hydrodynamic parameters, such

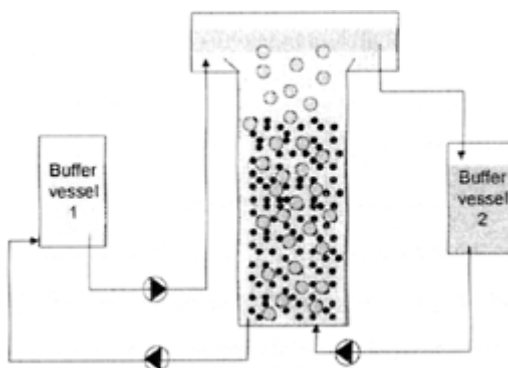


**Figure 12.3** Alternative process layout: water flows counter-current with respect to the droplets flow

as hold-up, were not determined; only visual observations were made on this operating strategy. Provided the solvent flux was higher than a minimal value, this three-phase system was stable for at least 24 hours.

As the droplet column with suspended gel beads worked well without any water flow, we also tried to operate the set-up with water flowing counter-currently, see Figure 12.3. The water flux puts a downward directed force on the gel beads, whereas the force put on the gel beads by the organic solvent flux is directed upwards. Obviously, when the water flux becomes too high, the gel beads will settle. Again, we only made visual observations for this set-up. These observations can be summarised as follows:

- at a fixed water flux, the organic solvent flux has to have a minimal value in order to make this system work. Increasing the organic solvent flux resulted in a larger bed height, i.e. a lower gel-bead hold-up;
- at a fixed organic solvent flux, higher than the minimum flux required for stable operation, the water flux can be increased to a maximum value. At higher values the system will not work, i.e. gel beads settle, and droplets coalesce.

This operating strategy gives a couple of advantages over a co-current strategy. In extraction processes counter-current operation is always better than co-current operation, as there is always a higher driving force for mass transfer. In co-current operation the gel-bead hold-up decreases with an increasing medium flux, whereas in counter-current operation the gel-bead hold-up increases with an increasing medium flux. It is also observed that at a higher organic solvent flux a higher water flux can be applied; this means that the throughput of substrate can be higher in counter-current operation.

#### *Loop reactors*

Another type of bioreactor is the so-called loop reactor: these reactors consist of two tubes connected to each other; internal and external designs exist (van 't Riet and Tramper, 1991). In order to function, there has to be a difference in density of the mixture

in both tubes. A density difference results in a pressure difference and water will flow between both tubes: the direction of this water flow goes from a high to a low density.

This principle has been applied in air-lift reactors (Chisti, 1989). The liquid analogue, droplets instead of gas bubbles, the so-called liquid-impelled loop reactor, has been described by Van Sonsbeek (1992a). This type of reactor with particles,  $\kappa$ -carrageenan gel beads, has been used by Mateus *et al.* (1996) and Vermuë *et al.* (1995) for biotransformations.

Figure 12.4 shows four possible reactor configurations for the application of a three-phase system in a loop reactor. First, it is assumed that the particles remain in one column, and are not circulating. Particles circulating between both tubes are discussed below. In parts A and B of this figure, a bed of biocatalytic particles and a spray extraction column are separated. In part C and D, conversion and extraction are fully integrated.

In part A droplets of an organic solvent rise from the bottom to the top of the column as their density is lower than the water density. Consequently, pressure is lower in the spray

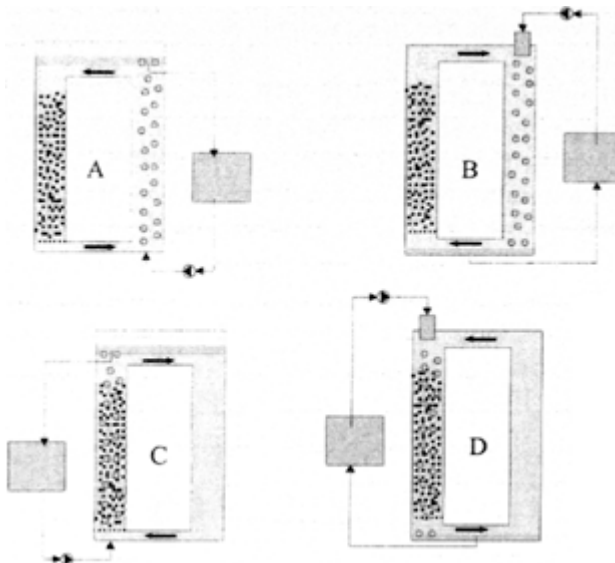


**Figure 12.4** Loop reactors (see text for explanation)

column, and water flows from top to bottom in the column with particles. If the density of the particles is higher than the water density, a packed bed will be formed. If the density of the particles is lower than the water density, and the water flux is larger than the rise velocity of the swarm of particles, a fluidised bed will be formed. This so-called inverse fluidisation has been studied by Fan *et al.* (1982).

In part B, droplets of an organic solvent settle from the top to the column, as the density is higher than the medium density. In this case, water flows from bottom to top in

the column with particles. This set-up will work if the particle density is higher than the water density. A fluidised bed will be observed, if the water flow is higher than the minimum fluidization velocity.

Part C of Figure 12.4 shows a three-phase mixture in one column and medium in the other column of the loop reactor. The density of the organic solvent is less than the medium density and solvent droplets will rise. A three-phase fluidised bed will only exist when the density of this mixture is less than the density of the medium in the other column. In that case water will flow from bottom to top in the three-phase column. For example, in our laboratory experiments have been done on the hold-ups in a three-phase system, i.e. water, dodecane and gel beads (density equals  $1060 \text{ kg/m}^3$ ). At a water flux of  $1.8 \times 10^2 \text{ m/s}$  and a dodecane flux of  $0.91 \times 10^2 \text{ m/s}$ , a gel bead hold-up of 0.20 and a dodecane hold-up of 0.08 was measured. This gives a mixture density of  $992 \text{ kg/m}^3$ . The density difference between both columns is in this case large enough to obtain this water flux of  $1.8 \times 10^2 \text{ m/s}$  (Van Sonsbeek *et al.*, 1990).

A different situation exists when the density in the three-phase system is larger than the density of the medium in the other column, due to a higher solids hold-up or a lower organic solvent hold-up. In this case water will flow from top to bottom. Provided the density of the solids is close to water, this configuration can also work (see the previous section "Counter-current water flow").

The column with only medium can be aerated. However, aeration results in a decrease of the mixture density in this column, and the circulation velocity of the medium between both columns is changed. In order for a three-phase fluidised bed to exist, the aeration must be carried out carefully. Aeration results in an air hold-up, and hence a smaller mixture density in the aerated column. Consequently, the density difference between both columns becomes less, and the circulation velocity decreases. At this smaller medium velocity a three-phase fluidised bed must still exist.

Part D of Figure 12.4 is the same as part C, but in this case the density of the organic solvent is larger than the density of water, hence droplets settle. Water will always flow in the direction indicated in this figure; from top to bottom in the three-phase column. Only if the biocatalytic particles have a density smaller than water, i.e. they rise in the column, will this configuration work.

So far it is assumed that the particles remain in a fluidised state. However, the water circulation velocity can be so high that it exceeds the terminal settling velocity of a single particle. In that case particles flow together with the water, and are present in both columns. This principle is widely used in air-lift bioreactors (Heijnen *et al.*, 1997).

## PERFORMANCE OF A CONVENTIONAL BIOREACTOR AND A THREE-PHASE FLUIDISED-BED BIOREACTOR

In the preceding section possible reactor configurations have been discussed. Whether such a three-phase reactor will work better than a conventional reactor is the topic of this section. We decided to compare a two-phase fluidised-bed bioreactor, the conventional reactor, with a three-phase liquid-liquid-solid fluidised-bed bioreactor. Comparing two different reactors, one should consider a fair comparison. This comparison can be based on cost, but in that case one should consider total cost, i.e. cost of a total production plant.

Making a total process design and optimising this design for both reactors goes beyond the scope of this paper. One can also compare both reactors on their performance, i.e. degree of conversion of the substrate, or synthesis rate of product.

Before we go into a detailed comparison of both bioreactors, the model used for the calculations is described.

### Model Derivation

A general total model for the design of a reactor is schematically shown in Figure 12.5. This model consist of three major parts:

- hydrodynamics of the reactor
- kinetics of the bioconversion
- mass transfer of compounds between the different phases

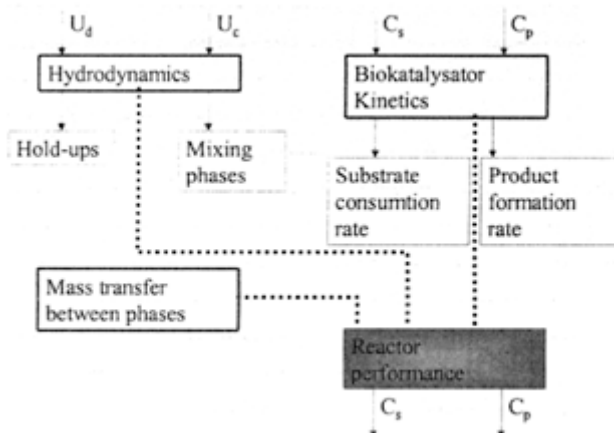


**Figure 12.5** Model outline

Together with mass balances over each phase for the different components, the total model is complete.

### Investigated system

In our laboratory hydrodynamic studies have been done on a three-phase system consisting of water, dodecane and gel beads. This system is used as the model system. Obviously, highly complicated bioconversions can be involved in producing industrially interesting products, in which more than one substrate and product influence the kinetics. We have chosen a very simple one-to-one conversion: substrate S gives product P. It is further assumed that substrate is dissolved in the medium and insoluble in the organic solvent, transported to the gel bead and then converted to product. The product itself is transported out of the gel bead to the medium phase and subsequently to the organic solvent phase.

### Hydrodynamics

This part of the model considers the hold-up and mixing of the different phases present. To model the medium flow, the fluidised bed is divided in a number of ideally mixed tanks. For a fluidised bed of 1 m high, and for medium fluxes between  $0.5 \times 10^{-2}$  and  $2 \times 10^{-2}$  m/s, the number of tanks has been experimentally determined. It appears that for medium fluxes the number of ideally mixed tanks is equal to 13 for the two-phase fluidised bed and 3 for the three-phase fluidised bed.

In order to make the reactor model less complicated, it is assumed that gel beads remain in one tank and do not circulate between the different tanks.

A model has been developed for predicting the hold-ups in a three-phase fluidised bed (van Zessen, 2000), but we chose to use the experimentally determined hold-ups as they are more accurate. The dodecane hold-up and gel bead hold-up as a function of medium flux and dodecane flux is shown in Figure 12.6.

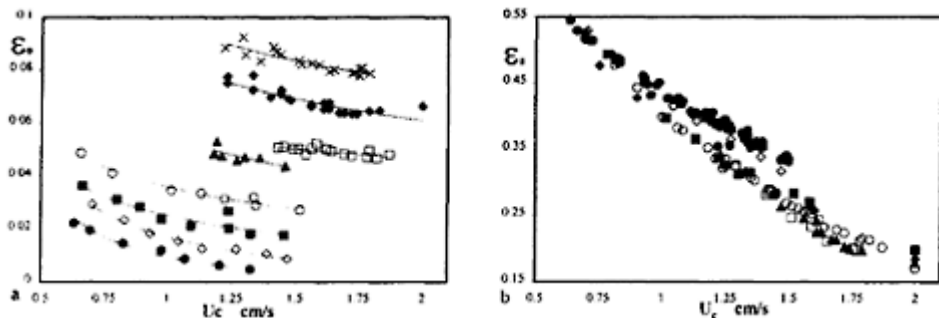


**Figure 12.6** a: droplet hold-up as a function of the water and dodecane flux. ●  $U_d=0.05\text{cm/s}$ , ◇  $U_d=0.10\text{ cm/s}$ , ■  $U_d=0.18\text{cm/s}$ , ▨  $U_d=0.27\text{ cm/s}$ , ▲  $U_d=0.44\text{cm/s}$ , □  $U_d=0.54\text{ cm/s}$ , ♦  $U_d=0.73\text{ cm/s}$ , ×  $U_d=0.91\text{ cm/s}$  b: Gel bead hold-up as a function of the water and dodecane flux. ●  $U_c=0\text{ cm/s}$ , ◇  $U_c=0.10\text{ cm/s}$ , ■  $U_c=0.29\text{ cm/s}$ , ♦  $U_c=0.42\text{ cm/s}$ , ▨  $U_c=0.54\text{ cm/s}$ , ▲  $U_c=0.75\text{ cm/s}$ , □  $U_c=0.91\text{ cm/s}$

Table 12.1 gives an overview of the assumptions made and the models used for determining the hold-up and mixing characteristics of both reactors.

### Mass transfer

Mass transfer between the different phases in a 2- or 3-phase system can be presented schematically as shown in Figure 12.7. To describe mass transfer inside the gel bead we used Fickian diffusion of substrate and product. For describing the mass transfer from gel bead interface to the bulk of the medium, we used the film model for substrate as well as product. The film model was also used for the mass transfer of the product from the bulk to the interface between medium and organic-solvent droplet. Mass transfer from this interface to the bulk of the organic-solvent droplet was also described by the film model. Further it is assumed that the distribution coefficient between gel bead and surrounding liquid is equal to one. Next, it is assumed that there is thermodynamic

**Table 12.1** Hydrodynamic characteristics for a liquid-fluidised bed and a liquid-liquid-solid fluidised bed

	2-phase fluidised bed	3-phase fluidised bed
<b>mixing</b>		
water phase	number of tanks-in-series (15)	number of tanks-in-series (3)
gel bead phase	ideally mixed per tank	ideally mixed per tank
droplet phase	—	plug flow
<b>hold-up</b>	Richardson and Zaki model with experimentally determined parameters $U_c = v_\infty \epsilon_w^n$	Experimentally determined, see Figure 12.6

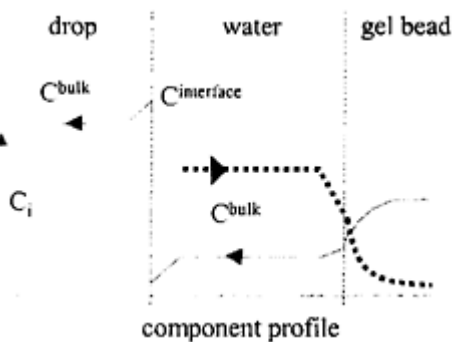


**Figure 12.7** Profiles in a multi-phase system:—product profile, ...substrate profile

equilibrium at the interface between droplet and medium. The equilibrium distribution at the interface can be described with a constant distribution coefficient ( $m$ ):

$$C_p^{o,int} = m C_p^{w,int}$$

The mass transfer rate between the different phases can be described with the equations given in Table 12.2; the rates are a combination of mass transfer per gel bead or droplet, and the number of gel beads or droplets present, respectively. The resulting rates are given per volume reactor.

The mass transfer coefficient for the transfer of product from medium to organic phase ( $K$ ) is a combination of the transfer coefficient from bulk to interface at both sides of the interface:

$$K = \left( \frac{1}{k_{drop,p}^w + \frac{1}{mk_{drop,p}^o}} \right)^{-1}$$

The mass transfer coefficients  $k_{bead,s}$ ,  $k_{bead,p}$ , and  $k_{drop,p}^w$  are calculated with the equation of Ranz and Marshall (1952); the mass transfer coefficient  $k_{drop,p}^o$  is calculated with the equation of Newman (1931); see appendix A for equations. As contact time in the latter equation, we used the residence time of a droplet ( $t = H_{bed} \varepsilon_0 / U_d$ ).

**Table 12.2** Substrate and product transfer rates between the different phases

	Medium/gel bead	Medium/droplet
substrate	$k_{bead,s} (C_s^{w,bulk} - C_s^{w,int}) \cdot \frac{6\varepsilon_s}{d_{bead}}$	no transfer to the droplet
product	$-k_{bead,p} (C_p^{w,bulk} - C_p^{w,int}) \cdot \frac{6\varepsilon_s}{d_{bead}}$	$\left( C_p^{w,bulk} - \frac{C_p^{d,bulk}}{m} \right) \cdot \frac{6}{d_{drop} \varepsilon_0}$

### Kinetics

Let us consider bioconversions carried out by either non-growing cells or enzymes immobilized in -carrageenan gel beads. It is further assumed that there is only one limiting substrate, which dissolves well in medium and not in the organic solvent. Medium is water containing all other essential nutrients. Straightforward Michaelis-Menten kinetics with first order product inhibition are considered:

$$-r_s = \frac{X v_{max} C_s}{K_m + C_s} \left( 1 - \frac{C_p}{C_p^{tox}} \right)$$

When the product concentration reaches the toxic concentration ( $(C_p^{tox})$ ) the substrate consumption rate is zero. More complicated kinetics can be used, but this is the most simple model to demonstrate the benefits for *in situ* extraction.

### Mass balances

Figure 12.8 shows how the liquid-liquid-solid three-phase fluidised bed is divided in stirred tanks to represent flow characteristics, see also Table 12.1. The total three-phase fluidised bed is divided in a number of tanks. The medium is perfectly mixed in each tank. The gel beads remain in each tank. The organic-solvent phase in each tank is divided into 15 perfectly mixed tanks-in-series to mimic plug flow behaviour. Mass balances are derived for single tanks. The total derivation of these balances is given in appendix A. The resulting dimensionless mass balances with the initial and boundary conditions are:

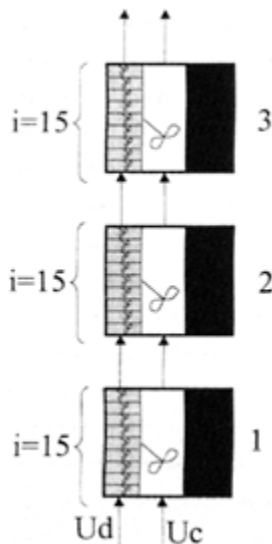


**Figure 12.8** Schematic representation of the three-phase fluidised bed

### Particle Mass Balances

substrate

$$\frac{\partial X_s^{p,n}}{\partial F_o} = \frac{\partial^2 X_s^{p,n}}{\partial z^2} + \frac{2}{z} \frac{\partial X_s^{p,n}}{\partial z} - (-r_s) \frac{r_p^2}{D_s C_s^{w,0}}$$

$$\forall t, z = 1, k_{bead,s}(X_s^{w,n} - X_s^{w,int,n}) = \left. \frac{D_s}{r_p} \frac{dX_s}{dz} \right|_{z=1}$$

$$\forall t, z = 0, \left. \frac{dX_s}{dz} \right|_{z=0} = 0$$

$$\forall z, t = 0, X = 0$$

product

$$\frac{\partial X_p^{p,n}}{\partial F_o} = \frac{D_p}{D_s} \frac{\partial^2 X_p^{p,n}}{\partial z^2} + \frac{D_p}{D_s} \frac{2}{z} \frac{\partial X_p^{p,n}}{\partial z} + (-r_s) \frac{r_p^2}{D_s C_s^{w,0}}$$

$$\forall t, z = 1, k_{bead,p} (X_p^{w,n} - X_p^{w,int,n}) = \frac{D_p}{r_p} \left. \frac{dX_p}{dz} \right|_{z=1}$$

$$\forall t, z = 0, \left. \frac{dX_p}{dz} \right|_{z=0} = 0$$

$$\forall z, t = 0, X_p = 0$$

### Medium-Phase Mass Balances

substrate

$$\frac{\partial X_s^{w,n}}{\partial F_o} = \frac{U_w}{\varepsilon_w H_t} \frac{r_p 2}{D_s} (X_s^{w,n-1} - X_s^{w,n}) - \frac{6}{d_{bead}} \frac{\varepsilon_s}{\varepsilon_w} k_{bead,s} \frac{r_p^2}{D_s} (X_s^{w,n} - X_s^{w,int,n})$$

batch operation

$$t = 0, X_s^w = 1 \text{ for each tank } n$$

continuous operation

$$t = 0, X_s^w = 0 \text{ for each tank } n$$

product

$$\frac{\partial X_p^{w,n}}{\partial F_o} = \frac{U_w}{\varepsilon_w H_t} \frac{r_p^2}{D_s} (X_p^{w,n-1} - X_p^{w,n}) + \frac{6}{d_{bead}} \frac{\varepsilon_s}{\varepsilon_w} k_{bead,p} \frac{r_p^2}{D_s} (X_p^{w,int,n} - X_p^{w,n}) - K \frac{6}{d_o} \frac{\varepsilon_o}{\varepsilon_w} X$$

$$\frac{r_p^2}{D_s} \left( X_p^{w,n} - \frac{\sum_{i=1}^{N_{dis}} X_p^{o,i}}{mN - dis} \right)$$

batch or continuous operation

$$t = 0, X_p^w = 0 \text{ for each tank } n$$

### Organic-Solvent-Phase Mass Balances

$$\frac{\partial X_p^{o,i}}{\partial F_o} = \frac{U_d}{\varepsilon_d H_{l,i}} \frac{r_p^2}{D_s} (X_p^{o,i-1} - X_p^{o,i}) + K \frac{6}{d_o} \frac{r_p^2}{D_s} \left( X_p^{w,n} - \frac{X_p^{o,i}}{m} \right)$$

batch or continuous operation

$$t = 0, X_p^{o,i} = 0 \text{ for each tank } i$$

Within this model two different kinds of parameters can be discerned:

1. parameters that can be manipulated easily by the designer; i.e. operating variables like the fluxes of the medium and organic solvent, and hence the hold-up of the different phases, initial concentration of substrate and product in the different phases, and reactor geometry.
2. parameters that are difficult to manipulate; e.g. the physical parameters like density and viscosity of the pure liquids, the mass transfer coefficients, and the diffusion coefficients of the compounds.

## Calculations

Before we compare a three-phase fluidised-bed bioreactor with its two-phase analogue, we will first show some typical results of the model. For these simulations we took a batch operation strategy for both liquids, with both liquids flowing co-currently, see also Figure 12.2. Figure 12.1 gives a short overview of the different simulations done. First we show a typical time course of substrate and product concentration inside the gel bead. Next the influence of the distribution coefficient and toxic product concentration is shown. These parameters are system dependent; a toxic product concentration depends on the micro-organism used, and can hardly be influenced; the distribution coefficient depends on the two liquids used, but can be influenced by adding specific compounds to the organic solvent for enlarging the distribution coefficient. The influence of the dodecane flux is discussed at the end of this section. The parameters that were used throughout the simulations are summarised in Table 12.3.

In Figure 12.9 a typical time course of substrate and product concentration inside the gel bead is shown. The maximum substrate conversion rate was  $0.01 \text{ mol}/(\text{m}^3 \text{ s})$ , the toxic product concentration was  $10 \text{ mol}/\text{m}^3$ , and the distribution coefficient was 1000. We took a medium flux of  $1.29 \times 10^{-2} \text{ m/s}$  and a dodecane flux of  $0.91 \times 10^{-2} \text{ m/s}$ , which resulted in gel bead hold-up of 0.32 and a dodecane hold-up of 0.093.

Figure 12.9a:

Substrate diffuses into the gel bead and gradually penetrates towards the centre of the gel bead. As time progresses the concentration increases, the profile flattens, and a maximum concentration is reached. As time period increases the concentration decreases as a result of consumption, until all substrate is converted into product. With the set of parameters used for calculating the profiles in Figure 12.9a, total conversion

**Table 12.3** Overview of parameters used in simulations

<i>Reactor Constants</i>		
# nozzles	209	
diameter nozzle	0.001	m
reactor height	1	m
reactor diameter	0.06	m
<i>Physical parameters</i>		
density medium	998	$\text{kg}/\text{m}^3$
density dodecane	742.7	$\text{kg}/\text{m}^3$
density gel bead	1065.1	$\text{kg}/\text{m}^3$
viscosity medium	0.0009325	Nm/s
viscosity dodecane	0.00135	Nm/s

surface tension between water and dodecane	0.040	N/m
diameter gel bead	2.76	mm
diffusion coefficient substrate	$10^{-9}$	m/s
diffusion coefficient product	$10^{-9}$	m/s
distribution coefficient	simulation depended	
<i>Hydrodynamics</i>		
hold-ups 3-phase fluidised bed	simulation depended	
Number of tanks per m reactor		
3-phase fluidised bed	3	
2-phase fluidised bed	13	
Richardson and Zaki constants 2-phase fluidisation		
n	2.35	
$v_\infty$	0.0377	m/s
<i>Kinetics</i>		
Michaelis-Menten constant	1	mol/m <sup>3</sup>
toxic product concentration	simulation depended	mol/m <sup>3</sup>
maximum substrate conversion rate	simulation depended	mol/(m <sup>3</sup> s)
<i>Operation parameters</i>		
medium flux	simulation depended	m/s
dodecane flux	simulation depended	m/s
initial substrate concentration	1000	mol/m <sup>3</sup>
initial product concentration	0	mol/m <sup>3</sup>

of substrate is reached. However, a combination of parameters is easily found for which the substrate is not completely converted, hence substrate concentration inside the gel bead is not equal to zero. Substrate will be converted to product, as long as the product concentration at any place inside the gel bead is less than the toxic product concentration.

Figure 12.9b:

As substrate is converted, product is formed. Early in the process little product is present. Gradually product appears throughout the whole gel bead. As product is initially formed near the surface of the gel bead, product not only diffuses out of the gel bead but also towards the centre; consequently a maximum concentration is found

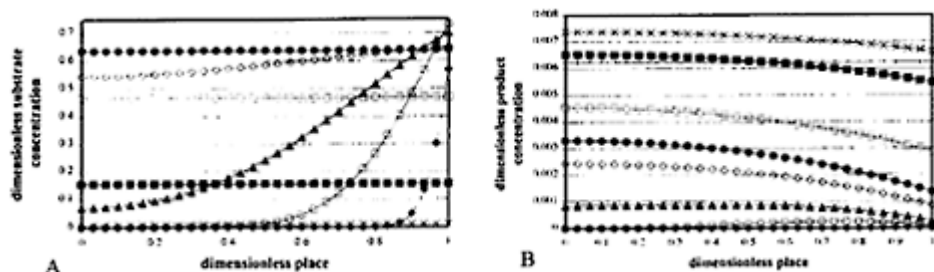


**Figure 12.9** Profile of substrate (A) and product (B) concentration in a gel bead particle.  $U_c=1.29 \text{ cm/s}$   $U_d=0.91 \text{ cm/s}$ ,  $\varepsilon_s=0.32$ ,  $\varepsilon_o=0.0925$ ;  $Xv_{\max}=0.01 \text{ mol/m}^3 \text{s}$ ,  $C^{tox}=10 \text{ mol/m}^3$ ,  $m=1000$ .

◆  $t=0:0:3$ , ▲  $t=0:0:33$ , ◇  $t=0:1:53$ , ◊  
 ■  $t=0:6:40$ , ●  $t=0:19:0$ , □  $t=19:6:0$ ,  
 ■  $t = 66:0:0$ , ×  $t = 98:0:0$ , +  $t = 111:0:0$

inside the gel bead. This maximum concentration progresses towards the centre of the gel bead over time. Hence, after some time, product concentration is highest in the centre. After some time a maximum concentration profile is also reached. If at this point in time, there is still mass transfer between the organic and medium phase, the product concentration inside the gel bead will decrease. This transfer of product will continue until equilibrium is reached between medium and organic phase.

Before discussing the influence of the distribution coefficient and toxic product concentration on the time course of the substrate concentration in the medium phase, and the time course of product concentration in the medium and organic phase, some general remarks can be made:

- The time course profile of the substrate concentration in the water phase shows two processes with a different time constant; the first process is completed after roughly 100 seconds, and is more or less independent of the distribution coefficient and the toxic product concentration. It can be seen in Figure 12.9b that around that point in time the gel bead is completely filled with substrate. The second process is the gradual conversion of substrate to product, and is dependent on the distribution coefficient and the toxic product concentration.
- Complete conversion of substrate can be reached with some combinations of distribution coefficient and toxic product concentration.
- If substrate is not completely converted, then the end-product concentration inside the gel bead and the medium phase is equal to the toxic product concentration.

- At the point in time where substrate is not longer converted, there is equilibrium for the product concentration between the medium phase and the organic phase.

The influence of the distribution coefficient ( $m$ ) is shown in Figure 12.10a-c. Figure 12.10a and 12.10b show the concentrations in the medium phase, whereas Figure 12.10c shows the product concentration in the dodecane phase. The maximum substrate conversion rate was  $0.01 \text{ mol}/(\text{m}^3 \text{ s})$ , and the toxic product concentration was  $10 \text{ mol}/\text{m}^3$ . We took a medium flux of  $1.29 \times 10^2 \text{ m/s}$  and a dodecane flux of  $0.91 \times 10^{-2} \text{ m/s}$ , which resulted in gel bead hold-up of 0.32 and a dodecane hold-up of 0.093. Figure 12.10a clearly shows that a larger  $m$  eventually results in a lower substrate concentration in the medium phase, hence substrate is converted to a higher degree. Naturally, when substrate is not converted totally, the product concentration in the medium phase is equal to the toxic product concentration (Figure 12.10b). As there is equilibrium between the medium and organic phase, the product concentration in the organic phase is higher for a higher  $m$ , Figure 12.10c. If the  $m$  is high enough, than at the end of the batch operation the product concentration in the medium phase will be lower than the toxic product concentration. Consequently, substrate is totally converted. This is observed for a distribution coefficient of 1000. The end of the batch operation is reached at an earlier time for a lower  $m$ .

The influence of the toxic product concentration ( $C_p^{\text{tox}}$ ) is shown in Figure 12.11. Figures 12.11a and 12.11b show the concentrations in the medium phase, whereas Figure 12.11c shows the product concentration in the dodecane phase. Obviously, a higher  $(C_p^{\text{tox}})$  results in a lower substrate concentration, hence there is a more complete conversion and the product concentration becomes  $(C_p^{\text{tox}})$ . This concentration is reached earlier for a lower  $(C_p^{\text{tox}})$ . At  $(C_p^{\text{tox}})$  equal to 100, substrate is completely converted, and  $(C_p^{\text{tox}})$  is not reached in the medium phase.

The influence of the organic solvent flux is shown in Figure 12.12. Figures 12.12a and 12.12b show the concentrations in the medium phase, whereas Figure 12.12c shows the product concentration in the dodecane phase. We kept the medium flux constant and changed the dodecane flux. The dodecane flux influences the hold-up of the different phases. At a constant medium flux, a higher dodecane flux gives a higher dodecane holdup, but a lower gel bead hold-up. Figure 12.12a shows that complete conversion of substrate is reached for the highest  $U_d$ , although the gel-bead hold-up is the lowest ( $U_d = 0.75 \times 10^{-2} \text{ m/s}$ ,  $\varepsilon_s = 0.26$ ;  $U_d = 0.14 \times 10^{-2} \text{ m/s}$ ,  $\varepsilon_s = 0.30$ ). So, at the highest dodecane flux, the product concentration in the medium phase is always below the toxic product concentration, Figure 12.12b. For the other dodecane fluxes applied in the simulations, the product concentration in the medium phase is equal to the toxic product concentration, Figure 12.12b. This concentration is reached at an earlier point of time for the lowest  $U_d$ . The time course of product concentration in the organic phase follows the time course for the product concentration in the medium phase.

## COMPARISON BETWEEN A TWO-PHASE AND A THREE-PHASE FLUIDISED-BED BIOREACTOR

In our comparison we did the simulations for batch operations:

Substrate is circulated until a certain amount of substrate is converted. In a two-phase fluidised bed substrate is not totally converted due to product inhibition. When the product concentration reaches the toxic product concentration in the medium phase, the conversion stops. At this moment, the product concentration inside the gel bead and in the medium phase are the same and equal to the toxic product concentration.

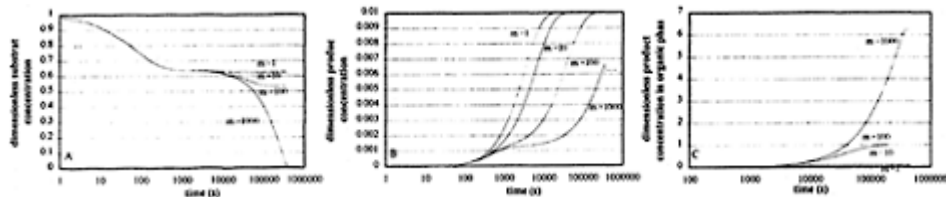


**Figure 12.10** Profile of substrate (10a) and product (10b) concentration in the medium phase at different distribution coefficients. Profile of product concentration in the dodecane phase (10c) at different distribution coefficients.

$$U_c = 1.29 \text{ cm/s}, U_d = 0.91 \text{ cm/s}, \varepsilon_s = 0.32, \\ \varepsilon_o = 0.0925; X_{V_{\max}} = 0.01 \text{ mol/m}^3 \text{ s}, C_p^{10x} = 10 \text{ mol/m}^3$$

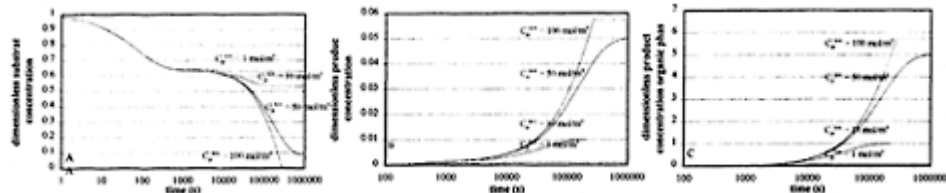


**Figure 12.11** Profile of substrate (11a) and product (11b) concentration in the medium phase at different toxic product concentrations. Profile of product concentration in the dodecane phase (11c) at different toxic product concentrations.

$$U_c=1.29 \text{ cm/s}, U_d=0.91 \text{ cm/s}, \epsilon_s=0.32, \\ \epsilon_o=0.0925; Xv_{\max}=0.01 \text{ mol/m}^3\text{s}, \\ m=100$$

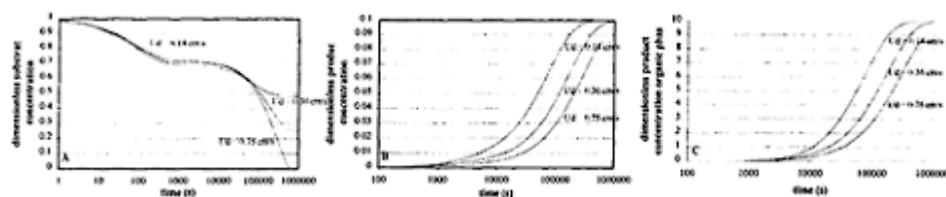


**Figure 12.12** Profile of substrate (12a) and product (12b) concentration in the medium phase at different fluxes of the organic phase. Profile of product concentration in the organic phase (12c) at different fluxes of the organic phase.

$$U_c=1.49 \text{ cm/s}, Xv_{\max}=0.01 \text{ mol/m}^3\text{s}, \\ m=100, C_p^{tox}=100 \text{ mol/m}^3. U_d=0.14 \\ \text{cm/s}, \epsilon_s=0.30, \epsilon_o=0.01 U_d=0.36 \text{ cm/s}, \\ \epsilon_s=0.27, \epsilon_o=0.036; U_d=0.75 \text{ cm/s}, \\ \epsilon_s=0.26, \epsilon_o=0.069.$$

So, the total amount of moles of product produced is equal to the toxic product concentration multiplied by the total reactor volume. In order to compare a three-phase fluidised bed with a two-phase fluidised bed we calculated the time necessary to reach 99% of the total amount that can be converted in a two-phase fluidised bed. Obviously, there is a lot of freedom in totally or partly recirculating the organic solvent in the three-phase fluidised-bed bioreactor, see Figure 12.2. In this strategy we used a total reflux as a fair comparison. An economic evaluation must show whether a total reflux yields the lowest cost, but this is not the topic of this chapter.

Comments on operating the bioreactor continuously may be found at the end of this chapter.

### Batch Operation

The comparison between both bioreactors was made for different combinations of medium and dodecane fluxes. Two different toxic product concentrations were used, i.e. 1 and 100 mol/m<sup>3</sup> with an initial substrate concentration of 1 kmol/m<sup>3</sup>.

Introducing an organic solvent in a three-phase fluidised bed, will in most cases result in a lower gel-bead hold-up. This means loss of biocatalytic activity per unit volume of bioreactor. This loss of activity has to be compensated for by lowering the product concentration in the gel beads, resulting in a higher substrate conversion rate. This is achieved by extracting the product into the organic solvent. The extraction rate is influenced by the distribution coefficient. As can be deduced from the equation in Table 12.2, a higher distribution coefficient gives a higher transfer rate.

So, at a given maximum substrate conversion rate, the time to reach a certain degree of conversion can be manipulated by the distribution coefficient ( $m$ ): a higher  $m$  results in a shorter time, see also Figure 12.10. Thus, to conclude whether a three-phase fluidised bed performs better than a two-phase fluidised bed, at a given maximum substrate conversion rate, a distribution coefficient is determined, that yields the same time to reach 99% of the total amount of moles converted in a two-phase fluidised bed. A higher distribution coefficient results in better performance, whereas a lower distribution coefficient gives a worse performance.

We chose to evaluate the performance of the bioreactor with two parameters, i.e. the maximum substrate conversion rate ( $X \cdot v_{\max}$ ) and the distribution coefficient ( $m$ ), and to keep the other parameters constant. The maximum substrate conversion rate can be influenced by using more or less biocatalyst, and the distribution coefficient might be influenced by adding specific compounds to the organic solvent for enlarging the distribution.

The distribution coefficient at a given maximum substrate conversion rate is thus calculated for which a three-phase fluidised bed performs the same as two-phase fluidised bed. This was done for a number of organic solvent fluxes and medium fluxes, and for different toxic product concentrations. The results are shown in Figures 12.13a-c. A three-phase fluidised bed performs better for combinations of the maximum substrate conversion rate ( $X \cdot v_{\max}$ ) and distribution coefficient in the area above the lines in these figures.

The distribution coefficient at each  $X \cdot v_{\max}$  in favour of the three-phase fluidised bed is relatively low, see Figures 12.13a-c, particularly when we consider the examples in Table 12.4 for distribution coefficients for different solutes for different liquid-liquid two-phase systems. Based on this table one might suggest that at any pre-set medium flux, a three-phase fluidised bed performs better than a conventional two-phase fluidised bed.

Looking in more detail at Figures 12.13a-c, the results in Figure 12.13a and Figure 12.13b—a lower water flux applied—show that a lower dodecane flux requires a higher distribution coefficient, whereas the results in Figure 12.13c—the highest water flux applied—show that a higher dodecane flux requires also a higher distribution coefficient. Although the latter observation might seem unexpected, both observations can be easily explained. In most cases the dodecane flux decreases the gel-bead hold-up and, as explained above, this decrease in gel-bead hold-up has to be compensated for with a high enough transfer rate to the dodecane phase. The transfer rate itself is influenced by the dodecane flux, as the dodecane flux determines largely the dodecane hold-up and the mass transfer coefficient, see also the equation in Table 12.2. A higher dodecane flux

results in a higher transfer rate. The transfer rate is also influenced by the distribution coefficient, a higher distribution coefficient gives also a higher transfer rate.

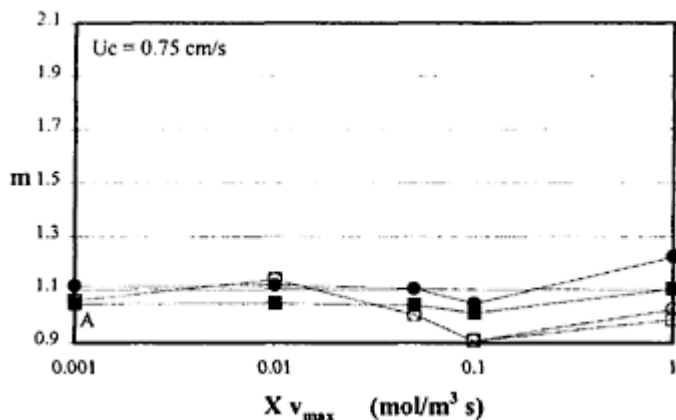


**Figure 12.13a** Distribution coefficient as a function of the maximum substrate conversion rate for which a three-phase fluidised bed performs equally well as a liquid fluidised bed.  $U_c=0.75 \text{ cm/s}$ , ■  $U_d=0.40 \text{ cm/s}$  ●  $U_d=0.14 \text{ cm/s}$ . Open symbols  $C_p^{\text{tox}}=1 \text{ mol/m}^3$ , closed symbols  $C_p^{\text{tox}}=100 \text{ mol/m}^3$

$X v_{\max} (\text{mol/m}^3 \text{ s})$	$t_{\text{batch}} (99\%) (\text{min})$	$C_p^{\text{tox}} = 1 \text{ mol/m}^3$	$C_p^{\text{tox}} = 100 \text{ mol/m}^3$
0.001		166.3	15545
0.01		22.13	1560
0.05		15.04	319.4
0.1		15.47	167.2
1		14.95	21.4

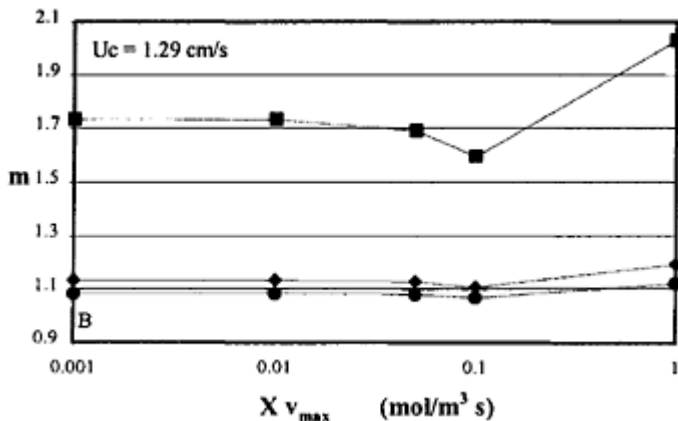


**Figure 12.13b** Distribution coefficient as a function of the maximum substrate conversion for which a three-phase fluidised bed performs equally well as a liquid fluidised bed.  $U_c=1.29 \text{ cm/s}$ ,  $C_p^{\text{tox}}=100 \text{ mol}/\text{m}^3$ , ■  $U_d=0.14 \text{ cm/s}$ , ◆  $U_d=0.55 \text{ cm/s}$  ●  $U_d=0.91 \text{ cm/s}$

$X v_{max} (\text{mol}/\text{m}^3 \text{ s})$	$t_{\text{batch}} (99\%) (\text{min})$	$C_p^{\text{tox}} = 100 \text{ mol}/\text{m}^3 \text{ mol}/\text{m}^3$
0.001		20950
0.01		2108
0.05		435.5
0.1		227.9
1		32.3

At the lower water fluxes, Figure 12.13a and Figure 12.13b, the decrease in gel-bead hold-up is not that large, less than 15% for all dodecane fluxes applied, and there is hardly any difference in gel-bead hold-up between the highest and lowest dodecane flux. Thus, the transfer rate in the three-phase fluidised beds, necessary to perform equally well as the two-phase fluidised bed, are more or less the same. So, at these water fluxes, a higher distribution coefficient is needed for the lower dodecane flux to establish a high enough transfer rate.

For the highest water flux applied, Figure 12.13c, there is a significant decrease in gelbead hold-up with an increasing dodecane flux (compared to the two-phase fluidised-bed analogue, 39% for the highest dodecane flux and 7% for the lowest). Consequently, the transfer rate must be higher for the higher dodecane fluxes. When a lower distribution coefficient is used for the higher dodecane fluxes, as above for the lower water fluxes, the resulting transfer rate is not enough for establishing the required transfer rate, although

dodecane hold-up is higher for a higher dodecane flux. Hence, the distribution coefficient has to be higher for the higher dodecane fluxes.

The open symbols in Figure 12.13a and c show the distribution coefficient as a function of the  $X \cdot v_{\max}$  for which the three-phase fluidised bed performs equally well for a low toxic product concentration ( $1 \text{ mol/m}^3$ , i.e. 0.1% of the initial substrate concentration). At the

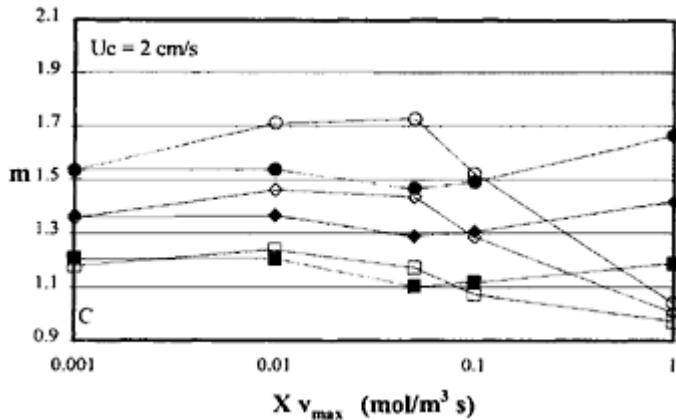


**Figure 12.13c** Distribution coefficient as a function of the maximum substrate conversion for which a three-phase fluidised bed performs equally well as a liquid fluidised bed.  $U_c=2 \text{ cm/s}$ , ■  $U_d=0.14 \text{ cm/s}$  ▲  $U_d=0.28 \text{ cm/s}$  ▽  $U_d=0.54 \text{ cm/s}$ . Open ● symbols  $C_p^{\text{tox}}=1 \text{ mol/m}^3$ , closed □ symbols  $C_p^{\text{tox}}=100 \text{ mol/m}^3$

$X \cdot v_{\max} (\text{mol/m}^3 \text{ s})$	$t_{\text{batch}}(99\%) \text{ (min)}$	$C_p^{\text{tox}}=1 \text{ mol/m}^3$	$C_p^{\text{tox}}=100 \text{ mol/m}^3$
0.001		355.8	32504
0.01		55.31	3278
0.05		23.81	699
0.1		19.63	361.4
1		17.02	55.94

**Table 12.4** Distribution coefficients for different liquid-liquid two-phase systems

Solute	Two-phase system	Distribution coefficient	Reference
--------	------------------	--------------------------	-----------

oxygen	FC40/water	12	Sonsbeek <i>et al.</i> , 1992a
	octene/water	11.4	Meer, 1993
propenoxide	toluene/water	3.5	Brink and Tramper, 1985
	butylacetate/water	4.6	Brink and Tramper, 1985
butanal	toluene/water	6.9	Kawakami, <i>et al.</i> , 1992
	hexadecane/water	1.52	Kawakami, <i>et al.</i> , 1992
tetraline	FC40/water	120	Vermudë, <i>et al.</i> , 1994
	dodecene/water	>5000	Vermudë, <i>et al.</i> , 1994
<b>Steroids</b>			
Androstenoloneactate	Hexane/water	1500	Boeren, <i>et al.</i> , 1992
4-Androstene-3,17-dione	Hexane/water	8.5	Boeren, <i>et al.</i> , 1992
dehydroepiandrosterone	Hexane/water	24	Boeren, <i>et al.</i> , 1992
phenylalanine	isobutyl methyl	123	Flashel, <i>et al.</i> , 1992
propyl ester	keton/water		

lower water flux, Figure 12.13a, the difference between both dodecane fluxes is almost insignificant. At the higher water flux, Figure 12.13b, this difference is a little more pronounced. A general remark about the difference between a high and low toxic product concentration can hardly be made: at  $X \cdot v_{\max}$  the distribution necessarily for giving an equal performance is sometimes lower other times higher.

### Continuous Operation

Executing a biotransformation continuously in a two-phase fluidised bed without a recycle is highly inefficient, as the medium flux is high compared to the maximum substrate conversion rate. Consequently the residence time is short and the conversion rate is low. Only for fast conversions or high reactors, a high degree of substrate conversion is possible, and hence a fluidised bed might be attractive. As an example, a substrate conversion of 1 mol/s, a medium velocity of 0.02 m/s, and a reactor height of 1 m results in conversion of 50 mol, assuming zero-order kinetics. This is 50% of the attainable conversion at a toxic product concentration of 100 mol/m<sup>3</sup>.

Otherwise one should use a set-up with a partial recycle and fresh substrate supply. In this case the incoming substrate concentration is kept constant. The product concentration in the medium phase will accumulate until steady state is reached. As the product concentration increases with an increasing recycle, substrate will be converted to a lesser amount. Application of an organic solvent, i.e. using a three-phase fluidised bed, will result in a higher conversion, as we calculated for the following case (the organic solvent was not recycled): medium flux  $0.75 \times 10^{-2}$  m/s, dodecane flux  $0.40 \times 10 m^2$  m/s, hence  $\varepsilon_s =$

$0.48$ ,  $\varepsilon_0 = 0.045$ ;  $X \cdot v_{\max} = 0.01$  mol/s,  $C_p^{\text{iox}} = 100$  mol/m<sup>3</sup>, and  $m=100$ . The dimensionless concentrations for a two-phase fluidised bed and three-phase fluidised bed are calculated and given in Table 12.5 for different recycles.

As little substrate is converted, only a small amount of product is made. The introduction of the organic solvent results in a smaller product concentration in the medium phase. In optimising a continuous operation, there is lot of freedom, e.g. the initial substrate concentration, recycle of medium and/or organic solvent. So, whether a continuous operation is feasible depends on a total cost calculation of the plant.

**Table 12.5** Dimensionless substrate and product concentrations in a continuously operated fluidised bed

Recycle	Two-phase fluidised bed		Three-phase fluidised bed		
	Substrate	Product	Substrate	Product	Product organic solvent
0.1	0.9993	6.50e-4	0.9994	6.07e-4	0.72e-4
0.9	0.9994	0.0061	0.9994	0.0019	2.98e-4
0.99	0.9996	0.0396	0.9994	0.005	8.5e-4

## CONCLUSIONS

In this chapter we explore different aspects of liquid-liquid-solid three-phase systems. The benefits of such a system for typical biotransformations have been discussed in literature. However, the ideal reactor configuration can still be argued. Different reactor configurations are discussed here, including a simple three-phase fluidised bed, but also more elaborate options, such as the different possibilities with a loop reactor. It can be concluded that building and operating a three-phase system is merely a minor extension of conventional bioreactors.

For a liquid-liquid-solid three-phase fluidised-bed bioreactor conditions have been established for which this reactor performs better than a conventional two-phase fluidised bed. Keeping all parameters constant, changing the operation variables, medium flux and organic solvent flux, the distribution coefficient is determined, at given maximum substrate conversion rate, for which the three-phase fluidised bed performs equally well. It appears that a low distribution coefficient (larger than 1 but less than 2) suffices for a better performance.

So, it can be concluded that a three-phase fluidised bed, or less simple three-phase bioreactors, are good options for operating specific biotransformations, provided *in situ* extraction is needed for such a specific biotransformation.

## NOMENCLATURE

$A_r$	area reactor	$\text{m}^2$
$C_i^j$	concentration component in phase j	$\text{mol}/\text{m}^3$
$C_s^w$	substrate concentration in medium phase at t=0	$\text{mol}/\text{m}^3$
$D_i$	diffusion coefficient component	$\text{m}^2/\text{s}$
$d_{\text{bead}}$	gel bead diameter	$\text{m}$
$d_{\text{drop}}$	droplet diameter	$\text{m}$
$d_{\text{noz}}$	nozzle diameter	$\text{m}$
$F_o$	dimensionless time	—
$g$	gravity constant	$\text{m}^2/\text{s}$
$H_{\text{bed}}$	height fluidised bed	$\text{m}$
$H_t$	height of one medium tank	$\text{m}$
$H_{t,i}$	height of disperse phase tank	$\text{m}$
$K$	overall mass transfer coefficient water/droplet	$\text{m}^3/(\text{m}_{\text{int}}^2 \text{ S})$
$K_m$	michaelis-menten constant	$\text{mol}/\text{m}^3$
$K_{\text{bead},i}$	mass transfer coefficient component i water/gel bead	$\text{m}^3/(\text{m}_{\text{int}}^2 \text{ S})$
$k_{\text{drop}}^0$	mass transfer coefficient interface droplet/bulk droplet	$\text{m}^3/(\text{m}_{\text{int}}^2 \text{ S})$
$k_{\text{drop}}^w$	mass transfer coefficient bulk water/interface droplet	$\text{m}^3/(\text{m}_{\text{int}}^2 \text{ S})$
$N_{\text{dis}}$	number of tanks in disperse phase per one medium tank	—
$m$	distribution coefficient organic/water	—
$R_p$	gel bead radius	$\text{m}$
$r$	space-coordinate in gel bead	$\text{m}$
$t$	time	$\text{s}$
$U_c$	medium phase flux	$\text{m}^3/(\text{m}^2 \text{s})$
$U_d$	organic solvent flux	$\text{m}^3/(\text{m}^2 \text{s})$
$V_r$	reactor volume	$\text{m}^3$
$V_\infty$	terminal rise velocity droplet	$\text{m/s}$
$v_{\text{max}}$	maximum substrate conversion rate	$\text{mol}/(\text{g}_{\text{cat}} \text{s})$
$v_{\text{wp}}$	slip velocity water particle	$\text{m/s}$
$v_{\text{wo}}$	slip velocity water droplet	$\text{m/s}$
$X$	concentration biocatalyst	$\text{g}_{\text{cat}}/\text{m}^3$
$X_i^j$	dimensionless concentration component in phase j	—

$z$  dimensionless space coordinate in gel bead —

### Subscripts

p	product
s	substrate

### Superscripts

bulk	bulk phase
int	at the interface between two phases
n	tank number in medium phase
o	organic solvent phase
p	gel bead phase
tox	toxic
w	medium phase

### Greek

$\eta_w$	viscosity medium phase	Nm/s
$\Delta\rho$	density difference	Kg/m <sup>3</sup>
$\varepsilon_0$	organic solvent phase hold-up	—
$\varepsilon_s$	gel bead phase hold-up	—
$\varepsilon_w$	medium phase hold-up	—
$\rho$	density	Kg/m <sup>3</sup>
$\sigma$	interfacial tension	N/m
$\phi_{pw}^p$	mass transfer flux of product gel bead/water	mol/s
$\phi_{wo}^p$	mass transfer flux of product water/organic solvent	mol/s
$\phi_{wp}^s$	mass transfer flux of substrate water/gel bead	mol/s

### REFERENCES

- Adlercreutz, P. (2000) Biocatalysis in non-conventional media, in *Applied Biocatalysis*, edited by A.J.J.Straathof and P.Adlercreutz, 2nd edn., pp. 295–316. Singapore: Harwood Academic Publishers.
- Boeren, S., Laane, C. and Hilborst, R. (1992) The effect of alkanes on viability, enzyme induction and enzyme activity in *Flavobacterium dehydrogenans*. In *Biocatalysis in Non-conventional media*, edited by J.Tromper, M.H.Verrnuë, H.H.Beeftink, U.von Stockar, pp. 637–643. Amsterdam: Elsevier Science Publ.

- Brink, L.E.S. and Tramper, J. (1985) Optimization of Organic Solvent in multiphase biocatalysis. *Biotechnol Bioeng.*, **27**, 1258–1269.
- Buitelaar, R.M., Langenhoff, A.A.M., Heidstra, R. and Tramper, J. (1991) Growth and Thiophene production by hairy root cultures of *tagetes patula* in various two-liquid-phase bioreactors. *Enzym. Microb. Techn.*, **13(6)**, 487–494.
- Chisti, M.Y. (1989) *Air lift Bioreactors*. London: Elsevier Science Publ.
- Fan, L-S., Muroyama, K. and Chern, S-H. (1982) Hydrodynamic Characteristics of inverse fluidization in liquid-solid and gas-liquid-solid systems. *Chem. Eng. J.*, **24**, 143–150.
- Flaschel, E., Crelier, S., Schulz, K., Huneke, F.-U. and Renken, A. (1992) Process Development for the optical resolution of phenylalanine by means of chymotrypsin in a liquid-liquid-solid three-phase reaction system. In *Biocatalysis in Non-conventional media*, edited by J.Tramper, M.H.Vermuë, H.H.Beeftink, U.von Stockar, pp. 637–643. Amsterdam: Elsevier Science Publ.
- Heijnen, J.J., Hols, J., van der Lans, G.J.M., van Leeuwen, H.L.J.M., Mulder, A. and Weltevreden, R. (1997) A simple hydrodynamic model for the liquid circulation velocity in a full scale two- and three-phase internal airlift reactor operating in the gas recirculation regime. *Chem. Eng. Sci.*, **52(15)**, 2527–2540.
- Hunik, J.H. and Tramper, J. (1993) Large Scale production of -carrageenan droplets for gel bead production: theoretical and practical limitations of size and production rate. *Biotech. Progress.*, **9**, 186–192.
- Kawakami, K. and Yosida, T. (1992) Kinetic study of enzymatic reaction in aqueous-organic two-phase systems—an example of enhanced production of aldehydes by alcohol oxidase. In *Biocatalysis in Non-conventional media*, edited by J.Tramper, M.H.Vermuë, H.H.Beeftink, U. von Stockar, pp. 637–643. Amsterdam: Elsevier Science Publ.
- Kumar, A. and Hartland, S. (1996) Unified correlations for the prediction of drop size in liquid liquid extraction columns. *Ind. Eng. Chem. Res.*, **35(8)**, 2682–2695.
- Mateus, D.M.R., Alves, S.S. and da Fonseca, M.M.R. (1996) Model for the production of L-tryptophan from L-serine and indole by immobilized cells in a three-phase liquid-impelled loop reactor. *Bioprocess. Eng.*, **14(3)**, 151–158.
- Meer, A.B. van der (1993) Multi-phase Fermentation: Reaction Engineering models for the production of optically active 1,2-epoxyoctane from 1-octene by free and immobilised *Pseudomonas oleovorans* cells. *ScD. thesis*, University of Groningen, Groningen, The Netherlands.
- Newman, A.B. (1931) The drying of porous solids: diffusion and surface emission equations. *Trans. Am. Int. Chem. Engrs.*, **27**, 203–220.
- Ranz, W.E. and Marshall, W.R. (1950) Evaporation from drop I+II. *Chem. Eng. Progr.*, **48**, 141–146, 173–180.
- Riet, K. van 't and J.Tramper (1991) *Basic Bioreactor Design*, 2nd edn. New York: Marcel Dekker.
- Sonsbeek, H.M. van, Beeftink, H.H. and Tramper J. (1993) Two-Liquid-phase bioreactors. *Enzyme. Microb. Technol.*, **15**, 722–729.
- Sonsbeek, H.M. van, Verduren, R.E.M., Verlaan, P. and Tramper, J. (1990) Hydrodynamic model for liquid-impelled loop reactors. *Biotech. Bioeng.*, **36**, 940–946.
- Sonsbeek, H.M. van (1992a) Physical aspects of liquid-impelled loop reactors. *ScD thesis*, Wageningen Agricultural University, Wageningen, The Netherlands.
- Sonsbeek, H.M. van, Blank, H.de and Tramper, J. (1992b) Oxygen transfer in liquid-impelled loop reactors using perfluorocarbon liquids. *Biotechnol. Bioeng.*, **40**, 713–718.
- Tramper, J., Wolters, I. and Verlaan, P. (1987) The liquid-impelled loop reactor: a new type of density-difference-mixed bioreactor. In *Biocatalysis in organic media* edited by C.Laane, J.Tramper and M.D.Lilly, pp. 311–316. Amsterdam: Elsevier Science Publ.
- Tramper, J., Vermuë, M.H., Beeftink, H.H. and Stockar, U.von (1992) *Biocatalysis in Non-conventional media*. Amsterdam: Elsevier Science Publ.
- Tweel, W.J.J. van den, Marsman, E.H., Vorage, M.J.A.W., Tramper, J. and De Bont, J.A.M. (1987) The application of organic solvents for the bioconversion of benzene to cis-benzene glycol. In

- Bioreactors and biotransformations* edited by G.W.Moody and P.B.Baker, pp. 231–241. London: Elsevier Science Publ.
- Vermüö, M.H. and Tramper, J. (1995a) Biocatalysis in non-conventional media; medium engineering aspects—a review. *Pure & Applied Chem.*, **67**, 345–373.
- Vermüö, M.H., Sikkema, J., Bakker, R., Janssen, G. and Tramper, J. (1995b) Strategy for selection of a suitable solvent for extractive biocatalysis in a liquid-impelled loop reactor. In *Biocatalysis in non-conventional media thermodynamic and kinetic aspects*, by M.H.Vermüö, *ScD thesis*, Wageningen Agricultural University, Wageningen, The Netherlands.
- Vermüö, M.H., Tacken, M. and Tramper, J. (1994) Tetralin and oxygen transfer in the liquid-impelled loop reactor. *Bioprocess Eng.*, **11**, 224–228.
- Wijffels, R.H., Buitelaar, R.M., Bucke, C. and Tramper, J. (1996) *Progress in Biotechnology 11 Immobilized cells: Basics and Applications*. Amsterdam: Elsevier.
- Zessen, E. van, Dierendonck, F. van, Rinzema A. and Tramper, J. (2000a) Solid and droplet phase hold-ups in a liquid-liquid-solid three-phase fluidised bed bioreactor, in preparation.
- Zessen, E. van, Keijzer, T., Rinzema, A. and Tramper, J. (2000b) Residence time distribution of the water phase in a liquid-liquid-solid three-phase fluidised bed bioreactor, in preparation.

## APPENDIX A DERIVATION OF MASS BALANCES FOR A THREE-PHASE FLUIDISED BED BIOREACTOR

In a three-phase fluidised bed three different phases are present. Mass balances are derived for the individual phases. As conversion we took one mol of substrate giving one mol of product. So, two components are present in the solid phase and the medium phase. Only product is present in the organic-solvent phase.

The total reactor is divided into a number of vertically stacked ideally stirred tank reactors, a tanks-in-series model (number of tanks is 3). We took a plug flow model for the organic-solvent phase. A tank-in-series model was applied with a large enough number of tanks to mimic plug flow. For simplicity we assumed that the gel beads did not circulate inside the reactor. Systematically the bioreactor looks as shown in Figure 12.8.

Mass transfer takes place from the medium phase to the gel beads for substrate. Product is transferred from the gel beads to the medium, and from medium to the organic solvent.

Mass balances for one tank, including the boundary and initial conditions, read as follows:

*The gel bead*

Substrate

$$\frac{\partial C_s^{p,n}}{\partial t} = D_s \frac{\partial^2 C_s^{p,n}}{\partial r^2} + \frac{2 \partial^2 C_s^{p,n}}{r \partial r} - (-r_s)$$

$$t = 0, \forall r, C_s^{p,n} = 0$$

$$r=0, \text{ centre of the gel } \left. \frac{\partial C_s^{p,n}}{\partial r} \right|_{r=0}$$

$$k_{\text{bead},s} (C_s^{w,n} - C_s^{w,int,n}) = D_s \left. \frac{\partial C_s^{p,n}}{\partial r} \right|_{r=R}$$

r=R, edge of the gel bead

Product

$$\frac{\partial C_p^{p,n}}{\partial t} = D_s \frac{\partial^2 C_p^{p,n}}{\partial r^2} + \frac{2 \partial C_p^{p,n}}{r \partial r} + r_p \quad \wedge \quad r_p = -r_s$$

$$t = 0, \forall r, C_p^{p,n} = 0$$

$$r=0, \text{ centre of the gel head} \quad \left. \frac{\partial C_s^{p,n}}{\partial r} \right|_{r=0}$$

$$r=R, \text{ edge of the gel bead} \quad k_{\text{bead},p} (C_p^{w,\text{int},n} - C_p^{w,n}) = -D_p \left. \frac{\partial C_p^{p,n}}{\partial r} \right|_{r=R}$$

*The medium phase*

Substrate

$$\varepsilon_w V_r \frac{dC_s^{w,n}}{dt} = U_c A_r (C_s^{w,n-1} - C_s^{w,n}) - \varphi_{wp}^s$$

$$t=0, C_s^{w,n}=0, \text{ batch operation}$$

$$C_s^{w,n}=0, \text{ continuous operation}$$

Product

$$\varepsilon_w V_r \frac{dC_p^{w,n}}{dt} = U_c A_r (C_p^{w,n-1} - C_p^{w,n}) + \varphi_{pw}^p - \sum_{i=1}^{No} (\varphi_{wo}^p)_i$$

$$t=0, C_p^{w,n}=0, \text{ batch operation and continuous operation}$$

*The organic solvent phase*

Product

$$\varepsilon_d \frac{V_r}{No} \frac{dC_p^{o,i,n}}{dt} = U_d A_r (C_p^{o,i-1,n} - C_p^{o,i,n}) - \varphi_{wo}^p$$

$$t = 0, C_p^{o,i,n} = 0$$

The different transfer fluxes are represented by:

$$\varphi_{wp}^s = k_{\text{bead},s} (C_s^{w,n} - C_s^{w,\text{int},n}) \frac{6}{d_{\text{bead}}} \varepsilon_s V_r$$

$$\varphi_{pw}^p = k_{\text{bead},p} (C_p^{w,\text{int},n} - C_p^{w,n}) \frac{6}{d_{\text{bead}}} \varepsilon_s V_r$$

$$\phi_{wd}^p, i = \left( \frac{1}{k_{\text{drop},p}^w} + \frac{1}{m k_{\text{drop},p}^d} \right)^{-1} \left[ C_p^{w,n} - \frac{C_p^{o,i,n}}{m} \right] \frac{6}{d_{\text{drop}}} \varepsilon_d \frac{V_r}{No}$$

The mass transfer coefficients  $k_{\text{bead},s}$ ,  $k_{\text{bead},p}$ , and  $k_{\text{drop},p}^w$  are calculated with the equation of Ranz and Marshall (1952):

$$\frac{k_{bead,i} d_{bead}}{D_i} = 2 + 0.57 \left( \frac{\rho_w v_{wp} d_{bead}}{\eta_w} \right)^{0.5} \left( \frac{\eta_w}{\rho_w D_i} \right)^{0.33}$$

$$\frac{k_{bead,p} d_{drop}}{D_p} = 2 + 0.57 \left( \frac{\rho_w v_{wo} d_{drop}}{\eta_w} \right)^{0.5} \left( \frac{\eta_w}{\rho_w D_p} \right)^{0.33}$$

with  $v_{wp}$  the slip-velocity between water and gel bead, and  $v_{wo}$  the slip-velocity between water and organic phase. The droplet diameter is calculated with the equation of Kumar and Hartland

$$d = \frac{d_{noz}}{0.55 Eo_{noz}^{0.33} + 0.0393 We_{noz}^{0.73} \left( \rho_d g d_{noz}^2 \right)^{-0.315}}$$

$$\text{with } Eo_{noz} = \frac{g \Delta \rho d_{noz}^2}{\sigma}, \text{ and } We_{noz} = \frac{\rho v_\infty^2 d_{noz}}{\sigma}$$

The rise velocity of a single droplet is calculated with Vignes' equation:

$$v_\infty = \frac{d}{4.2} \left( \frac{g \Delta \rho}{\rho} \right)^{\frac{1}{2}} \left( \frac{\rho}{\eta} \right)^{\frac{1}{2}} \left( 1 - \frac{Eo}{6} \right)$$

$$\text{with } Eo = \frac{g \Delta \rho d^2}{\sigma}$$

The mass transfer coefficient  $k_{drop,p}^d$  is calculated with the equation of Newman (1931).

$$k_{drop,p}^d = - \frac{d_{drop}}{6t} \ln \left( \frac{6}{\pi^2} \sum_{n=1}^{\infty} \frac{1}{n^2} \exp \left( -4n^2 \pi^2 D_{p,drop} \frac{t}{d_{drop}} \right) \right)$$

$t$  represents the contact time and is equal to:  $t = H_t \epsilon_0 / U_d$

The mass balances are made dimensionless by dividing with the initial substrate concentration, the bead diameter, and with  $D_s/R^2$ . The resulting dimensionless parameters are: dimensionless length inside the bead  $z=r/R$ , dimensionless concentration  $C/C_s^{w,0}$  and a dimensionless time  $Fo=D_s t / R^2$ .

The resulting mass balances with the implementation of the transfer flux relations are:

$$\frac{\partial X_s^{p,n}}{\partial Fo} = \frac{\partial^2 X_s^{p,n}}{\partial z^2} + \frac{2}{z} \frac{\partial X_s^{p,n}}{\partial z} - (-r_s) \frac{r_p^2}{D_s C_s^{w,0}}$$

$$\frac{\partial X_s^{p,n}}{\partial Fo} = \frac{D_p}{D_s} \frac{\partial^2 X_p^{p,n}}{\partial z^2} + \frac{D_p}{D_s} \frac{2}{z} \frac{\partial X_p^{p,n}}{\partial z} + (-r_s) \frac{r_p^2}{D_s C_s^{w,0}}$$

$$\frac{\partial X_s^{w,n}}{\partial Fo} = \frac{U_w}{\epsilon_w H_t D_s} \frac{r_p^2}{D_s} (X_s^{w,n-1} - X_s^{w,n}) - \frac{6}{d_{bead}} \frac{\epsilon_s}{\epsilon_w} k_{bead,s} \frac{r_p^2}{D_s} (X_s^{w,n} - X_s^{w,int,n})$$

$$\frac{\partial X_p^{w,n}}{\partial Fo} = \frac{U_w}{\epsilon_w H_t D_s} \frac{r_p^2}{D_s} (X_p^{w,n-1} - X_p^{w,n}) + \frac{6}{d_{bead}} \frac{\epsilon_s}{\epsilon_w} k_{bead,p} \frac{r_p^2}{D_s} (X_p^{w,int,n} - X_p^{w,n}) -$$

$$K \frac{6}{d_0} \frac{\varepsilon_o}{\varepsilon_w} \frac{r_p^2}{D_s} \left( X_p^{w,n} - \frac{\sum_{i=1}^{N_{dis}} X_p^{o,i}}{m N_{dis}} \right)$$

$$\frac{\partial X_p^{o,i}}{\partial F_O} = \frac{U_d}{\varepsilon_d H_{l,i}} \frac{r_p^2}{D_s} (X_p^{o,i-1} - X_p^{o,i}) + K \frac{6}{d_0} \frac{r_p^2}{D_s} \left( X_p^{w,n} - \frac{X_p^{o,i}}{m} \right)$$

The space co-ordinate in the gel bead mass balance is discretized, making the partial differential equation a set of ordinary differential equation (we took 31 grid points). To mimic the plug flow of the dispersed phase, we took 15 tanks per medium tank. Per medium tank  $2 \times 30 + 2 + 5 = 77$  differential equations were solved simultaneously with a solver for stiff differential equations.



# CHAPTER THIRTEEN

## FLOCCULATION BIOREACTORS

ANTÓNIO A. VICENTE, MANUEL MOTA AND JOSÉ A. TEIXEIRA

*Department of Biological Engineering, Universidade do Minho, 4710–057 Braga, Portugal*

### ABSTRACT

One of the main goals of bioprocess engineering is to increase the productivity of biotechnological processes and a vigorous progress has been observed in that field over the last decades. Fermentation based processes are not an exception and, in order to achieve those objectives, techniques such as the use of high cell density systems have been proposed and studied. The interest for such systems is increasing for they seem to be a very promising alternative to the traditional cell suspension fermentation. In fact, they may increase volumetric productivity, product concentrations in the outlet and conversion of raw materials, as a higher biomass concentration (biocatalyst) is present, at any moment, inside the bioreactor. Downstream processing will also be improved by the use of these technologies, as smaller amounts of biomass will be present in the effluent of the bioreactor.

To achieve this, several new processes were studied, changes in existing ones were introduced and technical developments were made. The examples are various and cover diverse applications such as ethanol, beer and antibiotics production, and waste water treatment, just to quote a few representative areas. Among the several immobilisation techniques, flocculation, although not being extensively considered, is one of the most attractive.

In this chapter, the main aspects associated with high cell density cultures using flocculating microorganisms will be considered. Aspects such as bioreactor design and performance, mass transfer limitations in cell aggregates and their relation with yeast cell activity, as well as applications, will be considered and discussed.

**Keywords:** floes, three-phase bioreactor, airlift, mass transfer, hydrodynamics, design

### INTRODUCTION

Systems using flocculating cultures (Abate *et al.*, 1996; Kida *et al.*, 1992; Kuriyama *et al.*, 1993; Roca *et al.*, 1995; Teixeira *et al.*, 1990; Wieczorek and Michalski, 1994) which take advantage of cell recycling by natural sedimentation of highly flocculating strains

are a very interesting technique due to their low operational costs (Sousa *et al.*, 1994a) and simplicity—no complex mechanical devices (e.g. centrifuges) are needed. In fact, construction costs are low and energy input is not very significant. Moreover, it allows a natural selection of the flocculating organisms in continuous fermentations, as the non-flocculating ones will be dragged out of the system together with the effluent. Further, the use of flocculating cells may provide important contributions for the improvement of separation processes in fermentation; besides being less aggressive than other separation techniques, a reduction in production costs is obtained since the amount of cells to be separated by centrifugation or filtration is significantly reduced (Teixeira and Mota, 1992). An additional advantage is obtained when using bioreactors operating with genetically modified flocculent microorganisms. In fact, such reactors are able to retain the genetically modified biomass, thus minimising the danger of spreading it into the environment, while exerting a permanent selective stress in the organism by expelling all the individuals that have lost flocculation ability.

Among the several possible bioreactor designs, reactors in which the power for mixing and mass transfer is introduced by injecting gas (such as bubble columns and airlifts) are better adapted to the culture conditions of flocculating microorganisms and present other advantages summarised by Michalski (1992):

- the construction is simpler and cheaper;
- compressors can easily be maintained or removed without the need to stop the process (as would be the case of e.g. a stirring motor);
- maintenance is simpler because there are no rotating parts below the liquid level; the maximum local shear stresses are much smaller than in other types of bioreactors;
- gas dispersion efficiency is good.

If a flocculent organism is used, the absence of an immobilisation support is also an advantage. In fact, it usually poses problems either in downstream processing (if it has to be separated from the product) or while recovering the biomass or the support itself (as it has to be separated from the cells), contributing to increased production costs. The environmental pollution can also become a worry when the disposal of the unrecoverable support is to be considered. Under such circumstances flocculation can be a solution, having no need for biomass/support separation and no additional environmental worries. However, in general and strongly associated with the flocculation ability of the microorganism used, there is a drawback concerning flocculation bioreactors when these are compared with those using an immobilisation support; while in continuous operation, the biomass concentration in the outlet stream is higher in the former than in the latter. Also, although present in most immobilisation systems, diffusional limitations may be a high concern in flocculation bioreactors.

### Flocculation

To clearly understand the operation of flocculation bioreactors, it is convenient to clarify the mechanism of cell flocculation.

Cell properties are the result of the permanent interaction between environmental, nutritional and genetic control; in the specific case of yeast, the effects on cell wall composition are the ones mainly responsible for the capacity of forming aggregates—

flocculation. In turn, the flocs will cause a change in both the individual cell metabolism and the environmental conditions.

The study of flocculation mechanisms has been centred on *Saccharomyces cerevisiae* as it has a capital importance in the brewing industry (Dengis *et al.*, 1995; Teixeira, 1988), although other microorganisms have been studied as well (Ananta *et al.*, 1995; Libicki *et al.*, 1988; Moradas-Ferreira *et al.*, 1994; Pereboom *et al.*, 1990; Teixeira *et al.*, 1995). Despite the wealth of works published on yeast aggregate formation and although it is accepted that flocculation is under genetic control, a fully explanatory interpretation of the phenomenon has not been given yet. It is a very complex process, depending on factors such as the microbial strain (growth, physiological state and metabolism), the composition of the culture medium and the culture conditions (temperature, pH, agitation and aeration) (Dengis *et al.*, 1995; Scares *et al.*, 1994).

Several mechanisms have been proposed to describe flocculation. Taylor and Orton (1975) found that  $\text{Ca}^{2+}$  induced a conformational change in certain proteins, allowing them to be recognised in the cell-cell adhesion process. Before, it was already known that  $\text{Ca}^{2+}$  was necessary for yeast flocculation, but its role was just thought to be a bridge between adjacent cells. Later on, Miki *et al.* (1982) suggested that the flocculation mechanism should involve a lectin-like protein, as some specific sugar molecules inhibited it. In fact, sugars like mannose and its derivatives were found to inhibit flocculation of *S. cerevisiae* strains, where the mechanism involves mannan receptors' recognition by lectins of an adjacent cell, requiring the presence of  $\text{Ca}^{2+}$  ions (Dengis *et al.*, 1995, Stratford, 1992). Other sugars (e.g. galactose and its derivatives) inhibit the flocculation of other yeast species (*Kluyveromyces bulgaricus* and *K.lactis*), as the cell-cell interactions involve a galactose-specific lectin (El-Behhari *et al.*, 1998). Also found in a flocculent bottom-fermenting brewer's yeast strain is a mannose/glucose-specific lectin-like protein; consequently the flocculation of this strain is inhibited by both glucose and mannose (Kobayashi *et al.*, 1998). In general, the mechanism above is a widely accepted one and is presently believed to explain the phenomenon of flocculation in yeast. It was shown, by studies on the interaction between flocculent and non-flocculent cells of *S. cerevisiae*, that cell-cell interaction corresponds to a true stable binding and not to a simple entrapment inside the floe matrix (Soares *et al.*, 1992).

It is also clear that hydrophobic interactions play a crucial role in microbial adhesion phenomena, having been demonstrated in e.g. *Saccharomyces* and *Kluyveromyces* strains that an increase in flocculation is strongly correlated with an increase in cell wall surface hydrophobicity (Azeredo *et al.*, 1997; Straver *et al.*, 1993; Teixeira *et al.*, 1995; van der Aar, 1996).

Although to a minor extent, other physicochemical properties such as cell walls' isoelectric point (Dengis *et al.*, 1995) or external medium properties such as pH (Stratford, 1996; Yang and Choi, 1998), ionic concentration (Dengis *et al.*, 1995) and organic solvent concentration (Teixeira, 1988) are also important in flocculation. In fact, all these factors together with the adequate  $\text{Ca}^{2+}$  concentration will enable sufficient bond strength between the cells (van Hamersveld *et al.*, 1997), which is fundamental for floe formation and stability.

When using flocculating microorganisms in bioreactors, the effects of physical parameters on flocculation are also very important. Namely, the cell concentration must be sufficient to provide an adequate number of collisions to form flocs (Glasgow, 1989;

van Hamersveld *et al.*, 1997) and the hydrodynamic conditions must be favourable, i.e. high enough collision rate and not too large break-up forces. These are mainly caused by the shear inside the bioreactor, which is ultimately determined by the kind of agitation used.

All the above is closely related to the type of bioreactor as well as to the design of its constitutive parts. This design must also have in mind the sedimentation characteristics of the flocs and should provide a convenient environment for floc settling in order to maximise biomass separation from the effluent (in continuous processes). Further, when porous pellets of any catalyst (flocs also included as a special kind of catalytic porous pellets) are used in a reactor, it is necessary to consider also mass transfer problems that are usually associated not only with the penetration of the substrate at a slower rate than it is being consumed, but also with the metabolite retention inside the flocs, which may increase product inhibition. As this clearly puts in evidence, a deep knowledge of the effects of the interaction between design and operational parameters of bioreactors and of floc properties is needed to optimise the operation of these systems. This is the focus of the next section.

### Bioreactor Design and Flocculation

The bioreactor is a vessel that should provide the nutritional and physiological environment required for microbial growth; it is the core of a bioprocess.

Immobilised catalysts (cells, enzymes, protoplasts, organelles) can be employed in various types of reactor, depending on the immobilisation technique, as well as on the type of process. The aim of such systems is to increase catalyst concentration while keeping it inside the bioreactor, in order to increase process productivity. An example of such high cell density systems is the production of ethanol using alginate-immobilised yeast (Gough and McHale, 1998; Joekes *et al.*, 1998; Nguyen and Shieh, 1992; Tyagi *et al.*, 1992) or flocculating yeast (Abate *et al.*, 1996; Sousa *et al.*, 1994a; Jianfeng *et al.*, 1998).

Basic bioreactor configurations are usually considered, namely the stirred tank, the packed bed, the fluidised bed, the bubble column and the airlift. To choose the best reactor type for such high cell density systems requires studies on mixing, heat and mass transfer between the different phases, as well as an evaluation of operational and maintenance costs.

With flocculating organisms, suitable hydrodynamic conditions must be provided (especially low shear stress) in order to maintain the adequate floc size, shape and density characteristics necessary to retain biomass inside the bioreactor as much as possible, although keeping the maximum possible activity. For these reasons, stirred vessels and packed beds are not recommended as flocculation bioreactors, although they are suitable for other immobilised cell systems which are mechanically more resistant. The fluidised bed is not very adequate for flocculating cultures either as the density difference between flocs and medium is rather small and fluidisation would be achieved at very low air/liquid flow rates. Bubble columns and especially airlift reactors are quite appealing to use with three-phase systems in processes involving flocculating organisms (Ganzeveld *et al.*, 1995; Kennard and Janekeh, 1991; Merchuk *et al.*, 1994; Onken and Weiland, 1983; Siegel and Robinson, 1992), so this section will be mainly devoted to these bioreactors.

The evaluation of the performance of flocculating cultures in airlift reactors depends on understanding of the following parameters (Michalski, 1992): gas hold-up, gas-liquid interfacial area, volumetric phase distribution, liquid mixing time, liquid circulation velocity, liquid and gas phase axial dispersion coefficients, fluid-wall heat transfer coefficients and cell retention capacity. Especially for this last parameter the flocculation ability of the microorganism is a major help as it contributes significantly to the cell retention capacity of the bioreactor (Sousa *et al.*, 1994a). The overall volumetric mass transfer coefficient as well as liquid-solid and intra-particle mass transfer are phenomena of capital importance, particularly in a flocculation bioreactor, that will be dealt with later on in a separate section. The relations between the variables in terms of their influence in bioreactor hydrodynamic behaviour have been summarised in Figure 13.1.

Independently of their oxygen transfer capability (which may or may not be needed, depending on the process), mixing (of both liquid and gas) must be adequate in order to minimise mass transfer resistance and to provide the desired homogeneity inside the bioreactor. Mixing time is a parameter directly related to mixing and it is useful to evaluate the degree of mixing in the bioreactor; gas flow rate is a good control variable as it directly influences not only liquid circulation velocity but also gas hold-up both in riser and downcomer. Thus, correct regulation of the gas flow rate will be crucial to keep solids

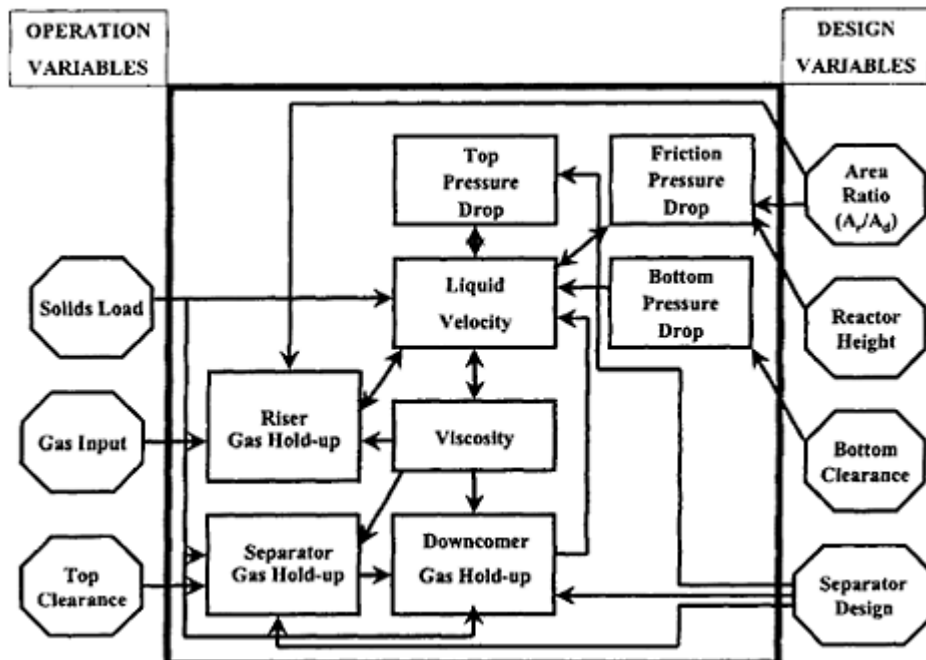


**Figure 13.1** Relations between variables in airlift reactors (adapted from Merchuk *et al.* 1996).

circulating as well as to optimise the hydrodynamic conditions inside the reactor. All the above-mentioned parameters are, in turn, influenced by the design of one or several of the parts that compose an airlift. The next sections are intended to give an idea of how those parameters are affected by reactor design and hence to give clues for the design of a flocculation bioreactor.

The effect of solid and liquid phases will be dealt with as well, in order to show their possible influence on reactor behaviour. Solids' characteristics such as density, size, shape and surface properties may change considerably the performance of the bioreactor, the same happening with the liquid phase properties.

As one of the main features of high cell density systems is the high hold-up of the solid phase (that can go up to 50–60% v/v of the total bioreactor volume, with the corresponding reduction in liquid-phase volume) a significant research effort has been devoted to optimise the design of several parts of three-phase airlift reactors, namely in those aspects related to their use as high cell density systems. As previously stated the use of flocculent microorganisms requires a great deal of attention when designing a reactor in order to retain flocs with the suitable characteristics for the process (shape, density and size, mainly).

### ***Gas-liquid separator***

The gas-liquid separator is the region at the top of an airlift reactor where riser and downcomer are connected. In systems operating with flocculating cultures, the design of this zone is a key factor, as its correct dimensioning is crucial in assuring biomass retention inside the system, particularly in continuous cultures. As a matter of fact, it has a major influence on the entire behaviour of the reactor; the gas recirculation rate is greatly affected by the gas-liquid separator's geometric configuration and by the liquid level in the separator, influencing the stability of the reactor (Siegel *et al.*, 1986). This section can be used to change the operating characteristics of an airlift reactor, making it possible to achieve operating patterns ranging from those of internal loop to those of external loop airlift reactors (Siegel and Merchuk, 1991). This may be important in giving more flexibility to this type of reactor.

Several studies have been done, characterising the effect of the design of this section of airlift bioreactor on hydrodynamic characteristics such as liquid circulation velocity, gas hold-up and liquid mixing, thus showing its importance. Russel *et al.* (1994) carried out yeast fermentations in a concentric tube airlift reactor and measured the influence of the top section height, which had a significant effect on liquid mixing by decreasing the mixing time as it was increased; liquid velocity and gas hold-up, on the other hand, were found to be independent from the top section height. Both the geometry and the design of that section, on the contrary, were found to have effects on hydrodynamic performance and oxygen transfer behaviour of airlifts by changing the liquid velocity, the gas hold-up in the downcomer, the mixing time and the overall volumetric gas-liquid oxygen transfer coefficient (Choi *et al.*, 1995). However, data describing how this section affects biomass retention in high cell density systems, particularly flocculation bioreactors, are scarce.

The introduction of an enlarged degassing zone in the top section (usually just an unbaffled extension of the riser and downcomer (Siegel and Merchuk, 1991)) of an airlift reactor not only enhances gas disengagement but also allows for a better solids settling.

These characteristics are especially useful in continuous three-phase reactors, where solids retention is a very important issue. It was possible to retain much more biomass during continuous fermentation with a highly flocculent strain of *S. cerevisiae* (NRRL Y265) by the introduction of an enlarged top section in a concentric tube type airlift bioreactor (Sousa *et al.*, 1994a). The results were encouraging, reaching total biomass concentrations of  $78 \text{ kg}\cdot\text{m}^{-3}$  (dry weight). In the absence of such an enlarged section, the biomass would have been mostly dragged out of the bioreactor, since most of the flocs would have had the time to settle and remain inside the vessel.

### ***Downcomer and riser dimensions***

The downcomer to riser cross sectional area ratio ( $A_d/A_r$ ) and the height of those sections also have a very important influence in the performance of the reactor. Studies on three-phase reactors are available and are a very useful contribution, as they provide insight into the possible behaviour of flocculating systems, despite the fact that the solid phase in such studies is usually not composed of cell flocs but plastic, gel or glass beads, typically used as models. Effects on the general hydrodynamic behaviour are to be expected with consequences on liquid circulation velocity, dispersion coefficient and gas and solid holdup in each section of the bioreactor, which are directly influencing overall parameters such as circulation and mixing times.

Kennard and Janekeh (1991) studied the mixing in a three-phase concentric tube airlift bioreactor using 2.5–4 mm Perlag® solid particles. Although  $A_d/A_r$  has not been varied, they have been able to conclude that this parameter might severely affect the operation of an airlift reactor. In fact, the decrease of  $A_d/A_r$  ratio and the increase of reactor height cause an increase of the liquid velocity with obvious consequences on the maximum solid hold-up with which the reactor can deal without the occurrence of stalling.

Solid particles of diverse polymeric materials (around 2.8 mm in diameter and with density values ranging from  $1202 \text{ kg}\cdot\text{m}^{-3}$  to  $1381 \text{ kg}\cdot\text{m}^{-3}$ ) were used to assess the importance of the reactor size in three-phase internal and external loop airlift reactors' behaviour (Kochbeck *et al.*, 1992). Both the liquid velocity and the dispersion coefficient were found to increase with reactor height, which is in agreement with other experimental works (Verlaan and Tramper, 1987). Also, Lu *et al.* (1995) found an increase of the liquid velocity with the riser height in three-phase internal loop airlift reactors with alginate beads.

Vicente and Teixeira (1995) investigated the effects of the  $A_d/A_r$  ratio and the riser height on mixing and circulation times and on critical (minimum) airflow rate in a three-phase airlift with an enlarged degassing zone. Alginate beads with two different density values ( $1016 \text{ kg}\cdot\text{m}^{-3}$  and  $1048 \text{ kg}\cdot\text{m}^{-3}$ ) were used as the solid phase. An optimal (minimum) value for the circulation time and for the critical airflow rate was obtained for a  $A_d/A_r$  ratio of 3.8. The minimum mixing time was obtained for a riser to downcomer height ratio of 0.80.

### ***Other design characteristics***

The design of other parts of the bioreactor may also affect its performance. In fact, there are studies on air sparger's design and location (Pollard *et al.*, 1996), on the top and

bottom clearances (i.e. the distance between the top of the draught tube, and the liquid surface and between the bottom of the reactor and the bottom of the draught tube, respectively) (Merchuk, *et al.*, 1994; Pollard *et al.*, 1996) as well as on the introduction of movable parts (Pollard *et al.*, 1997; Sisak *et al.*, 1990) or static mixers. In order to adequately design flocculation bioreactors, these studies must be extended to high solids loads.

In terms of flocculation bioreactor performance, the inclusion of static mixers has a particular importance. Experiments made with a 60 L external loop airlift reactor in the presence and in the absence of static mixers (Rüffer *et al.*, 1995) showed that these mixers are responsible for a reduction of the velocities of the liquid and gas phases, increasing therefore the circulation time; there is also an increase of the radial and axial liquid dispersion for lower aeration rates but not for higher aeration rates. As expected, static mixers also increase the shear stresses inside the bioreactor and those increased stresses may be used to decrease particle size if the particles are sufficiently fragile. Knowing that, static mixers were introduced in the riser of a three-phase airlift bioreactor, in order to diminish the floc size during fermentation with a highly flocculent strain of *S. cerevisiae* (Vicente *et al.*, 1999), and the average floc diameter decreased from 3 mm to 1 mm. As discussed later, this had favourable consequences in terms of a decrease in mass transfer limitations and an increase in overall system productivity.

### *Influence of the solid and liquid phases*

In order to increase biomass performance using yeast cell flocs, it is of crucial importance to characterise the properties of the solid phase (particularly solid phase hold-up) and the way it affects the hydrodynamics of flocculation bioreactors. However, no real data are available for flocculation bioreactors and so far, even when systems with similar properties have been used as models, only a few of them deal with solids loads as high as those found in flocculation bioreactors. Studies where gel beads (with a density similar to that of the flocs) are used as solid phase are particularly interesting, since the beads are easy to prepare and to handle and are, therefore, a very convenient model system.

The addition of solids may promote either bubble coalescence, bubble break up, or both, this effect being dependent on the concentration and size of the solid particles; this has consequences on the gas-liquid mass transfer efficiency (Smith and Skidmore, 1990). Also gas hold-up is affected: a reduction is observed when solids are added at low gas flow rate, but no effect is reported if the gas flow rate is high (Siegel *et al.*, 1988). In terms of superficial liquid velocity, the effect of solids can be negligible whereas their effect on circulation time may depend on the liquid phase; circulation time increases with solids for distilled water but decreases e.g. for carboxymethyl cellulose (CMC) solutions.

Liquid velocity and gas hold-up decrease were related to an increase in the particle diameter or increasing solids load (Lu *et al.*, 1995) in an internal loop airlift (containing Ca-alginate beads of 1 mm to 3.6 mm in diameter) and Ganzeveld *et al.* (1995) using split cylinder airlift bioreactors in order to study the effect of solids load (solid phase: cell microcarriers of  $0 \text{ kg}\cdot\text{m}^{-3}$  to  $30 \text{ kg}\cdot\text{m}^{-3}$ , with a particle size of 150  $\mu\text{m}$  to 300  $\mu\text{m}$  in diameter and density of  $1030 \text{ kg}\cdot\text{m}^{-3}$  to  $1050 \text{ kg}\cdot\text{m}^{-3}$ ) showed that, in the range of the solids load studied, increasing solids load provoked a decrease in liquid circulation velocity and an increase in mixing time.

As stated before, biomass retention in flocculation bioreactors is strongly improved when an enlarged top section is used as it permits better gas disengagement as well as enhanced solids settling. Using a 6 L airlift bioreactor with an enlarged top section, it was observed that both the critical airflow rate and the mixing time increased with the solids load, while the circulation time presented a maximum for a load of solids between 5% and 10% (v/v) (Vicente and Teixeira, 1995). Also, small changes in solids density (Ca-alginate beads,  $1016 \text{ kg}\cdot\text{m}^{-3}$  to  $1048 \text{ kg}\cdot\text{m}^{-3}$ ) were shown to have a significant influence on the critical airflow rate and on the mixing time. This is meaningful since the density range used includes that of yeast flocs (Vicente *et al.*, 1999), making it possible to have an idea of how a flocculation bioreactor will behave in identical situations. Nevertheless, the relatively small scale used (6 L) might have some influence in the results, so a 60 L concentric tube airlift bioreactor with an enlarged top section was tested instead (Freitas and Teixeira, 1997). The effects of solids load (Ca-alginate beads, with solids fractions varying from 5% to 30%) and density ( $1016 \text{ kg}\cdot\text{m}^{-3}$  and  $1038 \text{ kg}\cdot\text{m}^{-3}$ ) on gas and solids hold-up in the riser and the downcomer, on circulation and mixing times and on the interstitial liquid velocity were studied. It has been concluded that an increase in solids load and density causes an increase in riser and downcomer solids hold-up but provokes a decrease in the riser and downcomer gas hold-up. As before, circulation and mixing times decrease with the increase of airflow rate. It has also been confirmed that, while circulation time is practically independent of solids load and density, mixing time is strongly influenced by these two variables: it increases with solids load up to 20%, decreases with higher values and always increases with solids density. Increments of the airflow rate, solids load and solids density also cause an increase in the interstitial velocity.

A full characterisation of solid phase distribution inside the bioreactor was also done. The system (the same 60 L airlift bioreactor—see Figure 13.2) was divided into eight different sections (Freitas and Teixeira, 1998a) and, by using a special sampling device (Freitas *et al.*, 1997), it was observed that the solids hold-up increased, in general, from the wall to the middle of the separator (sections 1 to 3 and 4 to S) and from the top to the bottom of the reactor (sections 3, 5, 6 and 7/8). For all tested solids loads and gas flow rates, solids hold-up in the separator has been found to be lower than that in the riser or in the downcomer, thus proving the efficiency of this system in what concerns solids retention.

The effect of the presence of ethanol in system hydrodynamics is particularly relevant, since many applications of flocculation bioreactors deal with ethanol fermentation. When water is replaced by an ethanol solution ( $10 \text{ kg}\cdot\text{m}^{-3}$ ), a reduction in the surface tension occurs and changes significantly the response of the reactor in terms of the gas and solids hold-up in both riser and downcomer, the circulation and mixing times and the riser and downcomer interstitial velocity (Freitas and Teixeira, 1998b). In fact, an increase of the riser and downcomer gas hold-up is registered, together with the consequent decrease of solids hold-up in those sections and the resulting decrease of riser and downcomer interstitial velocity. However, the difference between gas and solids hold-up in the riser and in the downcomer remains practically constant when ethanol is added; the driving force for the circulation is thus maintained and so the presence of ethanol, while increasing mixing time, has no measurable effect on circulation time.

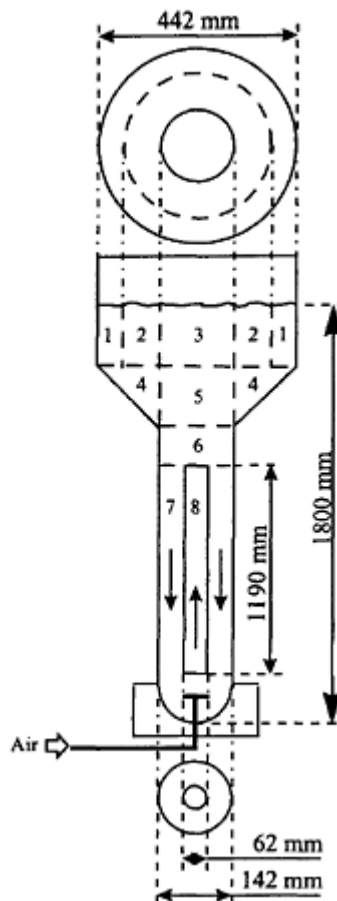


**Figure 13.2** Schematic diagram of the 60 L concentric tube airlift reactor. The reactor is divided in eight sections for sampling purposes (sections 1 to 5 correspond to the gas-liquid separator and section 6 is a transition section between the downcomer (7) and the riser (8)) (Freitas and Teixeira, 1998a).

#### CHARACTERISATION OF MASS TRANSFER MECHANISMS IN FLOCCULATING CELL CULTURES

In aerated fermentative process with flocculent cells, solute molecules must overcome several mass transfer resistances before they can reach the cells. Oxygen, for instance, must be transferred through the bubble's bulk gas phase (low resistance), then through the gas-liquid interface (very low resistance, if any) and through the liquid film surrounding the gas bubble (high resistance) to finally reach the bulk liquid (low resistance—well mixed reactor). Here, together with the other solutes (e.g. nutrients), the molecules must pass through the liquid film surrounding the flocs (which may have significant resistance), then through the floc-liquid interface (very low resistance, if any) and finally through the solid floc until the cells are reached (high resistance). Once these resistances are in series, only the high resistance mechanisms must be considered for mass transfer studies and so this section will be devoted to the main mass transfer mechanisms involved in a flocculation bioreactor: gas-liquid mass transfer of oxygen from the gas phase to the liquid medium through the liquid film surrounding the gas bubbles and solutes mass transfer inside the floc, with reference to a possible external mass transfer resistance around the floc.

### Gas-Liquid Mass Transfer of Oxygen

Especially in the case of aerobic fermentations, cell exposure to low or near zero dissolved oxygen concentrations may have a deleterious effect on metabolism, therefore affecting the overall yield of the process. This is likely to occur e.g. in the downcomer of an airlift bioreactor if the oxygen uptake rate of the culture is fast enough to cause a complete consumption of the dissolved oxygen during the residence time of the liquid in that unaerated part. The situation becomes critical in industrial scale airlifts due to their height, making it necessary either to induce gas recirculation into the downcomer by means of an increased liquid velocity or to sparge gas also into the downcomer. This simple example shows the importance of controlling the gas-liquid mass transfer during fermentation.

Due to the low solubility of oxygen in fermentation media, a continuous supply is needed, either pure or as part of a gaseous mixture (most frequently, air). During the mass transfer process from the gas phase to the medium or vice-versa (case of carbon dioxide), liquid film resistance at the gas-liquid interface is usually the limiting step. Therefore it is possible to express the rate of mass transfer of a component,  $dC_L/dt$ , as the product of a mass transfer coefficient,  $k_L$ , the specific gas-liquid interfacial area,  $a$ , and the transfer driving force, expressed as a difference between the concentration of the component in the liquid phase,  $C_L$ , and the saturation concentration of that component in the liquid,  $C^*$ :

$$\frac{dC_L}{dt} = K_L \cdot a \cdot (C^* - C_L) \quad (1)$$

In this case, Equation 1 has been written for gas which is being transferred into liquid.

The direct measurement of  $a$  is a rather imprecise procedure; being so, also the calculation of  $k_L$  from  $k_L a$  is not very reliable. Rather, the overall coefficient  $k_L a$  is preferred as it combines the information about the transfer area with that of the kinetics of the transport phenomena. Though quite convenient, this approach has nevertheless the shortcoming of preventing the independent study of transfer area and transport kinetics.

Several of the design parameters discussed in the previous sections as well as the presence of solids may affect gas-liquid oxygen transfer and that has been the object of several studies.

### ***Influence of the solid and liquid phases***

While studying the influence of solid phase, a widespread procedure is to replace immobilised biocatalysts (and microbial aggregates) by inert solid particles, which are easier to handle and pose no problems concerning biomass growth and maintenance. As regarding hydrodynamics, studies on the effect of high solids loads on gas-liquid mass transfer are scarce, at least in situations similar to those found in flocculation bioreactors. Verlaan and Tramper (1987) studied the gas-liquid oxygen transfer in a three-phase pilot plant airlift bioreactor (165 L). The solid phase consisted of polystyrene or Ca-alginate beads with a density of  $1050 \text{ kg}\cdot\text{m}^{-3}$  and diameters ranging from 2.4 mm to 2.7 mm. The maximum solids load at which the reactor could be operated was 40% (v/v) and it was found to provoke a decrease of  $k_{La}$  when compared to the value for two-phase operation, both for polystyrene and Ca-alginate beads. A similar effect has been found in a three-phase bubble column (Komáromy and Sisak, 1994). This decrease has been justified by a reduction of the specific area,  $a$ , due to an increase in coalescence provoked by the presence of the particles which cause an increase of the slurry viscosity. The viscosity increase is apparent, however, for it is effective only at a reactor scale, as the liquid viscosity remains the same and so the presence of solids is not expected to affect  $k_L$ . Even so, the reduction in  $k_{La}$  in the presence of alginate beads was slightly more significant than for polystyrene beads and this may be related to solids wettability, as pointed out by the authors (being Ca-alginate classified as perfectly wetted and polystyrene as poorly wetted). Siegel *et al.* (1988) also found a decrease in the overall mass transfer coefficient with increased solids load. Nevertheless, contrary to the previous authors, they state that the presence of non-wettable solids will have a profound (decreasing) effect on mass transfer coefficient, while wettable solids will cause a relatively smaller decrease in mass transfer. Correlations are presented for  $k_{La}$  as a function of the solids load and either the power input per degassed reactor volume or the superficial gas velocity. The results are classified into two groups, depending on whether the solid phase was composed of wettable or non-wettable particles.

Similar results were found in flocculent yeast cell cultures, as it is possible to observe a decrease of  $k_{La}$  values when biomass concentration increases (Sousa and Teixeira, 1996). As expected, this coincides with the behaviour observed when a non-living solid phase was used.

### ***Influence of design parameters***

The same design parameters referred to previously will exert their influence also in the oxygen transfer properties of a bioreactor, accordingly to Figure 13.1. The information on this is not abundant for three-phase reactors and data are even scarcer for flocculation bioreactors. As an example, the introduction of a draught tube in a three-phase fluidised bed (solid phase: polyurethane foam particles with an average size of 3 mm) increased the volumetric mass transfer rate of oxygen in the new bioreactor between one and a half

and three times (Karamanov *et al.*, 1992). The effect of the  $A_d/A_r$  ratio was also studied and a maximum  $k_{La}$  was obtained for a ratio value of three.

The assessment of  $k_{La}$  in different zones of a bioreactor is also important, as it may give insight into the limitations that a given reactor design might have. During the fermentation of a flocculating *S. cerevisiae* strain in a 5.4 L concentric tube airlift bioreactor with an aeration rate of 0.1 v.v.m., the value of  $k_{La}$  was significantly higher in the downcomer zone ( $0.12 \text{ min}^{-1}$ ), when compared with the riser ( $0.1 \text{ min}^{-1}$ ) and the gas-liquid separator ( $0.085 \text{ min}^{-1}$ ) (Sousa *et al.*, 1994b). Lübbert *et al.* (1988) suggest that the enhanced mass transfer in the downcomer is a consequence of the bigger difference between the gas and the liquid phase velocities in this zone, which means that a longer period of time is available for the bubbles to transfer oxygen into the liquid phase.

### Mass Transfer of Solutes in the Flocs

Diffusion is probably the most important mechanism of solute transport through cell aggregates and it is generally described using a single parameter, the effective diffusivity ( $D_e$ ) which relates the gradient of the characteristic concentration ( $c(r,t)$ ) along the coordinate  $r$  at time  $t$  to the average diffusive solute flux ( $J_D$ ) across the volume of the object in study, which is expressed by Fick's law:

$$J_D = -D_e \cdot \nabla c(r, t) \quad (2)$$

There are two distinct approaches for the calculation of effective diffusion coefficients, which are widely employed. In the first one, the effective diffusivity in the aggregates can be determined analysing the data by means of a reaction-diffusion model, knowing the consumption rate of the solute of interest and either the size of the aggregate or the solute's concentration profile in it; in the second, the assessment is made in steady state using Equation 2 in the absence of reaction. The techniques used in both approaches have advantages but also some limitations (Libicki *et al.*, 1988; Tanaka, *et al.*, 1984). In the first case, it is not necessary to destroy the flocs but some assumptions about the solutes consumption or production must be made, which can affect significantly the obtained results. In the second case, as no reaction is taking place, there is no need for assumptions about the kinetics of the solute consumption or production but, on the other hand, cell aggregates must usually be formed artificially or confined within a matrix (both procedures are likely to affect the results) and it is difficult to ensure that the solute does not react during the course of the experimental run. The option for either approach depends, therefore, on the system in question and on the experimental methods available.

In general, the diffusion coefficient of a component in a solvent is taken as a function of parameters such as temperature (Onuma *et al.*, 1985), pressure (in gaseous systems) and medium composition (Kurillová *et al.*, 1992). Very little work has been done in this area with flocs (Ananta *et al.*, 1995; Sousa and Teixeira, 1991; Teixeira and Mota, 1990) and the existing data on the diffusivity of glucose and oxygen do not usually refer to the case of cell aggregates (biofilms not included) (Libicki *et al.*, 1988). A very simple, yet valid, reason for this situation, already pointed out before, is their very fragile nature: in fact, flocs are very difficult to handle, as they are easily destroyed; further, this problem becomes more acute with the size increase, namely when dealing with diameters between

2 mm and 3 mm. Their geometry is seldom a perfectly defined sphere, contrary to the usual assumption; instead, flat cylinders and ellipsoids are the most common shapes and floc dimensions and shape are of capital importance to the assessment of  $D_e$ . Particularly, if the aggregates are assumed to be spherical or cylindrical, the determination of their diameter is crucial for the final result (Hamdi, 1995). One of the best ways to do this non-destructively is by image analysis. Such a technique applied to yeast flocs has been developed by Vicente *et al.* (1996), where both the floc size distribution of different populations and the number of flocs present in the treated samples have been determined by fitting a Gauss curve to the experimental data. From there, the values of the average floc size and their respective standard deviation can be calculated.

Most studies use the second approach mentioned above to calculate  $D_e$ . Some authors use non-reactive solutes: Libicki *et al.* (1988) calculated the effective diffusivity of nitrous oxide, a non-reactive solute, within cell aggregates of *Escherichia coli*. The effective diffusivity was found to decrease with increasing cell volume fraction. Other authors use inactivated cells, as is the case of Ananta *et al.* (1995), who measured the oxygen transfer characteristics of aggregates of *Solanum aviculare* with 3 mm to 12.5 mm in diameter. Effective diffusivity of oxygen in deactivated aggregates was found to increase with particle diameter varying between 2% and 40% of the molecular diffusivity of oxygen in water at the same temperature. The authors considered, therefore, that severe oxygen limitations occurred in the aggregate; nevertheless, one should pay attention when interpreting the results, since the measurements were made with inactivated cells, which may have a different behaviour from that of active cells.

Vicente *et al.* (1998) studied mass transfer characteristics (effective diffusivity,  $D_e$ , and external mass transfer coefficient,  $K_c$ ) of glucose and oxygen in flocs (0.90 mm to 2.42 mm in diameter) of *S. cerevisiae* using inactivated cells but a different technique. A modified diffusion cell (Figure 13.3) (Vicente *et al.*, 1997) was used in order to avoid floc destruction.  $D_e$  and  $K_c$  were calculated using two methods: a classical one, based on analytical solutions of Fick's law of diffusion and a numerical one, based on general mass balances of a component in flocs and bulk phase. Diffusion coefficients were found to be, for glucose, 17% of the diffusivity in water and, for oxygen, between 0.2% and 1% of the diffusivity in water, which is in agreement with the data from Ananta *et al.* (1995) if the size is considered.  $K_c$  values increased with the agitation rate, as expected, and have values which range from  $7.5 \times 10^{-9} \text{ m} \cdot \text{s}^{-1}$  to  $15 \times 10^{-9} \text{ m} \cdot \text{s}^{-1}$ . These values indicate that not only the mass transfer inside flocs, but also the one outside them, may be a limiting step in this process.

It is possible to calculate a floc critical diameter, defined as the diameter at which solid phase diffusion limitations become more important than liquid phase diffusion limitations (Hamdi, 1995). A floc diameter greater than its critical value can have consequences such as the presence of useless biomass inside the reactor, undesirable metabolite production by inactive biomass, or changes in chemical and biochemical characteristics of medium and microorganisms. The author, therefore, suggests a continuous disintegration of the flocs into a smaller size. In the same line, Webster (1981) developed criteria allowing the assessment of the importance of substrate diffusional limitations within cell flocs, depending on the rate law used to describe substrate consumption.

Teixeira and Mota (1990) proposed a membrane bioreactor for the assessment of internal diffusion limitations in yeast flocs (Figure 13.4). In this case a diffusion-reaction model (the first approach) was used and the authors found decreases in specific lactose uptake rate of flocculating *K. marxianus*, when compared with non-flocculating cells. This being so, the ratio between the specific lactose uptake rates of the flocculating strain over the non-flocculating strain (i.e., an effectiveness factor— $\eta$ ) could be calculated and its

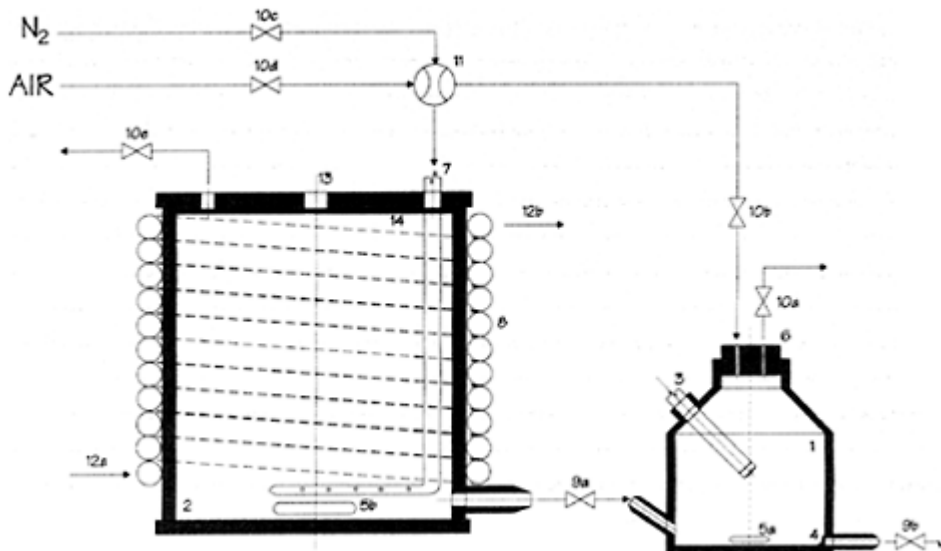


**Figure 13.3** Experimental set-up: (1) isolated measuring chamber (isolation not shown); (2) reservoir; (3) DO<sub>2</sub> probe; (4) stainless steel mesh; (5a,b) magnetic rod; (6) rubber sealing plug; (7) gas sparger; (8) temperature control jacket; (9a, b) and (10a-e) one-way-valves; (11) two-way valve; (12a, b) circulating temperature control liquid; (13) thermometer; (14) rubber sealing O-ring.

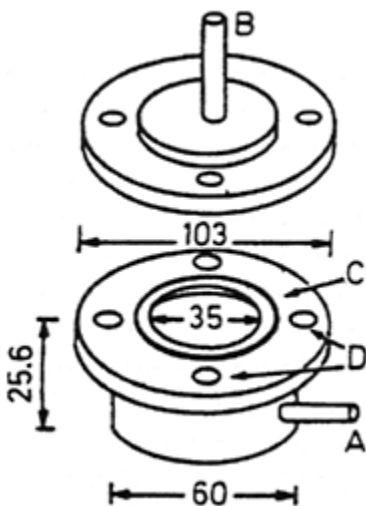


**Figure 13.4** Exploded view of the membrane microreactor: A—feed inlet; B—outlet; C—O—ring; D—sealing holes (internal diameter 5 mm). A membrane filter is placed between the upper and the lower chamber; the sealing is made with butterfly screws; all dimensions are in mm.

value related to the importance of mass transfer limitations inside the yeast flocs. The floc porosity was also determined by means of a thermogravimetric balance, obtaining a value of 50.5%.

This value increased about 10% when the flocs were grown in the presence of a polymeric flocculation additive (a cationic resin) causing a corresponding 10% increase in the value of the effectiveness factor.

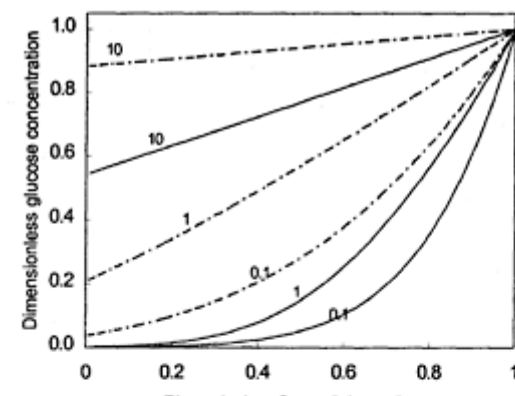
This is an example of one of many attempts that have been made in order to reduce diffusional limitations in flocs through the use of polymeric additives (Salt *et al.*, 1996; Sousa and Teixeira, 1991; Weir *et al.*, 1994). Those additives should enlarge the space between adjacent cells, extending the bridges that link the cells in a floc (Lima *et al.*, 1992). In fact, reductions in diffusional limitations have been reported suggesting an increase of the effective diffusion coefficients of the substrates in the floc, whenever some flocculating additives are used.

Lima *et al.* (1992) studied the influence of several polymeric additives on specific glucose uptake rate of flocs of *S. cerevisiae*, using the same system as in Figure 13.4. An increase of glucose uptake rate by cells in the flocs grown in the presence of additive was always observed when compared to those grown without additive: 19% for bis [polyoxyethylene-bis(amine)] 20 000, more than 50% for BPA 1000 and two-fold for

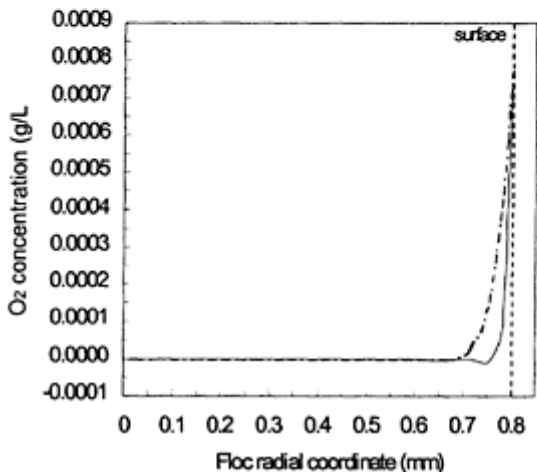
Magna Floc LT25. Floc porosity was measured and found to range from 55.7% (without additive) to 60.5%–63.0% (with additive). The authors proposed a model for the cell arrangement of yeast flocs, characterised by a cubic packing of the cells, which succeeded in explaining both the increase in the available area for substrate flux inside the floc provoked by the average 10% increase in floc porosity obtained with the flocculation additives tested and the consequent increase in the overall reaction rate. Sousa and Teixeira (1991) carried on the previous work by studying the influence of an anionic and a cationic polymer on the batch fermentation parameters of a flocculating strain of *S. cerevisiae*. While the cationic polymer showed little effect on the kinetic performance of the system, the anionic polymer caused a two-fold decrease in the time needed to obtain total glucose consumption, confirming its positive effect on the reduction of mass transfer limitations inside flocs. Through calculation of the effectiveness factor ( $\eta$ ), the same authors (Sousa *et al.*, 1994b) estimated the penetration depth of oxygen in the flocs, corresponding to fractions of cells in the floc having oxygen available ranging from 2.4% to 16.2%. This estimate was made considering that oxygen uptake by yeast follows zero-order kinetics. If this holds true, then a relation between  $\eta$  and the penetration depth can be established.

However, there are other means of estimating the penetration depth of the solutes in flocs e.g. by using data on substrate diffusion inside flocs and modelling diffusion-reaction phenomena. Concentration profiles of glucose and oxygen inside aggregates of *S. cerevisiae* were simulated and calculations were made for different possible sizes of the yeast flocs, considering also the presence or the absence of a polymeric additive (Vicente *et al.*, 1998) (Figure 13.5a, b).

From Figure 13.5 it can be seen that only a small percentage of the cells in the floc metabolise glucose oxidatively, due to severe oxygen limitations. The presence of the polymeric additive, however, increased the ratio of cells operating under respiratory metabolism over those under fermentative metabolism: from 0.4% to 5.7%, without additive, to 1.2% to 8.5%, with additive, depending on the bulk glucose concentration.



a



b

**Figure 13.5** Comparison of the concentration profiles for flocs grown with (dot-dashed lines) and without (solid lines) a flocculation additive, with a radius of 0.8 mm: a) dimensionless glucose concentration profiles (the parameters near the lines identify the values of the bulk concentration in  $\text{g}\cdot\text{L}^{-1}$  to which each

line corresponds); **b)** dissolved oxygen concentration profiles.

## OPERATION AND APPLICATIONS OF FLOCCULATION BIOREACTORS

As well as all the other factors pointed out through the preceding pages, the operational conditions under which a given bioreactor can be operated are also largely dependent on the flocculation ability of the microbial strain involved in the fermentation. If a highly flocculent strain is used, its continuance inside the bioreactor poses no problem even if “tough” operational conditions are used, such as high aeration and dilution rates (Vicente *et al.*, 1999). However, when a given strain has weak flocculation abilities, the reactor design plays a fundamental role, an airlift being one of the most appropriate, especially if equipped with a sedimentation zone (either at the top of the reactor, for an internal loop airlift, or at the top of the downcomer, for an external loop airlift). In Figure 13.6 it is possible to follow the operation of an external loop airlift with a sedimentation zone, a volume of 1.2 L and fed at different dilution rates, as shown (Teixeira and Mota, 1992).

This experiment was made with the yeast strain *K. marxianus* AJCC 10002 which, when inoculated in the bioreactor, had no flocculation ability. Being so, during the first 12 days there was no considerable difference between the biomass concentration in the effluent and inside the bioreactor. In the following days, however, flocs became apparent and the biomass concentration started to rise inside the bioreactor, while the effluent biomass concentration was kept near zero. This means that both the hydrodynamic conditions inside the reactor were favourable to the formation of flocs and that there was a selection of the most flocculent individuals to the detriment of the non-flocculating ones, due to the sedimentation characteristics of the former. Of particular importance is the fact that it has been possible to constantly maintain the flocculating characteristics of the strain used over a working period of two years. It is interesting to notice the effects of a sudden increase of the dilution rate (in days 39 to 41), when a peak of lactose concentration together with a drop of both ethanol and biomass concentrations are registered and are essentially due to a washout effect. However, the system reacts and, three days later, a new equilibrium state is reached. Also noteworthy is the biomass concentration in the effluent, which always has very small, near zero, values throughout the course of the experiment.

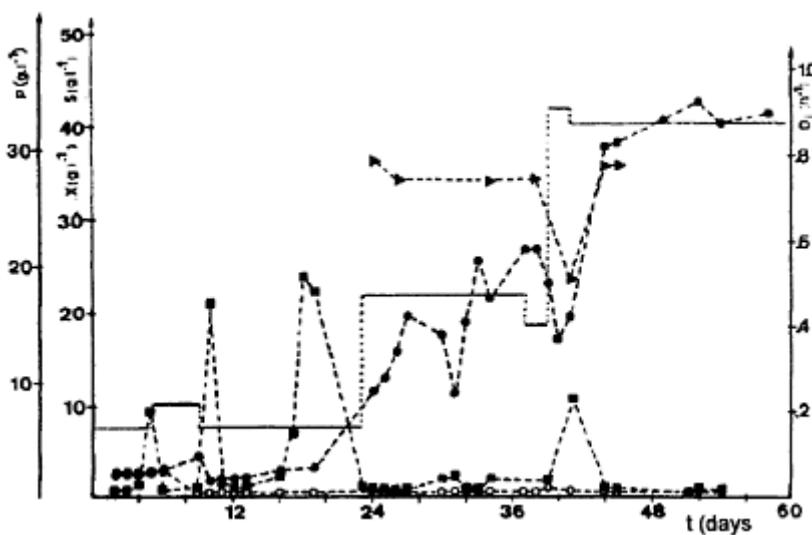


**Figure 13.6** Hocculcation bioreactor response to increasing dilution rate ( $D$ ) with a feed lactose concentration of  $57.2 \text{ g.L}^{-1}$ ; ●—biomass concentration in the bioreactor (X); —biomass concentration in the effluent (X); ■—lactose concentration (S); ▲—ethanol concentration(P).

With this system it has been possible to achieve a practically complete conversion of substrate during an alcoholic fermentation of lactose (Teixeira *et al.*, 1990). A maximum ethanol outlet concentration of  $44.8 \text{ g.L}^{-1}$  and a maximum ethanol productivity of  $24.4 \text{ g.L}^{-1}.\text{h}^{-1}$  were obtained.

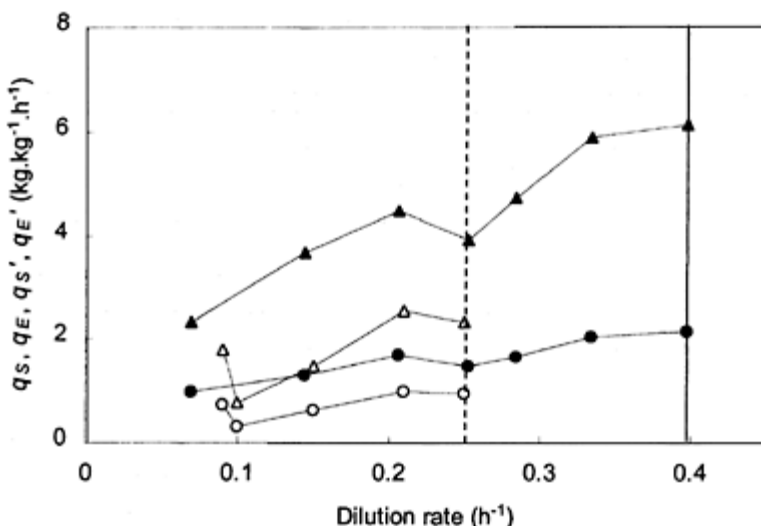
Considering the need to develop new and simpler fermentation systems and the suitability of the airlift bioreactor for cultures using flocculating microorganisms, a 5.4 L internal loop airlift bioreactor was tested and compared with the previous system (Sousa *et al.*, 1994a) using a highly flocculating strain of *S. cerevisiae* growing on glucose. A comparison was made in terms of start-up evolution, overall performance and power costs. The best ethanol productivity was obtained for the concentric tube airlift reactor ( $12.9 \text{ g.L}^{-1}\text{h}^{-1}$ ), but both systems behaved in a similar way and the productivity values were about seven times higher than in commercial systems. There was also a clear indication of a higher cell activity in the concentric tube airlift bioreactor when compared to the external loop airlift, thus compensating for the lower cell retention capacity of the former. The power cost analysis revealed differences only at laboratory and pilot scales; at industrial scale, however, the concentric tube airlift is advantageous because no mechanical parts are involved in cell recycling. The work proceeded, then, with the concentric tube airlift (Sousa *et al.*, 1994b), by studying the evolution of fermentation

parameters of the same flocculent strain of *S. cerevisiae* during the startup of a continuous fermentation. A strong influence of the dilution and aeration rates was found on both biomass and ethanol concentrations and kinetic parameters. The operating parameters, in turn, do not seem to affect glucose consumption rates but affect, instead, the stoichiometry of its conversion to either biomass or ethanol, suggesting a shift in the metabolic mechanisms as biomass builds up.

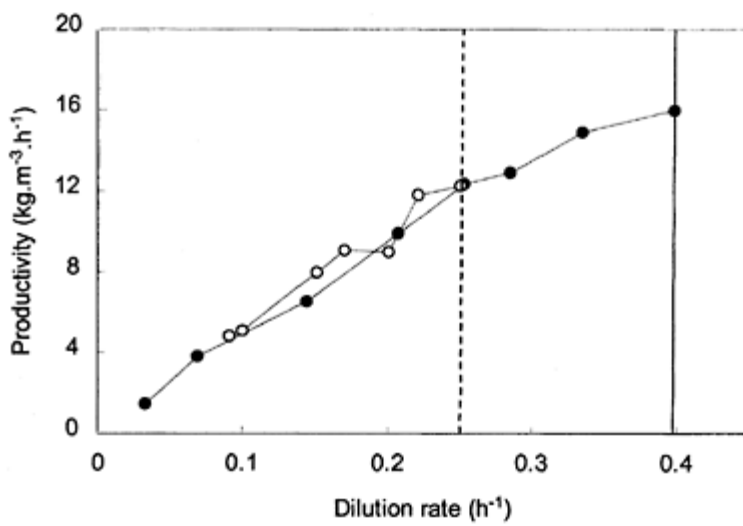
One of the shortcomings of flocculation bioreactors already mentioned is the presence of mass transfer limitations inside the flocs and it has been pointed out in the previous section that a reduction in floc size could be expected to bring a reduction in mass transfer limitations, leading to an increase of productivity. Vicente *et al.* (1999) introduced static mixers in the draught tube of the internal loop airlift bioreactor used by Sousa *et al.* (1994a, b), achieving an effective reduction of the floc size (3 mm to 1 mm in diameter). Steady state data at different dilution rates were measured for both systems (the original and the modified bioreactor) and the results were compared in terms of specific consumption/production rates and ethanol productivity (Figure 13.7a, b). A 40% increase was obtained in the maximum dilution rate at which a glucose conversion higher than 98% could be achieved. The respiratory quotient had a constant value (around 23) at all dilution rates, meaning that the metabolic state of the cells in flocs remained constant, having a strong fermentative metabolism.

The floc size reduction contributed to the higher observed reaction rates, not only by means of an increased dilution rate, but also because of reduced diffusional limitations, leading to a 30% increase of ethanol productivity when compared with the original system.

One of the first commercial applications of the sedimentation characteristics of flocculating microorganisms was made by the brewing industry, back in 1971, in order to facilitate the separation of the yeast cells from beer at the end of the process (Greenshields and Smith, 1971). Still, it is mostly in the brewing industry that flocculation bioreactors



a



b

**Figure 13.7** a) Comparison between specific rates of glucose consumption ( $q_s$  -  $\Delta$ ,  $q'_s$  -  $\blacktriangle$ ) and ethanol production ( $q_E$  -  $\circ$ ,  $q'_E$  -  $\bullet$ ) obtained with the original system (open symbols) and the modified system (solid symbols) vs. dilution rate; b) comparison between

ethanol productivity obtained with the original system ( ) and the modified system (●) vs. dilution rate.

are widely used. However, in this case, flocculation is essentially a separation technique and not a way to immobilise cells in continuous high cell density systems. Despite of this, work on flocculating bioreactors has been performed for some decades, as Smith and Greenshields (1974) have successfully grown flocculent strains of brewing yeast in bubble column fermenters. These ranged in capacity from 1 L to 50 L and a variety of media were used, from refinery by-product sugars and molasses to wort. They managed to maintain concentrations of flocculent yeast up to 17.5% (w/w) during continuous operation. Most brewing companies and brewing research groups have several research programmes running using high cell density bioreactors, mostly with airlift configuration, in order to investigate their potential use in continuous beer fermentation, with the advantages pointed out earlier (Dillenhöffer and Röhn, 1996; Dömeny *et al.*, 1998; Linko *et al.*, 1997; Masschlein, 1997; Mensour *et al.*, 1997; mogrovicová *et al.*, 1997; Tata *et al.*, 1999). Nevertheless, none of these works actually deals with flocculating cultures, though some mention them as a possible alternative to the existing processes, in particular beer maturation (Linko *et al.*, 1997).

The advantage of biomass retention in bioreactors makes the use of these systems particularly attractive in continuous fermentations. This is the case for flocculation bioreactors. In Table 13.1, a summary of works with flocculation bioreactors is presented, proving an emerging interest for this type of system. As can be seen, the majority of the work presented deals with flocculating microorganisms for continuous ethanol production, which is not surprising since, for the moment, continuous high cell density systems are adequate for high volume low added value products. As also indicated, most of the studies on flocculation bioreactors have been done using bench-scale apparatus due to the costs and complexity associated with larger scale research. This being so, further information on hydrodynamics and mass transfer needed for reactor scale-up is still missing and it is not surprising that, so far, industry still hesitates to select a flocculation-based process for commercial purpose, in spite of the operational advantages of these systems.

A particular reference must be made to the work of Domingues *et al.* (1999), who describe the use of a recombinant flocculating strain of *S. cerevisiae* expressing the *LAC4* (coding for  $\beta$ -galactosidase) and *LAC12* (coding for lactose permease) genes of *K. marxianus* to perform alcoholic fermentation of lactose with the previously described airlift bioreactor. In continuous operation, an ethanol productivity of  $11 \text{ g}\cdot\text{L}^{-1}\cdot\text{h}^{-1}$  was obtained (with a feed lactose concentration of  $50 \text{ g}\cdot\text{L}^{-1}$  and a dilution rate of  $0.55 \text{ h}^{-1}$ ), a productivity seven-times larger than that in conventional continuous systems. Despite the flocculence instability of the recombinant strain, a high biomass concentration was achieved inside the bioreactor as its design allowed for a selection of the most flocculating cells from a mixed culture, contributing thus to a selective pressure for the maintenance of the flocculating cells inside the bioreactor. The most direct application of this work is the high-productivity fermentation of the lactose present in cheese whey to produce ethanol, not only contributing towards the bioremediation of that by-product of

the dairy industry produced in large amounts, but also allowing for the production of a useful fuel.

There is the need for more research on high cell density systems, in general, and on flocculation bioreactors, in particular, in order to gather the necessary information to make them an interesting alternative to the processes used nowadays, which are in most cases very well established and studied. The potential surely exists in this new technology, but it has to be demonstrated before the industry risks investing largely in it.

**Table 13.1** Works with flocculation bioreactors

Organism	Reactor type	Volume [L]	Main substrate	Main product	Productivity [g·L <sup>-1</sup> b <sup>-1</sup> ]	Ref.
<i>S. cerevisiae</i>	bubble column	1–50	wort	beer	—	Smith and Greenshields, 1974
<i>S. cerevisiae</i>	bubble column	—	molasses	ethanol	25–30	Kida <i>et al.</i> 1989
<i>K. marxianus</i>	external loop airlift	1.2	lactose	ethanol	24.4	Teixeira <i>et al.</i> 1990
<i>S. cerevisiae</i>	external loop airlift	2	glucose/sucrose	ethanol	68	Fontana <i>et al.</i> 1992
<i>S. cerevisiae</i>	CSTR	3	glucose	ethanol	S	Kida <i>et al.</i> 1992
<i>S. cerevisiae</i>	series of 2 CSTR	0.5+1.5	molasses	ethanol	9.3	Kuriyama <i>et al.</i> 1993
<i>S. cerevisiae</i>	internal loop airlift	5.4	glucose	ethanol	—	Sousa <i>et al.</i> 1994b
<i>S. cerevisiae</i>	external+ internal loop airlift	1.2+ 5.4	glucose	ethanol	12.9	Sousa <i>et al.</i> 1994a
<i>S. cerevisiae</i>	fluidised bed	10	molasses	ethanol	15–20	Wieczorek and Michalski, 1994
<i>S. cerevisiae</i>	external loop airlift	2	sucrose	ethanol	—	Roca <i>et al.</i> 1995
<i>S. diastaticus</i>	external loop	2	Jerusalem artichoke	ethanol+ inulin	—	Schorr-Galindo <i>et al.</i>

	airlift	extract			1995
<i>Z. mobilis+</i> <i>Saccharomyces</i> sp.	agitated conical flasks	1	—	ethanol	1.5
<i>Rhodiola</i> <i>sachalinensis</i>	internal loop airlift	10–100	—	salidroside	—
<i>S. cerevisiae</i>	internal loop airlift	6	green beer	matured beer	—
<i>Schizosaccharomyces</i> <i>pombe</i>	external loop airlift	1.2	grape musts	deacidified grape musts	—
<i>S. cerevisiae</i>	internal loop airlift	1000	deproteinised cheese whey	ethanol	—
					Unpublished data

## REFERENCES

- Abate, C., Callieri, D., Rodríguez, E. and Garro, O. (1996) Ethanol Production by a Mixed Culture of Flocculent Strains of *Zymomonas mobilis* and *Saccharomyces* sp. *Appl. Microbiol Biotechnol.*, **45**, 580–583.
- Ananta, I., Subroto, M.A. and Doran, P.M. (1995) Oxygen Transfer and Culture Characteristics of Self-Immobilized *Solanum aviculare* Aggregates. *Biotechnol Bioeng.*, **47**, 541–549.
- Azeredo, J.; Ramos, I., Rodrigues L.; Oliveira, R. and Teixeira, J. (1997) Yeast Flocculation: A New Method for Characterising Cell Surface Interactions. *J. Inst. Brew.*, **103**, 359–361.
- Choi, K.H., Chisti, Y. and Moo-Young, M. (1995) Influence of the Gas-Liquid Separator Design on Hydrodynamic and Mass Transfer Performance of Split-Channel Airlift Reactors. *J. Chem. Biotechnol.*, **62**, 327–332.
- Dengis, P.B., Nélissen, L.R. and Rouxhet, P.G. (1995) Mechanisms of Yeast Flocculation: Comparison of Top- and Bottom-Fermenting Strains. *Appl. Environ. Microbiol.*, **61**, 718–728.
- Dillenöhffer, W. and Rönn, D. (1996) Continuous Maturation of Beer. *Beverage World International*, Nov./Dec., 34–36.
- Dömény, Z., Šmogrovicová, D., Gemeiner, P., Šturdík, E., Pátková, J., Malovíková, A. (1998) Continuous Secondary Fermentation using Immobilized Yeast *Biotechnol. Lett.*, **20**, 1041–1045.
- Domingues, L., Dantas, M.M., Lima, N. and Teixeira, J.A. (1999) Continuous Ethanol Fermentation of Lactose by a Recombinant Flocculating *Saccharomyces cerevisiae* Strain. *Biotechnol. Bioeng.*, **64**, 692–697.
- El-Behhari, M., Ekomé, J.N., Coulon, M., Pucci, B. and Bonaly, R. (1998) Comparative Extraction Procedures for a Galactose-specific Lectin Involved in Flocculation of *Kluyveromyces lactis* Strains. *Appl. Microbiol. Biotechnol.*, **49**, 16–23.
- Fontana, A., Ghommida, C., Guiraud, J.P. and Navarro, J.M. (1992) Continuous Alcoholic Fermentation of Sucrose Using Flocculating Yeast. The Limits of Invertase Activity. *Biotechnol. Lett.*, **14**, 505–510.
- Freitas, C., Vicente, A.A., Mota, M. and Teixeira, J.A. (1997) A New Sampling Device for Measuring Solids Hold-Up in a Three-Phase System. *Biotechnol. Tech.*, **11**, 489–492.

- Freitas, C. and Teixeira J.A. (1997) Hydrodynamic Studies in an Airlift Reactor with and Enlarged Degassing Zone. *Bioprocess Eng.*, **18**, 267–279.
- Freitas, C. and Teixeira J.A. (1998a) Solid-Phase Distribution in an Airlift Reactor with an Enlarged Degassing Zone. *Biotechnol. Tech.*, **12**, 219–224.
- Freitas, C., Teixeira, J.A. (1998b) Effect of Liquid-Phase Surface Tension on Hydrodynamics of a Three-Phase Airlift Bioreactor with an Enlarged Degassing Zone. *Bioprocess Eng.*, **19**, 451–457.
- Ganzeveld, K.J., Chisty, Y. and Moo-Young, M. (1995) Hydrodynamic Behaviour of Animal Cell Microcarrier Suspensions in Split-Cylinder Airlift Bioreactors. *Bioprocess Eng.*, **12**, 239–247.
- Glasgow, L.A. (1989) Effects of the Physicochemical Environment on Floc Properties. *Chem. Eng. Prog.*, August, 51–55.
- Gough, S. and McHale, A.P. (1998) Continuous Ethanol Production from Molasses at 45°C using Alginate-Immobilized *Kluyveromyces marxianus* IMB3 in a Continuous-Flow Bioreactor. *Bioprocess Eng.*, **19**, 33–36.
- Greenshields, R.N. and Smith, E.L. (1971) Tower-Fermentation Systems and their Applications. *Chem. Engineer*, May, 182–190.
- Hamdi, M. (1995) Biofilm Thickness Effect on the Diffusion Limitation in the Bioprocess Reaction: Biofloc Critical Diameter Significance. *Bioprocess Eng.*, **12**, 193–197.
- Jianfeng, X., Jian, X., Aiming, H., Pusun, F. and Zhiguo, S. (1998) Kinetic and Technical Studies on Large-Scale Culture of *Rhoiola sachalinensis* Compact Callus Aggregates with Air-Lift Reactors. *J. Chem. Technol. Biotechnol.*, **72**, 227–234.
- Joekes, I., Moran, P.J.S., Rodrigues, J.A.R., Wendhausen, R., Tonella, E. and Cassiola, F. (1998) Characterization of *Saccharomyces cerevisiae* Immobilized onto Chrysotile for Ethanol Production. *J. Chem. Technol. Biotechnol.*, **73**, 54–58.
- Karamanov, D.G., Nagamune, T. and Endo, I. (1992) Hydrodynamic and Mass Transfer Study of a Gas-Liquid-Solid Draft Tube Spouted Bed Bioreactor. *Chem. Eng. Sci.*, **47**, 3581–3588.
- Kennard, M. and Janekeh, M. (1991) Two-and Three-Phase Mixing in a Concentric Tube Gas-Lift Fermentor. *Biotechnol. Bioeng.*, **38**, 1261–1270.
- Kida, K., Kume, K., Morimura, S. and Sonoda, Y. (1992) Repeated-Batch Fermentation Process Using a Thermotolerant Flocculating Yeast Constructed by Protoplast Fusion. *J. Fermentation Bioeng.*, **47**, 169–173.
- Kida, K., Yamadaki, M., Asano, S.-L, Nakata, T. and Sonoda, Y. (1989) The Effect of Aeration on Stability of Continuous Ethanol Fermentation by a Flocculating Yeast. *J. Ferm. Bioeng.*, **68**, 107–111.
- Kobayashi, O., Hayashi, N., Kuroki, R. and Sone, H. (1998) Region of Flo 1 Proteins Responsible for Sugar Recognition. *J. Bacterial.*, **180**, 6503–6510.
- Kochbeck, B., Lindert, M. and Hempel, D.C. (1992) Hydrodynamics and Local Parameters in Three-Phase-Flow in Airlift-loop Reactors of Different Scale. *Chem. Eng. Sci.*, **47**, 3443–3450.
- Komáromy, P. and Sisák, C. (1994) Investigation of Gas-Liquid Oxygen Transport in Three-Phase Bioreactor. *Hungarian J. Ind. Chemistry*, **22**, 147–151.
- Kurillová, L'Ubica, Gemeiner, P., Ilavský, M., Štefuca, V., Polakovic, M., Welwardová, A. and Tóth, D. (1992) Calcium Pectate Gel Beads for Cell Entrapment. *Bioetchnol. Appl. Biochem.*, **16**.
- Kuriyama, H., Ishibashi, H., Miyagawa, H., Kobayashi, H. and Eiichi, M. (1993) Optimization of Two-Stage Continuous Ethanol Fermentation Using Flocculating Yeast. *Biotechnol. Lett.*, **15**, 415–420.
- Libicki, S.B., Salmon, P.M. and Robertson, C.R. (1988) The Effective Diffusive Permeability of a Nonreacting Solute in Microbial Cell Aggregates. *Biotechnol. Bioeng.*, **32**, 68–85.
- Lima, N., Teixeira, J.A. and Mota, M. (1992) Enhancement of Metabolic Rates of Yeast Flocculent Cells Through the Use of Polimeric Additives. *Bioprocess Eng.*, **7**, 343–348.
- Linko, M., Virkajarvi, I., Pohjala, N., Lindborg, K., Kronlöf, J., Pajunen, E. (1997) Main Fermentation with Immobilized Yeast—a Breakthrough?". *EBC Congress 1997*, 385–394.

- Lu, W.-J., Hwang, S.-J. and Chang, C.-M. (1995) Liquid Velocity and Gas Holdup in Three-Phase Internal Loop Airlift Reactors with Low Density Particles. *Chem. Eng. Sci.*, **50**, 1301–1310.
- Lübbert, A., Frölich, S., Larson, B. and Schügerl, K. In: King, R. ed. *Bioreactor Fluid Dynamics*. Cambridge: Elsevier, 1988, 379–393.
- Mafra, I., Cruz, J.M.M. and Teixeira, J.A. (1997) Beer Maturation in a Continuously Operating Bioreactor Using a Flocculation Brewer's Yeast Strain. *EBC Congress 1997*, 509–516.
- Masschelein, C.A. (1997) A Realistic View on the Role of Research in the Brewing Industry Today. *J. Inst. Brew.*, **103**, 103–113.
- Mensour, N.A., Margaritis, A., Briens, C.L., Pilkington, H., Russel, I. (1997) New Developments in the Brewing Industry Using Immobilized Yeast Cell Bioreactor Systems. *J. Inst. Brew.*, **103**, 363–370.
- Merchuk, J.C., Ladwa, N., Cameron, A., Bulmer, M. and Pickett, A. (1994) Concentric-Tube Airlift Reactors: Effects of Geometrical Design on Performance. *AIChE J.*, **40**, 1105–1117.
- Merchuk J.C., Ladwa, N., Cameron, A., Burmer, M., Berzin, I. and Pickett, A.M. (1996) Liquid Flow and Mixing in Concentric Tube Air-Lift Reactors. *J. Chem. Technol. Biotechnol.*, **66**, 174–182.
- Michalski, H.J. (1992) Air-Lift Bioreactors. In: M. Berovic and T. Koloini, eds. *Bioreactor Engineering Course Workshop Notes; Italy, 1992*.
- Miki, B.L.A., Poon, N.H., James, A.P. and Seligy, V.L. (1992) Possible Mechanisms for Flocculation Interaction Governed by Gene FLO 1 in *Saccharomyces cerevisiae*. *J. Bacteriol.*, **150**, 878–889.
- Moradas-Ferreira, P., Fernandes, P.A. and Costa, M.J. (1994) Yeast Flocculation—the Role of Cell Wall Protein. *Colloids Surf. B.*, **2**, 159–164.
- Nguyen, V.T., Shieh, W.K. (1992) Continuous Ethanol Fermentation Using Immobilized Yeast in a Fluidized Bed Reactor. *J. Chem. Tech. Biotechnol.*, **55**, 339–346.
- Onken, U. and Weiland, P. (1983) Airlift Fermenters: Construction, Behavior, and Uses. In: *Advances in Biotechnological Processes 1*. New York: Alan R.Liss, Inc., **1983**, 67–95.
- Omima, M., Omura, T., Umita, T. and Aizawa, J. (1985) Diffusion Coefficient and Its Dependency on Some Biochemical Factors. *Biotechnol. Bioeng.*, **27**, 1533–1539.
- Pereboom, J.H.F., van den Heuvel, J.C., Ottengraf, S.S.P., Huisman, J.W. and de Beer, D. (1990) Physical Transport Phenomena in Aggregated Microbial Systems. In: H.Breteler, R.F.Beuker and K.Ch.A.M.Luyben, eds. *Proceedings 3rd. Netherlands Biotechnology Congress 1990, Part II, Amsterdam 4th April 1990*.
- Pollard, D.J., Ison, A.P., Shamlow, P.A. and Lilly, M.D. (1997) Influence of a Propeller or *Saccharomyces cerevisiae* Fermentations in a Pilot Plant Scale Airlift Bioreactor. *Bioprocess Eng.*, **16**, 273–281.
- Pollard, D.J., Shamlow, P.A., Lilly, M.D. and Ison, A.P. (1996) *Saccharomyces cerevisiae* Fermentations in a Pilot Scale Airlift Bioreactor: Comparison of Air Sparger Configurations. *Bioprocess Eng.*, **15**, 279–288.
- Roca, E., Ghommidh, C., Navarro, J.M. and Lema, J.M. (1995) Hydraulic Model of a Gas-Lift Bioreactor with Flocculating Yeast. *Bioprocess Eng.*, **12**, 269–272.
- Rüffer, H.M., Bröring, S. and Schügerl, K. (1995) Fluiddynamic Characterization of Airlift Tower Loop Bioreactors With and Without Motionless Mixtures. *Bioprocess Eng.*, **12**, 119–130.
- Russel, A.B., Thomas, C.R. and Lilly, M.D. (1994) The Influence of the Vessel Height and Top-Section Size on the Hydrodynamic Characteristics of Airlift Fermentors. *Biotechnol. Bioeng.*, **43**, 69–76.
- Salt, D.E., Bentham, A.C., Hay, S., Idris, A., Gregory, J., Hoare, M. and Dunnill, P. (1996) The Mechanism of Flocculation of a *Saccharomyces cerevisiae* Cell Homogenate using Polyethyleneimine. *Bioprocess Eng.*, **15**, 71–76.
- Schorr-Galindo, S., Ghommidh, C. and Guiraud, J.P. (1995) Inulin Enrichment by Fermentation in a Flocculating Yeast Reactor. *Biotechnol. Lett.*, **17**, 1303–1310.

- Siegel, M.H., Hallaile, M., Herskowitz, M. and Merchuk, J.C. (1988) Hydrodynamics and Mass Transfer in a Three-Phase Airlift Reactor. In: R.King, ed. *2nd International Conference on Bioreactor Fluid Dynamics, 21–23 September 1988*.
- Siegel, M. and Merchuk, J.C. (1991) Hydrodynamics in Rectangular Airlift Reactors: Scale-up and the Influence of Gas-Liquid Separator Design. *Can. J. Chem. Eng.*, **69**, 465–473.
- Siegel, M.H., Merchuk, J.C. and Schügerl, K. (1986) Airlift Reactor Analysis: Interrelationships Between Riser, Downcomer, and Gas-Liquid Separator Behavior, Including Gas Recirculation Effects. *AICHE J.*, **32**, 1585–1596.
- Siegel, M.H. and Robinson, C.W. (1992) Applications of Airlift Gas-Liquid-Solids Reactors in Biotechnology. *Chem. Eng. Sci.*, **47**, 3215–3229.
- Smisák, C., Boross, L. and Szajáni, B. (1990) Stirred Fluidised-Bed Reactor Developed for Low Density Biocatalyst Supports. *Biotechnol. Tech.*, **4**, 15–20.
- Smith, B.C. and Skidmore, D.R. (1990) Mass Transfer Phenomena in an Airlift Reactor: Effects of Solids Loading and Temperature. *Biotechnol. Bioeng.*, **35**, 483–491.
- Smith, E.L. and Greenshields, R.N. (1974) Tower-Fermentation Systems and their Application to Aerobic Processes. *Chem. Engineer*, January, 28–34.
- Šmogrovicová, D., Dömeny, Z., Gemeiner, P., Malovíková, A. and Šturdík, E. (1997) Reactors for Continuous Primary Beer Fermentation using Immobilized Yeast *Biotechnol. Tech.*, **11**, 261–264.
- Scares, E.V., Teixeira, J.A. and Mota, M. (1992) Interaction Between Flocculent and Nonflocculent Cells of *Saccharomyces cerevisiae*. *Can. J. Microbiol.*, **38**, 969–974.
- Scares, E.V., Teixeira, J.A. and Mota, M. (1994) Effect of Cultural and Nutritional Conditions on the Control of Flocculation Expression in *Saccharomyces cerevisiae*. *Can. J. Microbiol.*, **40**, 851–857.
- Sousa, M.J., Teixeira, J.A. and Mota, M. (1993) Must Deacidification with an Induced Flocculant Yeast Strain of *Schizosaccharomyces pombe*. *Appl. Microbiol. Biotechnol.*, **39**, 189–193.
- Sousa, M.L., Mota, M. and Teixeira, J.A. (1994b) Influence of Operational Parameters on the Startup of a Flocculation Airlift Bioreactor. *Col. Surf. B: Biointerfaces*, **2**, 181–188.
- Sousa, M.L. and Teixeira, J.A. (1991) Reduction of Diffusional Limitations in Yeast Flocs. *Biotechnol. Lett.*, **13**, 883–888.
- Sousa, M.L. and Teixeira, J.A. (1996) Characterization of Oxygen Uptake and Mass Transfer in Flocculent Yeast Cell Cultures with or without a Flocculation Additive. *Biotechnol. Lett.*, **18**, 229–234.
- Sousa, M.L., Teixeira, J.A. and Mota, M. (1994a) Comparative Analysis of Ethanolic Fermentation in Two Continuous Flocculation Bioreactors and Effect of Flocculation Additive. *Bioprocess Eng.*, **11**, 83–90.
- Stratford, M. (1992) Lectin-mediated aggregation of yeast flocculation. *Biotechnol. Genet. Eng. Rev.*, **10**, 283–341.
- Stratford, M. (1996) Induction of Flocculation in Brewing Yeasts by Change in pH Value. *FEMS Microbiol. Lett.*, **136**, 13–18.
- Straver, M.J., van der Aar, P., Smit, G. and Kijne, J. (1993) Determinants of Flocculence of Brewers Yeast during Fermentation in Wort. *Yeast*, **9**, 527–532.
- Tanaka, H., Matsumura, M. and Veliky, L.A. (1984) Diffusion Characteristics in Ca-Alginate Gel Beads. *Biotechnol. Bioeng.*, **26**, 53–58.
- Tata, M., Bower, P., Bromberg, S., Duncombe, D., Fehring, J., Lau, V., Ryder, D., Stassi, P. (1999) Immobilized Yeast Bioreactor Systems for Continuous Beer Fermentation. *Biotechnol. Prog.*, **15**, 105–113.
- Taylor, N.W. and Orton, W.L. (1975) Calcium in Flocculence of *Saccharomyces cerevisiae*. *J. Inst. Brew.*, **81**, 53–57.
- Teixeira, J.A. (1988) Ph.D. Thesis: *Flocação da levedura Kluyveromyces marxianus*. Porto: Faculdade de Engenharia da Universidade do Porto.

- Teixeira, J.A. and Mota, M. (1990) Experimental Assessment of Internal Diffusion Limitations in Yeast Flocs. *Chem. Eng. J.*, **43**, B13-B17.
- Teixeira, J.A. and Mota, M. (1992) Flocculation Bioreactors. In: T.G.Villa and J.Abalde, eds. Profiles on Biotechnology. Spain: Servicio de Publicaciones, Universidade de Santiago, 1992, 413–428.
- Teixeira, J.A., Mota, M. and Goma, G. (1990) Continuous Ethanol Production by Flocculating Strain of *Kluyveromyces marxianus*: Bioreactor Performance. *Bioprocess Eng.*, **5**, 123–127.
- Teixeira, J.A., Oliveira, R., Azeredo, J., Sousa, M. and Sil, C. (1995) Cell Wall Surface Properties and Flocculence of a *Kluyveromyces marxianus* Strain . *Colloids Surfaces B: Biointerfaces*, **5**, 197–203.
- Tyagi, R.D., Gupta, S.K., Chand, S. (1992) Process Engineering Studies on Continuous Ethanol Production by Immobilized *S. cerevisiae*. *Proc. Biochem.*, **27**, 23–32.
- Van der Aar, P. (1996) Consequences of Yeast Population Dynamics with Regard to Flocculence. *Ferment.*, **9**, 39–42.
- van Hamersveld, E.H., van der Lans, R.G.J.M. and Luyben, K.C.A.M. (1997) Quantification of Brewers' Yeast Flocculation in a Stirred Tank: Effect of Physical Parameters on Flocculation. *Biotechnol. Bioeng.*, **56**, 190–200.
- Verlaan, P. and Tramper, J. (1987) Hydrodynamics, Axial Dispersion and Gas-Liquid Oxigen Transfer in an Airlift Loop Bioreactor with Three Phase Flow. In: *International Conference on Bioreactors and Biotransformations, Gleneagles, Scotland 9–12 November 1987*. 363–373.
- Vicente, A.A., Dluhy, M., Ferreira, E.C., Mota, M. and Teixeira, J.A. (1998) Mass Transfer Properties of Glucose and O<sub>2</sub> in *Saccharomyces cerevisiae* Flocs. *Biochemical Eng. J.*, **2**, 35–43.
- Vicente, A.A., Dluhy, M., Ferreira, E.C. and Teixeira, J.A. (1998) Modelling Diffusion-Reaction Phenomena in Yeast Flocs of *Saccharomyces cerevisiae* . *Bioprocess Eng.*, **18**, 335–342.
- Vicente, A.A., Dluhy, M. and Teixeira, J.A. (1997) A New Technique for Measuring Kinetic and Mass Transfer Parameters in Flocs of *Saccharomyces cerevisiae*. *Biotechnol Tech.*, **11**, 113–116.
- Vicente, A.A., Dluhy, M. and Teixeira, J.A. (1999) Increase of Ethanol Productivity in an Airlift Reactor with a Modified Draught Tube. *Can. J. Chem. Eng.*, **77**, 497–502.
- Vicente, A., Meinders, J.M. and Teixeira, J.A. (1996) Sizing and Counting of *Saccharomyces cerevisiae* Floc Populations by Image Analysis, Using an Automatically Calculated Threshold. *Biotechnol. Bioeng.*, **51**, 673–678.
- Vicente, A.A. and Teixeira, J.A. (1995) Hydrodynamic Performance of a Three-Phase Airlift Bioreactor with an Enlarged Degassing Zone. *Bioprocess Eng.*, **14**, 17–22.
- Webster, I.A. (1981) Criteria for the Prediction of Diffusional Control within Whole Cells and Cell Flocs. *J. Chem. Tech. Biotechnol.*, **31**, 178–182.
- Weir, S., Ramsden, D.K., Hughes, J. and Le Thomas, F. (1994) The Strength of Yeast Flocs Produced by the Cationic Flocculant Chitosan: Effect of Suspension Medium and of Pretreatment with Anionic Poly electrolytes . *Biotechnol. Tech.*, **8**, 129–132.
- Wieczorek, A. and Michalski, H. (1994) Continuous Ethanol Production by Flocculating Yeast in the Fluidized Bed Bioreactor. *FEMS Microbiol. Reviews*, **14**, 69–74.
- Yang, Y.L., Choi, C.Y. (1998) Induction of Flocculation of *Saccharomyces cerevisiae* by a pH-Upshift. *Biotechnol. Tech.*, **12**, 591–593.



# CHAPTER FOURTEEN

## BIOREACTOR DESIGN FOR PLANT CELL SUSPENSION CULTURES

PATRICIA M.KIERAN

*Department of Chemical Engineering, University College Dublin,  
Belfield, Dublin 4, Ireland*

### ABSTRACT

Plants are the natural source of a vast array of phytochemicals which are used as drugs, pesticides, flavourings and fragrances. In many cases, plant cell suspension culture is a viable production alternative to traditional cultivation methods or chemical synthesis. The use of suspension cultures for biotransformations and for the production of heterologous proteins has also been demonstrated. However, despite the obvious potential of these systems, fewer than a dozen products have been produced at commercial scale via the cell suspension route. Limited exploitation of the technology is largely attributable to economic factors, associated with both biological and engineering considerations. This chapter focuses on engineering aspects of bioreactor design for plant cell suspension cultures. Adaptation of bioreactor technology originally developed for microbial systems has obviously proven successful for the commercial processes now in existence. However, a fuller understanding of the distinguishing physical and physiological characteristics of plant cell suspension cultures is essential for the development of a broad-based and coherent strategy for scale-up. System morphology, rheology and shear sensitivity are identified as key factors for process design and optimisation. Existing and emerging trends in cultivation practice are reviewed.

**Keywords:** plant cells, bioreactor, shear sensitivity, scale-up, morphology, rheology

### INTRODUCTION

Plant cell culture technology facilitates the production of valuable plant material and phytochemicals under controlled and reproducible conditions; operation is independent of the geographical and climatic constraints of conventional crop cultivation. Plant cell cultures have traditionally been valued as a source of naturally occurring primary and secondary metabolites, for use in medicinal, food and cosmetic products (Sahai, 1994). They have been employed for biotransformations (Yokoyama, 1996) and it has been established that they can be used for the production of heterologous proteins (Franken *et*

al., 1997). Table 14.1 summarises current commercial/near commercial processes involving plant cell suspensions.

From an engineering perspective, the successful application of plant cell suspensions requires large-scale processing technology which supports high-density cultivation of high-yielding, stable cell lines. The processes identified in Table 14.1, coupled with additional, non-commercial, large-scale (>500 L) applications in Table 14.2, clearly illustrate the feasibility of this approach. However, given the diversity of phytochemicals, the range of cell lines and products involved is extremely limited. Cost factors clearly account for the modest exploitation of this inherently capital intensive technology. Economic analyses indicate the commercial viability of cell culture for the production of speciality chemicals (Verpoorte *et al.*, 1991; Sahai, 1994) and, assuming significant advances in system productivity and processing technology, of food and food ingredients (Goldstein, 1999). However, the absence of a consistent, broad-based approach to process design and scale-up indicates that there are still engineering challenges to be met.

This chapter takes a practical approach to engineering aspects of bioreactor design for plant cell cultures. The reader is also referred to other, comprehensive studies of this topic (Payne *et al.*, 1991; Doran, 1993; Singh and Curtis, 1994a). Only suspension cultures are considered here; tissue cultures, organ cultures and immobilised systems are covered elsewhere (*e.g.* Payne *et al.*, 1991; Doran, 1997; Singh and Curtis, 1994b). Where possible, reference is made to large-scale applications, although details of such processes are still generally proprietary.

## CHARACTERISATION OF PLANT CELLS AS BIOCATALYSTS

Many of the operational difficulties encountered with the scale-up of plant cell suspensions stem from the physical and physiological characteristics which distinguish plant cells from the microbial systems for which submerged cultivation technology was originally developed. As is apparent from Table 14.3, the most significant differences between plant cells in suspension cultures and microbial cells are in terms of cell size, shear sensitivity and growth rate. These three factors, coupled with broth rheology, which is significantly influenced by cell size and shape, impact directly on the engineering and commercial feasibility of cultivation in large-scale bioreactors. However, broad characterisation of plant cell suspension cultures is complicated by considerable variations between the performance of different cell lines and even, of the same cell line, under different cultivation conditions. Indeed, variability is a very important issue for the commercial application of cell suspension technology and has been identified as the most problematic factor for the use of *Taxus* cell cultures for paclitaxel production (Ketchum *et al.*, 1999).

### Morphology

In suspension culture, single plant cells are typically of the order of 10–100 µm in size, varying in shape from broadly spherical to cylindrical. Figure 14.1 shows micrographs of

**Table 14.1** Commerical/near-commercial processes involving plant cell suspension cultures

Product (system)	Application	Company	Scale/Configuration	Operating details	Reference
Berberine ( <i>Coptis japonica</i> )	medicinal	Mitsui Chemicals Inc., Japan	6000 L STR	fed-batch perfusion 2-stage continuous (not in production)	Fujita (1988b) Matsubara & Fujita (1991) Takahashi (1999)
Ginseng ( <i>Panax ginseng</i> )	health food additive	Nitto Denko Corporation, Japan	20 000 L, 25 000 L STR	pitched- blade disk turbine batch	Hibino (1999) Hibino & Ushiyama (1999)
Paclitaxel— Genexol® ( <i>Taxus</i> spp.)	medicinal	Samyang Genex Corporation, Korea	32 000 L STR		Kang (1999)
Paclitaxel— Taxol® ( <i>Taxus</i> spp.)	medicinal	Phyton Inc, USA/Germany	75 000 L STR		Venkat (1996)
Paclitaxel ( <i>Taxus</i> spp.)	medicinal	Mitsui Chemical Inc., Japan	200 L STR		Takahashi (1999)
Plant polysaccharides	food/pharmaceutical/ cosmetic additive	Cooperative Research Centre for Industrial Plant Biopolymers (CRCIPB), Australia	10 000 L STR 1000 L ALR	axial flow impeller semi- continuous mode	CRCIPB (1998) Doran (2000)
Plant polysaccharides ( <i>Polianthes tuberosa</i> )	cosmetics	Kao Corporation, Japan	4000 L, 10 000 L STR with draft tube	fed-batch or continuous mode	Takei <i>et al.</i> (1995) Otsuji (1999)
Shikonin ( <i>Lithospermum erythrorhizon</i> )	cosmetics	Mitsui Chemicals Inc., Japan	200 L, 750 L STR	two-stage batch	Fujita (1988a) Takahashi & Fujita (1991)

**Table 14.2** Other examples of (non-commercial) large-scale (>500 L) systems

System	Company	Scale/Operating Details	Reference
<i>Aralia cordata</i>	PCC Technology Inc., Japan	500 L STR N: 30 rpm semi-continuous	Kobayashi <i>et al.</i> (1993)
<i>Catharanthus roseus</i>	Metabogal, Israel	3000 L STR semi-continuous	Shaaltiel (1999)
<i>Catharanthus roseus</i>	GBF, Germany	5000 L STR D: 0.5 m; N: 30 rpm 3 Rushton turbines batch	Schiel & Berlin (1987)
<i>Echinacea purpurea</i>	Diversa, Germany	75, 750, 7500, 15 000, 75 000 L	Ritterhaus <i>et al.</i> (1990)
<i>Panax ginseng</i>		2-stage Intermig impellers; batch/semi-continuous mode	
<i>Rauwolfia serpentina</i>			
<i>Lithospermum erythrorhizon</i>	Mitsui Chemicals Inc., Japan	1000 L RDR	Takahashi & Fujita (1991)
<i>Nicotiana tabacum</i>	Japan Tobacco Inc., Japan	20 000 L STR (see Table 4) batch, continuous	Hashimoto & Azechi (1988)
		1500 L ALR	Kato <i>et al.</i> (1976)
<i>Panax ginseng</i>	Omutinsk Chemical Plant, Russia	630 L STR D: 0.9 m; N: 50 rpm	Shamakov <i>et al.</i> (1991)
<i>Taxus</i> spp.	ESCAgenetics Corporation, USA	2500 L STR	Smith (1995)

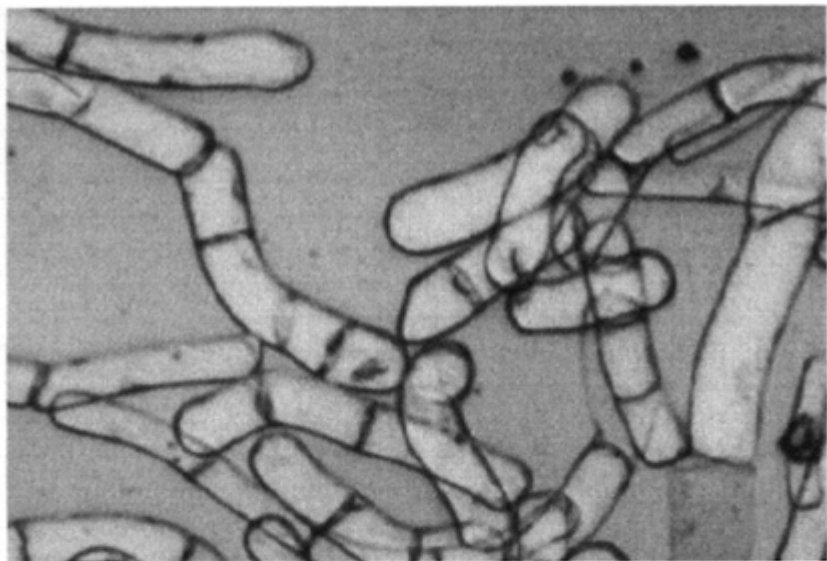
**Table 14.3** Comparison of biocatalyst properties

Biocatalyst	Shape	Size (μm)	Cell wall	Aggregates	Doubling time (h)	Shear tolerance	OUR (mmol L <sup>-1</sup> h <sup>-1</sup> )
Plant Cells	Spherical-Cylindrical	1:100–500 d: 20–50	Yes	Yes	20–100	low-moderate	10 <sup>1</sup>
Animal Cells	Spherical	d: 10–20	No	No	20	low	10 <sup>-1</sup>
Bacteria	Spherical Cylindrical Spiral	d: <1 1: <5	Yes	Yes/No	0.5–10	high	10 <sup>3</sup>
Yeasts	Spherical	d: 5–10	Yes	Yes/No	10	high	10 <sup>2</sup>
Moulds	Mycelial	d: 5–10	Yes	Yes/No	10–20	moderate-	10 <sup>2</sup>

1: <100

high

(a)



(b)

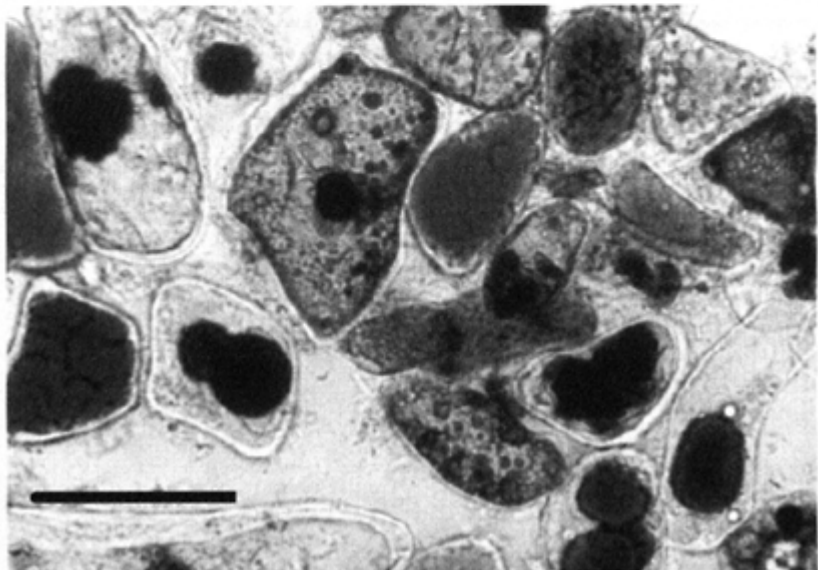


**Figure 14.1** Micrographs of (a) *M. citrifolia* and (b) *D. capensis* cells in

suspension culture, cultivated in shake flasks (Bar represents 50  $\mu\text{m}$ ).

(a) *Morinda citrifolia* and (b) *Drosera capensis* cells, cultivated in 250 mL shake flasks. *M. citrifolia* cells are characteristically cylindrical in shape and exist in the form of unbranched chains of between 2 and 15 cells. *D. capensis* grows in the form of aggregates which continuously slough off smaller aggregates and single cells into the suspending medium. Each plant cell is surrounded by a cell wall which defines cell size and shape and which plays a dynamic role in cellular expansion and osmo-regulation. Unlike microbial cells, a significant portion of the cellular volume is occupied by a vacuole, into which secondary metabolites are frequently sequestered and which is generally observed to increase in size during batch cultivation. With a view to ensuring system homogeneity and minimising mass transfer limitations, suspensions of single cells appear most desirable. However, aggregates, consisting of between 2 and many hundreds of cells, are most common. The predominance of aggregates is often associated with the presence of extracellular polysaccharides (ECPs), which may retard cell-cell separation after division. Cell and aggregate morphology vary with cell line, growth stage and cultivation conditions. For example, Curtis and Emery (1993) reported a switch between elongated and spherical cells in suspensions of *Nicotiana tabacum* cultivated under batch and semi-continuous conditions, respectively. Aggregation patterns are also known to be strongly influenced by hydrodynamic environment; transfer from shake flask to stirred tank reactor (STR) has been reported to both increase (e.g. Wagner and Vogelmann, 1977) and reduce (Takeda *et al.*, 1994) average aggregate size. In laboratory-scale bioreactors, sampling ports/devices designed for microbial broths are frequently unsuitable for aggregated plant suspensions and wider bores should be employed.

Cell-cell contact is generally regarded as advantageous for secondary metabolism and aggregate size-related variations in metabolite productivity have been attributed to a number of factors. Some degree of cellular organisation or differentiation is thought to be beneficial and is reflected in the heightened productivity reported for many tissue and organ cultures. Enhanced secondary metabolite production has been observed in compact aggregates of self-immobilised cells of *Solanum aviculare* (Tsoulpha and Doran, 1991) and *Rhodolia sachalinensis* (Xu *et al.*, 1998). The Nitto Denko ginseng process employs a highly aggregated *Panax ginseng* suspension (Hibino and Ushiyama, 1999) with aggregate equivalent diameters of up to 2 cm (Hibino, 1999). In this case, productivity is extremely sensitive to aggregate disruption and agitation rate has been identified as the most significant factor for secondary metabolite production. Diffusional limitations may prevail in larger aggregates and Hulst *et al.* (1989) estimated a critical diameter of approximately 3 mm for oxygen limitation, at a bulk oxygen concentration of 0.25 mmol L<sup>-1</sup>. At lower broth DO levels, the critical aggregate diameter will be reduced. However, even for aggregates of this size, or smaller, nutrient availability can be significantly influenced by the prevailing flow patterns: Singh and Curtis (1994a) observed hollow aggregates in an air-lift reactor (ALR), while solid aggregates of a comparable size were formed in the more turbulent flow field of a STR. Variations in light intensity may also occur throughout aggregates (Madhusudhan and Ravishankar, 1996), which will impact on photoautotrophic cultures and on systems in which metabolite production (e.g. anthocyanins) is stimulated or enhanced by light.

Many studies have focused on the identification of optimal aggregate size distributions for metabolite production (e.g. Hulst *et al.*, 1989; Hanagata *et al.*, 1993). However, Keßler *et al.* (1999) recently demonstrated that, on the basis of active biomass alone (*i.e.* excluding stored carbohydrates), specific ajmalicine production in suspensions of *Catharanthus roseus* was independent of aggregate size, for aggregate diameters of less than 250 µm. What is required for effective optimisation of any given cell line is the identification and maintenance of conditions supporting optimal productivity.

### Broth Rheology

By comparison with non-filamentous microbial systems, plant cell suspensions are commonly perceived as highly viscous fluids. However, it is important to note that plant systems are typically operated at significantly higher biomass levels than microbial suspensions. Curtis and Emery (1993) found that the apparent viscosities of plant cell suspensions were similar to those of yeast suspensions (Reuß *et al.*, 1979), at cell volume fractions of up to 0.3. Although rheological properties are strongly line-dependent and may also vary with cultivation conditions, data collected for a variety of suspensions give a good picture of typical trends. Relevant studies are summarised by Kieran *et al.* (1997). Analysis of the available data indicates that many suspensions exhibit non-Newtonian, shear-thinning characteristics. At higher biomass concentrations, some suspensions show evidence of a yield stress (e.g. Wagner and Vogelmann, 1977; Zhong *et al.*, 1992b). Thixotropic behaviour has been occasionally observed in some cell lines (e.g. Wagner and Vogelmann, 1977), but the data are extremely limited.

Broth rheology is strongly dependent on biomass concentration. For *Cudrania tricuspidata*, *C. roseus* and *N. tabacum* suspensions, Tanaka (1982) observed that broth apparent viscosity varied with biomass concentration (DW) raised to the power of 6.5. More recently, Curtis and Emery (1993) correlated broth viscosity with biomass (FW) concentration, expressed in terms of cell volume fraction. Because viscosity depends on the fractional volume of solid material present in the suspension, correlation with cell dry weight is less appropriate during the later stages of a batch growth cycle (Zhong *et al.*, 1992b) when, due to cellular expansion, fresh and dry weight profiles diverge.

In addition to biomass effects, increased broth viscosity is often attributed to the presence of ECPs in the suspending fluid. In cases where the ECP is the product of interest, high polysaccharide concentrations can significantly increase broth viscosity and, in turn, reduce mass transfer coefficients. Takei *et al.* (1995) reported mass transfer limitation in suspensions of *Polianthes tuberosa*, which are employed by Kao for ECP production. The viscosity of a 4 g L<sup>-1</sup> aqueous ECP solution was 550 cP. Mineral salt supplements reduced solution viscosity and the consequent increase in mass transfer rates facilitated enhanced ECP production, to a level of 6.5 g L<sup>-1</sup>; using a fed-batch system, the current ECP productivity is in excess of 20 g L<sup>-1</sup> month<sup>-1</sup> (Otsuji, 1999).

In general, however, only negligible or modest changes in filtrate viscosity have been recorded over the course of the growth cycle for many cell lines. Early studies of *N. tabacum* (Kato *et al.*, 1978) revealed pseudoplastic behaviour, with the broth apparent viscosity increasing by a factor of 27, while that of the cell-free broth varied only between 0.9 cP and 2.2 cP. Figure 14.2 shows broadly similar trends for suspensions of (a) *M. citrifolia* (Cusack and Kieran, 1998) and (b) *Papaver somniferum* (Curtis and

Emery, 1993). For comparison purposes, apparent viscosity values for the non-Newtonian *M. citrifolia* broth have been calculated at a nominal shear rate of  $150\text{ s}^{-1}$ , the broth filtrate exhibits Newtonian characteristics. Increases in the filtrate viscosity correlate well with ECP

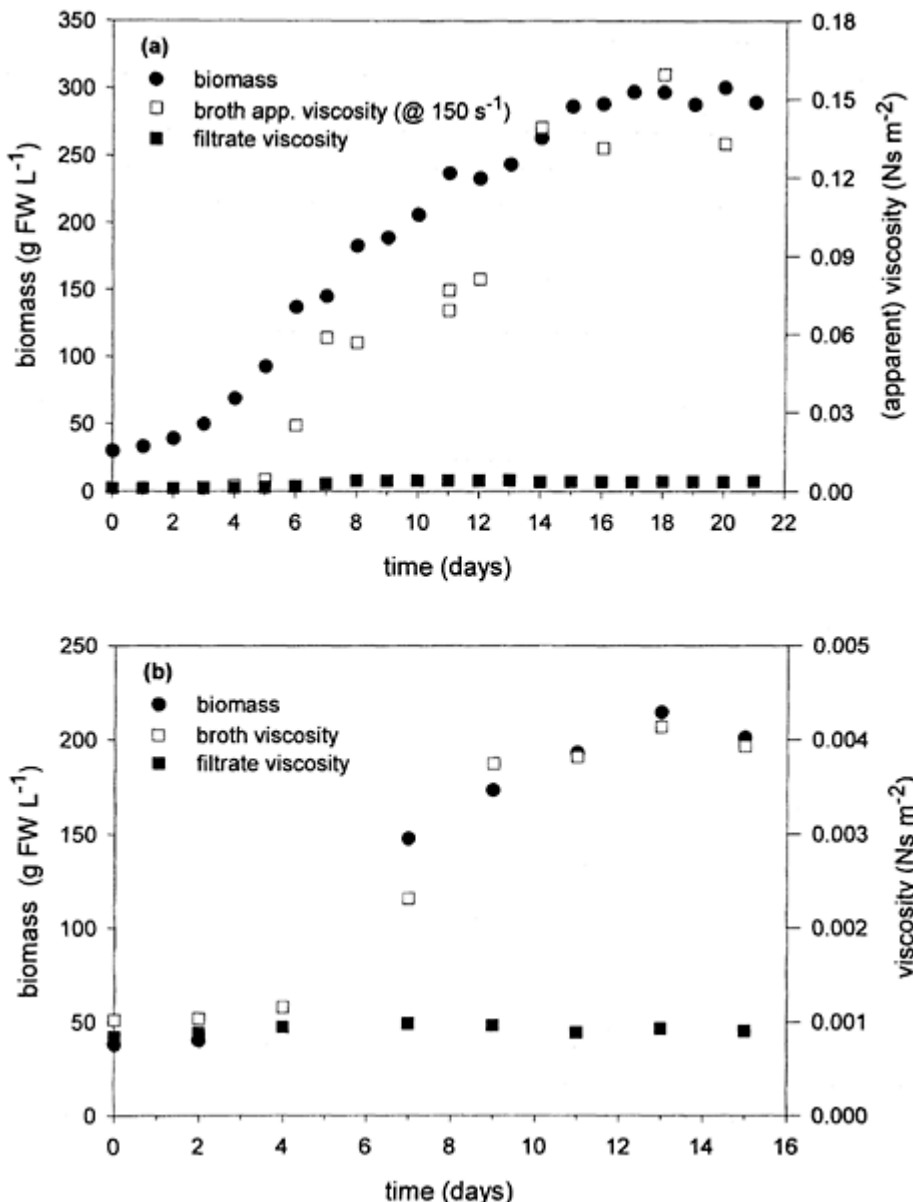


**Figure 14.2** Rheological profiles for batch cultures of (a) *M. citrifolia* (Cusack and Kieran, 1998) and (b) *P. somniferum* (Curtis and Emery, 1993) suspension cultures. (Figure 2(b) reproduced with permission. © 1993, Wiley-Liss, Inc., a subsidiary of John Wiley & Sons, Inc.)

concentration (data not shown), but are negligible compared to the corresponding increases in the whole broth viscosity. The poppy suspension filtrates display Newtonian behaviour at all stages. At a biomass level of 200 g FW L<sup>-1</sup>, the data in Figures 14.2(a) and (b) indicate approximately a 25-fold variation in the broth apparent viscosity between the *M. citrifolia* and poppy suspensions, which is most easily explained by the morphological differences between the two cultures. The influence of cell morphology and aggregation patterns on broth rheology has long been recognised (Wagner and Vogelmann, 1977; Tanaka, 1982). The *M. citrifolia* (Figure 14.1) cells are elongated and occur in unbranched, multi-cellular chains, while poppy cells are broadly spherical in shape. Curtis and Emery (1993) recorded low, Newtonian viscosities for a range of cell lines, all with roughly spherical cells. In *N. tabacum* batch cultures, cell elongation corresponded to increased viscosity and power law behaviour, while semi-continuous cultivation of the same cell line yielded spherical cells and low viscosity broths.

Cultivation conditions, as defined by reactor configuration and mode of operation may also influence rheology. Rodriguez-Monroy and Galindo (1999) observed Theological differences between *Beta vulgaris* suspensions cultivated in shake flasks and those from a 2 L STR. The higher viscosity of the bioreactor-cultivated suspensions was associated with a stress-induced increase in the level of extra-cellular compounds, possibly polysaccharides. There was no significant variation in cell/aggregate morphology.

The available data identify biomass level, cell line and morphological characteristics as determining factors for broth rheology. At the biomass levels necessary for commercially viable production, heightened viscosity can be expected in high ECP-yielding lines and, in particular, in suspensions of elongated cells. However, the data also highlight the potential for reducing broth viscosity by manipulating cell morphology.

### Fresh Weight/Dry Weight Ratio

In suspension culture, the ratio of fresh weight (FW) to dry cell weight (DW) varies significantly over the course of a batch cycle. A typical profile for *M. citrifolia* is presented in Figure 14.3. Broadly similar trends have been reported for a wide range of other cell lines (*e.g.* Park and Kim, 1993; Singh and Curtis, 1994a). However, absolute values of the FW/DW ratio are both line-specific and dependent on cultivation conditions. Curtis and Emery (1993) quoted values of between 7 and 25 for a range of late log/early stationary phase cell suspensions. These values reflect higher cellular water content and larger cell sizes than in bacterial systems. Some variation in cell size is associated with cell growth and division and is apparent during the early stages of the

batch cycle (Kieran *et al.*, 1993). However, the osmotic potential of the medium, which is predominantly determined by salt and sugar levels, has been identified as the most influential factor (*e.g.* Park and Kim, 1993; Zhang *et al.*, 1997). As the sugar supply in the medium is depleted, the osmotic pressure is reduced, and the cells expand, resulting in high FW/DW ratios towards the end of the growth cycle. For high-density perfusion cultures of *Anchusa officinalis* (Su *et al.*, 1993), reductions in average cell size were clearly associated with increased medium osmolarity.

Manipulation of the cell size via osmotic pressure regulation has been investigated as a strategy for reducing broth viscosity in cell suspensions of *Panax notoginseng* (Zhang *et al.*, 1997). In a 200 g FW L<sup>-1</sup> suspension subjected to a glucose shock (0.15 M glucose), aggregate shrinkage resulted in a reduction in broth apparent viscosity from 80 cP to 10 cP.

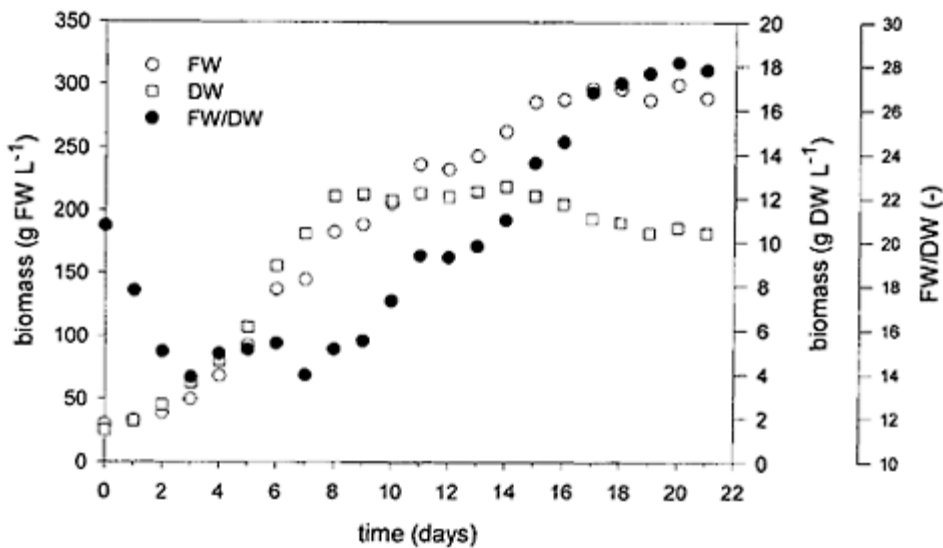


**Figure 14.3** Fresh weight (FW), dry weight (DW) and FW/DW profiles for *M. citrifolia* shake flask suspension cultures (Cusack, 1998).

This approach offers the possibility of increasing the sustainable biomass levels in a bioreactor. While some data are available to suggest that cells may be effectively adapted to high salt concentrations (Binzel *et al.*, 1985), studies must be performed to determine the effects of elevated osmotic potential on cell growth and secondary metabolism.

### Oxygen Requirements

By comparison with microbial systems, the oxygen requirements of plant cells are modest. Specific oxygen consumption rates ( $g_o$ ) depend on cell line, cultivation

conditions and growth phase, but are generally of the order of  $10^{-6}$  g O<sub>2</sub> (g DW)<sup>-1</sup> s<sup>-1</sup>. Maximum values typically occur early in the exponential growth phase (e.g. Dubuis *et al.*, 1995). In operational terms, it is the oxygen uptake rate (OUR), the product of  $q_o$  and biomass concentration,  $X$ , which is most relevant. Maximum OUR typically coincides with maximum (viable) biomass level, at the onset of the stationary growth phase. Reported data (e.g. Bond *et al.*, 1988; Ho *et al.*, 1995) typically refer to small scale systems, with relatively low biomass concentrations ( $\leq 12$  g DW L<sup>-1</sup>). However, assuming an upper  $q_o$  limit of about 0.6 mmol O<sub>2</sub> (g DW)<sup>-1</sup> h<sup>-1</sup>, an OUR of up to 12 mmol L<sup>-1</sup> h<sup>-1</sup> can be expected at a biomass level of 20 g DW L<sup>-1</sup>.

In strongly aerobic cultures, the rate of metabolic heat evolution ( $Q_{\text{met}}$ ) is directly proportional to the oxygen consumption rate (Cooney *et al.*, 1969), *viz.*

$$Q_{\text{met}} = (460 \text{ J mmol O}_2^{-1}) q_o X V \quad (1)$$

where  $V$  is the broth volume. Accordingly, lower oxygen consumption rates in plant systems result in correspondingly lower metabolic heat loads than in microbial systems. Metabolic heat generation rates of approximately 138 J (g DW)<sup>-1</sup> h<sup>-1</sup> were reported by Hashimoto and Azechi (1988) in a 20 m<sup>3</sup> *N. tabacum* chemostat culture (6.34 m<sup>3</sup> wv). At an average biomass level of 17 g L<sup>-1</sup>, this corresponds to a modest metabolic heat load of 652 W m<sup>-3</sup>. No data are available for overall heat transfer coefficients in aerated, agitated plant cell systems. However, Koloini (1990) reports values of between 100 and 200 W m<sup>-2</sup> K<sup>-1</sup> for viscous (xanthan) fermentation broths. Assuming similar values for a well-designed, jacketed plant bioreactor, metabolic heat removal should not constitute an operational difficulty, even allowing for less intense agitation conditions and the reduced driving force associated with a typical cultivation temperature of 25°C.

Critical dissolved oxygen (DO) concentrations ( $c_{\text{crit}}$ ) are generally assumed to be in the range 15–20% of air saturation. Values of 16% (Tate and Payne, 1991) and 25% (Dubuis *et al.*, 1995) have been reported for *C. roseus* and *Coffea arabica*, respectively. However, the  $c_{\text{crit}}$  value for metabolite synthesis may be substantially higher than that for biomass production. Recent studies of *C. roseus* (Schlatmann *et al.*, 1994b, 1995) indicate a critical DO value of 43% for ajmalicine production, although suspensions cultivated at high (85%) and low (18%) DO levels exhibited no significant differences in primary metabolism. Moreover, under oxygen limited conditions, biomass yields (g DW per g C-source) have been shown to be approximately constant (Tate and Payne, 1991) or to fall only slightly (Pareilleux and Vinas, 1983).

Expressed in terms of saturation-type (Monod) kinetics, the apparent oxygen saturation constant,  $K_{m,\text{app}}$  (Payne *et al.*, 1991) has been reported as 0.009 mmol L<sup>-1</sup> for *C. roseus* (Pareilleux and Vinas, 1983) and 0.078 mmol L<sup>-1</sup> for *C. arabica* (Dubuis *et al.*, 1995) suspensions with a mean aggregate diameter of 2 mm. Values are line-dependent and are also affected by system morphology and mass transfer characteristics. An oxygen maintenance coefficient of 6.26 mmol O<sub>2</sub> (C-mol biomass)<sup>-1</sup> h<sup>-1</sup> was determined for *N. tabacum* suspensions (van Gulik *et al.*, 1992). Assuming a molecular weight of approximately 30.7 (C-mol basis) for batch-cultured *N. tabacum* cells, this corresponds to a value of 0.204 mmol O<sub>2</sub> (g DW)<sup>-1</sup> h<sup>-1</sup>. However, on the basis of viable biomass alone, Ho *et al.* (1995) reported values of between 0.115 and 0.358 mmol O<sub>2</sub> (g DW)<sup>-1</sup> h<sup>-1</sup> for *N. tabacum*, accounting for 52% and 87% of respiration, respectively. The higher value was

recorded under high shear conditions, suggesting increased cellular maintenance requirements in cells under hydrodynamic stress.

### Shear Sensitivity

Reductions in plant system productivity on scale-up from shake flasks have been commonly attributed to the hydrodynamic stresses associated with aeration and agitation in bioreactors. Many of the shear sensitivity studies performed on plant cell suspensions have been highly specific, both in terms of cell line and operating conditions. However, they clearly reveal that susceptibility to shearing is not only line-dependent (e.g. Meijer, 1989) but is also strongly influenced by culture age, history and maintenance conditions. There is evidence that cultures may become adapted to high shear conditions (e.g. Allan *et al.*, 1988), possibly through regulation of cell wall synthesis (Tanaka *et al.*, 1988) or by preferential disruption of aggregates in a size-based sub-population which is more susceptible to damage. Reviews of shear sensitivity in plant cell suspensions are presented by Meijer *et al.* (1993) and Kieran *et al.* (2000). Early work focused on the identification of conditions leading to loss of viability. More recent studies have concentrated on sub-lethal metabolic responses (e.g. Takeda *et al.*, 1994, 1998), which may ultimately govern system productivity (Prokop and Bajpai, 1992; Namdev and Dunlop, 1995). Steward *et al.* (1999a,b) describe a method, based on esterase activity, for monitoring growth and lysis kinetics, as well as viability, in suspensions of *Medicago saliva* L., which might be usefully extended to other cell lines.

Shear sensitivity studies of plant cell suspension cultures can be broadly categorised in terms of the prevailing hydrodynamic environment, namely either well- or comparatively poorly-defined. In the first case, cells are exposed to well-characterised and reproducible flow conditions, in Couette-type, capillary or submerged-jet devices. Exposure may be continuous (Couette-type) or intermittent (capillary, submerged jet). Shear stresses, shear rates and, in turn, energy dissipation rates, may be many orders of magnitude higher than those prevailing under normal cultivation conditions (e.g. Kieran *et al.*, 1995; MacLoughlin *et al.*, 1998). As these devices are generally not designed for sterile operation, exposure times are usually short and thus do not allow for system analysis under growth conditions. Exceptions include the cultivation of *Pirus malus* suspensions in a 2 L sparged, concentric cylinder bioreactor (Soule *et al.*, 1987) and *Taxas cuspidata* suspensions grown in a 110 mL (wv) horizontal, rotating wall vessel with bubble-free aeration (Sun and Linden, 1999). In the short-term studies, suspension viability is most commonly used as a response indicator, which, in the context of bioreactor design, masks more subtle, non-lytic effects.

Shear studies under less well-defined conditions, in bioreactors designed for extended sterile operation, arguably offer more immediately applicable data on system scale-up prospects. Manipulation of the hydrodynamic environment is achieved via the rate or method of agitation and/or aeration. A strategy developed by Smith *et al.* (1990) for controlling dissolved oxygen and carbon dioxide concentrations, independently of total gas flow rate and agitation speed, allows for de-coupling of mechanical agitation and gassing effects. However, characterisation of the flow field in a multi-phase, bioreactor is a complex problem (Nienow, 1998). In the context of the shear sensitivity of plant cells, a number of approaches have been adopted. For STRs, the simplest analyses are based on

impeller agitation rate, and include rotational speed ( $N$ ) and impeller tip speed ( $\pi ND$ ). Kobayashi *et al.* (1993) successfully used an impeller speed of 30 rpm in a train of 3 vessels, ranging in volume from 10 L to 500 L, for the cultivation of *Aralia cordata* suspensions. Assuming geometric similarity between all three vessels, this corresponds to almost a 4-fold increase in tip speed, moving from the smallest to the largest vessel. Scragg *et al.* (1988) found cultures of *C. roseus* and *Helianthus annus* to be largely resistant to tip speeds of up to  $3.8 \text{ m s}^{-1}$ , for exposure times of up to 5 hours in a 3 L STR, with negligible loss of viability on subsequent regrowth. However, suspensions of *Cinchona robusta* and *Tabernaemontana divaricata* were growth-impaired at tip speeds in excess of  $0.6 \text{ m s}^{-1}$ , in a similar bioreactor (Meijer, 1989). Wu and Zhong (1999) present evidence that ginseng suspensions can be cultivated without any loss of productivity in a 2 L STR, equipped with a marine impeller, at tip speeds of 0.65 and  $2.5 \text{ m s}^{-1}$ . While appropriate for comparison purposes in a single vessel, neither impeller rotational speed nor tip speed is suitable for characterising flow conditions across different reactor/impeller geometries. As a scale-up parameter, it also should be noted that, for geometrically similar vessels and assuming comparable aeration conditions, constant impeller tip speed can be achieved only by a reduction in specific power input, with consequent reductions in mass transfer coefficients. Moreover, examination of the available data reveals that a comparatively narrow range of impeller tip speeds is typically employed in pilot-and production-scale STRs (Table 14.4). Time-averaged shear rates in a STR are frequently assumed to be proportional to  $N$ , although this simple relationship does not hold under turbulent conditions. Relevant, system specific expressions, for average and maximum shear rates are summarised by Chisti (1999) and Thomas (1990). In ALRs, average shear rates ( $\dot{\gamma}$ ) are usually correlated with superficial gas velocity ( $u_s$ ), using expressions of the form:

$$\dot{\gamma} = K u_s \quad (2)$$

although values of  $K$  vary widely and the general applicability of the relationship may be questionable. Characterisation of the intensity of the flow field in which plant cells are suspended has also been undertaken in terms of both the time-averaged shear stresses, and the so-called Reynolds stresses, associated with the very rapid fluctuations in turbulent flow (e.g. Meijer, 1989; Dunlop *et al.*, 1994). The Kolmogoroff length scale approach has been usefully applied to mammalian cell systems (e.g. Croughan *et al.*, 1989) and, to a lesser extent, to plant cell suspensions (Dunlop *et al.*, 1994; Huang *et al.*, 1998), but the larger dimensions of plant cells suggest that they may be more susceptible to eddies in the inertial subrange.

Considering agitation alone, energy dissipation rates in a STR can be calculated as:

$$\varepsilon = \frac{P}{\rho V} = \frac{N_p N^3 D^5}{V} \quad (3)$$

where  $(P/V)$  is the specific power impeller input ( $\text{W m}^{-3}$ ), based on an appropriate volume,  $V$ ,  $N$  is the impeller rational speed ( $\text{s}^{-1}$ ),  $D$  is the impeller diameter (m) and  $N_p$  is the power number for the relevant impeller, at the prevailing Reynolds number. In the high shear region surrounding the impeller, local turbulent energy dissipation rates may

be as high as 100 times the tank-averaged value  $\bar{\varepsilon}$ . In the remainder of the vessel, the local dissipation rate may fall to 0.25  $\bar{\varepsilon}$ . In bubble columns and ALRs, energy dissipation rates can be estimated using the following equations (Chisti, 1998):

$$\varepsilon = \frac{g u_{sr}}{1 + \frac{A_d}{A_r}} \quad (\text{ALR}) \quad (4)$$

$$\varepsilon = g u_{sr} \quad (\text{bubble column}) \quad (5)$$

where  $u_{sr}$  is the superficial gas velocity in the riser and  $A_d/A_r$  is the ratio of the downcomer-to-riser cross-sectional areas. Equations 3–5 indicate that energy dissipation rates are strongly dependent on impeller design and agitation rate in STRs, and on aeration rate and vessel geometry on ALRs. In an unaerated STR, average energy dissipation rates

**Table 14.4** System geometry and operating details for a train of commercial bioreactors (adapted from Hashimoto and Azechi, 1988)

V(L)	T(m)	H <sup>a</sup> (m)	H/T(–)	Agitation System	D/T(–)	N(rpm)	$\pi ND$ (m s <sup>–1</sup> )
20	0.24	0.33	1.38	2 turbines	0.40	125–1250	0.63–6.28
300	0.55	0.95	1.73	2 turbines	0.36	15–150	0.16–1.57
2000	1.25	1.22	0.98	2 turbines	0.34	10–100	0.22–2.20
20 000	2.50	3.06	0.92	2 4-blade paddles (45°)	0.50	10–40	0.65–2.62

<sup>a</sup>assuming a maximum working volume of 0.75V.

**Table 14.5** Representative energy dissipation levels in bioreactors used for the cultivation of plant cell suspension cultures

System	Vessel/Impeller configuration	Operating conditions	N <sub>p</sub> (–)	$\varepsilon$ (W kg <sup>–1</sup> ) <sup>a</sup>	Reference
<i>Catharanthus roseus</i>	11 L STR(10L wv) helical ribbon impeller $D: 0.21\text{ m}$	120 rpm surface aerated $\mu_a: 0.6\text{ Ns m}^{-2}$	~2	0.7	Kamen <i>et al.</i> (1992)
<i>Catharanthus roseus</i>	3 L STR (2 L wv) Rushton turbine $D: 0.045\text{ m}$	150 rpm	~5	0.007 <sup>b</sup>	Meijer <i>et al.</i> (1994)
<i>Nicotiana tabacum</i>	3 L STR (2L wv) marine propeller $D: 0.045\text{ m}$	100 rpm	~0.45	0.0002 <sup>b</sup>	Ho <i>et al.</i> (1995)
<i>Papaver</i>	300 L ALR	$Q_g: 0.05\text{ vvm}$	N/A	0.11	Park <i>et al</i>

<i>somniferum</i>	$A_d/A_r$ ; 1				(1992)
<i>Datura stramonium</i>	1.2L ALR $A_d/A_r$ ; 0.69	$Q_g$ : 0.69 vvm	N/A	0.05	Ballica & Ryu (1993)
<i>Chenopodium</i>	20 L ALR	$Q_g$ : 0.155 vvm	N/A	0.013	Fischer <i>et al.</i> (1994)
<i>rubrum</i>	$A_d/A_r$ ; 4				

<sup>a</sup>estimated using equation (3), for STRs, under non-aerated conditions; using equation (4) for ALRs; assumed broth density of 1000 kg m<sup>-3</sup>.

<sup>b</sup>apparent viscosity of 2 cP assumed by Meijer *et al.* (1994) and applied here to the data of Ho *et al.* (1995) for comparison purposes.

are of the order of 1 W kg<sup>-1</sup>, although levels can vary by an order of magnitude between laboratory and large-scale vessels. Representative values for plant cell systems are presented in Table 14.5. Reductions in power due to gassing are strongly dependent on impeller geometry, fluid viscosity and aeration conditions. Gassed-to-ungassed power ratios of about 0.4–0.6 are common for Rushton turbines, while values for up-pumping impellers are higher, typically about 0.8 (Nienow, 1998).

To take account of the combined effects of aeration and agitation, the initial oxygen mass transfer coefficient ( $k_{La}$ ), *i.e.* as measured in cell-free medium, has been employed as an indicator of the intensity of the environment (*e.g.* Kato *et al.*, 1975; Leckie *et al.*, 1991a). Application of initial  $k_{La}$  values as a design criterion is limited by subsequent variations in the prevailing  $k_{La}$ , due to increases in biomass levels and broth viscosity and addition/accumulation of surfactants including anti-foams and extracellular proteins. However, for individual cell lines, this approach can yield useful information.

More recently, the concept of a critical shear stress (*e.g.* Ballica and Ryu, 1993; Kieran *et al.*, 1995) or a critical energy dissipation rate has been superseded by the use of cumulative energy dissipation (*i.e.* the product of energy dissipation rate and exposure time) as a correlating parameter for cell damage. In an aerated, agitated bioreactor, a representative specific power input of 0.5 kW m<sup>-3</sup> corresponds to a daily cumulative energy dissipation level of approximately  $4 \times 10^7$  J m<sup>-3</sup>. However, evaluation of this quantity depends on the choice of an appropriate dissipation volume (*e.g.* the entire vessel

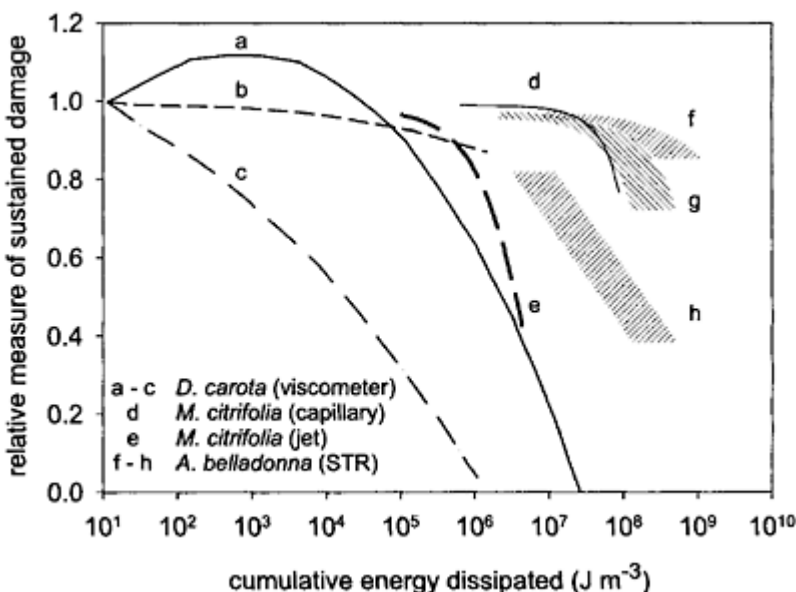


**Figure 14.4** Sustained damage in *D. carota* (Dunlop *et al.*, 1994), *M. citrifolia* (Kieran *et al.*, 1994; MacLoughlin *et al.*, 1998) and *A. belladonna* (Wongsamuth and Doran, 1997) suspensions, as a function of total energy expended.

Shearing/cultivation devices are as indicated. Response indicators: (a) aggregate size, (b) cell lysis, (c) mitochondrial activity, (d)-(f) viability (membrane integrity), (g) protein release, (h) cake permeability/aggregate size.

volume or the high shear region surrounding the impeller) and whether total energy dissipation is considered, or only that fraction dissipated on the biomass. Figure 14.4 uses cumulative energy dissipation to compare the effects of turbulent flow in capillary (Kieran *et al.*, 1995), jet (MacLoughlin *et al.*, 1998) and Couette (Dunlop *et al.*, 1994) devices and in a 2 L STR (Wongsamuth and Doran, 1997) for three different cell suspensions, using a variety of response indicators. Differences between the viability results for *M. citrifolia* in the capillary (curve (d)) and jet (curve (e)) trials are attributable to the choice of the active volume for estimation of the average energy dissipation rate.

The shaded regions for the *Atropa belladonna* data reflect the displacement of the data depending on whether total cumulative energy dissipated in the broth is considered, or that fraction to which the biomass alone is exposed (at a maximum level of 13 g DW L<sup>-1</sup>, which corresponds to an estimated 26% volume fraction, assuming a representative FW/DW ratio of 20). Overall, there is a good level of agreement between the response trends. The results suggest that cell metabolism, represented in this case by mitochondrial activity (curve (c)), may be affected at cumulative energy dissipation levels significantly below those required to cause detectable damage to the cell membrane (curve (a)). Doran (1999) used the *A. belladonna* data to identify a threshold level of 10<sup>7</sup> J m<sup>-3</sup> for shear-related damage in stirred bioreactors. Although undeniably valuable as a correlating parameter for cell response, the use of cumulative energy dissipation does not elucidate a mechanism for cell damage.

The current consensus on shear sensitivity is that plant cells are considerably more robust than was initially believed. Nonetheless, reduction in overall productivity on scaleup is common and, where cell death is not a factor, it reflects sub-lethal system responses. However, a full understanding of the key processes in stress perception and stress responses in plant cells has yet to be achieved. Identification of appropriate cultivation conditions can be approached using the guidelines presented in this section, but it is still a non-trivial, line specific task.

### Performance in Suspension Culture

In suspension culture, plant cells behave in a generally similar fashion to microbial systems. The most significant difference is the duration of batch processes. Typical doubling times for plant cells of between 1 and 4 days result in batch cultivation periods of between 5 and 25 days. Inoculum volumes are typically 5–15% of the total broth volume. Particularly low apparent growth rates may be attributable to appreciable levels of cell death and lysis, caused by sub-optimal cultivation conditions. For *M. sativa* L. suspensions in a 10 L STR, cell viability was observed to fall from 80% to 50%, over the first 3 days of cultivation, independent of nutrient limitation (Steward *et al.*, 1999b). Furthermore, from day 7 onwards, cell lysis accounted for more than 20% of total cell death. Accordingly, calculation of apparent specific growth rates, on the basis of whole cell counts alone, significantly underestimated actual rates of cell proliferation. Extended fermentation times challenge system sterility and make plant suspension processes inherently less commercially attractive, unless they have a competitive edge over existing or potential alternatives for the production of the same material.

Maximum biomass levels in the range 10–20 g DW L<sup>-1</sup> can now be routinely achieved with most cell lines. Biomass yields are approximately 0.5–0.6 g DW (g sucrose)<sup>-1</sup>; while a value of 0.78 g g<sup>-1</sup> has been reported (Pareilleux and Vinas, 1983), it is likely that this reflects conversion of the carbon source to intracellular stored carbohydrates, rather than to biomass. As with microbial systems, biomass levels can be augmented by optimisation of cultivation conditions, including substrate feeding and medium perfusion, and concentrations of 70 g DW L<sup>-1</sup> (Fujita, 1988b) have been reported. However, from the comparatively limited data available, it appears as if biomass levels for commercial and commercial-scale processes are typically in the range

15–20 g DW L<sup>-1</sup> (Hashimoto and Azechi, 1988; Ritterhaus *et al.*, 1990; Hibino and Ushiyama, 1999).

In most practical applications, it is a secondary metabolite which is of interest and not the biomass itself. Achievable levels of important metabolites have been enhanced through a combination of line selection and processing strategies (Buitelaar and Tramper, 1992) and novel approaches offer potential for further improvements (Shuler, 1999; Verpoorte *et al.*, 1999). Levels for commercially significant and/or high-yielding cell lines are summarised in a number of recent papers (Sahai, 1994; DiCosmo and Misawa, 1995; Curtis, 1999). The highest level achieved to date (36% of DW) is for rosmarinic acid in suspensions of by *Salvia officinalis* (Hippolyte *et al.*, 1992). Extracellular paclitaxel levels of up to 117 mg L<sup>-1</sup> have been detected in *Taxus canadensis* cultures (Ketchum *et al.*, 1999); Bringi *et al.* (1997) reported whole-broth paclitaxel titres of 902 mg L<sup>-1</sup> in fed-batch cultures of *Taxus* spp.. In general, secondary metabolite productivities are typically of the order of 10<sup>-2</sup>–10<sup>-1</sup> g L<sup>-1</sup> d<sup>-1</sup> (Scragg, 1995). From a processing perspective, it is important to note that many plant cells retain the metabolite of interest intracellularly, which complicates product recovery and which has led to an interest in the development of non-lethal methods for inducing product release. Growth-associated ECPs, which accumulate in the suspending medium, are an important exception. Use of a perfusion system for the high density cultivation of *A. officinalis* yielded a 2.4-fold increase in extracellular protein levels, compared to a batch system (Su *et al.*, 1996) and offers potential for the production of heterologous proteins.

Most plant cell suspensions can be cultivated at temperatures of between 15 and 35°C, with temperatures of 25–28°C most common. Limited studies of the effects of temperature on growth and product formation by *C. roseus* (Fowler, 1988) indicated maximum serpentine productivity at 25°C, with maximum growth rates observed at 30°C. However, this phenomenon may reflect the decoupling of biomass and secondary metabolite formation for non-or partially growth-associated product formation, rather than a temperature-specific effect.

## BIOREACTOR DESIGN AND OPERATION

### Mixing and Mass Transfer

In any bioreactor, the purpose of mixing is to ensure homogeneity with respect to biomass and nutrients, which includes effective gas phase dispersion. Plant cell broths are characterised by lower oxygen and cooling requirements (*Section on Oxygen Requirements*) than microbial fermentation fluids, but typically have higher apparent viscosities (*Section on Broth Rheology*). Reducing the intensity of the hydrodynamic environment to which potentially shear sensitive systems (*Section on Shear Sensitivity*) are exposed, may conflict with the need to prevent particle settling in heavily aggregated suspensions, with a solid specific gravity of approximately 1.02–1.03. Although particle sedimentation is generally not a problem in finely dispersed suspensions, increased aggregate size, which may be conducive to secondary metabolism and which, moreover, has been reported to occur on scale-up, leads to an increase in the minimum impeller speed ( $N_{js}$ ) required for particle suspension. Using the Zwietering (1958) correlation to

estimate  $N_{js}$ , Singh and Curtis (1994a) examine the interactions between aggregate size and agitation conditions on scale-up; on the basis of constant impeller tip speed, for example, the maximum aggregate size which can be suspended is reduced by approximately 70%, for a linear scale-up factor of 10.

Laboratory scale reactors have most frequently employed the near-ubiquitous Rushton turbine. However, with a turbulent power number of approximately S, the specific power input ( $P/V$ ) and energy dissipation rate ( $\epsilon$ ) (equation 3) will be higher for a Rushton turbine than for a marine impeller ( $N_p,_{turb} \sim 0.4$ ), a helical ribbon impeller ( $N_p,_{turb} \sim 0.3$ ), a paddle ( $N_p,_{turb} \sim 2$ ), a pitched blade turbine ( $N_p,_{turb} \sim 1$ ) or a two-stage Intermig ( $N_p,_{turb} \sim 0.7$ ), operated under comparable conditions in the same vessel. While data for most commercial applications are proprietary, data from laboratory and pilot-scale facilities indicates that axial flow impellers, including pitched blade impellers and marine propellers, are more appropriate for plant cell suspensions (e.g. Furuya *et al.*, 1984; Leckie *et al.*, 1991b). Hollow paddle impellers have been used with high density suspensions of *Coptis japonica* (Matsubara *et al.*, 1989) and helical ribbon impellers supported biomass levels in excess of 25 g DW L<sup>-1</sup> in suspensions of *C. roseus* (Kamen *et al.*, 1992; Jolicœur *et al.*, 1992) and *Vitis vinifera* (Cormier *et al.*, 1996). Novel agitation systems which have been employed or recommended for use with plant cell suspensions include a wide-bladed turbine impeller ( $w/D=1.84$ , compared to a value of 0.2 for a standard Rushton turbine) (Hooker *et al.*, 1990); a 2-blade "grid" paddle, employed in combination with a spiral sparger in a Maxblend Fermenter® (Yokoi *et al.*, 1993); tangential (Treat *et al.*, 1989) and centrifugal (Wang and Zhong, 1996) cell-lift impellers. However, there are no reports of large-scale plant cell suspension applications for any of these systems.

Because of the perceived low-shear advantage, as well as simplicity of operation, pneumatically impelled reactors, including bubble columns and ALRs (with both internal and external loops), have been widely used for plant cell applications. Tables 14.1 and 14.2 include references to 1000 L and 1500 L ALRs, used in development trials. Using available correlations for time-averaged shear rates and shear stresses, Doran (1993) estimated significantly lower average shear stresses in ALRs than in STRs, under representative operating conditions. However, for high density broths (>30 g DW L<sup>-1</sup>), mixing efficiency in the ALRs is sufficiently reduced to limit oxygen transfer in the broth and this factor largely explains the failure of this configuration to find wider application at industrial scale. It is also reflected in operational difficulties encountered in pilot scale systems (e.g. Park *et al.*, 1992) and experimental observations of pronounced inhomogeneity in bean suspensions in an internal loop ALR, at a biomass level of 12.5 g DW L<sup>-1</sup> (Assa and Bar, 1991). In this context, it is interesting to note that the two ALR systems referenced in Tables 14.1 and 14.2 were ultimately superseded by STRs.

In the design of large-scale microbial fermentation systems, oxygen transfer is often a limiting factor. On the basis of the lower characteristic oxygen requirements (Section on Oxygen Requirements), this is not expected to be the case for plant cell suspensions. The oxygen transfer rate (OTR) is defined as

$$OTR = k_L a (c^* - c_{crit}) \quad (6)$$

where  $k_{La}$  is frequently related to the operating conditions in a STR by correlations of the following form:

$$k_{La} = A \left( \frac{P_g}{V} \right)^a (u_s)^b \quad (7)$$

For ALRs, empirical correlations of the following form have been employed:

$$k_{La} = B(u_{sr})^f (\mu_a)^g \quad (8)$$

Evaluation of  $\mu_a$  depends, of course, on the specification of an appropriate shear rate (*Section on Shear Sensitivity*)

In practical terms, for a high density ( $30 \text{ g DW L}^{-1}$ ) suspension, with a  $q_o$  of  $0.3 \text{ mmol O}_2 \text{ (g DW)}^{-1} \text{ h}^{-1}$ , a  $c_{\text{crit}}$  of 25% and assuming an equilibrium dissolved oxygen concentration ( $c^*$ ) of  $0.25 \text{ mmol L}^{-1}$ , equation 6 indicates that the system oxygen demands can be met by a  $k_{La}$  of approximately  $48 \text{ h}^{-1}$ . This value lies comfortably within the performance range of conventional STRs and is representative of values reported for large-scale systems (e.g. Hashimoto and Azuchi, 1988). If either the biomass level or  $c_{\text{crit}}$  is higher than the assumed values, then a higher  $k_{La}$  will be required. It is obvious, from equations 7 and 8, that  $k_{La}$  can be increased by increasing  $N$  (and thus,  $P/V$ ) and/or the aeration rate (and thus,  $u_{sr}$ ). However, neither of these approaches may be appropriate for a shear-sensitive organism or a high-foaming broth. An alternative is to increase  $c^*$ , by either oxygen enrichment or increasing system pressure. Bioreactors are typically designed to withstand sterilisation and are generally rated for pressures of up to 2.5–2.7 bar. Thus, the costs associated with operating at pressures of up to 2 bar are minimal. However, although few organisms exhibit sensitivity to pressures within this range, the resulting effects of elevated concentration of other dissolved components, including CO<sub>2</sub> and ethylene (*Section on Aeration in Plant Bioreactors*) are still unclear. Oxygen enrichment is commonly employed in laboratory and pilot-scale fermentations, but is a costly exercise at industrial scale. This approach was adopted by Matsubara *et al.* (1989) to achieve  $k_{La}$  values of up to about  $80 \text{ h}^{-1}$ , at a gassing rate of 0.05 vvm, in a high density *C. japonica* system. Such higher values notwithstanding, analysis of the available data suggests that  $k_{La}$  values of between about 10 and  $30 \text{ h}^{-1}$  are typical for plant cell cultures. In the development of novel bioreactors/ mixing systems for use with plant cell suspensions, a premium has been placed on the achievement of high  $k_{La}$  values, under conditions of reduced aeration/agitation intensity (e.g. Tanaka *et al.*, 1983, Kamen *et al.*, 1992; Yokoi *et al.*, 1993).

In a recent analysis of mixing systems for plant cell suspension in STRs, Doran (1999) simultaneously considers the phenomena of gas dispersion, solids suspension, oxygen mass transfer and shear damage for a variety of impeller geometries, in a representative  $10 \text{ m}^3$  vessel of standard configuration. Large-scale commercial bioreactors typically have larger aspect ratios ( $H/T$ ) and consequently, are often equipped with more than one impeller. Nonetheless, the flow regime maps for a Rushton turbine (Figure 14.5 (a)) and an upward-pumping pitched blade turbine (Figure 14.5 (b)) give a clear, qualitative indication of the relative merits of these impellers and of the pertinent issues for mixing system design. The shaded regions, indicating approximate limits for shear-related damage, are evaluated on the basis of a maximum cumulative energy dissipation of  $10^7 \text{ J}$

$\text{m}^{-3}$  (Figure 14.4), combined with a model proposed by Jüsten *et al.* (1998) for fungal mycelial breakage. The aeration rates of 0.13 vvm (Rushton) and 0.17 vvm (upward-pumping) are specified so as to prevent oxygen mass transfer limitation in the broth. From the flow regime maps, it is apparent that the Rushton turbine may be unsuitable for this application. The minimum speed for complete solids and gas dispersion, which simultaneously satisfies oxygen mass transfer requirements, exceeds the limit for shear-related damage. In contrast, the upward-pumping impeller would appear to offer a wider range of potential operating conditions. Moreover, the minimum stirrer speeds required for solids suspension and gas dispersion are largely insensitive to aeration rate. Although there is experimental evidence of effective gas dispersion, stable operation and diminished power reduction on gassing with upward-pumping, axial flow agitators (Junker *et al.*, 1998a; Nienow, 1998), there is also some data (Junker *et al.*, 1998b) to suggest that such impellers cannot deliver the mass transfer rates required for high oxygen demand fermentations. To date, however, there are no reports of upward-pumping impellers employed with plant cell suspensions and they are certainly worthy of investigation.

### Aeration in Plant Bioreactors

To meet the oxygen demands of respiring plant cells in agitated bioreactors, aeration rates in the range 0.05–0.1 vvm are generally required, although values as high as 0.5 vvm are commonly reported. When higher rates are employed, gas flow dominates circulation patterns in the vessel, the air is poorly dispersed and the vessel essentially operates as an agitated bubble column. With a view to minimising agitation rates, spargers generating large numbers of small bubbles are more effective than single orifice nozzles (*e.g.* Treat *et al.*, 1989). High aeration rates, in addition to exacerbating foaming (*Section on Foaming and Wall Growth*), are associated with gas-stripping effects known to be inhibitory to plant cell systems. By recirculating the exhaust gas from a STR, Schlatmann *et al.* (1993) observed ajmalicine production profiles in *C. roseus* similar to those obtained in shake flasks, suggesting that valuable metabolites were removed during normal aeration. Carbon dioxide has been identified as an important gaseous component (*e.g.* Kobayashi *et al.*, 1991), although its effects are unrelated to photosynthetic activity. The volatile plant hormone, ethylene, is also susceptible to stripping and has been the subject of a number of related studies (Kim *et al.*, 1991; Mirjalili and Linden, 1995). Ethylene effects appear to be highly system specific, while both  $\text{CO}_2$  stripping and  $\text{CO}_2$  accumulation have been observed to have a negative influence on growth of *Cyclamen persicum* suspensions in bioreactors (Hone *et al.*, 1999). Schlatmann *et al.* (1994a) suggested that stripping of some other, unidentified volatile metabolite(s) was responsible for the reduction in secondary metabolism observed on scale-up from a shake flask to a sparged bioreactor. Currently available information on the effects of carbon dioxide, ethylene and oxygen accumulation

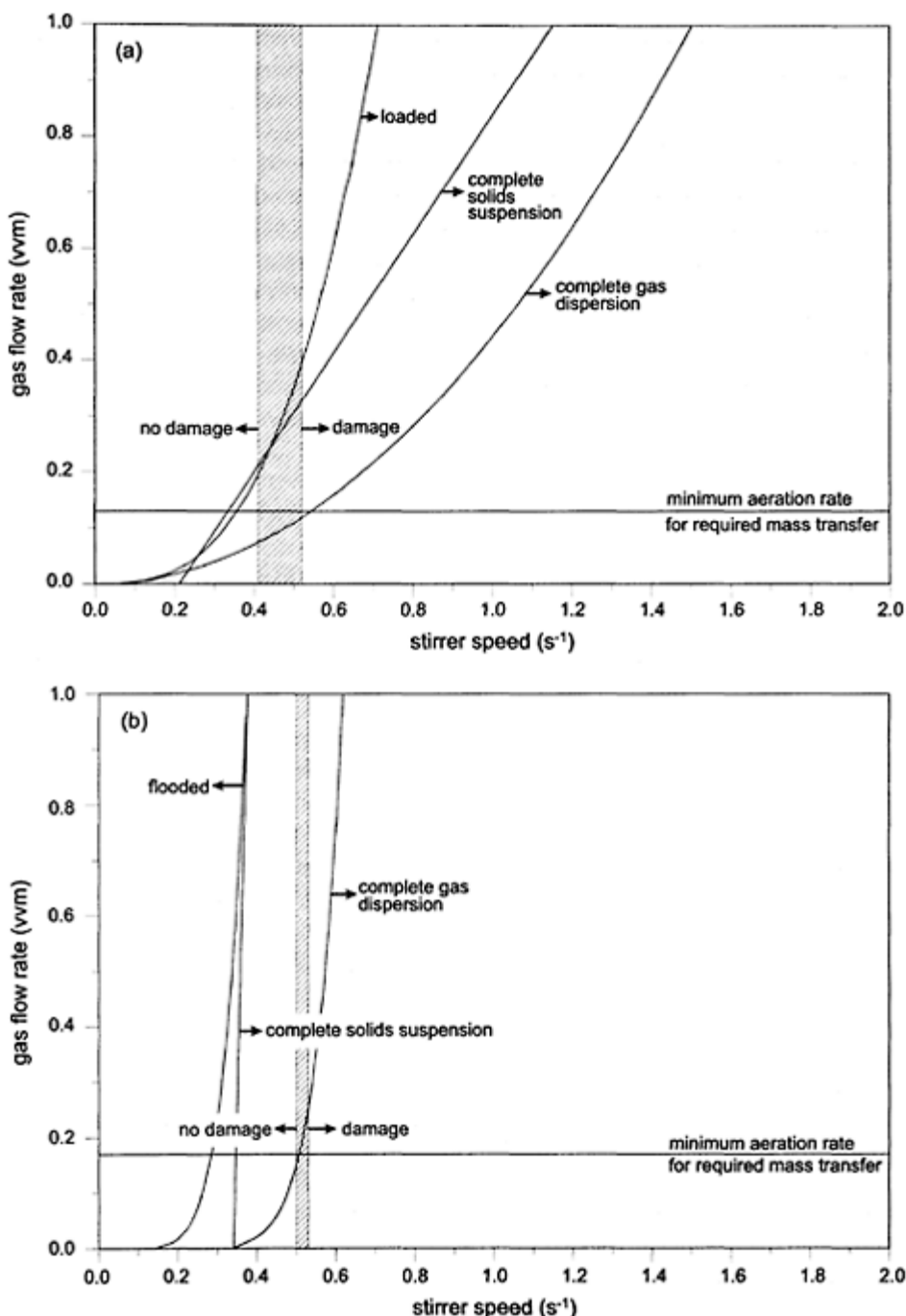


**Figure 14.5** Flow regime maps for (a) Rushton turbine ( $D=0.5T$ ) and (b) upward-pumping, 6-blade, pitched-blade turbine ( $D=0.57$ ). Redrawn, with permission, from Doran (1999). © ACS

is sparse and line specific and has, in general, been collected under conditions which make it difficult to draw comparisons between the results of different studies.

Extended oxygenation of plant bioreactors is most commonly achieved via direct sparging with air. Bubble-free aeration via porous membranes (e.g. Su and Humphrey, 1991) or surface aeration (Tanaka *et al.*, 1983; Jolicoeur *et al.*, 1992) and in a loop fluidised bed reactor (Dubuis *et al.*, 1995) has proven successful in laboratory/pilot-scale systems. In sparged, laboratory-scale bioreactors, the contribution of surface aeration to overall mass transfer may be significant (Singh and Curtis, 1994a) and head-space gassing with air or oxygen-enriched air may be used to reduce bulk sparging rates. Although more work is required in this area to develop a rational approach to optimisation of aeration conditions, current knowledge suggests that gassing rates in sparged systems should be maintained at the lowest level compatible with satisfying cellular oxygen demands and, where appropriate, mixing requirements. Oxygen supplementation may be beneficial.

### Foaming and Wall Growth

In aerated, laboratory/pilot-scale plant bioreactors, foaming is a common occurrence and can constitute a significant nuisance. Cells become entrained in a foam “meringue” which forms above the active broth level and which is fed by splashing. Although necrosis is inevitable in regions beyond the splash zone, significant cell/callus growth may occur on internal vessel surfaces. System productivity is reduced and, in severe cases, foam overflow may foul the exhaust filter and increase the risk of contamination. However, unlike animal cell systems, there is no evidence to suggest that plant cells are damaged by interactions with bursting bubbles, either during the gas disengagement process (Singh and Curtis, 1994a) or in the foam layer itself (Wongsamuth and Doran, 1994).

Foaming is strongly dependent on the aeration and agitation conditions and on the properties of the cell-free broth, particularly surface tension. Foaming studies with *A. belladonna* (Wongsamuth and Doran, 1994) and *M. citrifolia* (Cusack, 1998) broths in bubble columns have shown that, at a given aeration rate, foam formation is strongly, positively correlated with extracellular protein concentration, which is typically growth associated. Absence of foaming in aggregated, self-immobilised cultures (Xu *et al.*, 1998) has been attributed to reduced levels of metabolite secretion associated with cellular differentiation. Foaming typically commences during the exponential growth phase; release of additional proteinaceous material by cell lysis towards the end of the growth cycle may exacerbate the condition. Foaming patterns will be influenced by broth pH, which is generally uncontrolled in plant cell suspensions and which typically varies

between values of about 4 and 6. The stability of foam, once formed, is further enhanced by the presence of ECPs.

As with all fermentation processes, it is preferable to prevent foam formation rather than to destroy it, once formed. Efforts to prevent the onset of foaming include reducing aeration and agitation rates (without jeopardising system mixing and mass transfer) or, where practicable, employing surface aeration or bubble free-aeration. The most common approach is the use of antifoam, added directly to the medium prior to inoculation and/or as required during cultivation. Studies of the biocompatibility and effectiveness of a range of antifoams and other surfactants have been performed in shake flask cultures and, more valuably, under sparged conditions (*e.g.* Zhong *et al.*, 1992a; Li *et al.*, 1995). While the interaction between antifoaming agents and mass transfer is complex, experience with plant cells suggests that addition of antifoam is likely to reduce  $k_{La}$  values (Smart and Fowler, 1981; Wongsamuth and Doran, 1994). Mechanical foam breakers have traditionally been avoided with plant cell systems, for reasons of cost, complexity of operation and possible shear damage.

Once foam formation commences, it is difficult to prevent wall growth. As a general rule, it is advisable to minimise the internal surfaces available for wall growth by, for example, employing jackets rather than internal coils for temperature control. Removal of baffles has also been reported (Treat *et al.*, 1989) although, as this strategy will reduce bulk mixing efficiency for most agitation systems and is conducive to vortexing, it is not generally recommended. There is experimental evidence to show that substantially reduced  $\text{Ca}^{2+}$  levels in the medium (0.1–0.5 mM, as opposed to 3 mM in control medium) can significantly reduce foaming and wall growth in both shake flask (Takayama *et al.*, 1977) and chemostat (STR) cultures (Sahai and Shuler, 1982).

Data on foaming in large scale systems are sparse. Hashimoto and Azechi (1988) reported foam, rising to a height of 2 m during the exponential phase of a batch fermentation in a 20 m<sup>3</sup> vessel (10–15 m<sup>3</sup> wv). The performance of a 300 L, external loop ALR for the cultivation of *P. somniferum* (Park *et al.*, 1992) was limited by foaming. It is possible that the absence of more abundant data may reflect the fact that in commercial scale STRs, foaming may be less severe, due primarily to increased vessel aspect ratios (H/T) and lower aeration rates than those commonly employed in laboratory systems.

### **Bioreactor Configuration and Operation Mode**

The design of bioreactors for microbial systems is well-established (*e.g.* Winkler, 1990; Charles and Wilson, 1993). The same basic objectives apply to bioreactors for plant cell suspensions, namely the extended provision of reproducible conditions, supporting optimal system performance, evaluated in terms of biomass and/or product formation.

To date, most plant suspensions have been cultivated in either STRs or ALRs. Strategies for optimising the hydrodynamic environment in STRs have focused primarily on modifications to standard agitation (*Section on Mixing and Mass Transfer*) and aeration (*Section on Aeration in Plant Bioreactors*) regimes. Examples of variations on basic STR and ALR designs as well as rotating drum reactors, employed for plant cell suspensions, are summarised by Su (1995).

Assuming that a product market exists, there are two main routes to enhancing the commercial viability of plant cell-based processes, namely increasing system productivity

through a combination of biological and processing strategies, or reducing process costs. A stainless steel, sterilisable bioreactor constitutes a significant portion of the capital costs for any fermentation facility and a number of groups have begun to question traditional design philosophies and investigate the feasibility of innovative and less expensive but functional alternatives.

At laboratory scale, Fukui and Tanaka (1995) successfully employed a stationary, envelope-shaped culture vessel ("Culture Bag"), with a working volume of 25 mL, constructed of 12.5 $\mu\text{m}$  thick fluorocarbon polymer film, for the cultivation of *N. tabacum* and *L. erythrorhizon*. Biomass levels comparable to or better than those in shake flasks were achieved. The bag contents were not agitated and oxygen limitation accounted for reduced growth in thicker-walled bags. Singh (1999) describes a disposable, plastic-bag bioreactor (Wave Bioreactor®), mounted on a rocking table, which provides low-shear, wave-motion agitation. Although originally validated with animal cells, a similar reactor has been used with hairy root and embryogenic callus plant cultures (Eibl *et al.*, 1999). The system has been successfully scaled to 200 L (100 L wv) with maximum reported  $k_{L\alpha}$  values of 4 h<sup>-1</sup>. To date, there are no reports of trials with suspension cultures and oxygen transfer is likely to be the limiting factor for high-density cultivation. A promising option for such cultures is a bubble column reactor, comprising a sterilisable, plastic liner, clamped to a head-plate and supported within an inexpensive, non-sterilisable cylinder (Figure 14.6), developed by Curtis and co-workers (Hsiao *et al.*, 1999). Aeration, via an off-set sparger, coupled with contour baffles, ensures adequate fluid circulation within the vessel. The system has been demonstrated up to a working volume of 100 L (Curtis *et al.*, 1999), with biomass levels of up to 400 g FW L<sup>-1</sup>. And, although experience with ALRs (*Section on Mixing and Mass Transfer*) suggests that this configuration is unsuitable for higher density suspensions, the cost advantages make a multiple-vessel train commercially realistic.

Regardless of the bioreactor configuration employed, a bioreactor operating strategy must be selected, which supports high productivity and high product yield. The choice is

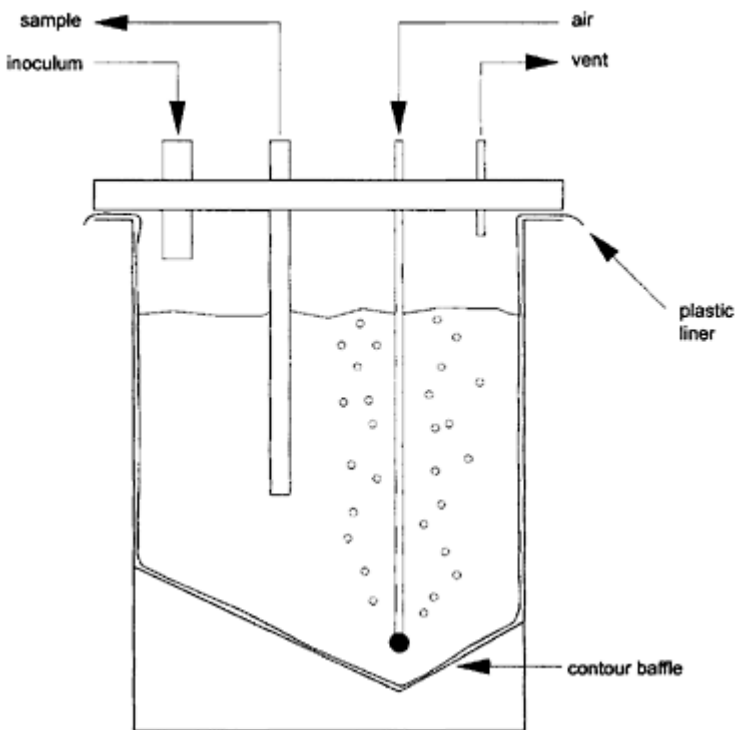


**Figure 14.6** Schematic diagram of a low cost bioreactor developed for plant cell suspension cultures. Redrawn, with permission, from Hsiao *et al.* (1999). © ACS.

essentially governed by (a) product synthesis patterns (*i.e.* growth-associated or non-growth associated) and (b) whether the product of interest is retained intracellularly or secreted into the medium. Table 14.6 summarises the appropriateness of the available options. Perfusion systems, on which comparatively little work has been performed, offer the prospect of high cell densities and are particularly suitable for extracellular products (*e.g.* Su *et al.*, 1993, 1996). The benefits of continuous culture (single-and two-stage) must be balanced against the sterility problems associated with extended operation. At laboratory scale, where continuous culture is a very useful tool for collecting stoichiometric and kinetic data (Wilson, 1980), other practical difficulties arise due to low growth rates, foaming and wall growth and the maintenance of a representative effluent (Sahai and Shuler, 1982, 1984; Schlatmann *et al.*, 1996). As is evident from Tables 14.1 and 14.2, repeated-batch ("draw-and-fill")/semi-continuous operation has proven extremely successful for a range of processes.

## CONCLUSIONS

Large-scale cultivation of plant cell suspensions for the production of valuable phytochemicals is certainly feasible, although commercial application has been comparatively limited. Under the current biological and processing conditions, plant cell-based processes are commercially viable only for high value products. Analysis of experience with plant cell suspensions, to date, suggests a framework for a rational approach to the design and scale-up of bioreactors, based on conventional microbial fermentation technology. However, a radical rethinking of conventional bioreactor design may facilitate wider application of the technology, by reducing processing costs. There are still significant gaps in our understanding of the interplay between the hydrodynamic environment in any bioreactor and the cellular metabolism. Slow system growth rates, coupled with the diversity and variability of plant cell lines, have been real obstacles to the accumulation of the same wealth of knowledge that exists for other, more commercially significant biocatalysts.

## ACKNOWLEDGEMENTS

The author is grateful for the co-operation of the following individuals in the preparation of this chapter: Professor Wayne Curtis, Professor Pauline Doran, Dr. Ken Hibino, Dr. Dermot Malone, Dr. Frank MacLoughlin, Dr. Kazuya Otsuji, Dr. Om Sahai, Dr. Yoseph Shaaltiel, Dr. Shigeru Takahashi and Dr. Graham Wilson.

## NOMENCLATURE

### Symbols

$A_d/A_r$	ratio of downcomer-to-riser cross sectional area (-)
$c_{\text{crit}}$	critical dissolved oxygen concentration (% of air saturation)
$c^*$	equilibrium dissolved oxygen concentration ( $\text{mmol L}^{-1}$ )

**Table 14.6** Choice of bioreactor operating strategy, based on product formation and location patterns  
(adapted from Payne *et al.*, 1991)

Product formation	Growth-associated	Non-growth-associated		
		extracellular	intracellular	extracellular
Operating strategy				intracellular
Batch	✓	✓	✓	✓
Fed-Batch	✓	✓	✓	✓
Reneated (fed) batch/semi-	✓	✓	✓	✓

continuous

Two-stage batch	—	—	✓	✓
Continuous (chemostat)	✓	✓	—	—
Two-stage continuous	—	—	✓	✓
Perfusion with cell retention	✓	—	✓	—
with cell bleed	✓	✓	—	—

$D$	impeller diameter (m)
$H$	liquid height (m)
$K_{m,app}$	apparent oxygen saturation constant (mmol O <sub>2</sub> L <sup>-1</sup> )
$k_L a$	volumetric oxygen mass transfer coefficient (h <sup>-1</sup> )
$N$	impeller rotational speed (s <sup>-1</sup> )
$N_S$	minimum impeller speed for particle suspension (s <sup>-1</sup> )
$N_p$	power number (—)
$P$	impeller power input (W)
$P_g$	gassed power input (W)
$q_o$	specific oxygen consumption rate (mmol O <sub>2</sub> g (DW) <sup>-1</sup> h <sup>-1</sup> )
$Q_g$	aeration rate (vvm)
$Q_{met}$	rate of metabolic heat generation (W)
$T$	vessel diameter (m)
$u_s$	superficial gas velocity (m s <sup>-1</sup> )
$u_{sr}$	superficial gas velocity in the riser (m s <sup>-1</sup> )
$V$	volume (m <sup>3</sup> )
$w$	impeller blade width (m)
$X$	biomass concentration (g DW L <sup>-1</sup> )

## Greek Symbols

$\epsilon$	energy dissipation rate (W kg <sup>-1</sup> )
$\dot{\gamma}$	shear rate (s <sup>-1</sup> )
$\rho$	density (kg m <sup>-3</sup> )
$\mu$	(apparent) viscosity (N s m <sup>-2</sup> )
$\tau$	yield stress (N m <sup>-2</sup> )

## Abbreviations

ALR	air-lift reactor
DO	dissolved oxygen

DW	dry weight
ECP	extracellular polysaccharide
FW	fresh weight
OTR	oxygen transfer rate
OUR	oxygen uptake rate
RDR	rotating drum reactor
STR	stirred tank reactor
vvm	volumes (gas) per volume (broth) per minute
wv	working volume

## REFERENCES

- Allan, E.J., Scragg, A.H. and Pugh, K. (1988) Cell suspension culture of *Picrasma quassoides*: the development of a rapidly growing, shear resistant cell line capable of quassin formation. *Journal of Plant Physiology*, **132**, 176–183.
- Assa, A. and Bar, R. (1991) Biomass axial distribution in an airlift bioreactor with yeast and plant cells. *Biotechnology and Bioengineering*, **38**, 1325–1330.
- Balica, R. and Ryu, D.D.Y. (1993) Effects of rheological properties and mass transfer on plant cell bioreactor performance: production of tropane alkaloids. *Biotechnology and Bioengineering*, **42**, 1181–1189.
- Binzel, M.L., Hasegawa, P.M., Handa, A.K. and Bressan, R.A. (1985) Adaptation of tobacco cells to NaCl. *Plant Physiology*, **79**, 118–125.
- Bond, P.A., Fowler, M.W. and Scragg, A.H. (1988) Growth of *Catharanthus roseus* suspensions in bioreactors: On-line analysis of oxygen and carbon dioxide levels in inlet and outlet gas streams. *Biotechnology Letters*, **10**, 713–718.
- Bringi, V., Karade, P., Prince, C.L. and Roach, B.L. (1997) Enhanced production of taxanes by cell cultures of *Taxus* species. Patent No. WO9744476.
- Buitelaar, R.M. and Tramper J. (1992) Strategies to improve the production of secondary metabolites with plant cell cultures: a literature review. *Journal of Biotechnology*, **23**, 111–141.
- Charles, M. and Wilson, J. (1993) Design of aseptic, aerated fermentors. In *Biotechnology: A multi-volume comprehensive treatise*, edited by H.-J.Rehm and G.Reed (2nd ed.), Volume 3 (edited by G.Stephanopoulos), pp. 401–26. Weinheim: VCH.
- Chisti, Y. (1998) Pneumatically agitated bioreactors in industrial and environmental bioprocessing: Hydrodynamics, hydraulics and transport phenomena. *Applied Mechanics Review*, **51**, 33–112.
- Chisti, Y. (1999) Shear sensitivity. In *Encyclopedia of Bioprocess Technology: Fermentation, Biocatalysis and Bioseparation*, edited by M.C.Flickinger and S.W.Drew, pp. 2379–2406. New York: John Wiley & Sons, Inc.
- Cooney, C.L., Wang, D.I.C. and Mateles, R.I. (1969) Measurement of heat evolution and correlation with oxygen consumption during microbial growth. *Biotechnology and Bioengineering*, **11**, 269–281.
- Cooperative Research Centre for Industrial Plant Biopolymers (1998) Annual Report 1997/98, Australia.
- Cormier, F., Brion, F., Do, C.B. and Moresoli, C. (1996) Development of process strategies for anthocyanin-based food colorant production using *Vitis vinifera* cell cultures. In *Plant Cell Culture Secondary Metabolism—Toward Industrial Application*, edited by F.DiCosmo, and M.Misawa, pp. 167–185. Boca Raton: CRC Press.

- Croughan, M.S., Sayre, E.S. and Wang, D.I.C. (1989) Viscous reduction of turbulent damage in animal cell culture. *Biotechnology and Bioengineering*, **33**, 862–872.
- Curtis, W.R. (1999) Achieving economic feasibility for moderate-value food and flavor additives: A perspective on productivity and proposal for production technology cost reduction. In *Plant Cell and Tissue Culture for the Production of Food Ingredients*, edited by T.-J.Fu, G.Singh and W.R.Curtis, pp. 225–236. New York: Kluwer Academic/Plenum Publishers.
- Curtis, W.R. and Emery, A.H. (1993) Plant cell suspension culture rheology. *Biotechnology and Bioengineering*, **42**, 520–526.
- Curtis, W.R., Bacani, F., Hsiao, T., Carvalho, E. and Srubar, C. (1999) Development and application of a low capital investment bioreactor. Poster presented at the 217th ACS National Meeting, Division of Biochemical Technology (BIOT), Paper No. 157, Anaheim, California.
- Cusack, W. (1998) Characterisation of foaming in cell suspension cultures of *Morinda citrifolia*. M.Sc. Thesis, Dublin City University, Dublin, Ireland.
- Cusack, W. and Kieran, P.M. (1998) Unpublished data.
- DiCosmo, F. and Misawa, M. (1995) Plant cell and tissue culture: alternatives for metabolite production. *Biotechnology Advances*, **13**, 425–53.
- Doran, P.M. (1993) Design of reactors for plant cells and organs. *Advances in Biochemical Engineering and Biotechnology*, **48**, 117–168.
- Doran, P.M. (ed.) (1997) *Hairy Roots: Cultures and Applications*. Amsterdam: Harwood Academic Publishers.
- Doran, P.M. (1999) Design of mixing systems for plant cell suspensions in stirred reactors. *Biotechnology Progress*, **15**, 319–335.
- Doran, P.M. (2000) Bioreactors: Stirred Tank. In *Encyclopedia of Cell Technology*, edited by R.E.Spier, pp. 249–278. New York: John Wiley & Sons, Inc.
- Dubuis, B., Kut, O.M. and Prenosil, J.E. (1995) Pilot-scale culture of *Coffea arabica* in a novel loop fluidised bed reactor. *Plant Cell, Tissue and Organ Culture*, **43**, 171–183.
- Dunlop, E.H., Namdev, P.K. and Rosenberg, M.Z. (1994) Effect of fluid shear forces on plant cell suspensions. *Chemical Engineering Science*, **49**, 2263–2276.
- Eibl, R., Lettenbauer, C., Eibl, D. and Röll, M. (1999) Experiences in the application of the Wave Bioreactor System 20 in cell culture technique. *BIOForum International*, **3**, 110–112.
- Fischer, U., Santore, U.J., Hüsemann, W., Barz, W. and Alfermann, A.W. (1994) Semi-continuous cultivation of photoautotrophic cell suspension cultures in a 20 L airlift-reactor. *Plant Cell Tissue and Organ Culture*, **38**, 123–134.
- Fowler, M.W. (1988) Problems in commercial exploitation of plant cell cultures. In *Applications of plant cell and tissue culture: Ciba Foundation Symposium 137*, edited by G.Bock and J.Marsh, pp. 239–253, Chichester: John Wiley & Sons, Inc.
- Franken, E., Teuschel, U. and Hain, R. (1997) Recombinant proteins from transgenic plants. *Current Opinion in Biotechnology*, **8**, 411–416.
- Fujita, Y. (1988a) Shikonin: production by plant (*Lithospermum erythrorhizon*) cell cultures. In *Biotechnology in Agriculture and Forestry: Medicinal and Aromatic Plants I*, edited by Y.P.S.Bajaj, Volume 4, pp. 225–236. Berlin: Springer-Verlag.
- Fujita, Y. (1988b) Industrial production of shikonin and berberine. In *Applications of plant cell and tissue culture: Ciba Foundation Symposium 137*, edited by G.Bock and J.Marsh, pp. 228–237, Chichester: John Wiley & Sons, Inc.
- Fukui, H. and Tanaka, M. (1995) An envelope-shaped film culture vessel for plant cell suspension cultures and metabolite production without agitation. *Plant Cell, Tissue and Organ Culture*, **41**, 17–21.
- Furuya, T., Yoshikawa, T., Orihara, Y. and Oda, H. (1984) Studies of the culture conditions for *Panax ginseng* cells in jar fermentors. *Journal of Natural Products*, **47**, 70–75.
- Goldstein, W.E. (1999) Economic considerations for food ingredients produced by plant cell and tissue culture. In *Plant Cell and Tissue Culture for the Production of Food Ingredients*, edited

- by T.-J.Fu, G.Singh and W.R.Curtis, pp. 195–213. New York: Kluwer Academic/Plenum Publishers.
- Hanagata, N., Ito, A., Uehara, H., Asari, F., Takeuchi, T. and Karube, I. (1993) Behaviour of cell aggregates of *Carthamus tinctorius* L. cultured cells and correlation with red pigment formation. *Journal of Biotechnology*, **30**, 259–269.
- Hashimoto, T. and Azechi, S. (1988) Bioreactors for large-scale culture of plant cells. In *Biotechnology in Agriculture and Forestry: Medicinal and Aromatic Plants I*, edited by Y.P.S.Bajaj, Volume 4, pp. 104–122. Berlin: Springer-Verlag.
- Hibino, K. (1999) Personal communication.
- Hibino, K. and Ushiyama, K. (1999) Commercial production of ginseng by plant tissue culture technology. In *Plant Cell and Tissue Culture for the Production of Food Ingredients*, edited by T.-J.Fu, G.Singh and W.R.Curtis, pp. 215–224. New York: Kluwer Academic/Plenum Publishers.
- Hippolyte, I., Marin, B., Baccou, J.C. and Jonard, R. (1992) Growth and rosmarinic acid production in cell suspension cultures of *Salvia officinalis*. *Plant Cell Reports*, **11**, 109–112.
- Ho, C.-H., Henderson, K.A. and Rorrer, G.L. (1995) Cell damage and oxygen mass transfer during cultivation of *Nicotiana tabacum* in a stirred-tank bioreactor. *Biotechnology Progress*, **11**, 140–145.
- Höne, A., Winkelmann, T. and Schwenkel, H.-G. (1999) CO<sub>2</sub> accumulation in bioreactor suspension cultures of *Cyclamen persicum* Mill, and its effect on cell growth and regeneration of somatic embryos. *Plant Cell Reports*, **18**, 863–867.
- Hooker B.S., Lee J.M. and An, G. (1990) Cultivation of plant cells in a stirred vessel: Effect of impeller design. *Biotechnology and Bioengineering*, **35**, 296–304.
- Hsiao, T.Y., Bacani, F.T., Carvalho, E.B. and Curtis, W.R. (1999) Development of a low capital investment reactor system: Application for plant cell suspension culture. *Biotechnology Progress*, **15**, 114–122.
- Huang S.-Y., Chen K.-W. and Chen, S.-Y. (1998) Hydrodynamic effect on the aggregate size of L-dopa producing *Stizolobium hassjoo* cells in suspension culture. *Journal of the Chinese Institute of Chemical Engineers*, **29**, 171–182.
- Hulst, A.C., Meyer, M.M.T., Breteler, H. and Tramper, J. (1989) Effect of aggregate size in cell cultures of *Tagetes patula* on thiophene production and cell growth. *Applied Microbiology and Biotechnology*, **30**, 18–25.
- Jolicoeur, M., Chavarie, C., Carreau, P.J. and Archambault, J. (1992) Development of a helical-ribbon impeller bioreactor for high-density plant cell suspension culture. *Biotechnology and Bioengineering*, **39**, 511–521.
- Junker, B.H., Stanik, M., Barna, C., Salmon, P., Paul, E. and Buckland, B.C. (1998a) Influence of impeller type on power input in fermentation vessels. *Bioprocess Engineering*, **18**, 401–412.
- Junker, B.H., Stanik, M., Barna, C., Salmon, P. and Buckland, B.C. (1998b) Influence of impeller type on mass transfer in fermentation vessels. *Bioprocess Engineering*, **19**, 403–413.
- Jüsten, P., Paul, G.C., Nienow, A.W. and Thomas, C.R. (1998) A mathematical model for agitation-induced fragmentation of *Pénicillium chrysogenum*. *Bioprocess Engineering*, **18**, 7–16.
- Kamen, A.A., Chavarie, C., André, G. and Archambault, J. (1992) Design parameters and performance of a surface baffled helical ribbon impeller bioreactor for the culture of shear sensitive cells. *Chemical Engineering Science*, **47**, 2375–2380.
- Kang, C.K. (1999) Personal communication.
- Kato, A., Shimizu, Y. and Nagai, S. (1975) Effect of initial  $k_L a$  on the growth of tobacco cells in batch culture. *Journal of fermentation technology*, **53**, 744–751.
- Kato, A., Kawazoe, S., Iijima, M. and Shimizu, Y. (1976) Biomass production of tobacco cells (II). *Journal of Fermentation Technology*, **54**, 82–87.
- Kato, A., Kawazoe, S. and Soh, Y. (1978) Viscosity of the broth of tobacco cells in suspension culture. *Journal of Fermentation Technology*, **56**, 224–228.

- Keßler, M., ten Hoopen, H.J.G. and Furusaki, S. (1999) The effect of aggregate size on the production of ajmalicine and tryptamine in *Catharanthus roseus* suspension culture. *Enzyme and Microbial Technology*, **24**, 308–315.
- Ketchum, R.E.B., Gibson, D.M., Croteau, R.B. and Shuler, M.L. (1999) The kinetics of taxoid accumulation in cell suspension cultures of *Taxus* following elicitation with methyl jasmonate. *Biotechnology and Bioengineering*, **62**, 97–105.
- Kieran, P.M., Malone, D.M. and MacLoughlin, P.P. (1993) Variation of aggregate size in plant cell suspension batch and semi-continuous cultures. *Food and BioProducts Processing, Trans. I. Chem. E. (C)*, **71**, 40–46.
- Kieran, P.M., O'Donnell, H.J., Malone, D.M. and MacLoughlin, P.P. (1995) Fluid shear effects on suspension cultures of *Morinda citrifolia*. *Biotechnology and Bioengineering*, **45**, 415–425.
- Kieran, P.M., P.F. MacLoughlin and D.M. Malone (1997) Plant cell suspension cultures—some engineering considerations, *Journal of Biotechnology*, **59**, 39–52.
- Kieran, P.M., MacLoughlin, P.F. and Malone, D.M. (2000) Effects of hydrodynamic and interfacial forces on plant cell suspension systems. *Advances in Biochemical Engineering and Biotechnology*, **67**, 139–177.
- Kim, D.-I., Pedersen, H. and Chin, C.-K. (1991) Cultivation of *Thalictrum rugosum* cell suspension in an improved airlift bioreactor: Stimulatory effect of carbon dioxide and ethylene on alkaloid production. *Biotechnology and Bioengineering*, **38**, 331–339.
- Kobayashi, Y., Fukui, H. and Tabata, M. (1991) Effect of CO<sub>2</sub> and ethylene on berberine production and cell browning in *Thalictrum minus* cell cultures. *Plant Cell Reports*, **9**, 496–499.
- Kobayashi, Y. et al. (1993) Large-scale production of anthocyanin by *Aralia cordata* cell suspension cultures. *Applied Microbiology and Biotechnology*, **40**, 215–218.
- Koloini, T. (1990) Heat and mass transfer in industrial fermentation systems. *Progress in Biotechnology*, **6**, 215–239.
- Leckie, F., Scragg, A.M. and Cliffe, K.C. (1991a) An investigation into the role of initial k<sub>L</sub>a on the growth and alkaloid accumulation by cultures of *Catharanthus roseus*. *Biotechnology and Bioengineering*, **37**, 364–370.
- Leckie, F., Scragg, A.H. and Cliffe, K.C. (1991b) Effect of impeller design and speed on the large scale cultivation of suspension cultures of *Catharanthus roseus*. *Enzyme and Microbial Technology*, **13**, 801–810.
- Li, G.-Q., Shin, J.H. and Lee, J.M. (1995) Mineral oil addition as a means of foam control for plant cell cultures in stirred tank fermenters. *Biotechnology Letters*, **9**, 713–718.
- MacLoughlin, P.F., Malone, D.M., Murtagh, J.T. and Kieran, P.M. (1998) The effects of turbulent jet flows on plant cell suspension cultures. *Biotechnology and Bioengineering*, **58**, 595–604.
- Madhusudan, R. and Ravishankar, G.A. (1996) Gradient of anthocyanin in cell aggregates of *Daucus carota* in suspension cultures. *Biotechnology Letters*, **18**, 1253–1256.
- Matsubara, K., Kitani, S., Yoshioka, T., Morimoto, T. and Fujita, Y. (1989) High density culture of *Coptis japonica* cells increases berberine production. *Journal of Chemical Technology and Biotechnology*, **46**, 61–69.
- Matsubara, K. and Fujita, Y. (1991) Production of berberine. In *Plant Cell Culture in Japan*, edited by A.Komamine, M.Misawa and F.DiCosmo, pp. 39–44. Tokyo: CMC.
- Meijer, J.J. (1989) Effects of hydrodynamic and chemical/osmotic stress on plant cells a stirred bioreactor. Ph.D. Thesis. Technical University of Delft, Delft, The Netherlands.
- Meijer, J.J., ten Hoopen, H.J.G., Luyben, K.Ch.A.M. and Libbenga, K.R. (1993) Effects of hydrodynamic stress on cultured plant cells: A literature survey. *Enzyme and Microbial Technology*, **15**, 234–238.
- Meijer, J.J., ten Hoopen, H.J.G., van Gameren, Y.M., Luyben, K.Ch.A.M. and Libbenga, K.R. (1994) Effects of hydrodynamic stress on the growth of plant cells in batch and continuous culture. *Enzyme and Microbial Technology*, **16**, 467–477.
- Mirjalili, N. and Linden, J.C. (1995) Gas phase composition effects on suspension cultures of *Taxus cuspidata*. *Biotechnology and Bioengineering*, **48**, 123–132.

- Namdev, P.K. and Dunlop, E.H. (1995) Shear sensitivity of plant cells in suspension. *Applied Biochemistry and Biotechnology*, **54**, 109–131.
- Nienow, A.W. (1998) Hydrodynamics of stirred bioreactors. *Applied Mechanics Review*, **51**, 3–32.
- Otsuji, K. (1999) Personal communication.
- Pareilleux, A. and Vinas, R. (1983) Influence of aeration rate on the growth yield in suspension cultures of *Catharanthus roseus*. *Journal of Fermentation Technology*, **61**, 429–433.
- Park, I.-S. and Kim, D.-I. (1993) Significance of fresh weight to dry cell weight ratio in plant cell suspension cultures. *Biotechnology Techniques*, **7**, 627–630.
- Park, J.M., et al. (1992) Production of sanguinarine by suspension cultures of *Papaver somniferum* on bioreactors. *Journal of Fermentation and Bioengineering*, **74**, 292–296.
- Payne, G.F., Bringi, V., Prince, C. and Shuler, M.L. (1991) *Plant Cell and Tissue Culture in Liquid Systems*. Munich: Carl Hanser Verlag.
- Prokop, A. and Bajpai, R.K. (1992) The sensitivity of biocatalysts to hydrodynamic shear stress. *Advances in Applied Microbiology*, **37**, 165–232.
- Reuß, M., Rosic, D., Popovic, M. and Brönn, W.K. (1979) Viscosity of yeast suspensions. *Applied Microbiology and Biotechnology*, **8**, 167–175.
- Ritterhaus, E., Ulrich, J. and Westphal, K. (1990) Large-scale production of plant cell cultures. *International Association of Plant Tissue Culture Newsletter*, **61**, 2–10.
- Rodriguez-Monroy, M. and Galindo, E. (1999) Broth rheology, growth and metabolite production of *Beta vulgaris* suspension culture: A comparative study between cultures grown in shake flasks and in a stirred tank. *Enzyme and Microbial Technology*, **24**, 687–693.
- Sahai, O. (1994) Plant tissue culture. In *Bioprocess Production of Flavor, Fragrance and Color Ingredients*, edited by A.Gabelman, pp. 239–275. New York: John Wiley & Sons, Inc.
- Sahai, O.P. and Shuler, M.L. (1982) On the non-ideality of chemostat operation using plant cell suspension cultures. *Canadian Journal of Botany*, **60**, 692–700.
- Sahai, O.P. and Shuler, M.L. (1984) Multi-stage continuous cultures to examine secondary metabolite formation in plant cells: phenolics from *Nicotiana tabacum*. *Biotechnology and Bioengineering*, **26**, 27–36.
- Schiel, O. and Berlin, J. (1987) Large-scale fermentation and alkaloid production of cell suspension cultures of *Catharanthus roseus*. *Plant Cell Tissue and Organ Culture*, **8**, 153–161.
- Schlattmann, J.E., Nuutila, A.M., van Gulik, W.M., ten Hoopen, H.J.G., Verpoorte, R. and Heijnen, J.J. (1993) Scale-up of ajmalicine production by plant cell cultures of *Catharanthus roseus*. *Biotechnology and Bioengineering*, **41**, 253–262.
- Schlattmann, J.E., Fonck, E., ten Hoopen, H.J.G. and Heijnen, J.J. (1994a) The negligible role of CO<sub>2</sub> and ethylene in ajmalicine production by *Catharanthus roseus* cell suspensions. *Plant Cell Reports*, **14**, 157–160.
- Schlattmann, J.E., Moreno, P.R.H., Vinke, J.L., ten Hoopen, H.J.G., Verpoorte, R. and Heijnen, J.J. (1994b) Effect of oxygen and nutrient limitation on ajmalicine production and related enzymes in high density cultures of *Catharanthus roseus*. *Biotechnology and Bioengineering*, **44**, 461–468.
- Schlattmann, J.E., Vinke, J.L., ten Hoopen, H.J.G. and Heijnen, J.J. (1995) Relation between dissolved oxygen concentration and ajmalicine production rate in high density cultures of *Catharanthus roseus*. *Biotechnology and Bioengineering*, **45**, 435–439.
- Schlattmann, J.E., ten Hoopen, H.J.G. and Heijnen, J.J. (1996) Large-scale production of secondary metabolites by plant cell cultures. In *Plant Cell Culture Secondary Metabolism—Toward Industrial Application*, edited by F.DiCosmo and M.Misawa, pp. Boca Raton: CRC.
- Scragg, A.H., Allan, E.J. and Leckie, F. (1988) Effect of shear on the viability of plant cell suspensions. *Enzyme and Microbial Technology*, **10**, 361–367.
- Scragg, A.H. (1995) The problems associated with high biomass levels in plant cell suspension cultures. *Plant Cell Tissue and Organ Culture*, **43**, 163–170.
- Shaaltiel, Y. (1999) Personal communication.

- Shamakov, N.V. *et al.* (1991) Large-scale ginseng cultivation in suspension II. *Soviet Biotechnology*, **1**, 41–44.
- Shuler, M.L. (1999) Overview of yield improvement strategies for secondary metabolite production in plant cell culture. In *Plant Cell and Tissue Culture for the Production of Food Ingredients*, edited by T.-J.Fu, G.Singh and W.R.Curtis, pp. 75–83. New York: Kluwer Academic/Plenum Publishers.
- Singh, G. and Curtis, W.R. (1994a) Reactor design for plant cell suspension culture. In *Biotechnological Applications of Plant Cultures*, edited by P.D.Shargool and T.T.Ngo, pp. 151–183. Boca Raton: CRC Press.
- Singh, G. and Curtis, W.R. (1994b) Reactor design for plant root culture. In *Biotechnological Applications of Plant Cultures*, edited by P.D.Shargool and T.T.Ngo, pp. 185–206. Boca Raton: CRC Press.
- Singh, V. (1999) Disposable bioreactor for cell culture using wave-induced action. *Cytotechnology*, **30**, 149–158.
- Smart, N.J. and Fowler, M.W. (1981) Effect of aeration on large-scale cultures of plant cells. *Biotechnology Letters*, **3**, 171–176.
- Smith, J.M., Davison, S.W. and Payne, G.F. (1990) Development of a strategy to control the dissolved concentration of oxygen and carbon dioxide at constant shear in a plant cell bioreactor. *Biotechnology and Bioengineering*, **35**, 1088–1101.
- Smith, M.A.L. (1995) Large scale production of secondary metabolites. In *Current Issues in Plant Molecular and Cellular Biology*, edited by M.Terzi, R.Cella, and A.Falavigna, pp. 669–674. Dordrecht: Kluwer Academic.
- Soule, J.J., Wilhelm, A.M., Riba, J.P. and Ambid, C. (1987) Bioréacteur à contraintes mécaniques contrôlées: Application à la culture in vitro de cellules végétales. *Entropie*, **23**, 24–32.
- Steward, N., Martin, R., Engasser, J.M. and Goergen, J.L. (1999a) Determination of growth and lysis kinetics in plant cell suspension cultures from the measurement of esterase release. *Biotechnology and Bioengineering*, **66**, 114–121.
- Steward, N., Martin, R., Engasser, J.M. and Goergen, J.L. (1999b) A new methodology for plant cell viability assessment using intracellular esterase activity. *Plant Cell Reports*, **19**, 171–176.
- Su, W.W. (1995) Bioprocessing technology for plant cell suspension cultures. *Applied Biochemistry and Biotechnology*, **50**, 189–230.
- Su, W.W. and Humphrey, A.E. (1991) Production of rosmarinic acid from perfusion culture of *Anchusa officinalis* in a membrane aerated bioreactor. *Biotechnology Letters*, **13**, 793–798.
- Su, W.W., Lei, F. and Su, L.Y. (1993) Perfusion strategy for rosmarinic acid production by *Anchusa officinalis*. *Biotechnology and Bioengineering*, **42**, 884–890.
- Su, W.W., He, B.J., Liang, H. and Sun, S. (1996) A perfusion air-lift bioreactor for high density plant cell cultivation and secreted protein production. *Journal of Biotechnology*, **50**, 225–233.
- Sun, X. and Linden, J.C. (1999) Shear stress effects on plant cell suspension cultures in a rotating wall vessel bioreactor. *Journal of Industrial Microbiology and Biotechnology*, **22**, 44–47.
- Takahashi, S. (1999) Personal communication.
- Takahashi, S. and Fujita, Y. (1991) Production of shikonin. In *Plant Cell Culture in Japan*, edited by A.Komamine, M.Misawa and F.DiCosmo, pp. 72–78. Tokyo: CMC.
- Takayama, S., Misawa, M., Ko, K. and Misato, T. (1977) Effect of culture conditions on the growth of *Agrostemma githago* cells in suspension culture and the concomitant production of an anti-plant virus substance. *Physiologia Plantarum*, **41**, 313–320.
- Takeda, T., Seki, M. and Furusaki, S. (1994) Hydrodynamic damage of cultured cells of *Carthamus tinctorius* in a stirred tank reactor. *Journal of Chemical Engineering of Japan*, **27**, 466–471.
- Takeda, T., Kitagawa, T., Takeuchi, Y., Seki, M. and Furusaki, S. (1998) Metabolic responses of plant cell culture to hydrodynamic stress. *Canadian Journal of Chemical Engineering*, **76**, 267–275.

- Takei, A., Shoga, Y., Hama, M., Honda, Y., Sugimura, Y. and Otsuji, K. (1995) Production of polysaccharides by liquid cultures of *Polianthes tuberosa* cells: high production by reduction in the viscosity of culture medium. *Biotechnology Techniques*, **9**, 253–258.
- Tanaka, H. (1982) Oxygen transfer in broths of plant cells at high density. *Biotechnology and Bioengineering*, **24**, 425–442.
- Tanaka, H., Nishijima, F., Suwa, M. and Iwamoto, T. (1983) Rotating drum fermenter for plant cell suspension cultures. *Biotechnology and Bioengineering*, **25**, 2359–2370.
- Tanaka, H., Semba, H., Jitsufuchi, T. and Harada, H. (1988) The effect of physical stress on plant cells in suspension cultures. *Biotechnology Letters*, **10**, 485–490.
- Tate, J.L. and Payne, C.F. (1991) Plant cell growth under different levels of oxygen and carbon dioxide. *Plant Cell Reports*, **10**, 22–25.
- Thomas, C.R. (1990) Problems of shear in biotechnology. In *Critical Reports on Applied Chemistry: Chemical Engineering Problems in Biotechnology*, edited by M.A.Winkler, Volume 29, pp. 23–94. London: Elsevier Applied Science.
- Treat W.J., Engler, C.R. and Soltes, E.J. (1989) Culture of photomixotrophic soybean and pine in a modified fermentor using a novel impeller. *Biotechnology and Bioengineering*, **34**, 1191–1202.
- Tsoulphar, P. and Doran, P.M. (1991) Solasodine production from self-immobilised *Solanum aviculare* cell. *Journal of Biotechnology*, **19**, 99–110.
- van Gulik, W.M., ten Hoopen, H.J.G., and Heijnen, J.J. (1992) Kinetics and stoichiometry of growth of plant cell cultures of *Catharanthus roseus* and *Nicotiana tabacum* in batch and continuous fermentors. *Biotechnology and Bioengineering*, **40**, 863–874.
- Venkat, K. (1996) Press Release, Phyton Inc., Ithaca, NY, August 21.
- Verpoorte, R., van der Heijden, R., ten Hoopen, H.J.G. and Memelink, J. (1999) Novel approaches to improve secondary metabolite production. In *Plant Cell and Tissue Culture for the Production of Food Ingredients*, edited by T.-J.Fu, G.Singh and W.R.Curtis, pp. 85–100. New York: Kluwer Academic/Plenum Publishers.
- Verpoorte, R., van der Heijden, R., van Gulik, W. and ten Hoopen, H.J.G. (1991) Plant biotechnology for the production of alkaloids: present status and prospects. In *The Alkaloids*, edited by A.Brossi, Volume 40, pp. 2–187, London: Academic Press.
- Wagner, F. and Vogelmann, H. (1977) Cultivation of plant tissue cultures in bioreactors and formation of secondary metabolites. In *Plant Tissue Culture and Its Biotechnological Applications*, edited by W.Barz, E.Reinhard and M.H.Zenk, pp. 245–252. Berlin: Springer-Verlag.
- Wang, S.-J. and Zhong, J.-J. (1996) A novel centrifugal impeller bioreactor I. Fluid circulation, mixing and liquid velocity profiles. *Biotechnology and Bioengineering*, **51**, 511–519.
- Wilson, G. (1980) Continuous culture of plant cells using the chemostat principle. *Advances in Biochemical Engineering*, **16**, 1–25.
- Winkler, M.A. (1990) Problems in fermenter design and operation. In *Critical Reports on Applied Chemistry: Chemical Engineering Problems in Biotechnology*, edited by M.A.Winkler, Volume 29, pp. 215–350. London: Elsevier Applied Science.
- Wongsamuth, R. and Doran, P.M. (1994) Foaming and cell floatation in suspended plant cell cultures and the effect of chemical antifoams. *Biotechnology and Bioengineering*, **44**, 481–488.
- Wongsamuth, R. and Doran, P.M. (1997) The filtration properties of *Atropa belladonna* plant cell suspensions; Effects of hydrodynamic shear and elevated carbon dioxide levels on culture and filtration properties. *Journal of Chemical Technology and Biotechnology*, **69**, 15–26.
- Wu, J. and Zhong, J.-J (1999) Production of ginseng and its bioactive components in plant cell cultures: Current technological and applied aspects. *Journal of Biotechnology*, **68**, 89–99.
- Xu, J.F., Su, Z.G. and Feng, P.S. (1998) Suspension culture of compact callus aggregate of *Rhodiola sachalinensis* for improved salidroside production. *Enzyme and Microbial Technology*, **23**, 20–27.

- Yokoi, H., Koga, J., Yamamura, K., Seike, Y. and Tanaka, H. (1993) High density cultivation of plant cells in a new aeration-agitation type fermenter, Maxblend Fermenter®. *Journal of Fermentation and Bioengineering*, **75**, 48–52.
- Yokoyama, M. (1996) Industrial application of biotransformations using plant cell cultures. In *Plant Cell Culture Secondary Metabolism—Toward Industrial Application*, edited by F.DiCosmo, and M.Misawa, pp. 79–121. Boca Raton: CRC Press.
- Zhang, Y.-H., Wang, H.-Q., Liu, S., Yu, J.-T. and Zhong, J.-J. (1997) Regulation of apparent viscosity and O<sub>2</sub> transfer coefficient by osmotic pressure in cell suspensions of *Panax notoginseng*. *Biotechnology Letters*, **19**, 943–945.
- Zhong, J.-J., Seki, T., Kinoshita, S.-I. and Yoshida, T. (1992a) Effect of surfactants on cell growth and pigment production in suspension cultures of *Perilla frutescens*. *World Journal of Microbiology and Biotechnology*, **8**, 106–109.
- Zhong, J.-J., Tatsuzi, S., Kinoshita, S.-I. and Yoshida, T. (1992b) Rheological characteristics of cell suspension and cell culture of *Perilla frutescens*. *Biotechnology and Bioengineering*, **40**, 1256–1262.
- Zwietering, T.N. (1958) Suspending of solid particles in liquid by agitators. *Chemical Engineering Science*. **8**, 244–253.

# CHAPTER FIFTEEN

## LETHAL EFFECTS OF BUBBLES IN ANIMAL-CELL CULTURE

DIRK E.MARTENS, MICHEL F.MULLER, CORNELIS D.DE  
GOOIJER AND JOHANNES TRAMPER

*Food and Bioprocess Engineering Group, Wageningen University, P.O.  
Box 8129, 6700 EV Wageningen, The Netherlands*

### ABSTRACT

One of the main problems in the scale-up of animal-cell cultures is supply of oxygen and removal of carbon dioxide. It has long been known that sparging causes excessive cell death due to the fragility of animal cells. There is convincing evidence that this cell death occurs at bubble rupture in the rapid retracting rim of the breaking bubble film and during the subsequent collapse of the bubble cavity. Although unlikely, cell death may also occur at the sparger during bubble formation either due to contact of the cell with a rapid expanding bubble surface or due to the local liquid flows. Also the subsequent rise of the bubble to the surface is very likely not to cause cell death. However, during bubble formation and rise cells may attach to the bubble and be transported to the surface where they are killed. The number of cells killed per bubble increases with bubble diameter for bubble diameters in the range from 0.5 mm to 6 mm. Cell death may be prevented through the addition of certain protective additives like Pluronics and Methocels. These additives protect the cells most probably through reducing the severity of the bubble burst and through strengthening the cell as a consequence of adsorption to the cell membrane. In addition, some of these compounds prevent adsorption of cells to the bubble surface and thus prevent the cells from being in the danger zone. Apart from adding these additives, cell death may be minimised by optimising the amount of oxygen transferred per bubble, through increasing the height of the reactor.

**Keywords:** Animal cell, bubble, cell death, shear, Pluronic

### INTRODUCTION

At present animal-cell culture is used for the production of a large number of pharmaceutical proteins. With over 1200 proteins in clinical trials in 1998 this number is expected to increase in the coming years. As a consequence there will be an increasing demand for medium-and large-scale production facilities. For medium-(10 to 1000 litre)

and large-scale (>1000 litre) production, suspension cultures are being used mostly. The major concern in scale-up of suspension cultures is the supply of oxygen and removal of carbon dioxide. Gas transfer may be enhanced by the direct sparging of gas into the culture medium and by dispersing the gas bubbles using high agitation speeds. However, animal cells are relatively fragile compared to microbial cells due to their larger size and lack of a protective cell wall. As a consequence, the hydrodynamic forces generated during sparging and bubble dispersion cause damage to the cells.

Oh *et al.* (1989, 1992) showed that in a 1.4 dm<sup>3</sup> bioreactor agitation up to 450 rpm does not damage cells as long as no sparging is used. Likewise, Chisti (1993) found that hybridoma cells can be cultured in a 0.3 m<sup>3</sup> stirred-tank reactor notwithstanding high (>1 m.s<sup>-1</sup>) impeller tip speeds and fluid turbulence. Finally, Kunas and Papoutsakis (1990) showed that as long as bubbles can not interact with a freely moving air-liquid interface, agitation becomes detrimental only at agitation rates far higher than those generally used in animal-cell bioreactors. Thus, it can be safely stated that cell death solely due to agitation does not occur under normal conditions. In contrast, the hydrodynamic forces associated with the presence of air bubbles have been shown to cause excessive damage to animal cells in numerous studies. There have been many reports trying to elucidate the mechanism of air-bubble-related cell death and model this process. For reviews the reader is referred to Chalmers (1994, 1996), Hua *et al.* (1993), Papoutsakis (1991a, 1991b) and Wu (1995b). Although progress has been made, the information is still quite scattered and incomplete. In this chapter the current knowledge is summarised and the remaining questions with respect to bubble-related cell death are discussed.

For optimal design and operation of a reactor in terms of minimising shear-related cell death one would like to be able to predict cell damage directly from design parameters using a mechanistic model. Essentially three types of knowledge are required for such a model (Zhang and Thomas, 1993a; Papoutsakis, 1991a). These concern knowledge about (i) the hydrodynamics in the reactor; (ii) the response of the individual cells in a cell population to hydrodynamic forces; and (iii) the mechanism by which the hydrodynamic forces interact with the cells. Because information on all three aspects mentioned above is not available, empirical models have been constructed just relating design parameters to cell death. The parameters of these models are determined from experiments. The main disadvantage of this approach is that extrapolation of the results to, for instance, different cell lines, medium formulations, and reactor scales is not allowed. The response of animal cells to hydrodynamic forces may range from increase in DNA-synthesis rate (Lakhotia and Papoutsakis, 1992) and metabolic rates (Al-Rubeai *et al.*, 1990) to cell death through apoptosis, necrosis or direct lysis (Al Rubeai *et al.*, 1995a, 1995b). Here we will only consider cell death.

From the start of animal-cell culture substances have been added that protect the cells against hydrodynamic forces (Papoutsakis, 1991b). Protective additives include Pluronic polyols, derivatised cellulose, polyethylene glycol (PEG), polyvinyl alcohol (PVA), dextran, and protein mixtures like serum. The protection mechanism is closely related to the damage mechanism and may be attributed to (i) increasing the strength of the cells, (ii) decreasing the hydrodynamic forces, and (iii) shielding the cells from the regions with damaging hydrodynamic forces. Therefore, these compounds and their protection mechanism will be treated throughout this chapter. In Table 15.1 some of the most common additives are listed together with their physical properties.

In this chapter empirical models describing the specific death rate due to sparging as a function of reactor parameters are first discussed. Next, current knowledge on the mechanism of cell death due to sparging is reviewed. For this it is necessary to have knowledge of the mechanical properties of animal cells and the interaction of cells with air bubbles, which are therefore discussed first. With this knowledge in mind, the possible mechanisms of cell death are reviewed for different regions in the reactor; the

**Table 15.1** Static surface tension  $\sigma_0$ , dynamic surface tension  $\sigma_d$ , surface viscosity  $\mu^s$ , and surface dilatational viscosity  $k^s$  of media with different additives

Medium	Cone (%)	$\sigma_0 \text{ mN.}^{-1}$	$\sigma_d \text{ mN.}^{-1}$	$\mu^s 10^{-4} \text{ N.m}^{-2}$	$k^s 10^{-4} \text{ N.m}^{-2}$	Ref.
HBBS			72.8			Chattopadhyay 1995b
RPMI		70			0.25	Dey 1997
TNM-FH		47.3	69.4			Chattopadhyay 1995b
SFM-L			64			Chattopadhyay 1995b
Serum free		61	70.8	5.1	0.46	Michaels 1995b
Serum	0.5		70.8			Michaels 1995b
	0.5	54				Dey 1999
	1.0		70.4			Michaels 1995b
	3.0		68.9	18200	1.36	Michaels 1995b
	5.0		69.2			Michaels 1995b
	5.0					Michaels 1995b
	5.0	52.4			1.5	Dey 1997
	10.0		68.8			Michaels 1995b
Pluronic F68	0.1	48	57.6	2.4	0.37	Michaels 1995b
	0.1	40				Dey <i>et al.</i> 1997
	0.1	44.1	56.1			Chattopadhyay 1995b
	0.2	38			2	Dey 1997
Methocel E50	0.1	52	55.7		<0.1	Michaels 1995b
	0.3	66.1	55.5			Chattopadhyay 1995b

PVA	0.1	47	65	2	1.24	Michaels 1995b
	0.1	48.7	71.5			Chattopadhyay 1995b
PVP	0.1	53	61.1	41600	0.25	Michaels 1995b
PEG 8000	0.1	52	62.3	77	<0.1	Michaels 1995b
PEG 4000	0.1	45.9	65.7			Chattopadhyay 1995b

sparger zone, the zone of bubble rise, the zone of bubble escape and the foam layer. The section on the mechanism of bubble-related cell death ends with a discussion on whether bubble break-up and coalescence may contribute to cell death and a summary of the protection mechanism of different additives. Finally, the chapter ends with a discussion on the possibility of reducing bubble-related cell death through proper reactor design.

## OVERALL THEORIES

Damaging effects of sparging were reported as early as 1965 (Telling and Elsworth 1965). Since then numerous studies have been devoted to the relation between air bubbles and cell death. Tramper *et al.* (1988) were the first to describe the amount of cell death due to sparging as a function of design parameters in their hypothetical-killing-volume theory. The main hypothesis of the theory is that a hypothetical volume,  $V_d$  ( $\text{m}^3$ ), associated with each air bubble during its life time exists, in which all viable cells are killed. A balance over the viable cells in the reactor assuming cell growth is negligible gives

$$V \frac{dC_v}{dt} = \xi \cdot C_v \cdot V_d = \frac{6F}{\pi \cdot d_b^3} \cdot C_v \cdot V_d \quad (1)$$

where  $V(\text{m}^3)$  is the reactor volume,  $C_v$  ( $\text{cells} \cdot \text{m}^{-3}$ ) is the concentration of viable cells,  $t$  (s) is the time,  $\xi$  ( $\text{s}^{-1}$ ) is the number of bubbles generated per second,  $F$  ( $\text{m}^3 \cdot \text{s}^{-1}$ ) is the gas-flow rate, and  $d_b$  (m) is the bubble diameter.

Assuming next that the hypothetical killing volume, the gas-flow rate, reactor volume, and bubble diameter are time independent, equation (1) can be written as

$$\frac{dC_v}{dt} = -k_d \cdot C_v \quad (2)$$

where  $k_d$  ( $\text{s}^{-1}$ ) is the first-order death-rate constant given by

$$k_d = \frac{6 \cdot F \cdot V_d}{\pi \cdot d_b^3 \cdot V} = \frac{24 \cdot F \cdot V_d}{\pi^2 \cdot d_b^3 \cdot T^2 \cdot H} \quad (3)$$

where  $T$  (m) is the reactor diameter and  $H$  (m) the reactor height. The model has been verified at lab scale by different authors. Table 15.2 summarises this work. Thus, it was shown that the killing volume is independent from the gas-flow rate, reactor height, and

reactor diameter. In Figure 15.1 an example is shown on the relation between the first-order death-rate constant and the gas-flow rate and reactor height (Martens *et al.* 1992). Furthermore, Tramper *et al.* (1988) showed that the hypothetical killing volume is proportional to the bubble volume.

Wu and Goosen (1995 a) derived an equation correlating the hypothetical killing volume of a gas bubble to its surface. They assumed that cell death occurs only at the medium surface, where bubble escape takes place. Furthermore, they made a distinction between the part of the bubble that is above the liquid level at burst (the bubble cap) and the part that is below the surface (the bubble cavity). Next, they proposed that the

**Table 15.2** Small-scale bubble-column (BC) and air-lift (AL) experiments

Reactor	Additives	Cell	F/V s <sup>-1</sup>	d <sub>b</sub> mm	v <sub>d</sub> 10 <sup>-10</sup> m <sup>3</sup>	Ref.
BC	0.1%MC10%FBS	Sf-21	0.016	3.5	0.4	Tramper 1988
BC	5% FCS	Hybridoma	0.001	1.6	0.06	Handa 1987
BC	none	Sf-21			7.0	Trinh 1994
BC	5%FBS	Sf-21	0.005	3.5 <sup>a</sup>	1.9	Wu 1995a
BC	1% FCS	Hybridoma	0.028	5 <sup>b</sup>	4.8	Jobses 1991
BC	none	Hybridoma	0.020	3.5 <sup>a</sup>	8.6	Pol 1992
BC	5% FCS	Hybridoma	0.020	3.5 <sup>a</sup>	1.7	Pol 1990
BC	5% FCS	Hybridoma	0.005	1.1	1.7	Orton 1992
AL	5% FCS	Vero	0.11	3.5 <sup>a</sup>	0.5	Martens 1992
AL	0.5% FCS	Hybridoma	0.028	3.5 <sup>c</sup>	2.1	Martens 1996
BC	0.1% Pluronic F68	Sf-21	0.20	5 <sup>c</sup>	1.4	Cherry 1992

<sup>a</sup>Value for the bubble diameter not given and arbitrary set at 3.5 mm.

<sup>b</sup>Average bubble diameter.

<sup>c</sup>Smallest measured bubble diameter.

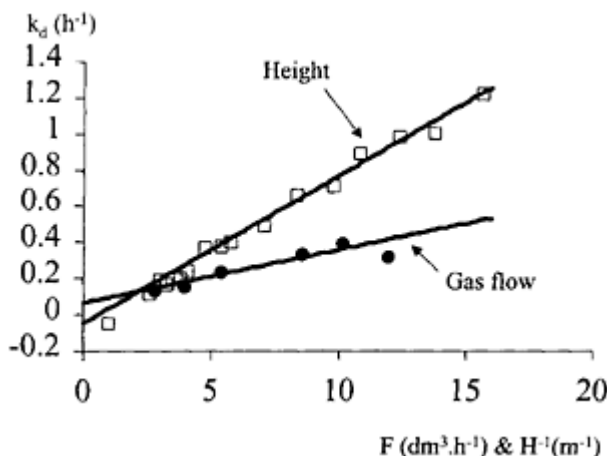


**Figure 15.1** First-order death-rate constant in a small bubble column as a function of the air-flow rate and reciprocal column height (Martens *et al.* 1992).

killing volume consists of the liquid present in the liquid film of the cap and in a thin liquid layer surrounding the bubble cavity. This led to the following equation for the killing volume:

$$V_d = k_1 \cdot (h_f \cdot A_f + h_c \cdot A_c) \quad (4)$$

where  $h_f, h_c$  (m) are the thickness of, respectively, the film and cavity layer,  $A_f, A_c$  ( $\text{m}^2$ ) are the surface areas of respectively the bubble cap and bubble cavity and  $k_1(-)$  is a dimensionless constant. Assuming a spherical bubble and an equal thickness of the bubble-cap film and the liquid layer around the cavity, this equation was simplified to

$$V_d = k_2 \cdot d_b^2 \quad (5)$$

where  $k_2$  (m) is a constant. If the film thickness in the bubble cap is different from that in the bubble cavity, it is necessary to calculate the surfaces of the cap and cavity separately. Wu and Goosen (1995a) derived equations for this on the basis of spherical bubbles, which, as they stated, is valid only for bubbles smaller than 2 mm. For bubbles between 2 and 5 mm the calculations are only approximate. Up to a bubble diameter of 3.5 mm they showed that less than 10% of the surface area belongs to the bubble cap and death is mainly attributed to the cavity. For bubbles larger than 5 mm a substantial part of the surface is located in the bubble cap, meaning that this cap becomes more important for cell death. They showed experimentally that the killing volume is proportional to the bubble surface area for bubble diameters ranging from 0.5–4.5 mm. This is different from

the findings of Tramper *et al.* (1988), who found that  $V_d$  is proportional to the bubble volume. It also differs from the findings of Handa *et al.* (1985), who found that smaller bubbles were more detrimental on a per bubble basis. Figure 15.2 summarises the data on the effect of bubble diameter on the hypothetical killing volume. The following equation is fitted to the data of Tramper *et al.* (1988) and Wu and Goosen (1995a):

$$V_d = V_{d0} + k \cdot d_b^p \quad (6)$$

where  $V_{d0}$  ( $\text{m}^3$ ) represents the part of the killing volume that is not a function of the bubble diameter,  $k$  (–) is a constant, and  $p$  (–) is the power coefficient. Table 15.3 gives the results

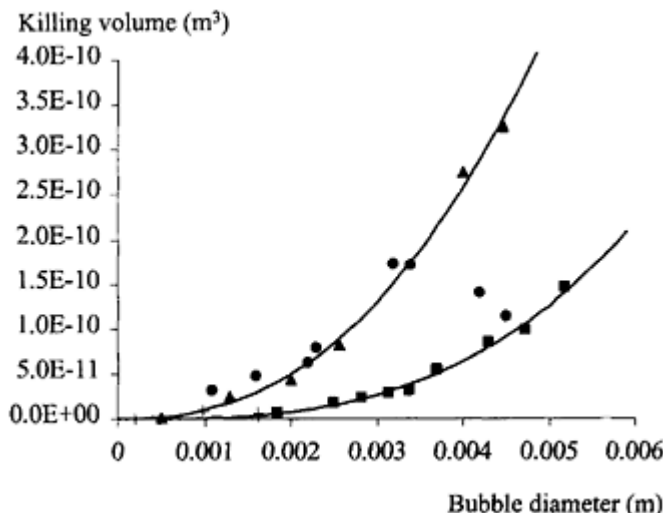


**Figure 15.2** Hypothetical killing volume as a function of bubble diameter. (■) Tramper *et al.* (1988), (▲) Wu and Goosen (1995a), (●) Orton (1992), (+) Handa *et al.* (1987) The lines represent the least-square regression lines of equation (6) through the data of Tramper *et al.* (1988) and Wu and Goosen (1995a).

**Table 15.3** Results of the fit of equation 6 to the data of Tramper *et al.* (1988) and Wu and Goosen (1995a) shown in Figure 15.2. Numbers between parentheses are the 95% confidence intervals

Parameter	Tramper <i>et al.</i> (1988)	Wu and Goosen (1995a)
$V_{d0}(\text{m}^3)$	$-5 (-176+166) 10^{-13}$	$-1 (-360+358) 10^{-13}$
k	0.001 ( $-0.005+0.008$ )	0.0001 ( $-0.0005+0.0008$ )
p	3.0 (2.0 4.1)	2.4 (1.4 3.3)
$r^2$	0.988	0.995
F-value	257	302
Data points	9	6

for the two data sets. The difference between the power coefficients is not significant and the values of 2 and 3 fall within the 95% confidence intervals for both sets. Consequently, on the basis of these data sets it is not possible to determine whether the killing volume is proportional to the bubble surface or bubble volume. The killing volumes of Wu and Goosen (1995a) are higher than those of Tramper *et al.* (1988) due to the fact that Tramper *et al.* (1988) used 10% FCS and 0.1% methyl-cellulose, while Wu and Goosen (1995a) only used 5% FBS. The data of Orton (1992) (taken from Meier *et al.* 1999) follow the curve of the data of Wu and Goosen (1995a) quite well, except for the last two points. In contrast to the above studies, which all showed that larger bubbles are more detrimental in the range of 0.5–5 mm, Handa *et al.* (1985) found that smaller bubbles (1 mm) were more damaging than larger bubbles (1.6 mm) on a per bubble basis. This difference may originate from the differences in experimental set-up. Handa *et al.* (1985) quantified cell damage from the maximum attained cell density in bubble columns operated in batch mode during three to four days at moderate sparging rates ( $10^{-4}$ – $10^{-3}$  vvm). The other authors studied the decrease in viable cells in small bubble columns for three to six hours at intense sparging conditions ( $5 \cdot 10^{-3}$ – $10^{-2}$  vvm).

Wang *et al.* (1994) presented a theory that is comparable in approach to the hypothetical-killing-volume theory. They defined an inactivation zone,  $\chi$  ( $\text{m}^3 \cdot \text{m}^{-3}$ ), around each bubble with a thickness  $s$  (m). Cells in this zone have a probability  $q$  of being inactivated. This resulted in the next Michaelis-Menten-like expression describing cell death:

$$\frac{dC_v}{dt} = \frac{k_2 \cdot a \cdot s \cdot C_v}{K + C_v} \quad (7)$$

where  $k_2$  ( $\text{cells} \cdot \text{m}^{-3} \cdot \text{s}^{-1}$ ) is the maximum inactivation rate reflecting the probability of a cell in the inactivation zone becoming inactivated,  $K$  ( $\text{cells} \cdot \text{m}^{-3}$ ) is the saturation constant expressing more or less the affinity for cells to be in the inactivation zone, and  $a$  is the specific surface area ( $\text{m}^{-1}$ ). When the unoccupied inactivation volume is much larger than that occupied by cells equation (7) can be simplified to

$$k_d = \frac{k_2 \cdot s}{K} \cdot a \quad (8)$$

For the case of a bubble column without coalescence and bubble break-up the specific surface area can be substituted giving

$$k_d = \frac{6 \cdot F}{V \cdot d_b^3} \cdot \frac{k_2}{K} \cdot d_b^2 \cdot s \quad (9)$$

This equation equals equation (3) for the hypothetical-killing-volume theory, with the killing volume being proportional to the bubble surface ( $V_d = (k_2/K)d_b^2 s$ ). Thus the main difference with the model of Tramper *et al.* (1988) is that the model of Wang *et al.* (1994) is proportional to the square of the bubble diameter instead of to the third power.

## MECHANISM OF CELL DEATH AND LOCATION OF THE KILLING VOLUME

The hypothetical-killing-volume theory of Tramper *et al.* (1988) does in fact not specify where the hypothetical killing volume is located. Although Wang *et al.* (1994) and Wu and Goosen (1995 a) suggested that the volume is located in a thin liquid layer around the bubble, experimentally a correlation is shown to exist only between their killing volume and the bubble diameter. A number of studies have been conducted to reveal the mechanism of cell damage and thereby the location of the killing volume. In the following section, first the mechanical properties of cells and the interaction of cells with air bubbles will be discussed. Next, possible mechanisms of cell death are reviewed for different zones in a bioreactor; the sparger zone, the zone of bubble rise, the zone of bubble escape and the foam layer. Finally, it is discussed whether bubble break-up and coalescence may contribute to cell death and a summary on the protection mechanism of different additives is given.

### Mechanical Properties of Animal Cells

In order to study the fragility of cells a number of authors have used simple shear devices like viscometers and capillary tubes. Table 15.4 gives an overview of the different methods used and the sensitivity of the cells. Abu-Reesh and Kargi (1989) exposed hybridoma cells for 30–180 minutes and found that cell damage in the turbulent-flow regime is more damaging than comparable shear stresses in the laminar-flow regime. To cause 50% loss of viable cells after one hour of shear, a shear level of about  $30 \text{ N.m}^{-2}$  was required for turbulent stress, while for laminar stress a level of  $55 \text{ N.m}^{-2}$  was required. McQueen and Bailey (1989) used hybridoma cells in a capillary system, wherein the flow was turbulent, and found a threshold wall shear stress of  $180 \text{ N.m}^{-2}$  below which no cell damage occurred. Tramper *et al.* (1986) found significant cell death in a viscometer after 3 hours at  $1 \text{ N.m}^{-2}$  in the presence of 0.1% methylcellulose (Methocel). After one hour only a small effect could be seen at  $55 \text{ N.m}^{-2}$ . For exposure times of 10 minutes Petersen *et al.* (1990) found already cell death at  $1 \text{ N.m}^{-2}$ . They observed that the shear sensitivity of cells in a batch culture is dependent on the phase of the culture and that this is not a consequence of changes in growth rate (Petersen *et al.* 1988, 1990). Michaels *et al.* (1991b) studied cells in viscometers in the presence of shear protecting agents. They

**Table 15.4** Shear sensitivity of different cells under different conditions. Presented is the lowest shear stress used in the reference and the exposure time required to cause about 10% loss in viable cells. For turbulent flows the average wall shear stress is given

Cell	Flow type	Shear stress N.m <sup>-2</sup>	Exposure time	Medium	Ref.
Hybridoma	Turbulent	5	1 h	15% FCS	Abu-Reesh 1989
Hybridoma	Laminar	20	1 h	15% FCS +dextran	Abu-Reesh 1989
Hybridoma	Laminar	86	10m		Augenstein 1971
Hybridoma	Laminar	200	10s	5% FCS+25% dextran	Born 1992
Blood cells	Laminar	10–20	10m	10% FCS	Chittur 1988
Tn-5, Sf-21	Laminar	7.3	20s	10% FCS	Goldblum 1990
Myeloma	Laminar	200	0.002s	10% FCS	McQueen 1989
Myeloma	Turbulent	180	0.01 s	10% FCS	McQueen 1989
Hybridoma	Laminar	5	10m	1% FCS	Petersen 1989
Hybridoma	Laminar	8	15 m	9% FBS	Ramirez 1990
Hybridoma	Laminar	15	3 m	10% FCS	Schuch 1988
Kidney	Laminar	2.6	1 h	10% FCS	Stathopoulos 1985
Sf 21	Laminar	55	1 h	10% FBS+ 0.1 %MC	Tramper 1986
Hybridoma	Turbulent	200	0.002s	5% FCS	Zhang 1993

found damaging shear stresses of 5 N.m<sup>-2</sup> for exposure times of 10 minutes. No short-term effect on shear sensitivity was observed for serum, Pluronic F68 and PEG, whereas long-term exposure to these compounds before shearing resulted in a decrease in shear sensitivity for serum only. Goldblum *et al.* (1990) studied the effect of Pluronic F68 on insect cells. They found that Pluronic F68 adsorbs to cell membranes and protect cells from shear. Al-Rubeai *et al.* (1995) and Murhammer and Goochee (1990a, 1990b) also suggested that Pluronic adsorbs to cell membranes. The latter authors showed that block-copolymers like Pluronics and reverse Pluronics may, depending on their structure either lyse cells, inhibit growth, or have no influence on cell growth and offer protection. Adsorption of Pluronics to the cell membrane is in accordance with studies of Ramirez and Mutharasan (1990, 1992). They showed that Pluronic as well as cholesterol, serum and a decrease of temperature reduce the plasma-membrane fluidity (PMF) and offer

protection when cells are exposed to laminar shear stresses of  $8 \text{ N.m}^{-2}$  for less than 20 minutes. EYL *et al.* (1992) reported that the PMF decreases during the batch growth phase and increases during the batch death phase, which agrees well with the findings of Petersen *et al.* (1988, 1990). With respect to Pluronic this does not agree with the results of Michaels *et al.* (1991b), who found no effect of Pluronic on the shear sensitivity of cells. Finally, Wu *et al.* (1997) actually measured the adsorption of Pluronic F68 and PEG to cells at different concentrations. Pluronic adsorption followed the Langmuir isotherm with maximum adsorption values of  $3.74 \mu\text{g}$  for  $10^6$  Sf-9 cells and  $4.54 \mu\text{g}$  for  $10^6$  Tn-5 cells. Half the maximum adsorption was reached at concentrations of  $2.8 \text{ g.m}^{-3}$  ( $0.0003\%$ ) and  $16 \text{ g.m}^{-3}$  ( $0.002\%$ ), respectively, which is far below concentrations normally used ( $0.1\%$ ). For PEG a plateau value was not observed and at a concentration of  $50 \text{ g.m}^{-3}$ ,  $30 \mu\text{g}$  and  $48.1 \mu\text{g}$  PEG was adsorbed per  $10^6$  sf-9 and Tn-5 cells, respectively. The main advantage of viscometer and capillary-tube studies over bioreactor studies is that they are done in a well-defined and controllable shear field. However, the shear sensitivity of the cells still cannot be separated from the interaction of the cells with the shear field. Thus, addition of protective compounds may affect the fragility of the cells as well as the interaction of the cells with the shear fields. Moreover, the exposure of cells is not comparable to the exposure in real bioreactors. For instance, exposure times are usually longer than the exposure occurring in bioreactors and besides the laminar and turbulent flows also elongational flows may occur as well (Garcia-Briones and Chalmers, 1994).

In the literature two methods are described to independently measure mechanical properties of individual cells. One method is the aspiration technique in which individual cells are sucked partly into a pipette (Sato *et al.*, (1987), Needham *et al.*, 1991). Assuming animal cells can be modelled as incompressible liquid drops with a constant cortical tension, Needham *et al.* (1991) calculated the cortical membrane tension, cell volume and apparent cell viscosity. According to Zhang and Thomas (1993a), this technique cannot be used to calculate the strength of individual cells, because it can only cause small deformations. Therefore, Zhang *et al.* (1991) developed a new micro-manipulation technique with which the force causing large deformations can be measured. In short, a cell is captured between two parallel surfaces (optic fibres) connected to a micro-manipulator. Next, the cell is squeezed by moving the surfaces towards each other, while at the same time the force applied is measured. From curves of the force applied versus the distance between the plates the bursting force and cell diameter can be obtained. Again modelling the cell as an incompressible liquid drop surrounded by a thin elastic membrane, the cell bursting membrane tension, bursting pressure and the elastic area compressibility modulus may be calculated.

Measurements with these techniques are carried out on whole cells in a time span of the order of 0.5 s. Interactions of cells with hydrodynamic forces may involve only part of the membrane and occur within milliseconds. Whereas, from a rational point of view, parameters like the bursting membrane tension are good measures of the strength of the membrane, the translation to situations in a real bioreactor remains a problem. To solve this problem, Born *et al.* (1992) developed models to describe the interaction of cells with laminar-shear fields in viscometers, while Zhang *et al.* (1993b) and Thomas *et al.* (1995) developed such models for turbulent-flow fields in capillary tubes. Upon shearing cells at high levels ( $200-600 \text{ N.m}^{-2}$ ) for short times (3 minutes) model predictions were within

30% of measured cell disruption, which ranged from 5 to 100%. For turbulent flow in a capillary good agreement was also obtained between measured data and model predictions, although the model still underestimated the cell death rate by 15%. Energy dissipation rates were about  $10^3 \text{ m}^2 \cdot \text{s}^{-3}$  corresponding to eddy lengths of  $5.9\mu\text{m}$ .

The technique is also very useful for comparing the fragility of different cells under different conditions. Thus, Zhang *et al.* (1992a, 1993c) showed that cells in the exponential phase of a batch culture are less fragile than cells in the death phase, which is in accordance with the data obtained by Petersen *et al.* (1991) and Ramirez and Mutharasan (1992). Furthermore, they showed that the cell fragility decreased in the presence of Pluronic F68 (Zhang *et al.* 1992b). There was a difference between long-term exposure, where 0.05% was sufficient and short-term exposure, where an effect was only seen above 0.1%. This is also in accordance with observations by Ramirez and Mutharasan (1991). Moreover, it is not difficult to imagine that a relation exists between plasma-membrane fluidity and the bursting membrane tension.

In conclusion, shear stresses at which cell damage occurs are in the order of  $1 \text{ N} \cdot \text{m}^{-2}$  and higher. The protective additive Pluronic F68 strengthens the cell probably through adsorption to the cell membrane. The shear stresses as measured in shear devices are, however, average shear stresses measured in shear devices for exposure times longer than minutes. The actual stresses cells are exposed to in these devices are somewhat higher than the average bulk shear stresses. Furthermore, exposure times are a factor 100–10,000 longer than those occurring in a bioreactor. Direct measurements of cell strength may be more informative. However, in this case additional models are required to connect the fragility of the cells to hydrodynamics of a bioreactor.

### Cell-Bubble Interaction

Bavarian *et al.* (1991) were the first authors to show attachment of insect cells to air bubbles. For successful cell attachment to air bubbles the free-energy change upon attachment must be negative and contact between cell and bubble is required. Wu *et al.* (1997) showed that cells attach to a water-hexadecane interface, thus demonstrating that a cell contains hydrophobic parts that in principle can also interact with air-liquid interfaces. Furthermore, they showed that addition of methyl-cellulose and Pluronic led to a dramatic decrease in adsorption to the hexadecane. In conjunction with the finding that Pluronic adsorbs to cells and that no stable droplets were formed at the interface, they deduced that the decrease in hydrophobicity of the cells is due to interaction of the cells with Pluronic and not due to adsorption of Pluronic to the hexadecane-water interface. Jordan *et al.* (1994) have experimentally shown that surfactants like Pluronics adsorb also to the bubble surface. Adsorption was due to convection rather than diffusion. Contact of cells with a bubble surface that contained no surfactants resulted in direct cell lysis, whereas contact with partially saturated covered bubble surface resulted in stable attachment of the cells to the surface. When the bubbles were completely saturated by adding 0.1% Pluronic or S% serum no interaction was observed. The fact that surfactants also adsorb to cells was not taken into account in this study.

Absalom *et al.* (1983) developed a model to describe adhesion of bacteria to surfaces based on changes in free enthalpy that in turn were related to interfacial tensions. Likewise, Chattopadhyay *et al.* (1995b) presented a thermodynamic approach to predict

whether a cell will adsorb to an air-bubble. Adsorption only occurs if the change in free energy upon adsorption is negative. This change is given by

$$dF^{ads} = \gamma_{final} - \gamma_{initial} = \gamma_{cv} - (\gamma_{lv} + \gamma_{cl}) \quad (10)$$

where  $\gamma_{cv}$  ( $N\cdot m^{-1}$ ) is the interfacial tension between the cells and the vapour,  $\gamma_{lv}$  ( $N\cdot m^{-1}$ ) is the interfacial tension between the liquid and the vapour,  $\gamma_{cl}$  ( $N\cdot m^{-1}$ ) is the interfacial tension between the cells and the liquid. Values for  $\gamma_{cv}$  and  $\gamma_{cl}$  were calculated by measuring the contact angle between a medium drop on a monolayer of cells. Assuming that the monolayer surface was chemically homogeneous and perfectly smooth and the system was in equilibrium, semi-empirical equations were used to calculate the values for the different surface tensions. Thus, they found that the values of  $\gamma_{cl}$  were very small ( $0-0.5\text{ mN}\cdot\text{m}^{-1}$ ) and do not contribute very much to the value of  $dF^{ads}$ , which is in accordance with the fact that cells are readily suspended in media. Values of  $\gamma_{cv}$  showed little variation and were usually in the range of  $60-70\text{ mN}\cdot\text{m}^{-1}$ . In the absence of additives the value of  $\gamma_{cv}\cdot\gamma_{lv}$  was of the order of  $-2\text{ mN}\cdot\text{m}^{-1}$ , indicating that adsorption can occur. Addition of 0.1% Pluronic or 0.3% Methocel resulted in a reduction of  $\gamma_{lv}$  with about  $10\text{ mN}\cdot\text{m}^{-1}$ . Because, complete wetting of the monolayer occurred in this case, the contact angle was zero and  $\gamma_{cv}$  could not be determined. However, as large changes in  $\gamma_{cv}$  are not expected, this made  $dF^{ads}$  positive. Consequently, adsorption will not occur, which is in accordance with the complete wetting of the monolayer surface.

In reality the membrane of a cell contains proteins (about 50%) and different lipids including glycosylated lipids and cholesterol. Thus, it is likely that the surface of a cell will be mainly hydrophilic, which is in accordance with the low  $\gamma_{cl}$ . However, parts of the cell surface will be hydrophobic, allowing for attachment to air bubbles. Furthermore, the membrane is fluid, meaning that with increasing contact time between a cell and a bubble, a redistribution of hydrophilic and hydrophobic parts may occur, with the hydrophobic parts concentrating on the cell-air interface. If we assume that the hydrophilic part is completely wetted by the liquid, the tension imposed on a cell is given by  $\gamma_{lv}$ . In order to prevent disruption of the cell, this tension is balanced by the surface tension of the cell  $\gamma_{cv}$ . If  $\gamma_{lv}$  is larger than  $\gamma_{cv}$ , the cell will be disrupted. However, this  $\gamma_{cv}$  is not the value determined by Chattopadhyay *et al.* (1995b), since their value is some kind of average value over the cell membrane. The value that should be filled in here should be representative of the value with which the cell membrane is held together.

Michaels *et al.* (1995a) measured the induction time ( $\tau$ ) for cell adhesion being the time cells should be in contact with a bubble in order to become attached. Measurements were done for serum-free medium with or without additives. Results are shown in Table 15.5. Clearly a negative free-energy change and cell-bubble contact is on itself not sufficient for attachment, but also the duration of contact is of importance. The increase in contact time for the different additives corresponds well with the decrease in surface tension, as would be expected from the results of Chattopadhyay *et al.* (1995b).

In conclusion, in the absence of surface-active compounds on the bubble surface cell-bubble contact may lead to direct cell death. In the presence of shear-protective additives cells may adsorb to the bubbles if they have been in contact with the bubble for a certain

**Table 15.5** Minimal contact time,  $\tau$ , for cell attachment to air bubbles cell movement and liquid drainage, and half life ( $t_{0.5}$ ) and height of the foam for different medium compositions (adapted from Michaels *et al.* (1995b) (see text for explanation of the parameters)

Medium formulation	$\tau$ ms	Cell movement	Thin film drainage	$t_{0.5}$	min	h cm
Basal medium	<10		Unstable			
Serum-free	50–100	Medium	Fast	4	7.4	
0.1% PVP	20–500	Slow	Slow	28	13.3	
0.1% PEG 8000	200–1000	Slow	Slow	7	15.0	
3%FBS	200–1000	Medium	Medium	65	21.4	
0.1% PVA	1000–10000	Fast	Fast	1	3.8	
0.1% Pluronic F68	5000–20000	Fast	Fast	0	2.0	
0.1%Methocel A15LV	no attachment	Fast	Fast	0	4.1	

required contact time. The length of this contact time depends on the type and concentration of the additive used.

### Cell Death at the Sparger

The bubble formation process at the sparger can be separated into two stages. In the first stage the bubble expands, while staying attached to the base. In the second stage the buoyancy force causes the bubble to move away from the base. Bubble growth continues through a narrowing neck connecting the bubble to the base. When this neck closes and the bubble detaches from the base, fluid rushes into the region of the bubble neck. Cell death near the sparger may have two causes.

One cause of cell death at the sparger may be the hydrodynamic forces associated with the flow of fluid around a growing and detaching bubble. The maximum velocity with which the bubble penetrates into the liquid may be calculated from

$$v_i = \frac{F}{n \cdot \pi \cdot d_i^2} \quad (11)$$

where  $n$  is the number of nozzles and  $d_i$  (m) is the diameter of a nozzle. Using this equation at  $F=1 \text{ dm}^3 \cdot \text{h}^{-1}$ ,  $n=1$  and  $d_i=1 \text{ mm}$  the injection velocity is equal to  $0.088 \text{ m} \cdot \text{s}^{-1}$ . Assuming the flow around the bubble is laminar, shear stresses associated with these flows may be estimated from

$$\tau = \mu \cdot \frac{dv}{dx} \quad (12)$$

where  $\mu$  is the dynamic viscosity, and  $dv/dx$  is the velocity gradient. For the velocity gradient  $dv$  is given by the maximum injector velocity,  $d_{vi}$ . It is more difficult to estimate  $dx$ , which depends on the thickness of the boundary layer around the bubble. Tramper *et al.* (1986) used the diameter of a cell for  $dx$ . For normal medium with a dynamic viscosity equal to that of water and a cell diameter of  $10\text{ }\mu\text{m}$  a shear stress of  $8.8\text{ N}\cdot\text{m}^{-2}$  is obtained, which is of the same order of magnitude as the shear stresses reported to damage cells. However, in these reports exposure times are of the order of minutes to hours while here a bubble is formed within 0.1 seconds, in which case much higher shear stresses may be required to damage cells.

Another possible mechanism of cell death may be through direct contact between cells and the bubble surface. During bubble formation the bubble surface is rapidly expanding. Absorption of surfactants on to the surface as well as distribution of these surfactants over the surface requires time. As a consequence, less surfactant molecules are present at the newly formed surface and the surface tension of a rapidly expanding surface (the dynamic surface tension) is higher than the static surface tension of a surface that is in equilibrium with the bulk liquid. Thus, depending on the speed of bubble formation and surfactant adsorption, cells may come in contact with a bubble surface that is not or only partly covered with surfactant molecules. As shown by Jordan *et al.* (1994) this may lead to direct cell death or adsorption of the cells to the bubble. Michaels *et al.* (1995b) and Jordan *et al.* (1994) looked at the speed of Pluronic F68 adsorption onto newly formed bubbles as a function of concentration. Both authors showed that at a concentration higher than 0.01% adsorption took place very rapidly ( $<0.1\text{ ms}$ ) at the source. This would mean that in order for the surface creation to be faster than the adsorption process, bubble formation should be very rapid.

Murhammer and Gooch (1990b) showed that the type of sparger influenced cell death by air-bubbles. They used two air-lift reactors with different sparger designs, a membrane gas distributor and a porous stainless-steel gas distributor. For the membrane distributor cells could be grown in the presence of 0.2% Pluronic F68, while for the stainless-steel distributor no growth occurred at 0.2% Pluronic F68. However, using 0.2% Pluronic L35, which has a lower molecular weight, or higher concentrations of Pluronic F68 (0.5%), growth was possible. They proposed that the increased pressure drop present for the stainless-steel distributor, which results in a higher gas entrance rate, was responsible for increased turbulence in the sparger region causing an increase in cell damage. The protective effect of higher Pluronic concentrations could then be due to either extra dampening of the hydrodynamic forces liberated at bubble formation, or more adsorption of Pluronic to the cells. However, the concentration at which saturation of adsorption to cells occurs is much lower than the 0.2% used here. Consequently, addition of extra Pluronic would be useless. Dey and Emery (1999) showed that the effect of Pluronic on the severity of bubble break-up was minimal after a concentration of 0.025%. Although this can not be directly translated to the situation of bubble formation, it suggests that the hypothesis of extra dampening is also unlikely. Possibly, in the stainless-steel distributor Pluronic adsorption cannot keep track with the very rapid formation of new bubble surface causing attachment of cells to the surface leading either to direct cell death or cell-bubble attachment and cell death later at the surface. Higher Pluronic concentrations lead to higher speeds of adsorption, which may explain the protection offered when more Pluronic F68 is added. Finally, another explanation is

given by Kioukia *et al.* (1992), who suggest that, although the mean bubble diameter was equal in both situations, the distribution of bubble sizes might have been different. More, smaller bubbles in the case of the stainless-steel distributor would result in higher death rates.

In conclusion, there is only one reported case in the literature indicating cell death at the sparger site. It seems unlikely that this is due to liquid flows in this region, although there is no clear proof for this. Furthermore, if adsorption of protective additives cannot keep up with the rapid expansion of the bubble surface at the sparger, bubble surface is created that is not or only partially covered with surfactants. If this surface comes into contact with a cell, it may lead to direct cell death in the case of surfactant-free surface or stable adsorption of the cell in the case of partially covered surface. However, to date there is no experimental proof for this mechanism either.

### Cell Death During Bubble Rise

Most studies on overall theories suggest that the specific death rate is proportional to the reciprocal height of the reactor or, in other words, the killing volume is independent from the residence time of a bubble (Tramper *et al.* 1988, Jöbses *et al.*, 1991, Martens *et al.*, 1992).

Hülscher and Onken (1992) derived an equation assuming that during the rise of a bubble, surface-active components adsorb to the bubble interface. Cells that come into contact with uncovered surface are eventually killed. They obtained the following equation to describe the first-order death-rate constant:

$$k_d = \frac{F}{V_b} \cdot \frac{1}{V_r} \cdot v_b \cdot A_{sb} \cdot k \cdot \frac{1}{-r} \cdot (1 - e^{-\frac{H}{v_b + v_l}}) \quad (13)$$

where  $v_b$  ( $\text{m.s}^{-1}$ ) is the rise velocity of the bubble,  $v_l$  ( $\text{m.s}^{-1}$ ) is the liquid velocity,  $A_{sb}$  ( $\text{m}^2$ ) is the cross-sectional area of the bubble,  $\kappa$  (-) is a model parameter containing the collision frequency and the tendency of a cell to interact with the bubble,  $r$  ( $\text{s}^{-1}$ ) is the surfactant adsorption rate, which is proportional to the surfactant concentration and  $V_b$  ( $\text{m}^3$ ) is the bubble volume. This equation again compares well to equation (3) of the hypothetical-killing-volume theory with

$$V_d = v_b \cdot A_{ab} \cdot k \cdot \frac{1}{-r} \cdot (1 - e^{-\frac{H}{v_b + v_l}}) \quad (14)$$

The model is in accordance with the results of Jordan *et al.* (1992) and Michaels *et al.* (1995), who showed that cells may interact with surfactant-free or partially saturated bubbles, which either leads to direct cell death or to cell attachment. Both groups also showed that surfactant adsorption to bubbles is very rapid. Jordan *et al.* (1992) showed that for medium containing one percent serum, bubbles were already saturated before they reached a height of 2.5 cm above the sparger. For equation (14) this would mean that for columns higher than this 2.5 cm  $V_d$  becomes height independent and the death-rate constant becomes proportional to the reciprocal column height. Since most sparging experiments are done in columns higher than 2.5 cm, this is in accordance with the finding that the killing volume is independent from reactor height. Furthermore,

according to this theory the killing volume would be proportional to the square of the bubble diameter, as is the case for the model of Wu and Goosen (1995a).

Meier *et al.* (1999) incorporated the adsorption of cells to bubbles in another way. They divided the hypothetical killing volume into two contributions: a rise-dependent ( $V_{d,rise}$  ( $\text{m}^3$ )) and a rise-independent ( $V_{d'}$  ( $\text{m}^3$ )) term:

$$k_d = \frac{F}{V_b} \cdot \left( \frac{V_{d,rise}}{V_r} + \frac{V_{d'}}{V_r} \right) \quad (15)$$

Cells are assumed to attach irreversibly to the bubble if they have been in contact with the bubble longer than a required contact time, which is in accordance with the experimental data of Michaels *et al.* (1995a). As the bubble rises from the sparger to the top of the reactor, it sweeps a certain volume in which the cells come in contact with the bubble for the desired time. This volume is given by

$$V_{d,rise} = h_r \cdot \pi \cdot R_p^2 \quad (16)$$

where  $R_p$  (m) is an effective radius projected by the rising bubble as shown in Figure 15.3. The projected radius is next calculated from the stream functions for creeping (equation 17) flow with a non-slip boundary condition and for potential flow (equation 18):

$$R_p = \left( \frac{R_c^2(R_b + 2R_c)}{2(R_b + R_c)} \right)^{0.5} \sec h \left[ \frac{\tau v_\infty (1 - \frac{3}{4} \frac{R_b}{R_b + R_c} - \frac{1}{4} \frac{R_b^3}{(R_b + R_c)^3})}{R_b + R_c} \right] \quad (17)$$

$$R_p = (3R_b R_c)^{0.5} \sec h \left[ \frac{3\tau v_\infty}{2R_b} \right] \quad (18)$$

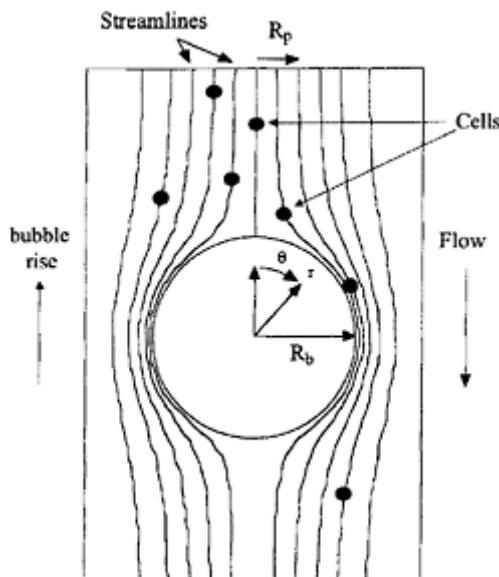


**Figure 15.3** Schematic drawing of the projected radius for a rising bubble  
(Adapted from Meier *et al.* (1999)).

where  $\tau(s)$  is the minimal contact time required for attachment of a cell to a bubble,  $R_b$  (m) is the bubble radius,  $R_c$  (m) is the cell radius, and  $v_\infty$  ( $m \cdot s^{-1}$ ) is the terminal rising velocity. In the creeping-flow regime, the Reynolds number for flow around the bubble is less than 1. For potential flow the Reynolds number is typically larger than 1000. In the absence of surfactants potential flow occurs at bubble diameters of 0.7 mm and higher. However, in the presence of surfactants the bubble surface becomes more rigid and also the larger bubbles fall within the creeping-flow regime. Michaels *et al.* (1995a) experimentally determined the required contact time needed for attachment of a cell to a bubble in the presence of protective compounds. Figure 15.4 shows the effect of reactor height and bubble diameter on the rise-dependent killing volume for a situation without

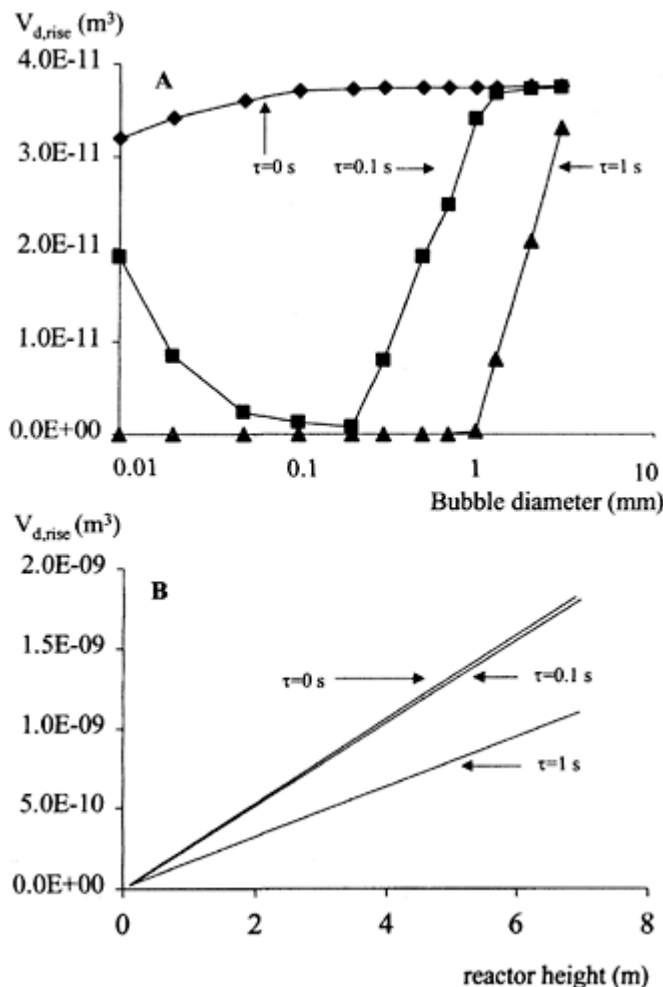


**Figure 15.4** Rise-dependent killing volume as a function of: A) bubble diameter and B) reactor height.  
Required contact times for attachment are 0, 0.1 and 1 second. Markers shown are points where the killing volume is calculated.

additives and with additives as calculated from the model of Meier *et al.* (1999). Without any protective compounds the contact time is 0.01 s. For a 3.5 mm bubble and a 15  $\mu\text{m}$  cell the projected radius is 9.2  $\mu\text{m}$ , which means that for each centimetre increase in height the  $V_{d,rise}$  increases with  $2.6 \times 10^{-12} \text{ m}^3$ . Assuming a killing volume of  $8.6 \times 10^{-10} \text{ m}^3$

for a 3.5 mm bubble (van der Pol *et al.* 1992), the contribution by the rise-dependent killing-volume would become significant only over a distance of one meter or more. In the presence of protective additives less attachment occurs and higher columns may be required for the rise-dependent killing volume to become significant, although also the rise-independent part will become smaller. Since most, if not all, studies on cell death are done in columns shorter than one meter, an effect of reactor height remains unnoticed. Meier *et al.* (1999) experimentally showed that for serum-free medium using columns of 0.34 m and 1.42 meter the killing volume is dependent on reactor height.

Bavarian *et al.* (1991), citing work of Kelly and Spottiswood on ore flotation, suggested that the rate of cell attachment is equal to the product of three factors being (i) the rate of collision, (ii) the probability of adhesion, (iii) the probability that an attached cell will not be detached. Sutherland (taken from Bavarian *et al.* 1991) derived the following equation for this:

$$p = [3\pi R_c R_b vC] \cdot \left[ \sec h^2 \left( \frac{3v\tau}{4R_b} \right) \right] \cdot p_s \quad (19)$$

where  $p$  is the probability per unit time of stable cell attachment to a bubble,  $v$  ( $\text{m}\cdot\text{s}^{-1}$ ) is the relative particle-bubble velocity,  $C$  ( $\text{particles}\cdot\text{m}^{-3}$ ) is the particle concentration, and  $p_s$  is the probability of a particle remaining attached to a bubble.

Apart from the possibility of detachment of attached cells, this equation is almost identical to the solution of Meier *et al.* (1999) for the potential-flow situation. Meier *et al.* (1999), however, stated that potential flow is in general not applicable, since surfactants are present that make the interface more rigid. Bavarian *et al.* (1991) use for part of their study bubbles with diameters smaller than 1 mm in the absence of surfactants, which in fact is in between the potential- and creeping-flow regime. Furthermore, as discussed by Bavarian *et al.* (1991), for large bubbles in the presence of surfactants a third hydrodynamic regime may occur referred to as large-wake hydrodynamics (Andrews *et al.*, 1988). In this situation cells may be captured in a wake behind the bubble without being attached. In terms of the model of Meier this would mean that the actual projected radius is larger than supposed or, in other words, cells that would normally get passed the bubble are now also captured in the wake. Consequently, effects of reactor height on the killing volume may become significant at lower heights.

All models assume that attachment of cells leads to cell death. As will be discussed further on, this is likely to occur when the bubble breaks up at the surface. Cell death at the surface would obscure any death of attached cells occurring during the rise of the bubble. Assuming a medium viscosity of  $10^{-3}$   $\text{N}\cdot\text{s}\cdot\text{m}^{-2}$ , a rising velocity of  $0.25 \text{ m}\cdot\text{s}^{-1}$  and a cell diameter of  $15 \mu\text{m}$  a shear stress of  $15 \text{ N}\cdot\text{m}^{-2}$  can be calculated (Tramper *et al.*, 1986). This stress is of the order of magnitude to cause damage for exposure times of minutes. Using a more detailed analysis Bavarian *et al.* (1991) estimated the maximum shear on a cell is about  $0.5 \text{ N}\cdot\text{m}^{-2}$  during the rise period of 17–270 s. For these exposure times this value is on the low side for shear stresses causing cell damage.

In conclusion, during rise of a bubble cells adsorb to its surface. In order to get adsorbed, cells must be in contact with the bubble for a certain required contact time, which depends on the type and concentration of protective additives used. Since cells are likely to be killed at the surface, the killing volume may become height dependent. In the absence of protective additives this dependence becomes only significant for reactors

higher than one meter, while in the presence of these additives the adsorption of cells to bubbles is minimal and the height dependence will be even less important. Finally, the rising of the bubble itself is not likely to result in cell death for either attached or non-attached cells. However, this is difficult to prove, since cell death during bubble rise will not be distinguishable from death at the surface.

### Cell Death at the Surface

There is ample experimental evidence that cell death occurs during bubble burst at the air-liquid interface. The bubble rupture process is schematically shown in Figure 15.5. As the bubble approaches the surface, liquid starts to drain from the top of the bubble due to gravity forces. A thin liquid cap is formed, from which liquid continues to drain due to gravity and the pressure differences caused by the negative curvatures at the film boundaries. At a given thickness a hole may be formed in the thinning film. Driven by surface tension the film retracts forming a growing toroidal rim, where the liquid is collected. Depending on variations in surface tension, thickness irregularities, and the escaping air, this rim may break up into small droplets, which are ejected from the film cap. The retraction process is very rapid (less than 1 ms) and cells in the bubble film essentially do not experience the presence of the toroidal rim until it reaches them, upon which the cells are rapidly accelerated to the speed of the rim. As the rim reaches the edge of the bubble cavity, it creates a small ripple that moves down the cavity during its collapse. The much slower process of cavity collapse (order of 5 ms) starts with liquid in a thin layer surrounding the bubble cavity flowing to the bottom of the cavity due to the surface tension and cavity curvature. The convergence of these liquid flows at the bottom of the cavity results in the formation of an upward and downward jet. The upward jet into the air breaks up into several drops depending amongst others on the original bubble diameter and surface properties. Maclntyre (1972) showed that the liquid in the upward jet originates from a small boundary layer around the bubble cavity as shown in Figure 15.5.

For describing cell death at bubble break-up, two regions or events may be discerned; the bubble cap including the thinning, breakage and retraction process and the bubble cavity and its collapse.

#### Bubble cap

Chalmers and Bavarian (1991) and Cherry and Hulle (1992) have visually observed the presence of cells in the bubble cap film. Trinh *et al.* (1994) captured the film cap and the cells therein by contacting the film cap with a haemacytometer before rupture. In the absence of surfactants about 300 cells were present in the film cap for a 3.5-mm bubble at a bulk cell concentration of about  $10^6$  cells/ml. By bursting bubbles using a pipette with the same cell suspension Trinh *et al.* (1994) found that 90% of the cells were killed upon

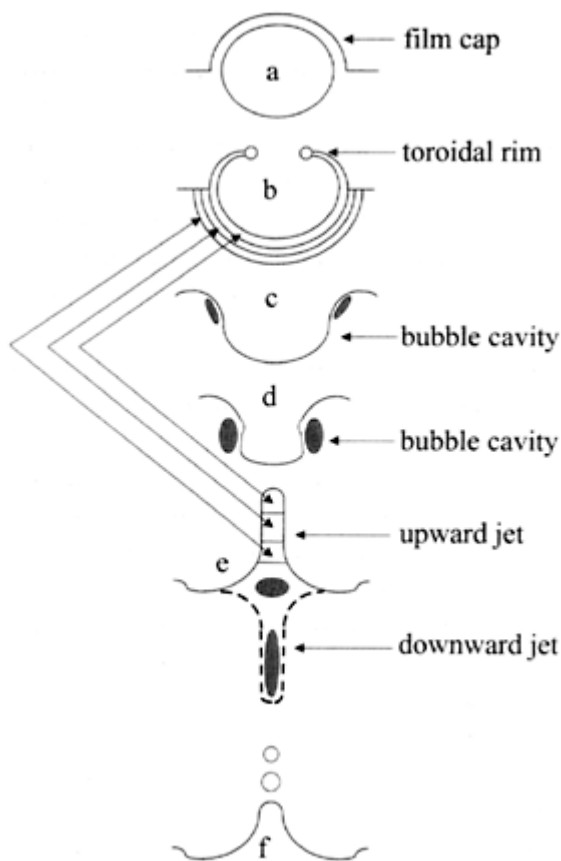


**Figure 15.5** Schematic drawing of the bubble burst process. Arrows on the left connecting b and e show the origin of the liquid present in the jet. Shaded areas represent the regions of high shear.

rupture of the film. Earlier Tramper *et al.* (1988) measured the effect of film rupture by repeated blowing of a bubble from a pipette and found that about 6% of the cells were killed upon rupture. Cherry and Hulle (1992) using a metal wire loop have also studied the effect of rupture of a single film. After spontaneous rupture they found that about 20% of the cells were killed. The cell death upon rupture found by Tramper *et al.* (1988) and Cherry and Hulle (1992) is thus significantly less than the value found by Trinh *et al.* (1994). This may be explained by the fact that protective additives were present in the media used by Cherry and Hulle (1992) (3% FBS) and Tramper *et al.* (10% FBS with 0.1% methyl-cellulose).

The entrapment and drainage of cells from a bubble film was studied by Michaels *et al.* (1995a) by microscopically looking at individual draining films. Results are presented in Table 15.5. In a serum-free medium they found that liquid draining was fast, while cells drained at medium rates, with some cells remaining entrapped in the film. In the presence of 0.1% PVP and 0.1% PEG drainage and cell movement was slow, leaving most cells entrapped in the film. With 3% serum both liquid drainage and cell drainage occurred at medium rates, leading to initial cell entrapment. However, with time the cells drained from the film. Finally, in the presence of PVA, Pluronic F68 and Methocel the drainage of liquid and cells was fast. These results indicate that PVA, Pluronic, Methocel and serum may offer protection by allowing cells to flow out of the danger zone before rupture. However, the experiments with PVP and PEG show that even if cells cannot drain from the film they are still protected. This indicates that other mechanisms like strengthening of the cells and reduction of the hydrodynamic forces associated with bubble burst may be more important in offering protection.

Several mechanisms may be responsible for cell death in the bubble film. During thinning of the liquid film in the bubble cap cells are exposed to capillary forces for a film thickness less than or equal to a cell diameter. Capillary pressures were estimated by Cherry and Hulle (1992) to be  $1.9 \cdot 10^4 \text{ N} \cdot \text{m}^{-2}$ . Comparing this to the resistance of a cell to deformation as calculated by Zhang *et al.* (1992a), which is in the order of  $600 \text{ N} \cdot \text{m}^{-2}$ , these forces can deform and crush a cell. Whether this actually occurs depends on the rate of film drainage compared to the rate with which a cell can be deformed and on the film thickness at breakage. Cherry and Hulle (1992) calculated that the thinning event is much faster than the deformation of the cell and thus assumed that these forces are not important for cell damage. On the other hand, Chalmers and Bavarian (1991) stated that they have observed cell deformation in the film cap together with what seemed to be leakage of cellular compounds from the cell.

In addition, draining of the film itself may impose stress upon the cells. Cell death due to direct contact of the cells with air can be excluded, because the exposure times are of the order of seconds at most, which is very short.

Finally, cell death may be due to events at bubble-film rupture i.e. in the rapidly retracting rim. The velocity of this rim may be estimated from the equation of Culick:

$$v = \left( \frac{2\sigma}{\rho h} \right)^{0.5} \quad (20)$$

where  $\sigma (\text{N} \cdot \text{m}^{-1})$  is the surface tension,  $\rho (\text{kg} \cdot \text{m}^{-3})$  is the density of the liquid, and  $h (\text{m})$  is the film thickness. The film thickness and surface tension are known to vary over a film. Together with difficulties in estimating the film thickness, this makes the outcomes of this equation questionable. At a film thickness of  $10 \mu\text{m}$  and a surface tension of  $64 \text{ mN} \cdot \text{m}^{-2}$  a velocity of  $3.5 \text{ m} \cdot \text{s}^{-1}$  can be calculated. This is sufficiently rapid for the film outside the rim not to notice of the film rupture, which means that cells are suddenly struck by the retracting rim. Chalmers and Bavarian (1991) calculated that acceleration rates experienced by cells are very high. Cherry and Hulle (1992) calculated the energy dissipation,  $(\text{m}^2 \cdot \text{s}^{-3})$ , in the retracting rim from the difference in surface energy ( $2\sigma A$ ) and kinetic energy of the rim using

$$\varepsilon = \frac{1}{\pi R_b^2} \left( \frac{2\sigma^3}{h\rho^3} \right)^{0.5} \quad (21)$$

where  $R_b$  (m) is the bubble radius. The rate of energy dissipation per unit mass for a surface tension of 64 mN·m<sup>-2</sup>, a hemispherical bubble of 3.5 mm diameter and a film thickness of 15 µm is 7000 m<sup>2</sup>·s<sup>-3</sup>. This value corresponds to a turbulent eddy size of 3.5 µm and a laminar shear stress of 95 N·m<sup>-2</sup>, which both can cause cell death. However, it is unknown how the energy released is dissipated in the rim. Kowalski and Thomas (1995) studied the breaking of a bubble in solution of SDS in water with and without Pluronic F68. Without Pluronic, rapid expansion of the hole was observed together with the tangential ejection of threads (20–60 in number) breaking up in small droplets (30–300 µm) at velocities of 10 m·s<sup>-1</sup>. Assuming a distance of acceleration of 1 mm, this results in a local energy dissipation of 10<sup>5</sup> m<sup>2</sup>·s<sup>-3</sup>, which is of the same order as the value calculated by Cherry and Hulle (1992). In the presence of Pluronic formation of the threads was suppressed, which was attributed to polymeric inhibition of the ultra-micro-scale motions.

In conclusion, in the absence of additives almost all cells present in the bubble film are killed upon rupture. This is most likely due to intense energy dissipation in the retracting rim, which results in the tangential ejection of liquid drops. This cell death can be prohibited by the addition of protective additives, primarily because the rupture process itself is less severe and cells have become less fragile. In addition, Pluronic, Methocel and PVA cause rapid draining of the cells out of the film and thus out of the danger zone.

### Bubble cavity

Chalmers and Bavarian (1991) calculated that the shear stresses associated with the collapse of the bubble cavity are of the order of 200 N·m<sup>-2</sup>, which is a magnitude larger than the shear stresses reported to cause cell damage. This is an average shear stress calculated on the assumption of simple boundary-layer flow. Garcia-Briones and Chalmers (1994) stated that for the more complex flows the shear stress does not represent the local state of stress. They suggested using two flow parameters of general nature to study hydrodynamic-related cell injury. These are the state of stress (characterised by the second invariant of the stress tensor) and the flow classification parameter  $R_D$ , which is related to the possibility of stress relaxation by rotation.  $R_D$  ranges from infinity for rigid-body rotation to unity for viscometric flows to zero for elongational flows. Flows with an  $R_D$  above unity are weaker than the viscometric flows and were assumed not to be able to damage cells (Garcia-Briones and Chalmers 1994). By numerically simulating the collapse of the bubble cavity during the bubble breakage process, Boulton-Stone and Blake (1993) and Garcia-Briones and Chalmers (1994) showed that the regions with the highest state of stress develop from the cavity edge, spread rapidly along the cavity interface and reach the highest value upon convergence at the bottom of the cavity, where two opposing jets are formed. Figure 15.5 schematically shows the regions of high state of stress during cavity collapse. Garcia-Briones and Chalmers (1994) showed that in particular for smaller bubbles (0.77 and 1.7 mm), a strong downward and upward jet are formed, which do not occur for a bubble of 6.3 mm in diameter. Furthermore, they showed that the magnitude of the stresses decreases

exponentially when the bubble diameter increases from 0.77 to 6.3 mm. This is in accordance with the finding of Handa *et al.* (1985) that smaller bubbles are more detrimental than larger bubbles. Table 15.6 shows maximum values for the flow parameters proposed by Garcia-Briones and Chalmers (1994) for different bubble sizes.

**Table 15.6** Flow parameters for three different bubble sizes, (adapted from Garcia-Briones and Chalmers 1994)

Bubble diameter (m)	State of stress (N.m <sup>-2</sup> )	R <sub>D</sub>	Time at maximum state of stress (s)	Total break-up time (s)
0.77 10 <sup>-3</sup>		479.7	0.02 0.43 10 <sup>-3</sup>	0.55 10 <sup>3</sup>
1.70 10 <sup>-3</sup>		199.8	0.02 1.4 10 <sup>-3</sup>	2.0 10 <sup>-3</sup>
6.32 10 <sup>-3</sup>		17.5	0.01 5.6 10 <sup>-3</sup>	10 10 <sup>-3</sup>

Comparing these values to the values known to damage cells as given in Table 15.3, they concluded that cells would be destroyed in a fraction of a second. Dey *et al.* (1997) experimentally studied and numerically calculated the effect of additives on the bubble burst process. The severity of the rupture process was assessed by measuring the Height of the Axis Node (HAN=depth of the cavity/initial bubble radius) as a function of time. Addition of surfactants resulted in a slower, less high jet with a wider base and narrower tip as opposed to the situation without surfactants, where a long, slender jet was formed. In addition, in the absence of surfactants four to five droplets were formed, whereas in the presence of 0.1% Pluronic only one droplet was formed and no droplets were formed at all when 5% serum was added. Thus, the presence of Pluronic clearly decreases the severity of the bubble burst, which may at least in part be the mechanism by which Pluronic offers protection. From the numerical simulation of the rupture process the most important parameter influencing this process was the surface dilatational viscosity. However, in order to obtain good agreement with the experimental data, the value of this parameter had to be made an order of magnitude higher than the experimentally determined value. It is stated that this may be due to the fact that the experimental method used to measure the surface dilatational viscosity may not give the correct value.

Trinh *et al.* (1994) tried to quantify the number of insect cells killed per bubble rupture as well as the location of cell death. From sparging experiments they found that at a cell concentration of about 2 10<sup>6</sup> cells per ml about 1150 insect cells were killed per burst of a 3.5 mm bubble, which corresponds to a killing volume of 6 10<sup>-10</sup> m<sup>3</sup>. Comparing this to other literature data, only van der Pol *et al.* (1992) present data obtained in a serum-free medium. From their data, assuming a bubble diameter of 3.5 mm, a hypothetical killing volume of 8.6 10<sup>10</sup> m<sup>3</sup> can be calculated. At a cell concentration of 2 10<sup>6</sup> cells per ml this means that about 1700 cells would be killed per bubble. Although of the same order of magnitude, these numbers are higher than those found by Trinh *et al.* (1994), which may be caused by the difference in cell types. Trinh *et al.* (1994) used insect cells, whereas van der Pol *et al.* (1992) used hybridoma cells. Trinh *et al.* (1994) also collected the liquid from the upward jet and found that in the absence of Pluronic about 1400 cells were present in this jet. Compared to the bulk liquid the viability in the jet was reduced

by 75%, meaning that about 900 cells were killed per bubble burst. This is somewhat lower than the value of 1150 cells found previously, which may be caused by the fact that not all liquid is collected and not all the cells that are affected by the bubble burst end up in the upward jet. For instance, the downward jet may also kill part of the cells. However, the variation in counts for both types of experiments was quite high and observed differences may not be significant. The cell concentration in the upward jet was about 2 times the bulk concentration indicating adsorption of cells to the bubble surface. For a total of 1400 cells this would mean adsorption of 700 cells per bubble.

Wen and Tan (1999) calculated the amount of CHO cells adsorbed per unit bubble surface using a foam-flotation technique. The amount of cells transferred to the foam will depend on the amount of liquid transferred to the foam, the cell concentration, the drainage of cells from the foam, and the adsorption of cells to the bubbles. They showed that the amount of cells transferred to the foam per unit bubble surface depended on the height of the column and the cell concentration. In serum-free medium without surfactants and at a cell concentration of  $10^6 \text{ cells.ml}^{-1}$  bubbles were saturated with cells at a height of 0.1 m. Assuming all cells present in the foam had adsorbed to the bubble, one can calculate that for a bubble with a diameter of 3.5 mm about 700 cells had adsorbed at saturation. Considering the high standard deviations and the differences in cell types and column height this agrees remarkably well with the value found by Trinh *et al.* (1994).

Using the theory of Meier *et al.* (1999) one can calculate the amount of cells that adsorb to the bubble during rise for the situation of Trinh *et al.* (1994) and Wen and Tan (1999). This results in a value of about 20 and 40 cells per bubble, respectively, which is substantially less than the experimental value of 700 cells per bubble. One explanation for this difference is that the model of Meier *et al.* (1999) only describes adsorption during bubble rise. Additional adsorption of cells may occur during bubble formation and break-up. Michaels *et al.* (1995a) showed that for serum-free medium liquid drains from the bubble film leaving the cells entrapped. With 300 cells present in the film (Trinh *et al.* 1994) this can at least in part explain the observed discrepancy. In addition, as mentioned, during bubble rise the flow patterns may not always resemble potential or creeping flow and cells may be captured in the wake of a bubble without having been in contact with the bubble. Finally, Dey *et al.* (1997) proposed on the basis of numerical simulation of the cavity collapse that the liquid flows occurring during the collapse might result in concentrating the cells near the axis of symmetry, where the highest rates of strain occur. In the presence of surfactant this concentration effect as well as the magnitude of the strain rates was much less resulting in less cells being subjected to less damaging flows.

Trinh *et al.* (1994) also studied the number of cells killed per bubble rupture and the number of cells in the upward jet in the presence of 0.1% Pluronic F68. The number of cells killed per bubble in their sparging experiments reduced to zero, while the concentration of cells in the upward jet was on average slightly lower than the bulk concentration. The reduced cell concentration in the upward jet is probably due to the prevention of cell attachment to bubbles, the rapid draining of cells from the bubble film in the presence of 0.1% Pluronic (Michaels *et al.*, 1995b) and reduction of the concentration effect as proposed by Dey *et al.* (1997). The reduced cell concentration is also in accordance with the decrease in adsorbed cells found by Wen and Tan in the

presence of Pluronic. However, in the presence of 0.1% Pluronic more liquid was present in the upward jet and Trinh *et al.* (1994) reasoned that this may have masked the occurrence of increased cell concentrations near the bubble surface. The higher volume also resulted in the number of cells in the jet being quite comparable to that for media without Pluronic. Because the viability of these cells was identical to that in the bulk, the main mechanism of protection does not seem to be the exclusion of cells from the danger zone. More likely protection is mainly caused by a reduction of the magnitude of the hydrodynamic forces or an increase in the strength of the cells or both. This is in accordance with the previously discussed protection offered by PVP and PEG, which cause an increased cell-bubble attachment but still offer protection.

Wu and Goosen (1994) developed a falling-film flow device in which they exposed cells to well-defined moving air-liquid interfaces in the presence of different additives. They showed that cell death was associated with the falling of the film into the bulk liquid and not with the interaction of cells with the air-liquid interface. Using this device, they showed that surface-active compounds like Pluronic F68 and methyl-cellulose had a protective effect, while additives that only enhanced the viscosity showed no clear effect. This suggests that protection is at least in part offered through interaction of the compounds with the cell membranes. The situation created in this device is, however, quite different from the situation in a bursting bubble. The film thickness (200–400  $\mu\text{m}$ ) is, for instance, significantly larger than the bubble film thickness (5–20  $\mu\text{m}$ ), which also results in larger amounts of liquid being involved. Furthermore, in the device the falling of the film is caused by gravity, while at bubble break-up interfacial tension is the main force. Finally, the liquid velocities ( $0.5\text{--}2 \text{ m}\cdot\text{s}^{-1}$ ) are somewhat lower than the retracting-rim velocity and the velocities around the bubble cavity ( $3\text{--}20 \text{ m}\cdot\text{s}^{-1}$ ).

In conclusion, numerical simulations of the cavity collapse show that for bubbles smaller than 6 mm hydrodynamic stresses occur around the bubble cavity that can potentially damage cells. This agrees with the fact that in the absence of protective additives all cells in the upward jet are dead. The hydrodynamic stresses associated with cavity collapse increase exponentially with a decrease in bubble size. For bubbles of 6 mm and larger no upward jet is formed anymore. However, cell death has not been studied for these large bubbles. To draw firm conclusions from the numerical simulations with respect to the mechanism of cell death, the interaction of the calculated flows with the cells as well as the strength of the cells should be included. Protection offered by additives seems most likely due to decreasing the severity of the hydrodynamic forces and strengthening of the cell. In addition, reducing the amount of cells in the danger zone may also contribute.

### Cell Death in a Foam

Chalmers and Bavarian (1991) showed that cells may be pushed into the foam. The situation with the presence of a foam layer differs essentially from the situation of bubble burst in the absence of a foam layer. In the foam layer only the retracting toroidal rim is present and not the flow of liquid into the cavity with the associated upward and downward jet. Cell death in a foam layer may be caused by liquid draining from the foam, breaking of films at foam rupture and nutrient exhaustion in the foam. Furthermore, foaming may cause cells to be physically lost from the bulk liquid. As

stated, the cell concentration in the foam will depend on the attachment of cells to bubbles, the cell concentration, the amount of liquid transferred to the foam and the drainage of liquid from the foam relative to the drainage of cells. The combination of cell attachment to bubbles and drainage of cells from the foam layer is studied in foam-fractionation studies. In these studies a foam layer formed by blowing air through a cell suspension is captured and the cell concentration in this captured foam is determined. Michaels *et al.* (1995b) and Wen and Tan (1999) did this kind of study in the presence of different additives. Michaels *et al.* (1995b) measured the following parameters: A cell separation factor being the cell concentration in the foam ( $C_{foam}$ ) divided by the cell concentration in the bulk ( $C_{bulk}$ ):

$$a_{sep} = \frac{C_{foam}}{C_{bulk}} \quad (22)$$

$C_{bulk}$  is the average cell concentration in the bulk at the start and end of a foaming experiment.

Fractional fluid transfer FL:

$$FL = \frac{\text{Fluid foam}}{\text{Fluid bulk initial}} \quad (23)$$

Since fluid transfer and cell adsorption may assumed to be related to the total surface area, both parameters may be corrected for the total surface area:

$$\langle a_{sep} \rangle = NF \frac{C_{foam}}{C_{bulk}} \quad (24)$$

$$\langle FL \rangle = NF \frac{\text{Fluid foam}}{\text{Fluid bulk initial}} \quad (25)$$

where NF is the ratio of the Sauter mean bubble diameter in a particular medium to the one in a serum-free medium.

The viabilities in the foam and bulk were quantified using the following normalised viabilities:

$$NCV_{bulk} = \frac{\text{final viability bulk}}{\text{initial bulk viability}} \quad (26)$$

$$NCV_{foam} = \frac{\text{final viability foam}}{\text{initial bulk viability}}$$

Of final interest is the fraction of cells removed through the foam corrected for the total surface area,  $b$ :

$$\langle b \rangle = NF \cdot FL \cdot a_{sep} \quad (27)$$

Finally, the foaming height and the half time for foam reduction may address the stability of the foam. Results are shown in Table 15.5 and Table 15.7 and can be summarised as follows:

In serum-free medium the separation factor was larger than unity indicating cell-bubble attachment, which is in agreement with previous results. The viability was reduced with about 56% including 12% lysis of cells. Remarkably, only a fraction of the cells were killed, indicating that the bursting of a foam is less detrimental than that of a bubble on a surface, in

**Table 15.7** Foaming experimental results from Michaels *et al.* (1995b) (see text for symbols).

	d32 mm	$a_{sep}$	FL	$\langle a_{sep} \rangle$	$\langle FL \rangle$	Column NCV	Foam NCV	$\langle b \rangle$
serum free	1.40	1.68	11.7	1.68	11.7	89.3	73.8	0.20
0.1% PVP	0.96	3.85	21.5	2.65	14.7	99.4	94.2	0.57
0.1% PEG	0.65	2.38	10.6	1.11	4.9	95.6	94.9	0.12
0.1% PVA	0.82	0.78	14.1	0.46	8.3	99.1	97.3	0.06
0.1% Pluronic	0.68	0.74	16.5	0.36	8.0	101.2	95.0	0.06
0.1% Methocel	1.21	0.64	8.4	0.55	7.3	99.0	98.1	0.05
0.5% FBS	1.43	1.91	11.9	1.95	12.2	88.9	78.4	0.23
5%FBS	0.98	0.50	26.5	0.35	18.6	100.1	95.6	0.09

which case all cells are killed. Addition of 0.1% PVA, Pluronic F68 and Methocel reduced the specific separation factor to 0.55 or less, indicating the absence of cell-bubble attachment and rapid draining of cells from the films. The retained viability in the foam after rupture for the remaining cells was 100%. Addition of serum up to a concentration of 5% led to a decrease in the specific separation factor to 0.35. Also the retained viability in the foam increased from 78 to almost 100% at 5% FBS. Finally, increasing serum concentrations led to an increasing fraction of fluid transferred. Addition of PVP and PEG resulted in specific separation factors still higher than unity. However, in this case also the viability in the foam was equal to the viability in the bulk. This again indicates that the protective mechanism of additives is primarily the reduction of hydrodynamic forces and strengthening of the cell rather than reducing the number of cells in the danger zone.

For a serum percentage of 3% Cherry and Hulle (1992) found a separation factor of 0.6, which is comparable to the value obtained by Michaels *et al.* (1995b). They proposed the following equation to describe cell death:

$$k_d = \psi \cdot \frac{C_{vf}}{C_{vb}} \cdot \left( \frac{3 \cdot h \cdot F}{R_b \cdot V} \right) \quad (28)$$

where  $\psi$  (–) is the fractional death in a bubble film,  $C_{vf}$  ( $\text{cells.m}^{-3}$ ) is the viable-cell concentration in the film,  $C_{vb}$  ( $\text{cells.m}^{-3}$ ) is the viable-cell concentration in the bulk,  $h$  (m) is the thickness of the film,  $F$  ( $\text{m}^3 \cdot \text{s}^{-1}$ ) is the gas-flow rate,  $R_b$  (m) is the bubble radius and  $V$  ( $\text{m}^3$ ) is the reactor volume. Using the cell separation value of 0.6 and the 20% cell death upon film rupture, Cherry and Hulle (1992) were able to accurately predict the first-order death-rate constant in a sparging experiment.

Finally, Murhammer and Goochee (1990a) showed that certain small molecular weight Pluronics, like Pluronic L35 and F38 offer just as good protection as Pluronic F68, but result in less foam formation.

In conclusion, the presence of a stable foam layer from which cells rapidly drain may be beneficial to the process, since in such a situation oxygen transfer is enhanced in the absence of cell death and physical loss of cells. Serum, PVP and PEG are not favoured as protective additives, since they result in increased foaming and cell entrapment.

### Bubble Coalescence and Break-up

It has been suggested in the literature that the coalescence and break-up of bubbles in sparged bioreactors may also be detrimental to animal cells (Oh *et al.*, 1989, 1992; Wang *et al.*, 1994; Yang and Wang, 1992). Until now the only studies available on these phenomena are done in sparged stirred-tank bioreactors (Gardner *et al.*, 1989; Kunas and Papoutsakis, 1990b; Michaels *et al.*, 1995a; Oh *et al.*, 1989, 1990; Wang *et al.*, 1994; Yang and Wang, 1992). In these reactors different situations may occur depending on the sparging rate, sparger position and the Froude number (Oh *et al.*, 1992):

$$Fr = \frac{N^2 \cdot D_i}{g} \quad (29)$$

where  $N$  ( $s^{-1}$ ) is the agitation speed,  $D_i$  (m) is the impeller diameter and  $g$  ( $m \cdot s^{-2}$ ) is the gravitational constant. The Froude number represents the balance between centrifugal inertial forces and buoyancy forces. In essence three situations may be discerned: (i) at high Froude numbers, i.e. at low agitation rates and low aeration rates, air is entrained in the trailing vortices of the impeller, where stable cavities are formed. Bubbles continuously coalesce with the cavity and break-up from the cavity; (ii) at low Froude numbers bubbles will be entrained in the vortex region but no stable cavities are formed. The bubbles are accelerated and may break-up; (iii) the agitation does not interfere with the bubbles.

As stated before, Wang *et al.* (1994) developed a generalised bubble break-up and coalescence model, that views bubble escape at the surface as a special case of coalescence. In this model the first-order death rate is proportional to the specific surface area. They used the data of Oh *et al.* (1989) to verify their theory. Oh *et al.* (1989, 1992) studied the reduction in growth rate of different cells as a function of gas flow, agitation speed and sparger position. They found that at a fixed gas-flow rate cell death increased with the agitation speed. However, since higher agitation speeds also gave rise to smaller and, consequently, more bubbles, it remained unclear whether bubble coalescence and break-up contributed to cell death. They concluded that in the absence of bubbles agitation rates can be much higher than previously assumed. This was confirmed by the study of Kunas and Papoutsakis (1990), who showed that in the absence of bubbles the agitation rate could be as high as 800 rpm. Above this rate the eddy size became so small that cells were damaged. Moreover, they showed that even in the presence of 5000 small (50–300 µm) bubbles per ml, but in the absence of a gas headspace, growth was not affected up to agitation rates of 600 rpm. This suggests that bubble coalescence and break-up does not significantly contribute to cell death. Using a bioreactor set-up specially designed to measure effects of bubble coalescence and break-up in the bulk,

Michaels *et al.* (1996) showed that these phenomena did not cause significant cell damage. Finally, Yang and Wang (1992) studied the reduction in growth of the alga *Ochromonas malhamensis* at different agitation and sparging rates. The first-order death-rate constant was proportional to the overall oxygen mass-transfer coefficient, which was used as a measure for the specific surface area. They concluded that the cell damage in a sparged and agitated bioreactor was higher than the damage at sparging or agitation alone. However, it is not clear whether this is due to the occurrence of damaging bubble coalescence and break-up in the bulk or due to the fact that bubbles are broken up resulting in more small bubbles causing more cell death at the surface.

In conclusion, there is no clear proof that cell death due to bubble coalescence and break-up is significant.

### Protective Additives

Protective additives prevent cell death by a combination of mechanisms depending on the type of additive. All additives adsorb to the cell membrane, making the cell less fragile. In addition, Pluronic moderates the bursting event. Finally, Pluronics, PVA and Methocel decrease attachment of cells to the air bubbles and cause rapid draining of cells and medium out of bubble films, which expels the cells from the danger zone. PVP and PEG cause an increase in cell concentration near the bursting bubbles due to increased cell-bubble attachment. In addition, cells and medium drain relatively slowly from the film. Despite this, these compounds effectively protect the cells against shear. This indicates that strengthening of the cells and reduction of hydrodynamic forces are the main protective mechanisms, although the effect of these additives on the burst process is not known. Also for Pluronic the drainage of cells out of the danger zone seems to not be required for offering protection. Finally, serum decreases cell attachment to bubbles and gives medium drainage rates of cells and medium from the bubble film. Furthermore, serum has also been shown to moderate the bursting event. Yet it only provides moderate protection compared to the other additives. Notably, in the absence of additives, medium drains faster than the cells, which may be partly responsible for the concentration factor of cells in the ejected liquid drops and in foams. With the use of Pluronic, which is the main additive used in commercial media, the problem of bubble-associated cell death is largely solved. However, one should consider that these additives might affect cell physiology. For instance, Al-Rubeai *et al.* (1992) showed that addition of Pluronic (0.025–0.1%) led to a decrease in cell concentration and increase in productivity in batch and steady-state continuous cultures. In addition, Pluronic may decrease the oxygen transfer coefficient (Murhammer and Pfalzgraf, 1992), thus leading to higher required gassing rates. Finally, upon using additives foaming may occur, which would result in physical loss of cells and operating problems. If possible, antifoam can be added. However, antifoam may make the cells more shear sensitive (van der Pol *et al.*, 1993) and often the use of antifoam is not allowed because of GMP regulations.

### REACTOR DESIGN

For designing bubble columns and airlift reactors the hypothetical-killing-volume theory of Tramper can be used. The killing volume can than be split into a rise-dependent and rise-independent part as in equations (14) and (15). The rise-dependent part will usually be negligible. The relation between the rise independent killing volume and different parameters is still not exactly known. From a mechanistic point of view it would be logical to assume that cells in the bubble film and in a small liquid layer around the bubble cavity are killed upon bubble rupture:

$$V_d = k_{film} \cdot h_{film} + k_{cavity} \cdot A_{cavity} \cdot h_{cavity} \quad (30)$$

with  $k$  (-) being a proportionality constant containing the fraction of cells killed and the concentration factor,  $A$  ( $\text{m}^2$ ) the surface area, and  $h$  (m) the film thickness, where cell death occurs. The surface area is proportional to the square of the bubble diameter meaning larger bubbles are more detrimental. On the other hand the forces associated with cavity collapse, which enter the above equations in the fraction killed and the thickness of the layer at the cavity wall, increase exponentially with decreasing bubble size. Thus, below a critical bubble diameter smaller bubbles can be more damaging. However, experimental proof for this is limited to one observation by Handa *et al.* (1985). In addition to a decrease in bursting forces, the proportion of the bubble that is above the surface at rupture will increase with increasing bubble diameter. Based on this a proportionality of the rise-independent killing volume to the square of the bubble diameter seems more logical than to the third power. As long as exact information on the mechanism is lacking we just assume that cells in a layer of thickness  $h$  around a bubble are killed. This results in

$$k_d = \frac{24F}{\pi^2 HT^2 d_b^3} (kh0.25\pi d_b^2 + H\pi r_p^2) = F \left( \frac{6kh}{HT^2 \pi d_b} + \frac{24r_p^2}{T^2 \pi d_b^3} \right) \quad (31)$$

From this equation it can be seen that for larger reactors the rise-dependent killing volume becomes relatively more important. The volumetric oxygen demand of the cells determines the minimal amount of sparging that is required:

$$q_o \cdot C_v = k_{ol} \cdot A \cdot (C_{ol}^* - C_{ol}) \quad (32)$$

Where  $q_o$  ( $\text{mol.cell}^{-1} \cdot \text{s}^{-1}$ ) is the specific oxygen consumption rate,  $k_{ol}$  ( $\text{m.s}^{-1}$ ) is the mass-transfer coefficient,  $A$  ( $\text{m}^{-1}$ ) is the specific surface area,  $C_{ol}^*$  ( $\text{mol.m}^{-3}$ ) is the saturation concentration of oxygen in medium, and  $C_{ol}$  ( $\text{mol.m}^{-3}$ ) is the oxygen concentration in medium. For bubble columns  $A$  is given by

$$A = \frac{24F}{\pi d_b v_{bw} T^2} \quad (33)$$

Combining equations (32) and (33), the gas flow rate required for a given cell concentration is given by

$$F = \frac{\pi d_b v_b T^2}{24} \frac{q_o C_v}{K_{ol}(C_{ol}^* - C_{ol})} \quad (34)$$

Combining this with equation (31) for the first-order death-rate constant gives

$$k_d = \frac{q_o C_v v_h}{k_{ol}(C_{ol}^* - C_{ol})} \left( \frac{kh}{4H} + \frac{r_p^2}{d_b^2} \right) \quad (35)$$

From this equation it is clear that increasing the reactor height decreases the death-rate constant until a certain plateau value given by the second part of equation (35). The effect of bubble diameter is difficult to deduce because it affects the following parameters:

*The bubble rise velocity.* For the creeping-flow regime the bubble rise velocity decreases with decreasing bubble diameter below diameters of 1 mm, which would also decrease the death-rate constant if the projected radius is not affected. However, the projected radius increases making the net effect difficult to predict.

*The combination "kh":* This factor in fact represents the amount of cells killed per unit bubble area. Garcia-Briones and Chalmers (1994) showed that the burst of smaller bubbles causes higher hydrodynamic forces. Therefore, a decrease in bubble diameter would be expected to lead to an increase in this factor and in the death-rate constant.

*Projected radius.* The projected radius is a function of the bubble and cell diameter, the bubble rise velocity and the required contact time. The relation is shown in Figure 15.4, where one can see that up to a bubble diameter of 0.2 mm the killing volume decreases with bubble diameter.

In conclusion, high reactors should be used to minimise cell death. For the bubble size many of the processes and parameters affecting cell death are not exactly known making it difficult to predict which bubble diameter should be used.

## CONCLUSIONS

Cell death due to sparging occurs at bubble break-up at the surface during retraction of the bubble film and the subsequent collapse of the bubble cavity. Numerical calculations modelling collapse of the cavity show that the hydrodynamic forces liberated are sufficient to kill the cells and increase with decreasing bubble diameter. When elucidating the exact mechanism of cell death and protection it is important to model the interaction of these forces with the cells. This might also give more insight into the effect of bubble diameter on cell death.

Cell death during bubble rise is highly unlikely. However, adsorption of cells occurs during bubble rise, which causes an increase of the number of cells in the danger zone at bubble break-up and thus an increase in cell death.

Although there is no clear proof of cell death at the sparger, this in principle may occur due to liquid flows at bubble formation and the contact between a cell and newly formed bubble surface that contains no surfactants. Modelling the flow patterns and hydrodynamic forces at the sparger as well as modelling the formation of new bubble surface in combination with adsorption of cells and surfactants would be of great importance for understanding events at the sparger.

With respect to the effect of bubble diameter, most observations on cell death show that the killing volume increases with bubble diameter in the range of 0.5 to 6 mm, which contradicts with the decrease of hydrodynamic forces for increasing bubble diameters. For larger bubbles a larger volume of medium and thus more cells are involved in the

rupture process, while apparently the hydrodynamic forces are still high enough to kill the cells in these larger volumes. Therefore, it would be interesting to study whether this still holds for bubbles larger than 6 mm, where the severity of the burst is even further reduced and no jet formation is observed anymore.

Certain surfactants like Pluronic F68 and Methocel can completely protect the cells against shear from bursting bubbles. These compounds adsorb on the cell membrane and the bubble surface and protect the cells by a combination of mechanisms primarily reduction of cell fragility and a decrease in hydrodynamic forces accompanying bubble rupture. In addition, some additives prevent attachment of cells to bubbles and allow cells to drain rapidly from bubble films. Thus, they cause a decrease in the cell concentration in the killing volume. Although this does not seem required for protection it prevents the physical loss of cells in case foaming occurs. With the application of additives like Pluronic and Methocel the problem of cell death due to sparging is largely solved. However, these compounds may have a negative effect on cell physiology and oxygen transfer.

For reactor design purposes the height of the reactor is the main design parameter, with higher reactors being more favourable for the growth of animal cells. With respect to bubble diameter the influence on reactor performance depends on a number of yet unknown effects and parameters and is therefore not clear. Finally, one of the major remaining problems associated with sparging will likely be foaming due to high cell and protein concentrations in the medium.

## REFERENCES

- Absalom, D.R., Lamberti, F.V., Policova, Z., Zing, W., van Oss, C.J., Neuman, A.W. (1983) Surface thermodynamics of bacterial adhesion. *Appl. Environ. Microb.* **46**, 90–97.
- Abu-Reesh, I., Kargi, F. (1989) Biological responses of hybridoma cells to defined hydrodynamic stress. *J.Biotechnol.* **9**, 167–178.
- Al-Rubeai, M., Oh, S.K.W., Musaheb, R. and Emery, A.N. (1990) Modified cellular metabolism in hybridomas subjected to hydrodynamic and other stresses. *Biotechnol. Lett.* **12**, 323–328.
- Al-Rubeai, M., Emery, A.N. and Chalder, S. (1992) The effect of Pluronic F-68 on hybridoma cells in continuous culture. *Appl. Microbiol. Biotechnol.* **37**, 44–45.
- Al-Rubeai, M., Emery, A.N., Chalder, S. and Goldman, M.H. (1993) A flow cytometric study of hydrodynamic damage to mammalian cells. *J.Biotechnol.* **31**, 161–177.
- Al-Rubeai, M., Singh, R.P., Goldman, H. and Emery, A.N. (1995a) Death mechanisms of animal cells in conditions of intensive agitation. *Biotechnol. Bioeng.* **45**, 463–472.
- Al-Rubeai, M., Singh, R.P., Emery, A.N. and Zhang, Z. (1995b) Cell cycle and cell size dependence of susceptibility to hydrodynamic forces. *Biotechnol. Bioeng.* **46**, 88–92.
- Andrews, G.F., Fike, R. and Wong, S. (1988). Bubble hydrodynamics and mass transfer at high Reynolds number and surfactant concentration. *Chem. Eng. Sci.* **43**, 1467–1477.
- Augenstein, D.C., Sinskey, A.J. and Wang, D.I.C. (1971) Effect of shear on the death of two strains of mammalian tissue cells. *Biotechnol. Bioeng.* **13**, 409–418.
- Bavarian, F., Fan, L.S. and Chalmers, J.J. (1991) Microscopic visualization of insect cell-bubble interactions: I: rising bubbles, air-medium interface, and the foam layer. *Biotechnol. Prog.* **7**, 140–150.
- Born, C., Zhang, Z., Al-Rubeai, M. and Thomas, C.R. (1992) Estimation of disruption of animal cells by laminar shear stress. *Biotechnol. Bioeng.* **40**, 1004–1010.

- Boulton-Stone, J.M. and Blake, J.R. (1993) Gas bubbles bursting at a free surface. *J. Fluid Mech.* **254**, 437–66.
- Chalmers, J.J. and Bavarian, F. (1991) Microscopic visualization of insect cell-bubble interactions. II: the bubble film and bubble rupture. *Biotechnol. Prog.* **7**, 151–158.
- Chalmers, J.J. (1994) Cells and bubbles in sparged bioreactors. *Cytotechnol* **15**, 311–320.
- Chalmers, J.J. (1996) Shear sensitivity of insect cells. *Cytotechnol* **20**, 163–171.
- Chattopadhyay, D., Rathman, J.F. and Chalmers, J.J. (1995a) The protective effect of specific medium additives with respect to bubble rupture. *Biotechnol. Bioeng.* **45**, 473–80.
- Chattopadhyay, D., Rathman, J.F. and Chalmers, J.J. (1995b) Thermodynamic approach to explain cell adhesion to air-medium interfaces. *Biotechnol. Bioeng.* **48**, 649–658.
- Cherry, R.S. and Hulle, C.T. (1992) Cell death in the thin films of bursting bubbles. *Biotechnol. Prog.* **8**, 11–18.
- Chisty, Y. (1993) Animal cell culture in stirred bioreactors: Observations on scale-up. *Bioproc. Eng.* **9**, 191–196.
- Chittur, K.K., McIntire, L.V. and Rich, R.R. (1988) Shear stress effects on human T cell function. *Biotechnol. Prog.* **4**, 89–96.
- Dey, D., Boulton-Stone, J.M., Emery, A.N. and Blake, J.R. (1997) Experimental comparisons with a numerical model of surfactant effects on the burst of a single bubble. *Chem. Eng. Sci.* **52**, 2769–2783.
- Dey, D. and Emery, A.N. (1999) Problems in predicting cell damage from bubble bursting. *Biotechnol. Bioeng.* **65**, 240–245.
- Eyl, V., Muller, S., Donner, M., Maugras, M. and Stoltz, J.-F. (1992) Use of fluorescence anisotropy determinations for indicating the physiological status of hybridoma cell cultures. *Cytotechnol.* **8**, 5–11.
- Garcia-Briones, M.A. and Chalmers, J.J. (1994) Flow parameters associated with hydrodynamic cell injury. *Biotechnol. Bioeng.* **44**, 1089–1098.
- Gardner A.R., Gainer, J.L. and Kirwan, D.J. (1989) Effects of stirring and sparging on cultured hybridoma cells. *Biotechnol. Bioeng.* **35**, 940–947.
- Goldblum, S., Bae, Y., Hink, W.F. and Chalmers, J.J. (1990) Protective effect of methylcellulose and other polymers on insect cells subjected to laminar shear stress. *Biotechnol. Prog.* **6**, 383–390.
- Handa, A., Emery, A.N. and Spier, R.E. (1985) On the evaluation of gas-liquid interfacial effects on hybridoma viability in bubble column bioreactors. *Dev. Biol. Stand.* **66**, 241–253.
- Handa-Corrigan, A., Emery, A.N. and Spier, R.E. (1989) Effect of gas- liquid interfaces on the growth of suspended mammalian cells: mechanisms of cell damage by bubbles. *Enzyme Microb. Technol.* **11**, 230–235.
- Hua, J., Erickson, L.E., Yiin, T.-Y. and Glasgow, L.A. (1993) A review of the effects of shear and interfacial phenomena on cell viability. *Crit. Rev. Biotechnol.* **13**, 305–328.
- Hülscher, M. and Onken, U. (1992) Mechanical damage of suspended animal cells in directly sparged bioreactors. In *Production of biologicals from animal cells in culture*, edited by Spier, R.E., Griffith, J.B. and MacDonald, C., pp. 195–202. Butterworths, Stoneham, MA.
- Jöbses, I., Martens, D. and Tramper, J. (1991) Lethal events during gas sparging animal cell culture. *Biotechnol. Bioeng.* **37**, 484–490.
- Jordan, M., Sucker, H., Einsele, A., Widmer, F. and Eppenberger, H.M. (1994) Interactions between animal cells and gas bubbles: The influence of serum and Pluronic F68 on the physical properties of the bubble surface. *Biotechnol. Bioeng.* **43**, 446–454.
- Kioukia, N., Nienow, A.W., Al-Rubeai, M. and Emery, A.N. (1996) Influence of agitation and sparging on the growth rate and infection of insect cells in bioreactors and a comparison with hybridoma culture. *Biotechnol Prog* **12**, 779–785.
- Kowalski, A.J. and Thomas, N.H. (1995) Bubbles burst the myth of shear damage in cell suspension bioreactors. *Adv. Biochem. Eng.* 82–84.

- Kunas, K.T. and Papoutsakis, E.T. (1990) Damage mechanisms of suspended animal cells in agitated bioreactors with and without bubble entrainment. *Biotechnol. Bioeng.* **36**, 476–483.
- Lakhotia, S. and Papoutsakis, E.T. (1992) Agitation induced cell injury in microcarrier cultures. Protective effect of viscosity is agitation intensity dependent: experiments and modeling. *Biotechnol. Bioeng.* **39**, 95–107.
- Lu, G.Z., Thompson, B.G. and Gray, M.R. (1992) Physical modeling of animal cell damage by hydrodynamic forces in suspension cultures. *Biotechnol. Bioeng.* **40**, 1277–1281.
- MacIntyre, F. (1972) Flow patterns in breaking bubbles. *J. Geophysical Research* **77**, 5211–5228.
- Martens, D.E., Gooijer, C.D. de, Beuvery, E.C. and Tramper, J. (1992). Effect of serum concentration on hybridoma viable-cell density and production of monoclonal antibodies in CSTRs and on shear sensitivity in air-lift loop reactors. *Biotechnol. Bioeng.* **39**, 891–897.
- Martens D.E., Gooijer C.D. de, Velden-de-Groot C.A.M. van der, Beuvery E.C. and Tramper J. (1993) Effect of dilution rate on growth, productivity, cell cycle and size, and shear sensitivity of a hybridoma cell in a continuous culture. *Biotechnol Bioeng.* **41**, 429–439.
- Martens, D.E., Nollen, E.A.A., Hardeveld, M., Velden-de-Groot, C.A.M. van der, Gooijer, C.D. de, Beuvery, E.C. and Tramper, J. (1996) Death rate in a small air-lift loop reactor of Vero cells grown on solid microcarriers and in macroporous microcarriers. *Cytotechnol* **21**, 45–59.
- McQueen, A. and Bailey, J.E. (1989). Influence of serum level, cell line, flow type and viscosity on flow-induced lysis of suspended mammalian cells. *Biotechnol. Lett.* **11**, 531–536.
- Meier, S.J., Hatton, T.A. and Wang, D.I.C. (1999). Cell death from bursting bubbles: Role of cell attachment to rising bubbles in sparged reactors. *Biotechnol. Bioeng.* **62**, 468–478.
- Michaels, J.D., Petersen, J.F., McIntire, L.V. and Papoutsakis, E.T. (1991) Protection mechanism of freely suspended animal cells (CRL 8018) from fluid-mechanical injury. Viscometric and bioreactor studies using serum, Pluronic F68 and polyethylene glycol. *Biotechnol. Bioeng.* **38**, 169–180.
- Michaels, J.D., Nowak, J.E., Mallik, A.K., Koczo, K., Wasan, D.T. and Papoutsakis, E.T. (1995a) Analysis of cell-to-bubble attachment in sparged bioreactors in the presence of cell-protecting agents. *Biotechnol. Bioeng.* **47**, 407–419.
- Michaels, J.D., Nowak, J.E., Mallik, A.K., Koczo, K., Wasan, D.T. and Papoutsakis, E.T. (1995b) Interfacial properties of cell culture media with cell-protecting additives. *Biotechnol. Bioeng.* **47**, 420–430.
- Michaels, J.D., Mallik, A.K. and Papoutsakis, E.T. (1996) Sparging and agitation-induced injury of cultured animal cells: Do cell-to-bubble interactions in the bulk liquid injure cells? *Biotechnol. Bioeng.* **51**, 399–409.
- Murhammer, D.W. and Goochee, C.F. (1988) Scale-up of insect cell cultures: Protective effects of Pluronic F-68. *Bio/Technol.* **6**, 1411–1418.
- Murhammer, D.W. and Goochee, C.F. (1990a) Structural features of nonionic polyglycol polymer molecules responsible for the protective effect in sparged animal cell bioreactors. *Biotechnol. Prog.* **6**, 142–148.
- Murhammer, D.W. and Goochee, C.F. (1990b) Sparged animal-cell bioreactors: mechanism of cell damage and Pluronic F-68 protection. *Biotechnol Prog.* **6**, 391–397.
- Murhammer, D.W. and Pfalzgraf, E.C. (1992) Effects of Pluronic F-68 on oxygen transport in an agitated, sparged bioreactor. *Biotechnol Techn.* **6**, 199–202.
- Needham, D., Ting-Beall, H.P. and Tran-Son-Tay, R. (1991) A physical characterization of GAP A3 hybridoma cells: morphology, geometry and mechanical properties. *Biotechnol Bioeng.* **38**, 838–852.
- Oh, S.K.W., Nienow, A.W., Al-Rubeai, M. and Emery, A.N. (1989) The effect of agitation intensity with and without continuous sparging on the growth and antibody production of hybridoma cells. *J. Biotechnol.* **12**, 45–62.
- Oh, S.K.W., Nienow, A.W., Al-Rubeai, M. and Emery, A.N. (1992) Further studies of the culture of mouse hybridomas in an agitated bioreactor with and without continuous sparging. *J. Biotechnol.* **22**, 245–270.

- Orton, D.R. 1992. Quantitative and mechanistic effects of bubble aeration on animal cells in culture. Ph.D. Thesis, Massachusetts Institute of Technology, Cambridge, MA.
- Papoutsakis, E.T. (1991a) Fluid mechanical damage of animal cells in bioreactors. *TIBTECH* **9**, 427–37.
- Papoutsakis, E.T. (1991b) Media additives for protecting freely suspended animal cells against agitation and aeration damage. *TIBTECH* **9**, 316–324.
- Petersen, J.F., McIntire, L.V. and Papoutsakis, E.T. (1988) Shear sensitivity of cultured hybridoma cells (CRL-8018) depends on mode of growth, culture age and metabolite concentration. *J. Biotechnol* **7**, 229–246.
- Petersen, J.F., McIntire, L.V. and Papoutsakis, E.T. (1990) Shear sensitivity of hybridoma cells in batch, fed-batch, and continuous cultures. *Biotechnol. Prog.* **6**, 114–120.
- Pol, L. van der, Zijlstra, C.M., Thalen, M. and Tramper, J. (1990) Effect of serum concentration on production of monoclonal antibodies and on shear sensitivity of a hybridoma. *Bioproc. Eng.* **5**, 241–245.
- Pol, L. van der, Bakker, W.A.M. and Tramper, J. (1992) Effects of low serum concentrations (0%–2.5%) on growth, production, and shear sensitivity of hybridoma cells. *Biotechnol. Bioeng.* **40**, 179–182.
- Pol, L. van der, Bonarius, D., Wouw, G.van der, and Tramper, J. (1993) Effect of silicone antifoam on shear sensitivity of hybridoma cells in sparged cultures. *Biotechnol. Prog.* **9**, 504–509.
- Ramirez, O.T. and Mutharasan, R. (1990) The role of the plasma-membrane fluidity on the shear sensitivity of hybridomas grown under hydrodynamic stress. *Biotechnol. Bioeng.* **36**, 911–920.
- Ramirez, O.T. and Mutharasan, R. (1992) Effect of serum on the plasma-membrane fluidity of hybridomas: An insight into its shear protective mechanism. *Biotechnol. Prog.* **8**, 40–50.
- Rooney, J.A. (1970) Hemolysis near an ultrasonically pulsating gas bubble. *Science* **169**, 869–871.
- Sato, M., Levesque, M.J. and Nerem, R.M. (1987) An application of the micropipette technique to the measurement of the mechanical properties of cultured bovine aortic endothelial cells. *J. Biochem. Eng.* **109**, 27–34.
- Schuch, U., Kramer, H.Einsele, A.Widmer, F. and Eppenberger, H.M. (1988). Experimental evaluation of laminar shear stress on the behavior of hybridoma mass cell cultures, producing monoclonal antibodies against mitochondrial creatine kinase. *J. Biotechnol.* **7**, 179–184.
- Smith, C.G., Greenfield, P.F. and Randerson, D.H. (1987) A technique for determining the shear sensitivity of mammalian cells in suspension culture. *Biotechnol. Technol.* **1**, 39–44.
- Stathopoulos, A. and Heliums, J.D. (1985) Shear stress effects on human embryonic kidney cells in vitro. *Biotechnol. Bioeng.* **27**, 1021–1026.
- Tan, W.S., Dai, G.C. and Chen, Y.L. (1995) Quantitative investigations of cell-bubble interactions using a foam fractionation technique. *Cytotechnol.* **15**, 321–328.
- Telling, R.C. and Elsworth, R. (1965) Submerged culture of hamster kidney cells in a stainless steel vessel. *Biotechnol. Bioeng.* **7**, 417–434.
- Thomas C.R., Al-Rubeai M. and Zhang, Z. (1995) Prediction of mechanical damage to animal cells in turbulence. *Cytotechnol.* **15**, 329–335.
- Tramper, J., Williams, J.B. and Joustra, D. (1986) Shear sensitivity of insect cells in suspension. *Enzyme Microbiol. Technol.* **8**, 33–36.
- Tramper, J., Smit, D., Straatman, J. and Vlak, J.M. (1988) Bubble-column design for growth of fragile insect cells. *Bioproc. Eng.* **3**, 37–41.
- Trinh, K., Garcia-Briones, M., Hink, F. and Charniers, J.J. (1994) Quantification of damage to suspended insect cells as a result of bubble rupture. *Biotechnol. Bioeng.* **43**, 37–45.
- Wang, N.S., Yang, J.-D., Calabrese, R.V. and Chang, K.-C. (1994) Unified modeling framework of cell death due to bubbles in agitated and sparged bioreactors. *J. Biotechnol.* **33**, 107–122.
- Wen, Z.Y. and Tan, W.S. (1999) Quantitative measurement of cell-bubble attachment in bubble columns using foam flotation techniques. *Biotechnol. Techn.* **13**, 131–135.
- Wu, J. and Goosen, M.F.A. (1994) Investigation of air-liquid damage of animal cells in a falling film-flow device. *Biotechnol. Techn.* **8**, 111–116.

- Wu, J. and Goosen, M.F.A. (1995a) Evaluation of the killing volume of gas bubbles in sparged animal cell culture bioreactors. *Enzyme Microbiol. Technol.* **17**, 241–247.
- Wu, J. (1995b) Mechanisms of animal cell damage associated with gas bubbles and cell protection by medium additives. *J. Biotechnol.* **43**, 81–94.
- Wu, J., Daugulis, A.J., Faulkner, P. and Goosen, M.F.A. (1995c) Protective effects of polymer additives on animal cells exposed to rapidly falling liquid films. *Biotechnol. Prog.* **11**, 127–132.
- Wu, J., Ruan, Q. and Lam, H.Y.P. (1997) Effects of surface active medium additives on insect cell surface hydrophobicity relating to cell protection against bubble damage. *Enzyme Microbiol. Technol.* **21**, 341–348.
- Yang, J.-D. and Wang, N.S. (1992) Cell inactivation in the presence of sparging and mechanical agitation. *Biotechnol. Bioeng.* **40**, 806–816.
- Zhang, Z., Ferenczi, M.A., Lush, A.C. and Thomas, C.R. (1991) A novel micro-manipulation technique for measuring the bursting strength of single mammalian cells. *Appl. Microbiol. Biotechnol.* **36**, 208–210.
- Zhang, Z., Al-Rubeai, M. and Thomas, C.R. (1992a) Mechanical properties of hybridoma cells in batch culture. *Biotechnol. Lett.* **14**, 11–16.
- Zhang, Z., Al-Rubeai, M. and Thomas, C.R. (1992b) Effect of Pluronic F-68 on the mechanical properties of mammalian cells. *Enzyme Microb. Technol.* **14**, 980–983.
- Zhang, S., Handa-Corrigan, A. and Spier, R.E. (1992c) Oxygen transfer properties of bubbles in animal cell culture media. *Biotechnol. Bioeng.* **40**, 252–259.
- Zhang, Z. and Thomas, C.R. (1993a) Micro-manipulation: A new approach to studying animal cell damage in bioreactors. *The genetic Engineer and Biotechnologist* **13**, 19–29.
- Zhang, Z., Al-Rubeai, M. and Thomas, C.R. (1993b) Estimation of disruption of animal cells by turbulent capillary flow. *Biotechnol. Bioeng.* **42**, 987–993.
- Zhang, Z., Al-Rubeai, M. and Thomas, C.R. (1993c) Comparison of the fragilities of several animal cell lines. *Biotechnol. Techn.* **7**, 117–182.

# CHAPTER SIXTEEN

## A LOW-COST TECHNOLOGY FOR ENTOMOPATHOGENIC NEMATODE LARGE-SCALE PRODUCTION

JOSÉ NEVES<sup>1</sup>, NELSON SIMÕES<sup>1</sup> AND MANUEL MOTA<sup>2</sup>

<sup>1</sup> Departamento de Biologia e Centro de Investigação em Recursos Naturais, Universidade dos Açores, 9501–801 Ponta Delgada, Portugal  
<sup>2</sup> Department of Biological Engineering, Universidade do Minho, 4710–057 Braga, Portugal

### ABSTRACT

Entomopathogenic nematodes of the genera *Steinernema* and *Heterorhabditis* may provide a valuable alternative to chemical insecticides. The characteristics that make them excellent biopesticides include their wide host spectrum, the ability to search for and kill hosts rapidly, and their high virulence and reproductive rates. Furthermore, they are considered environmentally safe. The major constraint to overcome before the onset of commercialisation is their mass production. Entomopathogenic nematodes are currently mass-produced *in vivo* or *in vitro*, either in solid culture or in liquid cultivation. An overview of these mass production methods and an analysis of three different bioreactor designs are presented. The progress achieved in liquid culture due to an improvement on sexual contact between adults (better mixture of the solid phase), which results in higher yields (RF), as compared with those reported before, is demonstrated. This improvement in the area of bioreaction engineering allowed these biopesticides to become more competitive compared to chemical insecticides. However, further technological advances and biological studies towards a better understanding of physiology and genetics of the complex nematode-bacterium are still required.

**Keywords:** biological control, biopesticide, entomopathogenic nematodes, mass production, liquid cultivation, airlift bioreactor

### INTRODUCTION

Nematodes are cylindrical roundworms that are unsegmented and lack appendages. They can be free-living, predaceous, or parasitic. Many of the parasitic species cause disease to plants, animals and humans. However, other species are beneficial in attacking insect

pests. Among them, entomopathogenic nematodes of the genera *Steinernema* and *Heterorhabditis* emerged as excellent candidates for biological control of insect pests.

Entomopathogenic nematodes form dauer (enduring) juveniles (DJs) which are morphologically and physiologically adapted for long-term survival in the soil (Figure 16.1). These DJs carry, in the anterior part of the intestine, an associated bacterium; *Xenorhabdus* spp. and *Photorhabdus* spp. in *Steinernema* and *Heterorhabditis* respectively.

When infective DJs locate a susceptible host insect, they enter through the natural body openings (mouth, spiracles and anus) or directly through the insect cuticle and invade its hemocoel, after which they release the bacteria. The bacteria multiply, killing the insect by septicaemia within 24–48 h of infection. The nematodes feed on the host tissue and cells of the symbiotic bacteria, develop into adults, mate, and reproduce inside the host, often for multiple generations. When host nutrients are depleted, DJs are produced and, upon leaving the dead insect, seek and infect new hosts.

Thus, entomopathogenic nematodes are a nematode-bacterium complex. In this complex the relationship between the nematode and the bacterium is symbiotic because nematode growth and complete development depend upon conditions established by the bacterial action and, as bacteria lack invasive capacity, they depend upon the nematode to enter the insect hemocoel, thereby causing infection.



### Figure 16.1 *Sieinernema carpocapsae* dauer juvénile.

#### Nematodes as Bioinsecticides

Since the 1930s steinernematids have been used as agents against agricultural pests. Particular characteristics of these entomopathogenic nematodes are their wide host spectrum, which include the majority of insect orders and families, their ability to search for and kill hosts rapidly, and their high virulence and reproductive rates. Moreover, the steinernematids are considered environmentally safe and non-toxic to mammals, being, thus, exempt from registration in the U.S. as well as in the majority of the E.U. countries.

As Djs spend their entire life cycle in the soil, they are ideal parasites of insects living in the soil and in cryptic habitats. Thus, the market for these nematodes are predominantly soildwelling insect pests that attack crops such as com, rice, vegetables and ornamentals, where nematodes can be used alone or combined with other agents. Examples of commercial nematode-based products that have been successfully used are: *Othyorinchus sulcatus* (black vine weevil), *Scapteriscus vicinus* (tawny mole crickets); *Fumibotys jumalis* (the mint root borer); *Chrysoteuchia topiaria* (the cranberry girdler); *Pachnaeus litus* (Florida citrus); *Diabrotica virgifera virgifera* (western corn rootworm); *Popillia japonica* (Japanese beetle); *Bradysia* spp (fungus gnat); and several *Noctuidae* in different crops.

Entomopathogenic complex insecticidal proteins have been sought since the 1990s. The infective DJ is able to invade insect tissues probably due to a combined mechanical and enzymatic activity and it has been proved that *S. carpocapsae* infective secretes, in artificial growth media, proteases shortly after its development starts. These proteases cause the histolysis of the insect mid-gut, suggesting that they participate in the invasive process (Simões *et al.*, 2000). Once inside the host hemocoel, *S. carpocapsae* infectives are able to escape insect defences, and to produce several other proteins, that cause the insect's immuno-depression (Götz *et al.*, 1981) and are toxic (Burman, 1982; Boemare *et al.*, 1982). Some of these proteins were obtained *in vitro* and it was shown that they cause mortality on insects (Simões & Rosa, 1996).

*Xenorhabdus nematophilus* are highly pathogenic to insects. They multiply quickly in insect hemocoel causing bacteraemia and releasing several enzymes and other proteins that cause toxæmia (Forst *et al.*, 1997). Recently, it has been suggested that two proteases released by the bacteria are involved in the pathogenic process.

#### Why Mass Produce Entomopathogenic Nematodes?

The main impetus for the commercialisation of insect biocontrol agents is the perception that regulatory pressures imposed by governmental agencies and public opinion will increase. Both demand insecticides with low toxicity and short-term persistence, low mobility in the soil to prevent ground-water contamination, limited effects on non-target organisms and a far greater reduction on chemical input into the environment. These prerequisites have reduced the chance of new active insecticides to be developed and successfully registered.

Entomopathogenic nematodes, because of all the characteristics stated above, can alternatively be used to control soil insects and even have substantial advantages over chemical insecticides.

## NEMATODE MASS PRODUCTION IN BIOREACTORS

Commercial exploitation of entomopathogenic nematodes, as of any biological control agent, depends on the selection of an adequate lineage and on the ability of industry to develop and commercialise *Steinernema* as a biopesticide. Until now, one of the most important limiting factors for the development of nematode-based products has been the inability of industry to develop an adequate productive process in order to obtain an economy of scale.

Over the past twenty years significant progress in our understanding of the nutritional requirements of entomopathogenic nematodes resulted in the development of mass production methods. Nowadays, and depending on the objective, three production systems are currently used: *in vivo*, solid culture and liquid cultivation.

### ***In Vivo* Production**

The first fully operational technique of mass production of *S. carpocapsae* was began in the United States (Dutky, 1964) and is based on parasitism of the greater wax moth, *Galleria mellonella*, by the nematode. It is a simple technique but the cost of production is high and it does not allow an economy of scale. In fact, the duplication of the production capacity requires the duplication of the area and the duplication of the capital. In addition, since the process requires a lot of hand labour, if it is not automated, the costs linearly increase with time. Moreover, the process requires the parallel multiplication of an insect host, which, in turn, also does not allow an economy of scale either. As important as the above aspects is the absence of an economy of quality as the production scale is increased. In fact, the opposite occurs: as scale increases, the *in vivo* nematode production is much more sensitive to insect disease outbreaks which are so characteristic of mass rearing.

### ***In Vitro* Production**

The limitations of *in vivo* production, coupled to the finding that entomopathogenic nematodes could grow in artificial medium with their symbiotic bacteria, the need for larger scale and more economical methods and the recent advances in the understanding of the nutritional requirements of steinernematids, resulted in the development of *in vitro* mass production methods.

#### ***Solid culture***

Bedding (1981, 1984) developed a system based on the use of small pieces of inorganic support (shredded sponge) soaked with protein-rich media (preferably chicken offal).

This substrate was autoclaved, inoculated with the symbiotic bacterium and incubated. After a two-day incubation, juveniles were inoculated and incubated.

This system promotes the aeration of the environment in nematode culture and a large area to volume ratio for the reproduction and development of the nematode/bacterium complex allowing yields of approximately  $10 \times 10^9$  dauer juveniles per 3-Kg bag of media.

The “Bedding-System” is a flexible method with low capital costs and it does not need specialised workmanship; therefore, it is attractive for many American, European and Chinese companies. It represents a significant improvement in the productive process of entomopathogenic nematodes. However, this system has some important disadvantages: its sensitivity to contamination, the need for large climate-controlled space for incubation, the considerable amounts of water necessary for downstream and the huge amount of solid waste material to be disposed of. In a scale-up model, Friedman (1990) reported that the “Bedding-System” was economically feasible up to a production level of approximately  $10 \times 10^{12}$  DJs per month. For nematode production beyond this level, labour costs increase significantly suggesting that more advanced technology is needed to support larger scale production of entomopathogenic nematodes.

### *Liquid culture*

Nowadays, it is consensual that the technology of cultivation in liquid medium could be the best method for the mass production of these biopesticides, as the maximisation of volumetric productivity allows the minimisation of the capital invested (Bonifassi & Neves, 1990, Friedman, 1990; Ehlers, 1996). On the other hand, liquid medium culture simplifies the “scale-up” and downstream processing thus allowing their cost reduction.

The first reference to the culture of *Steinernema* in liquid medium goes back to the 1940s (Glaser, 1931, 1940). Since then, the growth of nematodes in liquid medium has been firmly established. Several studies showed that the biological and physiological needs of the nematodes could be satisfied in liquid medium; first in small volumes (Stoll, 1961; Jackson, 1973; Buecher & Popiel, 1989) and later in larger volumes (Georgis & Hague, 1991).

Pace *et al.* (1986) obtained concentrations of  $90 \times 10^3$  DJs/ml in a 10L stirred tank bioreactor. Friedman *et al.* (1989) reported concentrations above  $95 \times 10^3$  DJs/ml in an airlift bioreactor. Despite these progresses, the production costs are still high, thereby limiting the use of these biopesticides to control insect pests in high-value crops. Therefore, it is crucial to improve the biotechnological process acting at the level of the bioreaction engineering and more specifically in the bioreactor design.

## BIOREACTORS FOR ENTOMOPATHOGENIC NEMATODE PRODUCTION

*Steinernematid* mass production in liquid culture is a highly complex process when compared with the liquid culture of yeast or bacteria. Indeed, we are discussing a mixed multiphasic system. In this system the solid phase is not homogeneous. Furthermore, the reproduction of these organisms is only sexual, involving therefore a correct blending

between sexually dimorphic males and females, with different lengths and densities (Neves *et al.*, 1996), and these adults coexist with several other developmental stages.

To this solid phase, we must add a liquid phase where the nutrients are dissolved and, because nematodes are aerobes, abundant aeration to the liquid medium, where the solubility of oxygen is very low. Thus, in the case of liquid culture of entomopathogenic nematodes we are compelled to take into account at least two solid phases—one for each sex, if one disregards the influence of the intermediate juvenile nematode stages—a liquid phase and a gaseous phase. The need for an appropriate mating rate coupled with the different shear sensitivity of all stages present in the bioreactor lead to the conclusion that traditional stirred bioreactors are definitely not appropriate for achieving high nematode productivities. A multiphase bioreactor is therefore needed.

Airlift systems are becoming everyday more important (Siegel & Robinson, 1992) and should be considered as an alternative to the stirred bioreactor. In an airlift system, the fluidisation of solids is not a direct consequence of the bubbling of gas, but rather due to the liquid circulation within the bioreactor. This system creates an environment of relatively low shear forces ideal for the culture of sensible cells, e.g. those of mammals, vegetables and nematodes, and is especially appropriate for three-phase systems (Kargi & Cervoni, 1983; Kloosterman & Lilly, 1985; Kennard & Janekeh, 1991). There should be a potential application of airlift systems in three-phase processes where gas, liquid and solids must be brought into contact, which is the case for nematode cultivation.

### **Bioreactor Design**

The design of a bioreactor—the heart of a cultivation process where a favourable environment is maintained—must satisfy the biological and technological requirements of the process in cause. Pace *et al.* (1986) and Friedman *et al.* (1989) verified that aeration was the most difficult requirement to meet and that shear sensitivity was the most significant limitation for efficient nematode production. Neves *et al.* (1998) pointed out the low copulation rates, resulting from high aeration and agitation rates, as a factor of great importance in the low yields obtained. Due to the particular characteristics of entomopathogenic nematodes—namely shear sensitivity and sexual dimorphism—mass production in liquid cultivation cannot follow the traditional concepts normally used in the stirred bioreactors. Two major factors have been mandatory in the choice of the bioreactor design: i) an adequate blending of the two sexes; and ii) an appropriate oxygen supply with an acceptable shear stress.

The following examples illustrate the use of several airlift configurations in the liquid cultivation of entomopathogenic nematodes.

#### ***Internal-loop airlift***

An internal-loop airlift bioreactor, was constructed in Perspex (Figure 16.2). The total height was 0.30 m, a downcomer (D) with 0.23 m of height and an inside diameter of 0.032 m, containing a concentric 0.125 m high and 0.016 m diameter draft tube (R). The ratio of the cross-sectional area of the riser to the down-comer (AR/AD) was 0.28. The top section was of the one of cylindrical conical type. The angle of the conical sector with

the main body of the reactor was 45° and the height and diameter of the cylindrical part were, respectively, 0.11 m and 0.06 m.

The air was injected beneath the riser annulus by means of a nozzle injector with 0.5 mm diameter.

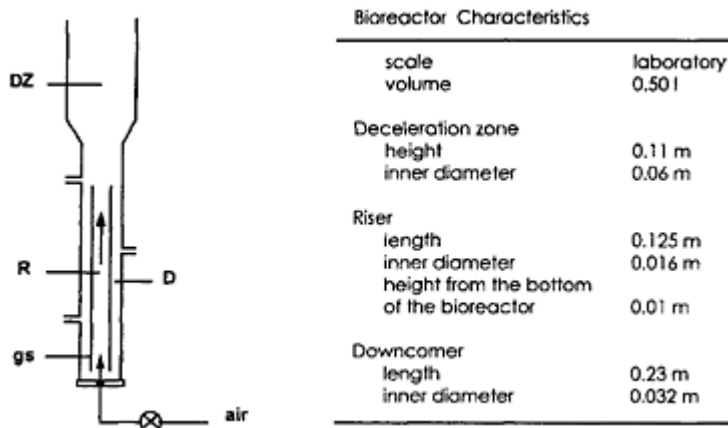


**Figure 16.2** Schematic diagram of the internal-loop bioreactor. R (riser); D (down-comer); DZ (deceleration zone); gs (gas sparger).

#### *Conventional external-loop airlift*

The schematic diagram of the conventional external-loop airlift is shown in Figure 16.3. It consisted of a Plexiglas bioreactor and was composed of a riser (R) with an inside diameter of 0.032 m and a downcomer with an inside diameter of 0.016 m. The ratio of the cross-sectional area of the downcomer (D) to the riser (AD/AR) was 0.28. The top of the riser—deceleration zone (DZ)—was of cylindrical conical type, to facilitate the solid phase (nematodes) deceleration. The height and diameter of this enlarged part were 0.11 m and 0.06 m, respectively. All other dimensions are shown in Figure 16.3. The riser, down-comer and connecting pipes were tubular and, in order to avoid a settling zone, the down-

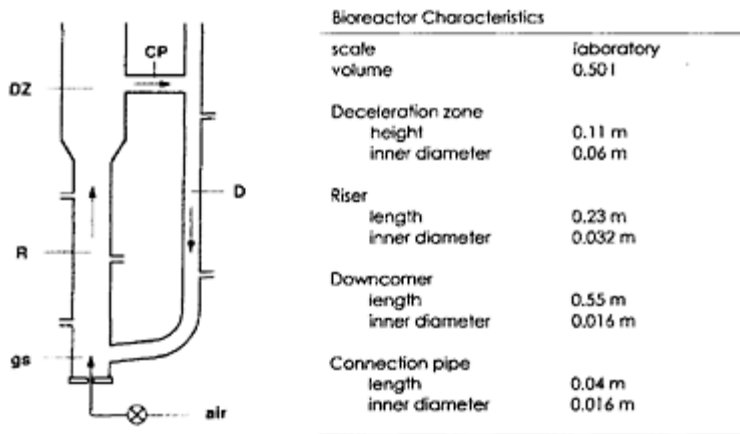


**Figure 16.3** Schematic diagram of the conventional external-loop bioreactor.  
R (riser); D (down-comer); DZ (deceleration zone); gs (gas sparger); CP (connection pipe).

most connection pipe between the riser and down-comer was inclined. The airlift vessel contained a non-aerated working volume of 0.5 L. Air was sparged into the bioreactor through a nozzle injector with a 0.5 mm diameter placed beneath the riser.

#### *Non conventional external-loop airlift*

The most important design characteristics are shown in Figure 16.4. The bioreactor included a circulation zone (CZ) and a deceleration zone (DZ). The circulation zone was composed by two connected pipes: one of 0.23 m and 0.032 m and the other of 0.55 m and 0.0016 m, height and diameter respectively. The height of the deceleration zone was 0.11 m and the diameter 0.06 m. This zone had 2 concentric bulkheads to decrease the liquid circulation velocity. To avoid solids settling, the connection pipe between the circulation zone and the deceleration zone was inclined.

#### Experimentation

The experimentation included i) the hydrodynamic characterisation of each bioreactor (measurement of mixing parameters and of oxygen mass transfer) and ii) the determination of the bioreactors efficiency concerning adult distribution, mass transfer and yields.

With the internal-loop airlift bioreactor, the circulation and hence the distribution of both adult forms was uniform across the different sections of the bioreactor. One of the basic premises was the improvement in contact between the two sexes: the experimental

results obtained with this configuration proved its inadequacy to promote an increase in the mating rate.

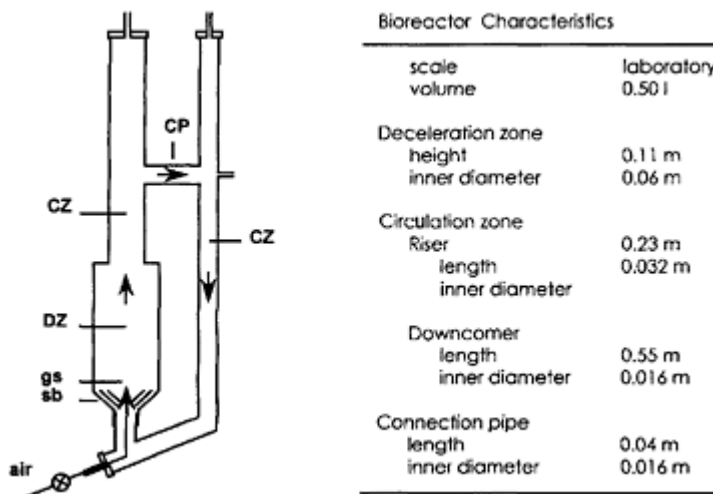


**Figure 16.4** Schematic diagram of the experimental non-conventional external-loop bioreactor. CZ (circulation zone); DZ (deceleration zone); CP (connection pipe); gs (gas sparger); sb (setting baffles).

The experiments with the external-loop airlift bioreactor clearly showed that male and female distribution was affected differently (Figure 16.5) (Neves, 1994). The distribution of males (Figure 16.5A) was independent of the airflow rate, whereas the female distribution pattern showed a strong dependence on the aeration (Figure 16.5B). This is not surprising and should be expected considering the differences between males and females in the physical properties concerned, namely size and density. Indeed, *S. carpocapsae* females are much bigger than males and have a different density (Neves *et al.*, 1996b). These differences led to different sedimentation rates and, under different airflow rates, to different distribution patterns. At 0.05 vvm, the liquid circulation velocity ( $0.30 \text{ cms}^{-1}$ ) was slightly lower than the sedimentation rate of the nematode females in Tyrodes' solution ( $0.37 \text{ cms}^{-1}$ ). Under these conditions, it was possible to retain 60.6 % of the females in the deceleration zone. When the airflow rate was 0.09 vvm, females tended to distribute evenly between the different sections of the bioreactor and this tendency became more prominent at 0.15 vvm. At this airflow rate, the liquid circulation velocity increased to  $0.62 \text{ cms}^{-1}$  and the percentage of females retained in the deceleration zone decreased to 38.9%. In general, it may be concluded that high airflow rates bring about a uniform nematode distribution.

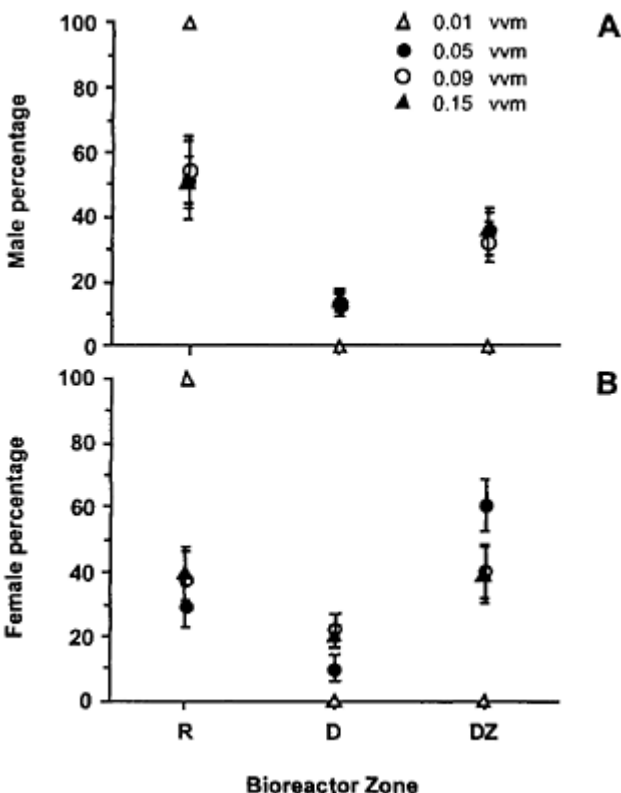


**Figure 16.5** Distribution of males (A) and females (B) in the conventional external-loop bioreactor at different airflow rates.

The mass transfer coefficient ( $k_{L}a$ ) was measured for different airflow rates. Increasing the airflow rate increased the  $k_{L}a$ , with  $9.3\text{ h}^{-1}$  at 0.05 vvm as the highest value. This value is insufficient to fulfil the oxygen requirements of nematode cultures (Neves *et al.*, 1996a) and lower than the one reported by other authors (Chisti, 1989) for identical systems. The small dimensions of the bioreactor and the design of the air distribution system could account for the low  $k_{L}a$  observed.

Concerning yields obtained after 15 days operation, at 0.05 vvm the DJs production in the bioreactor attained  $30 \times 10^6$  ( $60 \times 10^3/\text{ml}$ ). This value underwent a 39% reduction when an airflow rate of 0.15 vvm was used. In these conditions the maximum number of DJs obtained was just  $19 \times 10^6$  ( $38 \times 10^3/\text{ml}$ ).

It is important to notice that the above set of results shows the heterogeneity of adult distribution pattern when different airflow rates are used. These experimental observations appear to agree with similar findings by Siegel *et al.* (1989) and Assa and Bar (1991). The solid phase heterogeneity can be very important when this solid phase is

composed of particles with different physical properties such as nematodes in which males and females have different sizes and densities (Neves *et al.*, 1996b). In order to maximise egg productivity, which after hatching will give rise to juveniles, as many females as possible must be fertilised. Therefore, it is important to concentrate females in one region of the bioreactor, so that mating between the retained females and the circulating males will be favoured.

On the other hand, as shown in Figure 16.5, with the exception of 0.01 vvm the region where the maximum number of females is observed—always above 40% of the total—corresponds, in all aeration rates, to the deceleration zone. Furthermore, the aeration which maximises the number of males is in DZ is 0.05 vvm. On the contrary, for 0.15 vvm, a smaller number of males will be present in DZ. Thus, it is quite reasonable to admit that the encounters between males and females are favoured by an aeration rate of 0.05 vvm. Since it was shown that the yield was at its maximum at 0.05 vvm, it is also probable that mating occurs mainly in DZ.

Analysis of the data obtained with the conventional external-loop airlift bioreactor showed that it was possible to improve the mixing and increase  $k_{La}$  and consequently increase yields (exploiting the particularities of the solid phase, namely the density differences between adults) by coupling a decanter to the bioreactor. Therefore, a non-conventional external-loop airlift bioreactor was designed. In this bioreactor, the enlarged part of the riser—deceleration zone—acted as a “gynaeceum” where the mating rate was enhanced.

The experimental results obtained with the novel bioreactor confirmed expectations. For airflow rates of 0.3 vvm, male concentrations in the deceleration zone were close to 60% (Figure 16.6A). For higher airflow rates, the male distribution was uniform. Similarly, at airflow rates between 0.3 and 0.8 vvm it was possible to retain 70% of females in the deceleration zone (Figure 16.6B). For higher airflow rates, the female DZ concentration was reduced and females tended to uniformly distribute across all sections of the bioreactor.

It is important to notice that the airflow rates used in this reactor were tenfold greater than on the other bioreactors used. As a consequence, the volumetric oxygen mass transfer coefficient increased significantly, varying between  $40.9\text{ h}^{-1}$  and  $138\text{ h}^{-1}$  for 0.3 vvm

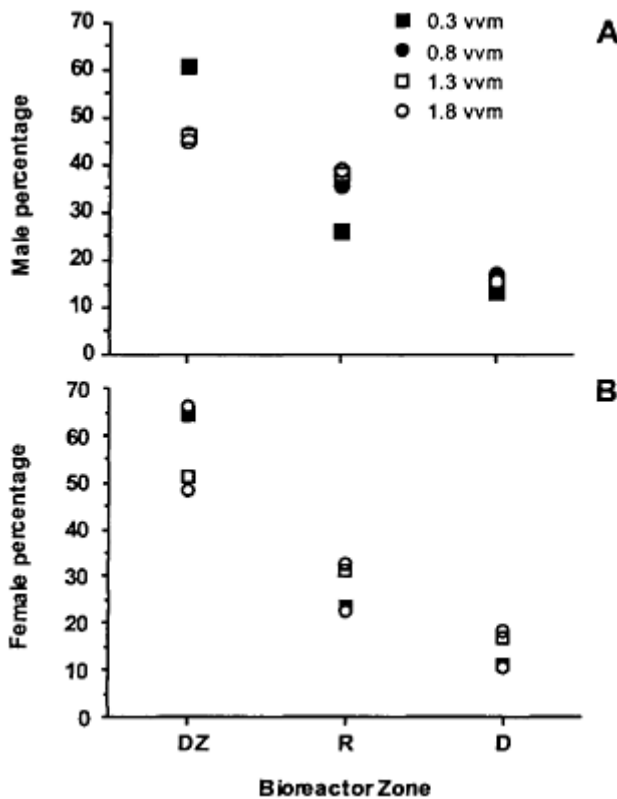


**Figure 16.6** Distribution of males (A) and females (B) in the non-conventional external-loop bioreactor at different airflow rates.

and 2.8 vvm respectively. For 0.8 vvm, the airflow rate which promotes the biggest concentration of females (70%), the  $k_{La}$  was  $50.9\text{ h}^{-1}$ . Under these conditions, after 15 days of operation, it was possible to obtain a total number of DJs of  $59 \times 10^6$  ( $97.5 \times 10^3/\text{ml}$ ) (Neves *et al.*, 1998).

## CONCLUSIONS

Recent developments in bioreactor design have attempted to either address some of the limitations of existing bioreactors or open new avenues in bioprocessing. The further development of innovative bioreactor designs remains a high priority, since a single bioreactor configuration will never provide universal solution. In many instances, progress in a reactor design will require preliminary advances in the biological fundamentals. Conversely, many questions addressed to biologists by bioprocess

engineers may provide new fields for fundamental research. The answers found in the meantime may then give rise to a more rational, creative and focused approach to bioreactor design.

The data obtained in this work show that the airlift system proposed is rather more efficient than those reported before (e.g., Pace *et al.*, 1986 and Friedman *et al.*, 1989) (Table 16.1). The advantage of the proposed bioreactor design results from the improvement of sexual contact between adults by creating a zone of low liquid velocity where a high concentration of females is maintained, thus increasing the mating opportunities with males that circulate in the bioreactor. In fact, although uniform distribution of the solid and liquid phases throughout the airlift vessel is generally sought, it is sometimes desirable to create non-homogenous distribution patterns of the solid phase in particular cases. By associating the differences in the physical properties of the components of the solid phase—namely, male and female nematodes—with an adequate design for the bioreactor, it was possible to develop a more efficient system for nematode production in submerged cultures.

The improvement obtained with this design becomes more clear if the yield achieved, i.e., the reproductive factor ( $RF = \text{final concentration}/\text{inoculum concentration}$ ), is compared with those obtained with other *S. carpocapsae* production systems. As may be seen in Table 16.1, with the novel bioreactor design, a 2-fold improvement in yield was achieved. The data also show that the aeration rate could not be directly responsible for production differences, since a lower aeration rate induced a higher production. The significantly higher yield must be associated with an increase in the mating rate due to a lower liquid circulation velocity.

In spite of these data, there are still some questions to be answered, which may bring about a great impact. Coupled with the advances in bioreaction engineering, particularly in bioreactor design and process control, optimisation of the cultivation environment (physical and chemical) is of utmost importance for maximising development, copulation, fecundity and formation of dauer juveniles.

Organism development is also a key area in liquid culture. Thus, a better understanding of both nematode and bacterial biology, especially genetics and physiology, is required.

The process of exit from enduring infective stage (recovery) is crucial. The importance of recovery lies on its influence on population dynamics, the duration of the cultivation process and, certainly, on the final yield. The percentage of in vitro culture recovery is very low, but so far little is known about the factor(s) that control this process, urging the need to better understand its regulatory mechanisms.

**Table 16.1** Yield comparison among different bioreactor designs for production of *Steinernema carpocapsae* in liquid medium

Bioreactor	Duration (Days)	Inoculum (DJs/ml)	Final (DJs/ml)	Rf
stirred tank bioreactor (a)	20	2000	90000	45
internal-loop airlift bioreactor (b)	15	1000	95000	95

internal-loop airlift bioreactor (c)	15	500	60000	120
external-loop airlift bioreactor (c)	15	500	97500	195

Rf (reproduction factor)=Final concentration/Inoculum concentration,

(a) Pace *et al.* (1986); (b) Friedman *et al.* (1989); (c) our work

On the other hand, the importance of *Xenorhabdus* spp. in nematode production is well-documented (Akhurst & Boemare, 1990). The bacterium has two phases, the primary and secondary, the primary being the only phase that supports greater nematode production. Both, genetic and physiological approaches must be used in order to know i) the dynamics of the two phases in the bioreactor; ii) the stability of the primary form of the bacteria; and iii) the interaction between bacteria and nematodes.

In conclusion, the progress achieved in liquid cultivation of steiner nematids is nothing but another step forward to make entomopathogenic nematodes competitive with chemical insecticides in medium and high-value crops on the basis of cost/benefit ratio and ease of application.

## REFERENCES

- Akhurst, R.J. and Boemare, N. (1990). Biology and taxonomy of *Xenorhabdus*. In *Entomopathogenic Nematodes in Biological Control*, edited by R. Gaugler and H.K. Kaya, pp. 75–90. Boca Raton: CRC Press.
- Assa, A. and Bar, R. (1991) Biomass axial distribution in airlift bioreactor with yeast and plant cells. *Biotechnology and Bioengineering*, **38**, 1325–1330.
- Bedding, R.A. (1981) Large scale production, storage and transport of insect-parasitic nematodes *Neoplectana* spp. and *Heterorhabditis* spp. *Annals of Applied Biology*, **104**, 117–120.
- Bedding, R.A. (1984) Low cost in vitro mass production species of *Neoplectana* and *Heterorhabditis* for field control of insect pests. *Nematologica*, **27**, 109–114.
- Boemare, N., Laumond, C. and Luciani, J. (1982) Mise en évidence d'une toxicogénèse provoquée par le nematode axénique entomophage *Neoplectana carpocapsae* Weiser chez l'insect axénique *Galleria mellonella* L. *Comptes Rendus de l'Académie de les Sciences, Série D*, 543–546.
- Bonifassi, E. and Neves, J.M. (1990) La production en masse des nématodes entomopathogènes *Steinernematidae* et *Heterorhabditidae*. In *Les Colloques n° 58*, edited by INRA, pp. 125–132, Paris.
- Buecher, E. and Popiel, I. (1989) Growth of *Steinernema feltiae* in liquid culture. *Journal of Nematology*, **21**, 500–504.
- Burman, M. 1982. *Neoplectana carpocapsae*: toxin production by axenic insect parasitic nematodes. *Nematologica*, **28**, 62–70.
- Chisti, M.Y. (1989) *Airlift Bioreactors*. Elsiever Science Publishers, Barking, U.K.
- Dutky, S.R., Thompson, J.V. & Cantwell, G.W. (1964) A technique for the propagation of the DD-136 nematode. *Journal of Insect Pathology*, **6**, 417–422.
- Ehlers, R.U. (1996) Current and future use of nematodes in biocontrol: Practice and commercial aspects with regard to regulatory policy issues. *Biocontrol Science and Technology*, **6**, 303–316.
- Friedman, M.J., Langton, S.E. and Pollitt, S. (1989) Mass production in liquid culture of insect-killing nematodes. *Patent International Publication Number WO 89/04602*, 1–24.

- Friedman, M.J. (1990) Commercial production and development. In *Entomopathogenic Nematodes in Biological Control*, edited by R.Gaugler and H.K.Kaya, pp. 153–172. Boca Raton: CRC Press.
- Forst, S., Dowds, B., Boemare, N. and Stackebrandt, E. (1997) *Xenorhabdus* and *Photorhabdus* spp.: Bugs that kill bugs. *Annual Review Microbiology*, **51**, 47–72.
- Glaser, R.W. (1931) The cultivation of a nematode parasite of an insect. *Science*, **73**, 614–615.
- Georgis, R. (1992) Present and future for entomopathogenic nematode products. *Biocontrol Science and Technology*, **2**, 83–99.
- Georgis, R. and Hague, N.G.M. (1991) Nematodes as biological insecticides. *Pesticide Outlook*, **2**, 29–32.
- Glaser, R.W. (1940) The bacteria-free culture of a nematode parasite. *Proceedings of the Society of Experimental Biology and Medicine*, **43**, 512–514.
- Götz, P., Boman, A. and Boman, H.G. (1981) Interaction between insect immunity and an insectpathogenic nematode with symbiotic bacteria. *Proceedings Royal Society London*, **212**, 333–350.
- Jackson, G.J. (1973) *Neoplectana glaseri*: essential amino acids. *Experimental Parasitology*, **34**, 111–114.
- Kargi, F. and Cervoni, T.D. (1983) An airlift-recycle fermentor for microbial dessulfurization of coal. *Biotechnology Letters*, **5**, n° 1, 33–38.
- Kennard, M. and Janekeh, M. (1991) Two-and three-phase mixing in a concentric draft tube gas-lift fermentor. *Biotechnology and Bioengineering*, **38**, 1261–1270.
- Kloosterman, I.V. and Lilly, M.D. (1985) An airlift loop reactor for the transformation of steroids by immobilised cells. *Biotechnology Letters*, **7**, n° 1, 25–30.
- Neves, J.M. (1994) Distribution Analysis of the solid phase (*Steinernema carpocapsae* Az20 strain) in airlift bioreactor. *Comunication to the II Congresso Ibérico de Biotecnologia, 2–4 Out. Univ. Algarve, Portugal*.
- Neves, J.M., J.Teixeira, N.Simões & M.Mota. (1996a) Determinação das condições de arejamento necessárias à produção de nemátodos em bioreactor. *Actas da V Conferência Nacional sobre a Qualidade do Ambiente*, 1937–1943
- Neves, J.M., Mota, M., Simões, N., Teixeira, J.A. (1996b) A rapid method for adults separation from a mixed population of *Steinernema carpocapsae* (Nematoda: Steinernematidae). *Fundamental and Applied Nematology*, **19**, 103–106.
- Neves, J.M., J.A.Teixeira, N.Simões & M.Mota (1998) Produção de nemátodos entomopatogénicos *Steinernema* spp. em fermentador airlift não convencional: Avaliação da Eficácia. *Biotec'98*, 216.
- Pace, G.W., Grote, W. and Pitt, J.M. (1986) Liquid cultures of nematodes. *Patent International Publication Number WO 86/01094*, 1–16.
- Richardson, P.N. (1990) Uses for parasitic nematodes in insect control strategies in protected crops. *Aspects of Applied Biology*, **24**, 205–210.
- Siegel, M.H., Hallaile, M., Herskowitz, M. and Merchuck, J.C. 1989. Hydrodynamics and transfer in a three-phase airlift reactor. In *Bioreactor fluid dynamics*, edited by R.King, pp. 337–352, London: Elsevier.
- Siegel, M.H. and Robinson, C.W. (1992) Applications of airlift gas-liquid-solid reactors in biotechnology. *Chemical Engineering Science*, **47**, 3215–3229.
- Simões, N. and Rosa, J.S. (1996). Pathogenicity and host specificity of entomopathogenic nematodes. *Biocontrol Science and Technology*, **6**, 403–411.
- Simões, N., Caldas, C., Rosa, J.S., Bonifassi E. and C.Laumond. (2000) Pathogenicity Caused by a High Virulent and a Low Virulent Strains of *Steinernema carpocapsae* on *Galleria mellonella*. *Journal of Invertebrate Pathology*, **75**, 47–54.
- Stoll, N. (1961) Favoured RLE for axenic culture of *Neoplectana glaseri*. *Journal of Helminthology, R.T. Leiper Supplement*, 169.

# **CHAPTER SEVENTEEN**

## **MARINE SPONGES AS**

## **BIOCATALYSTS**

RENÉ H. WIJFFELS<sup>1</sup>, RONALD OSINGA<sup>1</sup>, SHIRLEY POMPONI<sup>2</sup>  
AND JOHANNES TRAMPER<sup>1</sup>

<sup>1</sup> *Food and Bioprocess Engineering Group, Wageningen University, P.O. Box 8129, 6700 EV Wageningen, The Netherlands*

<sup>2</sup> *Division of Biomedical Marine Research, Harbor Branch Oceanographie Institution, Inc. 5600 US 1 North, Fort Pierce, Florida 34946, USA*

### **ABSTRACT**

There is an increasing interest in biotechnological production of marine-sponge biomass, due to the discovery of many commercially important secondary metabolites in this group of animals. Sponges produce a variety of interesting compounds: cytotoxic compounds that may be used as anti-cancer drugs, antibiotics, anti-viral agents and compounds with anti-inflammatory and cardiovascular properties, and compounds that can be used as anti-fouling agent. Sponges as production organisms are therefore very interesting. Direct harvesting from the ocean, however, would be environmentally unacceptable. Production of metabolites using sponge cells could therefore be the best production method.

Two possibilities are presently in study in our group: growth of sponges as aggregates (primmorphs) and growth of immobilised sponge cells.

Primmorphs and immobilisation of axenic dissociated sponge cells could be a major breakthrough in sponge-cell culture research. Cell-cell contacts are an essential prerequisite for growth of sponges. Both methods described have the advantage that cell-cell contacts are maintained in axenic sponge-cell cultures. In the case of primmorphs, cells re-aggregate and in the case of immobilised sponge cells, the cells are stimulated to divide by growth factors and once small aggregates have been formed growth can continue.

### **INTRODUCTION**

Marine organisms are scientifically of great importance for two reasons (National Science and Technology Council USA, 1995). First, they constitute a major share of the Earth's biological resources. Second, marine organisms often possess unique structures,

metabolic pathways, reproductive systems, and sensory and defense mechanisms, because they have adapted to extreme environments ranging from the cold polar seas to the great pressures of the ocean floor. Most major classes of the Earth's organisms are primarily or exclusively marine, so the oceans represent a source of unique genetic information. The oceans therefore offer abundant resources for research and development. Yet the potential of this domain as the basis for new biotechnologies remains largely unexplored. The vast majority of marine organisms have yet to be identified.

The marine environment is a plentiful source of interesting new products for human society. It is therefore striking that so few of these marine natural products (Table 17.1) have reached the stage of commercial production (Pomponi, 1999). Words such as "promising" and "potential" dominate the literature on marine natural products, while papers describing successful application of these products remain scarce. The gap from "promising" to products and processes of interest to industry and society needs to be closed. Research on marine biotechnology, the practical use of marine organisms it under controlled conditions, is therefore an important new development in this respect (Cowan 1997; Zaborsky 1995).

## SPONGES

There is an increasing interest in biotechnological production of marine-sponge biomass, due to the discovery of many commercially important secondary metabolites in this group

**Table 17.1** Some examples of marine bioproducts commercially available (From: Pomponi, 1999).

Product	Application	Source
Ara-A	antiviral drug	microbial culture (original source: marine sponge)
Ara-C	anticancer drug	chemical synthesis (original source: marine sponge)
okadaic acid	molecular probe: phosphatase inhibitor	dinoflagellate
manoalide	molecular probe: phospholipase A2 inhibitor	marine sponge
Vent DNA polymerase	polymerase chain reactions	deep sea hydrothermal vent bacterium
Formulaid®	nutritional supplement	additive: fatty acid produced by marine microalga
Aequorin	bioluminescent calcium indicator	bioluminescent jellyfish, <i>Aequorea victoria</i>
Green Fluorescent Protein (GFP)	reporter gene	bioluminescent jellyfish, <i>Aequorea victoria</i>

---

phycoerythrin	conjugated antibodies used in ELISAs and flow cytometry	red algae
Resilience®	skin creams	additive: extract of Caribbean sea fan

---

of animals. Sponges produce a variety of interesting compounds: cytotoxic compounds that may be used as anti-cancer drugs, antibiotics, anti-viral agents and compounds with anti-inflammatory and cardiovascular properties and compounds that can be used as anti-fouling agents. In Figure 17.1 screening results for different organisms are given (Munro *et al.*, 1999). Shown is the percentage of organisms tested in which components have been found with a positive cytotoxic activity. Compounds with cytotoxic activity can potentially be used as anti-tumour agents. Less than 0.5% of the micro-organisms tested have cytotoxic activity. In this respect marine animals are potentially much more interesting as in almost 2% of the tested animals compounds with cytotoxic activity were found. Sponges form a part of this group; in 10% of the sponges tested cytotoxic activity was found.

Sponges are classified within the animal kingdom as the phylum Porifera, which consists of approximately 10,000 described species. Some examples of the morphological diversity within the phylum Porifera are given in Figure 17.2. With respect to the level of body organisation, sponges (Porifera) represent one of the two most primitive groups of multicellular animals (Metazoa). Together with the phylum Placozoa, Porifera form the Parazoa, multicellular animals without organs and with poorly defined tissues. Hence, the structure of the sponge body is simple: the tissue is built around a network of channels and chambers, through which water is pumped continuously (Figure 17.3). This network, which is called the aquiferous system, has numerous small inflowing openings (ostia) and one or two outflowing openings. The biological material around the aquiferous system basically consists of three tissue-like components: i. Pinacoderm, a thin layer of flat skin cells (pinacocytes). ii; Choanoderm, a layer of flagellate cells (choanocytes) that line the walls of the chambers. The beating of these flagellae generates the water current through the sponge body, iii; The mesohyl, which is a gelatinous matrix containing free living cells and skeletal components. Most of these free living cells are termed archaeocytes. Archaeocytes are totipotent, multifunctional cells that can develop into any other cell type present in sponges.

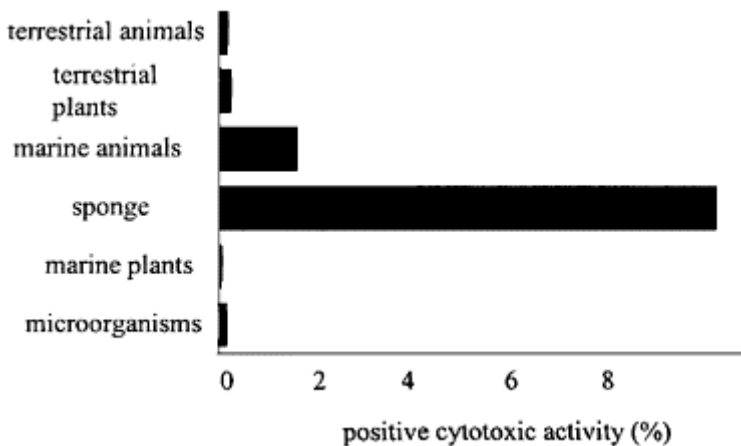


**Figure 17.1** Percentage of organisms with a positive cytotoxic activity (Munro *et al.*, 1999)

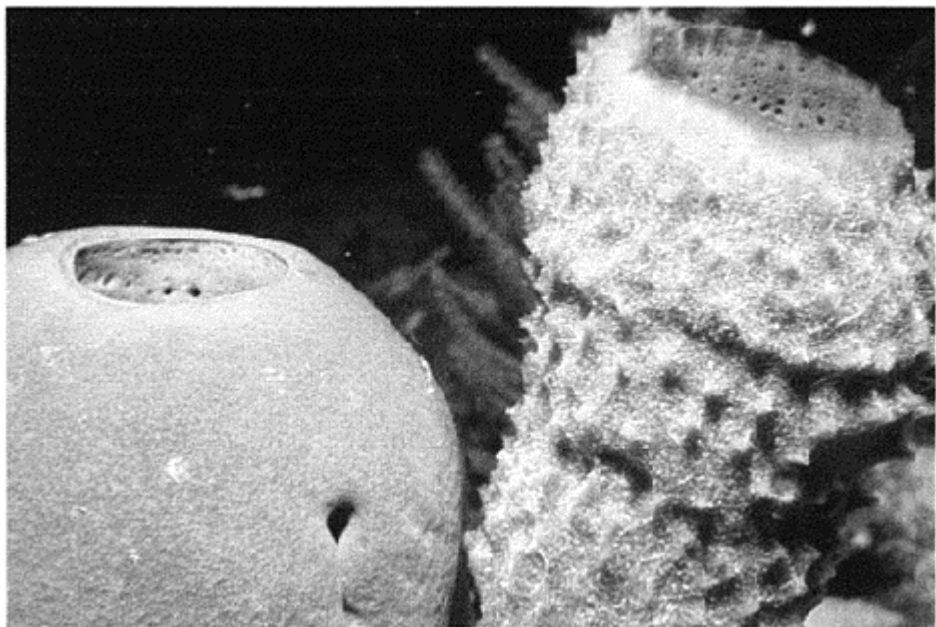


**Figure 17.2** Examples of sponges  
(Picture: Ronald Osinga)

Although many uncertainties still exist about sponge cell biology, the general view is that sponge cells can reversibly alter their function, with only a few cell types being terminally differentiated. For example, a pinacocyte can become an archaeocyte and vice versa. This feature and the low organisational level of the sponge body are responsible for another important property of sponges: their strong regenerative power. It was discovered a long time ago that cuttings of mature sponges can regenerate into full-grown, functional sponges. This property is important for biotechnology: cloning of sponges is much easier than cloning of higher animals.

In addition to their ability to reproduce asexually, sponges also have sex. Formation and release of eggs and sperm cells occurs. Some sponge species are hermaphrodite, egg and sperm production taking place within the same individual. Other species have male and female individuals, which both release their gametes into the surrounding water so that fertilisation takes place outside the sponge body.

Sponges are filterfeeders: they filter small organic particles (microalgae, bacteria, dead organic particles) out of the surrounding water. It is generally assumed that the upper size limit of particles that can be taken up (i.e. the size of the inflowing pores) is around 50  $\mu\text{m}$ . Larger particles are trapped where the inflowing channels become narrower. The particle is then ingested by an archaeocyte cell via phagocytosis. After taking up the particle, the archaeocytes move through the mesohyl matrix towards an outflowing

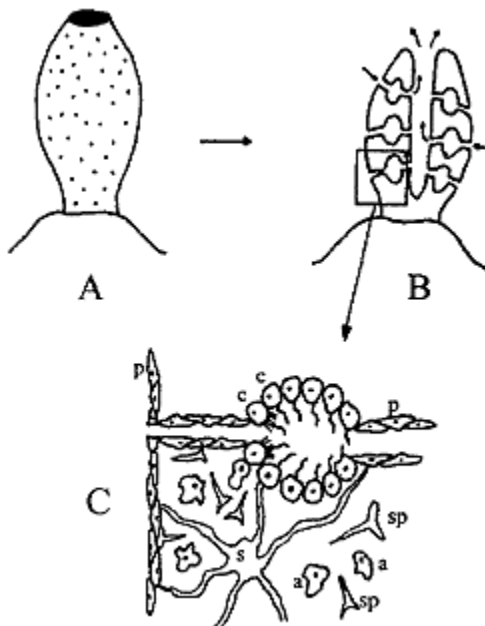


**Figure 17.3** Body structure of a sponge. A. Macroscopic observation. B. Cross-section, showing a canal system through which media is

pumped and in which particles are filtered. C. Detail of a channel, a flagellated chamber and the mesohyl.  
p=pinacocyte (skin cell),  
c=choanocyte, a=archaeocyte (free floating cell), s=sponge, sp=spicula.

channel while digesting the particle. Undigestible parts of the food particle are released into the outflowing channel.

Smaller particles are trapped by the choanocytes in the choanocyte chambers. The flagellae of the choanocytes are surrounded by a collar of so-called microvilli. This collar acts as a sieve with a very small mesh size. Sponges are capable of trapping even the smallest picoplanktonic particles such as ultramicrobacteria and prochlorophytes. Particles trapped in the collar are transported into the choanocyte cells, where some particles are digested and others are stored in food vacuoles. The content of these food vacuoles is regularly transferred to archaeocytes that make cell-to-cell contact with the choanocytes to take up the food. Similar to the processing of larger particles, the undigestible parts are released by the archaeocytes into the outflowing channels.

Metabolites of interest produced by the sponges or their endosymbionts are often present only in trace amounts. Several authors have stressed the fact that much greater sponge biomass is needed for commercial production of these sponge metabolites than can be harvested from the seas (Munro *et al.*, 1999, Pomponi *et al.*, 1994, Osinga *et al.*, 1998, 1999, Ilan *et al.*, 1996). Currently, this "supply problem" still hampers the development of many promising metabolites from sponges and other marine macroorganisms (Munro *et al.*, 1999; Pomponi *et al.*, 1999). A good example is the case of halichondrin B, one of several compounds that have been isolated from *Halichondria okadai* and *Lissodendorix* sp. This potential anti-cancer agent has successfully proceeded through the first preclinical test phase, but can not be studied further until the supply of sufficient material has been solved (Munro *et al.*, 1999).

In order to give an idea of the amount of sponge biomass that is necessary to produce one kg of final product, two examples are given: i. Latrunculins are cytotoxic compounds isolated from the sponge *Latrunculia magnifica* (Ilan *et al.*, 1996). The latrunculin concentrations in the sponge tissue are relatively low (up to 0.35% of the dry weight). For the production of 1 kg lactrunculin 286 kg dry sponge or 9.5 m<sup>3</sup> of sponge biomass needs to be produced; ii. The anti-bacterial polybrominated biphenyl ethers in the Indo-Pacific, encrusting sponge *Dysidea herbacea* can make up to 12% of the sponge dry weight (Unson *et al.*, 1994). Production of a kilogram of target compound would in this case require 8.3 kg dry sponge or 0.3 m<sup>3</sup> of sponge volume.

Commercialisation of bio-active compounds from sponges has been limited so far. The molecules are often very complex which makes them difficult to synthesize chemically. The metabolic pathways are unknown, which make it difficult to transfer the genetic information for the metabolite production into other organisms.

Sponges as production organisms are therefore very interesting. Direct harvesting from the ocean, however, would be environmentally unacceptable. Production of metabolites with sponge cells could therefore be the best production method.

Developments are in the initial phase and more remains unknown than known. We have tried to give the first steps in the development of processes for the production of sponge metabolites under controlled conditions.

## MARICULTURES

Descriptions of large-scale bath sponge maricultures in several parts of the world are given in several publications (Cahn, 1948; Storr, 1964; Shubow, 1969; Vacelet, 1985; Verdenal and Vacelet, 1990; Adams *et al.*, 1995; Battershill and Page, 1996).

In New Zealand, progress is being made with maricultures of sponges for metabolite production (Battershill *et al.*, 1998; Pomponi 1999). Here, not only do sponges have to be grown fast and economically, but they also need to be cultured in a manner which promotes target metabolite synthesis. Recently, five species of marine sponges (*Latrunculia brevis*, *Lissodendoryx* n.sp., *Mycale murryi*, *Polymastia croceus* and *Raspailia agminata*) were grown in sea-based cultures with maintenance of target metabolite synthesis (Battershill *et al.*, 1998; Duckworth *et al.*, 1998). *In situ* sponge aquacultures, based on old methods to produce commercial bath sponges, are still the cheapest and easiest way to obtain bulk amounts of sponge biomass. However, the cultivation success of this method strongly depends on the unpredictable and often suboptimal natural environment. Production of compounds for pharmaceuticals needs well defined, controlled conditions in order to guarantee a defined product quality. For this reason production of sponge metabolites should preferably be done in pure cultures.

## SPONGE-CELL CULTURES: A FUTURE OPTION FOR METABOLITE PRODUCTION

*In vitro* culture of sponges as axenic (i.e. free of bacteria and other microbial contaminants) dissociated sponge cells or tissue will provide a clean, defined system for the production of sponge metabolites, a prerequisite for the biotechnological production of pharmaceuticals. Culture of animal cells and tissue is commonly used in biotechnology and medical science. Until now, however, all attempts to establish a continuous cell line from a sponge have failed. Primary cell cultures of sponges can be produced, but the axenic, dissociated cells seem to lack the stimulus to divide, despite the use of very rich media. In contrast to other animal cells (for instance mammalian cells and insect cells), the primary sponge cell lines do not proliferate in media containing fetal calf serum. This is in contradiction to the undetermined nature and strong regenerative power of sponge cells, which are believed to be capable of forming a functional sponge from a single cell. Phytohemagglutinin (a lectin that induces mitosis in mammalian cells) can be used to stimulate cell division in primary cell cultures, but this only results in a few cell-division cycles, after which the proliferation stops completely. The occurrence of microbial contaminants further complicates the establishment of a clean cell line. Bacteria, fungi and unicellular eukaryotes easily overgrow sponge cell cultures and can sometimes hardly be distinguished from sponge cells. Because of these problems, cell culture must

at present be considered a future option for the biotechnological production of natural products from sponges.

A potential risk of using sponge cell or tissue cultures for metabolite production is that the sponge cells may lose the ability to produce the target compound when grown in axenic culture. It has been shown that in the culture of *T. morchella*, the cells were still able to produce the target metabolite, even after artificially induced cell division (Pomponi *et al.*, 1997).

### DISSOCIATION OF SPONGE TISSUE

Artificial dissociation of the sponge tissue is the first step to obtain primary cell cultures. Both mechanical and chemical dissociation methods exist. A combination of these usually gives the best result. The mechanical part consists of cutting the sponge tissue into small pieces, which are then squeezed through a cloth or another fine mesh to dissociate the tissue and separate the cells from non-cellular components such as spicules. The resulting suspension of cells and small aggregates is collected in CMF-ASW, artificial seawater that does not contain calcium and magnesium ions.  $\text{Ca}^{2+}$  and  $\text{Mg}^{2+}$  play a crucial role in the binding between sponge cells, and the absence of these ions not only causes the cell-to-cell bond to break, but also prevents the cells from re-aggregating (Ilan *et al.*, 1996; Pomponi *et al.*, 1997).

After the dissociation step, the cells are treated with antibiotics and antimycotics. The ultimate goal of this step is to obtain axenic (contamination-free) cell cultures, although complete removal of all contaminants has proven to be a difficult task. However, if properly used, the antibiotics will at least prevent overgrowth of the primary sponge cell culture by microorganisms. The treatment with antibiotics is a very critical step, because excessively high antibiotic concentrations may kill the sponge cells, while very low concentrations will not sufficiently inhibit all contaminants. A combination of rifampicin (a broad spectrum antibiotic) and amphotericin (an antifungal compound) has been used successfully to obtain axenic cell cultures of *Hymeniacidon heliophila* and *Teichaxinella morchella*. The concentrations used were  $1.16 \mu\text{M}$  and  $2.5 \text{ mg dm}^{-3}$  respectively. However, dose-response relations have to be determined for every new combination of sponges and antibiotics. A basal sponge culture medium has been described in the literature in which primary sponge cells can be maintained for a limited period (Pomponi *et al.*, 1997; Pomponi and Willoughby, 1994).

### SPONGE-CELL GROWTH

Of the several cell types found in sponges, archaeocytes and choanocytes most often show mitotic activity. Hence, growth in sponges is thought to take place by proliferation of these two cell types partially followed by functional differentiation of the newly formed archaeocytes. Archaeocytes show better survivability in primary cell cultures than choanocytes. The totipotent nature of the archaeocytes and their better survival in primary cell cultures make these cells the best candidates for developing continuous cell lines.

Techniques are available to separate different cell fractions. Usually, a crude cell suspension is put into a density gradient consisting of two or more layers with increasing density, followed by centrifugation at ~600 g. Density gradients can be made of Ficoll or Percoll solutions, commercially available fluids with a high density, that can be diluted with CMF-ASW. The bands of cells that are formed at the interfaces between layers must be carefully collected, for instance by using a pasteur pipet, and transferred to clean CMF-ASW or sterilised seawater. In this way fractions that are enriched in specific cell types such as archaeocytes can be obtained.

So far it has not been possible to produce a continuous cell line. Cell division was successfully stimulated with different growth factors, but a continuous cell line could still not be established. Only initial cell proliferation could be stimulated (Ilan *et al.*, 1996, Pomponi *et al.*, 1997).

Once more, we emphasize that despite their totipotency and high proliferative capacity in functional sponges, even archaeocytes have not been shown capable of growing in suspension. Potential causes and possible solutions are:

### **1. Immortal Sponge Cells are not Available**

Animal cell lines from insects and mammals usually consist of cells that are immortal; they have an unlimited capacity to proliferate. Immortal cells of mammals can be obtained from tumour tissue. Immortality can also be induced artificially, either by hybridisation of normal cells with immortal cells (e.g. hybridoma's) or by subjecting the cells to mutagenic agents such as carcinogenic compounds, viruses or radioactivity. Sometimes immortal cells evolve spontaneously by mutation of normal cells growing in rich media. It is unknown to us to what extent these methods have been applied to sponge cells; no reports on successful immortalisation of sponge cells have yet been published. It should be borne in mind here that out of a thousand attempts to establish mammalian and insect cell lines, only a few are successful. It is therefore well worth continuing attempts to develop immortal, continuous sponge cell lines, by using both existing techniques and by applying the methods mentioned above to produce immortal sponge cells.

An advantage of sponge archaeocytes over other animal cells is their free-living nature. They are not part of multicellular tissues, which may reduce the time the cells need to adapt to life in suspension. Another advantage is that sponge cells have a high telomerase activity. This enzyme stimulates the restoration of the telomeric ends of the chromosomes after mitosis, which is assumed to be a crucial process for cells continuing their division cycle. In theory, somatic sponge cells can thus maintain the mitotic cycle longer than somatic cells of other animals. In other words they are closer to immortal cells than most other somatic cells. However, the contrasting inability of sponge cells to proliferate in rich media containing foetal calf serum remains a serious obstacle, because this considerably reduces the possibility that an immortal cell line evolves spontaneously by mutation.

### **2. Cell-to-cell Contact Stimulates Telomerase Activity**

Why do dissociated sponge cells hardly proliferate in media containing foetal calf serum? Apparently, the media used until now to culture sponge cells do not sufficiently resemble

their natural environment (the sponge mesohyl) and/or may not contain the molecular growth factors needed to induce mitosis. Although some response to mammalian growth factors has been found, sponge cells may have their own, specific growth factors, which remain to be identified. It has been demonstrated that the lack of cell-to-cell contact after artificial dissociation of sponge tissue considerably reduces the high telomerase activity of the cells, indicating that the loss of proliferative capacity is caused by dissociation. Although the exact mechanism is unknown, cell-to-cell contact or cell-to-matrix contact apparently stimulates the production of growth factors and telomerase (Custodio *et al.*, 1998; Koziol *et al.*, 1998).

With respect to the facts and hypotheses mentioned above, the potential way to improve sponge cell-culture techniques is by growing sponge cells as axenic, multicellular aggregates formed from suspended sponge cells after treatment with antibiotics and antimycotica. Cell-to-cell contact is then restored, thus re-initiating the processes of mitosis and growth.

Two possibilities are presently in study in our group: growth of sponges as primmorphs and growth of immobilised sponge cells. In both cases sponge cells are grown as cells with cell-to-cell contact. The present state of this novel research is described below. It should be remembered that developments in sponge-cell cultivation are in an initial phase. It is difficult to draw general conclusions about applicability and feasibility in these circumstances.

## PRIMMORPHS

Growing sponges as axenic, multicellular aggregates has been attempted. To obtain such aggregates, sponges are first dissociated in CMF-ASW and treated with antibiotics. If the dissociated cells are then transferred back into normal seawater (with antibiotics), they will reaggregate and form spherical clumps of cells (primmorphs) within a few weeks (Custodio *et al.*, 1998; Müller 1998). The formation of these primmorphs is illustrated for *Styliissa massa* (Figure 17.4). If a cell suspension of *Styliissa massa* is shaken gently, after only a few hours the cells start to reaggregate (Figure 17.5A). After a few days the aggregates becomes smoother (Figure 17.5B) and after 11 days strong smooth spherical

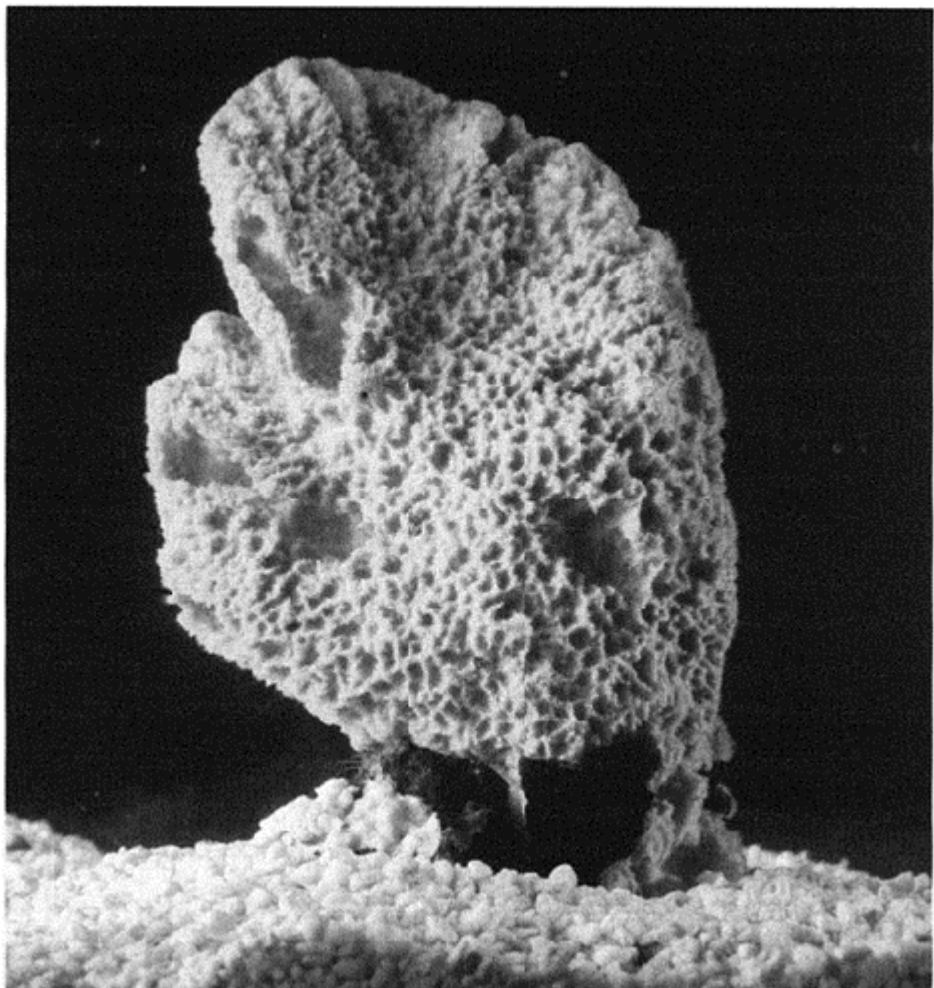


**Figure 17.4** *Styliissa massa*

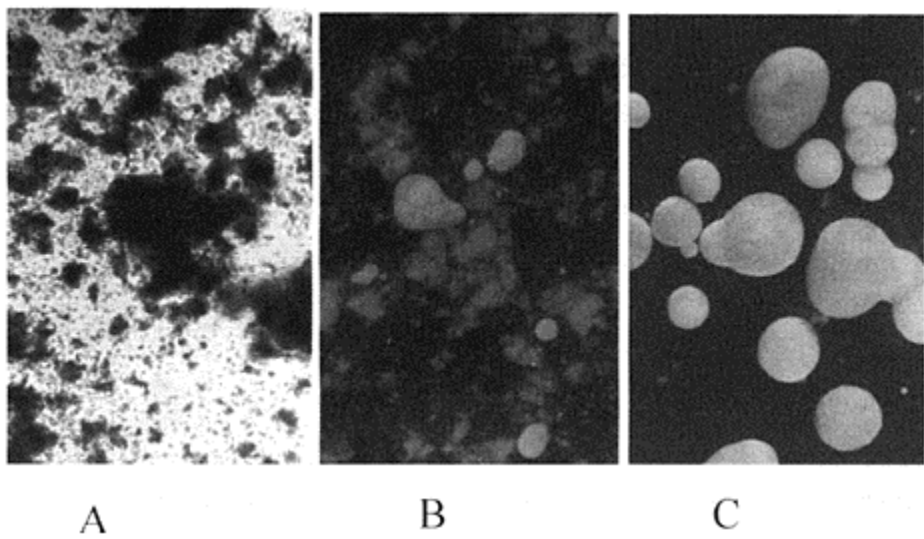


**Figure 17.5** Formation of primmorph from *Stylissa massa* cells after 3 hours (A), 5 days (B) and 11 days (C) aggregation.

particles are obtained (Figure 17.5C), the primmorphs. Primmorphs were observed more closely with electron microscopy. Figure 17.6A shows the very smooth surface of such a primmorph. Figure 17.6B shows a cross section, it can clearly be seen that the smooth surface is like a skin around the reaggregated sponge cells. Primmorphs are usually a few mm in size. Custodio *et al.* (1998) showed that cells inside the primmorphs showed a high telomerase activity. This means that cells should be able to continue their cell divisions.

The morphology of primmorphs resembles that of gemmules and buds, structures found in many sponges in nature. Gemmules and buds are asexually-produced reproductive stages that can be released by the parent sponge. The densely packed and well-protected cells in gemmules and buds can survive long periods of starvation and low temperature. When conditions are favourable again, the released gemmules and buds will hatch; they attach to a solid surface and start to develop into functional sponges. The striking morphological similarity between primmorphs and gemmules/buds, together with the ability of primmorphs to be maintained under conditions of complete starvation for long periods, has given rise to the idea that primmorphs are artificially created, axenic resting stages. Although DNA replication in primmorphs has been demonstrated, growth (of new biomass) has not yet been observed. Long term experiments with growth media have not been conducted so far. Another important lesson about the development of cells or primmorphs into functional sponges can be learned from older experimental sponge embryology. By removing specific areas from larval tissue, it was demonstrated that at least two cell types have to be present in sufficient amounts to allow further development:

archaeocytes and collencytes (a specific cell type that is known to produce collagen fibers). The presence of sufficient collencytes is obligatory to form a basal lamina on the substrate because only collencytes can differentiate into the specific type of pinacocyte

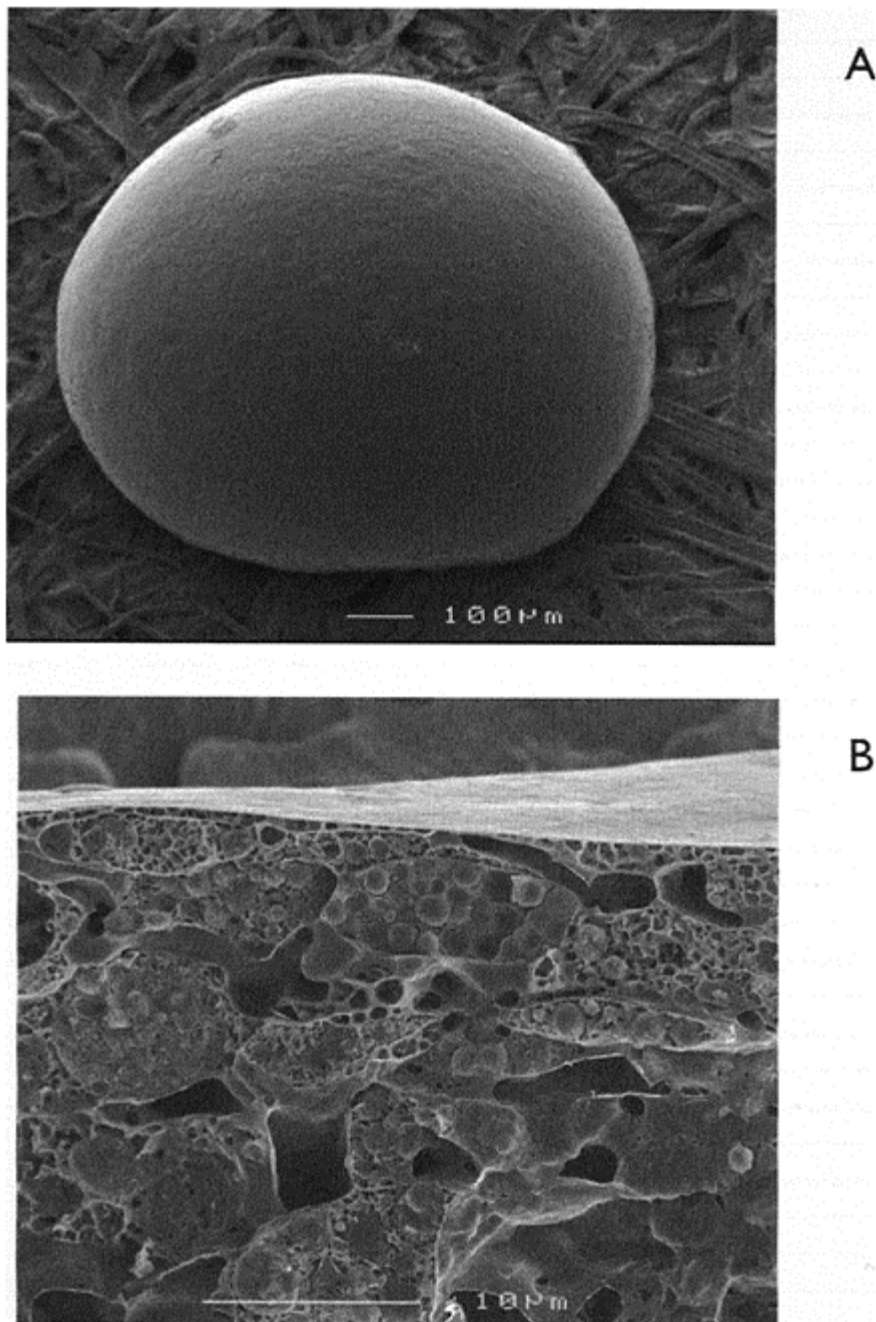


**Figure 17.6** Scanning electron microscopy observations of

primmorphs from *Styliissa massa* cells  
 32 days after aggregation: a surface  
 (A) and a cross section (B) are shown

that can attach to a surface (basopinacocytes). Here, the totipotency of the archaeocytes shows a deficiency, because only after the formation of a basal lamina are archaeocytes able to form new collencytes. Hence, if the initial number of collencytes is too low, the development of the sponge is terminated in an early stage. It is not known to what extent collencytes survive the dissociation protocol executed by most researchers. It is also not known whether the results of this embryologic study are representative for all sponges or not. These are interesting subjects for further study by both marine biotechnologists and sponge biologists.

### IMMOBILISED SPONGE CELLS

A drawback of primmorphs is that their formation is slow (11 days) and the particles are relatively fragile. Artificial immobilisation in gel supports could be an alternative. Division of the immobilised cells can then be promoted by the use of growth stimulating lectin phytohemagglutin, similar to that in dissociated cell cultures (Pomponi and Willoughby, 1994). After division the cells can form an aggregate in the gel, so that cell-to-cell contact is restored and further growth triggered. In addition, the gel provides a solid matrix for the aggregates enabling them to develop further into axenic functional sponges.

In order to show that immobilisation of sponge cells is possible and that immobilised sponge cells can proliferate, some initial experiments were done with different sponges (*Halichondria melanodocia*, *Teichaxinella murchella*, *Agelas clathrodes*, *Spongisorites* sp. and *Forcepia* sp.). Dissociated cells were immobilised in a thermogelating gel. Immobilisation conditions were very mild. Immobilisation was carried out using agarose with a low gelling temperature (25 °C). For bioprocess purposes immobilisation is usually done in gel beads. Gel beads can easily be kept in suspension in bioreactors up to a holdup of 25%. In order to show effects of immobilisation on cell viability and proliferation capacities, gel layers were made that could easily be observed microscopically. The gel with cells was brought into multiwell-plates to form a layer of 1–3 mm thickness. These layers were covered with growth medium.

Microscopic observations revealed that many cells survived the immobilisation step. In most experiments, both single cells and small aggregates were present and these could be kept in an apparently viable state for at least two weeks. In addition, the gel material often remained free of overgrowth by contaminating micro-organisms. As an example results are given of *Halichondria melanodocia*. Individual cells were immobilised. After 9 days of cultivation all cells developed in aggregates due to growth, as is shown in Figure 17.7. Cell proliferation was very similar to the development of micro-colonies that are normally observed when immobilised micro-organisms are grown. In other experiments aggregates of *Agelas clathrodes* also showed some growth during the first week. In addition their outer appearance changed from rather irregularly shaped clumps to spherical aggregates with a smooth surface. The best results were obtained with

*Teichaxinella morchella*. In several wells a considerable increase in sponge biomass was found. A micro-colony of *T. morchella* is shown in Figure 17.8.

A production system was developed by immobilising the sponge cells in agarose beads instead of layers. The gel beads with sponge cells can easily be fluidised and continuously

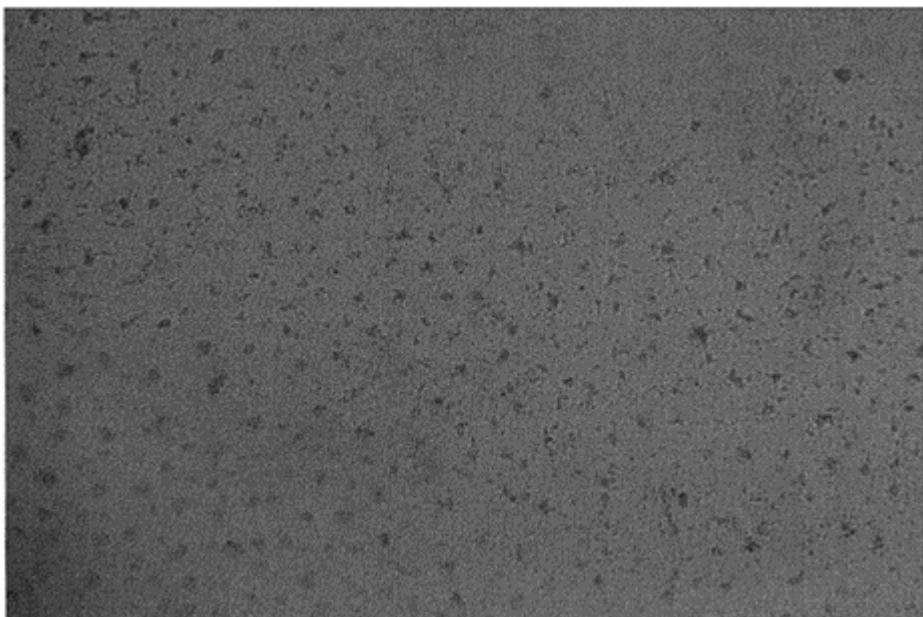


**Figure 17.7** Aggregates of immobilised cells of *Halichondria melanadocia* after 9 days of cultivation (magnification 40  $\times$ )

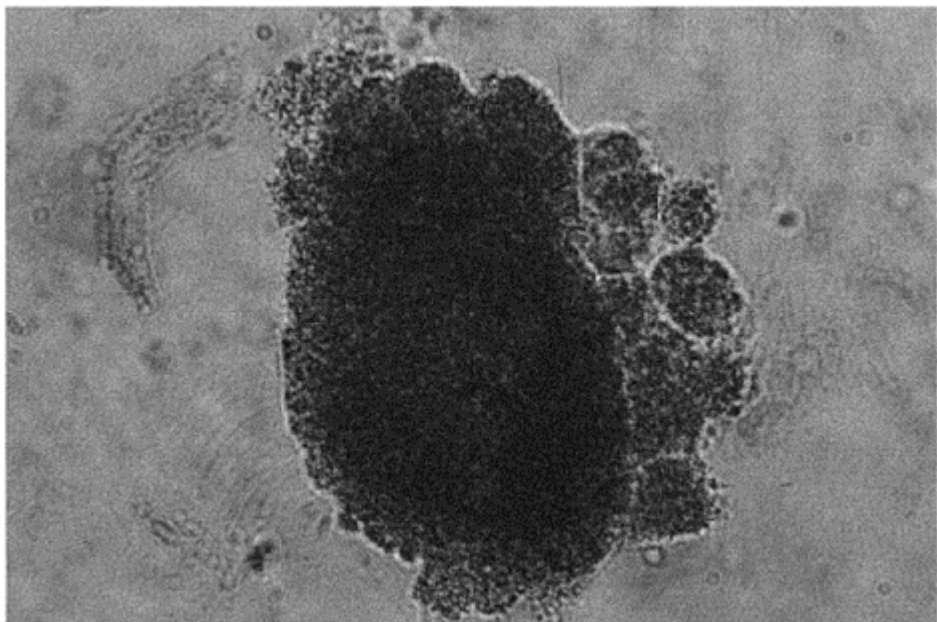


**Figure 17.8** Aggregates of immobilised *Teichaxinella morchella* after 19 days of cultivation (magnification 400  $\times$ )

fed and aerated in bioreactors. Initial experiments were done in spinner flasks. Proliferation of sponge cells into micro-colonies could be observed in the gel beads as well.

#### PERSPECTIVES

Primmorphs and immobilisation of axenic dissociated sponge cells could be a major breakthrough in sponge-cell culture research. Cell-cell contacts are an essential prerequisite for growth of sponges. Both methods described above have the advantage that cell-cell contacts are maintained in axenic sponge-cell cultures. In the case of primmorphs, cells re-aggregate and in the case of immobilised sponge cells, the cells are stimulated to divide by growth factors and once small aggregates have been formed growth can continue.

So far only initial growth has been shown for both systems. Long term growth needs to be studied. How growth proceeds is not known at the present time. It is possible that micro-colonies develop further in the same fashion as in the case of immobilised microorganisms, and diffusion limitation across the biocatalyst particles will occur. On the other hand the primmorphs or immobilised sponge cells might be able to differentiate

as the aggregates increase in size and the primmorph or gel bead may act as seed for axenic functional sponges. Further research should answer these issues. In all cases, however, primmorphs and immobilised sponge cells are potentially interesting systems for the production of sponge metabolites. The potential production mechanisms could be:

1. Sponge biomass in primmorphs or in the support material grows. The particles are harvested and secondary metabolites are recovered;
2. Sponge biomass in primmorphs or in the support material increases and differentiates into functional sponges. The axenic sponges can be cultivated in closed controlled bioreactors;
3. Sponge biomass in primmorphs or in the support material increases and at a certain size excess biomass is excreted from the particles. Excreted cells are harvested and secondary metabolites are recovered from the cells;
4. Primmorphs or immobilised sponge cells are used as a biofactory. Secondary metabolites are excreted into the bioreactor medium and can be recovered from there.

Another fact that may cause problems in sponge cell cultures in relation to food is that sponge cells ingest small organic particles and pass organic substances from cell to cell rather than excreting it in the mesophyl. Hence, the capacity of sponge cells to take up dissolved organic matter through their cell membrane might be limited, although it has been shown that sponge cells can take up dissolved amino acids. In addition, it is not known to what extent mammalian cell culture media can replace the natural diet of sponges. Addition of marine-based food supplements (bacterial or algal extracts) may increase the nutritive value of a sponge cell culture medium.

Especially in the case of primmorph or immobilised sponge cells that develop into functional sponges, the organisms could be fed as normal sponges; this means by food particles. A possible strategy is growing the axenic sponges with media consisting of micro-algae. The product is a photobioreactor in which micro-algae is fed to a sponge bioreactor (Osinga *et al.*, 1998).

Methods for cultivation of sponges and production of sponge metabolites are still in the initial phases of development. The metabolites with bio-active properties are of high value. For this reason it is highly worthwhile to continue this research. Recent progress indicates that possibilities for sponge cultivation are realistic.

#### ACKNOWLEDGEMENTS

We thank Cindy Stoffelen for her contributions in the experiments with immobilised sponge cells. We would like to thank Robin Willoughby for her help in making primary cell lines. Rutger van Wielink is thanked for his work on primmorphs and Werner Müller and Renate Steffen for all the valuable advise on the production of primmorphs.

#### REFERENCES

- Adams C., Stevely J.M. and Sweat D. (1995) Economic feasibility of small-scale sponge fanning in Pohnpei, Federated States of Micronesia. *J. World Aquacult Soc* **26**:132–142.

- Battershill C.N. and Page M. (1996) Sponge aquaculture for drug production. *Aquaculture Update*, Spring 1996:5–6.
- Battershill C.N., Page M.J., Duckworth A.R., Miller K.A., Bergquist P.R., Blunt J.W., Munro M.H.G., Northcote P.T., Newman, D.J. and Pomponi, S.A. (1998) Discovery and sustainable supply of marine natural products as drugs, industrial compounds and agrochemicals: chemical ecology, genetics, aquaculture and cell culture. In: Origin and Outlook, 5th International Sponge Symposium, Brisbane, p. 16.
- Cahn A.R. (1948) Japanese sponge culture experiments in the South Pacific Islands. US Fish Wildl Serv, Fish Leaflet 309.
- Cowan D.A. (1997) The marine biosphere: a global resource for biotechnology. *Trends in Biotechnology* **15**, 129–131.
- Custodio M.R., Prokic I., Steffen R., Koziol C., Borojevic R., Brümmer F., Nickel M. and Müller W.E.G. (1998) Primmorphs generated from dissociated cells of the sponge *Suberites domuncula*: a model system for studies of cell proliferation and cell death. *Mech Ageing Dev* **105**:45–59.
- Duckworth A.R., Battershill C.N., Schiel D.R. and Bergquist P.R. (1998) Drug farming in the 21st century. In: Origin and Outlook, 5th International Sponge Symposium, Brisbane, p. 15.
- Ilan M., Contini H., Caraieli S. and Rinkevich B. (1996) Progress towards cell cultures from a marine sponge that produces bioactive compounds. *J. Mar. Biotechnol* **4**:145–149.
- Koziol C., Borojevic R., Steffen R. and Müller W.E.G. (1998) Sponges (Porifera) model systems to study the shift from immortal to senescent somatic cells: the telomerase activity in somatic cells. *Mech. Ageing Dev.* **100**:107–120.
- Müller W.E.G.: Herstellung von Primmorphe® aus dissoziierten Zellen von Schwämmen, Korallen und weiteren Invertebraten: Verfahren zur Kultivierung von Zellen von Schwämmen und weiteren Invertebraten zur Produktion und Detektion von bioaktiven Substanzen, zur Detektion von Umweltgiften und zur Kultivierung dieser Tiere in Aquarien und im Freiland. AZ 198 24 384 [30.05.1998] (Patent application).
- Munro M.H.G., Blunt J.W., Dumdei E.J., Hickford S.J.H., Lill R.E. Li S., Battershill C.N. and Duckworth A.R. (1999) The discovery and development of marine compounds with pharmaceutical potential. *J. Biotechnology* **70**, 15–25.
- National Science and Technology Council USA (1995) Biotechnology for the 21st century: opportunities in marine biotechnology and aquaculture, <http://www.nalusda.gov/bic/bio21/aqua.html>.
- Osinga R., Tramper J. and Wijffels R.H. (1998) Cultivation of marine sponges for metabolite production: applications for biotechnology? *Trends Biotechnol* **16**:130–134.
- Osinga R., Tramper J. and Wijffels R.H. (1999) Cultivation of marine sponges. *Marine Biotechnology* **1**:509–532.
- Pomponi S.A. and Willoughby R. (1994) Sponge cell culture for production of bioactive metabolites. In: Van Soest R.W.M., Van Kempen T.M.G. and Braekman J.C. (eds) *Sponges in time and space*. A.A.Balkema, Rotterdam, pp. 395–400.
- Pomponi S.A., Willoughby R., Kaighn M.E. and Whright A.E. (1997) Developments of techniques for in vitro production of bioactive natural products from marine sponges. In: Maramorosch K. and Mitsuhashi J. (eds) *Invertebrate cell culture. Novel directions and biotechnology applications*. Science Publishers, USA, pp. 231–237.
- Pomponi S.A. (1999) The bioprocess-technological potential of the sea. *J. Biotechnol.* **70**, 5–13.
- Rinkevich B. (1999) Cell cultures from marine invertebrates: obstacles, new approaches and recent improvements. *J. Biotech* **70**:133–153.
- Shubow D. (1969) The Florida sponge industry. MSc Thesis, Univ Miami, Coral Gables, Florida.
- Storr J.F. (1964) Ecology of the Gulf of Mexico commercial sponges and its relation to the fishery. Special Scientific Report—Fisheries no. 466, United States Department of the Interior.

- Unson M.D., Holland N.D. and Faulkner D.J. (1994) A brominated secondary metabolite synthesized by the cyanobacterial symbiont of a marine sponge and accumulation of the crystalline metabolite in the sponge tissue. *Mar. Biol.* **119**:1–11.
- Vacelet J. (1985) Bases historiques et biologiques de eventuelle spongiculture. *Océanis* **11**: 551–584.
- Verdenal B. and Vacelet J. (1990) Sponge culture on vertical ropes in the Northwestern Mediterranean Sea. In: Rützler K. (ed) New Perspectives in Sponge Biology. Smithsonian Institution Press, pp. 416–424.
- Zaborsky O.R. (1995) Bioprocess engineering: now and beyond 2000. *FEMS Microbiology Reviews* **16**. 277–285.

# INDEX

Aerated Slurry Systems, 1, 2

Animal Cells

cell-bubble interactions, 437

cell death, 434, 439, 441, 445, 451

culture, 427, 434

gas bubble, 427, 430

gas transfer, 428

hydrodynamics, 427, 430

image analysis, 34

lethal effects, 427

reactor design, 455

Automation, 69

Back-mixing. *see* dispersion

Binding problem, 25

Biocatalysis, 115, 185

Biofilm

concept, 271

growth equation, 300

properties, formation and performance, 279

reactor calculation, 293

reactor modelling, 284

reactor start-up, 278

reactor types, 271–274

Biofilms vs. suspended biomass, 283

Biological activity in biofilms, 282

Biomass characterisation, 28

Bioreactor Imaging, 35

Biot number, 103

Biotransformation, 136, 151, 152

Biosensors, 59

BSTR, *see* batch stirred tank reactor

Bubble shape image analysis, 39, 40

Charged compounds, *see* electrostatic interactions

Conventional external-loop airlift for nematode production, 469

Cofactor

reactions with, 151, 157, 158

regeneration, 157, 160, 169

Concentrate, 137, 142, 149

Concentration polarisation, 141, 148, 150, 151

Conformational effects, 87, 88, 110

- Control, 69
  - closed-loop, 73
  - implementation, 78–80
  - model based, 76
  - optimal open loop, 72
  - optimal, 77
  - PID, 75, 76
- Conversion degree, 104, 106, 107, 109
- CSTR, *see* continuous feed stirred tank
- Data Acquisition, 61, 78–80
- Dauer juveniles, 464
- Dean vortices, 142
- Diffusion coefficients in biofilms, 296
- Diffusion-reaction parameters in biofilm reactors, 295
- Dispersion coefficient, 110
- Distributing plate geometry, 2
- Distribution models, 193
- Down-comer and riser dimensions, 369
- Driving force, 136, 145, 169
- Dynamics of biofilm formation, 280
- Effectiveness factor, 95, 98, 99, 101, 102, 103 110, 111
- Electrical conductivity detection method, 3
- Electrostatic interactions, 87, 88
- Energy effectiveness of gas-liquid, 14
- Enlarged degassing zone, 368
- Enthomopathogenic Nematodes, 463
- Enzyme solid/gas reactors, 248
- Enzyme
  - activity, 88, 104, 107, 111
  - compartmentalisation, 136
  - poisoning, 148
  - immobilisation, 115, 136, 139, 181, 331
  - inactivation, 111
  - retention
    - adsorption, 139, 147, 148, 150, 151
    - chemical coupling, 139
    - electrostatic repulsion, 138, 160
    - entrapment, 139
    - immobilisation, 138, 139, 147
    - isoelectric trapping, 138
    - size exclusion, 138, 160
- Esterification, 154, 155
- Fick's law, 97, 98
- Filamentous fungi and filamentous bacteria, 28
- Filtration, 141, 142, 144, 151
- Flat sheet membrane, 142
- Flocculating cultures performance, 367
- Flocculation Bioreactors, 363

- Flocculation Mechanisms, 364, 365
- Flow
  - main, 142
  - recirculation, 143
  - secondary, 142
- Flow Injection Analysis, 59
- Flow pattern studies, 19
- Gas hold-up, 10
- Gas-liquid separator, 368
- Gas pulsation, pellet morphology control, 322
- Geometrical factors, 97
- Hollow fibre, 142, 145, 146, 147, 156, 161, 164, 165, 168
- Hydrolysis, 115, 149, 151, 152, 153, 156, 165, 168
- Image analysis, 25
- Image processing, 26, 27
- Immobilised
  - biocatalyst, 85, 89, 95, 96, 97, 105, 106, 110, 111, 115, 331
  - enzyme, 87, 88, 94, 103, 104, 105, 106, 107, 109, 110, 111
- In vitro* production of nematodes, 466
- In vivo* production of nematodes, 466
- Infective DT, 464
- Influence of design parameters, 374
- Influence of solid and liquid phases, 373
- Inhibition
  - competitive product, 90
  - non-competitive product, 90
  - simultaneous substrate and competitive product, 90
  - substrate, 90, 95, 105, 107, 109
- Internal loop airlift reactor, 2
- Internal-loop airlift for nematode production, 468
- Kinetics
  - first order, 97, 101, 109
  - irreversible reaction, 90
  - Michaelis-Menten, 90
  - reversible Michaelis-Menten, 95, 110, 111
  - two-liquid phase, 122, 123
  - zero order, 93, 97, 109
- Latrunculins, 482
- Limiting substrate in biofilm reactor modelling, 291
- Liquid culture of nematodes, 467
- Liquid velocity and gas hold-up in flocculation bioreactors, 370
- Longitudinal mixing, 6
- Marine bioproducts, 478
- Marine sponges as biocatalysts, 477

- Marine sponges, compounds from, 478  
Mass transfer  
  coefficients, 89, 90  
  effects, 98, 101, 105, 109, 110, 111  
  external, 101, 104, 105  
  internal, 101, 105  
  mechanisms in flocculating cell cultures, 372  
  three-phase fluidised bed, 338, 340  
  two liquid phase, 122, 123  
MBR, *see* membrane bioreactor  
Membrane  
  asymmetric, 141  
  bioreactor, 122, 135, 136, 151, 169, 181, 192, 198  
  dialysis, 143, 144, 145  
  fouling, 148, 150, 151  
  module  
    hollow fibre, 145, 146, 147, 164, 165, 168  
    plate and frame, 142  
    spiral wound, 142, 154, 166  
    tubular, 142, 143, 167  
  molecular weight cut-off, 149, 150, 200  
  properties, 200  
  reactor  
    advantages, 135, 136, 148, 149  
    applications, 135, 151, 152, 156, 160, 161, 163, 164, 165, 168  
    classification, 122, 135, 143, 192, 198  
    configuration, 143, 144, 147, 149, 161, 165, 169  
    dead-end, 142, 143, 144  
    dialysis, 143, 144  
    diffusion, 145, 146, 168  
    direct contact, 143, 152  
    disadvantages, 144, 145, 148, 149, 161  
    multiphase, 141, 146, 147, 156,  
    recycle, 143, 147, 150, 165  
  rejection coefficient, 202  
  resistance, 202  
  separation, 135, 137, 141  
  structure, 141, 146  
Microbial solid/gas reactors, 250  
Microemulsions, 184  
Minimum mixing time for recirculation, 369  
Mixing  
  axial, 107  
  radial, 107  
Modelling, 55  
  Artificial Neural Networks, 68, 69  
  basic concepts, 63  
  cell models, 64  
  continuous MBR, 209  
  fuzzy, 67, 69  
  hybrid, 68, 69  
  knowledge integration, 66

- model identification, 66
- Monitoring, biomass, 55, 58
  - carbon dioxide, 57
  - ex situ*, 58
  - FIA, 59
  - in situ*, 54
  - inferential measuring, 70
  - measuring dynamics compensation, 74
  - model based, 75
  - oxygen, 57
  - pH, 56
  - pressure, 56
  - software sensors, 75
- Multiple steady states, 90
- Nanofiltration, 142, 159
- Nernst layer, 89
- Non-conventional external-loop airlift for nematodes, 470
- Non-filamentous bacteria, 30
- Operation and applications of flocculation bioreactors, 379
- Optical resolutions, 151, 161, 162
- Organic phase, 117, 118, 119, 127
- Organic media, 183
- Organic solvent, 191, 332, 344
- Overall model for biofilm transient development, 298
- Particle imaging velocimetry, 39
- Particle streak velocimetry, 39
- Particle tracking velocimetry, 39
- Partitioning effects, 87, 88, 89, 97
- Permeate
  - flux, 141, 151
  - stream, 140, 142, 149, 150, 152
- Permeation, 140, 141, 142, 144, 145, 150, 151
- PFR, *see* plug flow reactor
- Plant cell bioreactors
  - aeration, 412
  - operating strategy, 418
  - configuration and operation mode, 415
  - design and operation, 409
  - energy dissipation levels, 406
  - foaming and wall growth, 414
  - mixing and mass transfer, 409
  - system geometry, 405
- Plant cell suspension cultures, 391
  - broth rheology, 398
  - cell-cell contact, 397
  - commercial processes, 393–395
  - critical shear stress, 407
  - fresh weight/dry weight, 400

- morphology, 392
- oxygen requirements, 401
- performance, 408
- rheological profiles, 399
- shear sensitivity, 402
- Plant cells image analysis, 33
- Practical design problems in biofilm reactors, 297
- Primmorphs formation, 487
- Primmorphs morphology, 487
- Primmorphs, 477, 486
- Process
  - integration, 135, 169
  - intensification, 135, 169
  - scale-up, 127
- Product
  - inhibition, 148, 149, 166
  - separation, 136, 139
- Protozoan image analysis, 34
- Pulsator
  - elastic membrane, 313
  - piston, 310
  - pneumatic, 310
  - self-propelled, 310
- Pulsed packed-bed reactor, 315
  - axial dispersion, 315, 316
- Pulsing bioreactors, 309
  - alcoholic fermentation, 318
  - bioreactor performance, 319
  - biotechnological processes, 317
  - citric acid production, 325
  - efficiency, 320
  - enzyme hydrolysis of starch, 318
  - gas-phase, 321
  - Mn-Peroxidase production, 324
  - synthetic dyes decolourisation, 326
- Pulsing devices, types, 309
- Pulsing plates column, 310
- Pulsing systems in biochemical reactors, 312
- Pulsing systems, uses, 311
- Rate
  - diffusion, 93
  - kinetic, 95
  - observed reaction, 95, 99
  - overall reaction, 97
  - transport, 90
- Rate parameters
  - effective, 88
  - inherent, 88
  - intrinsic, 88
- Reactor

- basket, 104
- batch, 104, 106, 204
- batch stirred tank, 105, 106, 107, 109, 110, 111
- biofilm, 271–274
- choice, 105
- continuous, 104, 107, 206, 209
- continuous feed stirred tank, 104, 105, 106, 109, 110, 111, 112, 136, 139, 140, 143, 144
- differential, 104, 206
- fluidised bed, 104, 105, 110, 331, 334, 335, 337, 347, 358
- ideal, 104, 105, 106, 110
- immobilised viable cell, 112
- integral, 206
- liquid-impelled loop, 122, 332
- liquid-liquid-solid, 331
- loop, 331, 336, 337
- packed bed, 105
- plug flow, 104, 105, 106, 107, 109, 110, 111 210
- pulsing, 309
- real, 110
- reversed micellar, 181, 198
- series, 212, 214
- stirred tank, 104
- tubular, 104
- Recovery, 474
- Rejection coefficient, 137, 139, 140, 202
- Reproductive factor, 474
- Residence time, 107, 109
- Reversed micelles, 181, 183, 184, 186
  
- Sectionalised bubble columns, 1, 2
- Segmentation, 27, 28
- SOLD method, 43
- Solid culture of nematodes, 465
- Solid phase distribution in flocculation bioreactors, 371
- Solid phase distribution, 5
- Solid-gas bioreactors
  - alcohol dehydrogenase, 261
  - atmospheric and reduced pressure, 252
  - hydration level, 259
  - lipolytic enzymes, 256
  - operating, 250
  - packed-bed, 253, 254
  - review, 247
  - thermodynamic parameters, 251
  - reduction of hexanal, 263
  - thermal stability, 260
  - water activity, 260, 263
- Solid-gas systems, 247
- Solid-to-solid bioconversions, 225
- Solid-to-solid bioconversions
  - batch and continuous crystallisers, 238–240

biocatalyst immobilisation, 233

classification, 227

continuous, 231

conversion and scale, 229

costs batch vs. continuous, 241

downstream processing, 236

equipment design, 233

kinetics, 230

overall costs, 238

process control, 235

rate-limiting, 237

Sponge cells, immobilised, 489

Sponge tissue dissociation, 483

Sponge-cell cultures, 483

Sponge-cell growth, 484, 485

Sponges

body structure, 481

classification, 479

maricultures, 482

Stability, 85, 87, 88, 91, 103, 105, 111, 211

Staining techniques, 28–30

Steinerinema, 463

Steric effects, 87, 88

Substrate

inhibition, 139, 148

modulus, 90, 93

retention, 139, 140

Surfactant, 181, 182

Support in biofilm reactors, 276

Synthesis of peptides, 151, 161, 162

Taylor vortices, 142

Thiele modulus, 98, 99, 101

Three-phase fluidised bed bioreactor, 334, 335, 337, 347, 358

batch operation, 350

continuous operation, 354

hydrodynamics, 339

kinetics, 338, 342

mass transfer, 338, 340

Transesterification, 152, 154, 181

Two liquid phase

biocatalysis, 115, 130

biocatalytic processes, 116, 117, 126

biocatalytic reactors, 115, 121

biocatalytic systems, 331, 353

downstream processing, 116, 118, 129, 132

kinetics, 122, 123

log P, 119, 120

mass transfer, 122, 123

reactor operation, 124

Ultrafiltration

cell, 142, 144, 153, 154, 155, 158, 162, 168  
membrane, 141, 169

Volumetric gas-liquid mass transfer coefficient, 13

*Xenorhabdus nematophilus*, 465

Yeasts, image analysis, 31